

DYNAMIC MODELING OF VERTICAL U-TUBE STEAM  
GENERATORS FOR OPERATIONAL SAFETY SYSTEMS

(Vol. I)  
by

WALTER HERBERT STROHMAYER

B. S. Rensselaer Polytechnic Institute  
(Dec. 1976)

S. M. Massachusetts Institute of Technology  
(June 1978)

SUBMITTED TO THE DEPARTMENT OF  
NUCLEAR ENGINEERING IN PARTIAL  
FULFILLMENT OF THE  
REQUIREMENTS FOR THE  
DEGREE OF

DOCTOR OF PHILOSOPHY

at the

MASSACHUSETTS INSTITUTE OF TECHNOLOGY

August 1982

© Walter Herbert Strohmayer 1982

Signature of Author \_\_\_\_\_

Department of Nuclear Engineering  
August 1982

Certified by \_\_\_\_\_

Professor John E. Meyer  
Thesis Supervisor

Accepted by \_\_\_\_\_

Professor Allan F. Henry  
Chairman, Departmental Graduate Committee

Science

MASSACHUSETTS INSTITUTE  
OF TECHNOLOGY

JAN 18 1983

LIBRARIES

# DYNAMIC MODELING OF VERTICAL U-TUBE STEAM GENERATORS FOR OPERATIONAL SAFETY SYSTEMS

by

Walter Herbert Strohmayer

Submitted to the Department of Nuclear Engineering  
on August 25, 1982, in partial fulfillment of the  
requirements for the degree of Doctor of Philosophy  
in Nuclear Engineering.

## ABSTRACT

Currently envisioned operational safety systems require fast running computer models of major power plant components in order to generate reliable estimates of significant safety-related parameters. The objectives of this research are to develop and to validate such a model for a vertical U-tube natural circulation steam generator.

The model is developed using a first principles application of the one-dimensional conservation equations of mass, momentum, and energy. Two-phase flow is treated by using the drift flux model. Two salient features of the model are the incorporation of an integrated secondary-recirculation-loop momentum equation and the retention of all nonlinear effects. The inclusion of the integrated loop momentum equation permits calculation of the steam generator water level. The use of a nonlinear model, as opposed to a linearized model, allows accurate calculation of steam generator conditions for transients with large changes from nominal operating conditions.

The model is validated over a wide range of steady-state conditions and a spectrum of transient tests ranging from turbine trip events to a milder full-length control-element assembly drop transient. The results of the validation effort are encouraging, demonstrating that the model is suitable for application to a broad range of operational transients.

Execution speed of the model appears to be fast enough to achieve real-time execution on plant process computers. Real Time-to-CPU Time ratios for running the computer program on an Amdahl 470 V/8 computer range from 47 to 200, with integration time step sizes of 0.1 to 0.4 seconds, respectively. When the model is run on a Digital Equipment Corp. VAX 11/780 computer using an integration time step of 0.25 seconds, the Real Time-to-CPU Time ratio is 11.

Thesis Supervisor: John E. Meyer  
Title: Professor of Nuclear Engineering

Thesis Reader: David D. Lanning  
Title: Professor of Nuclear Engineering

## ACKNOWLEDGMENTS

I would like to express my heartfelt appreciation to my thesis supervisor, Professor John E. Meyer, for his invaluable support, advice, and assistance. His willingness to discuss, at any time, topics related to this project has made my association with him a privileged and rewarding experience.

Thanks are also due to Professor David D. Lanning who served as the reader of this thesis and motivated the advanced control systems group.

I wish to express my gratitude to Professor Allan F. Henry for his encouragement throughout my stay at M.I.T.

The work was funded through the fellowship program at The Charles Stark Draper Laboratory. This allowed me to work with a group of professionals who truly enriched my own professional development. I wish to acknowledge: Dr. John Hopps, for his support and advice; Mr. James Deckert for his valuable comments, help, and advice during the research; Dr. Jay Fisher, for his support and thoughtful suggestions, particularly during the validation phase of the study; Dr. Asok Ray, whose technical expertise and willingness to share his knowledge contributed in no small way to my education; and, Mr. Renato Ornedo, for his advice, constructive criticism, and friendship.

The RD-12 boiler data was acquired through the courtesy of Mr. C.G. Mewdell of Ontario Hydro, and Mr. W.C. Harrison of the Whiteshell Nuclear Research Establishment.

Thanks are due to:

- Jon, Bob, Patrick, Ed, Jim, Dale, Mike, and Lucy, my officemates, for their friendship and moral support;
- Derek Ebeling-Koning, for his friendship;
- Peggy Conley, for her help;
- Jean Nolley, who made the bad times good;
- Edward Carbrey and his staff, for their help in the preparation of this thesis;
- Kathleen Rogness, who typed the majority of this thesis and did so with a cheerfulness and zeal that, despite my constant revisions, was truly appreciated; and,
- Lisa Kern, for typing various figures, and Laura Burkhardt, for typing various figures and some of the text, and Vugraphs.

This thesis is dedicated to my parents for their love, support and encouragement.

Finally, thanks are due to Dr. P. Bergeron of Yankee Atomic Co. for providing information related to the Maine Yankee plant.

The information contained in this thesis cited as deriving from "Maine Yankee", however, should not be considered as representing that actual system in its current or projected operating configuration, but as an idealization

thereof. In particular, the results so identified in this report have not been either reviewed or approved by the Yankee organization.

I hereby assign my copyright of this thesis to The Charles Stark Draper Laboratory, Inc., Cambridge, Massachusetts.

---

Walter Herbert Strohmayer

Permission is hereby granted by The Charles Stark Draper Laboratory, Inc. to the Massachusetts Institute of Technology to reproduce any or all of this thesis.

## TABLE OF CONTENTS

	<u>Page</u>
Abstract.....	ii
Acknowledgements.....	iii
List of Figures.....	xii
List of Tables.....	xix
Chapter 1. INTRODUCTION.....	1-1
1.1 Background and Motivation.....	1-1
1.2 Research Objectives.....	1-5
1.3 Previous Work.....	1-7
1.4 Organization of Report.....	1-9
Chapter 2. STEAM GENERATOR MODEL: OVERVIEW.....	2-1
2.1 Description of Steam Generator.....	2-1
2.2 Model Regions.....	2-1
2.3 Auxiliary Models.....	2-8
Chapter 3. SECONDARY SIDE MODEL.....	3-1
3.1 Tube Bundle Region.....	3-1
3.1.1 Mass and Energy Equations.....	3-1
3.1.2 Integration by Profiles.....	3-4
3.1.3 Detailed Profiles.....	3-5
3.1.4 Approximate Profiles.....	3-12
3.1.5 Approximation Errors.....	3-17
3.1.6 State Variables.....	3-21

TABLE OF CONTENTS (Cont.)

	<u>Page</u>
3.2 Riser Region.....	3-27
3.2.1 Mass and Energy Equations.....	3-27
3.2.2 Profiles.....	3-28
3.2.3 State Variables.....	3-29
3.3 Steam Dome and Downcomer.....	3-31
3.3.1 Case 1 Conservation Equations.....	3-34
3.3.2 Case 1 State Variables.....	3-38
3.3.3 Case 2 Conservation Equations.....	3-41
3.3.4 Case 2 State Variables.....	3-50
3.4 Momentum Equation for the Recirculating Flow.....	3-56
3.5 Closure of Equations.....	3-71
3.6 Main Steam and Feedwater System Models.....	3-76
3.7 Discussion of Model.....	3-83
Chapter 4. PRIMARY SIDE MODEL.....	4-1
4.1 Primary Fluid System.....	4-1
4.1.1 Plenum Model.....	4-1
4.1.2 Tubeside Model.....	4-6
4.2 Heat Transfer Model.....	4-9
4.2.1 Tube Metal Conduction.....	4-11
4.2.2 Tube Metal Temperature Response.....	4-15
4.2.3 Heat Transfer Model.....	4-19

## TABLE OF CONTENTS (Cont.)

	<u>Page</u>
Chapter 5. NUMERICAL SOLUTION.....	5-1
5.1 Equation System.....	5-1
5.1.1 Primary Side Equations.....	5-1
5.1.2 Secondary Side Equations.....	5-2
5.2 Steady State Solution.....	5-9
5.2.1 Primary Side Steady State Solution.....	5-9
5.2.2 Secondary Side Steady State Solution.....	5-18
5.3 Decoupling of Primary and Secondary Transient Solutions.....	5-23
5.4 Transient Solution Boundary Conditions.....	5-29
5.5 Primary Transient Solution.....	5-30
5.6 Secondary Transient Solution.....	5-31
5.7 Transient Heat Transfer Rate.....	5-38
5.8 Numerical Analysis of Secondary Side Equations.....	5-41
Chapter 6. VALIDATION.....	6-1
6.1 Preview.....	6-1
6.2 Argonne National Laboratory Test Loop.....	6-6
6.2.1 Background Information.....	6-6
6.2.2 Results.....	6-7
6.3 RD12 Boiler Tests.....	6-12
6.3.1 Background Information.....	6-12
6.3.2 Steady State Tests.....	6-18
6.3.3 Additional Information for Transient Simulations.....	6-30



TABLE OF CONTENTS (Cont.)

	<u>Page</u>
6.3.4 Power Increase Test.....	6-34
6.3.5 Power Decrease Test.....	6-41
6.3.6 Primary Flowrate Decrease Test.....	6-47
6.3.7 Primary Flowrate Increase Test.....	6-54
6.3.8 Secondary Pressure Increase Test.....	6-60
6.3.9 Feedwater Transient.....	6-66
6.3.10 Oscillating Pressure Test.....	6-72
6.4 Arkansas Nuclear One - Unit 2.....	6-74
6.4.1 Background Information.....	6-74
6.4.2 Full Length CEA Drop Test.....	6-82
6.4.3 Sensitivity of Level to Feedwater Flowrate.....	6-90
6.4.4 Turbine Trip Test.....	6-97
6.4.5 Loss of Primary Flow.....	6-112
6.5 Program Execution Time.....	6-129
Chapter 7. SUMMARY, CONCLUSIONS, AND RECOMMENDATIONS.....	7-1
7.1 Summary.....	7-1
7.2 Conclusions.....	7-3
7.3 Recommendations for Future Work.....	7-8
Appendix A. TWO-PHASE FLOW.....	A-1
Appendix B. GENERAL CONSERVATION EQUATIONS.....	B-1
B.1 Mass Conservation Equation.....	B-2

TABLE OF CONTENTS (Cont.)

	<u>Page</u>
B.2 Energy Conservation Equation.....	B-4
B.3 Momentum Conservation Equation.....	B-5
B.4 Enthalpy Reference Point and the Energy Equation.....	B-10
B.5 Application of Conservation Equations.....	B-13
Appendix C. EMPIRICAL CORRELATIONS.....	C-1
C.1 Vapor Volume Fraction.....	C-1
C.2 Frictional Pressure Drop.....	C-6
C.3 Heat Transfer.....	C-8
Appendix D. CROSS FLOW LOSS COEFFICIENT.....	D-1
Appendix E. LINEAR PROFILE ERRORS.....	E-1
Appendix F. CONVECTIVE DIFFERENCING SCHEMES.....	F-1
Appendix G. CALCULATING STEAM AND FEEDWATER FLOWRATES USING WATER LEVEL AND PRESSURE AS INPUTS.....	G-1
G.1 Introduction.....	G-1
G.2 Model Modification.....	G-2
G.3 Results.....	G-5
G.4 Conclusions and Recommendations.....	G-10
Appendix H. ADDITIONAL VALIDATION AND GEOMET- RIC INPUT.....	H-1
H.1 Maine Yankee.....	H-1
H.1.1 Steady State Results.....	H-2
H.1.2 Transient Tests of 106 per cent Power.....	H-2
H.1.3 Transient Tests at Full Power.....	H-15

TABLE OF CONTENTS (Cont.)

	<u>Page</u>
H.2 Calvert Cliffs.....	H-23
H.2.1 Licensing Calculations.....	H-24
H.2.2 Startup Test Results.....	H-30
H.3 Geometric Input for All Test Cases and Comments Regarding Special Fea- tures in Some Test Cases.....	H-38
Appendix I. PROGRAM INPUT - OUTPUT.....	I-1
I.1 Input.....	I-1
I.2 Sample Output.....	I-9
Appendix J. CODE LISTING.....	J-1
Appendix K. DOWNCOMER GEOMETRIC REPRESENTATION FOR WATER LEVEL CALCULATION.....	K-1
NOMENCLATURE.....	Nom-1
REFERENCES.....	Ref-1
BIOGRAPHICAL NOTE.....	Bio-1

## LIST OF FIGURES

	<u>Page</u>
1.1-1 Analytic measurement.....	1-2
1.1-2 Decision/estimator.....	1-3
1.1-3 Generation of a best estimate value of quantity A.....	1-4
2.1-1 Representative U-Tube steam generator.....	2-2
2.2-1 Primary side regions.....	2-6
2.2-2 Secondary side regions.....	2-7
2.3-1 Typical main steam system.....	2-9
2.3-2 Block diagram of typical feedwater controller.....	2-12
3.1-1 Secondary nomenclature.....	3-2
3.1-2 Heat transfer regimes.....	3-6
3.1-3 Profiles at 100 per cent power.....	3-13
3.1-4 Profiles at 40 per cent power.....	3-14
3.1-5 Profiles at 5 per cent power.....	3-15
3.1-6 Integrated energy content per unit mass.....	3-20
3.3-1 Steam dome - downcomer.....	3-33
3.3-2 Case 2 block diagram and nomenclature.....	3-44
3.3-3 Mass balance jump condition.....	3-46
3.4-1 Notation for momentum equation.....	3-58
3.6-1 Steam dump valve control program.....	3-82
4.1-1 Primary side nomenclature.....	4-3
4.2-1 Heat transfer mechanisms.....	4-10
4.2-2 Nomenclature for equation 4.2-3.....	4-13

LIST OF FIGURES (Cont.)

	<u>Page</u>
4.2-3 System for calculation of temperature response time.....	4-16
4.2-4 Primary temperature distribution at heat transfer calculation transition.....	4-22
4.2-5 Histogram representation of profile shown in Figure 4.2-4.....	4-22
4.2-6 Generalized histogram representation of temperature profile.....	4-24
5.2-1 Flowchart of steady state primary temperature calculation.....	5-12
5.2-2 Bisection method for heat transfer calculation.....	5-14
5.2-3 Bisection method for downcomer flowrate calculation.....	5-21
5.2-4 Flowchart of steady state calculation of recirculation flowrate.....	5-24
5.6-1 Flowchart of secondary transient solution.....	5-35
6.2-1 Argonne National Laboratory test loop configuration.....	6-8
6.2-2 Downcomer flowrate versus power.....	6-9
6.3-1 Test loop arrangement.....	6-13
6.3-2a Schematic of RD12 steam generator.....	6-14
6.3-2b Steam generator with integral preheater.....	6-16
6.3-3 Slip ratio in riser vs. power.....	6-19
6.3-4 Mean vapor velocity at riser inlet vs. volumetric flux.....	6-21
6.3-5 Riser inlet vapor volume fraction vs. power.....	6-22
6.3-6 Downcomer flowrate vs. power.....	6-22

LIST OF FIGURES (Cont.)

	<u>Page</u>
6.3-7 Kiser inlet vapor volume fraction vs. power.....	6-24
6.3-8 Downcomer flowrate vs. power.....	6-27
6.3-9 Input for power increase test.....	6-36
6.3-10 Steam Generator response for power increase test.....	6-38
6.3-11 Input for power decrease test.....	6-43
6.3-12 Steam generator response for power decrease test.....	6-45
6.3-13 Input for primary flowrate decrease test.....	6-48
6.3-14 Steam generator response for primary flowrate decrease test.....	6-50
6.3-15 Downcomer vapor volume fraction during primary flowrate decrease test.....	6-53
6.3-16 Input for primary flowrate increase test.....	6-56
6.3-17 Steam generator response for primary flowrate increase test.....	6-58
6.3-18 Input for secondary pressure increase test.....	6-62
6.3-19 Steam generator response for secondary pressure increase test.....	6-64
6.3-20 Input for feedwater transient test.....	6-68
6.3-21 Steam generator response for feedwater transient test.....	6-70
6.4-1 Arkansas Nuclear One - Unit 2 schematic.....	6-75
6.4-2 Short term input for full length CEA drop, steam generator 1.....	6-85
6.4-3 Long term input for full length CEA drop, steam generator 1.....	6-86

LIST OF FIGURES (Cont.)

	<u>Page</u>
6.4-4 Short term full length CEA drop response, steam generator 1.....	6-87
6.4-5 Long term full length CEA drop response, steam generator 1.....	6-88
6.4-6 Short term input for full length CEA drop, steam generator 2.....	6-91
6.4-7 Long term input for full length CEA drop, steam generator 2.....	6-92
6.4-8 Short term full length CEA drop response, steam generator 2.....	6-93
6.4-9 Long term full length CEA drop response, steam generator 2.....	6-94
6.4-10 Long term full length CEA drop response using feedwater controller, steam generator 2.....	6-96
6.4-11 Comparison of feedwater flowrates.....	6-98
6.4-12 Short term input for turbine trip, steam generator 1.....	6-101
6.4-13 Long term input for turbine trip, steam generator 1.....	6-102
6.4-14 Short term turbine trip response, steam generator 1.....	6-104
6.4-15 Long term turbine trip response, steam generator 1.....	6-105
6.4-16 Short term input for turbine trip, steam generator 2.....	6-107
6.4-17 Long term input for turbine trip, steam generator 2.....	6-108
6.4-18 Short term turbine trip response, steam generator 2.....	6-109
6.4-19 Long term turbine trip response, steam generator 2.....	6-111

LIST OF FIGURES (Cont.)

	<u>Page</u>
6.4-20 Primary flowrate used for loss of flow calculations.....	6-115
6.4-21 Short term input for loss of primary flow test, steam generator 1.....	6-117
6.4-22 Long term input for loss of primary flow test, steam generator 1.....	6-118
6.4-23 Short term loss of primary flow response, steam generator 1.....	6-120
6.4-24 Long term loss of primary flow response, steam generator 1.....	6-122
6.4-25 Short term input for loss of primary flow test, steam generator 2.....	6-124
6.4-26 Long term input for loss of primary flow test, steam generator 2.....	6-125
6.4-27 Short term loss of primary flow response, steam generator 2.....	6-126
6.4-28 Long term loss of primary flow response, steam generator 2.....	6-128
B-1 Channel geometry.....	B-3
C-1 Drift Flux Model - Weighted Mean Vapor Velocity vs. Volumetric Flux.....	C-3
C-2 Void Distribution Profiles in a Round Tube.....	C-4
D-1 Arrangement of tubes in tube bundle for cross flow.....	D-4
E-1 Internal energy profile.....	E-4
G-1 Steam and feedwater flows obtained using 4-digit accuracy for input level and pressure.....	G-7
G-2 Steam and feedwater flows obtained using 7-digit accuracy for input level and pressure.....	G-9



LIST OF FIGURES (Cont.)

		<u>Page</u>
G-3	Steam and feedwater flows obtained using smoothed level and pressure inputs.....	G-11
H.1-1	Feedwater temperature vs. power.....	H-3
H.1-2	Primary average temperature vs. power.....	H-3
H.1-3	Steady state results.....	H-4
H.1-4	Input for CEA withdrawal incident.....	H-6
H.1-5	Steam generator response for CEA withdrawal incident.....	H-8
H.1-6	Input for loss of load incident.....	H-10
H.1-7	Steam generator response for loss of load incident.....	H-11
H.1-8	Input for loss of feed incident.....	H-13
H.1-9	Steam generator response for loss of feed incident.....	H-14
H.1-10	Input for reactor trip.....	H-16
H.1-11	Steam generator response for reactor trip.....	H-17
H.1-12	Input for turbine trip with steam dump.....	H-19
H.1-13	Steam generator response for turbine trip with steam dump.....	H-20
H.1-14	Input for turbine trip without steam dump.....	H-21
H.1-15	Steam generator response for turbine trip without steam dump.....	H-22
H.2-1	Input for CEA withdrawal incident.....	H-26
H.2-2	Steam generator response for CEA withdrawal incident.....	H-27
H.2-3	Input for the loss of load incident.....	H-28
H.2-4	Steam generator response for the loss of load incident.....	H-29

LIST OF FIGURES (Cont.)

	<u>Page</u>
H.2-5 Input for turbine trip test.....	H-32
H.2-6 Steam generator response for turbine trip test.....	H-33
H.2-7 Primary flowrate during loss of primary flow test.....	H-34
H.2-8 Input for loss of primary flow at 40% power.....	H-36
H.2-9 Steam generator response for loss of primary flow at 40% power.....	H-37
K-1 Idealized steam dome - downcomer repre- sentation.....	K-2

## LIST OF TABLES

	<u>Page</u>
1.3-1 Typical Computation Times for Detailed Steam Generator Codes.....	1-8
3.1-1 Representative Fluid Transport Times.....	3-5
3.1-2 Inputs for Detailed Profile Calculations.....	3-11
3.1-3 Results of Detailed Profile Calculations - Bubble Departure and Saturation Lengths.....	3-12
3.1-4 Errors Introduced by Linear Profile Approximation.....	3-19
3.1-5 Partial Derivatives for Eqs. 3.1-11 and 3.1-12.....	3-23
3.1-6 Property Derivatives.....	3-26
3.2-1 Partial Derivatives of $M_R$ and $E_R$ .....	3-32
3.3-1 Partial Derivatives for Equation 3.3-10.....	3-40
3.3-2 Partial Derivatives Appearing in Equation 3.3-11.....	3-42
3.3-3 Partial Derivatives Appearing in Equation 3.3-27.....	3-52
3.3-4 Partial Derivatives Appearing in Equation 3.3-29.....	3-55
3.5-1 Equations Available for Solution.....	3-72
3.5-2 Partial Derivatives Appearing in Equation 3.5-4.....	3-75
3.5-3 Secondary Side Unknowns.....	3-76
3.5-4 Secondary Side Equations.....	3-77
4.1-1 Representative Primary Side Transport Times.....	4-2
4.2-1 Representative Steam Generator Parameters.....	4-18

LIST OF TABLES (Cont.)

	<u>Page</u>
5.1-1 Components of A Matrix.....	5-6
5.2-1 Derivative of Equation 5.2-3.....	5-19
5.8-1 Eigenvalues of the Sixth Order System for Maine Yankee.....	5-47
5.8-2 Eigenvalues of the Seventh Order System for Maine Yankee.....	5-50
6.1-1 Test Cases Used for Model Validation.....	6-2
6.1-2 Breakdown of Validation Program.....	6-3
6.2-1 Test Loop Operating Conditions.....	6-7
6.3-1 Steam Generator Conditions for Fouling Factor Calculations.....	6-31
6.3-2 Initial Conditions for Power Increase Test.....	6-35
6.3-3 Initial Conditions for Power Decrease Test.....	6-42
6.3-4 Initial Conditions for Primary Flowrate Decrease Test.....	6-52
6.3-5 Initial Conditions for Primary Flowrate Increase Test.....	6-55
6.3-6 Initial Conditions for Secondary Pres- sure Increase Test.....	6-61
6.3-7 Initial Conditions for Feedwater Transient.....	6-67
6.4-1 Arkansas Nuclear One - Unit 2 Steam Generator Design Operating Parameters.....	6-76
6.4-2 RTD Response Times.....	6-78
6.4-3 Primary Flowrates and Tube Fouling Factors Used in Initialization Calcula- tions for Each Transient.....	6-80

LIST OF TABLES (Cont.)

	<u>Page</u>
6.4-4 Full Length CEA Drop Initial Conditions, Steam Generator 1.....	6-84
6.4-5 Full Length CEA Drop Initial Conditions, Steam Generator 2.....	6-90
6.4-6 Turbine Trip Initial Conditions, Steam Generator 1.....	6-100
6.4-7 Turbine Trip Initial Conditions, Steam Generator 2.....	6-110
6.4-8 Decay Power Parameters.....	6-116
6.4-9 Loss of Primary Flow Initial Conditions, Steam Generator 1.....	6-119
6.4-10 Loss of Primary Flow Initial Conditions, Steam Generator 2.....	6-123
6.5-1 Real Time-to-CPU Time Ratio for Execution on Amdahl 470 V/8 System.....	6-129
H.1-1 Steady State Operating Parameters for Maine Yankee.....	H-5
H.1-2 Initial Conditions for Maine Yankee Transient Tests at 106 percent Power.....	H-7
H.1-3 Initial Conditions for Maine Yankee Transient Tests at Full Power.....	H-15
H.2-1 Initial Conditions for Calvert Cliffs Licensing Calculations.....	H-24
H.2-2 Initial Conditions for Turbine Trip Test.....	H-30
H.2-3 Initial Conditions for Loss of Primary Flow at 40 per cent Power.....	H-35
H.3-1 Input Geometry for Test Cases.....	H-39
K-1 Region Volumes.....	K-4
K-2 Water Level Equations.....	K-7

## Chapter 1

### INTRODUCTION

The goal of this thesis is to develop a fast running computer model of a vertical U-tube natural circulation steam generator. In this chapter we first discuss possible applications for this model in the context of current safety issues and concerns. Having demonstrated a need for such a model, we then clearly define the research task and follow up with a brief review of previous work.

#### 1.1 BACKGROUND AND MOTIVATION

Major efforts are being made to improve the safety of nuclear power plants by developing systems to assist operators in taking appropriate corrective action during off-normal plant transients. Two such systems are the utility-funded Electric Power Research Institute's disturbance analysis and surveillance system (DASS) (Refs. (E2) and (M6)), and the Nuclear Regulatory Commission - mandated safety parameter display system (SPDS) (Ref. (H4)). Both of these systems should be predicated upon the concept of information reliability. That is, the creation and maintenance of a validated data base consisting of best estimate values of processed sensor signals to be used in generating reliable estimates of parameters relevant to plant safety (Refs. (H4) and (D1)). Systems that achieve information reliability can

be used by power plant operators with a high degree of confidence, particularly during off-normal plant events when crucial decisions have to be made. In addition to improving plant safety, these systems should also improve plant availability, providing an economic incentive for their development.

Given that information reliability is desirable, how can it be achieved? One approach to this question is addressed elsewhere (Refs. (H4) and (D1)) and will only be discussed briefly here. We consider a situation where we have sensors to measure four quantities: A, B, C, and D (this example is taken from Ref. (D1)). In fact, we have two sensors to measure quantity A and one each for quantities B, C, and D. We also have a plant component X which defines a physical relationship between quantity A and quantities B, C, and D. We define an analytic measurement of quantity A to be the output of an analytic model of component X using as input the measured quantities B, C, and D. This relationship is defined in Fig. 1.1-1.

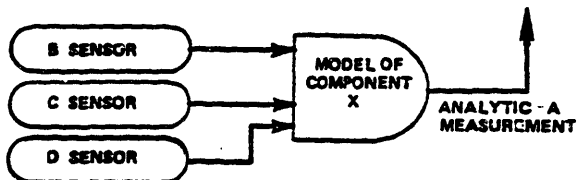


Figure 1.1-1. Analytic Measurement (Ref. (D1)).

Before pursuing this example any further, we pause here to define a decision/estimator (D/E). The inputs to a D/E consist of all measurements of a quantity of interest; these measurements can be both direct sensor measurements or analytic measurements. The D/E performs two functions:

- 1.) detection and isolation of inconsistencies in the multiple measurements for a given variable; and,
- 2.) uses remaining consistent input measurements to obtain a single estimate of the given variable.

Figure 1.1-2 shows the symbol used to represent a D/E. The D/E shown in this figure has three input measurements and one output corresponding to the estimated value of the measurement. The arrow emerging from the side of the D/E indicates the detection and isolation of inconsistencies in the input measurements.



Figure 1.1-2. Decision Estimator (Ref. (D1)).

Returning to our example, we use the two direct sensor measurements of quantity A together with the analytic measurement of A as inputs to a D/E, as shown in Fig. 1.1-3. The output of the D/E is then a good, or reliable, estimate



of the value of the measured quantity A. There are several comments regarding Fig. 1.1-3:

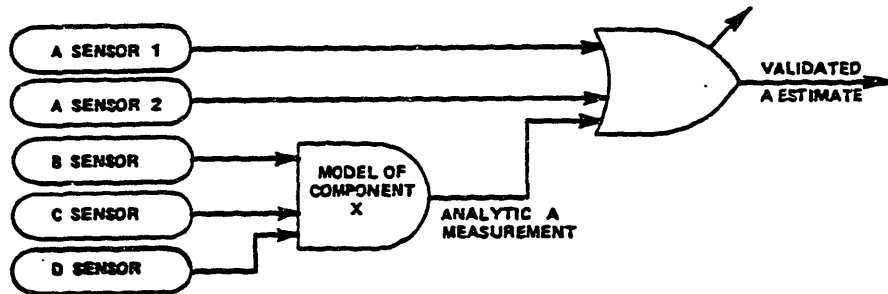


Figure 1.1-3. Generation of a Best Estimate Value of Quantity A (Ref. (D1)).

- 1.) The inputs to the model of component X could consist of validated estimates from other D/Es, as well as direct sensor measurements;
- 2.) The method usually does not require installation of additional sensors in power plants, particularly in major plant systems; and,
- 3.) The methodology has fault detection capability (Ref. (D1)).

In order to generate an analytic measurement, we need a model of plant component X. This model is required to run in real time, or faster, in parallel with all other plant computer tasks. The model should be derived from physical laws applying to the component in question. A physically based model is preferred to an empirically constructed model because a model derived from basic physical laws can often

be applied to a wide range of operating conditions while empirical models are generally limited to the narrow range of operating conditions for which they are obtained. Both the DASS and SPDS need plant component models in order to generate parameters relevant to plant safety. For this application, the models are also required to run in real time and should be physically derived. Finally, if we obtain much faster than real time computing capability, then these models can be used in a predictive manner to aid operations personnel in making decisions concerning alternate control actions to be initiated during off-normal plant transients.

In summary, the judicious application of physically derived, accurate, faster than real time computer models of major plant components can result in systems that improve the reliability of information displayed to plant operators or used in closed loop control, improve plant availability, and provide the operator with predictive capability.

## 1.2 RESEARCH OBJECTIVES

The main objectives of this work are to develop and validate an analytic model of a vertical U-tube natural circulation steam generator, which is a major component in many pressurized water reactor (PWR) plants (the other type of steam generator in PWR plants is the once-through steam generator). The model should satisfy the criteria set down in the previous section, which are:

- 1.) Real time operation of the model; and,
- 2.) Model development based on the application of fundamental physical laws rather than an empirically derived model.

Model development is accomplished by the application of the laws of conservation of mass, momentum, and energy to control volumes constituting the steam generator. The control volumes selected and the physical assumptions used in these control volumes are based on considerations such as geometric configuration, the physics occurring within the various steam generator regions, and constraints arising from numerical solution techniques.

The task of model validation is the comparison of the computer model results with experimental data and/or results generated by other computer codes that have been well validated. This step ensures model fidelity and helps determine the limits of model applicability. A thoroughly validated model can be used with confidence in an operational safety system.

An additional dividend resulting from the development of a fast, physically based steam generator model is that such a model bridges the gap between simplified boiler-pot models and the more complex, computer-time-consuming codes such as RETRAN (Ref. (M8)), URSULA2 (Ref. (K2)), and COBRA-TF(EPRI) (Ref. (S2)).

### 1.3 PREVIOUS WORK

Little literature exists relevant to the real time modeling of steam generators. However, there is a fair amount of information available dealing with steam generator modeling in general. A good literature survey of transient modeling of nuclear steam generators is given in Ref. (L2), so a literature review will not be given here.

Much of the recent work in steam generator modeling involves detailed, three-dimensional, two-fluid representations of the boiling side of the steam generator (Refs. (K2), (M7), (S2), and (I2)). The computer models derived in the references given above are used to generate detailed flow conditions for either steady state or transient cases. The detail is obtained only by spending large amounts of computing time as shown in Table 1.3-1. Note that the geometric detail of these models ranges from 4900 cells to about 500 cells, while the model developed in this work has 4 cells. Less detailed computer models are developed in Refs. (V1), (H5), and (L3); these models use one-dimensional, slip-flow (not two-fluid) representations of the boiling side of the steam generator. The TRANSG code (Ref. (L3)) when used to model a once-through steam generator with a fixed time step size of 0.05 seconds requires 16 seconds of computer time to simulate 10 seconds of real time on an Amdahl 470/V6 computer system. (Computation time results quoted here vary with the size of the problem being solved - for the TRANSG problem mentioned above this is 20 cells for

Table 1.3-1  
 Typical Computation Times for Detailed Steam Generator  
 Codes (Times as reported in cited references).

Code	Computing Time	Computer	Comments
THIRST (Ref. (I2))	210 seconds per steady state calculation	CDC-CYBER-175	4900 cells. Homogeneous model. Steady state only.
URSULA2 (Ref. (M7))	Homogeneous model: 180 seconds per steady state calculation 30-100 seconds per time step*  Two-fluid model: 288 seconds per steady state calculation 48-160 seconds per time step* *Time step size = 4 seconds	CDC-7600	936 cells. 936 cells.  936 cells. 936 cells.
COBRA-TF(EPRI) (Ref. (S2))	9 hours per steady state calculation 1 hour per steady state calculation	VAX CDC-7600	-500 cells.

both the primary and secondary sides.) Although none of the works cited here deal with real time modeling of steam generators, they are useful guides in developing real time computer models since they provide insightful information concerning steam generator dynamics and modeling.

The most relevant work with respect to real time modeling is a thesis by Clarke (Ref. (C2)). In this work Clarke uses a lumped parameter approach in the treatment of the secondary regions of the steam generator. The model is simple, but it retains the essential physical features necessary to reproduce gross steam generator dynamics.

#### 1.4 ORGANIZATION OF REPORT

Chapter 2 is an overview of the steam generator model developed in this work. Chapter 3 provides detailed information regarding the development of the secondary side model. The primary side model, along with the heat transfer model, is developed in Chapter 4. The numerical solution scheme, including a discussion of stability concerns, is given in Chapter 5. Model validation is discussed in Chapter 6 and Appendix H. Conclusions and recommendations, as well as a summary, are given in Chapter 7. Appendices I and J contain a description and listing of the computer program. An interesting attempt to use boundary conditions for transient calculations other than those given in the main text is presented in Appendix G. The remaining appendices (A, B, C, D, E, F, and K) contain supplementary details.

## Chapter 2

### STEAM GENERATOR MODEL: OVERVIEW

#### 2.1 DESCRIPTION OF STEAM GENERATOR

Heat generated by the nuclear chain reaction in the core of a pressurized water reactor is removed by the primary coolant and is transferred to the secondary coolant via the steam generators. This heat transfer results in the production of secondary steam which is then used to drive a turbine-generator set.

A representative U-tube steam generator (UTSG) is shown in Fig. 2.1-1. The unit consists of two interacting fluid systems: the hot primary fluid system and the colder secondary fluid system. The primary and secondary sides are linked by heat transfer through the tube walls. The primary fluid system consists of the hot reactor coolant on the tube side of the tube bundle, as well as the primary coolant contained in the inlet and outlet plena located at the bottom of the steam generator. Hot reactor water enters the steam generator through the primary inlet nozzle. It then flows inside the U-tubes, first upward and then downward, where it transfers heat to the secondary fluid. The coolant then leaves the outlet plenum through the outlet nozzle.

The secondary fluid has two distinct regions: an upflow region and a downflow region. These regions are separated by a wrapper with the inner (upflow) region consisting of

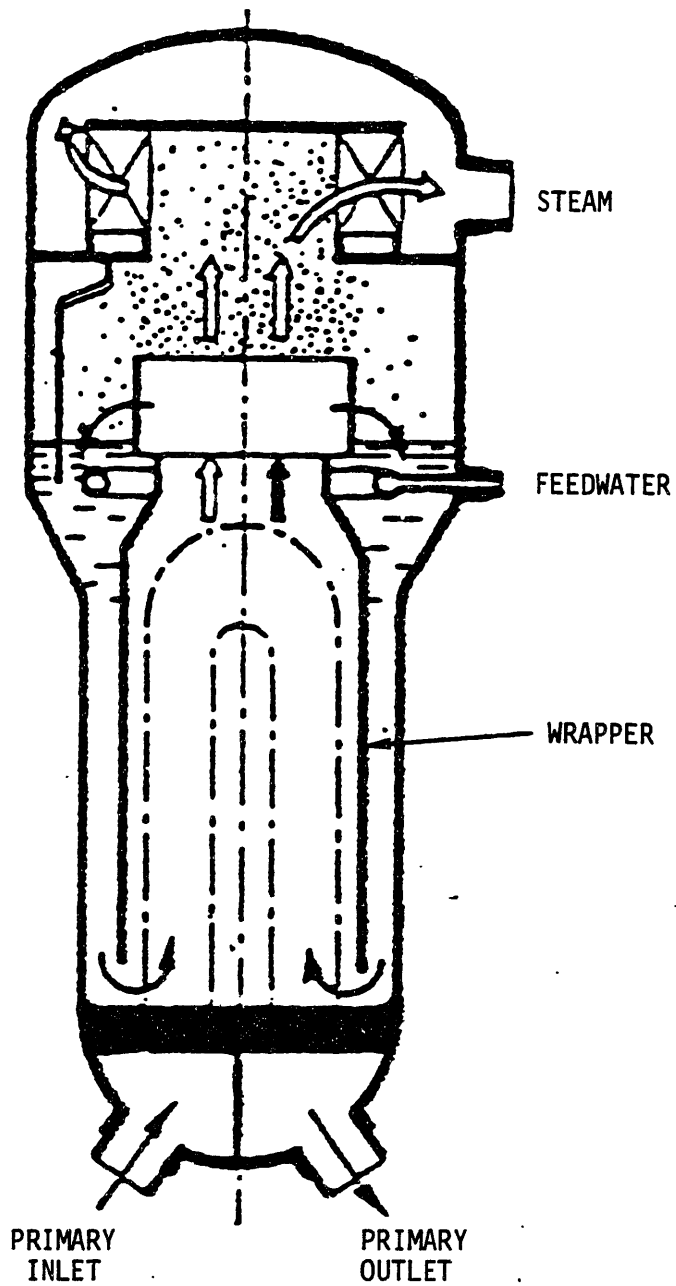


Figure 2.1-1 Representative U-Tube Steam Generator (Ref. (B1)).



the tube bundle and riser, and the outer (downflow) region consisting of the downcomer and feedwater mixing region. Subcooled feedwater is introduced into the steam generator via the feedwater nozzle and is distributed throughout the feedwater mixing region by the feedwater ring. There it mixes with the recirculating saturated liquid returning from the steam separation devices. The resulting subcooled liquid flows downward through the annular downcomer region formed by the wrapper and the steam generator outer shell. At the bottom of the downcomer, the water is turned and flows upward through the shell side of the tube bundle region, where it is heated to saturation and boils. The secondary fluid exits the tube bundle region as a saturated two-phase mixture and flows upward through the riser into the steam separating equipment. Steam separation is achieved by using a combination of centrifugal steam separators, for bulk liquid-vapor separation, and chevron type steam dryers, for the removal of any residual moisture. The relatively dry steam leaves through the steam outlet nozzle at the top of the steam generator, while the saturated water is directed downward to mix with the entering feedwater.

The secondary fluid path just described constitutes a natural circulation loop. The driving head for this recirculation flow is provided by the density difference between the subcooled column of liquid in the downcomer region and the two-phase mixture in the tube bundle and riser. This

driving head is counterbalanced by the various pressure losses in the loop, such as frictional losses in the tube bundle and the losses within the steam separators.

Load changes in UTSG units are accompanied by changes in the secondary pressure, primary coolant inlet temperature, feedwater flowrate, and feedwater temperature. Since the steam generator heat transfer rate is essentially proportional to the difference between the primary coolant temperature and the secondary saturation temperature, and since the saturation temperature is a function of saturation pressure, a change in secondary pressure results in a change in the primary-to-secondary heat transfer rate. For example, a load demand increase may be satisfied by increasing both the primary inlet temperature and feedwater flowrate, along with a decrease in secondary pressure.

## 2.2 MODEL REGIONS

For the purposes of developing a model of the steam generator, it is necessary to divide both the primary and secondary sides into several regions. As a matter of practicality, these model regions correspond to actual physical regions of the steam generator. This allows us to specify with greater accuracy the different physical processes occurring within each region. For instance, in the downcomer we are primarily interested in the flow of a subcooled liquid, while in the tube bundle portion of the secondary side

we are interested in describing a two-phase flow with heat addition. These are two essentially different physical processes requiring different modeling techniques; hence, we require two separate model regions. However, one must avoid the temptation to use too many model regions since this can result in a large and computationally costly model, which is contrary to the goals of this work.

The steam generator model developed in this work has four model regions on the secondary side and three model regions on the primary side. The primary side regions consist of the inlet plenum, the fluid volume within the tubes of the tube bundle, and the outlet plenum (Fig. 2.2-1). The four secondary regions are: the tube bundle region; the riser region; and, the steam dome-downcomer region, which is divided into a saturated volume and a subcooled volume (Fig. 2.2-2). The saturated and subcooled volumes have a movable interface; thus these volumes are not constant. However, the sum of their volumes is constant and equal to the total volume of the steam dome-downcomer region. There are three constraints imposed on the model of the regions contained within the steam dome-downcomer. The first is that the interface between the saturated and subcooled regions can never be above the level of the feedwater ring. This constraint is motivated by physical considerations, since one would not expect to find subcooled liquid above the feedwater ring because the feedwater ring sprays highly

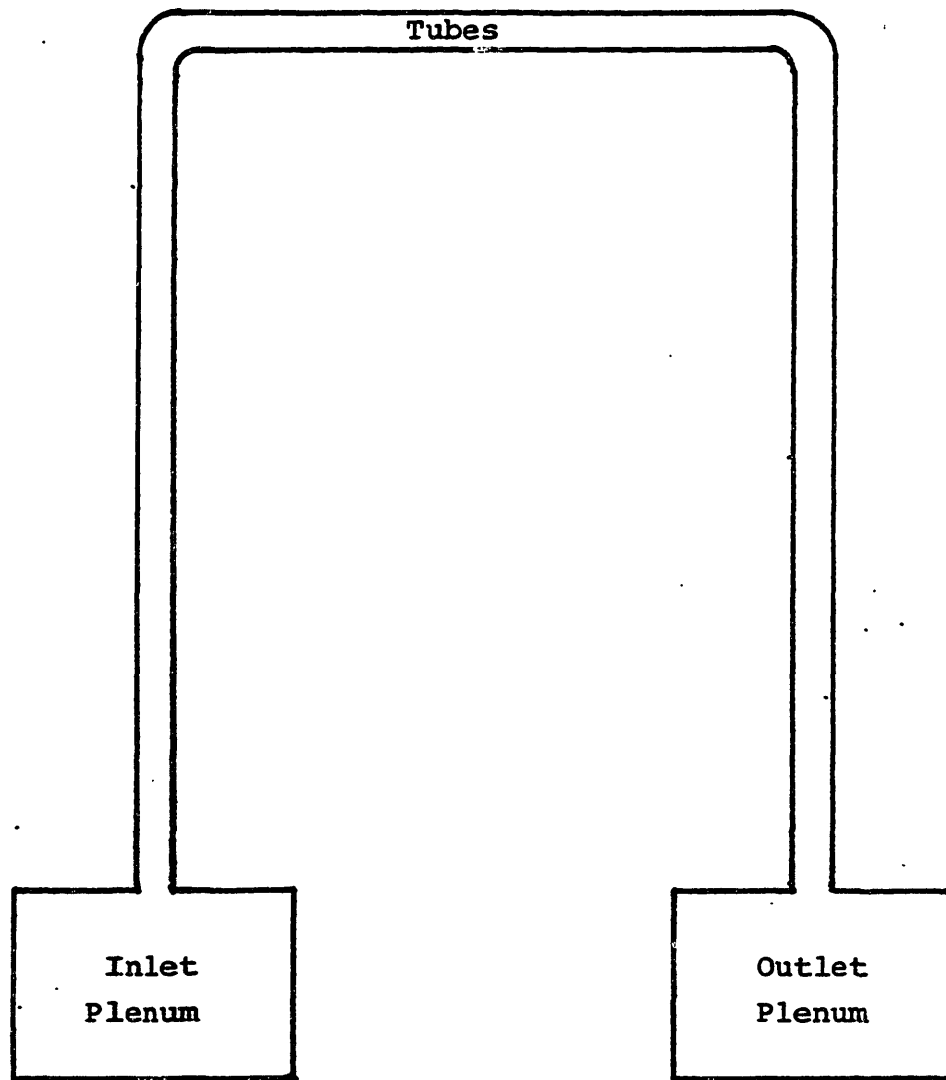


Figure 2.2-1 Primary Side Regions

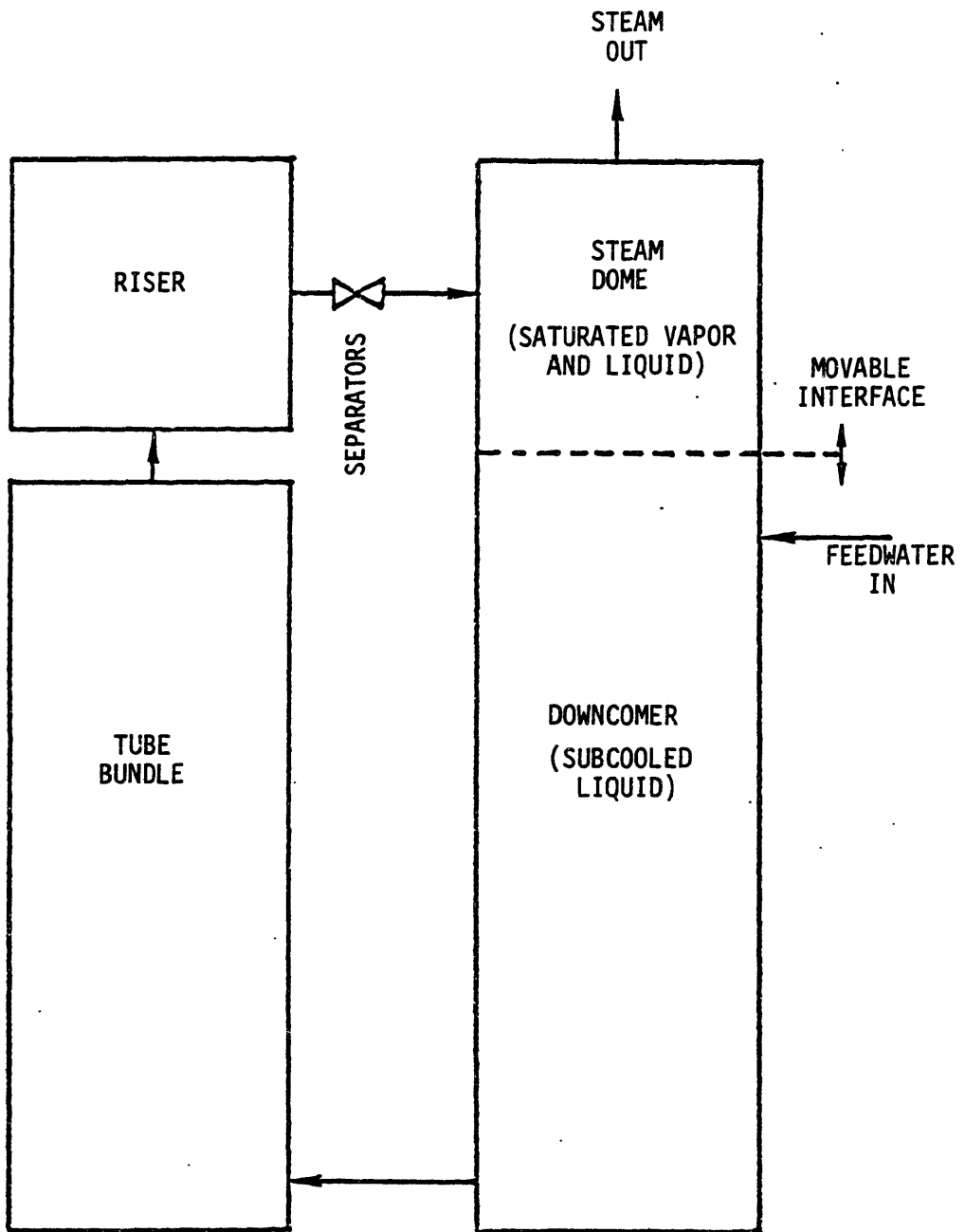


Figure 2.2-2 Secondary Side Regions

subcooled water downward. The second constraint is that there is always a minimum amount of saturated liquid present in the saturated region. The final constraint is that the feedwater is always added to the subcooled region, although this is not always true during steam generator off-normal operation. The last two constraints are discussed at length in Section 3.3. The steam separators, although not explicitly treated, are accounted for by assigning a loss coefficient for pressure drop calculations and by assuming that they always accomplish complete phase separation.

### 2.3 AUXILIARY MODELS

In order to simulate the effects of control actions initiated in the main steam and feedwater systems on steam generator performance, we have included simple models of these systems in the overall steam generator model as an alternative to providing the time-dependent steam and feedwater flows as input. These models are fully developed in Section 3.6; here we simply describe the systems and their operation.

A schematic of a typical main steam system is shown in Fig. 2.3-1. The main steam line extends from the steam generator steam outlet nozzle to the high pressure turbine main stop and control valve. The main steam line is also provided with a main steam isolation valve (MSIV), which

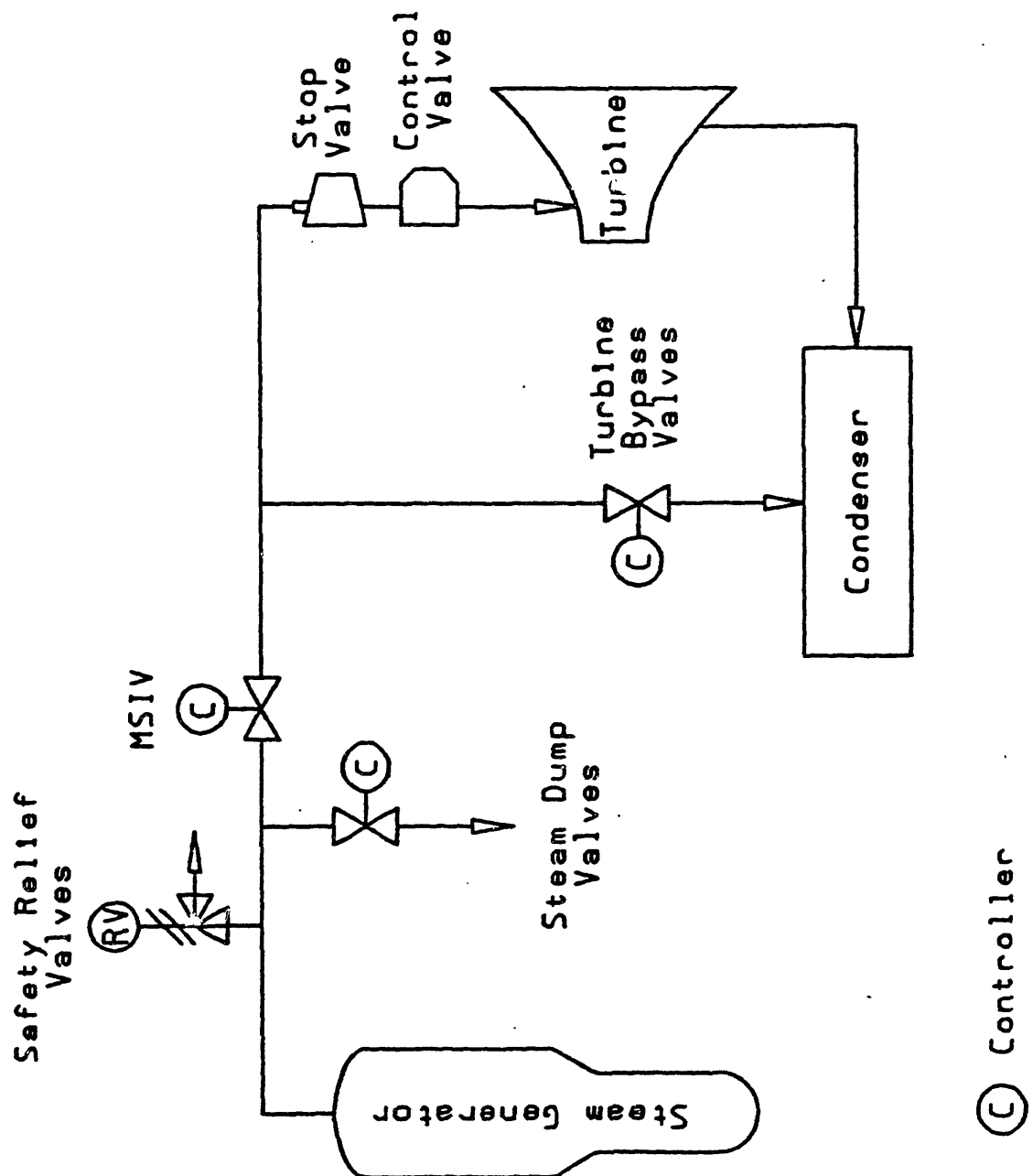


Figure 2.3-1 Typical Main Steam System

serves to isolate each steam generator in the event of a main steam line break and thereby limits the steam generator inventory loss. The MSIV also closes on a low steam generator pressure signal in order to prevent overcooling of the primary system fluid. There are also a number of steam relief systems associated with the main steam line. These are the steam dump, turbine bypass, and safety relief valve systems. The steam dump system vents to the atmosphere. The turbine bypass system diverts steam directly to the condensers and serves to limit steam pressure during operational transients. The bypass system is also used during hot standby and shutdown cooling. Both the steam dump and turbine bypass systems are used during load rejections in order to limit the ensuing secondary pressure rise. This action maintains the steam generator heat removal capability and prevents excessive increases in primary system temperatures. The safety relief valve system consists of a number of pressure relief valves located upstream of the MSIV. This is a passive system requiring no operator or control system action since the valves are spring loaded and open if the steam pressure is greater than the spring force. The steam relief capacity of this system is generally 5 to 6 per cent larger than the main steam flowrate at full power conditions.

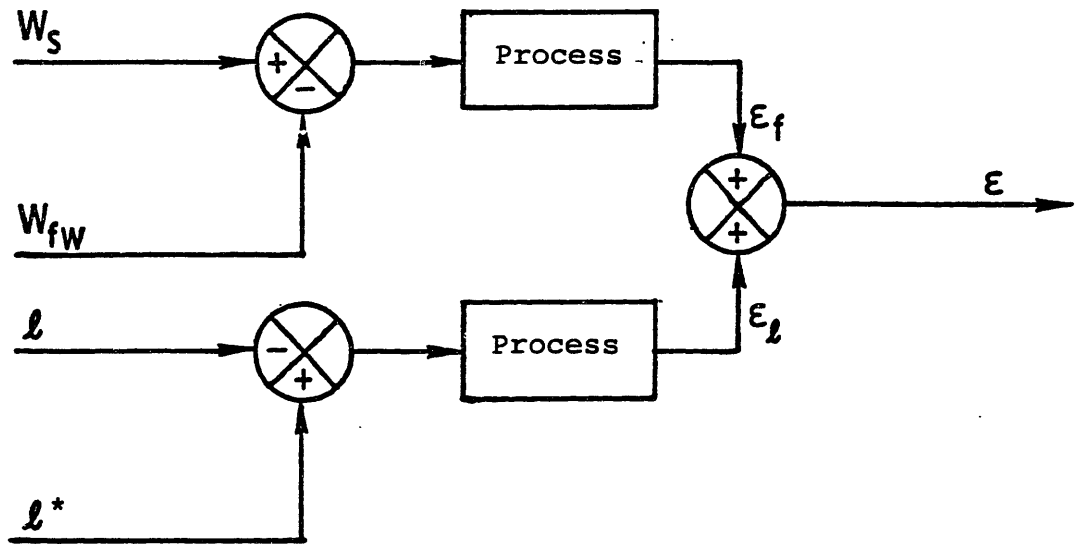
The feedwater system consists of the feedwater heaters, feedwater pumps and feedwater regulating valves. Modeling



of this system in itself is a difficult task and is not attempted in this work. The feedwater temperature, in particular, is a required input to the steam generator model since determining this quantity would require a model of the feedwater train, including extraction steam, which is beyond the scope of this work.

A simple model of the feedwater control system is incorporated into the overall steam generator model so that one can simulate controller effects on feedwater flowrate. The feedwater flow controller is a three-element controller that monitors steam flowrate, feedwater flowrate, and steam generator water level. The controlled quantity is the steam generator water level, and its control is accomplished by regulating the feedwater flowrate. Figure 2.3-2 is a block diagram of the controller. The measured steam and feedwater flowrates are compared and processed to provide a flow mismatch error signal. The measured water level is compared to the desired water level, and the difference between them is processed to provide a level error signal. The flow mismatch and level error signals are then combined to produce a feedwater flowrate demand signal that either increases or decreases the feedwater flowrate.

In Chapters 3 and 4 we develop in detail the steam generator primary and secondary side models, as well as the models of the peripheral systems.



- $W_s$  - Measured Steam Flowrate
- $W_{fw}$  - Measured Feedwater Flowrate
- $l$  - Measured Water Level
- $l^*$  - Desired Water Level
- $\epsilon_f$  - Flow Mismatch Error Signal
- $\epsilon_l$  - Level Error Signal
- $\epsilon$  - Feedwater Demand Signal

Figure 2.3-2 Block Diagram of a Typical Feedwater Controller

## Chapter 3

### SECONDARY SIDE MODEL

The most challenging part of the steam generator from a modeling point of view is the secondary side. The modeling difficulties are due to the following:

- 1.) Strong coupling between all regions of the secondary side;
- 2.) Natural recirculation flow;
- 3.) Both two-phase and single phase conditions exist; and,
- 4.) Geometry.

The following sections describe in detail the development of the secondary side model.

#### 3.1 TUBE BUNDLE REGION

##### 3.1.1 Mass and Energy Equations

As described in Chapter 2, the recirculating secondary fluid is heated and boils in the tube bundle region. A block diagram indicating the secondary side regions and the variables of interest is shown in Fig. 3.1-1 (see Nomenclature for variable identification). As discussed in Appendix B, we are using a model in which all system fluid properties are evaluated at a single, time-dependent reference pressure. It should be noted that the flow pattern and heat transfer distribution are not uniform in the tube bundle.

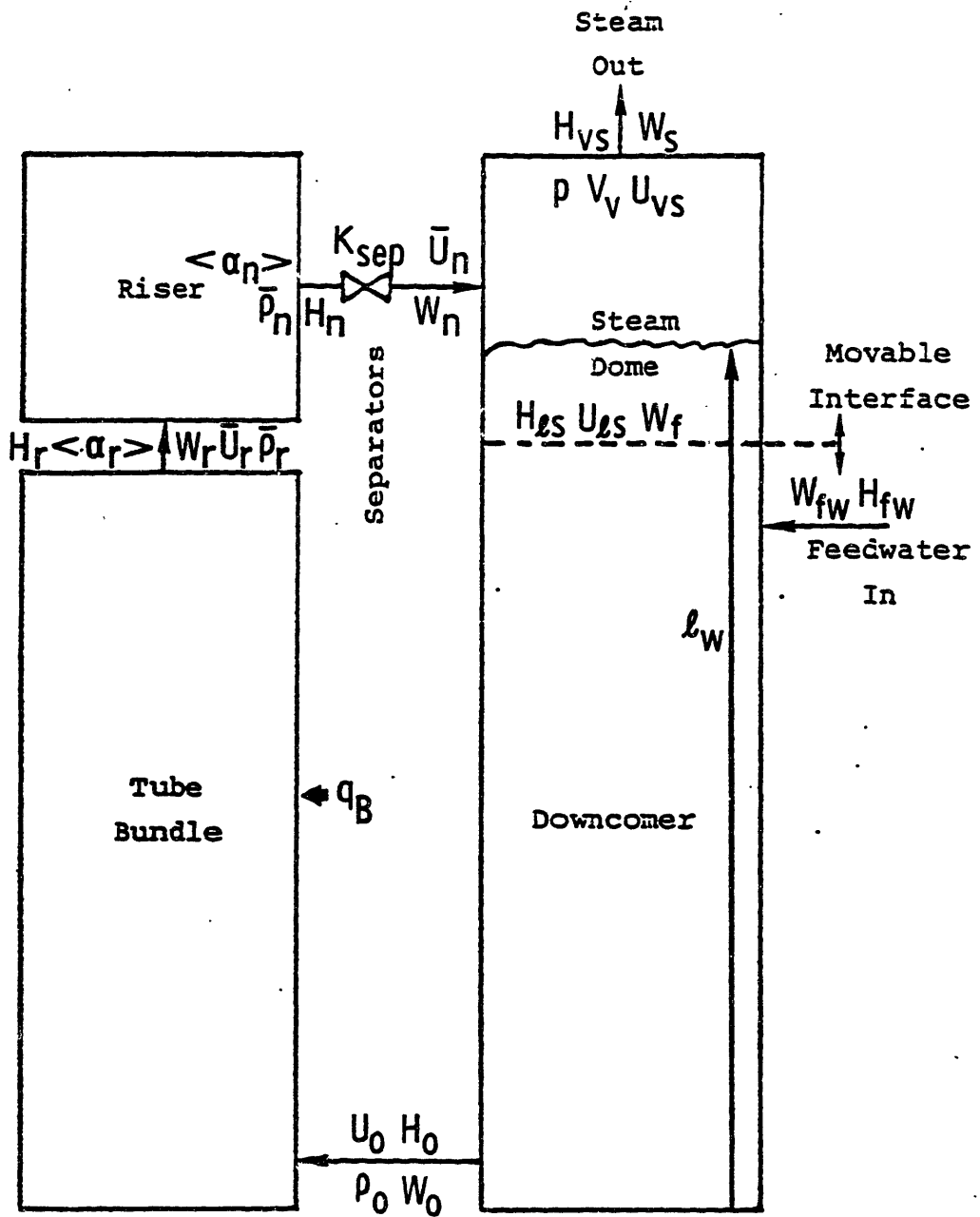


Figure 3.1-1. Secondary nomenclature.

Since the primary fluid is cooled during its journey through the tubes, the heat transfer rate varies along the length of the tubes. This results in a "hot side" and a "cold side" of the steam generator, which correspond to the upflow and downflow portions of the tubeside fluid. This spatially non-uniform heat transfer causes the secondary side flow pattern in the tube bundle to be non-uniform. In addition, there is a flow redistribution within the crossflow region of the tube bundle. Thus, although we use a one-dimensional treatment for the fluid on the shell-side of the tube bundle, the flow conditions are truly three-dimensional.

Using the mass and energy equations developed in Appendix B and neglecting heat transfer to the steam generator structural material, we obtain:

$$\frac{dM}{dt}_{TB} = W_0 - W_r \quad (3.1-1)$$

and,

$$\frac{dE}{dt}_{TB} = W_0 H_0 - W_r H_r + q_B \quad (3.1-2)$$

Solving Eq. (3.1-1) for  $W_r$  and substituting the result into Eq. (3.1-2) yields,

$$\frac{dE}{dt}_{TB} - H_r \frac{dM}{dt}_{TB} = W_0 (H_0 - H_r) + q_B \quad (3.1-3)$$

Equation (3.1-3) is in a form which is independent of enthalpy reference point (see Appendix B, Section 4).

### 3.1.2 Integration by Profiles

In order to solve Eq. (3.1-3) we need to determine  $E_{TB}$  and  $M_{TB}$ . Both of these quantities are integrals of either the density or the product of density and internal energy over the tube bundle volume. Since we are using a one-dimensional approach we really need only integrate over the length of the tube bundle taking into account, of course, flow area changes. Thus, the problem is reduced to finding, or making an approximation regarding, the axial profiles of the fluid density and internal energy in the tube bundle. Determining the transient axial profiles of these quantities is a time consuming task, and since we are interested in computational speed we choose to make some approximations in obtaining these profiles. One condition that seems appropriate for these profiles to satisfy is that they reduce to the correct steady state profiles. In addition, we are interested in transients which are significantly longer in time span than the fluid transport time through the tube bundle (see Table 3.1-1 for representative transport times). Therefore, it is reasonable to assume that each transient profile adjusts slowly and is similar to some steady state profile. So now the question is: What are the steady state profiles?

Table 3.1-1  
Representative Fluid Transport Times

Percent Power	Tube Bundle	Riser	Downcomer	Steam Dome
100	4.5 sec	1.4 sec	1.7 sec	9.2 sec
10	13.8 sec	7.7 sec	2.3 sec	11.5 sec

### 3.1.3 Detailed Profiles

Before we can answer this question we must take a closer look at the tube bundle region and the physical processes occurring there. This is best accomplished by performing a detailed one-dimensional steady state thermal-hydraulic analysis of the tube bundle region. In this region we can identify three flow and heat transfer regimes (see Fig. 3.1-2):

- 1.) Heat transfer by forced convection to a subcooled liquid;
- 2.) Heat transfer via subcooled nucleate boiling; and,
- 3.) Heat transfer by saturated nucleate boiling.

Clearly our detailed analysis should account for these processes.

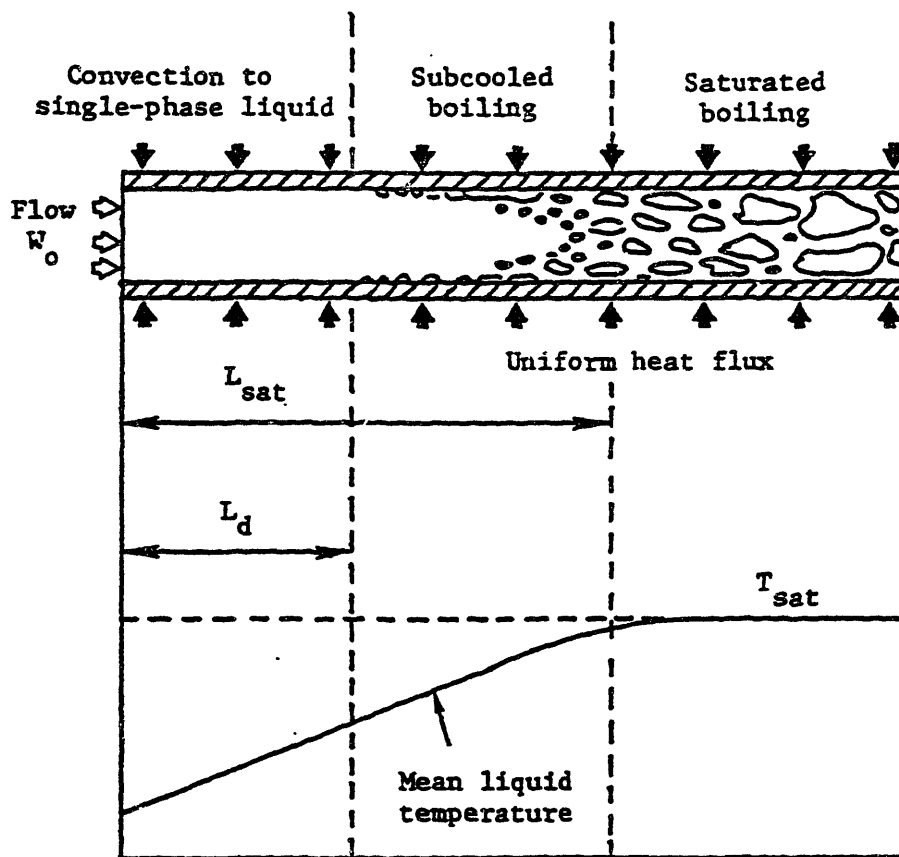


Figure 3.1-2. Heat transfer regimes (Ref. (C1)).



The approach taken here is to develop a detailed computer model subject to the following:

- 1.) Uniform axial heat flux;
- 2.) Single pressure for property evaluation;
- 3.) Onset of subcooled boiling determined by the empirical bubble departure criterion of Saha and Zuber (Ref. (L1));
- 4.) Subcooled and saturated flow quality distributions provided by a profile-fit model (Ref. (L1)); and
- 5.) Vapor volume fraction-flow quality relationship described by the drift flux model (Appendices A and C).

In this detailed model we use steady state heat balances to determine the fluid axial enthalpy distribution. Thus, the axial position at which the fluid bulk temperature reaches the saturation temperature is given by,

$$L_{SAT} = \frac{W(H_{LS} - H_{IN})}{A_{HT}q''} \quad (3.1-4)$$

However, subcooled boiling occurs before the bulk of the fluid is at saturation. The subcooled boiling region is further divided into two regimes. In the first region vapor is generated, but the vapor bubbles collapse immediately after they detach from the wall. In the second region the bulk fluid temperature is high enough so that the vapor

bubbles do not collapse immediately after they detach from the wall. This second region starts at the so-called bubble departure point and is the more important of the two regions. We will, therefore, neglect the first region and assume that the onset of subcooled boiling is coincident with the bubble departure point. The Saha-Zuber criterion for the bubble departure point is:

$$H_{ls} - (H_l)_d = (0.0022) \frac{Pe q''}{G} \quad Pe < 70,000$$

$$H_{ls} - (H_l)_d = \frac{154 q''}{G} \quad Pe \geq 70,000$$

where

$$Pe \equiv \text{Peclet Number} = \frac{G D_h C_{pl}}{K_l}$$

and  $(H_l)_d \equiv$  fluid bulk enthalpy at the bubble departure point.

So the axial position at which subcooled boiling occurs is

$$L_d = \frac{W ((H_l)_d - H_{IN})}{A_{HT} q''} \quad (3.1-5)$$

Upstream of  $L_d$  is very little vapor, between  $L_d$  and  $L_{SAT}$  the bulk fluid temperature is less than the prevailing saturation temperature but there is a net production of vapor, and downstream of  $L_{sat}$  the fluid is a mixture of saturated

liquid and vapor. Thus, the density and internal energy distributions are

$$\begin{aligned}\bar{\rho} &= \rho_{\ell} & z < L_d \\ \bar{U} &= U_{\ell}\end{aligned}$$

$$\bar{\rho} = \langle \alpha \rangle \rho_{vS} + (1 - \langle \alpha \rangle) \rho_{\ell} \quad L_d \leq z < L_{SAT}$$

$$\bar{U} = [ \langle \alpha \rangle \rho_{vS} U_{vS} + (1 - \langle \alpha \rangle) \rho_{\ell} U_{\ell} ] / \bar{\rho}$$

$$\bar{\rho} = \langle \alpha \rangle \rho_{vS} + (1 - \langle \alpha \rangle) \rho_{\ell S} \quad z \geq L_{SAT}$$

$$\bar{U} = [ \langle \alpha \rangle \rho_{vS} U_{vS} + (1 - \langle \alpha \rangle) \rho_{\ell S} U_{\ell S} ] / \bar{\rho}$$

We still need to determine the distribution of  $\langle \alpha \rangle$ . By using the drift flux model we can obtain  $\langle \alpha \rangle$  once we know  $x$ . As mentioned earlier, we are using a profile-fit model to predict the flow quality distribution. In the profile-fit model we assume that the mean liquid enthalpy,  $H_{\ell}$ , is the following function of the enthalpy,  $H'$ ,

$$\frac{(H_{\ell S} - H_{\ell})}{[H_{\ell S} - (H_{\ell})_d]} = \exp \left\{ - \frac{[H' - (H_{\ell})_d]}{[H_{\ell S} - (H_{\ell})_d]} \right\} = \xi$$

but,

$$H' = H_{\ell} (1 - x) + H_{vS} x$$

so,

$$x = \frac{(H - H_{\ell S}) + [H_{\ell S} - (H_{\ell})_d] \xi}{\{H_{\ell VS} + [H_{\ell S} - (H_{\ell})_d] \xi \}}$$

At this point we have completely specified and solved the problem. All that remains is a discussion of how this scheme is implemented on the computer.<sup>1</sup> Simply stated, the tube bundle is divided into a number of nodes and the various parameters of interest ( $H'$ ,  $x$ ,  $\langle \bar{\alpha} \rangle$ ,  $\bar{\rho}$  and  $U$ ) are then calculated. The nodalization scheme is determined by  $L_d$  and  $L_{SAT}$ . The length extending from the tube bundle inlet to  $L_d$  is divided into five nodes, as is the distance between  $L_d$  and  $L_{SAT}$ . The remaining length from  $L_{SAT}$  to the tube bundle outlet is divided into ten nodes.

The required inputs for this calculation are the power, system pressure, inlet flowrate, inlet density, and inlet internal energy. The system conditions used for the calculations presented here are representative of current nuclear U-tube steam generators. These parameters are listed in Table 3.1-2.

---

<sup>1</sup> This is a preliminary calculation for verification purposes only. This scheme is not used in the final steam generator model.

Table 3.1-2  
Inputs for Detailed Profile Calculations

Percent Power	$P_{sat}$ (MPa)	U (MJ/kg)	$\rho$ (kg/m <sup>3</sup> )	W (kg/s)
100	5.6	1.141	785.4	2250
80	5.67	1.146	783.9	2309
60	5.74	1.153	781.4	2310
40	5.81	1.164	777.5	2208
20	5.88	1.177	772.4	1869
5	5.93	1.191	767.2	992

Table 3.1-3 lists the fractional lengths at which bubble departure is calculated, and the fractional lengths at which bulk saturation conditions occur. The results clearly indicate that subcooled boiling, as predicted by the bubble departure criterion, plays a significant role at all power levels. That is, anywhere from 9 percent to 12 percent of the tube bundle length is in subcooled boiling. Thus, flow quality and vapor volume fraction profiles start well before bulk saturation conditions exist.

Table 3.1-3  
Results of Detailed Profile Calculations  
Bubble Departure and Saturation Lengths

Percent Power	$L_d/L_{Tot}$	$L_{SAT}/L_{Tot}$
100	0.0	0.1187
80	0.0269	0.1526
60	0.0641	0.1897
40	0.0993	0.2248
20	0.1406	0.2662
5	0.2039	0.2966

#### 3.1.4 Approximate Profiles

Figures 3.1-3 through 3.1-5 are plots of  $\langle \alpha \rangle$ ,  $\bar{\rho}$ ,  $\bar{v}$  ( $\bar{v} = 1/\bar{\rho}$ ) and  $\bar{U}$  versus fractional length for power levels of 100%, 40%, and 5% of the nominal power (817 MWt). The plots of interest are those of  $\bar{v}$  and  $\bar{U}$ . The figures show that these quantities are nearly linear functions of position. This observation, together with the fact that subcooled boiling starts very near the tube bundle inlet, leads us to the assumptions that the density varies inversely with axial position, while the internal energy varies in direct proportion to the axial position.

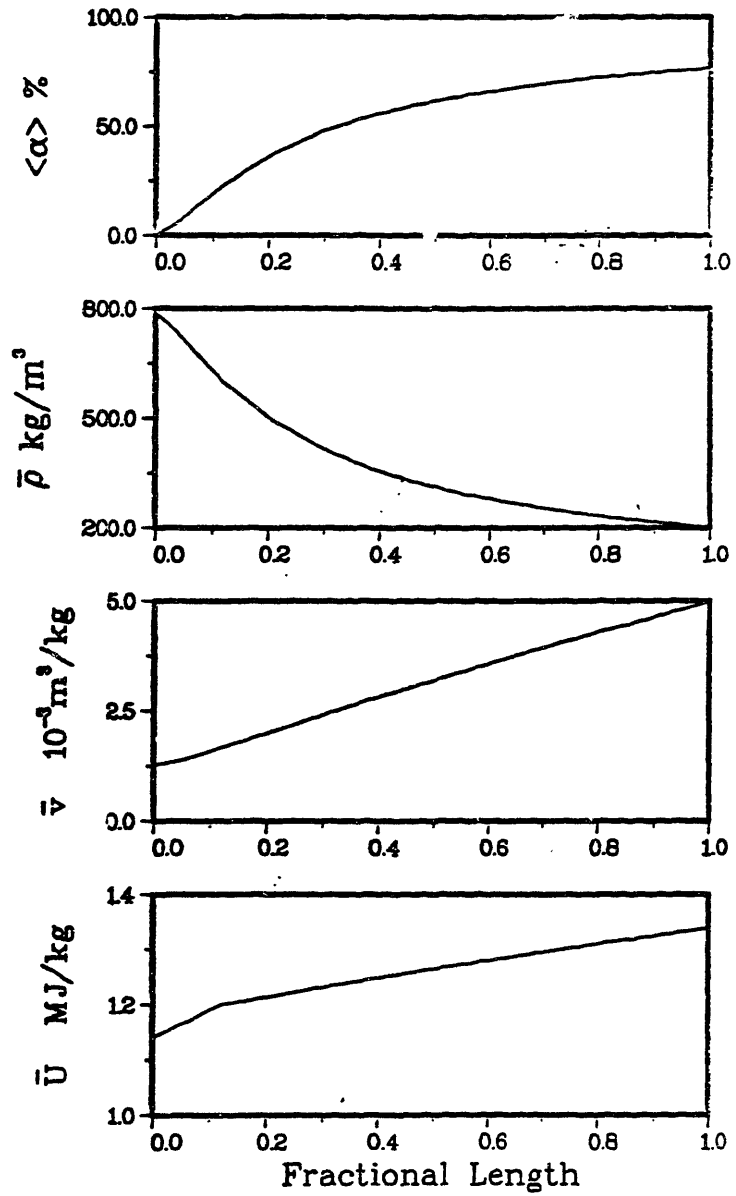


Figure 3.1-3. Profiles at 100 per cent power.

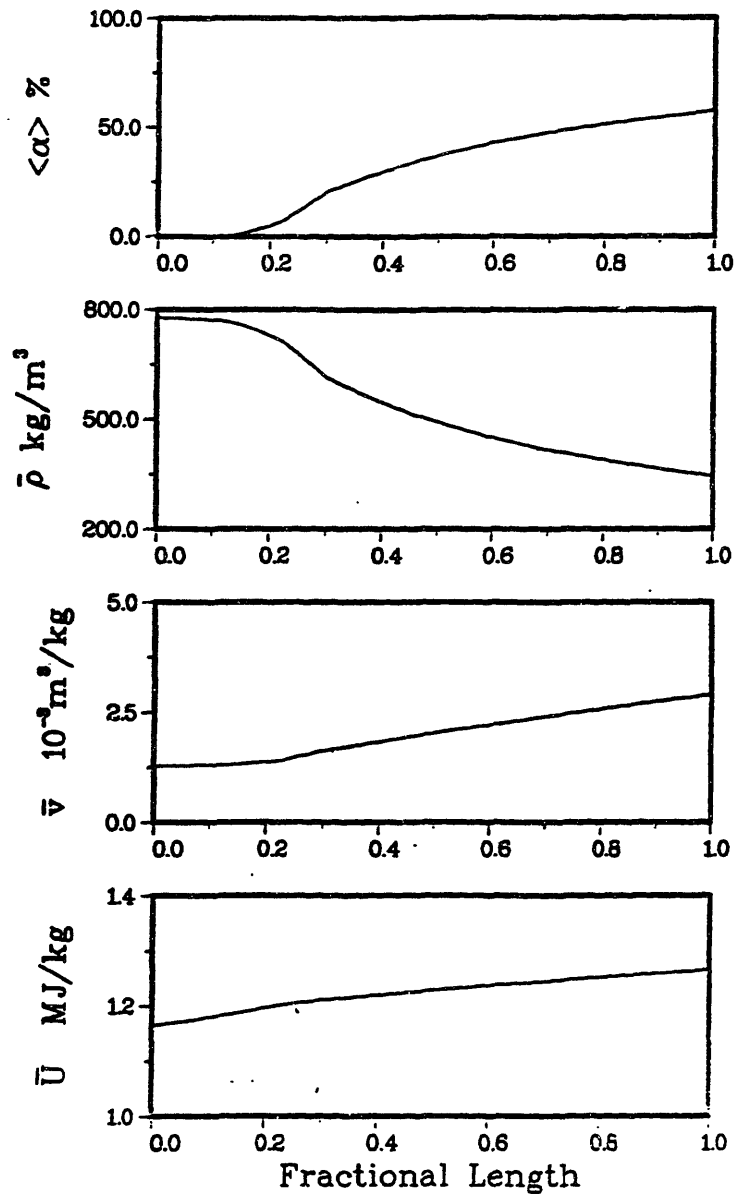


Figure 3.1-4. Profiles at 40 per cent power.



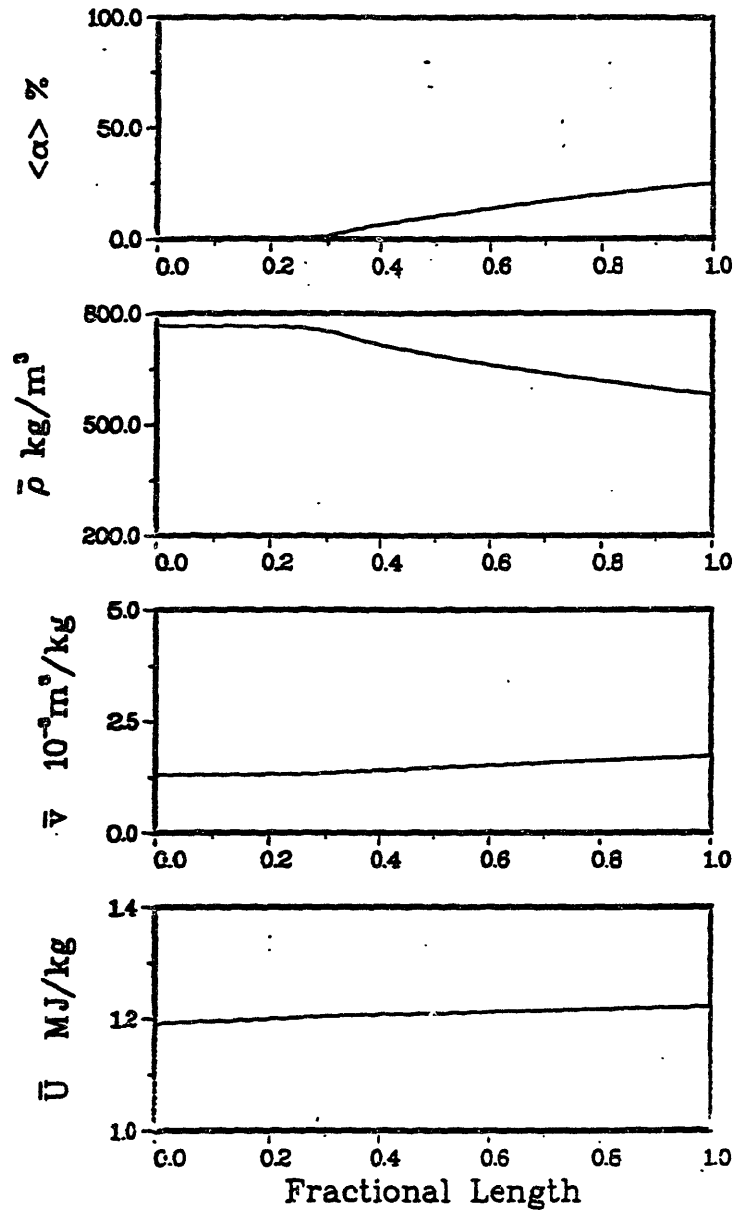


Figure 3.1-5. Profiles at 5 per cent power.

It might seem at first glance that these assumptions are not self-consistent. However, we will show that they are indeed consistent in saturated two-phase regions, and that assuming one profile directly implies the other. Starting with the density being inversely proportional to axial position we have,

$$\frac{1}{\bar{\rho}} = Az + B \quad (3.1-6)$$

But

$$\bar{U} = \frac{\rho_{ls} U_{ls}}{\bar{\rho}} + \frac{\langle \alpha \rangle}{\bar{\rho}} (\rho_{vs} U_{vs} - \rho_{ls} U_{ls}) \quad (3.1-7)$$

$$\text{and } \langle \alpha \rangle = \frac{\rho_{ls} - \bar{\rho}}{\rho_{ls} - \rho_{vs}} \quad \text{or} \quad \frac{\langle \alpha \rangle}{\bar{\rho}} = \frac{\frac{\rho_{ls}}{\bar{\rho}} - 1}{\rho_{ls} - \rho_{vs}}$$

Substituting Eq. (3.1-6) into the previous expression yields,

$$\frac{\langle \alpha \rangle}{\bar{\rho}} = \frac{\rho_{ls}(Az + B) - 1}{\rho_{ls} - \rho_{vs}} = Cz + D$$

Substituting this result and Eq. (3.1-6) into Eq. (3.1-7),

$$\bar{U} = \rho_{ls} U_{ls} (Az + B) + (Cz + D)(\rho_{vs} U_{vs} - \rho_{ls} U_{ls})$$

or

$$\bar{U} = Ez + F \quad (3.1-8)$$

Thereby demonstrating that if  $\bar{\rho}$  is inversely proportional to axial position, then  $\bar{U}$  is directly proportional to axial position in saturated two-phase regions.

### 3.1.5 Approximation Errors

In order to gain insight into the magnitude of the error generated by extending linear profiles to other regions, we can perform some straightforward calculations. Equation (3.1-6) can be written as

$$\frac{1}{\bar{\rho}} = \left[ \frac{1}{\bar{\rho}_r} - \frac{1}{\bar{\rho}_0} \right] \frac{z}{L_{TB}} + \frac{1}{\bar{\rho}_0}$$

Substituting this expression into the definition of  $M_{TB}$  yields

$$M_{TB} = \int_0^{V_{TB}} \bar{\rho} dV = \left( \frac{V_{TB} \bar{\rho}_0 \bar{\rho}_r}{\bar{\rho}_0 - \bar{\rho}_r} \right) \ln \frac{\bar{\rho}_0}{\bar{\rho}_r} \quad (3.1-9)$$

Equation (3.1-8) can be written as,

$$\bar{U} = (\bar{U}_r - U_0)z/L_{TB} + U_0$$

So,  $E_{TB}$  is,

$$E_{TB} = \int_0^{V_{TB}} \bar{\rho} \bar{U} dV = M_{TB} \frac{\bar{U}_r - U_0}{\ln(\rho_0/\bar{\rho}_r)} + \frac{(\rho_0 U_0 - \bar{\rho}_r \bar{U}_r)}{\rho_0 - \bar{\rho}_r} \quad (3.1-10)$$

By comparing the values of  $M_{TB}$  and  $E_{TB}$  calculated using Eqs. (3.1-9) and (3.1-10) to the values obtained using the detailed profiles generated earlier we can determine the error introduced by using linear profiles. The error in mass content is calculated as the difference between the "approximate" mass and the "exact" mass, divided by the "exact" mass. The error introduced by using linear profiles for  $\bar{\rho}$  and  $\bar{U}$  when calculating  $E_{TB}$  is determined by the following:

$$\frac{\left( \frac{1}{M_{TB}} \int_0^{V_{TB}} \bar{\rho} (\bar{U} - U_{IN}) dV \right)_{\text{Approximate}} - \left( \frac{1}{M_{TB}} \int_0^{V_{TB}} \bar{\rho} (\bar{U} - U_{IN}) dV \right)_{\text{Exact}}}{\left( \frac{1}{M_{TB}} \int_0^{V_{TB}} \bar{\rho} (\bar{U} - U_{IN}) dV \right)_{\text{Exact}}}$$

The quantity,

$$\frac{1}{M_{TB}} \int_0^{V_{TB}} \bar{\rho} (\bar{U} - U_{IN}) dV$$

is essentially the energy content per unit mass of the tube bundle fluid over and above the internal energy of the fluid

at the inlet, as shown in Fig. 3.1-6. This method of calculating the error avoids the ambiguity that could arise due to the arbitrariness of property table reference point for internal energy since only differences in internal energy appear in the calculation.

Table 3.1-4 shows the results of the error calculations. The linear profiles tend to underestimate both  $M_{TB}$  and  $E_{TB}$ . The error in mass content is never greater than six percent, which indicates that using a linear profile for  $\bar{v}$  is a relatively good approximation. The error in energy content, on the other hand, lies in the range of 13 to 22

Table 3.1-4  
Errors Introduced by Linear Profile Approximation

Percent Power	Mass Content Error (%)	Energy Content Error (%)
100	-0.389	-21.21
80	-4.081	-18.38
60	-5.531	-17.06
40	-5.836	-15.47
20	-5.159	-13.46
5	-3.163	-12.98

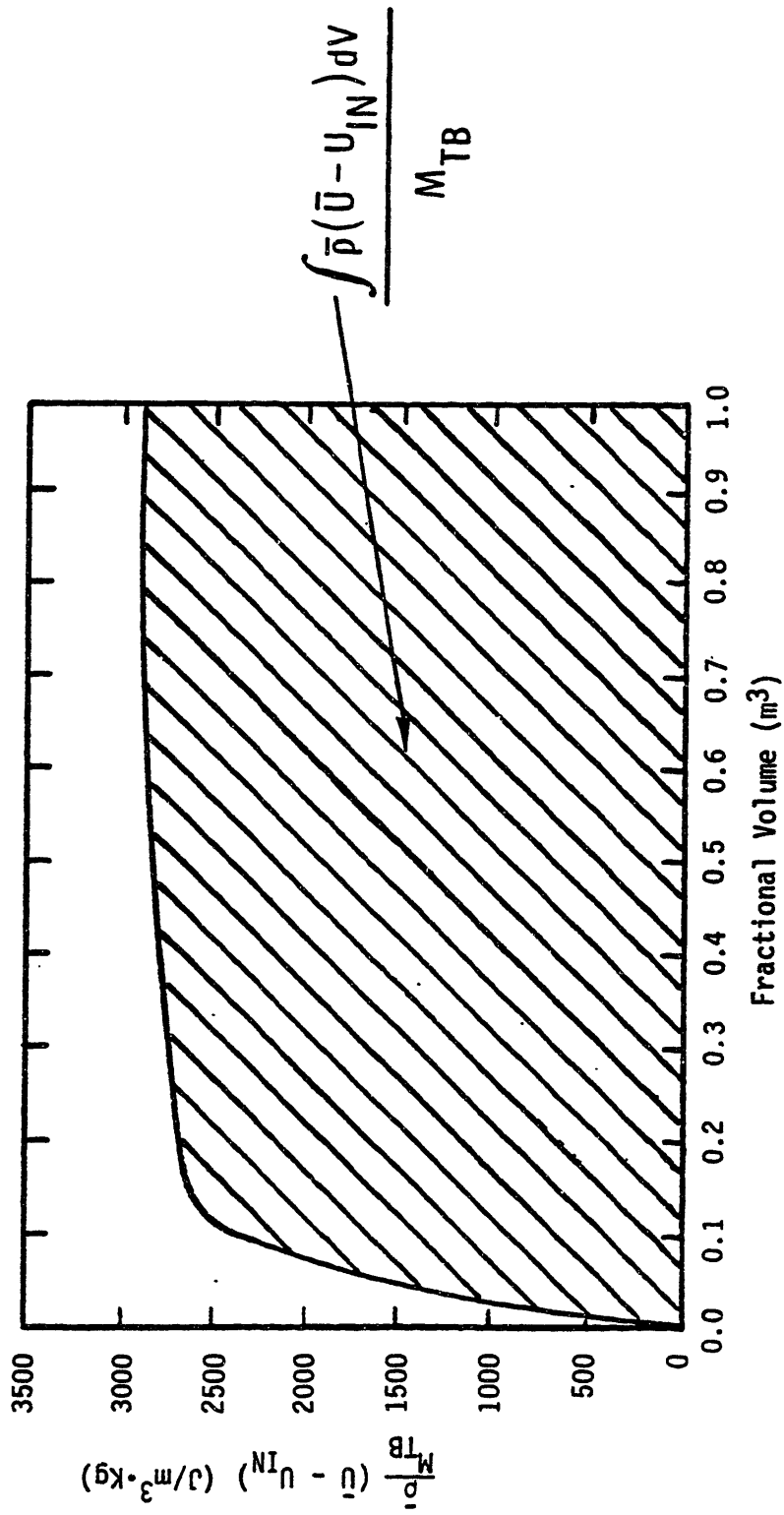


Figure 3.1-6. Integrated energy content per unit mass.

percent, with the error decreasing as the power decreases. A discussion of the sources of error is included in Appendix E.

### 3.1.6 State Variables

We are almost ready to return to Eq. (3.1-3) and proceed with determining the time derivatives of  $M_{TB}$  and  $E_{TB}$ . However, we still need to specify the state variables. As can be seen from Eqs. (3.1-9) and (3.1-10), both  $M_{TB}$  and  $E_{TB}$  depend only on the values of the fluid properties at the inlet and outlet of the tube bundle. These properties obviously depend on pressure, which is, therefore, one of our state variables. For the subcooled fluid at the entrance we require an additional state variable in order to completely specify its thermodynamic state. This state variable could be temperature, density, enthalpy, or internal energy. For our purposes it is convenient to use the liquid internal energy as the additional state variable. The fluid at the tube bundle exit is a saturated mixture of liquid and vapor, so its thermodynamic properties are known if we know the pressure. However, in order to specify its thermodynamic state, we need to know the relative proportions of liquid and vapor present. Hence, we need the vapor volume fraction as an additional state variable. In summary, our state variables are: the system pressure,  $p$ ; the subcooled liquid internal energy,  $U_0$ ; and the vapor volume fraction at the tube bundle exit,  $\langle \alpha_r \rangle$ .

The total derivatives of  $M_{TB}$  and  $E_{TB}$  can now be written as,

$$\begin{aligned} \frac{dM_{TB}}{dt} = & \left( \frac{\partial M_{TB}}{\partial U_0} \right)_{\langle \alpha_r \rangle, p} \frac{dU_0}{dt} + \left( \frac{\partial M_{TB}}{\partial \langle \alpha_r \rangle} \right)_{U_0, p} \frac{d\langle \alpha_r \rangle}{dt} \\ & + \left( \frac{\partial M_{TB}}{\partial p} \right)_{U_0, \langle \alpha_r \rangle} \frac{dp}{dt} \end{aligned} \quad (3.1-11)$$

and

$$\begin{aligned} \frac{dE_{TB}}{dt} = & \left( \frac{\partial E_{TB}}{\partial U_0} \right)_{\langle \alpha_r \rangle, p} \frac{dU_0}{dt} + \left( \frac{\partial E_{TB}}{\partial \langle \alpha_r \rangle} \right)_{U_0, p} \frac{d\langle \alpha_r \rangle}{dt} \\ & + \left( \frac{\partial E_{TB}}{\partial p} \right)_{U_0, \langle \alpha_r \rangle} \frac{dp}{dt} \end{aligned} \quad (3.1-12)$$

The partial derivatives appearing in Eqs. (3.1-11) and (3.1-12) and associated property derivatives are shown in Tables 3.1-5 and 3.1-6. Thus Eq. (3.1-3) can be written as,

$$B_1 \frac{dU_0}{dt} + B_2 \frac{d\langle \alpha_r \rangle}{dt} + B_3 \frac{dp}{dt} = W_0 (H_0 - H_r) + q_B \quad (3.1-13)$$



Table 3.1-5.  
 Partial Derivatives for Eqs. 3.1-11 and 3.1-12

Quantity	Expression
$\left(\frac{\partial M_{TB}}{\partial U_0}\right) \langle \alpha_r \rangle, p$	$\frac{\bar{\rho}_r}{\rho_0 - \bar{\rho}_r} \left( V_{TB} - \frac{M_{TB}}{\rho_0} \right) \left( \frac{\partial \rho_0}{\partial U_0} \right) p$
$\left(\frac{\partial M_{TB}}{\partial \langle \alpha_r \rangle}\right) U_0, p$	$\frac{\rho_0}{\rho_0 - \bar{\rho}_r} \left( \frac{M_{TB}}{\rho_r} - V_{TB} \right) \left( \frac{\partial \bar{\rho}_r}{\partial \langle \alpha_r \rangle} \right) p$
$\left(\frac{\partial M_{TB}}{\partial p}\right) \langle \alpha_r \rangle, U_0$	$\frac{\left(\frac{\partial M_{TB}}{\partial U_0}\right) \langle \alpha_r \rangle, p}{\left(\frac{\partial \rho_0}{\partial U_0}\right) p} + \frac{\left(\frac{\partial M_{TB}}{\partial \langle \alpha_r \rangle}\right) U_0, p}{\left(\frac{\partial \bar{\rho}_r}{\partial \langle \alpha_r \rangle}\right) p}$

Table 3.1-5 (Contd.)  
 Partial Derivatives for Eqs. 3.1-11 and 3.1-12

Quantity	Expression
$\left(\frac{\partial E_{TB}}{\partial U_0}\right) \langle \alpha_r \rangle, p$	$\frac{E_{TB}}{M_{TB}} \left(\frac{\partial M_{TB}}{\partial U_0}\right) \langle \alpha_r \rangle, p + M_{TB} \left[ \frac{\rho_0}{\rho_0 - \bar{\rho}_r} - \frac{1}{\ln(\rho_0/\bar{\rho}_r)} \right] + M_{TB} \left[ \frac{U_0 - \bar{U}_r}{\rho_0 \ln^2(\rho_0/\bar{\rho}_r)} - \frac{\bar{\rho}_r (U_0 - \bar{U}_r)}{(\rho_0 - \bar{\rho}_r)^2} \right] \left(\frac{\partial \rho_0}{\partial U_0}\right) p$
$\left(\frac{\partial E_{TB}}{\partial \langle \alpha_r \rangle}\right) U_0, p$	$\frac{E_{TB}}{M_{TB}} \left(\frac{\partial M_{TB}}{\partial U_0}\right) \langle \alpha_r \rangle, p + M_{TB} \left[ \frac{1}{\ln(\rho_0/\bar{\rho}_r)} - \frac{\bar{\rho}_r}{\rho_0 - \bar{\rho}_r} \right] \left(\frac{\partial U_r}{\partial \langle \alpha_r \rangle}\right) p + M_{TB} \left[ \frac{\rho_0 (U_0 - \bar{U}_r)}{(\rho_0 - \bar{\rho}_r)^2} - \frac{(U_0 - \bar{U}_r)}{\bar{\rho}_r \ln^2(\rho_0/\bar{\rho}_r)} \right] \left(\frac{\partial \bar{\rho}_r}{\partial \langle \alpha_r \rangle}\right) p$

Table 3.1-5 (Contd.)  
 Partial Derivatives for Eqs. 3.1-11 and 3.1-12

Quantity	Expression
$\left(\frac{\partial E_{TB}}{\partial p}\right) \langle \alpha_r \rangle, U_0$	$\begin{aligned} & \frac{E_{TB}}{M_{TB}} \left(\frac{\partial M_{TB}}{\partial p}\right) U_0, \langle \alpha_r \rangle + M_{TB} \left[ \frac{1}{\ln(\rho_0/\bar{\rho}_r)} - \frac{\bar{\rho}_r}{\rho_\ell - \bar{\rho}_r} \right] \left(\frac{\partial U_r}{\partial p}\right) \langle \alpha_r \rangle, \langle \alpha_n \rangle \\ & + M_{TB} \left[ \frac{(U_0 - \bar{U}_r)}{\bar{\rho}_r \ln^2(\rho_0/\bar{\rho}_r)} - \frac{\rho_0(U_0 - \bar{U}_r)}{(\rho_0 - \bar{\rho}_r)^2} \right] \left(\frac{\partial \bar{\rho}_0}{\partial p}\right) U_0, \langle \alpha_r \rangle \\ & + M_{TB} \left[ \frac{\rho_0(U_0 - \bar{U}_r)}{(\rho_0 - \bar{\rho}_r)^2} - \frac{(U_0 - \bar{U}_r)}{\bar{\rho}_r \ln^2(\rho_0/\bar{\rho}_r)} \right] \left(\frac{\partial \bar{\rho}_r}{\partial p}\right) \langle \alpha_r \rangle, \langle \alpha_n \rangle \end{aligned}$

Table 3.1-6  
Property Derivatives

Quantity	Expression
$\left(\frac{\partial \bar{\rho}}{\partial \langle \alpha \rangle}\right)_p$	$\rho_{vs} - \rho_{\lambda s}$
$\left(\frac{\partial \bar{\rho}}{\partial p}\right) \langle \alpha \rangle$	$\langle \alpha \rangle \frac{d\rho_{vs}}{dp} + (1 - \langle \alpha \rangle) \frac{d\rho_{\lambda s}}{dp}$
$\left(\frac{\partial \bar{U}}{\partial \langle \alpha \rangle}\right)_p$	$\frac{\rho_{vs} \bar{U}_{vs} - \rho_{\lambda s} \bar{U}_{\lambda s}}{\bar{\rho}} - \frac{\bar{U}}{\bar{\rho}} \left(\frac{\partial \bar{\rho}}{\partial \langle \alpha \rangle}\right)_p$
$\left(\frac{\partial \bar{U}}{\partial p}\right) \langle \alpha \rangle$	$\frac{\langle \alpha \rangle \frac{d}{dp} [U_{vs} \rho_{vs}] + (1 - \langle \alpha \rangle) \frac{d}{dp} [\rho_{\lambda s} U_{\lambda s}]}{\bar{\rho}} - \frac{\bar{U}}{\bar{\rho}} \left(\frac{\partial \bar{\rho}}{\partial p}\right) \langle \alpha \rangle$

where

$$B_1 = \left( \frac{\partial E_{TB}}{\partial U_0} \right)_{\langle \alpha_r \rangle, p} - H_r \left( \frac{\partial M_{TB}}{\partial U_0} \right)_{\langle \alpha_r \rangle, p}$$

$$B_2 = \left( \frac{\partial E_{TB}}{\partial \langle \alpha_r \rangle} \right)_{U_0, p} - H_r \left( \frac{\partial M_{TB}}{\partial \langle \alpha_r \rangle} \right)_{U_0, p}$$

$$B_3 = \left( \frac{\partial E_{TB}}{\partial p} \right)_{\langle \alpha_r \rangle, U_0} - H_r \left( \frac{\partial M_{TB}}{\partial p} \right)_{\langle \alpha_r \rangle, U_0}$$

This completes the derivation of the tube bundle energy equation.

### 3.2 RISER REGION

#### 3.2.1 Mass and Energy Equations

The riser region is the unheated upflow region located just above the tube bundle. The mass and energy conservation equations for this region are (neglecting heat transfer to steam generator structure):

$$\frac{dM_R}{dt} = W_r - W_n \quad (3.2-1)$$

and

$$\frac{dE_R}{dt} = W_r H_r - W_n H_n \quad (3.2-2)$$

Solving Eq. (3.2-1) for  $W_n$  and substituting the result into into Eq. (3.2-2) yields:

$$\frac{dE_R}{dt} - H_n \frac{dM_R}{dt} = W_r(H_r - H_n) \quad (3.2-3)$$

### 3.2.2 Profiles

As in the case of the tube bundle, we need to know the profiles of the density and the product of the internal energy and density in order to evaluate  $M_R$  and  $E_R$ . For the riser we will assume that the average vapor volume fraction,  $\langle \alpha \rangle$ , is a linear function of riser volume. By definition we know the following (Appendix A):

$$\bar{\rho} = \rho_{ls} + \langle \alpha \rangle (\rho_{vs} - \rho_{ls})$$

and

$$\bar{\rho} \bar{U} = \rho_{ls} U_{ls} + \langle \alpha \rangle (\rho_{vs} U_{vs} - \rho_{ls} U_{ls})$$

Since the saturated thermodynamic properties are not functions of position, which is a result of our single pressure assumption, both the density and the product of density and internal energy are linear functions of riser volume. Thus,

$$M_R = \int_{V_R} \bar{\rho} dV = \frac{V_R}{2} (\bar{\rho}_r + \bar{\rho}_n) \quad (3.2-4)$$

and

$$E_R = \int_{V_R} \bar{\rho} \bar{U} dV = \frac{V_R}{2} (\bar{\rho}_r \bar{U}_r + \bar{\rho}_n \bar{U}_n) \quad (3.2-5)$$

### 3.2.3 State Variables

From these equations it is clear that  $M_R$  and  $E_R$  are functions of the fluid thermodynamic state at the inlet and outlet of the riser, as well as the riser volume, which is constant. The thermodynamic state of the fluid at the riser inlet is a function of the system pressure,  $p$ , and the inlet vapor volume fraction,  $\langle \alpha_r \rangle$ . At the riser outlet we need the system pressure and the exit vapor volume fraction,  $\langle \alpha_n \rangle$ , to determine the fluid state. Therefore, our state variables for the riser region are: system pressure,  $p$ ; inlet vapor volume fraction,  $\langle \alpha_r \rangle$ ; and exit vapor volume fraction,  $\langle \alpha_n \rangle$ .

Taking the total derivatives of  $M_R$  and  $E_R$  yields:

$$\begin{aligned} \frac{dM_R}{dt} = & \left( \frac{\partial M_R}{\partial \langle \alpha_r \rangle} \right)_{\langle \alpha_n \rangle, p} \frac{d\langle \alpha_r \rangle}{dt} + \left( \frac{\partial M_R}{\partial \langle \alpha_n \rangle} \right)_{\langle \alpha_r \rangle, p} \frac{d\langle \alpha_n \rangle}{dt} \\ & + \left( \frac{\partial M_R}{\partial p} \right)_{\langle \alpha_r \rangle, \langle \alpha_n \rangle} \frac{dp}{dt} \end{aligned} \quad (3.2-6)$$

and

$$\begin{aligned} \frac{dE_R}{dt} = & \left( \frac{\partial E_R}{\partial \langle \alpha_r \rangle} \right)_{\langle \alpha_n \rangle, p} \frac{d\langle \alpha_r \rangle}{dt} + \left( \frac{\partial E_R}{\partial \langle \alpha_n \rangle} \right)_{\langle \alpha_r \rangle, p} \frac{d\langle \alpha_n \rangle}{dt} \\ & + \left( \frac{\partial E_R}{\partial p} \right)_{\langle \alpha_r \rangle, \langle \alpha_n \rangle} \frac{dp}{dt} \end{aligned} \quad (3.2-7)$$

Substituting Eqs. (3.2-6) and (3.2-7) into Eq. (3.2-3)

yields:

$$B_4 \frac{d\langle \alpha_r \rangle}{dt} + B_5 \frac{d\langle \alpha_n \rangle}{dt} + B_6 \frac{dp}{dt} = W_r (H_r - H_n) \quad (3.2-8)$$

where

$$B_4 = \left( \frac{\partial E_R}{\partial \langle \alpha_r \rangle} \right)_{\langle \alpha_n \rangle, p} - H_n \left( \frac{\partial M_R}{\partial \langle \alpha_r \rangle} \right)_{\langle \alpha_n \rangle, p}$$

$$B_5 = \left( \frac{\partial E_R}{\partial \langle \alpha_n \rangle} \right)_{\langle \alpha_r \rangle, p} - H_n \left( \frac{\partial M_R}{\partial \langle \alpha_n \rangle} \right)_{\langle \alpha_r \rangle, p}$$

$$B_6 = \left( \frac{\partial E_R}{\partial p} \right)_{\langle \alpha_r \rangle, \langle \alpha_n \rangle} - H_n \left( \frac{\partial M_R}{\partial p} \right)_{\langle \alpha_r \rangle, \langle \alpha_n \rangle}$$



The partial derivatives of  $M_R$  and  $E_R$  appearing above are shown in Table 3.2-1. Equation (3.2-8) is our energy equation for the riser region.

### 3.3 STEAM DOME AND DOWNCOMER

The steam dome consists of the steam generator volume above the separator deck and the feedwater ring. The downcomer is the annular region formed by the steam generator outer shell and the tube bundle wrapper (Fig. 3.3-1). During normal operation the steam dome contains saturated vapor and liquid, while the downcomer contains subcooled liquid. During off-normal transients it is possible for the liquid level to fall below the feedwater ring. In this case, the steam dome contains saturated or superheated steam, while the downcomer contains both saturated and subcooled liquid.

In order to describe the liquid behavior in the steam dome - downcomer we consider two cases:

- 1.) Liquid volume in these regions greater than a pre-specified volume; and,
- 2.) Liquid volume less than a pre-specified volume.

The pre-specified volume is generally taken to be the volume of the downcomer plus some fraction (in our model 25 per cent) of the volume of saturated liquid at normal operating conditions. For Case 1, the steam dome is treated as a volume containing only saturated liquid and vapor, while the downcomer is treated as a volume containing only subcooled

Table 3.2-1  
Partial Derivatives of  $M_R$  and  $E_R$

Quantity	Expression
$\left(\frac{\partial M_R}{\partial \langle \alpha_r \rangle}\right)_{\langle \alpha_n \rangle, p}$	$\frac{V_R}{2} \left(\frac{\partial \bar{\rho}_r}{\partial \langle \alpha_r \rangle}\right)_p$
$\left(\frac{\partial M_R}{\partial \langle \alpha_n \rangle}\right)_{\langle \alpha_r \rangle, p}$	$\frac{V_R}{2} \left(\frac{\partial \bar{\rho}_n}{\partial \langle \alpha_n \rangle}\right)_p$
$\left(\frac{\partial M_R}{\partial p}\right)_{\langle \alpha_r \rangle, \langle \alpha_n \rangle}$	$\frac{V_R}{2} \left[ \left(\frac{\partial \bar{\rho}_r}{\partial p}\right)_{\langle \alpha_r \rangle} + \left(\frac{\partial \bar{\rho}_n}{\partial p}\right)_{\langle \alpha_n \rangle} \right]$
$\left(\frac{\partial E_R}{\partial \langle \alpha_r \rangle}\right)_{\langle \alpha_n \rangle, p}$	$\frac{V_R}{2} \left[ U_r \left(\frac{\partial \bar{\rho}_r}{\partial \langle \alpha_r \rangle}\right)_p + \bar{\rho}_r \left(\frac{\partial \bar{U}_r}{\partial \langle \alpha_r \rangle}\right)_p \right]$
$\left(\frac{\partial E_R}{\partial \langle \alpha_n \rangle}\right)_{\langle \alpha_r \rangle, p}$	$\frac{V_R}{2} \left[ U_n \left(\frac{\partial \bar{\rho}_n}{\partial \langle \alpha_n \rangle}\right)_p + \bar{\rho}_n \left(\frac{\partial \bar{U}_n}{\partial \langle \alpha_n \rangle}\right)_p \right]$
$\left(\frac{\partial E_R}{\partial p}\right)_{\langle \alpha_r \rangle, \langle \alpha_n \rangle}$	$\frac{V_R}{2} \left[ U_r \left(\frac{\partial \bar{\rho}_r}{\partial p}\right)_{\langle \alpha_r \rangle} + \bar{\rho}_r \left(\frac{\partial \bar{U}_r}{\partial p}\right)_{\langle \alpha_r \rangle} \right]$  $+ \frac{V_R}{2} \left[ U_n \left(\frac{\partial \bar{\rho}_n}{\partial p}\right)_{\langle \alpha_n \rangle} + \bar{\rho}_n \left(\frac{\partial \bar{U}_n}{\partial p}\right)_{\langle \alpha_n \rangle} \right]$

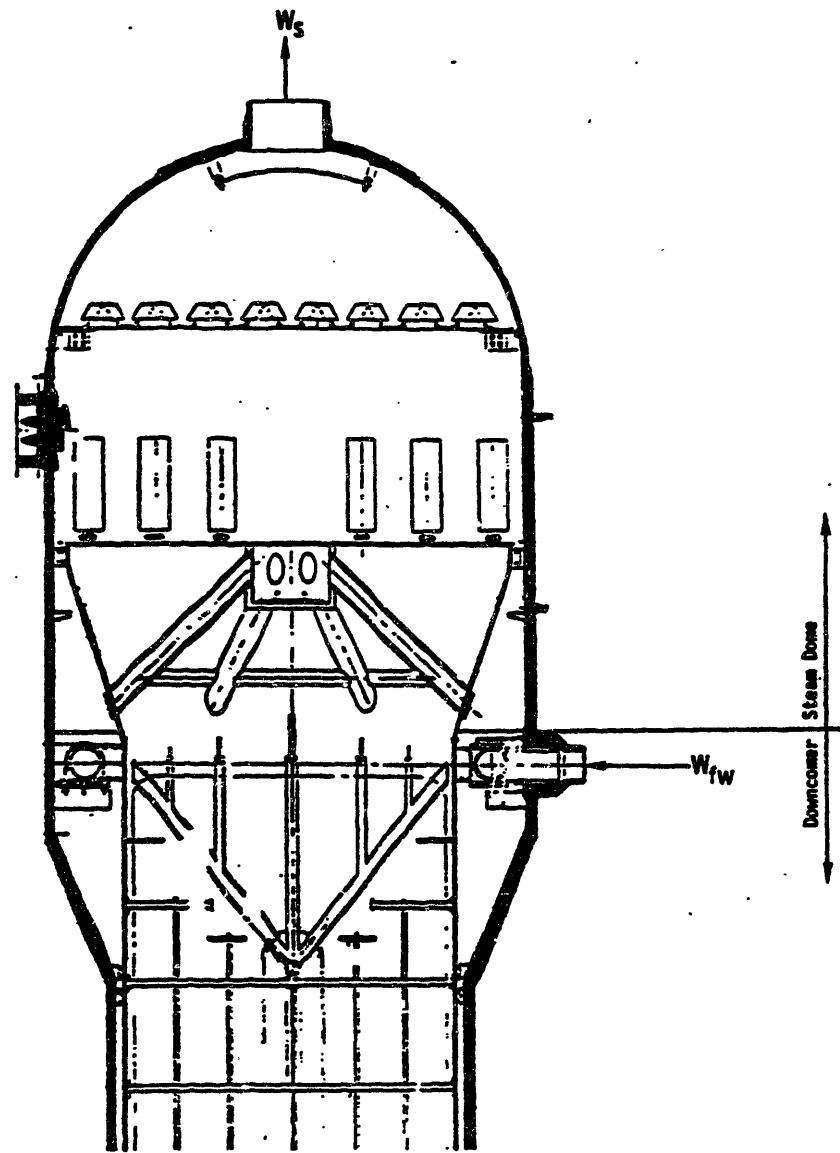


Figure 3.3-1. Steam dome - downcomer.

liquid. For Case 2, the steam dome and downcomer are not treated as separate control volumes. Rather, the steam dome - downcomer is divided into a saturated region and a subcooled region. These regions share a common interface which is allowed to move with time. During the movement, the volume of saturated liquid is kept constant. The sum of the saturated and subcooled region volumes is constant and equal to the total steam dome - downcomer volume. We will now develop the conservation equations for both Case 1 and Case 2.

### 3.3.1 Case 1 Conservation Equations

For Case 1 we make the following assumptions:

- 1.) Only saturated vapor and liquid in the steam dome (thermodynamic equilibrium);
- 2.) Only subcooled liquid in the downcomer;
- 3.) Instantaneous and perfect mixing in the downcomer;
- 4.) No vapor below the liquid-vapor interface;
- 5.) Neglect heat transfer to structural material;
- 6.) No vapor carry-under or liquid carry-over;  
and,
- 7.) Neglect liquid held up in separator return pipes or running down steam generator structure.

The first assumption is reasonable since we are interested in modeling relatively slow operational transients

where we would not expect to see significant departures from thermodynamic equilibrium. In addition, the feedwater ring sprays the feedwater downward so that we would not expect to find much subcooled liquid above the feedwater ring. The second assumption is justified by the fact that pressure reductions occurring during transients of interest to us are expected to be slow enough and mild enough so that the downcomer fluid does not start boiling. The third assumption is physically reasonable since the fluid transport time in the downcomer is relatively small compared to the lengths of the transients we wish to model. This assumption is also important from a numerical standpoint (donor cell differencing), as is discussed in Appendix F.

The fourth assumption regarding a lack of vapor below the liquid-vapor interface is essentially equivalent to assuming that we will deal only with a collapsed liquid level. This assumption is excellent for dealing with the gravitational component of the momentum equation, but introduces some error when calculating the mass or energy content of regions with varying cross-sectional flow areas.

Neglecting heat transfer to steam generator structural material is reasonable since this is a small contribution in the energy equation. Steam separating equipment in the steam dome of the steam generator is designed to minimize liquid carry-over, so neglecting this effect during operational transients is reasonable. The assumption regarding vapor carry-under is not justifiable since there is no

evidence as to whether or not carry-under is significant. The same comment applies to liquid held up in separator return lines and on structure walls.

The conservation of mass and energy equations for the steam dome are:

$$\frac{dM_{SAT}}{dt} = W_n - W_s - W_f \quad (3.3-1)$$

$$\frac{dE_{SAT}}{dt} = W_n H_n - W_s H_{vs} - W_f H_{ls} \quad (3.3-2)$$

Multiplying Eq. (3.3-1) by  $H_{ls}$  and subtracting the result from Eq. (3.3-2) yields:

$$\frac{dE_{SAT}}{dt} - H_{ls} \frac{dM_{SAT}}{dt} = W_n (H_n - H_{ls}) - W_s H_{lvs} \quad (3.3-3)$$

By definition we have,

$$\begin{aligned} M_{SAT} &= \int_0^{V_{SD}} \rho \, dV + \int_0^{V_{STM}} \rho \, dV \\ &= \rho_{ls} V_{SD} + (\rho_{vs} - \rho_{ls}) V_v + \rho_{vs} V_{STM} \end{aligned} \quad (3.3-4a)$$

$$\begin{aligned}
E_{SAT} &= \int_0^{V_{SD}} V \rho U \, dV + \int_0^{V_{STM}} \rho U \, dV \\
&= \rho_{lS} U_{lS} V_{SD} + (\rho_{vS} U_{vS} - \rho_{lS} U_{lS}) V_V + \rho_{vS} U_{vS} V_{STM}
\end{aligned}
\tag{3.3-4b}$$

where,  $V_{SD}$   $\equiv$  volume of steam dome;

$V_V$   $\equiv$  volume of saturated steam in the steam dome; and,

$V_{STM}$   $\equiv$  volume of main steam line.

In Eqs. (3.3-4) we have included the volume of the main steam line. In this formulation we have assumed that there is only saturated steam in the main steam line and we have neglected changes in properties caused by the pressure drop experienced by the steam flowing in the pipes.

The mass and energy conservation equations for the downcomer are:

$$\frac{dM_{SUB}}{dt} = W_{fw} + W_f - W_0 \tag{3.3-6}$$

$$\frac{dM_{SUB}}{dt} = W_{fw} H_{fw} + W_f H_{lS} - W_0 H_0 \tag{3.3-7}$$

Multiplying Eq. (3.3-6) by  $H_{lS}$  and subtracting the result from Eq. (3.3-7) yields,

$$\frac{dE_{SUB}}{dt} - H_{ls} \frac{dM_{SUB}}{dt} = W_{fw}(H_{fw} - H_{ls}) - W_0(H_0 - H_{ls}) \quad (3.3-8)$$

Using the instantaneous and perfect mixing assumption to determine  $M_{SUB}$  and  $E_{SUB}$  gives:

$$M_{SUB} = \int_0^{V_D} \rho \, dV = \rho_0 V_D \quad (3.3-9a)$$

$$E_{SUB} = \int_0^{V_D} \rho U \, dV = \rho_0 U_0 V_D \quad (3.3-9b)$$

where  $V_D$  is the downcomer volume.

### 3.3.2 Case 1 State Variables

It is apparent from Eqs. (3.3-4) that  $M_{SAT}$  and  $E_{SAT}$  are functions of pressure and vapor volume alone, so these quantities are chosen to be our state variables. Taking the total derivatives of  $M_{SAT}$  and  $E_{SAT}$  and substituting them into Eq. (3.3-3) yields:

$$B_7 \frac{dV_v}{dt} + B_8 \frac{dp}{dt} = W_n(H_n - H_{ls}) - W_s H_{lvs} \quad (3.3-10)$$



where,

$$B_7 = \left( \frac{\partial E_{SAT}}{\partial V_V} \right)_P - H_{LS} \left( \frac{\partial M_{SAT}}{\partial V_V} \right)_P$$

and,

$$B_8 = \left( \frac{\partial E_{SAT}}{\partial P} \right)_{V_V} - H_{LS} \left( \frac{\partial M_{SAT}}{\partial P} \right)_{V_V}$$

Table 3.3-1 shows the partial derivatives appearing in Eq. (3.3-10).

Equations (3.3-9a and b) show that both  $M_{SUB}$  and  $E_{SUB}$  are functions of pressure. Since the downcomer fluid is subcooled we need to know an additional thermodynamic property to completely specify the state of the fluid. In the derivation of the tube bundle energy equation we use the internal energy of the subcooled fluid as this additional state variable, so we will do the same here. Taking the total derivatives of  $M_{SUB}$  and  $E_{SUB}$  and substituting into Eq. (3.3-8) yields:

$$B_9 \frac{dU_0}{dt} + B_{10} \frac{dp}{dt} = W_{fw}(H_{fw} - H_{LS}) - W_0(H_0 - H_{LS})$$

Table 3.3-1  
 Partial Derivatives for Equation 3.3-10.

Quantity	Expression
$\left(\frac{\partial M_{SAT}}{\partial V_v}\right)_p$	$(\rho_{vs} - \rho_{ls})$
$\left(\frac{\partial M_{SAT}}{\partial p}\right)_{V_v}$	$\frac{d\rho_{ls}}{dp} (V_{SD} - V_v) + \frac{d\rho_{vs}}{dp} (V_v + V_{STM})$
$\left(\frac{\partial E_{SAT}}{\partial V_v}\right)_p$	$\rho_{vs} U_{vs} - \rho_{ls} U_{ls}$
$\left(\frac{\partial E_{SAT}}{\partial p}\right)_{V_v}$	$\left(\rho_{ls} \frac{dU_{ls}}{dp} + U_{ls} \frac{d\rho_{ls}}{dp}\right)(V_{SD} - V_v)$ $+ \left(\rho_{vs} \frac{dU_{vs}}{dp} + U_{vs} \frac{d\rho_{vs}}{dp}\right)(V_v + V_{STM})$

where,

$$B_g = \left(\frac{\partial E_{SUB}}{\partial U_0}\right)_p - H_{ls} \left(\frac{\partial M_{SUB}}{\partial U_0}\right)_p \quad (3.3-11)$$

and,

$$B_{10} = \left( \frac{\partial E_{SUB}}{\partial p} \right) U_0 - H_{1s} \left( \frac{\partial M_{SUB}}{\partial p} \right) U_0$$

The partial derivatives appearing in Eq. (3.3-11) are shown in Table 3.3-2.

### 3.3.3 Case 2 Conservation Equations

For Case 2 we make the same assumptions as for Case 1 with the following additional assumptions:

- 1.) The saturated liquid volume is constant and equal to some specified fraction of the volume of saturated liquid present during normal operation; and,
- 2.) The feedwater is always added to the sub-cooled region.

The first assumption listed above is difficult to justify, except to note that we would expect to find saturated liquid present even if the water level is below the feedwater ring. A similar assumption (assuming a constant per cent of the total liquid mass) has been used with success (Ref. (S1)). The results of calculations using the constant saturated liquid volume depend on the size of the volume. In this work we use a value of 25 per cent of the saturated liquid volume at normal full power operation.

Table 3.3-2  
 Partial Derivatives Appearing in Equation 3.3-11.

Quantity	Expression
$\left(\frac{\partial M_{SUB}}{\partial U_0}\right)_p$	$v_D \left(\frac{\partial \rho_0}{\partial U_0}\right)_p$
$\left(\frac{\partial M_{SUB}}{\partial p}\right)_{U_0}$	$v_D \left(\frac{\partial \rho_0}{\partial p}\right)_{U_0}$
$\left(\frac{\partial E_{SUB}}{\partial U_0}\right)_p$	$v_D \rho_0 + v_D U_0 \left(\frac{\partial \rho_0}{\partial U_0}\right)_p$
$\left(\frac{\partial E_{SUB}}{\partial p}\right)_{U_0}$	$v_D U_0 \left(\frac{\partial \rho_0}{\partial p}\right)_{U_0}$

The second assumption listed above is not always true in off-normal plant transients. However, in situations where the liquid inventory becomes low enough for Case 2 to be implemented, the feedwater flowrate is usually small enough so assuming that the feedwater is added directly to the subcooled region introduces a small error.

It should be noted that situations in which the water level is low enough for us to use Case 2 for calculations

are infrequent and generally occur during transients for which the steam generator model developed here rapidly becomes invalid.

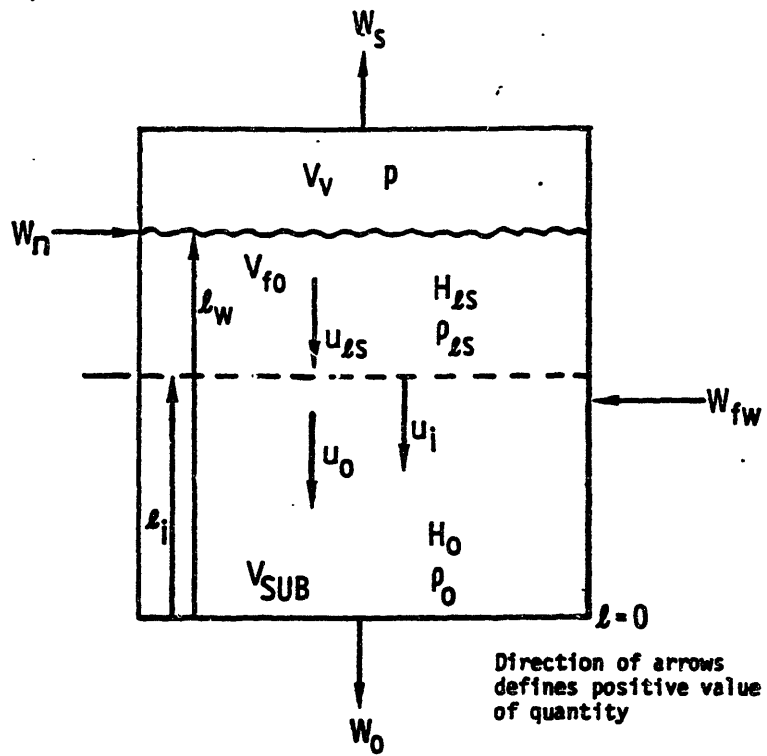
As mentioned at the beginning of this section we use control volumes with a common interface that moves with time. The conservation equations for each region comprising this system are somewhat different from those used for fixed control volumes. Here we must account for two effects:

- 1.) Addition or loss of fluid due to the motion of the interface; and,
- 2.) Work done by or on the control volume due to expansion or contraction.

Before we formulate the conservation equations for Case 2 it is necessary to clearly define the system and the variables of interest. Figure 3.3-2 is a block diagram of the steam dome-downcomer showing the variables of interest. One of the more important quantities is the velocity of the interface,  $u_i$ . This quantity is given by,

$$u_i = - \frac{d\ell_i}{dt} \quad (3.3-12)$$

where the minus sign is introduced because a positive interface velocity is defined to be in the direction of decreasing interface height. The rate at which volume is swept out by the interface (the rate at which the saturated region volume changes) is given by



- |  |  |
|--|--|
| $l_W$ - Water level                            | $u_i$ - Velocity of interface                                |
| $l_i$ - Level of interface                     | $u_{2S}$ - Velocity of saturated liquid just above interface |
| $V_V$ - Saturated vapor volume                 | $u_o$ - Velocity of subcooled liquid just above interface    |
| $V_{SUB}$ - Subcooled liquid volume            |  |
| $V_{fo}$ - Constant volume of saturated liquid |  |

Figure 3.3-2. Case 2 block diagram and nomenclature.

$$\frac{dV_{\text{sat}}}{dt} = A_i u_i = - \frac{A_i dl_i}{dt} \quad (3.3-13)$$

Since the volume of saturated liquid is assumed to be constant Eq. (3.3-13) becomes

$$\frac{dV_v}{dt} = \frac{dV_{\text{sat}}}{dt} = A_i u_i \quad (3.3-14)$$

Returning to Fig. (3.3-2), the rate at which mass is added to the saturated region due to both the motion of the interface and flow across the interface is given by,

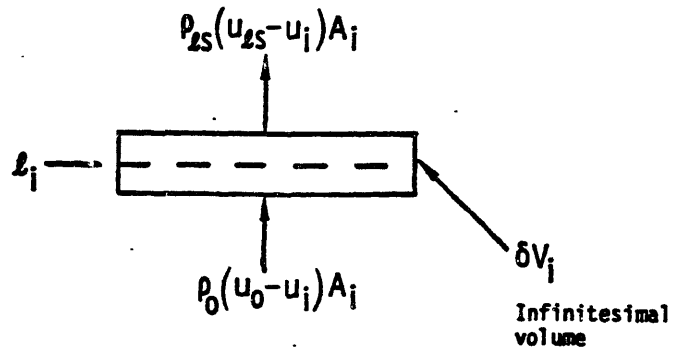
$$\rho_{ls}(u_{ls} - u_i)A_i \quad (3.3-15a)$$

Likewise, for the subcooled region we have

$$\rho_0(u_0 - u_i)A_i \quad (3.3-15b)$$

The relationship between Eqs. (3.3-15a) and (3.3-15b) can be found by performing a mass balance for an infinitesimal volume,  $\delta V_i$ , around the interface (see Fig. 3.3-3). We do not allow the accumulation of mass in this infinitesimal volume, which results in the so-called jump condition:

$$\rho_{ls}(u_{ls} - u_i)A_i = \rho_0(u_0 - u_i)A_i \quad (3.3-16)$$



OR

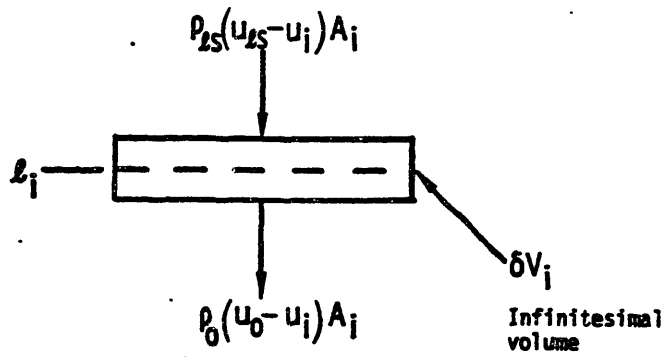


Figure 3.3-3. Mass balance jump condition.



Performing a mass balance for the saturated region results in:

$$\frac{dM_{SAT}}{dt} = W_n - W_s - \rho_{lS}(u_{lS} - u_i)A_i \quad (3.3-17)$$

The quantity  $\rho_{lS}u_{lS}A_i$  is equal to the flowrate across the interface if the interface was stationary,  $W_f$ , and the quantity  $\rho_{lS}u_iA_i$  is a term which accounts for the motion of the interface. Substituting  $W_f$  for  $\rho_{lS}u_{lS}A_i$  and Eq. (3.3-14) for  $A_iu_i$  yields:

$$\frac{dM_{SAT}}{dt} = W_n - W_s - W_f + \rho_{lS} \frac{dV_v}{dt}$$

or

$$\frac{dM_{SAT}}{dt} - \rho_{lS} \frac{dV_v}{dt} = W_n - W_s - W_f \quad (3.3-18)$$

Comparing Eqs. (3.3-18) and (3.3-1) we see that the only difference between them is the term  $\rho_{lS} dV_v/dt$  appearing on the left hand side of Eq. (3.3-18). Clearly this term accounts for the fact that the control of volume is not fixed.

For the subcooled volume a mass balance yields:

$$\frac{dM_{SUB}}{dt} = W_{fw} - W_0 + \rho_0(u_0 - u_i)A_i \quad (3.3-19)$$

Substituting Eq. (3.3-16) into the expression gives:

$$\frac{dM_{SUB}}{dt} = W_{fw} - W_0 + \rho_{ls}(u_{ls} - u_i)A_i$$

Performing the same manipulations that gave us Eq. (3.3-18) from Eq. (3.3-17) results in:

$$\frac{dM_{SUB}}{dt} + \rho_{ls} \frac{dV_v}{dt} = W_{fw} - W_0 + W_f \quad (3.3-19)$$

When writing the energy equation for the saturated region we must account for the motion of the interface. First, we must account for the work done by or on the control volume due to expansion or contraction. Second, we must properly account for energy convected through the interface due to both the motion of the interface and the fluid velocity. The work term is given by,

$$-p \frac{dV_{SAT}}{dt} = -p \frac{dV_v}{dt} \quad (3.3-20)$$

while, the convective term is given by,

$$-\rho_{ls}(u_{ls} - u_i)A_i H_k \quad (3.3-21)$$

where

$$H_k \begin{cases} = H_{ls} & \text{if } u_{ls} \geq u_i \\ = H_0 & \text{if } u_{ls} < u_i \end{cases}$$

Thus, the energy equation for the saturated region is:

$$\frac{dE_{SAT}}{dt} = W_n H_n - W_s H_{lvs} - \rho_{ls}(u_{ls} - u_i)A_i H_k - p \frac{dV_v}{dt}$$

Substituting for  $\rho_{ls} u_{ls} A_i$  and  $A_i u_i$  yields:

$$\frac{dE_{SAT}}{dt} - (\rho_{ls} H_k - p) \frac{dV_v}{dt} = W_n H_n - W_s H_{vs} - W_f H_k \quad (3.3-22)$$

Using the same arguments for the subcooled region yields:

$$\frac{dE_{SUB}}{dt} + (\rho_{ls} H_k - p) \frac{dV_v}{dt} = W_{fw} H_{fw} + W_f H_k - W_0 H_0 \quad (3.3-23)$$

Multiplying Eq. (3.3-18) by  $H_k$  and subtracting the result from Eq. (3.3-22) gives:

$$\frac{dE_{SAT}}{dt} - H_k \frac{dM_{SAT}}{dt} + p \frac{dV_v}{dt} = W_n(H_n - H_k) - W_s(H_{vs} - H_k) \quad (3.3-24)$$

Multiplying Eq. (3.3-19) by the  $H_k$  and subtracting from Eq. (3.3-23) gives:

$$\frac{dE_{SUB}}{dt} - H_k \frac{dM_{SUB}}{dt} - p \frac{dV_v}{dt} = W_{fw}(H_{fw} - H_k) - W_0(H_0 - H_k) \quad (3.3-25)$$

### 3.3.4 Case 2 State Variables

The mass and energy contents of the saturated region are given by

$$\begin{aligned} M_{SAT} &= \int_0^{V_{SAT}} \rho \, dV \\ &= V_{f0} \rho_{ls} + (V_v + V_{STM}) \rho_{vs} \end{aligned} \quad (3.3-26a)$$

and,

$$\begin{aligned}
 E_{\text{SAT}} &= \int_0^{V_{\text{SAT}}} \rho U \, dV \\
 &= V_{f0} \rho_{\ell s} U_{\ell s} + (V_v + V_{\text{STM}}) \rho_{vs} U_{vs}
 \end{aligned}
 \tag{3.3-26b}$$

From Eqs. (3.3-26) it is clear that both  $M_{\text{SAT}}$  and  $E_{\text{SAT}}$  are functions of pressure,  $p$ , and steam volume,  $V_v$ . Therefore, these quantities are again chosen as state variables. Taking the total derivative of  $M_{\text{SAT}}$  and  $E_{\text{SAT}}$ , and substituting the result into Eq. (3.3-24) gives:

$$B_{11} \frac{dV_v}{dt} + B_{12} \frac{dp}{dt} = W_n (H_n - H_k) - W_s (H_{vs} - H_k)$$

where,

$$B_{11} = \left( \frac{\partial E_{\text{SAT}}}{\partial V_v} \right)_p - H_k \left( \frac{\partial M_{\text{SAT}}}{\partial V_v} \right)_p + p \tag{3.3-27}$$

and,

$$B_{12} = \left( \frac{\partial E_{\text{SAT}}}{\partial p} \right)_{V_v} - H_k \left( \frac{\partial M_{\text{SAT}}}{\partial p} \right)_{V_v}$$

$$H_k \left\{ \begin{array}{l} = H_{\ell s} \text{ if } u_{\ell s} \geq u_i \\ = H_0 \text{ if } u_{\ell s} < u_i \end{array} \right.$$

The partial derivatives appearing above are shown in Table 3.3-3.

Table 3.3-3  
Partial Derivatives Appearing in Equation 3.3-27.

Quantity	Expansion
$\left(\frac{\partial M_{SAT}}{\partial V_v}\right)_p$	$\rho_{vs}$
$\left(\frac{\partial M_{SAT}}{\partial p}\right)_{V_v}$	$(V_v + V_{STM}) \frac{d\rho_{vs}}{dp} + V_{fo} \frac{d\rho_{\ell s}}{dp}$
$\left(\frac{\partial E_{SAT}}{\partial V_v}\right)_p$	$\rho_{vs} U_{vs}$
$\left(\frac{\partial E_{SAT}}{\partial p}\right)_{V_v}$	$(V_v + V_{STM}) \left( U_{vs} \frac{d\rho_{vs}}{dp} + \rho_{vs} \frac{dU_{vs}}{dp} \right) + V_{fo} \left( U_{\ell s} \frac{d\rho_{\ell s}}{dp} + \rho_{\ell s} \frac{dU_{\ell s}}{dp} \right)$

For the subcooled region we have,

$$M_{\text{SUB}} = \int_0^{V_{\text{SUB}}} \rho \, dV = (V_{\text{TOT}} - V_{\text{v}} - V_{\text{fo}}) \rho_0 \quad (3.3-28a)$$

and,

$$E_{\text{SUB}} = \int_0^{V_{\text{SUB}}} \rho U \, dV = (V_{\text{TOT}} - V_{\text{v}} - V_{\text{fo}}) \rho_0 U_0 \quad (3.3-28b)$$

where,  $V_{\text{TOT}} \equiv$  Volume of steam dome and downcomer

$= V_{\text{SD}} + V_{\text{D}}$ ; and,

$V_{\text{fo}} \equiv$  Volume of saturated liquid.

Both  $M_{\text{SUB}}$  and  $E_{\text{SUB}}$  depend on pressure, and since the fluid is subcooled we also need the fluid internal energy to completely specify its thermodynamic state. In addition, since the vapor volume appears in Eq. (3.3-28) it is also one of our state variables. Thus,

$$\frac{dM_{\text{SUB}}}{dt} = \left( \frac{\partial M_{\text{SUB}}}{\partial U_0} \right)_{V_{\text{v}}, p} \frac{dU_0}{dt} + \left( \frac{\partial M_{\text{SUB}}}{\partial V_{\text{v}}} \right)_{U_0, p} \frac{dV_{\text{v}}}{dt} + \left( \frac{\partial M_{\text{SUB}}}{\partial p} \right)_{U_0, V_{\text{v}}} \frac{dp}{dt}$$

and,

$$\frac{dE_{\text{SUB}}}{dt} = \left(\frac{\partial E_{\text{SUB}}}{\partial U_0}\right)_{V_v, p} \frac{dU_0}{dt} + \left(\frac{\partial E_{\text{SUB}}}{\partial V_v}\right)_{U_0, p} \frac{dV_v}{dt} + \left(\frac{\partial E_{\text{SUB}}}{\partial p}\right)_{U_0, V_v} \frac{dp}{dt}$$

Substituting the above expressions into Eq. (3.3-25) yields:

$$B_{13} \frac{dU_0}{dt} + B_{14} \frac{dV_v}{dt} + B_{15} \frac{dp}{dt} = W_{fw}(H_{fw} - H_k) - W_0(H_0 - H_k)$$

where

$$B_{13} = \left(\frac{\partial E_{\text{SUB}}}{\partial U_0}\right)_{V_v, p} - H_k \left(\frac{\partial M_{\text{SUB}}}{\partial U_0}\right)_{V_v, p} \quad (3.3-29)$$

$$B_{14} = \left(\frac{\partial E_{\text{SUB}}}{\partial V_v}\right)_{U_0, p} - H_k \left(\frac{\partial M_{\text{SUB}}}{\partial V_v}\right)_{U_0, p} - p$$

and,

$$B_{15} = \left(\frac{\partial E_{\text{SUB}}}{\partial p}\right)_{U_0, V_v} - H_k \left(\frac{\partial M_{\text{SUB}}}{\partial p}\right)_{U_0, V_v}$$

The partial derivatives appearing in Eq. (3.3-29) are shown in Table 3.3-4. This completes the derivation of the steam dome - downcomer conservation equations.



Table 3.3-4  
 Partial Derivatives Appearing in Equation 3.3-29.

Quantity	Expression
$\left(\frac{\partial M_{SUB}}{\partial U_0}\right)_{V_0, P}$	$(V_{SD} - V_v - V_{f0}) \left(\frac{\partial \rho_0}{\partial U_0}\right)_P$
$\left(\frac{\partial M_{SUB}}{\partial V_v}\right)_{U_0, P}$	$-\rho_0$
$\left(\frac{\partial M_{SUB}}{\partial p}\right)_{U_0, V_v}$	$(V_{SD} - V_v - V_{f0}) \left(\frac{\partial \rho_0}{\partial p}\right)_{U_0}$
$\left(\frac{\partial E_{SUB}}{\partial U_0}\right)_{V_v, P}$	$(V_{SD} - V_v - V_{f0}) (\rho_0 + U_0 \left(\frac{\partial \rho_0}{\partial U_0}\right)_P)$
$\left(\frac{\partial E_{SUB}}{\partial V_v}\right)_{U_0, P}$	$-\rho_0 U_0$
$\left(\frac{\partial E_{SUB}}{\partial p}\right)_{U_0, V_v}$	$(V_{SD} - V_v - V_{f0}) U_0 \left(\frac{\partial \rho_0}{\partial p}\right)_{U_0}$

### 3.4 MOMENTUM EQUATION FOR THE RECIRCULATING FLOW

In this section we develop the momentum equation used for calculating the recirculating flow pattern. As mentioned in Chapter 2, the secondary side of the steam generator forms a boiling natural circulation system. The driving head for the natural circulation flow is provided by the density difference between the subcooled downcomer fluid and the two phase mixture in the tube bundle and riser. This driving head is offset by the various pressure losses in the loop, such as friction and turning losses.

The form of the momentum equation used here is derived formally in Appendix B. We apply the equation to a one-dimensional loop consisting of connected flow paths through the tube bundle, riser, steam dome, and downcomer. The coordinate  $s$  is used to denote distance along the flow path. The momentum equation for this loop is:

$$I \frac{d\bar{W}}{dt} = \cancel{\Delta P}^0 - F \quad (3.4-1)$$

where

$$I = \oint \frac{ds}{A};$$

$$\bar{W} = \oint \frac{W ds}{A} / I$$

$\Delta p = \oint \left( - \frac{\partial p}{\partial s} \right) ds = 0$  since the loop is closed; and,

$$F = \oint \frac{1}{A} d \left( \frac{v' W^2}{A} \right) + \oint \frac{fW/W/ds}{2c D_n A^2} + \oint \rho g \sin \theta ds + \sum_i \frac{K_i W_i^2}{2\rho_i A_i^2}$$

In order to determine  $\bar{W}$  we must first find an expression for  $\oint \frac{Wds}{A}$ . This is best done by performing the required integration in a piecewise manner, i.e.,

$$I\bar{W} = \oint \frac{Wds}{A} = \int_0^{L_{TB}} \frac{Wds}{A} + \int_0^{L_R} \frac{Wds}{A} + \int_0^{l_w} \frac{Wds}{A}$$

Tube Bundle	Riser	Steam Dome - Downcomer
----------------	-------	---------------------------

(3.4-2)

In Eq. (3.4-2) we have defined a new origin for each sub-volume so that the limits of each piecewise integration can be written simply. The tube bundle portion of the flow path can be divided into two parts (see Fig. 3.4-1):

- 1.) a parallel flow portion in which flow is essentially parallel to the tubes; and,
- 2.) a crossflow portion in which flow is predominantly transverse to the tubes.

The flow path length associated with the radial inflow at the bottom of the tube bundle is neglected. In the parallel flow portion of the tube bundle the flow area,  $A_{TB}$ , is

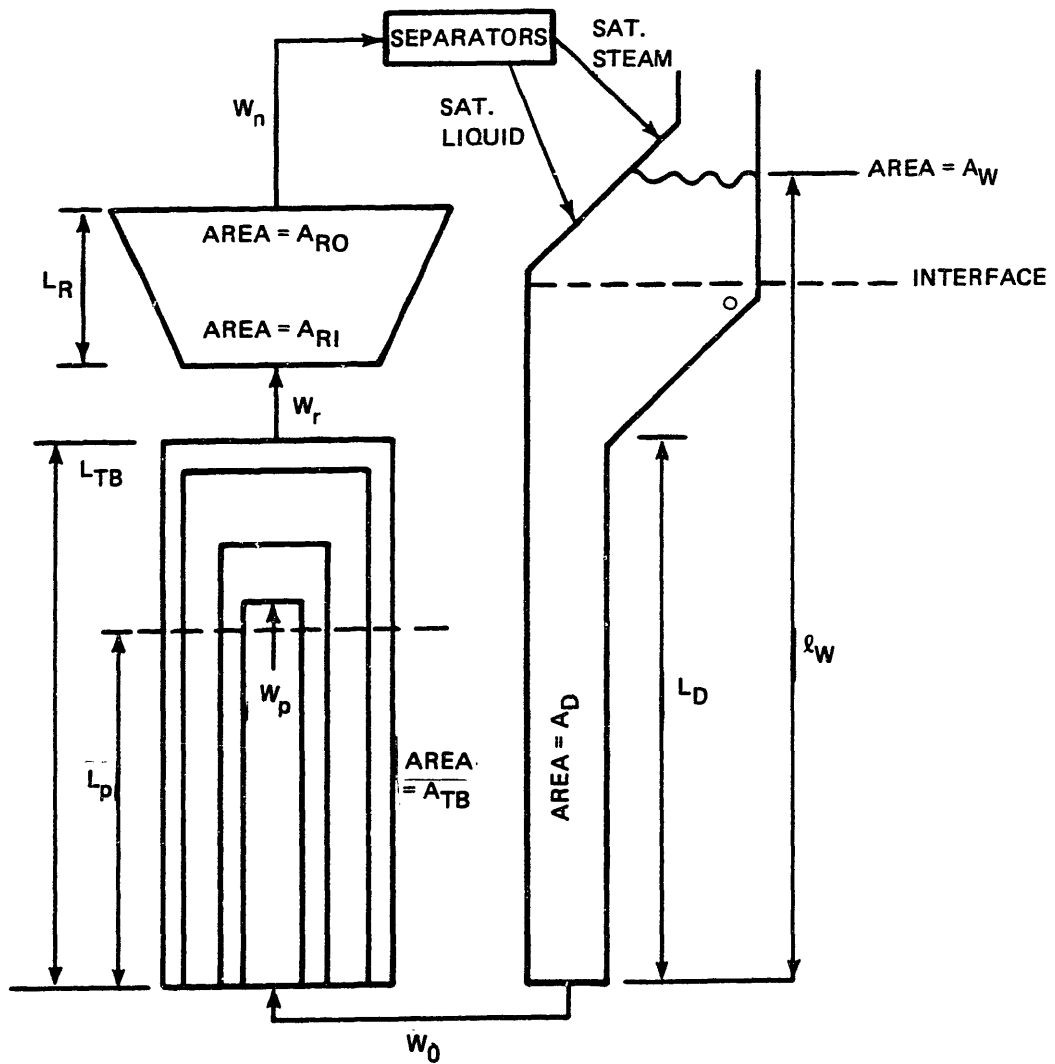


Figure 3.4-1. Notation for momentum equation.

constant. Denoting the length of the parallel flow region by  $L_p$  we can rewrite the first term of Eq. (3.4-2) as:

$$\int_0^{L_{TB}} \frac{Wds}{A} = \frac{1}{A_{TB}} \int_0^{L_p} Wds + \int_{L_p}^{L_{TB}} \frac{Wds}{A} \quad (3.4-3)$$

The integrations indicated in Eq. (3.4-3) require that we know the axial profile of the flowrate. Unfortunately, we do not know what this profile is in transient situations, so we must make an assumption regarding this profile. We use the trapezoidal rule to perform the integrations, which is equivalent to assuming that the quantity  $W/A$  (the mass flux) has a linear profile. Thus,

$$\begin{aligned} \int_0^{L_{TB}} \frac{Wds}{A} &= \frac{(W_0 + W_p)L_p}{2A_{TB}} + \frac{(L_{TB} - L_p)}{2} \left( \frac{W_p}{A_{TB}} + \frac{W_r}{A_{RI}} \right) \\ &= \left( \frac{L_p}{2A_{TB}} \right) W_0 + \left( \frac{L_{TB}}{A_{TB}} \right) W_p + \left( \frac{L_{TB} - L_p}{2A_{RI}} \right) W_r \end{aligned} \quad (3.4-4)$$

Similarly for the riser, we obtain,

$$\begin{aligned} \int_0^{L_R} \frac{Wds}{A} &= \frac{L_R}{2} \left( \frac{W_r}{A_{RI}} + \frac{W_n}{A_{RO}} \right) \\ &= \left( \frac{L_R}{2A_{RI}} \right) W_r + \left( \frac{L_R}{2A_{RO}} \right) W_n \end{aligned} \quad (3.4-5)$$

For the steam dome - downcomer portion of the recirculation loop the situation is complicated by the addition of feedwater. Thus, we will ignore the addition of feedwater and we will characterize the flowrate within this region by  $W_0$ , the downcomer flowrate. This is justifiable since only a small portion of the flow path is above the feedwater ring and since the flow is essentially constant in density. Thus, we obtain,

$$\begin{aligned} \int_0^{\ell_w} \frac{W ds}{A} &= W_0 \int_0^{L_D} \frac{ds}{A} + W_0 \int_0^{\ell_w} \frac{ds}{A} \\ &= \frac{(\ell_w - L_D)}{2} \left( \frac{1}{A_w} + \frac{1}{A_D} \right) + \frac{L_D}{A_D} W_0 \end{aligned} \quad (3.4-6)$$

In deriving Eq. (3.4-6) we have implicitly assumed that the water level,  $\ell_w$ , is greater than the height of the downcomer,  $L_D$ . It turns out, however, that Eq. (3.4-6) reduces to a correct result even when the water level is less than the downcomer height. In this case  $A_w$  is equal to  $A_D$  so Eq. (3.4-6) becomes;

$$\int_0^{\ell_w} \frac{W ds}{A} = \left( \frac{\ell_w}{A_D} \right) W_0$$

which is the correct result when  $\ell_w$  is less than  $L_D$ .

Eq. (3.4-1) is derived with the assumption that the inertance,  $I$ , is time invariant. This is not strictly true for the steam dome - downcomer since we have a moving free surface, i.e. the water level. We will allow the inertance to vary with time; however, we will neglect the time derivative of the inertance. This is justifiable since in most situations of interest to us the derivative of Eq. (3.4-6) is small. When  $l_w$  is less than  $L_D$  this is not true, but in this case there is probably a breakdown in the natural recirculation flow and our formulation of the momentum equation is invalid.

Substituting Eqs. (3.4-4), (3.4-5), and (3.4-6) into Eq. (3.4-2) and collecting terms yields:

$$\begin{aligned}
 I\bar{W} &= \frac{(l_w - l_D)}{2} \left( \frac{1}{A_w} + \frac{1}{A_D} \right) + \left[ \frac{L_D}{A_D} + \frac{L_D}{2A_{TB}} \right] W_0 \\
 &+ \left( \frac{L_{TB}}{A_{TB}} \right) W_p + \left( \frac{L_{TB} - L_p + L_R}{2A_{RI}} \right) W_R + \left( \frac{L_R}{2A_{RO}} \right) W_n \\
 I\bar{W} &= \beta_1 W_0 + \beta_2 W_p + \beta_3 W_R + \beta_4 W_n \quad (3.4-6)
 \end{aligned}$$

The inertance,  $I$ , is determined by using the following equality:

$$\oint \frac{ds}{A} = \int_0^{L_{TB}} \frac{ds}{A} + \int_0^{L_R} \frac{ds}{A} + \int_0^{\ell_w} \frac{ds}{A} \quad (3.4-7)$$

Tube
Riser
Steam Dome -  
Bundle

Downcomer

A consistent evaluation of I can therefore be obtained by equating all flows to unity in Eq. (3.4-6):

$$I = \frac{L_p}{A_{TB}} + \frac{(L_{TB} - L_p)}{2} \left( \frac{1}{A_{TB}} + \frac{1}{A_{RI}} \right) + \frac{L_R}{2} \left( \frac{1}{A_{RI}} + \frac{1}{A_{RO}} \right) + \frac{(\ell_w - L_D)}{2} \left( \frac{1}{A_w} + \frac{1}{A_D} \right) + \frac{L_D}{A_D} \quad (3.4-8)$$

Using Eqs. (3.4-6) and (3.4-8) gives:

$$\bar{W} = \beta_1' W_D + \beta_2' W_p + \beta_3' W_r + \beta_4' W_n \quad (3.4-9)$$

where  $\beta_i' = \beta_i / I$ , and  $\sum_{i=1}^4 \beta_i' = 1$ .

It is important to note that the sum of the  $\beta_i'$ s is unity.

The last quantity of interest in Eq. (3.4-1) is the term F, which consists of acceleration, friction, shock, and gravitation components. We will derive each component for the entire loop in turn.



## Friction

The frictional term can be written as:

$$\oint \frac{f|W|W}{2\rho D_h A^2} ds = \int_0^{L_{TB}} \frac{fW|W|}{2\rho D_h A^2} ds + \int_0^{L_R} \frac{fW|W|}{2\rho D_h A^2} ds + \int_0^{L_W} \frac{fW|W|}{2\rho D_h A^2} ds \quad (3.4-10)$$

We will neglect frictional losses in the riser and steam dome, since in these regions the hydraulic diameter and flow area are large resulting in a small frictional pressure gradient. Equation (3.4-10) then becomes:

$$\oint \frac{fW|W|}{2\rho D_h A^2} ds = \int_0^{L_{TB}} \frac{fW|W|}{2\rho D_h A^2} ds + \int_0^{L_D} \frac{fW|W|}{2\rho D_h A^2} ds \quad (3.4-11)$$

Characterizing the flowrate in the downcomer by  $W_0$  yields:

$$\int_0^{L_D} \frac{fW|W|}{2\rho D_h A^2} ds = \frac{f_D W_0 |W_0| L_D}{2\rho_0^D D_{hD} A_D^2} \quad (3.4-12)$$

This result is based on a flowrate in the downcomer assumed to be spatially constant at any instant in time. This is reasonable since the downcomer fluid is virtually constant

in density. The downcomer fluid is thermally expandable, but this has a negligible effect on the flow rate.

The tube bundle can be split into two regions: a parallel flow region and a cross-flow region. Thus,

$$\int_0^{L_{TB}} \frac{fW|W|}{2\rho D_h A^2} ds = \int_0^{L_p} \frac{fW|W|}{2\rho D_h A^2} ds + \int_{L_p}^{L_{TB}} \frac{fW|W|}{2\rho D_h A^2} ds \quad (3.4-13)$$

The first term in this equation is evaluated using the trapezoidal rule, giving:

$$\int_0^{L_p} \frac{fW|W|}{2\rho D_h A^2} ds = \frac{L_p}{4D_{hTB} A_{TB}^2} \left[ \frac{f_0 W_0 |W_0|}{\rho_0} + \frac{f_{\ell s, p} W_p |W_p|}{\rho_{\ell s}} \phi_{\ell 0, p}^2 \right] \quad (3.4-14)$$

where  $\phi_{\ell 0, p}^2$  is the two-phase multiplier evaluated at the junction of the parallel and cross-flow regions (see Appendices A and C).

The cross-flow component of the frictional pressure gradient in the tube bundle is difficult to evaluate. Here we use the following expression for the frictional pressure drop:

$$\int_{L_p}^{L_{TB}} \frac{fW|W|}{2\rho D_h A^2} ds = \frac{K_c}{2\phi_{ls}} [W_p|W_p|\phi_{ls,p}^2 + W_r|W_r|\phi_{l0,r}^2] \quad (3.4-15)$$

The quantity  $K_c$  appearing in Eq. (3.4-15) is a cross-flow frictional loss coefficient for saturated single-phase flow and it is formally defined in Appendix D.

Substituting Eqs. (3.4-12), (3.4-13), (3.4-14), and (3.4-15) into Eq. (3.4-11) gives:

$$\begin{aligned} \oint \frac{fW|W|}{2\rho D_h A^2} ds &= \left[ \frac{f_D L_D}{2\rho_0^D h D A^2} + \frac{L_p f_0}{4\rho_0^D h T_B A^2} \right] W_0|W_0| \\ &+ \left[ \frac{L_p f_{ls,p}}{4\phi_{ls}^D h T_B A^2} + \frac{K_c}{2\phi_{ls}} \right] W_p|W_p|\phi_{l0,p}^2 \\ &+ \left( \frac{K_c}{2\phi_{ls}} \right) W_r|W_r|\phi_{l0,r}^2 \end{aligned} \quad (3.4-16)$$

### Acceleration

The acceleration term can be written as:

$$\oint \frac{1}{A} d \left( \frac{v'W^2}{A} \right) = \int_0^{L_{TB}} \frac{1}{A} d \left( \frac{v'W^2}{A} \right) + \int_0^{L_R} \frac{1}{A} d \left( \frac{v'W^2}{A} \right) + \int_0^{L_W} \frac{1}{A} d \left( \frac{v'W^2}{A} \right)$$

(3.4-17)

where the integration limits indicate the s positions at which the definite integral is to be evaluated. In the parallel flow region of the tube bundle the flow area is constant, so we have:

$$\int_0^{L_{TB}} \frac{1}{A} d \left( \frac{v'W^2}{A} \right) = \frac{1}{A_{TB}^2} \int_0^{L_P} d(v'W^2) + \int_{L_P}^{L_{TB}} \frac{1}{A} d \left( \frac{v'W^2}{A} \right)$$

Using the trapezoidal rule on the third term in this equation yields

$$\int_0^{L_{TB}} \frac{1}{A} d \left( \frac{v'W^2}{A} \right) = \frac{1}{A_{TB}^2} (W_P^2 v'_P - \frac{W_0^2}{\rho_0}) + \frac{1}{2} \left[ \frac{v'_R W_R^2}{A_{RI}} - \frac{v'_P W_P^2}{A_{TB}} \right] \left[ \frac{1}{A_{RI}} + \frac{1}{A_{TB}} \right]$$

(3.4-18)

Similarly for the riser we obtain:

$$\int_0^{L_R} \frac{1}{A} d \left( \frac{v' W^2}{A} \right) = \frac{1}{2} \left[ \frac{v'_n W_n^2}{A_{RO}} - \frac{v'_r W_r^2}{A_{RI}} \right] \left[ \frac{1}{A_{RI}} + \frac{1}{A_{RO}} \right] \quad (3.4-19)$$

In the steam dome - downcomer we will neglect momentum effects caused by the introduction of feedwater, and we will only account for acceleration due to changes in flow geometry. To do this we will characterize the flowrate and density by the downcomer outlet flowrate,  $W_0$ , and the downcomer density,  $\rho_0$ . These assumptions yield:

$$\begin{aligned} \int_{z_w}^0 \frac{1}{A} d \left( \frac{v' W^2}{A} \right) &= \frac{W_0^2}{\rho_0} \int_{A_w}^{A_D} \frac{1}{A} d \left( \frac{1}{A} \right) \\ &= \frac{W_0^2}{2\rho_0} \left( \frac{1}{A_D} - \frac{1}{A_w} \right) \end{aligned} \quad (3.4-20)$$

Substituting Eqs. (3.4-18), (3.4-19), and (3.4-20) into Eq. (3.4-17) gives:

$$\begin{aligned}
\int \frac{1}{A} d \left( \frac{v' W^2}{A} \right) &= \left[ \frac{1}{A_D^2} - \frac{1}{A_W^2} - \frac{2}{A_{TB}^2} \right] \frac{W_0^2}{2\rho_0} + \left[ \frac{1}{A_{TB}} - \frac{1}{A_{RI}} \right] \frac{v'_p W_p^2}{2A_{TB}} \\
&+ \left[ \frac{1}{A_{TB}} - \frac{1}{A_{RO}} \right] \frac{v'_r W_r^2}{2A_{RI}} + \left[ \frac{1}{A_{RO}} + \frac{1}{A_{RI}} \right] \frac{v'_n W_n^2}{2A_{RO}}
\end{aligned}
\tag{3.4-21}$$

### Gravity

The gravitational term can be written as

$$\int \rho g \sin \theta ds = \int_0^{L_{TB}} \bar{\rho} g ds + \int_0^{L_R} \bar{\rho} g ds - \int_0^{l_w} \rho g ds
\tag{3.4-22}$$

From Section 3.1 we know that the density profile in the tube bundle is given by:

$$\frac{1}{\rho} = \frac{1}{\rho_0} + \left( \frac{1}{\rho_r} - \frac{1}{\rho_0} \right) \frac{s}{L_{TB}}$$

Using this expression in the first term on the right hand side of Eq. (3.4-22) gives:

$$\int_0^{L_{TB}} \bar{\rho} g ds = \frac{L_{TB} \rho_0 \bar{\rho}_r g}{\rho_0 - \bar{\rho}_r} \ln \left( \frac{\rho_0}{\bar{\rho}_r} \right)
\tag{3.4-23}$$

In the riser we assume the vapor volume fraction axial profile is linear, which implies that the axial profile of the density is linear. Thus,

$$\int_0^{L_R} \bar{\rho} g \, ds = \frac{L_R g}{2} (\bar{\rho}_r + \bar{\rho}_n) \quad (3.4-24)$$

Finally in the steam dome - downcomer region we obtain

$$\int_0^{l_w} \rho g \, ds = \rho_{lS} g l_{SAT} + \rho_0 g l_{SUB} \quad (3.4-25)$$

where  $l_{SAT}$  is the vertical length of the saturated region and  $l_{SUB}$  is the vertical length of the subcooled region. Substituting Eqs. (3.4-23), (3.4-24), and (3.4-25) into Eq. (3.4-22) yields:

$$\oint \rho g \sin \theta \, ds = g \frac{L_{TB} \rho_0 \bar{\rho}_r}{\rho_0 - \bar{\rho}_r} \ln \left( \frac{\bar{\rho}_0}{\bar{\rho}_r} \right) + \frac{L_R}{2} (\bar{\rho}_r + \bar{\rho}_n) - \rho_{lS} l_{SAT} - \rho_0 l_{SUB} \quad (3.4-26)$$

### Other Losses

There are three major sources of pressure drop other than those already derived. One is the turning and shock loss occurring at the bottom of the downcomer. Another is the pressure drop caused by tube supports in the tube bundle. The last is the pressure drop experienced by the two-phase mixture as it flows through the separators. We will not deal directly with tube support losses; rather, we will combine those losses with the separator loss and assign a single loss coefficient,  $K_{SEP}$ , to account for both pressure drops. This loss coefficient is based on the velocity of the fluid at the top of the riser and is given by:

$$\Delta p = K_{SEP} \frac{v' W_n^2}{2A_{RO}^2} \quad (3.4-27)$$

The loss at the bottom of the downcomer is given by:

$$\Delta p = K_D \frac{W_0^2}{2\rho_0 A_D^2} \quad (3.4-28)$$

### Overall Loss

Adding Eqs. (3.4-16), (3.4-21), (3.4-26), (3.4-27) and (3.4-28) yields:



$$F = M_1 W_0 + W_2 W_p + M_2 W_r + M_4 M_n + M_5 \quad (3.4-29)$$

where,

$$M_1 = \frac{1}{2\rho_0} \left[ \left( \frac{1 + K_D}{A_D^2} - \frac{1}{A_w^2} - \frac{2}{A_{TB}^2} \right) W_0 + \left( \frac{f_D L_D}{D_{hD} A_{TB}^2} + \frac{L_p f_0}{2D_{hTB} A_{TB}^2} \right) |W_0| \right];$$

$$M_2 = \left[ \frac{1}{A_{TB}} - \frac{1}{A_{RI}} \right] \frac{v'_p W_p}{2A_{TB}} + \left[ \frac{L_p f_{\ell s, p}}{2D_{hTB} A_{TB}^2} + K_c \right] \frac{\phi_{\ell 0, p}^2 |W_p|}{2\rho_{\ell s}};$$

$$M_3 = \left[ \frac{1}{A_{TB}} - \frac{1}{A_{RO}} \right] \frac{v'_r W_r}{2A_{RI}} + \frac{K_c \phi_{\ell 0, r}^2}{2\rho_{\ell s}} |W_r|;$$

$$M_4 = \left[ \frac{K_{SEP} + 1}{A_{RO}} + \frac{1}{A_{RI}} \right] \frac{v'_n W_n}{2A_{RO}}; \text{ and,}$$

$$M_5 = g \left[ \frac{L_{TB} \rho_0 \bar{\rho}_r}{\rho_0 - \bar{\rho}_r} \ln \left( \frac{\rho_0}{\bar{\rho}_r} \right) + \frac{L_R}{2} (\bar{\rho}_r + \bar{\rho}_n) - \rho_{\ell s} \ell_{SAT} - \rho_0 \ell_{SUB} \right]$$

### 3.5 CLOSURE OF EQUATIONS

At this point it is worthwhile to take a look at the number of unknown quantities that we have, as well as the number of equations available for solution. There are 11

unknowns:  $\bar{U}_0$ ,  $V_v$ ,  $\langle \alpha_r \rangle$ ,  $\langle \alpha_n \rangle$ ,  $p$ ,  $\bar{W}$ ,  $W_0$ ,  $W_p$ ,  $W_r$ ,  $W_n$ , and  $W_f$ . We have derived 10 equations, as shown in Table 3.5-1. In order to have closure we require an additional equation. Further examination of the unknowns reveals that the required equation should involve  $W_p$ , the flowrate at the parallel to cross-flow transition in the tube bundle. This flowrate was introduced in the momentum equation and does

Table 3.5-1.  
Equations Available for Solution

Conservation Equation	Equation Number in Text
Tube Bundle Mass	3.1-1
Tube Bundle Energy	3.1-13
Riser Mass	3.2-1
Riser Energy	3.2-8
Saturated Region Mass	3.3-1 or 3.3-18
Saturated Region Energy	3.3-10 or 3.3-27
Subcooled Region Mass	3.3-6 or 3.3-19
Subcooled Region Energy	3.3-11 or 3.3-29
Momentum	3.4-1
Definition of $\bar{W}$	3.4-9

not appear in any equations prior to that. The simplest equation that incorporates  $W_p$  is a mass conservation equation for the cross-flow region of the tube bundle. This equation is:

$$\frac{dM_{TBC}}{dt} = W_p - W_r \quad (3.5-1)$$

where,

$$M_{TBC} = \int_{V_p}^{V_{TB}} \bar{\rho} dV \quad (3.5-2)$$

In section 3.1 we make the assumption that the density profile is inversely proportional to axial position in the tube bundle. Using this assumption in Eq. (3.5-2) yields:

$$M_{TBC} = \frac{V_{TB} \rho_0 \bar{\rho}_r}{\rho_0 - \rho_r} \ln \left( \frac{\bar{\rho}_p}{\bar{\rho}_r} \right) = \frac{\ln \left( \frac{\bar{\rho}_p}{\bar{\rho}_r} \right)}{\ln \left( \frac{\rho_0}{\rho_r} \right)} M_{TB} \quad (3.5-3)$$

The quantity,  $\bar{\rho}_p$ , is a known function of  $\rho_0$  and  $\bar{\rho}_r$ , the tube bundle inlet and outlet densities. Thus Eq. (3.5-3) is a function of pressure,  $p$ , inlet internal energy,  $U_0$ , and outlet vapor volume fraction,  $\langle \alpha_r \rangle$ . These variables are all part of our set of unknowns so we have not introduced

any new unknowns with Eq. (3.5-1). Expanding the left hand side of Eq. (3.5-1) into its total derivative yields:

$$\begin{aligned} \frac{dM_{TBC}}{dt} = & \left( \frac{\partial M_{TBC}}{\partial U_0} \right)_{\langle \alpha_p \rangle, p} \frac{dU_0}{dt} + \left( \frac{\partial M_{TBC}}{\partial \langle \alpha_r \rangle} \right)_{U_0, p} \frac{d\langle \alpha_r \rangle}{dt} \\ & + \left( \frac{\partial M_{TBC}}{\partial p} \right)_{\langle \alpha_r \rangle, U_0} \frac{dp}{dt} = W_p - W_r \end{aligned} \quad (3.5-4)$$

The partial derivatives appearing in Eq. (3.5-4) are shown in Table 3.5-2. Tables 3.5-3 and 3.5-4 list the unknowns and equations that constitute the secondary side model.

Evaluation of the various fluid properties and fluid property derivatives dictates the need for a comprehensive set of fluid property tables. The model incorporates a complete set of thermodynamic property fits for both saturated and subcooled conditions, as well as fits for various transport properties such as fluid viscosity. The property fits are those used in the TRAC code (Ref (L4)) and the THERMIT code (Ref (K3)). The fits can be found in subroutines THERM and PRMPRO in the code listing given in Appendix J.

The last element needed to ensure closure is a relationship between the vapor volume fraction,  $\langle \alpha \rangle$ , and the flow quality,  $x$ . As mentioned previously we use the drift flux model to satisfy this requirement. The drift flux

Table 3.5-2  
 Partial Derivatives Appearing in Equation 3.5-4.

Quantity	Expression*
$\left(\frac{\partial M_{TBC}}{\partial U_0}\right) \langle \alpha_r \rangle, p$	$\frac{V_{TB}^2 (1 - \gamma)}{[(\rho_0 - \bar{\rho}_r) \gamma \rho_0 + (1 - \gamma) \bar{\rho}_r]} - \frac{M_{TBC} \bar{\rho}_r}{\rho_0 (\rho_0 - \bar{\rho}_r)} \left(\frac{\partial \rho_0}{\partial U_0}\right) p$
$\left(\frac{\partial M_{TBL}}{\partial \langle \alpha_r \rangle}\right) U_0, p$	$\frac{\rho_0}{\rho_0 - \bar{\rho}_r} \left(\frac{M_{TBC}}{\bar{\rho}_r} - v_{TB}\right) + \frac{V_{TB}^2 \gamma}{(\rho_0 - \bar{\rho}_r) [\gamma \rho_0 + (1 - \gamma) \bar{\rho}_r]} \left(\frac{\partial \rho_r}{\partial p}\right) \langle \alpha_p \rangle$
$\left(\frac{\partial M_{TBC}}{\partial p}\right) \langle \alpha_r \rangle, U_0$	$\frac{\left(\frac{\partial M_{TBC}}{\partial U_0}\right) \langle \alpha_r \rangle, p}{\left(\frac{\partial \rho_0}{\partial U_0}\right) p} + \frac{\left(\frac{\partial M_{TBC}}{\partial \langle \alpha_r \rangle}\right) U_0, p}{\left(\frac{\partial \rho_r}{\partial p}\right) \langle \alpha_r \rangle} + \frac{\left(\frac{\partial M_{TBC}}{\partial p}\right) U_0, p}{\left(\frac{\partial \rho_r}{\partial \langle \alpha_r \rangle}\right) p}$

$$*\gamma = \frac{L_p}{L_{TB}}$$

Table 3.5-3  
Secondary Side Unknowns.

Symbol	Definition
$U_0$	Internal energy of subcooled fluid
$V_v$	Volume of vapor in saturated region
$\langle \alpha_r \rangle$	Vapor volume fraction at tube bundle outlet
$\langle \alpha_n \rangle$	Vapor volume fraction at riser outlet
$p$	System pressure
$\bar{W}$	Geometrically averaged flowrate
$W_0$	Downcomer flowrate
$W_p$	Flowrate at parallel-to-crossflow interface
$W_r$	Tube bundle exit flowrate
$W_n$	Riser exit flowrate
$W_f$	Flowrate of sub-liquid from Saturated to subcooled region

model is derived in Appendix A, and the various empirical parameters needed to use this model are discussed in Appendix C.

### 3.6 MAIN STEAM AND FEEDWATER SYSTEM MODELS

Control actions initiated in the main steam and feedwater systems can have profound effects on steam generator performance. The operation of these systems is usually

Table 3.5-4  
Secondary Side Equations.

Conservation Equation	Equation Number In Text
Tube Bundle Mass	3.1-1
Tube Bundle Energy	3.1-13
Riser Mass	3.2-1
Riser Energy	3.2-8
Saturated Region Mass	3.3-1 or 3.3-18
Saturated Region Energy	3.3-10 or 3.3-27
Subcooled Region Mass	3.3-6 or 3.3-19
Subcooled Region Energy	3.3-11 or 3.3-29
Momentum	3.4-1
Definition of $\bar{W}$	3.4-9
Tube Bundle Cross-flow Region Mass	3.5-4

automatic and is governed by sensor signals concerning such quantities as steam pressure, steam generator water level, primary average temperature, trip alarms, steam flowrate, and feedwater flowrate. The net result of control actions taken in the main steam and feedwater systems is a change in steam flowrate and/or feedwater flowrate. Both of these flowrates are boundary conditions for our model and are

required as input to the computer program. As an alternative to directly inputting the steam and feedwater flowrates we provide simple models of the main steam and feedwater systems to calculate these flowrates given the system operating conditions.

The feedwater system itself is not modeled since this would require accounting for feedwater heaters, pumps and valves, which is beyond the scope of this work. We simply model the control actions of a three-element feedwater flowrate controller. This three-element controller monitors the steam flowrate, the feedwater flowrate, and the steam generator water level, and generates a feedwater flowrate demand signal. The demand signal consists of components due to a steam flow-feed flow mismatch error and a level error, where the level error is the difference between the desired level and the measured level. This control scheme is represented by the following differential equation:

$$\frac{dW_{fw}}{dt} = C_w(W_s - W_{fw}) + C_l(l^* - l_w) \quad (3.6-1)$$

where  $C_w$  and  $C_l$  are controller parameters that must be determined for each plant, and  $l^*$  is the desired level.

The main steam system accomplishes its control functions by the opening and closing of valves. Therefore, the major component model for this system is a valve model.



There are generally four sets of valves that discharge steam from the main steam system. They are:

- 1.) steam dump valves discharging to the atmosphere;
- 2.) bypass valves diverting steam to the condenser;
- 3.) turbine stop and control valves which regulate steam flow to the turbine; and
- 4.) secondary safety relief valves.

The steam dump, bypass and secondary relief valves discharge steam at a much lower pressure than that in the main steam system. Hence, it is reasonable to assume that the flow through these valves is choked and can be simulated using a critical flow model. This is not necessarily the case for the turbine stop and control valves. Nonetheless, the assumption of choked flow through the stop and control valves is commonly used and will be applied here. Dry steam at high pressure behaves very much like an ideal gas so critical flow equations derived for an ideal gas can be used to model choking in steam systems. The flowrate of an ideal gas in critical flow is given by:

$$W_s = K_s p / \sqrt{T} \quad (3.6-2)$$

where the valve flow constant,  $K_s$ , is a function of flow area, gas specific heat ratio, gas atomic mass, and the

universal gas constant. We use Eq. (3.6-2) to determine the steam flowrate through the valves of the main steam system.

The valve flow constant for the fully opened valve can be obtained from the rated valve capacity and is denoted by the additional subscript 0 i.e.  $K_{S0}$ . The valve capacity is given in terms of a flowrate at a specified pressure, and, since the steam is saturated, once we know the steam pressure we also know its temperature. Thus, Eq. (3.6-2) can be solved for  $K_{S0}$ . The value of the valve constant,  $K_S$ , for other valve openings is directly proportional to the valve flow area at that opening divided by the maximum valve flow area. Therefore:

$$\begin{aligned} W_s &= \left( \frac{A}{A_{MAX}} \right) K_{S0} p / \sqrt{T} & (3.6-3) \\ &= f_v p / \sqrt{T} \end{aligned}$$

where  $f_v$  is the fractional valve opening. Given the fractional valve opening and the pressure we can use Eq. (3.6-3) to determine the valve flowrate.

The way in which the steam dump and bypass systems operate varies from plant to plant. We will describe here the operation of these systems for the Maine Yankee Nuclear Power Plant (Ref. (C-2)). The steam dump valves open only after a turbine trip. Once opened by a turbine trip signal, the dump valve opening is controlled by a reactor coolant

temperature error signal. This error signal is the steam generator average primary temperature minus the zero load reference temperature. The rate at which the dump valves open following a trip is governed by the magnitude of the temperature error signal (Fig. 3.6-1). The valves open rapidly to their fully open position when the temperature error signal at the time of the trip is larger than a pre-specified amount,  $\Delta T_{Fast}$ . If the temperature error signal at the time of the trip is less than a minimum temperature difference,  $\Delta T_{min}$ , then the dump valves will not open until the temperature error signal reaches  $\Delta T_{min}$ . If the temperature error signal is within the range of  $\Delta T_{min}$  to  $\Delta T_{Fast}$ , then the dump valves are opened at normal speed to a proportional position as shown in Figure 3.6-1. Once the dump valves are opened they are modulated by the reactor coolant temperature error signal (Figure 3.6-1). When the error signal is less than  $\Delta T_{Close}$  the valves are fully closed, thereby ensuring that steam is not continuously bled from the system as the plant approaches zero load. Once the valves are closed a temperature error signal greater than  $\Delta T_{min}$  is required to reopen them.

The bypass system operates to maintain the secondary pressure at or below the zero load steam pressure. After a turbine trip the bypass valves open rapidly. Once open, the steam bypass system receives the higher of the dump system temperature error signal and a secondary pressure signal.

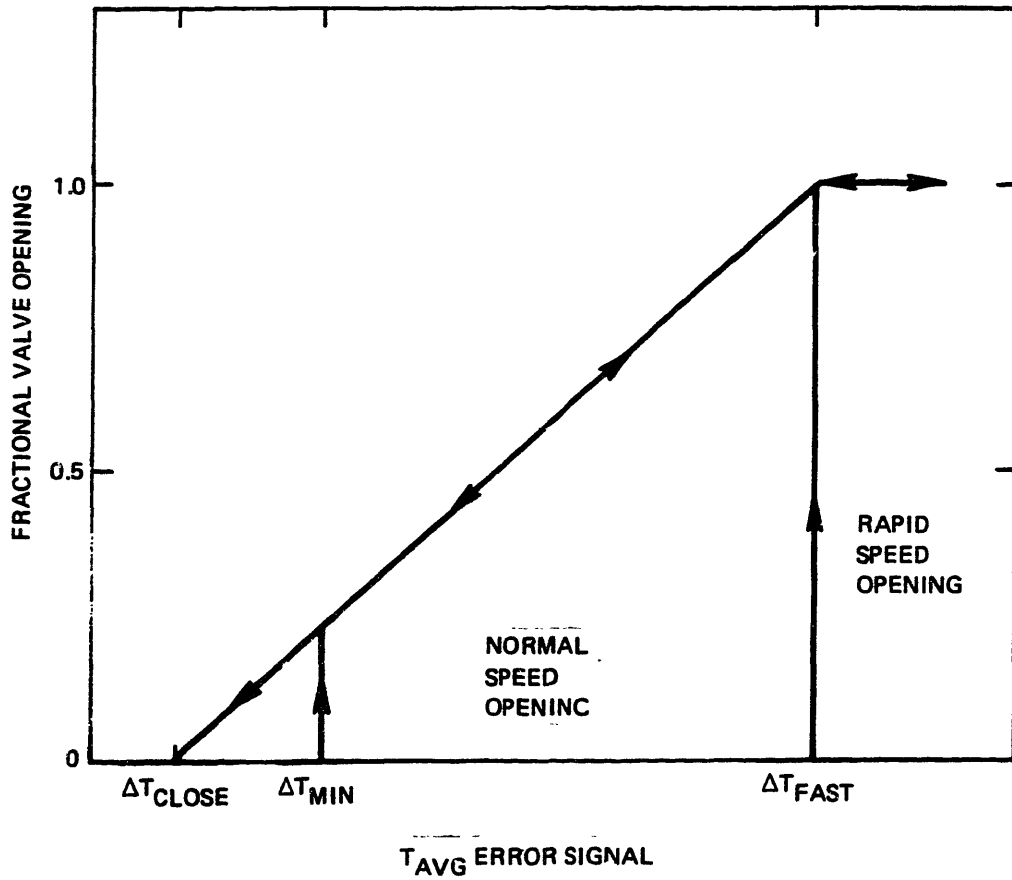


Figure 3.6-1. Steam dump valve control program (Ref. (C2)).

As hot standby is approached, the bypass valves are positioned to maintain the secondary pressure at the zero load pressure and the reactor coolant temperature near the zero power level value.

The secondary safety relief valves provide overpressure protection for the shell side of the steam generator. This system for the Maine Yankee plant consists of four banks of valves, each bank having its own set-point. The steam flow through these valves is choked and can be modeled by using Eq. (3.6-3).

The turbine stop and control valve is modeled using a critical flow equation (Eq. (3.6-3)). The model allows the user to input the time at which turbine trip occurs, as well as the valve closing time, and when the trip time is reached in the simulation the computer code automatically starts closing the stop valve. In addition, we can also simulate load maneuvering by specifying the percent full power valve position as a function of time in tabular form.

We should emphasize here that the main stream system described above is characteristic of the Maine Yankee Plant. Other plants may or may not have the same operational characteristics.

### 3.7 DISCUSSION OF MODEL

The preceding sections define in detail the steam generator secondary side model. It is now worthwhile to summarize the limitations on the use of the model. The model

cannot be used to simulate situations where flow reversal can occur, since we implicitly assume that the flow is in one direction only. We also assume that natural circulation flow is always maintained. Therefore, cases in which a breakdown in the natural circulation flow (i.e. riser exit quality greater than or equal to 1.0) cannot be treated by using this model. Finally, the model is not valid for transients in which there is significant amount of boiling in the downcomer.

## Chapter 4

### PRIMARY SIDE MODEL

The model of the primary side of the steam generator consists of three model regions:

- 1.) The primary inlet plenum;
- 2.) The primary fluid volume contained within the tubes of the tube bundle; and,
- 3.) The primary outlet plenum.

In this chapter we develop a set of conservation equations for these regions. In addition, we develop the model used to determine the heat transfer from the primary coolant to the secondary fluid.

#### 4.1 PRIMARY FLUID SYSTEM

Modeling of the primary fluid system requires that we develop two component models. We need a model for the plenum and a model for the primary fluid in the tubes.

##### 4.1.1 Plenum Model

The one-dimensional conservation equations for the inlet plenum are (Appendix B):

$$\frac{dM_1}{dt} = W_{IN} - W_1 \quad (4.1-1)$$

$$\frac{dE_1}{dt} = W_{IN}H_{IN} - W_1H_1 \quad (4.1-2)$$

where the primary side nomenclature is defined in Fig. 4.1-1. Multiplying Eq. (4.1-1) by  $\frac{(H_1 + H_{IN})}{2}$  and subtracting the result from Eq. (4.1-2) yields:

$$\frac{dE_1}{dt} - \frac{(H_1 + H_{IN})}{2} \frac{dM_1}{dt} = \frac{(W_{IN} + W_1)}{2} (H_{IN} - H_1) \quad (4.1-3)$$

In order to evaluate  $M_1$  and  $E_1$  we invoke the instantaneous, perfect mixing assumption, which is justified since the transport time in either the inlet or outlet plenum is short compared to the time span of transients of interest to us (Table 4.1-1).

Table 4.1-1  
Representative Primary Side Transport Times

Region	Transport Time* (s)
Plenum	0.67
Tubes	2.73

\* Transport time =  $\int \rho dV/W$



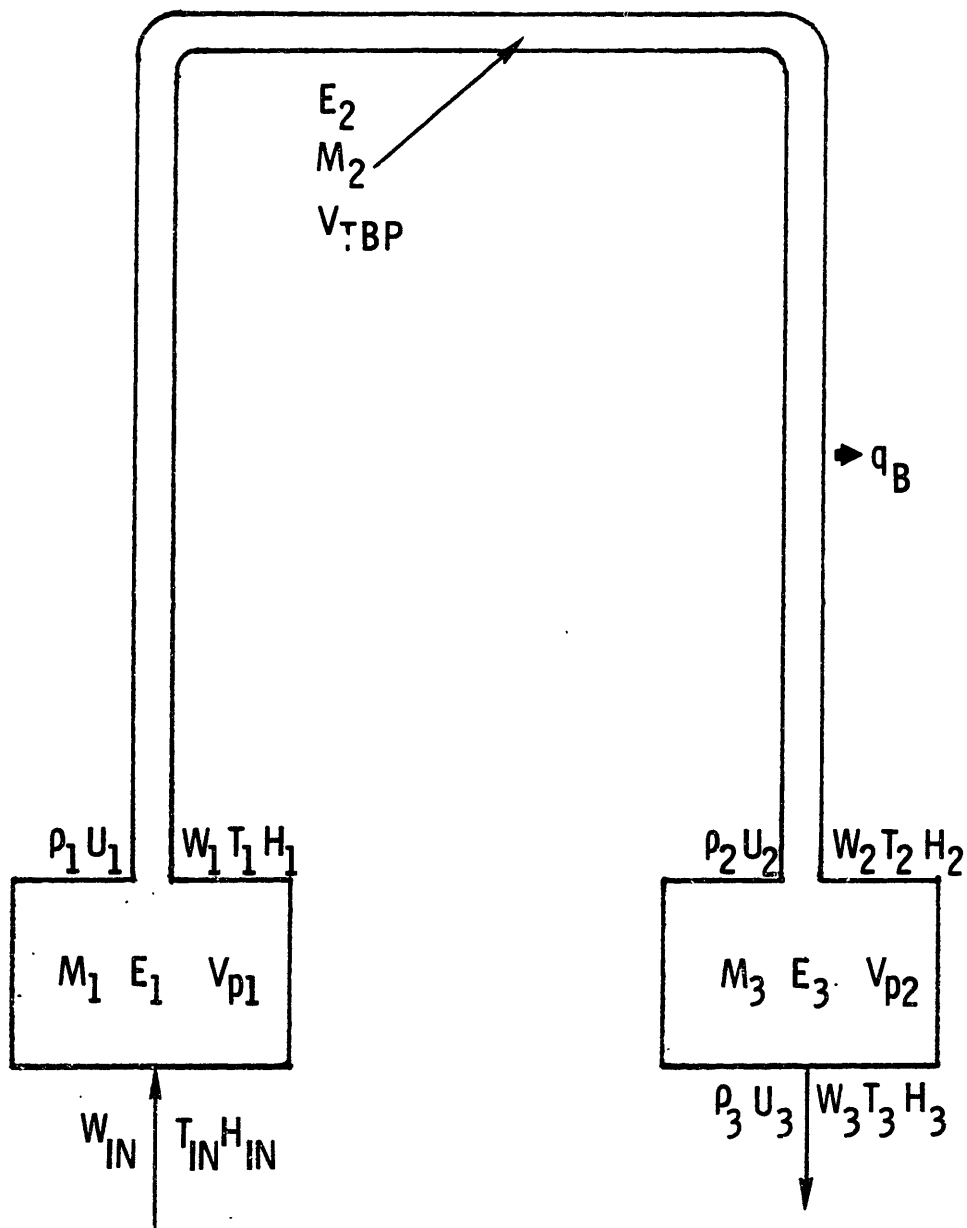


Figure 4.1-1. Primary side nomenclature.

Thus:

$$M_1 = \int_0^{V_{p1}} \rho \, dV = \rho_1 V_{p1} \quad (4.1-4a)$$

and,

$$E_1 = \int_0^{V_{p1}} \rho U_1 \, dV = \rho_1 U_1 V_{p1} \quad (4.1-4b)$$

For a subcooled fluid we need two thermodynamic properties in order to specify its thermodynamic state. Since the pressure dependence of properties for a fluid in a highly subcooled state is weak we will neglect the pressure derivatives of the primary fluid properties and assume that the pressure is either a known function of time or constant. This leaves us with one state variable, which we will take to be fluid temperature. Thus:

$$\frac{dM_1}{dt} = V_{p1} \left( \frac{d\rho_1}{dT_1} \right) \frac{dT_1}{dt} \quad (4.1-5a)$$

and

$$\frac{dE_1}{dt} = v_{p1} \left[ \rho_1 \left( \frac{\partial U_1}{\partial T_1} \right)_p + U_1 \left( \frac{\partial \rho_1}{\partial T_1} \right)_p \right] \frac{dT_1}{dt} \quad (4.1-5b)$$

Substituting Eqs. (4.1-5) into Eq. (4.1-3) gives:

$$C_1 \frac{dT_1}{dt} = \frac{(W_{IN} + W_1)}{2} (H_{IN} - H_1)$$

where,

$$C_1 = v_{p1} \left[ \rho_1 \left( \frac{\partial U_1}{\partial T_1} \right)_p + \left( U_1 - \frac{(H_1 + H_{IN})}{2} \right) \left( \frac{\partial \rho_1}{\partial T_1} \right)_p \right]$$

We will further assume that the flowrate throughout the primary portion of the steam generator is spatially constant, but that changes in the primary inlet flow are felt instantaneously at all points in the primary flow path. This assumption allows us to ignore the conservation of mass equation (Eq. (4.1-1)), leaving us the following equation as the sole conservation equation for the inlet plenum.

$$C_1 \frac{dT_1}{dt} = W_{IN} (H_{IN} - H_1) \quad (4.1-6)$$

The conservation equation for the outlet plenum is derived in an analogous manner, which yields:

$$C_3 \frac{dT_3}{dt} = W_{IN}(H_2 - H_3) \quad (4.1-7)$$

where

$$C_3 = v_{p2} \left[ \rho_3 \left( \frac{\partial U_3}{\partial T_3} \right)_p + \left[ U_3 - \frac{(H_2 + H_3)}{2} \right] \left( \frac{\partial \rho_3}{\partial T_3} \right)_p \right]$$

Note that the primary inlet flowrate  $W_{IN}$ , appears in Eq. (4.1-7) since we have assumed a spatially constant primary flowrate.

#### 4.1.2 Tubeside Model

The conservation equations for the primary fluid within the tubes of the tube bundle are:

$$\frac{dM_2}{dt} = W_1 - W_2 \quad (4.1-8)$$

$$\frac{dE_2}{dt} = W_1 H_1 - W_2 H_2 - q_B \quad (4.1-9)$$

Multiplying Eq. (4.1-8) by  $\frac{(H_1 + H_2)}{2}$  and subtracting the result from Eq. (4.1-9) yields:

$$\frac{dE_2}{dt} - \frac{(H_1 + H_2)}{2} \frac{dM_2}{dt} = \frac{(W_1 + W_2)}{2} (H_1 - H_2) - q_B$$

(4.1-10)

We will evaluate  $M_2$  and  $E_2$  by using the instantaneous, perfect mixing assumption. This assumption can be justified, to some extent, by the fact that the transport time through the tubes is short relative to the length of transients of interest to us. This assumption does, however, tend to deviate from reality when calculating energy transport. That is, tube outlet temperatures calculated using this assumption tend to respond to transient perturbations faster than they would in reality. In particular, during a primary flow coastdown, when the tube transport time becomes long, characterizing the tube region temperature by the tube outlet temperature is inappropriate and leads to difficulties in calculating the heat transfer rate. In section 4.2.3 we develop a method to deal with this special situation.

The instantaneous, perfect mixing assumption is useful for two reasons. First, it is easy to apply to Eq. (4.1-10) without loss of physical plausibility. Second, it has desirable properties from a numerical standpoint (see Appendix F). Thus we will retain this assumption despite the shortcomings mentioned previously. The mass and energy content of the tubes are then given by:

$$M_2 = \int_0^{V_{TBP}} \rho \, dV = \rho_2 V_{TBP} \quad (4.1-11a)$$

and

$$E_2 = \int_0^{V_{TBP}} \rho U \, dV = \rho_2 U_2 V_{TBP} \quad (4.1-11b)$$

As stated in the development of the plenum model, we will neglect the pressure derivatives of the primary fluid properties, so that we deal only with temperature derivatives. Therefore:

$$\frac{dM_2}{dt} = V_{TBP} \left( \frac{\partial \rho_2}{\partial T_2} \right)_p \frac{dT_2}{dt} \quad (4.1-12a)$$

and

$$\frac{dE_2}{dt} = V_{TBP} \left[ \rho_2 \left( \frac{\partial U_2}{\partial T_2} \right)_p + U_2 \left( \frac{\partial \rho_2}{\partial T_2} \right)_p \right] \frac{dT_2}{dt} \quad (4.1-12b)$$

Since the primary flowrate is assumed to be constant, Eq. (4.1-10) becomes:

$$C_2 \frac{dT_2}{dt} = W_{IN}(H_1 - H_2) - q_B \quad (4.1-13)$$

where,

$$C_2 = V_{TBP} \left[ \rho_2 \left( \frac{\partial U_2}{\partial T_2} \right)_p + \left[ U_2 - \frac{(H_1 + H_2)}{2} \right] \left( \frac{\partial \rho_2}{\partial T_2} \right)_p \right]$$

Eqs. (4.1-6), (4.1-7), and (4.1-13) comprise our primary fluid system model. By assuming a spatially constant flowrate we have essentially reduced the problem to one of determining energy transport and have thereby obviated any need for the mass conservation equations.

#### 4.2 HEAT TRANSFER MODEL

The primary to secondary heat transfer occurs primarily through three mechanisms:

- 1.) single-phase forced convection heat transfer from primary fluid to tube inner wall;
- 2.) conduction heat transfer through the tube metal; and,
- 3.) boiling heat transfer from tube outer wall to secondary fluid.

This situation is illustrated in Fig. 4.2-1. In this section we develop the heat transfer model. Details regarding heat transfer correlations can be found in Appendix C.

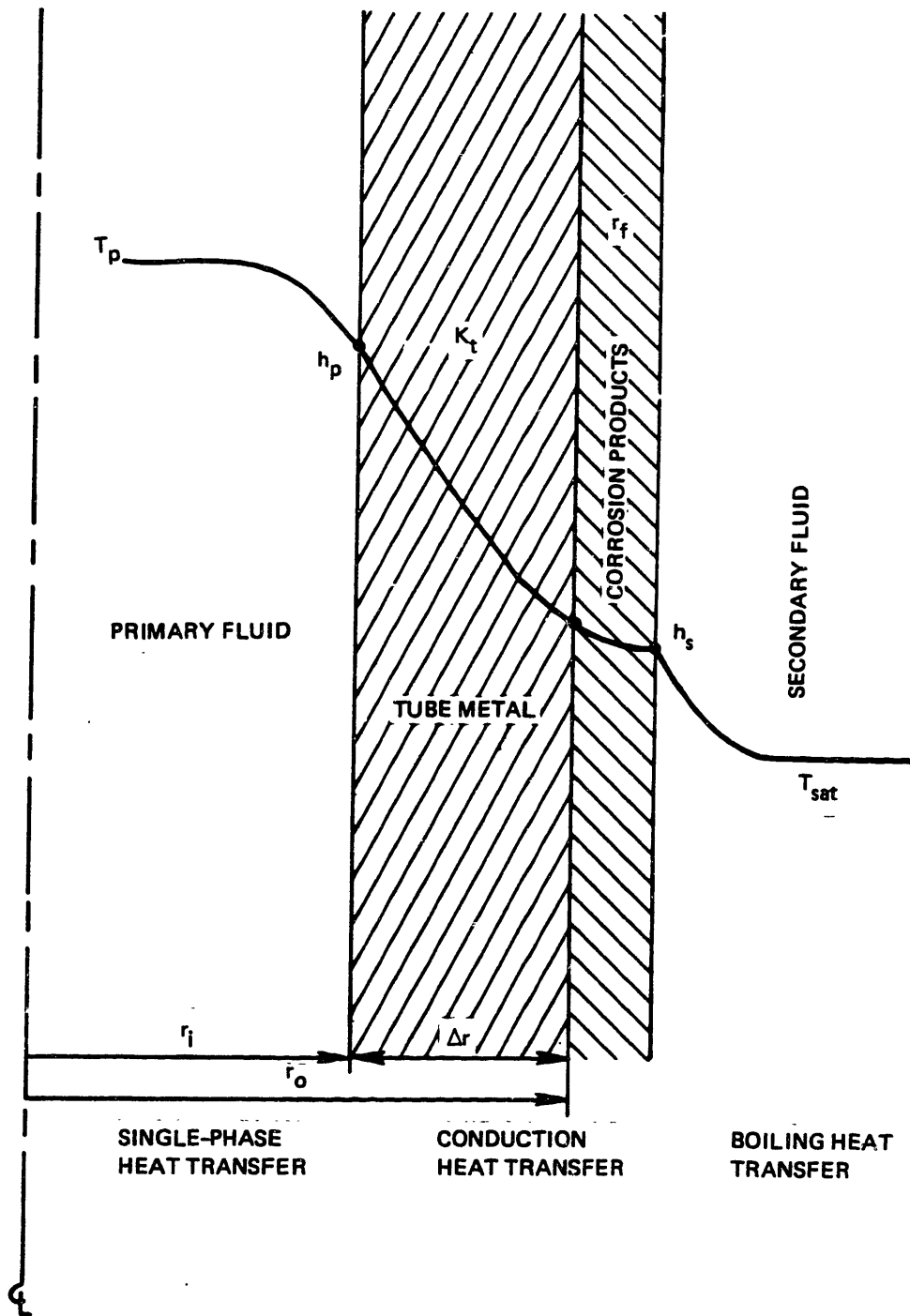


Figure 4.2-1. Heat transfer mechanisms.



#### 4.2.1 Tube Metal Conduction

The heat conduction equation is (Ref (B2)):

$$\rho_t C_{pt} \frac{\partial T_t}{\partial t} = \nabla \cdot k_t \nabla T_t$$

Assuming that heat conduction is significant only in the radial direction of a cylindrical geometry, and assuming that the thermal conductivity is constant yields:

$$\rho_t C_{pt} \frac{\partial T_t}{\partial t} = \frac{K_t}{r} \frac{\partial}{\partial r} \left( \frac{r \partial T_t}{\partial r} \right) \quad (4.2-1)$$

Equation (4.2-1), along with appropriate boundary conditions, is the formal equation we should solve to determine the heat transfer rate. We would like to avoid solving this equation in the interests of computational speed and efficiency. One way to do this is to use a technique which is analogous to a lumped parameter approach. This technique will now be described.

Since the tube wall is thin we can approximate Eq. (4.2-1) by its rectangular coordinate analogue:

$$\rho_t C_{pt} \frac{\partial T_t}{\partial t} = K_t \frac{\partial^2 T_t}{\partial x^2} \quad (4.2-2)$$

where the coordinate  $x$  replaces the radial coordinate of Eq. (4.2-1). The steady state solution of Eq. (4.2-2) is:

$$T_t = \left( \frac{T_0 - T_i}{r_0 - r_i} \right) (x - r_i) + T_i \quad (4.2-3)$$

where the nomenclature is defined by Fig. 4.2-2. Clearly this temperature profile is linear. If the response of the tube metal temperature to transient perturbations is fast, we can assume that the tube metal temperature retains a linear profile during transients. Thus, the energy stored per unit volume of tube metal is given by:

$$\frac{E_{\text{tube}}}{V_{\text{TM}}} = \rho_t C_{\text{pt}} \frac{(T_i + T_0)}{2} \quad (4.2-4)$$

For constant tube metal properties the energy storage rate per unit volume becomes:

$$\frac{1}{V_{\text{TM}}} \frac{dE_t}{dt} = \frac{\rho_t C_{\text{pt}}}{2} \left( \frac{dT_0}{dt} + \frac{dT_i}{dt} \right) \quad (4.2-5)$$

Eq. (4.2-5) is basically the left hand side of Eq. (4.2-2). Finally, if we assume that  $(T_2 + T_{\text{SAT}})/2$  is approximately equal to  $(T_0 + T_i)/2$ , then Eq. (4.2-5) becomes:

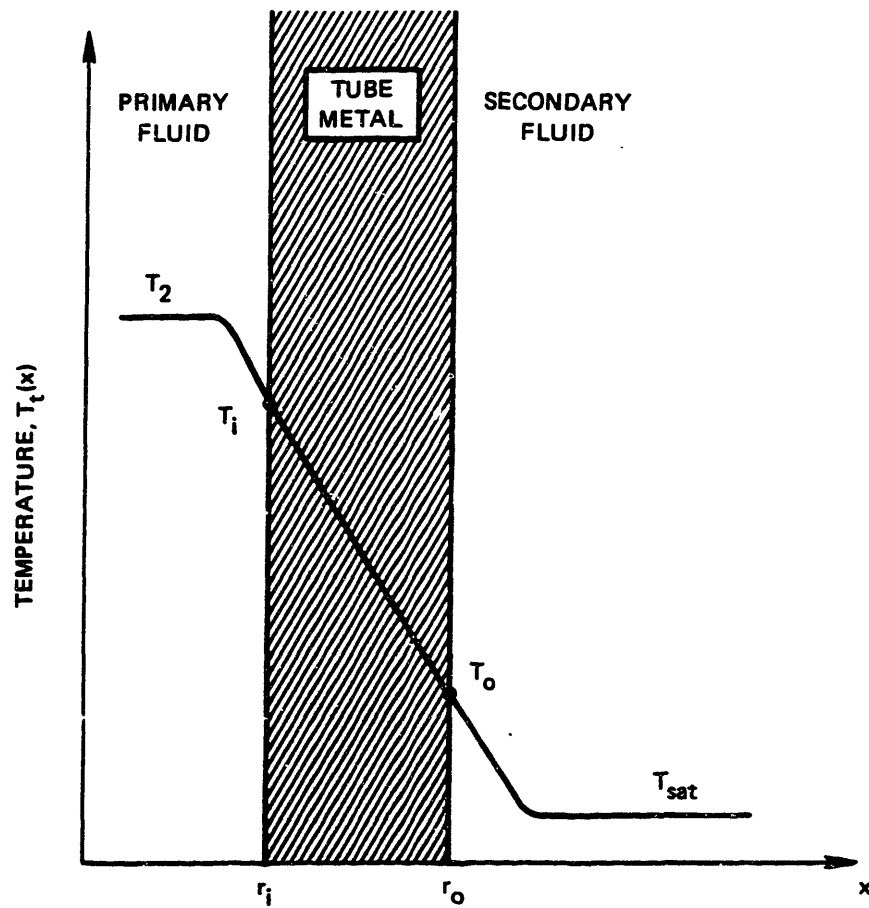


Figure 4.2-2. Nomenclature for equation 4.2-3.

$$\frac{1}{V_{TM}} \frac{dE_t}{dt} = \frac{\rho_t C_{pt}}{2} \left( \frac{dT_0}{dt} + \frac{dT_{SAT}}{dt} \right) \quad (4.2-6)$$

Eq. (4.2-6) suggests a method which we can use to account for energy storage in the tube metal without solving the conduction equation. We can simply lump half the tube metal heat capacity in the primary side tube fluid energy equation and the other half in the secondary side tube bundle energy equation. Thus, the coefficient  $C_2$  in Eq. (4.1-13) becomes:

$$C_2 = V_{TBP} \left[ \rho_2 \left( \frac{\partial U_2}{\partial T_2} \right)_p + \left[ U_2 - \frac{(H_1 + H_2)}{2} \right] \left( \frac{\partial \rho_2}{\partial T_2} \right)_p \right] + \frac{V_{TM} \rho_T C_{pt}}{2} \quad (4.2-7)$$

and the coefficient  $B_3$  in Eq. (3.1-13) becomes:

$$B_3 = \left( \frac{\partial E_{TB}}{\partial p} \right)_{\langle \alpha_r \rangle, U_0} - H_r \left( \frac{\partial M_{TB}}{\partial p} \right)_{\langle \alpha_r \rangle, U_0} + \frac{V_{TM} \rho_t C_{pt}}{2} \frac{dT_{SAT}}{dp} \quad (4.2-8)$$

The overall heat transfer rate,  $q_B$ , is then calculated using a log mean temperature difference, as discussed in Section 4.2.3.

### 4.2.2 Tube Metal Temperature Response

An essential assumption made in the derivation appearing above is that the response of the tube metal temperature to transient perturbations is fast. We can justify this assumption by performing a simple calculation for the system shown in Fig. 4.2-3. This system consists of an infinite slab of metal surrounded by a fluid at a uniform temperature. The fluid temperature is increasing in a ramp manner such that the metal temperature reaches and maintains an asymptotic shape with a continuously increasing magnitude. The temperature time derivative at all points in the metal region is then given by:

$$\frac{\partial T}{\partial t}(x, t) = a$$

where  $a$  is constant.

The one-dimensional conduction equation for this system is:

$$\rho C_p \frac{\partial T}{\partial t}(x, t) = K \frac{\partial^2 T(x, t)}{\partial x^2}$$

or,

$$K \frac{\partial^2 T(x, t)}{\partial x^2} = \rho C_p a$$

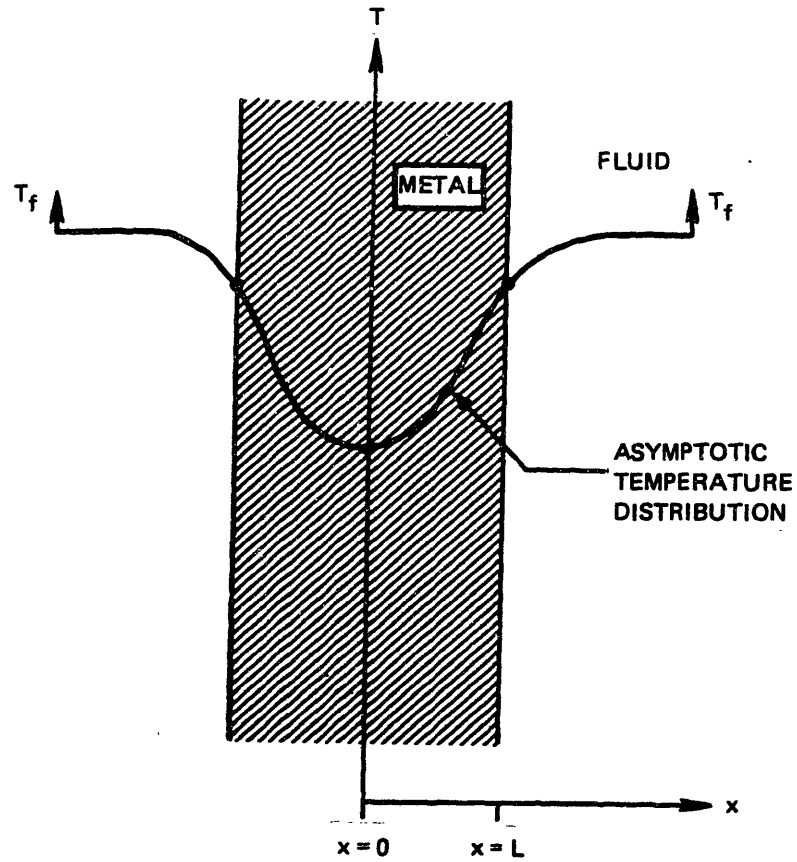


Figure 4.2-3. System for calculation of temperature response time.

subject to the boundary conditions:

$$\frac{\partial T(0,t)}{\partial x} = 0 \text{ and } K \frac{\partial T}{\partial x} (L,t) = h(T_f(t) - T(L,t))$$

The solution to this equation is:

$$T(x,t) = \frac{\rho C_p a}{2K} x^2 + T_f - \rho C_p a L \left[ \frac{1}{h} + \frac{L}{2K} \right] \quad (4.2-9)$$

We can define the time constant,  $\tau$ , for the metal temperature response as:

$$\tau = \frac{T_f(t) - T(0,t)}{a} \quad (4.2-10)$$

Equation (4.2-10) simply defines the time span by which the metal center-line temperature lags the fluid temperature. Substituting Eq. (4.2-9) into Eq. (4.2-10) yields:

$$\tau = \rho C_p L \left[ \frac{1}{h} + \frac{L}{2K} \right] \quad (4.2-11)$$

Table 4.2-1 lists some representative numbers for the quantities appearing in Eq. (4.2-11). Using these numbers yields:

Table 4.2-1  
Representative Steam Generator Parameters

Quantity	Value
$\rho_t C_{pt}$	4.1338 MJ/m <sup>3</sup> - °C
$K_t$	18.6005 W/m - °C
h	$3.2671 \cdot 10^4$ W/m <sup>2</sup> - °C
L	$6.0 \cdot 10^{-4}$ m

$$\tau = 0.12s$$

This is indeed a relatively fast response time compared to other characteristic times for the steam generator (i.e. transport times) and, therefore, justifies our assumption that the tube metal temperature response to transient perturbations is fast.



### 4.2.3 Overall Heat Transfer

The overall heat transfer,  $q_B$ , is calculated using the log-mean temperature difference and the overall heat transfer coefficient (Ref. (H2)). That is:

$$q_B = U_0 A_0 \Delta T_{LM} \quad (4.2-12)$$

where,

$\Delta T_{LM} \equiv$  log-mean temperature difference

$$\equiv \frac{T_1 - T_2}{\ln \left( \frac{T_1 - T_{SAT}}{T_2 - T_{SAT}} \right)} ;$$

$A_0 \equiv$  total outside surface area of tubes; and,

$U_0 \equiv$  overall heat transfer coefficient based on outside surface area of tubes.

The derivation of log-mean temperature difference is valid for steady state heat transfer involving fluids with constant specific heats. Extension of this formulation to transient calculations is, perhaps, questionable. However, the log-mean temperature difference is based on an exponential temperature profile along the tube length, and since the transport time for the primary fluid in the tubes is short relative to the time span of transients of interest to us, we can assume that we maintain temperature profiles similar to the steady state profile. The log-mean temperature difference defined in Eq. (4.2-12) is based on the heat

sink being uniformly at the saturation temperature. This is not quite the case in reality since there is some subcooled fluid located near the inlet to the tube bundle, so the log-mean temperature difference is actually greater than that obtained using the saturation temperature for the secondary side fluid. Using our expression for the log-mean temperature difference will result in our calculating too low a heat transfer rate. But, as is shown in Chapter 3, the majority of the tube bundle region is in either subcooled or saturated nucleate boiling, which is a more efficient mode of heat transfer than forced convection. Since we use a secondary side heat transfer coefficient for nucleate boiling in evaluating the overall heat transfer coefficient (see Appendix C), we will obtain a value of  $U_0$  that is larger than it should be. This offsets, to some extent, the low log-mean temperature difference that we calculate using Eq. (4.2-12). Further discussion of the overall heat transfer coefficient,  $U_0$ , and correlations related to it can be found in Appendix C.

There are situations where using the log-mean temperature difference to calculate the heat transfer rate is inappropriate. We can envision a transient in which the primary flow coasts down while the secondary pressure undergoes a fairly rapid increase. For this case, our primary fluid system model using the instantaneous, perfect mixing assumption for the fluid in the tubes does not do a good job in simulating energy transport since the fluid transport time

is long. In addition, since the primary flowrate is small and the secondary pressure is increasing quickly, we can have a temporary situation where the tube outlet temperature is below the secondary saturation temperature. When this occurs, the log-mean temperature difference is undefined and we must seek another method to calculate the heat transfer rate.

The transition from the log-mean temperature difference method for obtaining the heat transfer rate to the alternative method used in the special case mentioned in the preceding paragraph must be smooth. A method that satisfies this criterion will now be developed.

The first step in developing this alternate heat transfer model is to define at what point we switch from the log-mean temperature difference approach. We define this transition point to correspond to the time when the tube outlet temperature,  $T_2$ , reaches a value that is  $\epsilon$  degrees above the prevailing secondary saturation temperature. We denote the log-mean temperature difference for this particular point by  $\Delta T_{LM}^*$ , which is given by:

$$\Delta T_{LM}^* = \frac{T_1 - T_2 - \epsilon}{\ln \left( \frac{T_1 - T_{SAT}}{\epsilon} \right)} \quad (4.2-13)$$

The primary fluid temperature distribution corresponding to Eq. (4.2-13) is shown in Fig. 4.2-4. We represent this

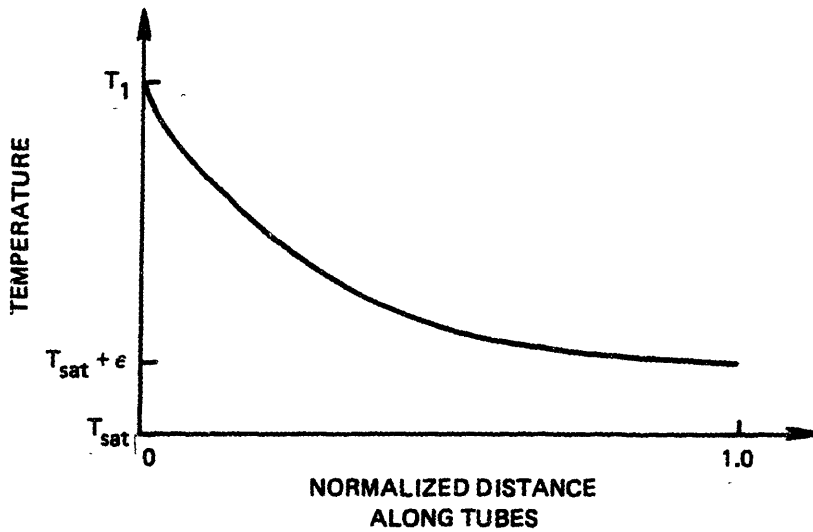


Figure 4.2-4. Primary temperature distribution at heat transfer calculation transition.

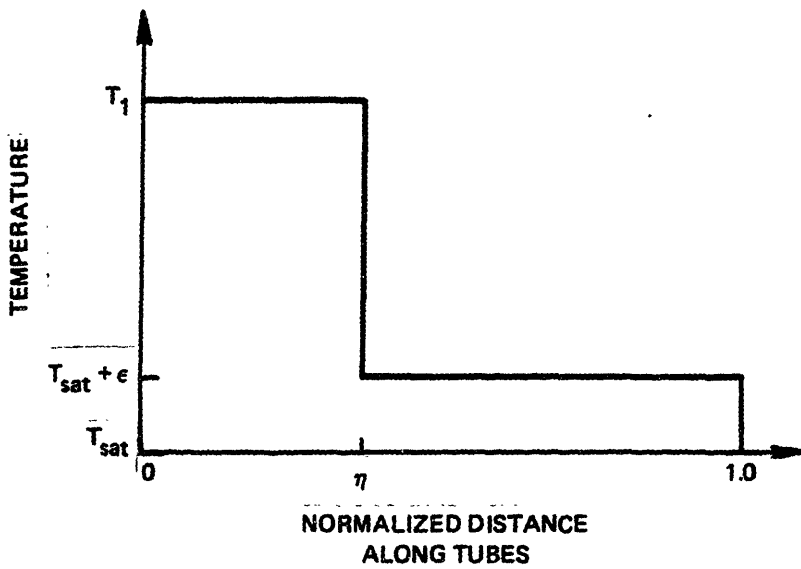


Figure 4.2-5. Histogram representation of profile shown in Figure 4.2-4.

profile by an equivalent histogram-like temperature distribution as shown in Fig. 4.2-5. We then define a weighting factor,  $\eta$ , such that:

$$\eta(T_1 - T_{SAT}) + (1 - \eta)\epsilon = \Delta T_{LM}^* \quad (4.2-14)$$

We now define the following average temperature difference:

$$\Delta \bar{T} = \eta(T_1 - T_{SAT}) + (1 - \eta)(T_2 - T_{SAT}) \quad (4.2-15)$$

with the heat transfer rate given by:

$$q_B = U_0 A_0 \Delta \bar{T} \quad (4.2-16)$$

Equation (4.2-16) is exact when  $T_2$  is equal to  $T_{SAT} + \epsilon$ . If we assume that we can use Eqs. (4.2-13) through (4.2-16) when  $T_2$  is less than  $T_{SAT} + \epsilon$ , then we can use this method to calculate the heat transfer rate for situations such as the one illustrated in Fig. 4.2-6. The calculational scheme is as follows:

- 1.) Find the weighting factor,  $\eta$ , using Eqs. (4.2-13) and (4.2-14);
- 2.) Use this value of  $\eta$  in Eq. (4.2-15) to calculate  $\Delta \bar{T}$ ; and,
- 3.) Calculate  $q_B$  using Eq. (4.2-16).

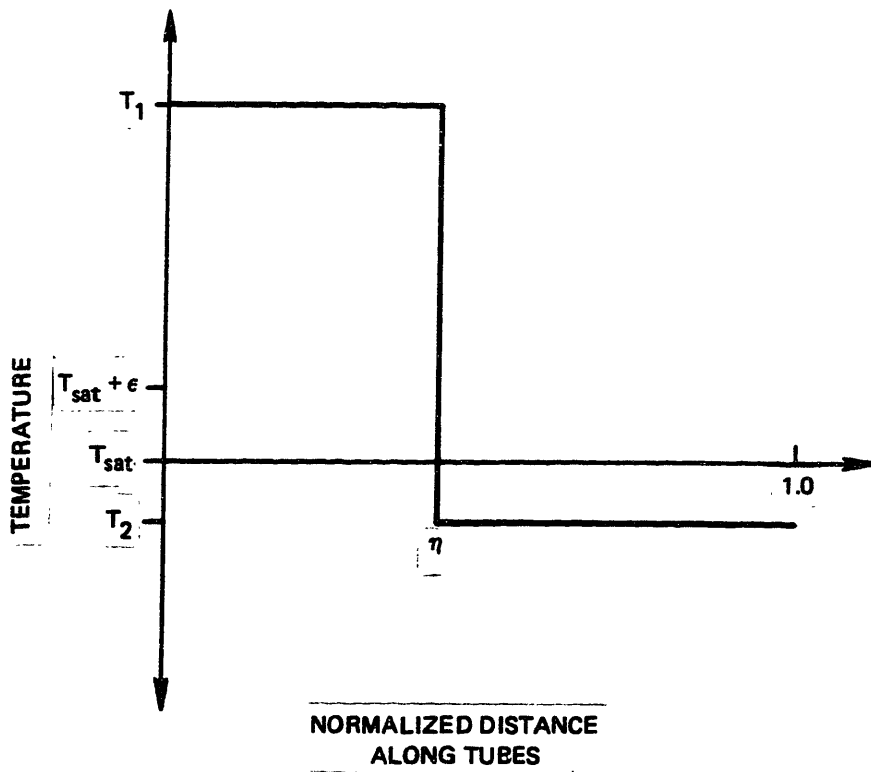


Figure 4.2-6. Generalized histogram representation of temperature profile.

Note that this scheme results in a continuous transition since Eqs. (4.2-13) through (4.2-16) reduce to Eq. (4.2-12) when  $T_2$  is equal to  $T_{SAT} + \epsilon$ .

There are several comments regarding this alternate heat transfer calculation. First, it is based on the assumption that we can extend the exact histogram representation to situations where  $T_2$  is not equal to  $T_{SAT} + \epsilon$ . This assumption is difficult to justify; however, situations where we make use of the alternate heat transfer calculational scheme are rare and of short duration. Second, this alternate method allows us to "ride through" transients which we would not be able to simulate otherwise.

## Chapter 5

### NUMERICAL SOLUTION

In this chapter we discuss the formulation and implementation of a numerical scheme for solving the model equations given in Chapters 3 and 4. A brief, but illuminating, discussion of solution techniques for ordinary differential equations may be found in Reference (H3).

#### 5.1 EQUATION SYSTEM

We have developed a set of equations which can be broken down into two subsets. One subset is comprised of the primary fluid system equations, while the second set consists of the secondary side equations. We will deal with each subset individually.

##### 5.1.1 Primary Side Equations

For the primary fluid system model we have a set of three differential equations in three unknowns. This set of equations can be written compactly as:

$$\underline{\underline{C}} \dot{\underline{T}} = \underline{g} \quad (5.1-1)$$



where,

$$\underline{\underline{C}} = \text{Diag}[C_1, C_2, C_3];$$

$$\underline{T} = \text{Col}[T_1, T_2, T_3]; \text{ and,}$$

$$\underline{g} = \text{Col}[W_{IN}(H_{IN} - H_1), W_{IN}(H_1 - H_2) - q_B, W_{IN}(H_2 - H_3)]$$

### 5.1.2 Secondary Side Equations

The secondary side equations consist of mass and energy conservation equations for each region of the steam generator as well as a loop momentum equation. Not all of these equations are differential equations; some are algebraic relationships. We will now derive and define the differential, or state, equations.

By manipulating the various individual region mass balances along with an overall mass balance for the steam generator, we obtain the following equations:

$$W_p = W_0 - \frac{dM_{TB}}{dt} + \frac{dM_{TBC}}{dt} \quad (5.1-2a)$$

$$W_r = W_0 - \frac{dM_{TB}}{dt} \quad (5.1-2b)$$

$$W_n = W_0 - \frac{dM_{TB}}{dt} - \frac{dM_R}{dt} \quad (5.1-2c)$$

Substituting these equations into the defining equation for  $\bar{W}$  (Eq. 3.4-9) and noting that  $\sum_{i=1}^4 \beta'_i = 1$  yields:

$$\bar{W} = W_0 + \beta'_2 \frac{dM_{TBC}}{dt} - (\beta'_2 + \beta'_3 + \beta'_4) \frac{dM_{TB}}{dt} - \beta'_4 \frac{dM_R}{dt}$$

or

$$\bar{W} = W_0 + E_1 \frac{dU_0}{dt} + E_2 \frac{d\langle \alpha_r \rangle}{dt} + E_3 \frac{d\langle \alpha_n \rangle}{dt} + E_4 \frac{dp}{dt} \quad (5.1-3)$$

where,

$$E_1 = \beta'_2 \left( \frac{\partial M_{TBC}}{\partial U_0} \right)_{p, \langle \alpha_r \rangle} - (\beta'_2 + \beta'_3 + \beta'_4) \left( \frac{\partial M_{TB}}{\partial U_0} \right)_{p, \langle \alpha_r \rangle}$$

$$E_2 = \beta'_2 \left( \frac{\partial M_{TBC}}{\partial \langle \alpha_r \rangle} \right)_{p, U_0} - (\beta'_2 + \beta'_3 + \beta'_4) \left( \frac{\partial M_{TB}}{\partial \langle \alpha_r \rangle} \right)_{p, U_0} \\ - \beta'_4 \left( \frac{\partial M_R}{\partial \langle \alpha_r \rangle} \right)_{p, \langle \alpha_n \rangle}$$

$$E_3 = -\beta'_4 \left( \frac{\partial M_R}{\partial \langle \alpha_n \rangle} \right)_{p, \langle \alpha_r \rangle}$$

and,

$$E_4 = \beta'_2 \left( \frac{\partial M_{TBC}}{\partial p} \right) \langle \alpha_r \rangle, U_0 - (\beta'_2 + \beta'_3 + \beta'_4) \left( \frac{\partial M_{TB}}{\partial p} \right) \langle \alpha_r \rangle, U_0 \\ - \beta'_4 \left( \frac{\partial M_R}{\partial p} \right) \langle \alpha_r \rangle, \langle \alpha_n \rangle$$

Substituting Eqs. (5.1-2a,b,c) and (5.1-3) into the various energy equations derived in Chapter 3, summing up the mass conservation equations, and retaining the momentum equation yields:

$$\underline{\underline{A}} \dot{\underline{\underline{x}}} = \underline{\underline{f}} \quad (5.1-4)$$

or,

$$\underline{\underline{A}} \frac{d}{dt} \begin{bmatrix} U_0 \\ V_v \\ \langle \alpha_r \rangle \\ \langle \alpha_n \rangle \\ p \\ \bar{W} \end{bmatrix} = \begin{bmatrix} \bar{W}(H_0 - H_r) + q_B \\ \bar{W}(H_r - H_n) \\ \bar{W}(H_n - H_k) - W_s(H_{vs} - H_k) \\ W_{fw}(H_{fw} - H_k) - \bar{W}(H_0 - H_k) \\ W_{fw} - W_s \\ -F \end{bmatrix}$$

$$H_k \begin{cases} = H_{ls} & V_v \leq V_{ref} \text{ or } u_i \leq u_f \\ = H_0 & u_i > u_f \text{ and } V_v > V_{ref} \end{cases}$$

(5.1-5)

where the components of the matrix A are shown in Table 5.1-1.

Equation (5.1-5) shows us that we have six equations in six unknowns. We will call these six unknowns the state variables of our system, so that  $\underline{x}$  is our state vector. The six equations are the differential, or state, equations of our secondary side model, and can be solved to determine the state variables and their derivatives at any time. Knowing the derivatives of the state variables allows us to determine the mass storage rates for the various regions of our model. Then, using Eqs. (5.1-3) and (5.1-2a,b,c) as algebraic relationships we can find  $W_0$ ,  $W_p$ ,  $W_r$ , and  $W_n$ . The flowrate of saturated liquid leaving the saturated region,  $W_f$ , is then found from:

$$W_f = \frac{dM_{SUB}}{dt} - W_{fw} + W_0 \quad V_v \leq V_{ref} \quad (5.1-6)$$

or

$$W_f = \frac{dM_{SUB}}{dt} - W_{fw} + \rho_s \frac{dV_v}{dt} + W_0 \quad V_v > V_{ref}$$

where  $V_{ref}$  is the vapor volume at which we switch from a fixed control volume steam dome - downcomer to a variable volume steam dome - downcomer.

Table 5.1-1  
Components of A Matrix

Component	Expression
A <sub>11</sub>	B <sub>1</sub> in Eq. (3.1-13) + E <sub>1</sub> (H <sub>0</sub> - H <sub>r</sub> )
A <sub>12</sub>	0
A <sub>13</sub>	B <sub>2</sub> in Eq. (3.1-13) + E <sub>2</sub> (H <sub>0</sub> - H <sub>r</sub> )
A <sub>14</sub>	0
A <sub>15</sub>	B <sub>3</sub> in Eq. (4.2-8) + E <sub>4</sub> (H <sub>0</sub> - H <sub>r</sub> )
A <sub>16</sub>	0
A <sub>21</sub>	$\left[ \left( \frac{\partial M_{TB}}{\partial U_0} \right)_{\langle \alpha_r \rangle, p} + E_1 \right] (H_r - H_n)$
A <sub>22</sub>	0
A <sub>23</sub>	$B_4 \text{ in Eq. (3.2-8)}$ $+ \left[ \left( \frac{\partial M_{TB}}{\partial \langle \alpha_r \rangle} \right)_{U_0, p} + E_2 \right] (H_r - H_n)$
A <sub>24</sub>	B <sub>5</sub> in Eq. (3.2-8) + E <sub>3</sub> (H <sub>r</sub> - H <sub>n</sub> )
A <sub>25</sub>	$B_6 \text{ in Eq. (3.2-8)}$ $+ \left[ \left( \frac{\partial M_{TB}}{\partial p} \right)_{U_0, \langle \alpha_r \rangle} + E_4 \right] (H_r - H_n)$
A <sub>26</sub>	0

Table 5.1-1  
Components of A Matrix (Cont.)

Component	Expression
$A_{31}$	$\left[ \left( \frac{\partial M_{TB}}{\partial U_0} \right) \langle \alpha_r \rangle, p + E_1 \right] (H_n - H_k)$
$A_{32}$	$B_7$ or $B_{11}$ is Eqs. (3.3-10 or 27)
$A_{33}$	$\left[ \left( \frac{\partial M_{TB}}{\partial \langle \alpha_r \rangle} \right) U_{0,p} + \left( \frac{\partial M_R}{\partial \langle \alpha_r \rangle} \right) \langle \alpha_n \rangle, p + E_2 \right] (H_n - H_k)$
$A_{34}$	$\left[ \left( \frac{\partial M_R}{\partial \langle \alpha_n \rangle} \right) \langle \alpha_n \rangle, p + E_3 \right] (H_n - H_k)$
$A_{35}$	$B_8$ or $B_{12}$ in Eqs. (3.3-10 or 27) + $\left[ \left( \frac{\partial M_{TB}}{\partial p} \right) U_{0, \langle \alpha_r \rangle} + \left( \frac{\partial M_R}{\partial p} \right) \langle \alpha_r \rangle, \langle \alpha_n \rangle + E_4 \right] (H_n - H_k)$
$A_{36}$	0
$A_{41}$	$B_9$ or $B_{13}$ in Eqs. (3.3-11 or 29) - $E_1 (H_0 - H_k)$
$A_{42}$	0 or $B_{14}$ in Eq. (3.3-29)
$A_{43}$	$-E_2 (H_0 - H_k)$
$A_{44}$	$-E_3 (H_0 - H_k)$

Table 5.1-1  
Components of A Matrix (Cont.)

Component	Expression
A <sub>45</sub>	B <sub>10</sub> or B <sub>15</sub> in Eq. (3.3-11) or 29) - E <sub>4</sub> (H <sub>0</sub> - H <sub>k</sub> )
A <sub>46</sub>	0
A <sub>51</sub>	$\left(\frac{\partial M_{TB}}{\partial u_0}\right) \langle \alpha_r \rangle, p + \left(\frac{\partial M_{SUB}}{\partial u_0}\right) p$ or $p, v_v$
A <sub>52</sub>	$\left(\frac{\partial M_{SAT}}{\partial v_v}\right) p + \left(\frac{\partial M_{SUB}}{\partial v_v}\right) p, U_0$
A <sub>53</sub>	$\left(\frac{\partial M_{TB}}{\langle \alpha_r \rangle}\right) p, U_0 + \left(\frac{\partial M_R}{\partial \langle \alpha_r \rangle}\right) \langle \alpha_r \rangle, p$
A <sub>54</sub>	$\left(\frac{\partial M_R}{\partial \langle \alpha_n \rangle}\right) \langle \alpha_r \rangle, p$
A <sub>55</sub>	$\left(\frac{\partial M_{TB}}{\partial p}\right) \langle \alpha_r \rangle, U_0 + \left(\frac{\partial M_R}{\partial p}\right) \langle \alpha_r \rangle, \langle \alpha_n \rangle$ $+ \left(\frac{\partial M_{SAT}}{\partial p}\right) v_v$ $+ \left(\frac{\partial M_{SUB}}{\partial p}\right) U_0$ or $U_0, v_v$
A <sub>56</sub>	0

Table 5.1-1  
Components of A Matrix (Cont.)

Component	Expression
$A_{61}, A_{62},$	0
$A_{63}, A_{64}, A_{65}$	0
$A_{66}$	I in Eq. (3.4-8)

## 5.2 STEADY STATE SOLUTION

The steady state solution of our model equations provides a starting point for transient calculations. The primary and secondary side solutions are coupled through the heat transfer rate. In the steady state the heat transfer rate is constant, so we can present the primary and secondary steady state solutions independently.

### 5.2.1 Primary Side Steady State Solution

The primary side steady state solution is obtained by solving the primary side model equations with all derivatives set equal to zero. The solution is calculated for two sets of initial conditions: full power operation and other than full power operation. The solution for full power operation is always calculated and is used to determine the tube fouling factor (see Appendix C) for subsequent heat



transfer calculations. The other than full power primary steady state solution is then calculated if an input flag indicates that the power plant is operating at a power different from full power. We will now describe each solution scheme separately.

### Full Power Solution

To obtain the steady state solution for the primary fluid system we must solve the following equations:

$$H_1 = H_{IN}$$

$$W_{IN}(H_1 - H_2) = q_B; \quad (5.2-1)$$

$$H_3 = H_2; \text{ and}$$

$$q_B = U_0 A_0 \Delta T_{LM}.$$

The necessary inputs for this calculation are:

- 1.) The primary average temperature,  $T_{avg} = \frac{T_{IN} + T_3}{2}$ ;
- 2.) The primary flowrate,  $W_{IN}$ ;
- 3.) The primary system pressure,  $p_p$ ;
- 4.) The power corresponding to full power; and,
- 5.) The secondary pressure,  $p$ .

The secondary pressure enters into this calculation since we need the secondary saturation temperature to evaluate the log-mean temperature difference. The calculated outputs are the primary fluid temperatures  $T_1$ ,  $T_2$ , and  $T_3$ , and the fouling factor,  $r_f$ .

The solution is obtained in two steps. We first calculate the primary fluid temperatures, then we calculate the fouling factor. A flowchart for the primary temperature calculation is shown in Fig. 5.2-1. The numerical scheme shown in this figure uses the bisection method to converge to the correct temperatures. Given the full power operating conditions we first calculate the required enthalpy drop of the primary fluid,  $\Delta H^*$ . To start off the bisection method we make a guess at  $T_{IN}$  which is sufficiently large so as to ensure that our first estimate of the primary enthalpy drop,  $\Delta H$ , is larger than  $\Delta H^*$  (see Fig. 5.2-2). To do this we add  $100^\circ\text{C}$  to the given primary average temperature, which is equivalent to estimating that the primary temperature drop is on the order of  $200^\circ\text{C}$ . This temperature drop is, as required, too large. Having an estimate for  $T_1$  we can calculate a consistent estimate for  $T_2$  by using the definition of  $T_{avg}$ . Now we are in a position to evaluate  $H_1$  and  $H_2$  by using fluid property routines and, therefore, we can calculate an estimated primary enthalpy drop,  $\Delta H$ . Since our first estimate for the primary enthalpy drop is larger than  $\Delta H^*$ , we obtain our second estimate for  $T_1$  by averaging our old value of  $T_1$  and  $T_{avg}$ . By going through the

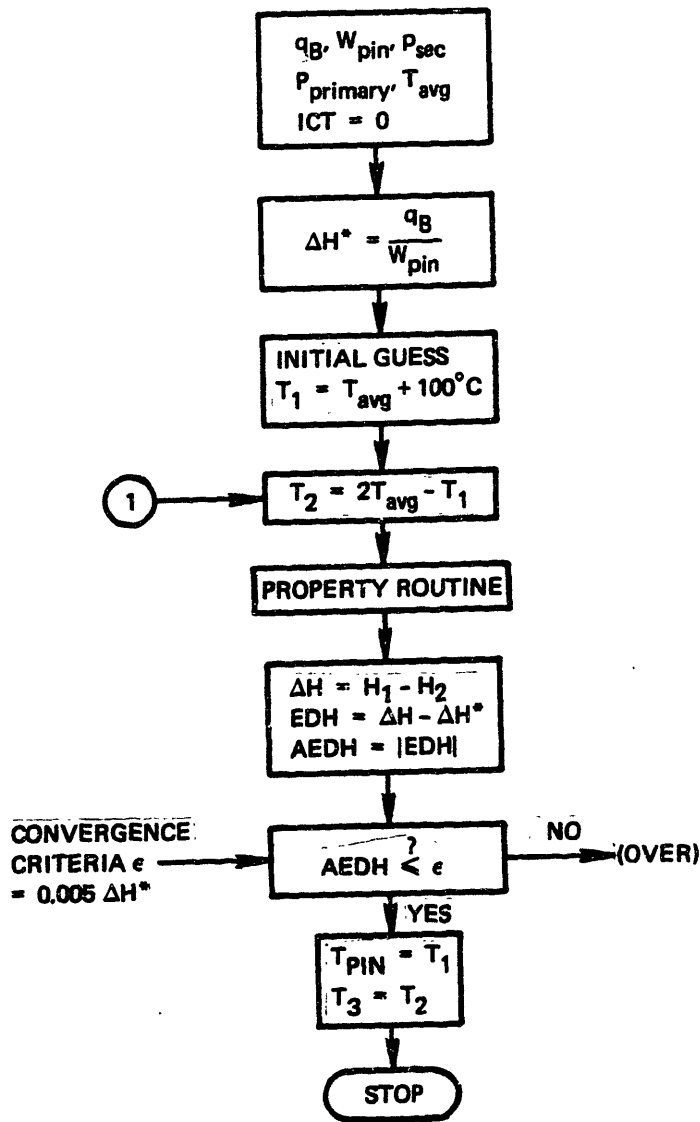


Figure 5.2-1. Flowchart of steady state primary temperature calculation.

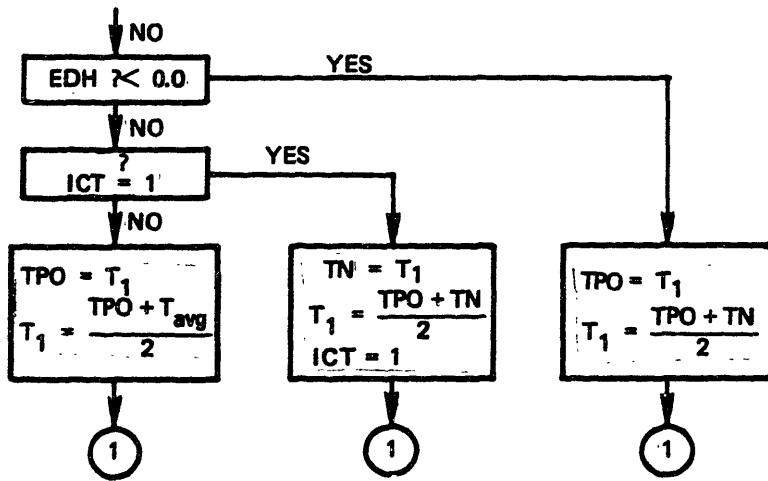


Figure 5.2-1. Flowchart of steady state primary temperature calculation (Cont.).

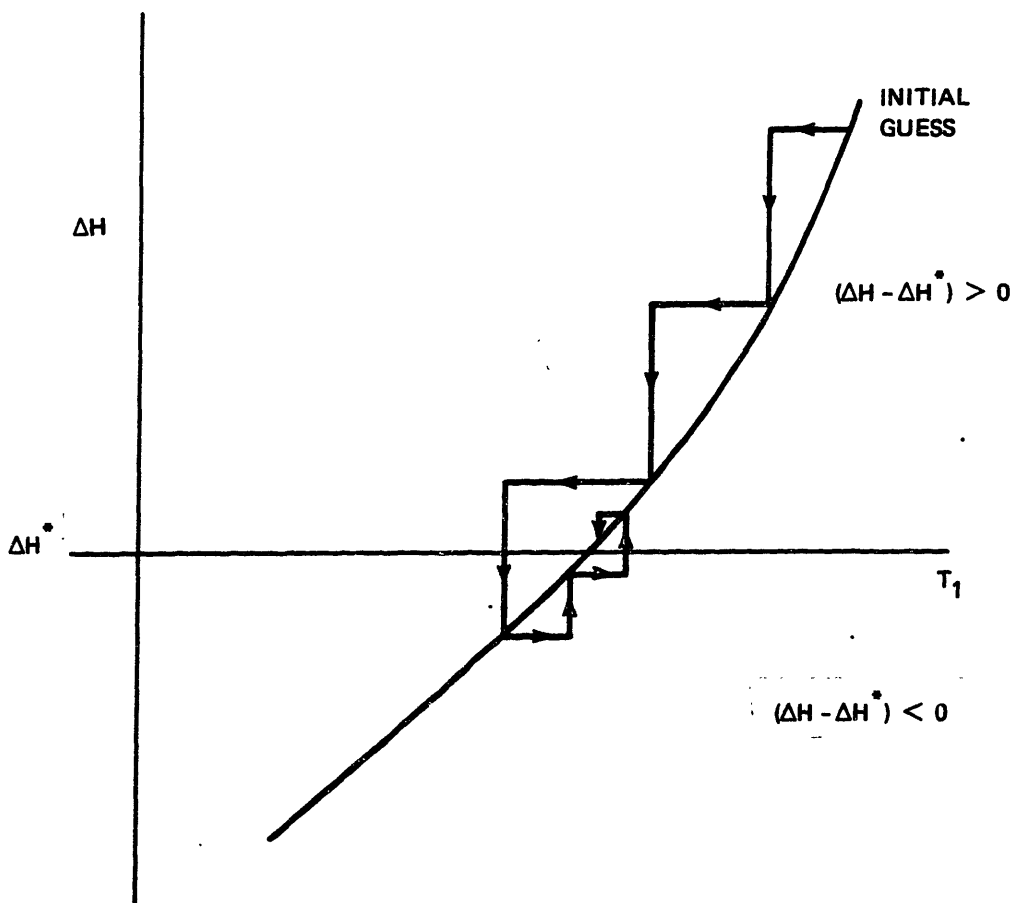


Figure 5.2-2. Bisection method for heat transfer calculation.

process described above we obtain an updated estimate of  $\Delta H$ , which we then compare to  $\Delta H^*$ . If  $\Delta H$  is still greater than  $\Delta H^*$  we again average the old value of  $T_1$  and  $T_{avg}$  to obtain a new estimate for  $T_1$ , and we continue to do this until  $\Delta H$  is less than  $\Delta H^*$ , or until the absolute value of the difference between  $\Delta H$  and  $\Delta H^*$  is less than some specified convergence criteria (usually 0.5% of  $\Delta H^*$ ). Once  $\Delta H$  has been less than  $\Delta H^*$  we average, or bisect, the last value of  $T_1$  to give us a positive value of  $(\Delta H - \Delta H^*)$  with the last value of  $T_1$  to give us a negative value of  $(\Delta H - \Delta H^*)$ , to generate a new estimate for  $T_1$ . We continue to do this until the convergence criteria is satisfied. Figure 5.2-2 shows how the bisection method is used to converge on the correct value of  $\Delta H$ . At this point we have obtained  $T_1$  and  $T_2$ , and since  $T_{IN}$  is equal to  $T_1$  and  $T_3$  is equal to  $T_2$ , we have completed the solution for the primary fluid temperatures.

We can readily obtain the fouling factor by inverting (see Appendix C),

$$q_B = U_0 A_0 \Delta T_{LM}$$

to obtain,

$$r_f = \frac{A_0 \Delta T_{LM}}{q_B} - \frac{A_0}{A_i h_p} - \frac{r_0^{0.8} n \left( \frac{r_0}{r_i} \right)}{K_t} - \frac{1}{h_s} \quad (5.2-2)$$

All the quantities on the righthand side of Eq. (5.2-2) are known, or can be determined from quantities already calculated.

#### Solution at Other Powers

For calculation of the primary side conditions at power levels other than full power we use a somewhat different calculational scheme. For these cases, a fouling factor is calculated assuming full power conditions, and this fouling factor is then used in heat transfer calculations to calculate the secondary pressure which results in a heat balance for the given power level. The inputs required for this calculation are:

- 1.) The primary average temperature,  $T_{avg}$ , corresponding to this power level;
- 2.) The primary flowrate,  $W_{IN}$ ;
- 3.) The primary system pressure,  $p_p$ ; and,
- 4.) The power level,  $q_B$ .

The first step in this calculation is to obtain the fouling factor at full power, using the scheme discussed in the preceding section. If the plant is operating at full power then the primary steady state calculation stops here.

If not, the conditions pertaining to the current plant power level are read in and the primary fluid temperatures are calculated in the same manner as they are for full power conditions. Next, the heat transfer equation,

$$q_B = U_0 A_0 \Delta T_{LM}$$

is solved for the saturation temperature. Since both  $U_0$  and  $\Delta T_{LM}$  are functions of the saturation temperature, the equation given above is a nonlinear, transcendental equation and a straightforward solution for  $T_{SAT}$  is impossible. However, we can use Newton's method to solve for the root of the following rearranged form of this equation:

$$\frac{q_B}{U_0 A_0} - \Delta T_{LM} = 0 = H(T_{SAT}) \quad (5.2-3)$$

where the notation  $H(T_{SAT})$  indicates that the left-hand expression in Eq. (5.2-3) is a function of  $T_{SAT}$ . Newton's method for finding the root of Eq. (5.2-3) is given by:

$$T_{SAT}^{\delta+1} = T_{SAT}^{\delta} - \frac{H(T_{SAT}^{\delta})}{\left. \frac{dH}{dT_{SAT}} \right|_{T_{SAT}^{\delta}}} \quad (5.2-4)$$



where the superscript  $\delta$  indicate the last iterate value, and  $\delta + 1$  indicates the new iterate value. We need an initial estimate for  $T_{SAT}$  and we use  $T_{avg} - 30^{\circ}C$  as this starting value. The iteration indicated by Eq. (5.2-4) is continued until the difference between prior and current iterates (i.e.  $T_{SAT}^{\delta+1} - T_{SAT}^{\delta}$ ) is less than  $0.1^{\circ}C$ . The derivative appearing in Eq. (5.2-4) is shown in Table 5.2-1. Once we have a converged value for  $T_{SAT}$ , it is simply a matter of using property tables to find the corresponding secondary pressure.

### 5.2.2 Secondary Side Steady State Solution

The purpose of the secondary side steady state solution is to determine the steady state flow pattern and downcomer density. The bisection method is used to numerically solve the recirculation-loop momentum equation. The initial conditions required as input for the solution are:

- 1.) Secondary pressure,  $p$ , either input or determined by a prior heat transfer calculation;
- 2.) Power level,  $q_B$ ;
- 3.) Water level in downcomer; and,
- 4.) Feedwater temperature,  $T_{fw}$ .

The first step in the calculation is to determine the steady state steam and feedwater flowrates, which are equal. They are calculated using a heat balance for the entire secondary side of the steam generator:

Table 5.2-1  
Derivative of Equation 5.2-3

$$\frac{d}{dT_{SAT}} H(T_{SAT}) = \frac{q_B}{A_0} \left[ r_0^{2n} \left( \frac{r_0}{r_i} \right) \frac{d}{dT_{SAT}} \left( \frac{1}{K_t} \right) + \frac{d}{dT_{SAT}} \left( \frac{1}{h_s} \right) \right] - \frac{d\Delta T_{LM}}{dT_{SAT}}$$

where,

$$\frac{d}{dT_{SAT}} \left( \frac{1}{K_t} \right) = -\frac{1}{K_t^2} \frac{dK_t}{dT_{SAT}} = -\frac{0.016}{K_t^2} \left[ \frac{1}{2} \frac{d\Delta T_{LM}}{dT_{SAT}} + 1 \right]$$

$$\frac{q_B}{A_0} \frac{d}{dT_{SAT}} \left( \frac{1}{h_s} \right) = -22.65 \left[ \frac{q_B}{10^6 A_0} \right]^{\frac{1}{2}} \cdot \frac{\exp\left(\frac{-P_{SAT}}{87 \cdot 10^5}\right)}{87 \cdot 10^5} \cdot \frac{dP_{SAT}}{dT_{SAT}}$$

$$\frac{d\Delta T_{LM}}{dT_{SAT}} = -\frac{\Delta T_{LM}^2}{(T_1 - T_{SAT})(T_2 - T_{SAT})}$$

Note: Explicit correlations for  $h_s$  and  $K_t$  are given in Appendix C.

$$W_s = W_{fw} = \frac{q_B}{H_{vs} - H_{fw}} \quad (5.2-5)$$

The next step is to solve the steady state loop momentum equation for the downcomer flowrate,  $W_0$ , which is, from Chapter 3:

$$F = (M_1 + M_2 + M_3 + M_4)W_0 + M_5 = 0 \quad (5.2-6)$$

where the  $M_i$  are complex functions of  $W_0$ . A representative plot of the left hand side of Eq. (5.2-6) is shown in Fig. 5.2-3. The solution we seek is shown in Fig. 5.2-3 as the intersection of the curve representing  $F$  and the  $W_0$  axis. In order to start the bisection method we need an estimate of  $W_0$  sufficiently large so that  $F$  is positive. In the steady state the tube bundle exit quality exit is equal to the steam flowrate divided by the downcomer flowrate; hence,

$$W_0 = \frac{W_S}{x_R} \quad (5.2-7)$$

If we choose a sufficiently low value for  $x_R$ , then  $W_0$  will be large and  $F$  will be positive. Thus, we use 0.01 as a starting value for  $x_R$ . Before continuing with the calculation we must determine the fluid properties at various locations on the secondary side of the steam generator. In the steady state the tube bundle exit quality,  $x_R$ , is equal to the riser exit quality,  $x_n$ . Using the drift flux model (see Appendices A and C) we can then calculate  $\langle \alpha_R \rangle$  and  $\langle \alpha_n \rangle$ , and, since we know the secondary pressure, we also know the saturation properties of the water, so we can

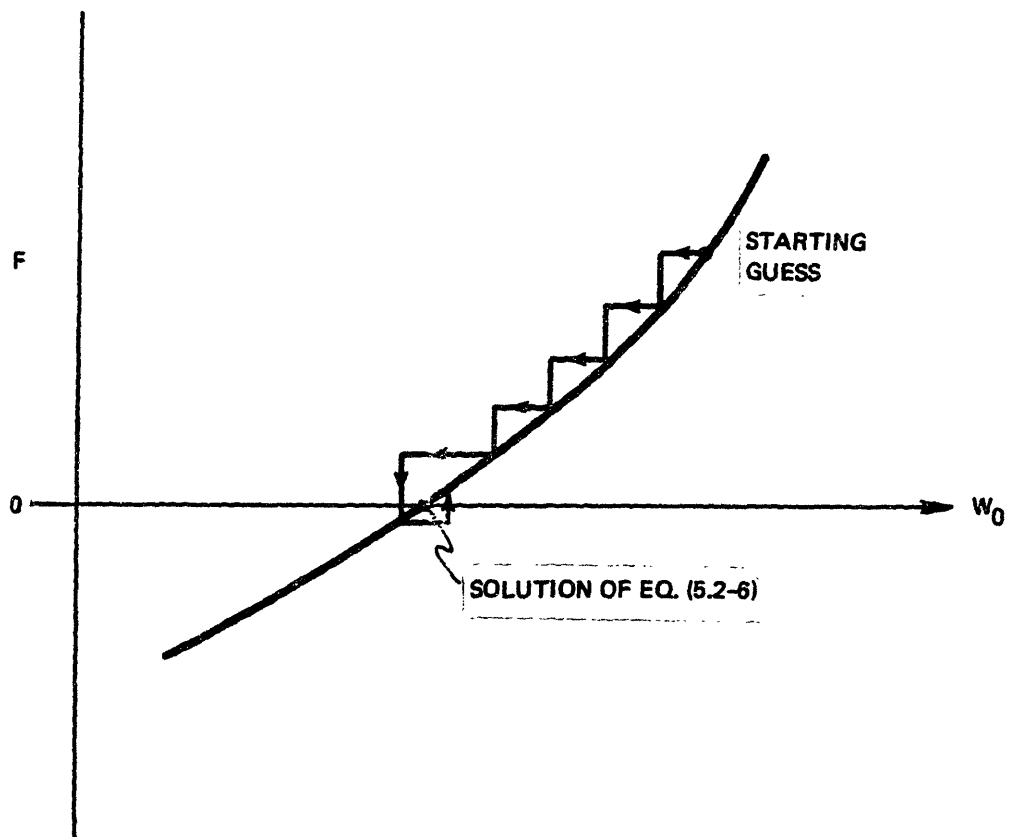


Figure 5.2-3. Bisection method for downcomer flowrate calculation.

evaluate  $\bar{\rho}_r$  and  $\bar{\rho}_n$ . The downcomer density,  $\rho_0$ , is determined by performing a steady state mixing calculation for the subcooled region. An energy balance for this region yields:

$$H_0 = x_r H_{fw} + (1 - x_r) H_{ls}$$

Knowing the subcooled fluid enthalpy and the secondary pressure we can determine the subcooled fluid density,  $\rho_0$ , from fluid property routines. Given the location of the parallel to cross flow transition,  $L_p$ , as well as  $\bar{\rho}_r$  and  $\rho_0$  it is a simple matter to determine  $\rho_p$ , and hence  $\langle \alpha_p \rangle$ , from the assumed linear profile of  $1/\bar{\rho}$  in the tube bundle region. The flow quality at this point,  $x_p$ , can be obtained from  $\langle \alpha_p \rangle$  by using the drift flux model. Finally, the fluid viscosities are obtained from property routines. We are now in a position to evaluate Eq. (5.2-6). For the first estimate of  $x_r$  we know that  $F$  is greater than zero, so for our next estimate  $x_r$  is increased by adding 0.05 to the original value of  $x_r$ . Then the whole process described above is repeated until either  $F$  is less than zero or the absolute value of  $F$  is less than some convergence criteria (in our model we use 0.1 Pa as this convergence criteria). If the convergence criteria is satisfied then we can proceed to the next step in the solution. Otherwise, we average the last value of  $W_0$  which gave us a negative

value of  $F$  and the last value of  $W_0$  which gave us a positive value of  $F$  to obtain a new estimate for  $W_0$  (and  $x_r$  through the relation  $x_r = W_s/W_0$ ). This process is continued until the convergence criteria is met. Figure 5.2-4 is a flowchart of this solution scheme.

The next step is to determine  $W_f$  which is simply  $W_0$  minus  $W_{fw}$ . Then the steady state masses of the various regions are calculated and summed to obtain the total mass of fluid contained in the steam generator, which completes the steady state solution for the secondary side.

### 5.3 DECOUPLING OF PRIMARY AND SECONDARY TRANSIENT SOLUTIONS

In the steady state solution scheme it is permissible to decouple the primary and secondary solutions since the heat transfer rate is constant. This is not the case for the transient solution because the heat transfer rate is not constant and depends on the instantaneous conditions present in both the primary and secondary fluid systems. We can, however, make reasonable arguments for decoupling the primary and secondary solution by using an explicit representation for the heat transfer rate. That is, we can use a heat transfer rate calculated from system parameters obtained at a previous time step to calculate the advanced time condition in the time differenced version of our model equations. For instance, consider a system consisting of two concentric cylinders with the outer cylinder insulated

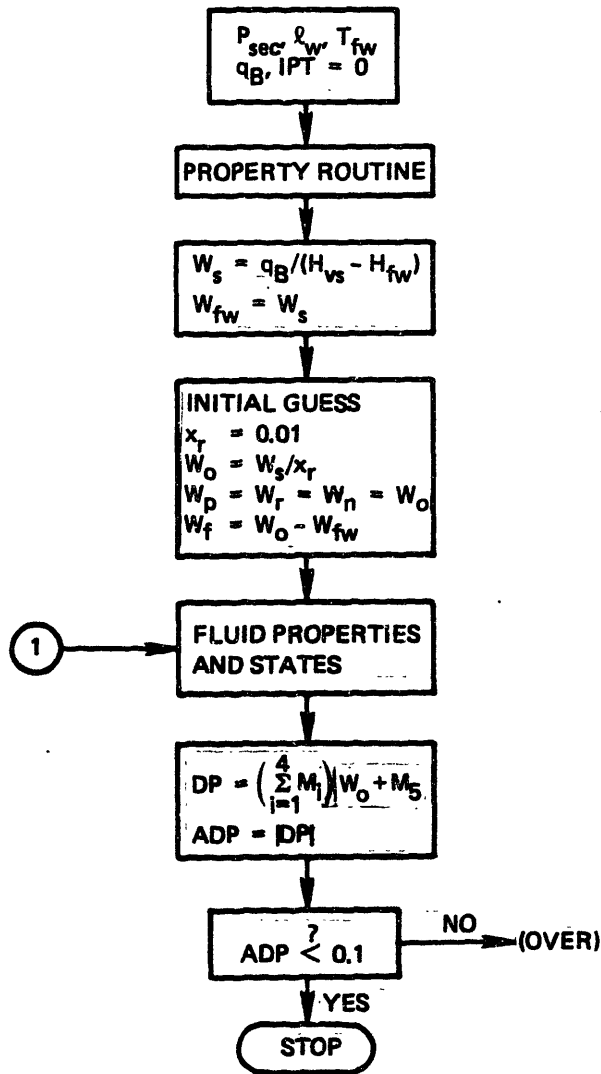


Figure 5.2-4. Flowchart of steady state calculation of recirculation flowrate.

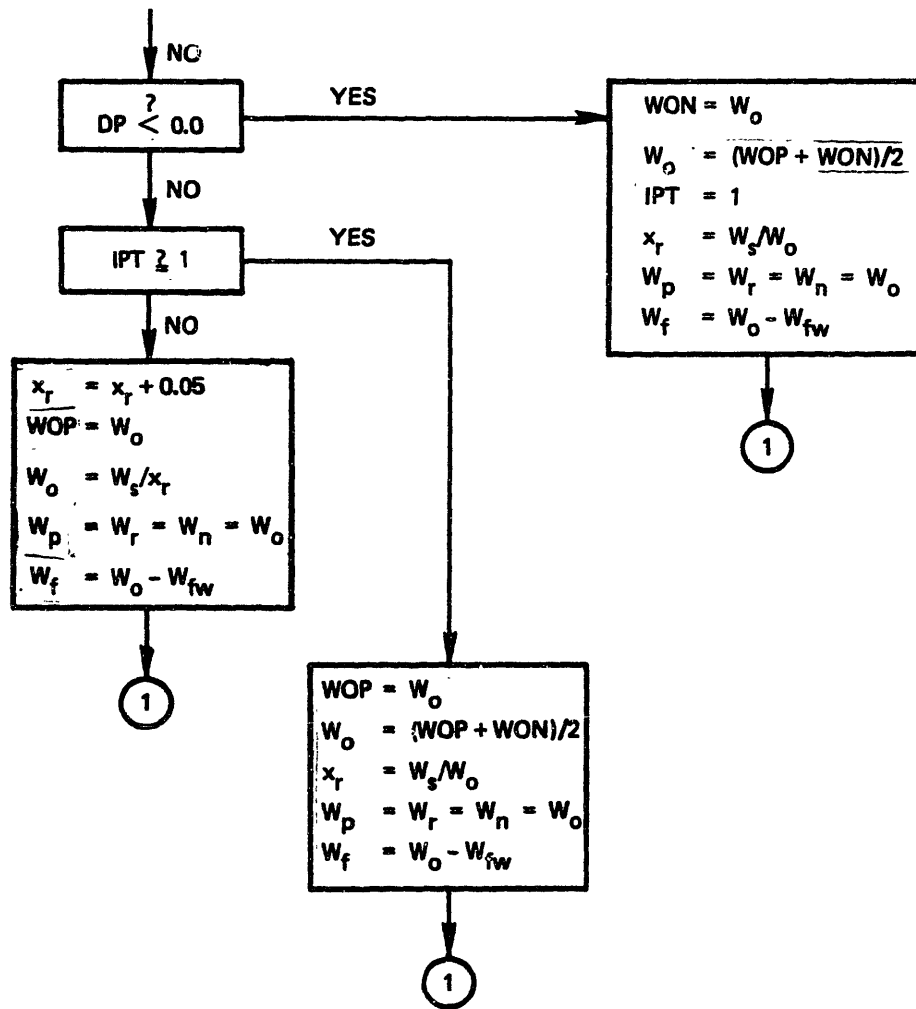


Figure 5.2-4. Flowchart of steady state calculation of recirculation flowrate (Cont.).



over its outer surface. The inner cylinder has a hot fluid flowing inside it, while the annulus formed by the two cylinders contains a colder fluid flowing in the opposite direction. The colder fluid is heated by heat transfer from the hot fluid through the wall of the inner cylinder. We denote quantities associated with the flow in the annulus by the subscript a, and those associated with the flow in the inner cylinder by the subscript i. We also make the following assumptions:

- 1.) the pressure for both fluids is constant;
- 2.) we can neglect the heat capacity of the cylinders;
- 3.) we can use the log-mean temperature difference to calculate the transient heat transfer rate;
- 4.) instantaneous, perfect mixing for both fluids;
- 5.) constant flowrates for both fluids; and,
- 6.) inlet temperatures are known functions of time.

The energy equations for the system are:

$$(\rho C_p V)_i \frac{dT_{i \text{ OUT}}}{dt} = W_i (H_{i \text{ IN}} - H_{i \text{ OUT}}) - q \quad (5.3-1)$$

$$(\rho C_p V)_a \frac{dT_{a \text{ OUT}}}{dt} = W_a (H_{a \text{ IN}} - H_{a \text{ OUT}}) + q \quad (5.3-2)$$

where

$$q = UA_{HT} \frac{(T_{i \text{ IN}} - T_{a \text{ OUT}}) - (T_{i \text{ OUT}} - T_{a \text{ IN}})}{\ln \left[ \frac{T_{i \text{ IN}} - T_{a \text{ OUT}}}{T_{i \text{ OUT}} - T_{a \text{ IN}}} \right]}$$

Time differencing these equations in an explicit fashion yields,

$$(\rho C_p V)_i \frac{T_{i \text{ OUT}}^{n+1} - T_{i \text{ OUT}}^n}{\Delta t} = W_i (H_{i \text{ IN}} - H_{i \text{ OUT}})^n - q^n \quad (5.3-3)$$

$$(\rho C_p V)_a \frac{T_{a \text{ OUT}}^{n+1} - T_{a \text{ OUT}}^n}{\Delta t} = W_a (H_{a \text{ IN}} - H_{a \text{ OUT}})^n + q^n \quad (5.3-4)$$

where the superscript  $n$  denotes the old time level, and  $n+1$  the new time level. All the quantities on the right hand side of Eqs. (5.3-3) and (5.3-4) are known so that  $T_{i \text{ OUT}}^{n+1}$  and  $T_{a \text{ OUT}}^{n+1}$  can be calculated independently. This would not be the case if we used  $q_B^{n+1}$  in Eqs. (5.3-3) and (5.3-4), since these equations would be coupled through the log-mean

temperature difference in the heat transfer rate equation. Solution for the new time level outlet temperatures in this case would require simultaneous solution of Eqs. (5.3-3) and (5.3-4).

The argument just given is also true for the solution of the primary and secondary side equations. Thus, we can perform the primary and secondary side transient solutions independently by using explicit time differencing for the heat transfer rate.

We can justify the use of explicit time differencing for two reasons. First, when time differencing differential equations, it is somewhat arbitrary as to when quantities not appearing in time derivatives are evaluated within the time step. They can be evaluated at the beginning of the time step, the end, or somewhere in between, as long as the difference equations reduce to the differential equations in the limit of  $\Delta t$  approaching zero. Explicit time differencing satisfies this condition. Second, heat transfer transients occur on a longer time scale than fluid flow transients. That is pressure disturbances propagate at the sonic velocity (in our case at an infinite velocity since we assume a uniform system pressure) and affect flowrates in the time it takes a sonic wave to travel from the source of the disturbance to the location of interest. Heat transfer and energy transport disturbances propagate at speeds on the order of the fluid velocity for convective heat transfer, and on a time scale on the order of tenths of a second for

conduction heat transfer. Hence, using explicit time differencing for the heat transfer rate should introduce little error in the calculations, although we recognize the possibility of introducing instability in the calculation when using an explicit form for  $q_B$ .

#### 5.4 TRANSIENT SOLUTION BOUNDARY CONDITIONS

Steam generator transients are initiated and maintained by events occurring in the primary system, the main steam system, or the feedwater system. Therefore, the boundary conditions, or forcing function inputs, are quantities that define the changes at the interfaces between these systems and the steam generator. Boundary conditions related to the primary system are:

- 1.) Primary fluid temperature at the steam generator inlet;
- 2.) Primary flowrate; and
- 3.) Primary system pressure.

Feedwater related boundary conditions are:

- 1.) Feedwater flowrate; and,
- 2.) Feedwater temperature.

The last boundary condition is the steam flowrate, which is related to the main steam system.

All the boundary conditions listed above are required as input for a transient calculation. The quantities can be obtained from measurements, or from a suitable model of the system.

## 5.5 PRIMARY TRANSIENT SOLUTION

The primary fluid system transient solution is obtained by using an explicit time differencing scheme for Eq. (5.1-1). That is,

$$\underline{\underline{C}}^n \frac{\underline{T}^{n+1} - \underline{T}^n}{\Delta t} = \underline{g}^n \quad (5.5-1)$$

or,

$$\underline{T}^{n+1} = \underline{T}^n + [\underline{\underline{C}}^n]^{-1} \Delta t \underline{g}^n \quad (5.5-2)$$

But,  $\underline{\underline{C}}$  is diagonal so we can write:

$$T_1^{n+1} = T_1^n + \frac{\Delta t W_{IN}^n}{C_1^n} (H_{IN} - H_1)^n;$$

$$T_2^{n+1} = T_2^n + \frac{\Delta t}{C_n^n} [W_{IN}^n (H_1 - H_2)^n - q_B^n];$$

and

$$T_3^{n+1} = T_2^n + \frac{\Delta t W_{IN}^n}{C_3^n} (H_2 - H_3)^n.$$

(5.5-3)

Equations (5.5-3) constitute the transient solution for the primary fluid system.

### 5.6 SECONDARY TRANSIENT SOLUTION

The equations making up the transient model of the secondary side consist of a mixture of differential and algebraic equations. In section 5.1.2 we isolate the differential equations and write them in compact form as:

$$\underline{\underline{A}} \dot{\underline{x}} = \underline{f}$$

where

$$\underline{x} = \text{Col}[U_0, V_v, \langle \alpha_r \rangle, \langle \alpha_n \rangle, p, \bar{W}]$$

It is worthwhile to take a look at the structure of the matrix  $\underline{\underline{A}}$  to see whether or not we can take advantage of the structure in our numerical solution. The structure is as follows:

$$\underline{\underline{A}} \equiv \begin{array}{|c|c|c|c|c|c|} \hline X & 0 & X & X & X & 0 \\ \hline X & 0 & X & X & X & 0 \\ \hline X & X & X & X & X & 0 \\ \hline X & X & X & X & X & 0 \\ \hline X & X & X & X & X & 0 \\ \hline 0 & 0 & 0 & 0 & 0 & X \\ \hline \end{array}$$

X ≡ nonzero entry

0 ≡ zero entry

The structure shown above indicates that the last equation, which is the momentum equation, is independent of the other equations. This is not really the case, and the reason why the momentum equation appears to be independent of the other equations is because we did not substitute Eqs. (5.1-2a,b,c) and (5.1-3) into the right hand side of the momentum equation. This substitution step is omitted since it results in nonlinear algebraic expressions involving the derivatives of the state variables, which is a situation we want to avoid. Therefore, we will assume that the momentum equation can be solved independently of the other state equations at any time step. The result of this assumption is that instead of having to solve a set of six coupled differential equations we now have to solve a set of five coupled differential equations. We will represent this reduced set of equations by:

$$\underline{\underline{R}} \dot{\underline{y}} = \underline{h} \quad (5.6-1)$$

where  $\underline{\underline{R}}$  is the matrix formed by deleting the sixth row and column from  $\underline{\underline{A}}$ ,  $\underline{y}$  is the corresponding reduced state vector, and  $\underline{h}$  is the reduced vector corresponding to  $\underline{f}$ .

Differencing Eq. (5.6-1) in an explicit manner yields:

$$\underline{\underline{R}}^n \underline{\underline{y}}^n = \underline{h}^n$$

or,

$$\dot{\underline{y}}^n = [\underline{\underline{R}}^n]^{-1} \underline{h}^n \quad (5.6-2)$$

$$\underline{y}^{n+1} = \underline{y}^n + \Delta t \dot{\underline{y}}^n \quad (5.6-3)$$

where,

$$\dot{\underline{y}}^n = \frac{\underline{y}^{n+1} - \underline{y}^n}{\Delta t}$$

Equation (5.6-2) gives us the time derivatives of the reduced set of state variables, while Eq. (5.6-3) gives us the new time values of the reduced set of state variables. Before we update the state variables, we substitute the derivatives of the reduced set of state variables into Eq. (5.1-3) to obtain  $W_0^n$ . Further substitution of these derivatives into Eqs. (3.1-11), (3.2-6), and (3.5-4) yields the derivatives of the mass contents appearing in Eqs. (5.1-2a,b,c), which then gives us  $W_p^n$ ,  $W_r^n$  and  $W_n^n$ . The flowrate  $W_f^n$  is obtained by using Eq. (5.1-6). Note that the flowrates obtained in this manner are not the current flowrates but flowrates at the old time. This is so because we used an



explicit method to obtain  $\dot{\underline{y}}^n$  and a typical mass conservation equation differenced in a corresponding manner is:

$$W_{IN}^n - W_{OUT}^n = \frac{dM^n}{dt} = \xi(\dot{\underline{y}}^n)$$

where  $\xi(\dot{\underline{y}}^n)$  indicates that  $dM^n/dt$  can be written as an algebraic function of  $\dot{\underline{y}}^n$ . Therefore, solving the mass conservation equations (Eqs. (5.1-2a,b,c)) together with the definition of  $\bar{W}^n$  (Eq. (5.1-3)) yields the flowrates at time level  $n$ .

The next step (see Fig. 5.6-1 for a flowchart of the secondary solution) in the secondary solution is to update the reduced set of state variables using Eq. (5.6-3) and then evaluate the secondary fluid properties. Following this we calculate the downcomer water level in a way that guarantees that we conserve mass for the entire steam generator unit. The steps followed to obtain the water level are:

- 1.) Calculate the total mass of the steam generator fluid at the new time using:

$$M_{TOT}^{n+1} = M_{TOT}^n + (W_{fw}^{n+1} - W_s^{n+1})\Delta t;$$

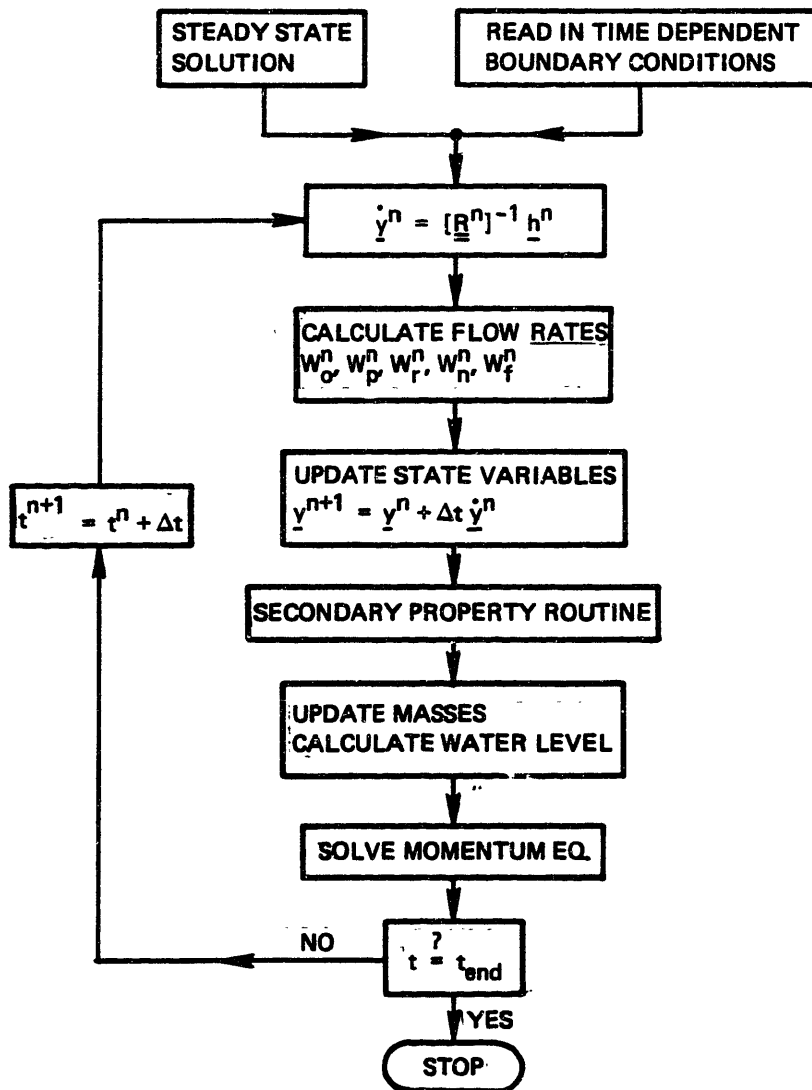


Figure 5.6-1. Flowchart of secondary transient solution.

- 2.) Calculate the new time values of the tube bundle and riser mass contents ( $M_{TB}^{n+1}$  and  $M_R^{n+1}$ ) using Eqs. (3.1-9), (3.2-4), and  $y^{n+1}$ ;
- 3.) Subtract the results of Step 2 from the result of Step 1 to obtain the new time mass contained in the steam dome - downcomer, i.e.

$$M_{SD}^{n+1} = M_{SUB}^{n+1} + M_{SAT}^{n+1} = M_{TOT}^{n+1} - M_{TB}^{n+1} - M_R^{n+1};$$

- 4.) At this point we must determine whether or not the water level is low enough so that we are using a steam dome - downcomer model with variable volumes. To do this we can calculate the mass content of the steam dome - downcomer as if the water level was exactly at the level where the switch from a constant volume approach to a variable volume approach is made. Call this mass  $M_{CUT}^{n+1}$ . Then,

$$V_v^{n+1} = \frac{V_{SD} \rho_{ls}^{n+1} + V_{TOT} \rho_0^{n+1} + V_{STM} \rho_{vs}^{n+1} - M_{SD}^{n+1}}{(\rho_{ls} - \rho_{vs})^{n+1}}$$

$$\text{if } M_{CUT}^{n+1} < M_{SD}^{n+1}$$

or,

$$V_v^{n+1} = \frac{V_{STM} \rho_{vs}^{n+1} + V_{f0} \rho_{ls}^{n+1} + (V_{TOT} - V_{f0}) \rho_0^{n+1} - M_{SD}^{n+1}}{(\rho_0 - \rho_{vs})^{n+1}}$$

$$\text{if } M_{CUT}^{n+1} < M_{SD}^{n+1}$$

5.) Using  $V_v^{n+1}$  and the steam generator geometry calculate  $z_w^{n+1}$  (Appendix K).

The final step in the numerical solution of the secondary side equations is to solve the momentum equation:

$$I^n \frac{\bar{W}^{n+1} - \bar{W}^n}{\Delta t} = -F(\underline{y}^{n+1}, W^n)$$

or

$$\bar{W}^{n+1} = \bar{W}^n - \frac{\Delta t}{I^n} F(\underline{y}^{n+1}, W^n) \quad (5.6-4)$$

In Eq. (5.6-4) we indicate that  $F$  is evaluated as a function of the new time state variables and the old time flowrates. This may seem inconsistent, but recall that when time differencing equations the matter of where quantities are evaluated is arbitrary so long as the difference equation reduces to the correct differential equation when  $\Delta t$  is allowed to approach zero. Equation (5.6-4) satisfies this requirement.

This completes the discussion of the secondary side numerical solution.

### 5.7 TRANSIENT HEAT TRANSFER RATE

In this work we assume that the transient heat transfer rate is given by (see Chapter 4):

$$q_B = U_0 A_0 \Delta T_{LM} \quad (5.7-1)$$

Solving this equation for  $q_B$  is not as straightforward as it seems, since  $U_0$  depends on  $q_B$  through  $h_s$ , the secondary side heat transfer coefficient. Writing out  $U_0$ :

$$U_0 = \left[ \frac{A_0}{A_i h_p} + \frac{r_0 \ln \left( \frac{r_0}{r_i} \right)}{K_t} + \frac{1}{h_s} + r_f \right]^{-1} \quad (5.7-2)$$

The secondary side heat transfer coefficient,  $h_s$ , is given by (Appendix C):

$$h_s = \frac{q_B}{A_0 (T_w - T_{SAT})} \quad (5.7-3)$$

But, using Eq. (C-13) from Appendix C:

$$A_0(T_w - T_{SAT}) = 22.65 \left[ \frac{q_B}{10^6 A_0} \right]^{\frac{1}{2}} A_0 \exp \left( \frac{-p}{87.0 \cdot 10^5} \right)$$

or

$$A_0(T_w - T_{SAT}) = z_2 \sqrt{q_B} \quad (5.7-4)$$

Substituting Eq. (5.7-4) into Eq. (5.7-3) yields:

$$h_s = \frac{\sqrt{q_B}}{z_2} \quad (5.7-5)$$

Defining:

$$Z = \frac{A_0}{A_i h_p} + \frac{r_0 \ln \left( \frac{r_0}{r_i} \right)}{K_t} + r_f$$

and using Eq. (5.7-5), Eq. (5.7-2) becomes:

$$U_0 = \left[ z_1 + \frac{z_2}{\sqrt{q_B}} \right]^{-1} \quad (5.7-6)$$

Substituting Eq. (5.7-6) into Eq. (5.7-1) gives:

$$q_B = \left[ z_1 + \frac{z_2}{\sqrt{q_B}} \right]^{-1} z_3$$

where,  $z_3 \equiv A_0 \Delta T_{LM}$ . This equation can be written as:

$$z_1 q_B + z_2 \sqrt{q_B} - z_3 = 0 \quad (5.7-7)$$

Equation (5.7-7) is a quadratic equation in  $\sqrt{q_B}$ , and the solution is given by:

$$\sqrt{q_B} = \frac{-z_2 \pm \sqrt{z_2^2 + 4z_1 z_3}}{2z_1} \quad (5.7-8)$$

Equation (5.7-8) indicates that we have two solutions for  $\sqrt{q_B}$ . However, in order to satisfy Eq. (5.7-5) we must select the positive value of  $\sqrt{q_B}$  since both  $h_s$  and  $z_2$  are always positive, so the correct solution for  $\sqrt{q_B}$  is:

$$\sqrt{q_B} = \frac{-z_2 + \sqrt{z_2^2 + 4z_1 z_3}}{2z_1} \quad (5.7-9)$$

Therefore the transient heat transfer is given by:

$$q_B = \left[ \frac{-z_2 + \sqrt{z_2^2 + 4z_1 z_3}}{2z_1} \right]^2 \quad (5.7-10)$$

## 5.8 NUMERICAL ANALYSIS OF SECONDARY SIDE EQUATIONS

It is useful to develop some insight into the stability characteristics of the secondary side solution scheme. This is difficult to do for the nonlinear set of equations which we have developed for the secondary fluid system. However, if we linearize the state equations we can then perform a straightforward analysis of the stability of the linear system, which, for small perturbations about the linearization point, gives us a good feel for the stability characteristics of our nonlinear model.

Taking Eq. (5.1-4) and solving for  $\dot{\underline{x}}$  yields:

$$\dot{\underline{x}} = \underline{\underline{A}}^{-1} \underline{f} \quad (5.8-1)$$

Let us linearize Eq. (5.8-1) about an operating point  $\underline{x}_0$  such that:

$$\underline{x} = \underline{x}_0 + \tilde{\underline{x}} \quad (5.8-2)$$

where  $\tilde{\underline{x}}$  is small. Now we make a Taylor expansion of the right hand side of Eq. (5.8-1) about the point  $\underline{x}_0$  to obtain:

$$\underline{\underline{A}}^{-1} \underline{f} = \underline{\underline{A}}^{-1} \underline{f} \Big|_{\underline{x}_0} + \underline{\underline{J}}_{\underline{x}_0} \tilde{\underline{x}} + \text{Higher order terms} \quad (5.8-3)$$



where  $\underline{J}_{\underline{x}_0}$  is the Jacobian matrix of  $\underline{A}^{-1}\underline{f}$  with respect to  $\underline{x}$  evaluated at  $\underline{x}_0$ , that is:

$$[\underline{J}_{\underline{x}_0}]_{i,j} = \left. \frac{\partial (\underline{A}^{-1}\underline{f})_i}{\partial x_j} \right|_{\underline{x}_0}$$

If the perturbation is small enough we can neglect the higher order terms in Eq. (5.8-3). Then substituting Eqs. (5.8-2) and (5.8-3) into Eq. (5.8-1) yields:

$$\dot{\underline{x}} = \underline{J}_{\underline{x}_0} \underline{x} \quad (5.8-4)$$

The stability properties of the linear system described by Eq. (5.8-4) are directly linked to the eigenvalues of the matrix  $\underline{J}_{\underline{x}_0}$ . Before continuing any further we should define exactly what we mean by stability. We define a system of equations to be stable if when we introduce a small, but arbitrary, perturbation into the system, this perturbation does not grow in time as the equations are solved. We will denote this small, arbitrary perturbation by  $\underline{x}_0$  for the system of equations defined in Eq. (5.8-4).

We now derive the solution for Eq. (5.8-4). In this derivation we assume that the matrix  $\underline{J}_{\underline{x}_0}$  has a full set of linearly independent eigenvectors, where each eigenvector,  $\underline{\sigma}_i$ , has a corresponding eigenvalue,  $\lambda_i$ . The diagonalizing matrix  $\underline{S}$  of  $\underline{J}_{\underline{x}_0}$  is a matrix with columns consisting of

the eigenvectors of  $\underline{\underline{J}}_{\underline{\underline{x}}_0}$  (Ref. (S3)). The diagonalized form of  $\underline{\underline{J}}_{\underline{\underline{x}}_0}$  is then given by:

$$\underline{\underline{S}}^{-1} \underline{\underline{J}}_{\underline{\underline{x}}_0} \underline{\underline{S}} = \underline{\underline{\Lambda}} = \begin{bmatrix} \lambda_1 & & & & & \\ & \lambda_2 & & & & \\ & & \ddots & & & \\ & & & & & \\ & & & & & \lambda_6 \end{bmatrix} \quad (5.8-5)$$

where the diagonal matrix  $\underline{\underline{\Lambda}}$  has the eigenvalues of  $\underline{\underline{J}}_{\underline{\underline{x}}_0}$  as diagonal elements. If we define a vector  $\underline{\underline{v}}$  such that:

$$\underline{\underline{x}} = \underline{\underline{S}} \underline{\underline{v}}$$

then Eq. (5.8-4) becomes:

$$\dot{\underline{\underline{v}}} = \underline{\underline{S}}^{-1} \underline{\underline{J}}_{\underline{\underline{x}}_0} \underline{\underline{S}} \underline{\underline{v}} = \underline{\underline{\Lambda}} \underline{\underline{v}} \quad (5.8-6)$$

The solution of this equation, subject to the initial condition  $\underline{\underline{v}}_0 = \underline{\underline{S}}^{-1} \underline{\underline{x}}_0$ , is simply (Ref. (B-6)):

$$\underline{\underline{v}} = \underline{\underline{S}}^{-1} \sum_{i=1}^6 C_{i\sigma} e^{\lambda_i t}$$

where the  $C_i$  are determined from

$$\tilde{\underline{v}}_0 = \underline{\underline{S}}^{-1} \sum_{i=1}^6 C_i \underline{\sigma}_i$$

or, in terms of  $\tilde{\underline{x}}$ :

$$\tilde{\underline{x}} = \sum_{i=1}^6 C_i \underline{\sigma}_i e^{\lambda_i t} \quad (5.8-7)$$

with,

$$\tilde{\underline{x}}_0 = \sum_{i=1}^6 C_i \underline{\sigma}_i$$

In order for the initial perturbation,  $\tilde{\underline{x}}_0$ , to not increase with time, the real parts of the eigenvalues appearing in Eq. (5.8-7) must be less than or equal to zero. If this is the case then our differential equations, by our definition, are stable. What this means is that if the system is operating in the steady state and there is a small perturbation to the state vector, then the system will eventually return to the steady state.

We now ask ourselves the question: can we perform a similar analysis for the difference equation analogue to Eq. (5.8-4)? The answer to this question is yes, we can.

We can write the explicit time differenced form of Eq. (5.8-6) as:

$$\left[ \frac{\underline{\tilde{v}}^{n+1} - \underline{\tilde{v}}^n}{\Delta t} \right] = \underline{\underline{\Lambda}} \underline{\tilde{v}}^n$$

or,

$$\underline{\tilde{v}}^{n+1} = [\underline{\underline{I}} + \Delta t \underline{\underline{\Lambda}}] \underline{\tilde{v}}^n \quad (5.8-8)$$

Starting with  $\underline{\tilde{v}}_0$  and performing successive substitutions we can rewrite Eq. (5.8-8) as:

$$\underline{\tilde{v}}^{n+1} = [\underline{\underline{I}} + \Delta t \underline{\underline{\Lambda}}]^{n+1} \underline{\tilde{v}}_0 \quad (5.8-9)$$

Since  $[\underline{\underline{I}} + \Delta t \underline{\underline{\Lambda}}]$  is a diagonal matrix, each element of the vector  $\underline{\tilde{v}}^{n+1}$  is given by:

$$v_i^{n+1} = (1 + \Delta t \lambda_i)^{n+1} v_{0i} \quad i = 1, 2, \dots, 6 \quad (5.8-10)$$

Equation (5.8-10) satisfies our definition of stability if the largest magnitude of  $(1 + \Delta t \lambda_i)$  is less than or equal to one. We use the term magnitude rather than absolute

value since some of the  $\lambda_i$  may be complex. Expanding each eigenvalue in complex form yields:

$$\lambda_i = a_i + b_i I$$

where either  $a_i$  or  $b_i$  may be zero, and  $I = \sqrt{-1}$ . Using this expression for the  $\lambda_i$  in Eq. (5.8-10) yields the following stability criterion for our discrete-time system:

$$(1 + \Delta t a_i)^2 + (\Delta t b_i)^2 \leq 1 \quad \text{for all } i.$$

After some manipulation we obtain:

$$\Delta t \leq \frac{-2a_i}{a_i^2 + b_i^2} \quad (5.8-11)$$

Since  $\Delta t$  must be positive,  $a_i$  must be negative to satisfy Eq. (5.8-11). But  $a_i$  is the real part of  $\lambda_i$ , so this is the same condition that we require for stability of the continuous time system of equations. Therefore, in addition to satisfying the same stability condition as the continuous time system our explicit discrete time system must also satisfy the more stringent requirements of Eq. (5.8-11).

We have performed the analysis given above for the Maine Yankee nuclear power plant. The Jacobian is obtained by numerical differentiation and the operating point for the

linearization is at 106 per cent full power steady state operation. The eigenvalues for our sixth order set of differential equations are shown in Table 5.8-1.

Table 5.8-1  
Eigenvalues of the Sixth Order System for Maine Yankee.

i	$\lambda_i$
1	-2.0490
2	-0.4718 + 1.0270i
3	-0.4718 - 1.0270i
4	-0.2155
5	-0.0348
6	0.0

As can be seen the eigenvalues all have real parts that are less than or equal to zero, indicating that our differential equations are stable. That is, a small disturbance to our state vector in the steady state will eventually die out, returning our system to the steady state. Using Eq. (5.8-11) to determine the critical time step size for our linear discrete time system yields 0.73 seconds, which corresponds to the complex conjugate pair  $\lambda_2$  and  $\lambda_3$ . This may or may not be the critical time step size for our

nonlinear system. (Note that the zero eigenvalue does not make  $\Delta t$  undefined since it satisfies  $(1 + \Delta t \lambda_6) \leq 1$ ).

Transient tests indicate that the critical time step size for our nonlinear model is around 0.65 seconds, which is 11 per cent less than the time step size obtained using a linear analysis. It is important to note that the critical time step size calculated here is for the secondary side model and not for the entire steam generator model. When both the primary and secondary sides are modeled, testing shows the critical time step size to be on the order of 0.45 seconds rather than 0.65 seconds. For the primary side, which is donor cell differenced (see Appendix F), the critical time step size is on the order of the transport time through the plena. For Maine Yankee this transport time is 0.67 seconds. However, the critical time step size for the entire steam generator is neither the critical time step size for the primary side nor the critical time step size for the secondary side. This is because there is a coupling between the primary and secondary sides through the heat transfer rate and this heat transfer rate is treated in an explicit fashion in the difference equations. This explicit treatment of the heat transfer rate introduces a more stringent requirement on integration time step size.

Finally, there is the matter of a zero eigenvalue ( $\lambda_6$ ). This eigenvalue corresponds to what is referred to in linear control system analysis as a free integrator. This means that we are integrating a system of equations

which has an output that responds in an unbounded manner to a persisting error in the inputs. Specifically, for our model, we are talking about the response of the steam generator water level to the feedwater flowrate. To clarify this, we can draw an analogy between our steam generator model and a tank with a single inflow and outflow. For this tank, in the steady state, the flowrate into the tank is equal to the flowrate out of the tank so that the tank water level is constant. This tank also has a water level controller which regulates the flowrate into the tank in a way that maintains a constant water level. Let us assume that a model for this tank exists, but that a model of the controller is not used. Rather, the flowrate into the tank is specified as input. Consider that there is a slight error in input to the model such that the steady state flowrate in is marginally greater than the flowrate out. Integration of the model equations yields the result that the steady state tank water level increases continuously in time, which is physically incorrect. However, if we were to use a tank model which included a model of the water level controller, this problem would not arise.

A similar situation exists for the steam generator model; therefore, it seems appropriate to add an equation simulating the feedwater controller to our existing set of six equations and then to redo the eigenvalue analysis. The controller equation we use is:



$$\frac{dW_{fw}}{dt} = C_w(W_s - W_{fw}) + C_l(l^* - l_w)$$

with  $C_w$  equal to 0.025 and  $C_l$  equal to 0.05. The eigenvalues for this seventh order model, again for Maine Yankee, are shown in Table 5.8-2. The first three eigenvalues shown

Table 5.8-2  
Eigenvalues of the Seventh Order System for Maine Yankee.

i	$\lambda_i$
1	-2.0490
2	-0.4718 + 1.0270i
3	-0.4718 - 1.0270i
4	-0.2172
5	-0.0288 + 0.0112i
6	-0.0288 - 0.0112i
7	-0.0005

in this table are identical to the first three shown in Table 5.8-1. In addition, the zero eigenvalue has disappeared. As for the sixth order system, the critical time step size is 0.73 seconds and is determined by the complex conjugate pair  $\lambda_2$  and  $\lambda_3$ . Hence, the conclusions drawn

regarding stability for the sixth order system apply equally for the seventh order system.

The presence of a free integrator in our model in the absence of an accurate feedwater controller model is significant. It indicates that small errors in the feedwater flowrate input can be integrated over a long time span into a sizable error in the calculated water level. This fact must be kept in mind when comparing results calculated using the steam generator model to experimental results.

## Chapter 6

### VALIDATION

#### 6.1 PREVIEW

An important step in the development of a computational model is the validation and testing of the model. This step serves two purposes: First, it allows us to establish working limits on the applicability of the model. Second, it serves to give us confidence in the predictions of the model within its applicable limits.

The steam generator model developed here has been extensively tested against the predictions of other computer programs and experimental results, for both steady state and transient conditions. Table 6.1-1 lists the test cases used in the model validation effort. This table lists the test facilities along with representative numbers for steam generator operating pressure and full power heat transfer rate. These test cases can be further subdivided into test case runs; that is, conditions simulated using the steam generator computer model. Table 6.1-2 gives a breakdown of conditions simulated for each test case. Also listed in this table are text references where specific information regarding each test run may be found, as well as a classification as to whether the test run is compared to experimental results or results calculated using another computer program.

Table 6.1-1  
Test Cases Used for Model Validation.

Test Case	Power per Steam Regener- ator (MWf)	Operating Pressure (MPa)
Maine Yankee	817	5.6
Arkansas Nuclear One - Unit 2	1408	6.2
Calvert Cliffs	1280	5.8
Argonne National Laboratory Tests	0.12	3.5
RD-12 Boiler Experiments	1.2	4.6

As can be seen in Table 6.1-2, only three of the five test cases are discussed in this chapter, while two are presented in Appendix H. The two test cases presented in Appendix H, Maine Yankee and Calvert Cliffs, are test cases in which the transient boundary conditions are not well known. That is, the steam flowrate, feedwater flowrate, and feedwater temperature are not given as functions of time. For these cases we used models of the main steam and

Table 6.1-2  
Breakdown of Validation Program.

Test Case	Type of Validation	Test Case Conditions	Text Reference
1.) Maine Yankee	Computer Computer Computer Computer Computer Computer	A) Steady State B) Control Element Assembly Withdrawal from 106% Power C) Turbine Trip from 106% Power D) Total Loss of Feedwater Accident from 106% Power E) Reactor Trip from Full Power F) Turbine Trip from Full Power With Steam Dump G) Turbine Trip from Full Power Without Steam Dump	Appendix H Appendix H Appendix H Appendix H Appendix H Appendix H Appendix H
2.) Arkansas Nuclear One - Unit 2	Experimental Experimental Experimental Experimental	A) Turbine Trip - Steam Generator 1 B) Turbine Trip - Steam Generator 2 C) Loss of Primary Flow - Steam Generator 1 D) Loss of Primary Flow - Steam Generator 2	6.4.4 6.4.4 6.4.5 6.4.5

Table 6.1-2  
Breakdown of Validation Program (Cont.)

Test Case	Type of Validation	Test Case Conditions	Text Reference
2.) Arkansas Nuclear One - Unit 2	Experimental	E) Full Length Control Element Assembly Drop - Steam Generator 1	6.4.2
	Experimental	F) Full Length Control Element Assembly Drop - Steam Generator 2	6.4.2
3.) Calvert Cliffs	Computer Computer Experimental Experimental	A) Control Element Withdrawal	Appendix H
		B) Turbine Trip	Appendix H
		C) Loss of Primary Flow	Appendix H
		D) Turbine Trip	Appendix H
4.) Argonne National Laboratory Tests	Experimental	A) Downcomer Flowrate versus Power for Operating Pressures of:	6.2.2
		- 2.17 MPa - 2.86 MPa - 3.55 MPa	

Table 6.1-2  
Breakdown of Validation Program (Cont.)

Test Case	Type of Validation	Test Case Conditions	Text Reference
5.) RD-12 Boiler Experiments	Experiment Experiment Experiment Experiment Experiment Experiment Experiment	A) Steady State B) Power Increase C) Power Decrease D) Primary Flow Increase E) Primary Flow Decrease F) Boiler Pressure Increase G) Feedwater Transient H) Oscillating Secondary Pressure	6.3.2 6.3.4 6.3.5 6.3.7 6.3.6 6.3.8 6.3.9 6.3.10

feedwater systems to calculate the feed and steam flowrates, while the feedwater temperature was held constant. It is not known whether or not these models predict steam and feedwater flowrates comparable to those in the test case transients, so it is difficult to draw any firm conclusions regarding the steam generator model accuracy. These cases do provide, however, a confidence that the model behaves well over a wide range of interesting conditions.

The remaining three test cases, on the other hand, are well documented. The Argonne National Laboratory data are for steady state operation and all the input necessary for simulation is documented. The Arkansas Nuclear One - Unit 2 data was acquired during preoperational testing, and the transient boundary conditions for the steam generator are known, with the exception of the transient feedwater temperature. The RD-12 Boiler data is complete, allowing us to wholly specify the transient boundary conditions. Thus, for these three test cases we can perform model validation under carefully specified conditions and, therefore, more readily draw conclusions regarding model accuracy and validity.

## 6.2 ARGONNE NATIONAL LABORATORY TEST LOOP

### 6.2.1 Background Information

This test case is a set of measurements made during the steady state operation of a natural circulation test loop at the Argonne National Laboratory (Ref. (P2)). Data appearing



in Ref. (P2) is taken from Refs. (A1) and (A2). The measurements were made for various loop geometries; however, we are interested in only one test loop configuration, which is shown in Fig. 6.2-1. For this geometry the loop was operated at a series of pressures, and at each pressure the heat input was incremented until a steady flow oscillation was observed in the downcomer. After each power increment the steady state downcomer flow was measured. Table 6.2-1 shows the test loop operating conditions. Information regarding geometric input can be found in Appendix H.

Table 6.2-1  
Test Loop Operating Conditions.

Quantity	Value
Operating Pressure	Variable (2.17, 2.86, 3.55 MPa)
Feedwater Temperature	32.25°C
Heat Input <sup>1</sup>	Variable (20, 30, 40 kW, ...)
Water Level <sup>2</sup>	1.93 m

<sup>1</sup> Heat losses in downcomer neglected.

<sup>2</sup> From bottom of heated section.

### 6.2.2 Results

The results of calculations for the test loop are shown in Fig. 6.2-2 in the form of downcomer flowrate vs. power

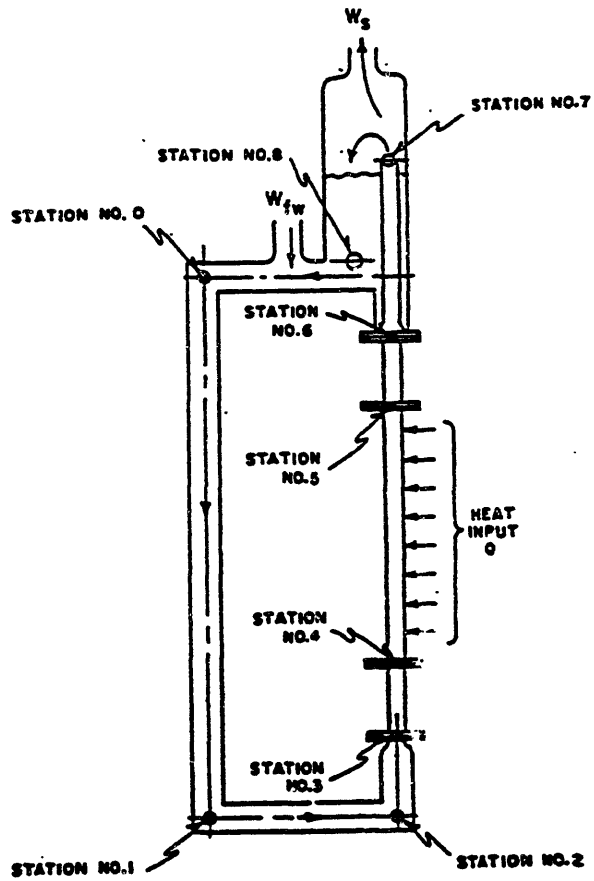


Figure 6.2-1. Argonne National Laboratory test loop configuration (Ref. P2)).

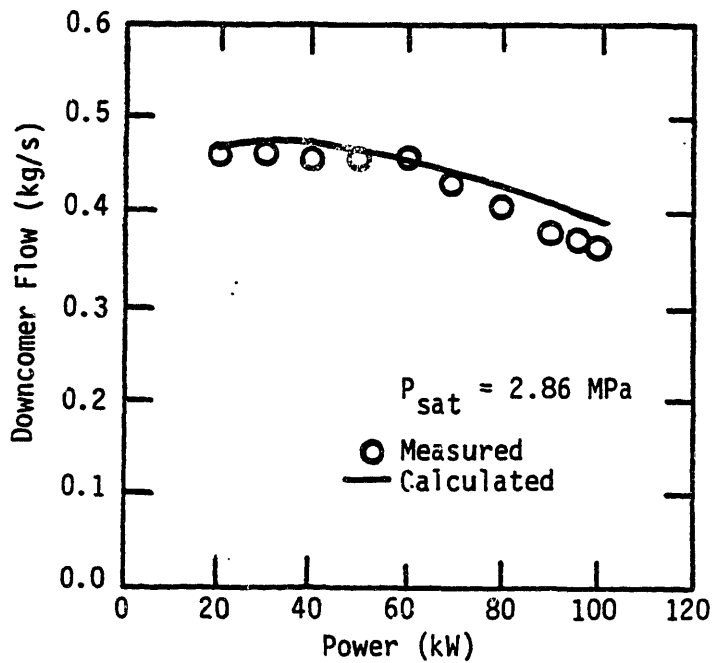
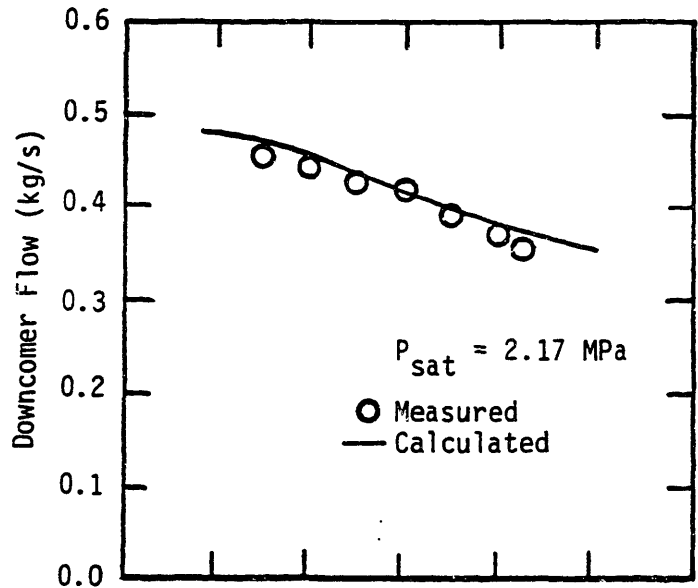


Figure 6.2-2. Downcomer flowrate versus power.

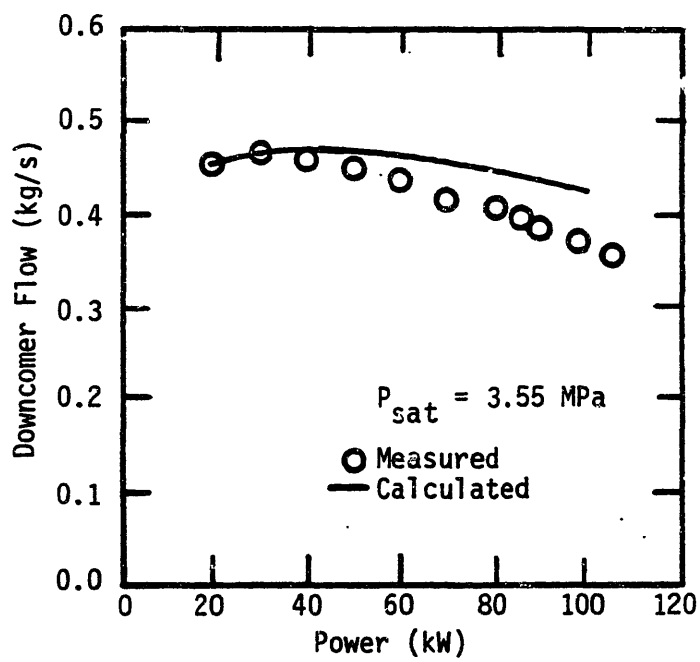


Figure 6.2-2. Downcomer flowrate versus power. (Continued)

curves for three different operating pressures. As can be seen, the agreement between calculation and experiment is generally good. For the lower pressures (2.17 and 2.86 MPa), in particular, the shapes and magnitudes of the calculated downcomer flowrate vs. power curves are in excellent agreement with the measured data. The calculated downcomer flowrate vs. power curve for the case where the operating pressure is 3.55 MPa is in good agreement with the data at low power. But, at higher powers (greater than 50 kW) the calculated downcomer flowrate tends to be larger than the measured flowrate. This could be due to either inaccuracies in calculating two-phase friction losses in the tube bundle, or calculating too high a vapor volume fraction in two phase regions, or both. If the calculated friction losses in the tube bundle are too low, then the calculated downcomer flowrate will exceed the measured flowrate because the calculated loop losses must balance out the calculated natural circulation driving head. If the calculated vapor volume fraction is too high, then the calculated driving head will be too large which results in calculating a larger downcomer flowrate than is measured.

One of the objectives of the tests made on the Argonne test loop was to determine the power, at a given pressure, that caused a sustained oscillation of the downcomer flowrate. We attempted to simulate this situation by inputting the measured critical power and performing a steady state calculation. A transient was then run in which the power

was increased by 2 per cent at time zero, and the behavior of the downcomer flowrate was observed. At all pressures the calculated downcomer flowrate did indeed oscillate, but the oscillation was damped rather than sustained. This result is to be expected, since the model developed here does not account for transport effects in a detailed manner, and the experimentally observed downcomer flowrate oscillation is greatly influenced by transport effects in the heated region.

### 6.3 RD12 BOILER TESTS

#### 6.3.1 Background Information

The RD12 test loop is an experimental facility at the Whiteshell Nuclear Research Establishment in Pinawa, Canada. It is a scale version of the heat transport system of a CANDU (CANada Deuterium Uranium) reactor system designed to provide experimental data for use in the validation of analytic models for the transient behavior of such heat transport systems. The test loop has scaled versions of the major components of a CANDU system including heated sections to simulate the reactor core, primary pumps, and natural circulation U-tube steam generators. Reference (M4) states that the test loop primary fluid is H<sub>2</sub>O and not D<sub>2</sub>O, which is the primary fluid in CANDU reactors.

A diagram of the test loop arrangement for the tests discussed here is shown in Fig. 6.3-1. Details regarding

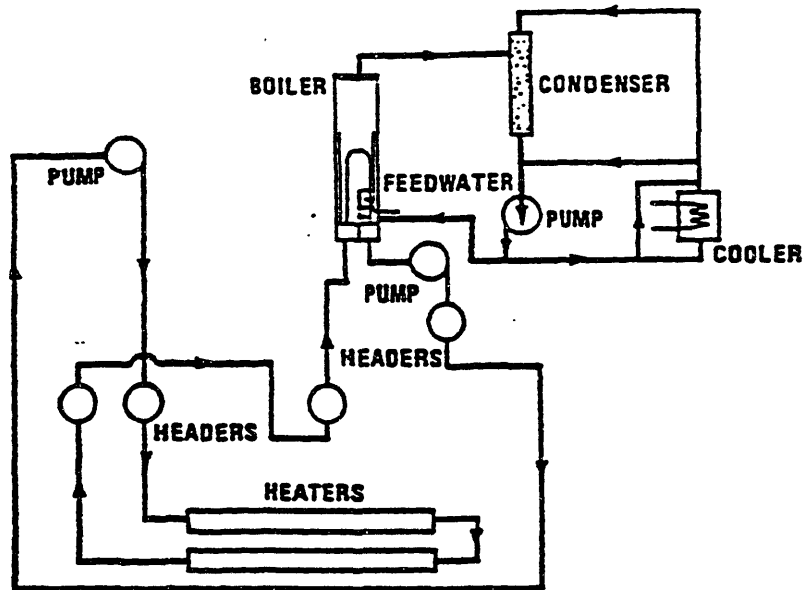


Figure 6.3-1. Test loop arrangement (Ref. (M4)).

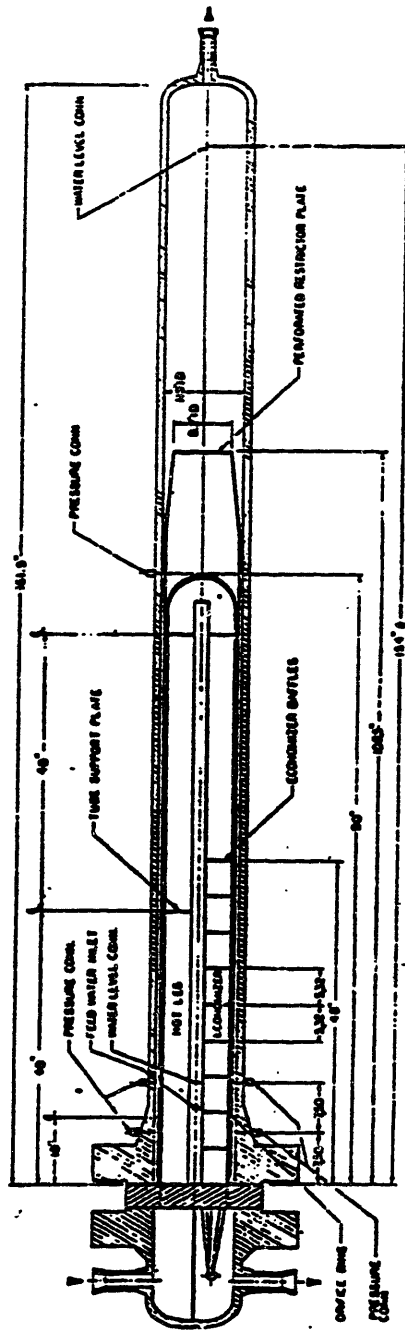


Figure 6.3-2a Schematic of RD12 steam generator (Ref. B2).



the test loop design and operation can be found in Refs. (M4) and (B3). A schematic of the RD12 steam generator is shown in Fig. 6.3-2a. The steam generator is instrumented to measure the following parameters:

- 1.) Primary inlet temperature;
- 2.) Primary outlet temperature;
- 3.) Primary pressure;
- 4.) Primary flowrate;
- 5.) Feedwater flowrate;
- 6.) Steam flowrate;
- 7.) Downcomer flowrate;
- 8.) Steam generator level; and,
- 9.) Vapor volume fraction at various elevations.

The list given above does not include all the measured quantities available, just those quantities of interest to us.

Temperature measurements are made using both resistance temperature detectors (RTDs) and thermocouples. The RTDs have time constants on the order of 28 seconds, so they are only used for steady state measurements. The thermocouple time constants are on the order of 0.1 seconds, which is fast enough to avoid having to account for sensor dynamics during transient tests.

The RD12 steam generators have integral preheaters (economizers) where the entering feedwater is heated before mixing with the recirculating saturated fluid (see Fig. 6.3-2b). This geometry is somewhat different from that for

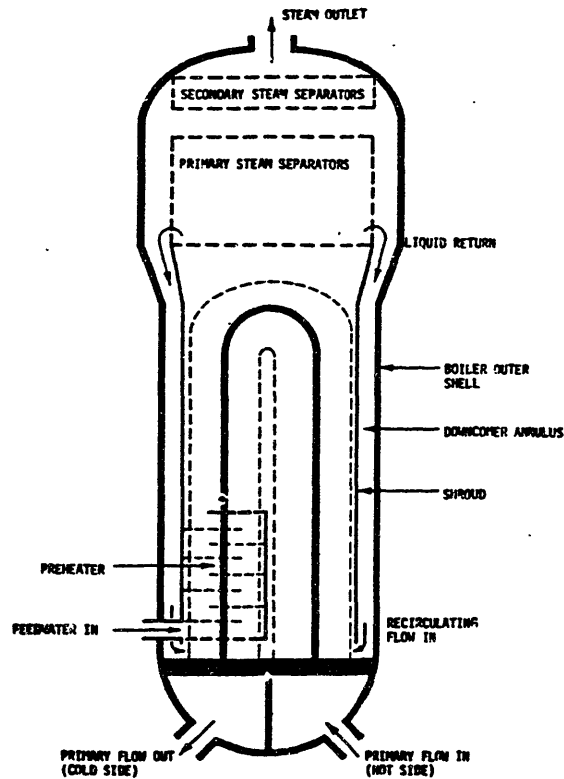


Figure 6.3-2b. Steam generator with integral preheater (Ref. (I2)).

which our steam generator model is developed. However, during operation of the RD12 steam generator it was found that there is a significant amount of preheater leakage (Refs. (M4) and (M3)). That is, there is some mixing of the feedwater with the saturated recirculating fluid in the lower portion of the steam generator. We can approximate the situation in our steam generator model by introducing the feedwater at the bottom of the downcomer and using a very small subcooled region volume located at the bottom of the downcomer.

The RD12 steam generators do not have steam separating equipment. The two phase mixture exits the riser through a perforated plate and then the steam separates from the water by means of free separation.

Both steady state and transient tests were performed using the loop configuration shown in Fig. 6.3-1. During the steady state tests measurements were made of the down-comer flowrate and the riser inlet vapor volume fraction for various powers and pressures (other parameters were also measured, but only those listed are of immediate interest).

The transient tests are:

- 1.) Power increase;
- 2.) Power decrease;
- 3.) Primary flow decrease;
- 4.) Primary flow increase;
- 5.) Secondary pressure increase;
- 6.) Feed flow transient; and,
- 7.) Oscillating secondary pressure.

Calculated results for the transients listed above, except for the oscillating secondary pressure, are presented in the following sections. The calculation for the oscillating secondary pressure was unsuccessful and the reasons why are discussed in 6.3.10. The geometric input for the RD12 steam generator is given in Appendix H.

### 6.3.2 Steady State Tests

Data acquired during steady state tests were used to determine some parameters relevant to two-phase flow modeling, in particular the drift flux model (Ref. (M4)). Figure 6.3-3 shows the slip ratio inferred from data taken in the riser as a function of power. This plot clearly indicates that the homogeneous model (slip ratio equal to one) for calculating the vapor volume fraction (see Appendix A) is inappropriate and that a model accounting for the relative motion between the phases should be used. The drift flux model (Appendices A and C) satisfies this requirement. In Appendix C we state that we use the following drift flux parameters:

$$C_0 = 1.13; \text{ and,}$$

$$u_{vj} = 1.41 \left[ \frac{\sigma g (\rho_{ls} - \rho_{vs})}{\rho_{ls}^2} \right]^{\frac{1}{4}}$$

However, data presented in Ref. (M4) and transient calculations reported in Ref. (M4) indicate that the drift flux parameters that are appropriate for the RD12 steam generators are:

$$C_0 = 1.12; \text{ and,}$$

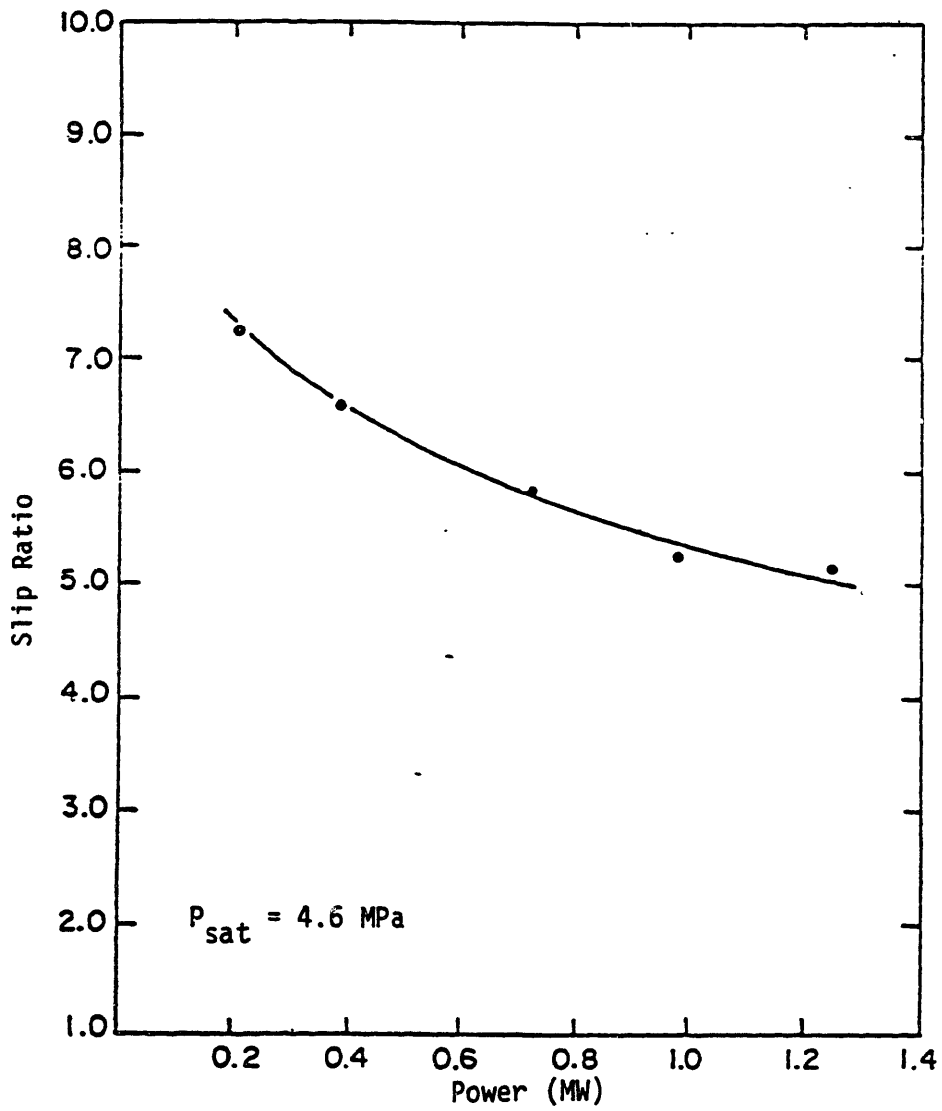


Figure 6.3-3. Slip ratio in riser vs. power (Ref. (M4)).

$$u_{vj} = 2.54 \left[ \frac{\sigma g (\rho_{ls} - \rho_{vs})}{\rho_{ls}^2} \right]^{\frac{1}{4}} \quad (6.3-1)$$

The coefficient 2.54 appearing in the correlation for  $u_{vj}$  is obtained by fitting the data at a pressure of 4.6 MPa. It appears that Eq. (6.3-1) is valid within a pressure range of approximately 3.6 to 5.6 MPa. The secondary pressure during all transient tests is within this range, so the use of Eq. (6.3-1) to calculate  $u_{vj}$  does not introduce significant error. Figure 6.3-4 is a plot of  $\langle u_v \rangle_v$  versus  $\langle j \rangle$  at 4.6 MPa using the drift flux parameters given above. Also shown in this figure are experimental data taken at 4.6 MPa (Ref. (M4)).

Figures 6.3-5 and 6.3-6 are taken from Ref. (M4). Figure 6.3-5 shows the experimentally determined steady state vapor volume fraction at the riser inlet as a function of steam generator power at various pressures. Figure 6.3-6 is a similar plot for the measured downcomer flowrate. Before trying to reproduce these curves analytically it is necessary to determine values for the parameters  $K_{SGP}$  and  $K_D$  appearing in the momentum equation for the recirculating flow (see Chapter 3). These parameters are chosen so that the calculated downcomer flowrate curve matches the experimental curve at 3.9 MPa. The parameters thus obtained, by trial and error, are:

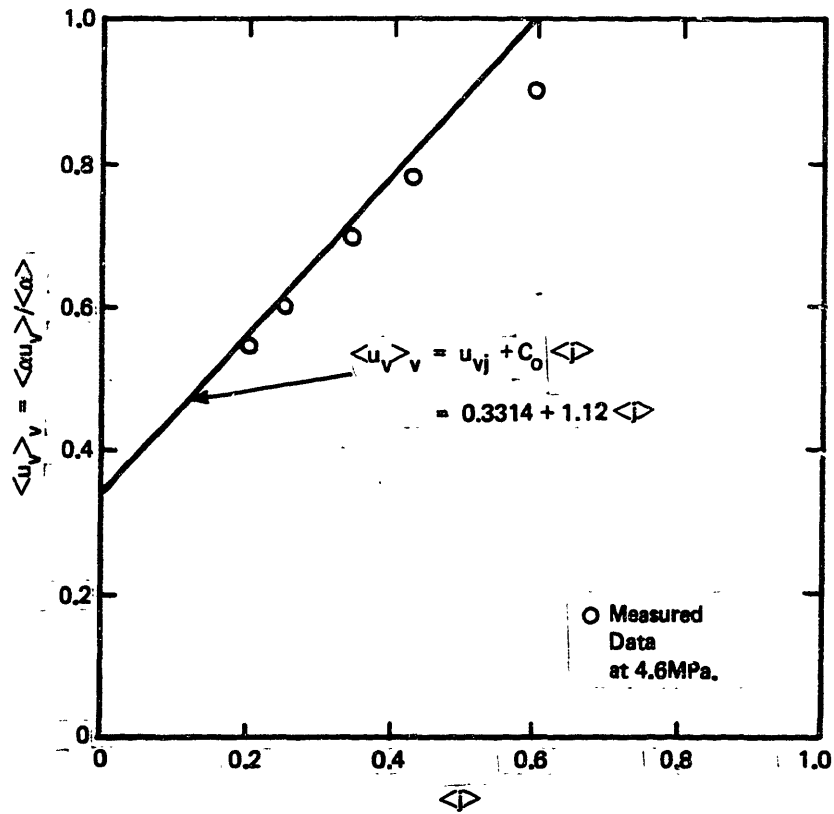


Figure 6.3-4. Mean vapor velocity at riser inlet vs volumetric flux.

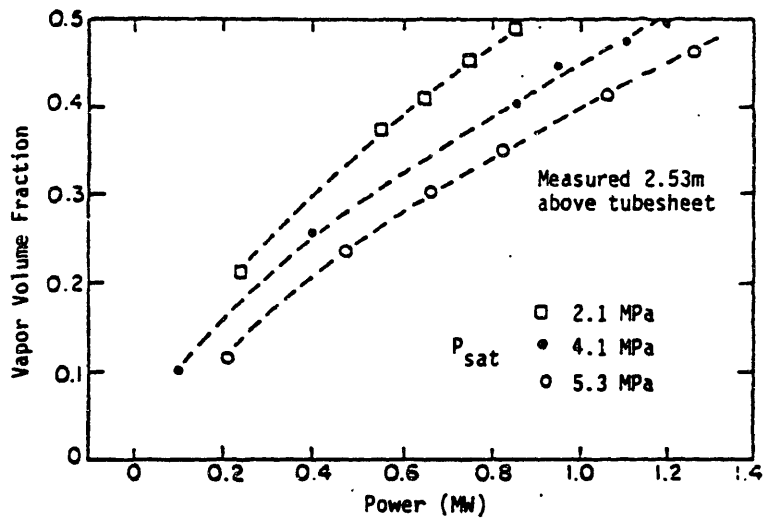


Figure 6.3-5. Riser inlet vapor volume fraction vs. power (Ref. (M4)).

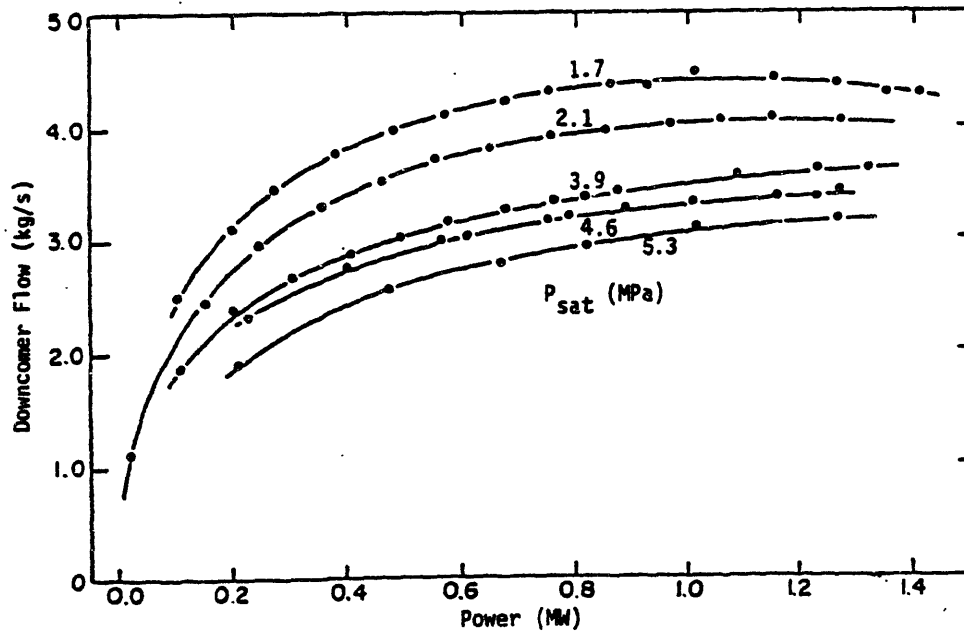


Figure 6.3-6. Downcomer flowrate vs. power (Ref. (M4)).



$$K_{SEP} = 124; \text{ and,}$$

$$K_D = 39.$$

It is interesting to note that both the shape and the magnitude of the downcomer flowrate versus power curve can be controlled by juggling the values of  $K_{SEP}$  and  $K_D$ . This observation has significant ramifications from a model adaptation viewpoint, in that it implies that both  $K_{SEP}$  and  $K_D$  are probable model adaptation parameters and can be modified in order to correct for model deviations from actual plant performance.

Now that all model parameters have been specified we may compare model calculations to measured data. Figure 6.3-7 is a set of plots of the riser inlet vapor volume fraction as a function of power for three pressures: 2.1 MPa, 4.1 MPa and 5.3 MPa. The calculations are in good agreement with the measured data for pressures of 4.1 MPa and 5.3 MPa. For a secondary pressure of 2.1 MPa the calculated vapor volume fraction is greater than the measured vapor volume fraction at all powers, although it follows the same trend as the measured data. This discrepancy is most likely due to the fact that the pressure, 2.1 MPa, is outside of the range of validity of Eq. (6.3-1), which is used to calculate  $u_{vj}$ . It is apparent that a larger value of  $u_{vj}$  than that obtained from Eq. (6.3-1) would result in

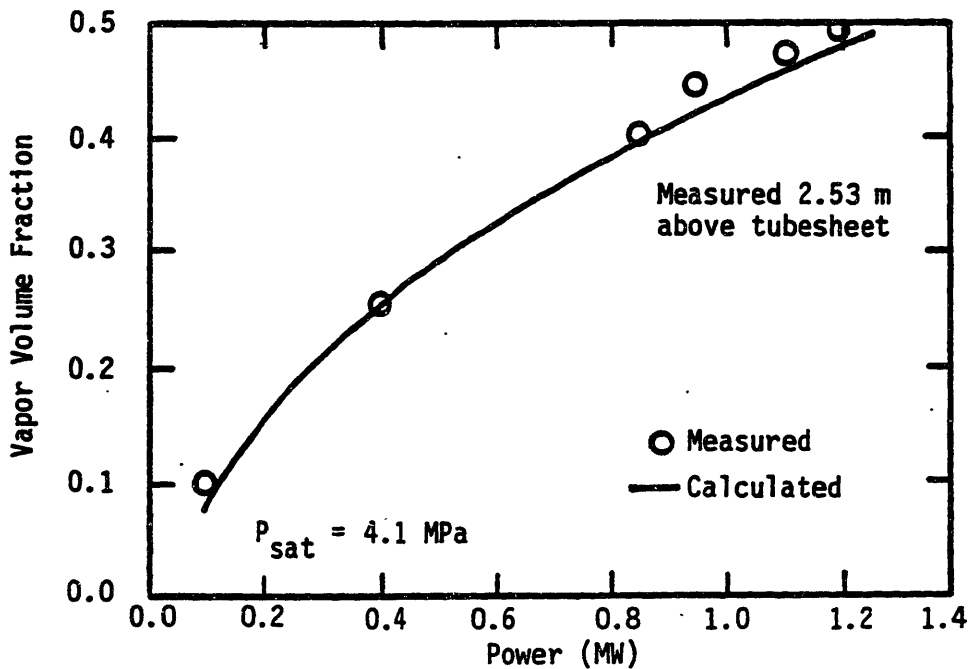
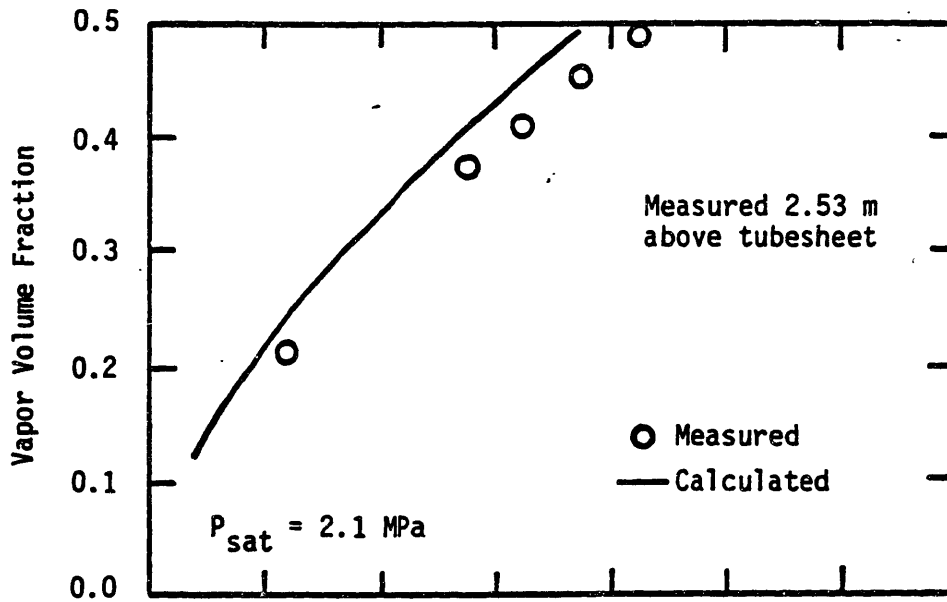


Figure 6.3-7. Riser inlet vapor volume fraction vs. power.

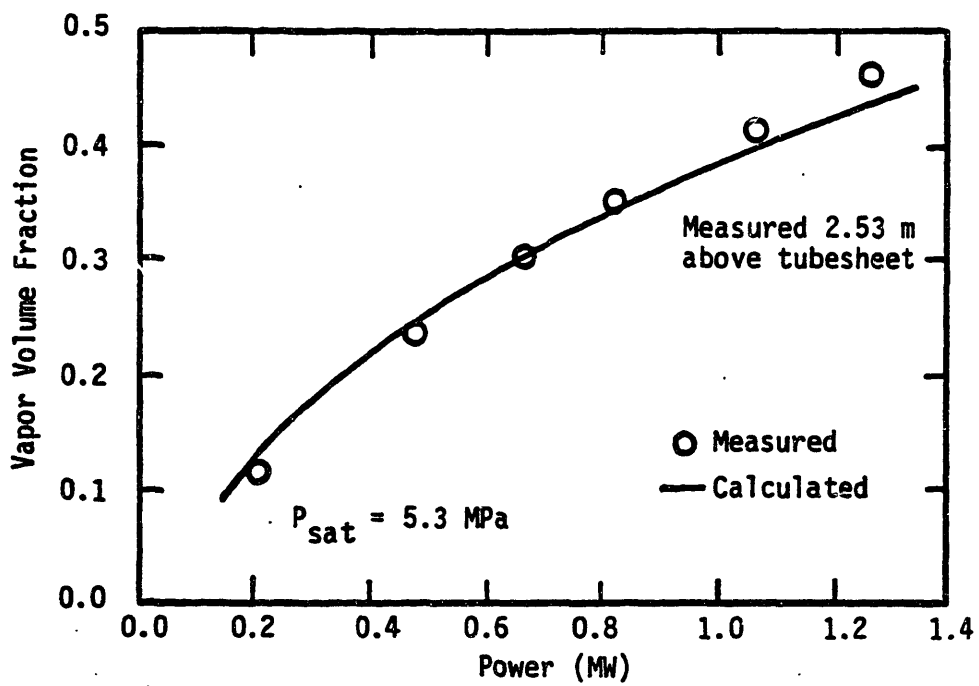


Figure 6.3-7.. Riser inlet vapor volume fraction vs. power. (Continued)

better agreement between calculated and measured vapor volume fractions. Data presented in Ref. (M4) supports this conclusion.

Figure 6.3-8 is a set of plots of the downcomer flowrate as a function of steam generator power for five pressures: 5.3 MPa, 4.6 MPa, 3.9 MPa, 2.1 MPa, and 1.7 MPa. Since the measured data at 3.9 MPa are used to determine  $K_{SEP}$  and  $K_D$  it is not surprising that the calculated downcomer flowrate is in excellent agreement with the data at this pressure. The comparison is also excellent at a secondary pressure of 4.6 MPa. The calculated results at a pressure of 5.3 MPa are in good agreement with the measured downcomer flowrate, although slightly high. At 2.1 MPa the calculated downcomer flows are somewhat larger than the measured flows at powers less than 1 MW and agreement is good at higher powers. Some of the deviation between calculation and experiment seen here can be attributed to errors in calculating  $u_{vj}$  and losses in the tube bundle and riser, i.e.  $K_{SEP}$  and  $K_D$ . Although  $K_{SEP}$  and  $K_D$  are assumed to be constant, they are in reality dependent on flow conditions in the tube bundle and riser. To some extent they account for the distribution (in an integral sense) of the pressure loss experienced by the fluid in the heated and unheated upflow portion of the steam generator. This distribution certainly depends on the mean system pressure in a boiling channel.

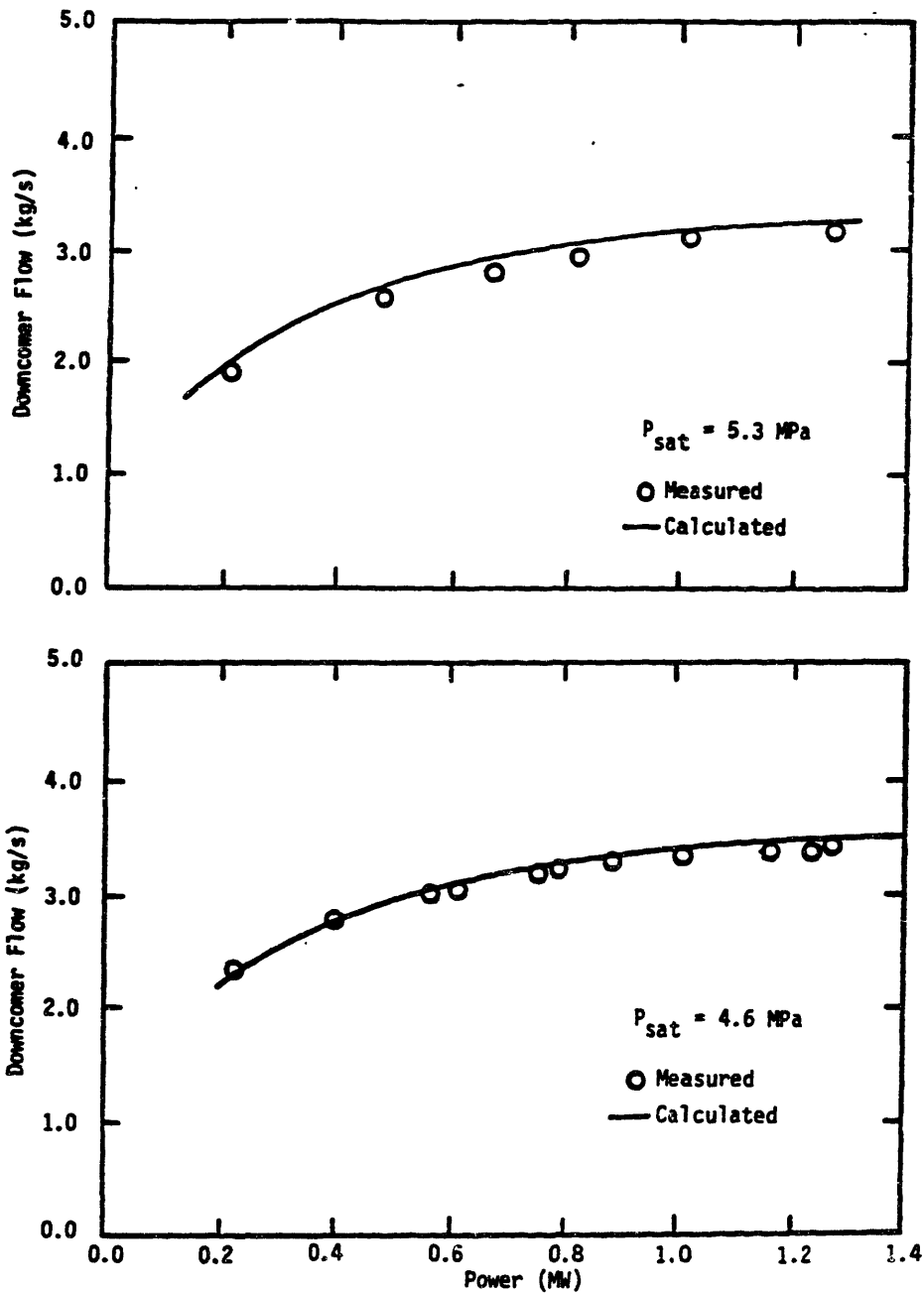


Figure 6.3-8. Downcomer flowrate vs. power.

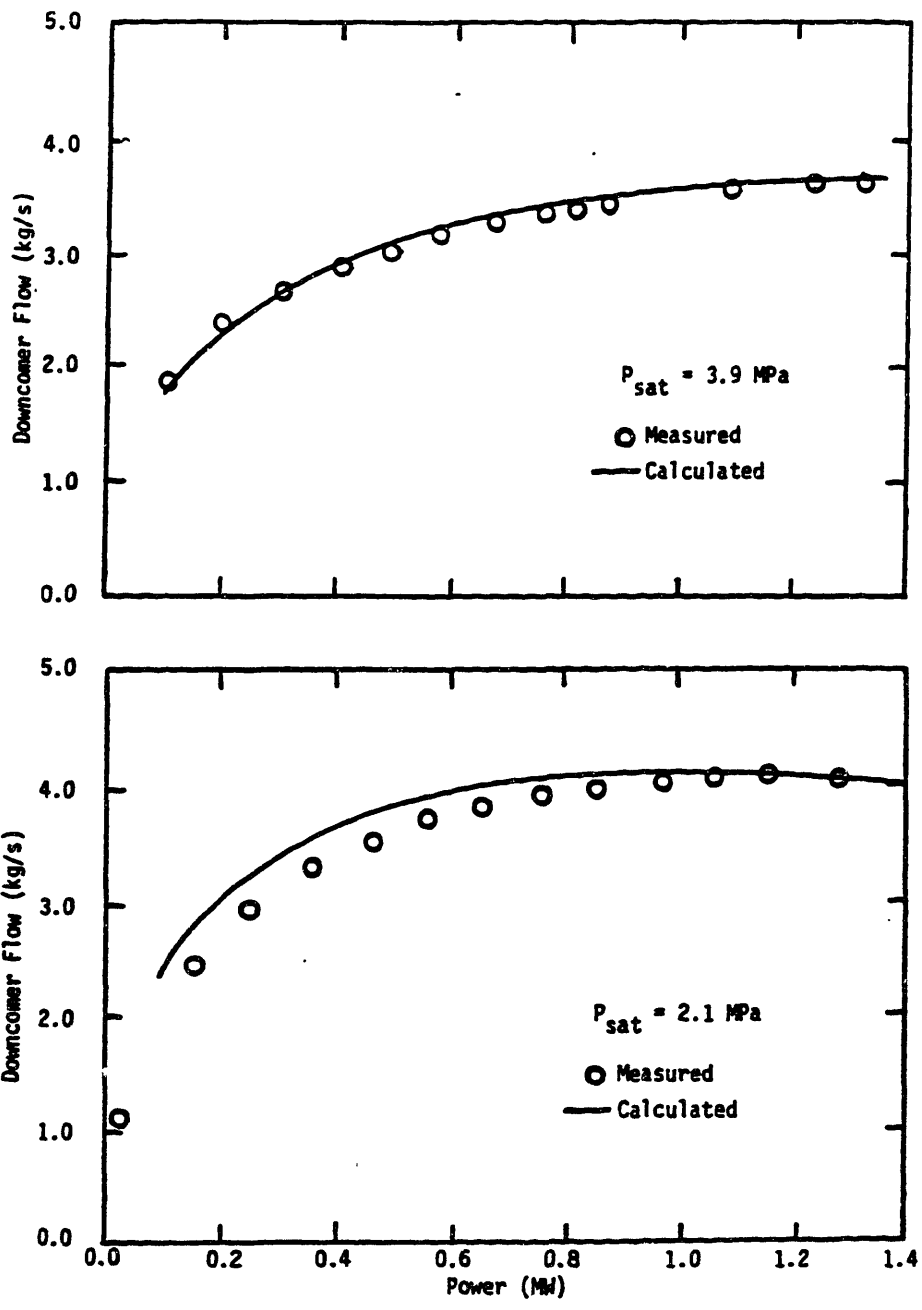


Figure 6.3-8. Downcomer flowrate vs. power. (Continued)

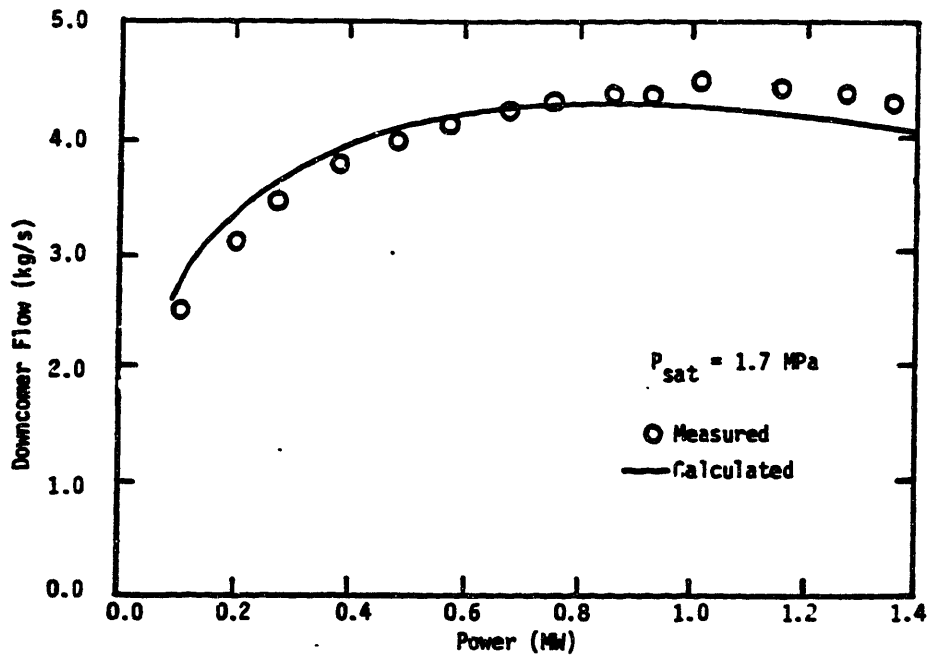


Figure 6.3-8. Downcomer flowrate vs. power. (Continued)

Finally, calculated downcomer flowrates at 1.7 MPa agree fairly well with the measured flowrates, although the shape of the calculated downcomer flowrate curve is slightly different from the shape of the measured flowrate variation with power. As with the 2.1 MPa calculations, the differences can be partially accounted for by errors in calculating  $u_{vj}$  and by using fixed values for  $K_{SEP}$  and  $K_D$ .

### 6.3.3 Additional Information for Transient Simulations

The fouling factor for heat transfer calculations still needs to be specified. Reference (M3) provides a number of measured steady state primary side temperature distributions and we used one of these measured curves to calculate a nominal fouling factor. Table 6.3-1 shows the steam generator operating conditions for this calculation. The nominal fouling factor obtained is  $1.29 \cdot 10^{-4} \text{ m}^2 \cdot \text{°K/W}$ . This fouling factor is used in all transient calculations. In Ref. (M3) the fouling factor used is  $1.25 \cdot 10^{-4} \text{ m}^2 \cdot \text{°K/W}$ , which compares favorably with our value for the fouling factor.

The initial heat transfer rate for any given transient is determined from a heat balance on the secondary side of the steam generator using measured data. Thus, the initial steady state heat transfer rate is given by:



Table 6.3-1  
 Steam Generator Conditions for Fouling Factor Calculation.

Quantity	Value
Power	1.05 MWt
Steam Pressure	4.6 MPa
Feedwater Temperature	80°C
Primary Inlet Temperature	301°C
Primary Outlet Temperature	269.5°C
Primary Flowrate	6.4 kg/s

$$W_{PIN} = \frac{q_B}{(H_{IN} - H_{OUT})} = \frac{W_S (H_{VS} - H_{FW})}{(H_{IN} - H_{OUT})} \quad (6.3-3)$$

In transients where the measured primary volumetric flowrate changes, we vary the input primary flowrate by the same fractional amount of the steady state flowrate. That is, if the measured primary volumetric flowrate changes by a factor of 0.5 based on the initial steady state volumetric flowrate, then we change the input primary flowrate by a factor of 0.5 based on the initial steady state calculated primary flowrate given by Eq. (6.3-3).

Two level measurements are presented in Ref. (M4). The level measurements presented are actually calculated from static level measurements. The first level presented in Ref. (M4), referred to in that work as the apparent level, is calculated assuming that the measured static head is caused by saturated liquid only. This assumption is probably not true when the water level is above the top of the riser, since free separation is used instead of separators. In addition, flashing can occur in the downcomer, which will also affect the level. The second level presented in Ref. (M4) is calculated in a manner that attempts to account for these effects. Pressure taps in the downcomer are used to measure the static head and the downcomer density is inferred from this. The density of the riser flow (which can be inferred from vapor volume fraction measurements at the riser inlet) is assumed to prevail above the riser outlet in the steam dome. These two densities along with a measurement of the static head from the bottom of the downcomer to the top of the steam generator are then used to calculate the level. We use this technique to calculate the level, except we assume that the downcomer fluid does not boil. Thus, the scheme used here to calculate the water level is slightly different from that presented in Chapter 5. The steps used in this case are:

- 1.) Determine  $M_{TOT}^{n+1}$  from:

$$M_{TOT}^{n+1} = M_{TOT}^n + \Delta t (W_{fw}^{n+1} - W_s^{n+1})$$

- 2.) Obtain  $M_{SD}^{n+1}$  (the advanced time steam dome - downcomer mass content) from:

$$M_{SD}^{n+1} = M_{TOT}^{n+1} - M_{TB}^{n+1} - M_R^{n+1}$$

- 3.) Calculate the steam dome - downcomer mass content that corresponds to a water level coincident with the top of the riser. Call this mass content  $M_{CUT}^{n+1}$ :

$$M_{CUT}^{n+1} = V_{TOP} \rho_{vs}^{n+1} + (V_{SD} - V_{TOP}) \rho_{\ell s}^{n+1} + V_{SUB} \rho_0^{n+1}$$

where,

- $V_{TOP} \equiv$  Volume of steam dome above riser exit;  
 $V_{SD} \equiv$  Volume of steam dome - downcomer excluding the small subcooled volume at bottom of downcomer;  
 $V_{SUB} \equiv$  Volume of small subcooled region at bottom of downcomer.

- 4.) If  $M_{SD}^{n+1} \geq M_{CUT}^{n+1}$ , then the following equation is used to calculate  $V_v$ :

$$v_v^{n+1} = \frac{V_{TOP} \rho_r^{-n+1} + (V_{SD} - V_{TOP}) \rho_{\ell s}^{n+1} + V_{SUB} \rho_0^{n+1} - M_{SD}^{n+1}}{(\rho_r^{-n+1} - \rho_{vs}^{n+1})}$$

Otherwise we use:

$$v_v^{n+1} = \frac{V_{SD} \rho_{\ell s}^{n+1} + V_{SUB} \rho_0^{n+1} - M_{SD}^{n+1}}{(\rho_{\ell s}^{n+1} - \rho_{vs}^{n+1})}$$

- 5.) Using  $v_v^{n+1}$  and the known steam generator geometry we can calculate  $\ell_w^{n+1}$ , the water level at the advanced time.

#### 6.3.4 Power Increase Test

The initial conditions used in the simulation of the power increase test are given in Table 6.3-2. Plots of the input used to conduct the simulation are shown in Fig. 6.3-9. The measured and calculated responses of the RD12 steam generator are shown in Fig. 6.3-10. The calculated riser inlet vapor volume fraction is in excellent agreement with the measured data. The same comment applies to the measured and calculated level. The calculated downcomer flowrate matches the measured downcomer flowrate for the first 25 seconds, which is actually a period of steady state operation. As the power increase is initiated, the calculated downcomer flowrate first dips and then starts to increase.

Table 6.3-2  
Initial Conditions for Power Increase Test.

Quantity	Value
Power	0.2704 MWt
Water Level*	0.2501 m
Downcomer Flowrate	2.366 kg/s
Steam Pressure	4.6 MPa
Steam Flowrate	0.11 kg/s
Feedwater Temperature	79.55°C
Riser Inlet Vapor Volume Fraction	0.1751
Primary Inlet Temperature	271.9°C
Primary Outlet Temperature	262.4°C
Primary Flowrate	5.66 kg/s

\* Referenced to top of riser.

The measured downcomer flowrate does not exhibit an initial dip; rather, it starts increasing as soon as the power increase starts. This difference in behavior between the measured and calculated downcomer flowrates is probably due to three dimensional effects that are not accounted for in our one-dimensional model. In our one-dimensional, large control volume model, the dip in the calculated downcomer flowrate is caused by the increased boiling occurring in the

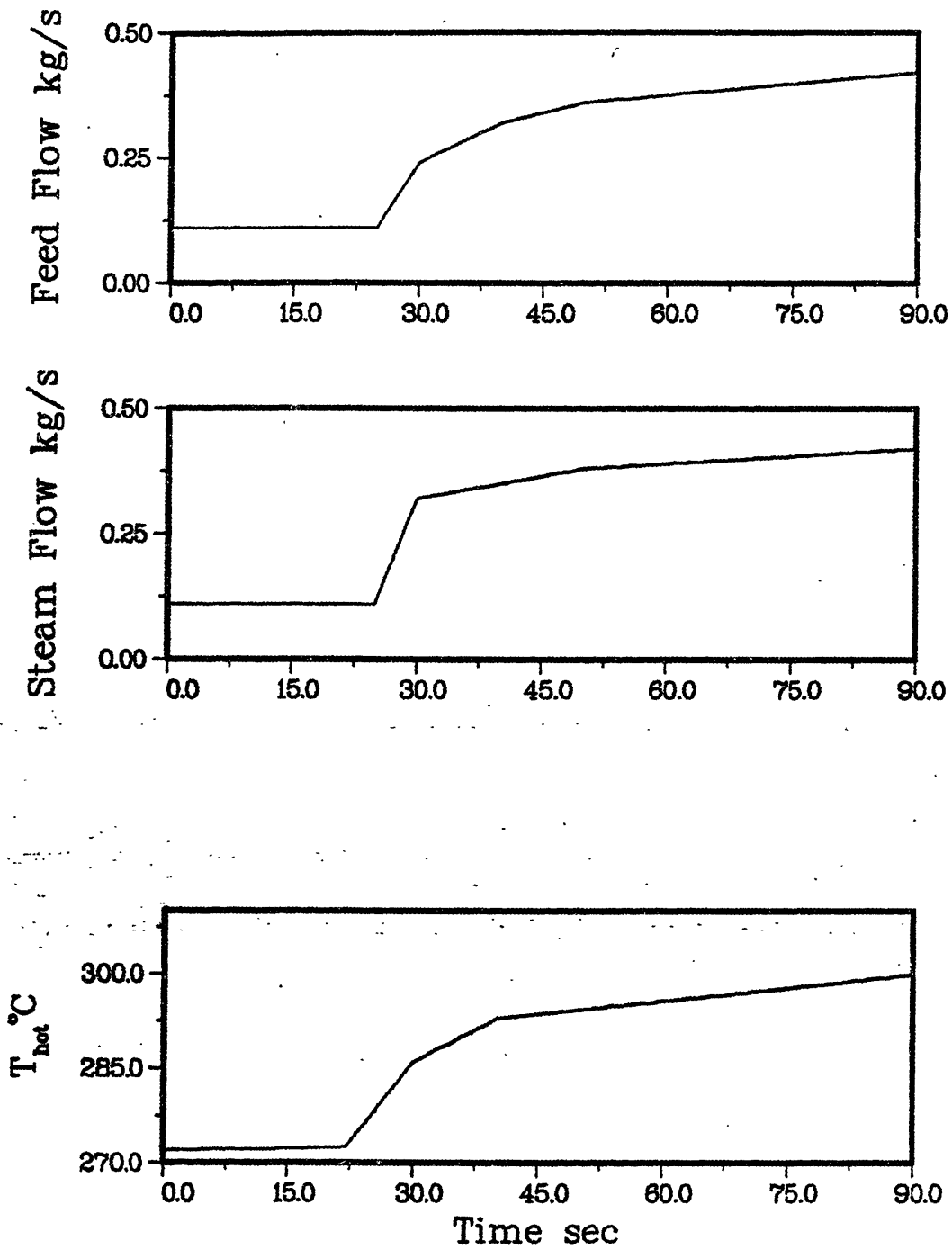


Figure 6.3-9. Input for power increase test.

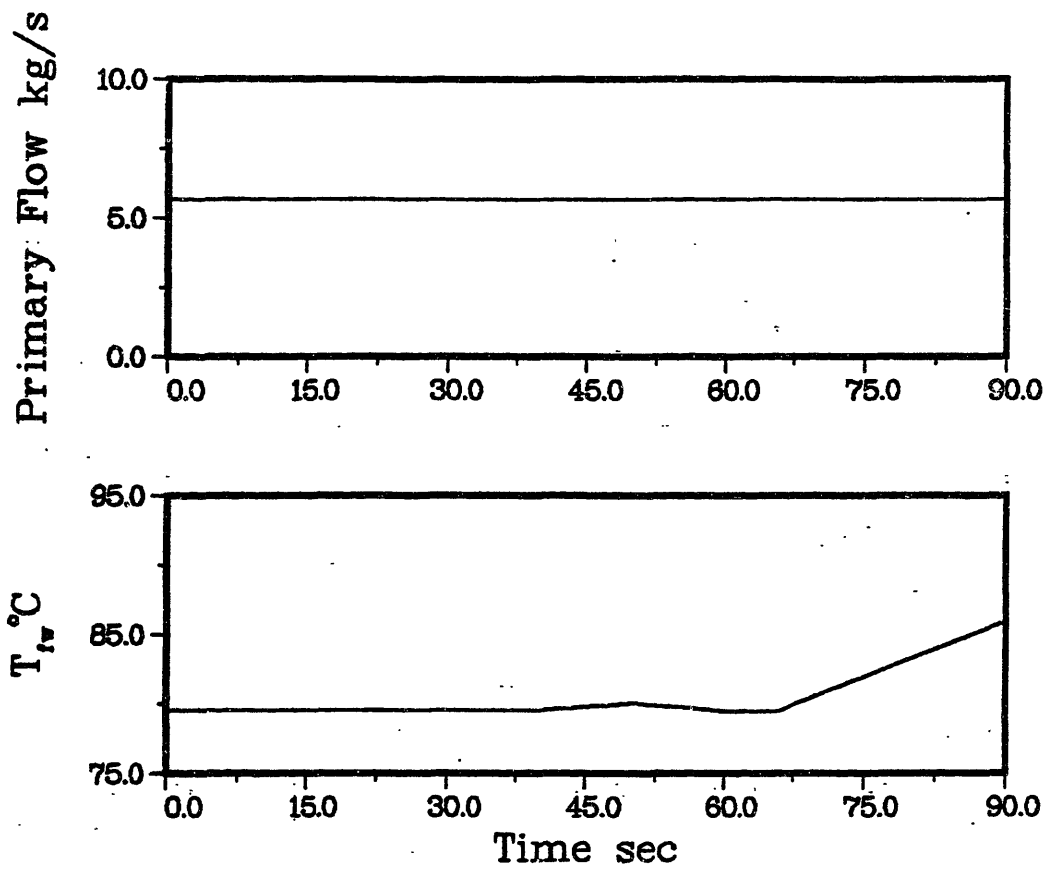


Figure 6.3-9. Input for power increase test. (Continued)

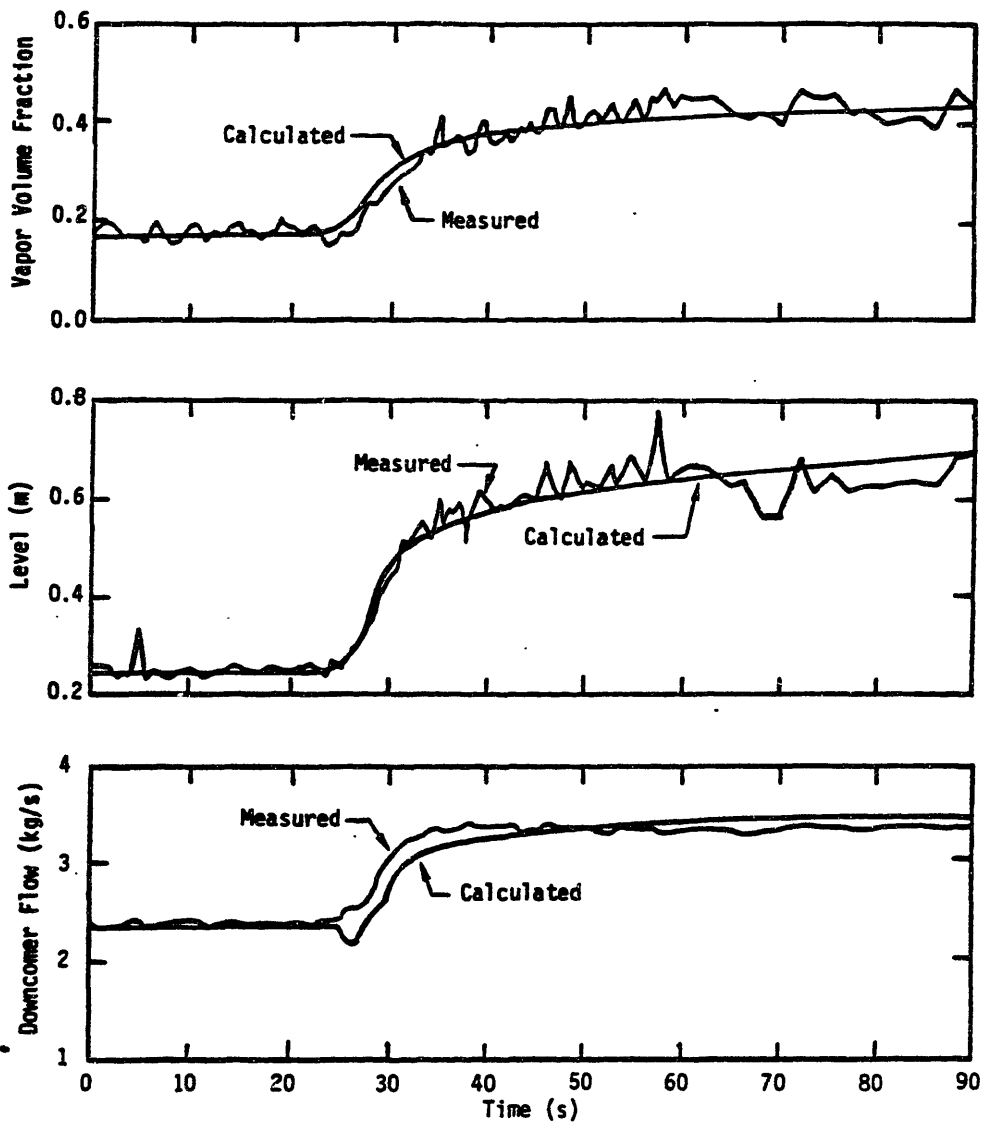


Figure 6.3-10. Steam generator response for power increase test.



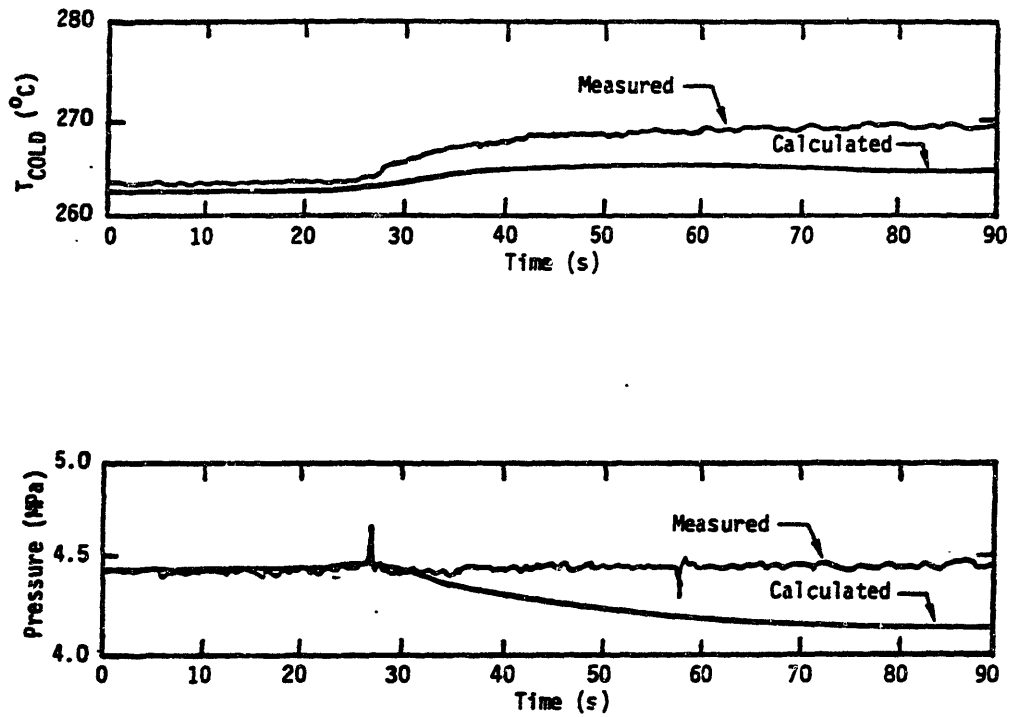


Figure 6.3-10 Steam generator response for power increase test. (Continued)

tube bundle as the result of the increased heat transfer rate. This increased boiling expels mass from our one-dimensional volume resulting in an increase in the exit flowrate and a decrease in the inlet flowrate (i.e. the downcomer flowrate). This calculated decrease in the downcomer flowrate is eventually offset by the increased natural circulation driving head caused by the increased vapor volume fraction in the tube bundle and riser. In the actual steam generator the increased boiling causes a three-dimensional redistribution of the flowrate rather than the one-dimensional adjustment that we calculate, thereby softening or eliminating the effect on the downcomer flowrate. Once the calculated downcomer flowrate has recovered from its initial dip, the calculated flowrate is in good agreement with the measured data.

The results for the primary outlet temperature ( $T_{\text{COLD}}$ ) and the secondary pressure must be considered together. As can be seen, both the calculated cold leg temperature and secondary pressure are less than the corresponding measured quantities. The calculated response of the cold leg temperature is directly linked to the calculated response of the secondary pressure through the heat transfer rate. Thus, we would expect to see the cold leg temperature follow the trend set by the secondary pressure. The cold leg temperature is also affected by the behavior of the hot leg temperature. The calculated cold leg temperature shows a less marked increase than the measured cold leg temperature. The

increasing hot leg temperature causes the calculated cold leg temperature to increase, however, the decreasing calculated secondary pressure limits, or holds down, the increase in the cold leg temperature. Therefore, the error in the behavior of the cold leg temperature can be traced to the error in the behavior of the calculated secondary pressure. The behavior of the calculated secondary pressure is strongly influenced by the input steam flow, so it is reasonable to assume that some of the error in the calculated pressure can be attributed to the input steam flow. In addition, we account for the integral preheater present in the RD12 steam generator by using an approximation in our model which may not properly represent the heat transfer dynamics, although it is not clear what effect this has on the calculated cold leg temperature and secondary pressure.

#### 6.3.5 Power Decrease Test

The initial conditions for the power decrease test simulation are given in Table 6.3-3. Figure 6.3-11 shows the inputs used to drive the simulation. The measured and calculated response of various steam generator parameters are shown in Fig. 6.3-12.

The calculated and measured riser inlet vapor volume fractions are in excellent agreement. The calculated steam generator level is in good agreement with the data, although after 40 seconds the calculated level is less than the measured level. This difference could be due to integration of

Table 6.3-3  
Initial Conditions for Power Decrease Test.

Quantity	Value
Power	1.154 MWt
Water Level*	0.4410 m
Downcomer Flowrate	3.415 m
Steam Pressure	4.6 MPa
Steam Flowrate	0.4699 kg/s
Feedwater Temperature	80.05°C
Riser Inlet Vapor Volume Fraction	0.4409
Primary Inlet Temperature	305.4°C
Primary Outlet Temperature	270.6°C
Primary Flowrate	6.208 kg/s

\*Referenced to top of riser.

any error in the measured feedwater and steam flowrates used as input. The calculated downcomer flowrate is in good agreement with the measured downcomer flowrate, except for the time period extending from 22 to 35 seconds. During this time span the calculated downcomer flow shows a slight increase before it starts to decrease. The reason for this behavior is analogous to the reason given for the dip in the downcomer flowrate in the power increase test, except here

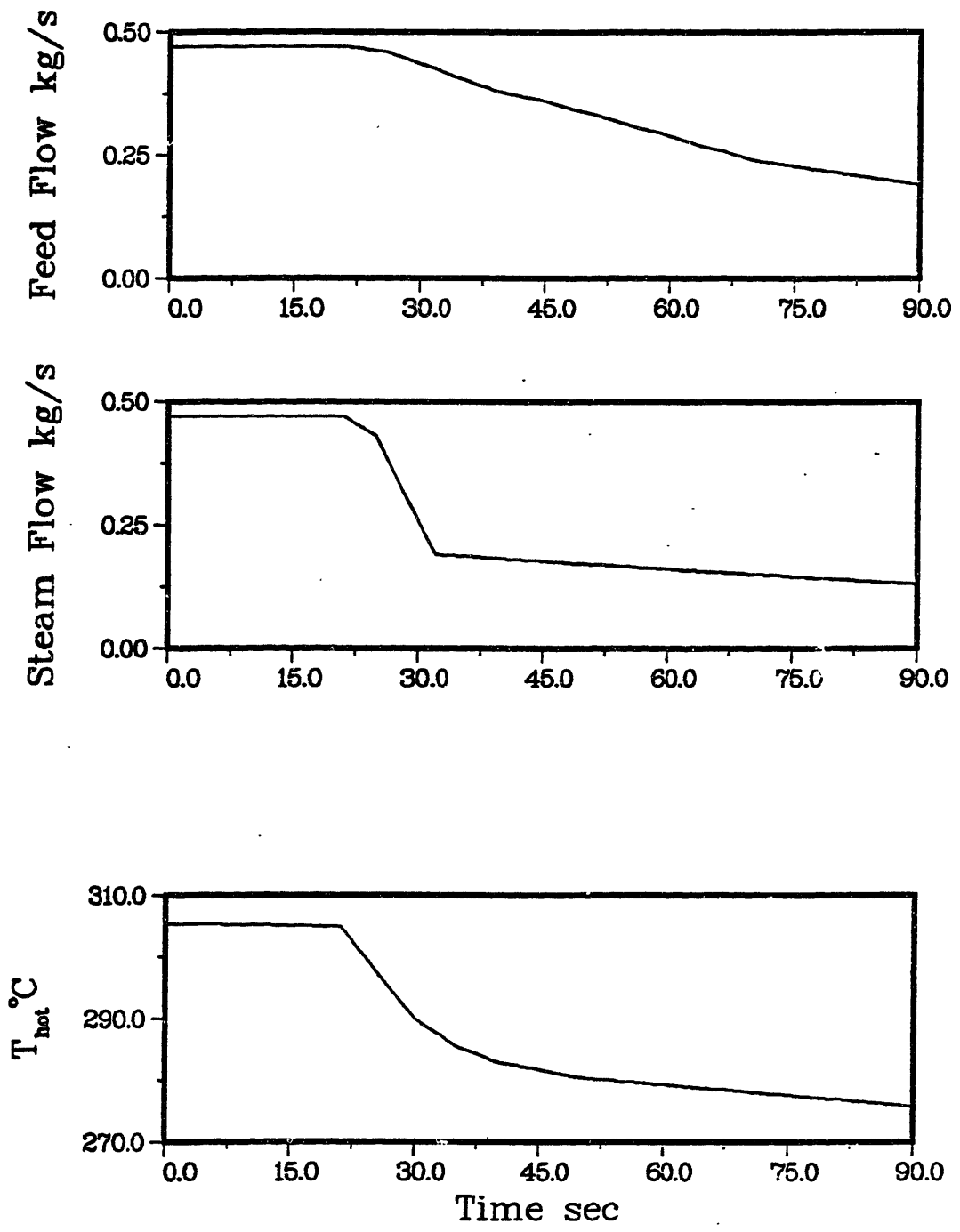


Figure 6.3-11. Input for power decrease test.

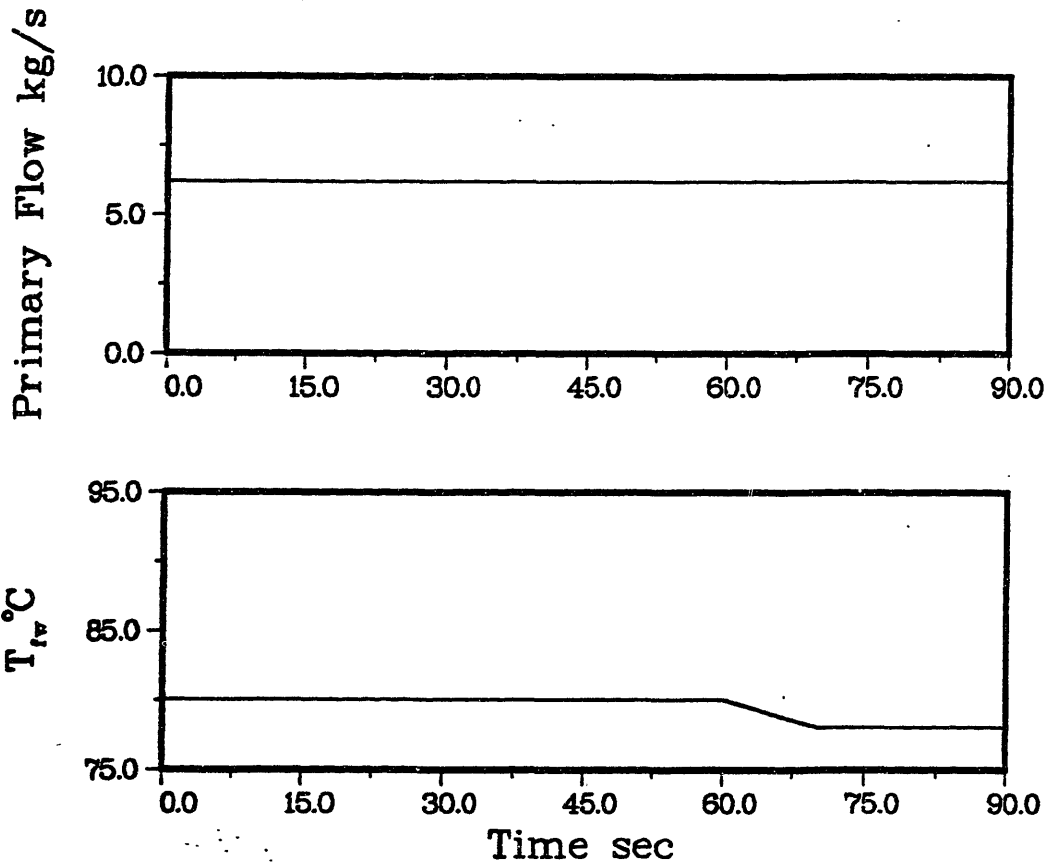


Figure 6.3-11. Input for power decrease test. (Continued)

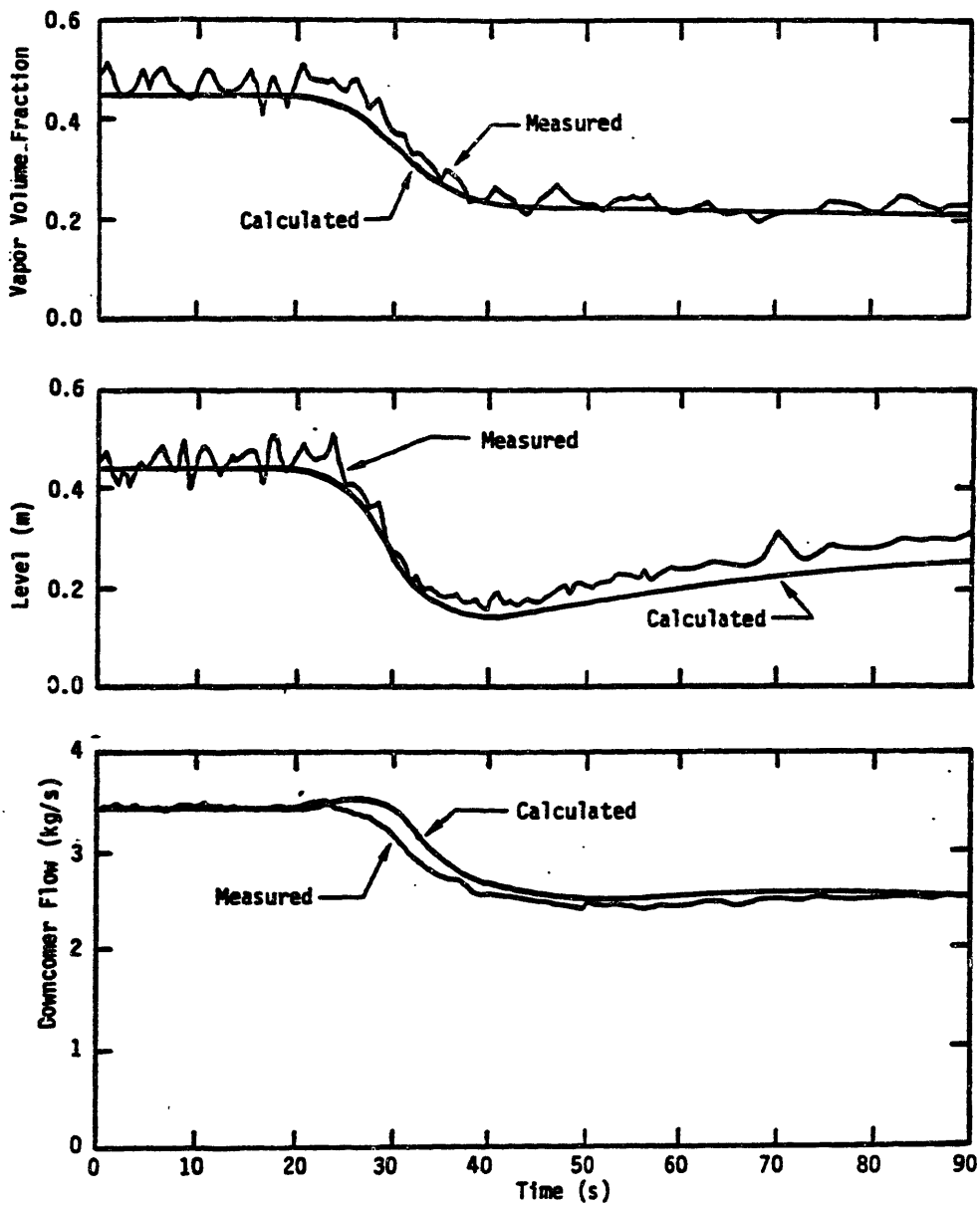


Figure 6.3-12. Steam generator response for power decrease test.

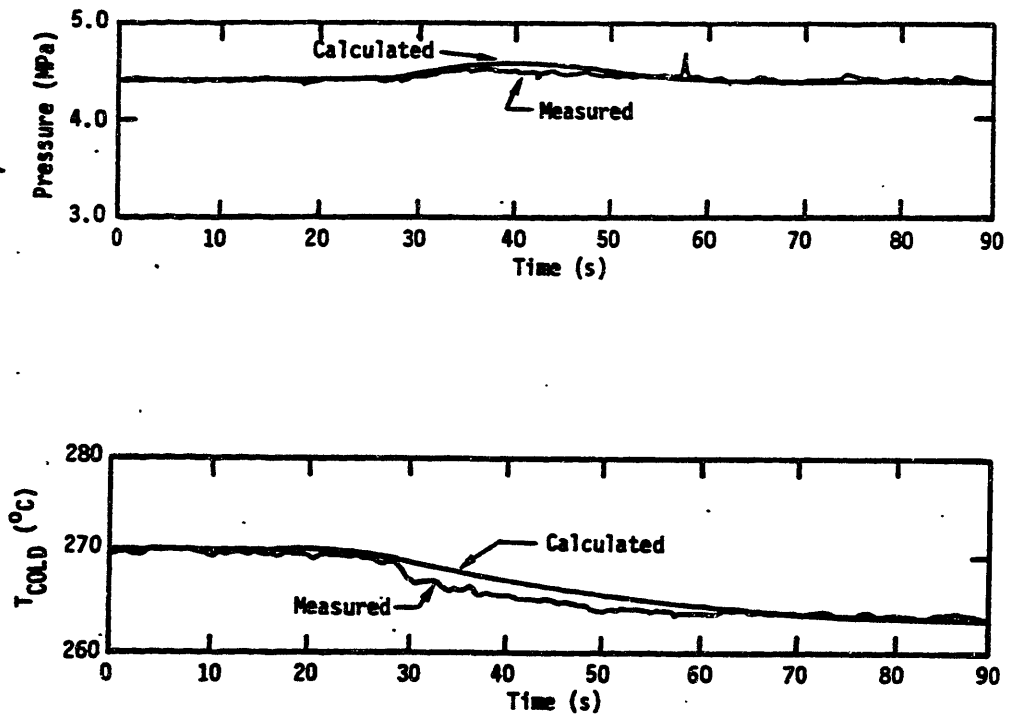


Figure 6.3-12. Steam generator response for power decrease test. (Continued)



the decreased boiling in the tube bundle causes a "shrink" in that volume resulting in a decrease in the exit flow and an increase in the inlet flow. Again, we can attribute the stronger response of the calculated downcomer flowrate to using a one-dimensional model to represent a three-dimensional effect. The increased calculated downcomer flowrate also affects the calculated level and contributes to the error seen between the calculated and measured levels.

The calculated pressure is in excellent agreement with the measured pressure. The calculated cold leg temperature matches the measured temperature except for the time span extending from 28 to 60 seconds. In this interval the calculated cold leg temperature is a little larger than the measured cold leg temperature. This may be due in part to the heat transfer dynamics associated with the integral preheater, which are modeled approximately in our calculation.

#### 6.3.6 Primary Flowrate Decrease Test

The initial conditions for the primary flowrate decrease test are given in Table 6.3-4. The inputs used to drive the transient are shown in Fig. 6.3-13. The measured and calculated responses of the RD12 steam generator are shown in Fig. 6.3-14.

The calculated riser inlet vapor volume fraction is in excellent agreement with the measured results. The calculated level follows the same trend as the measured level,

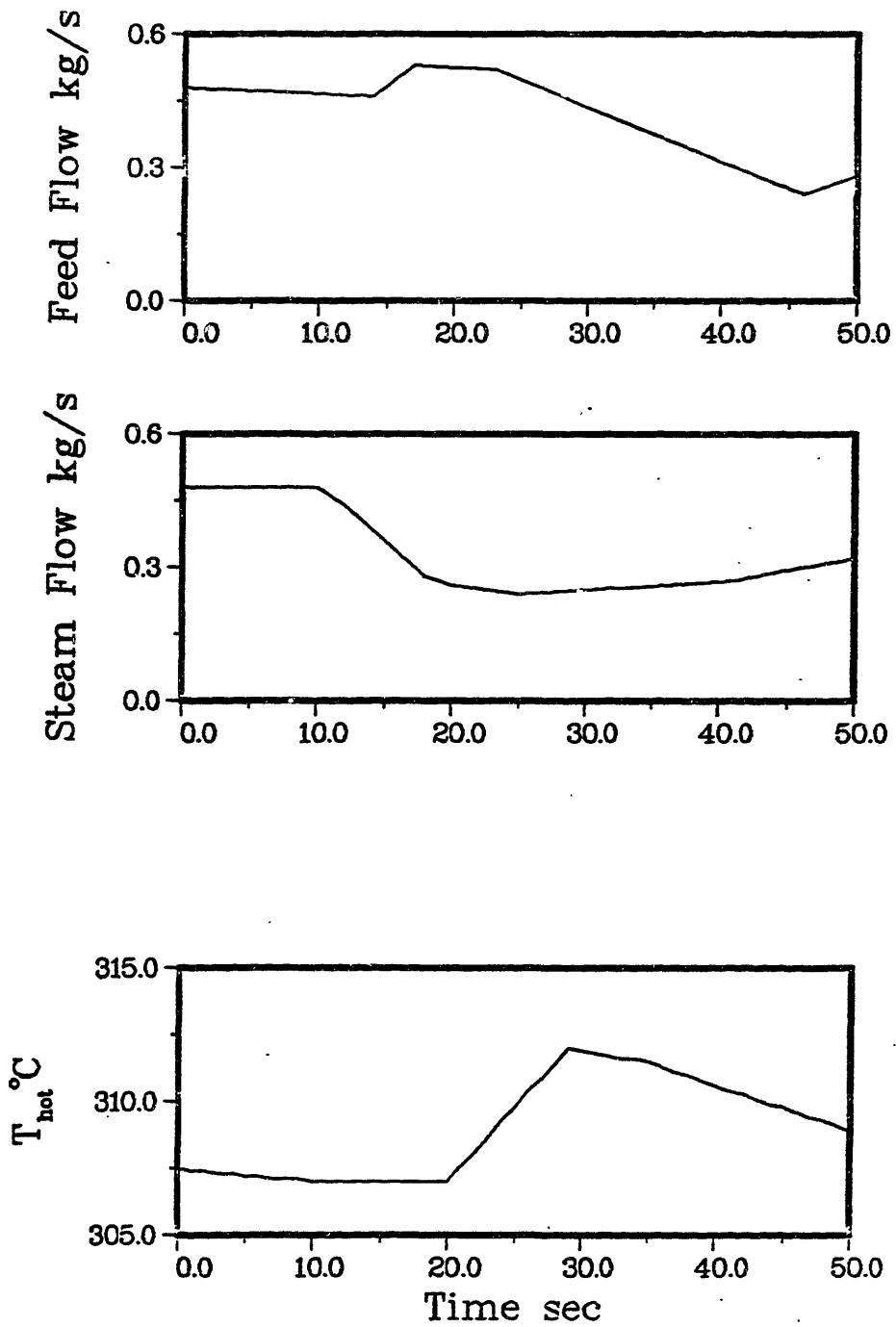


Figure 6.3-13. Input for primary flowrate decrease test.

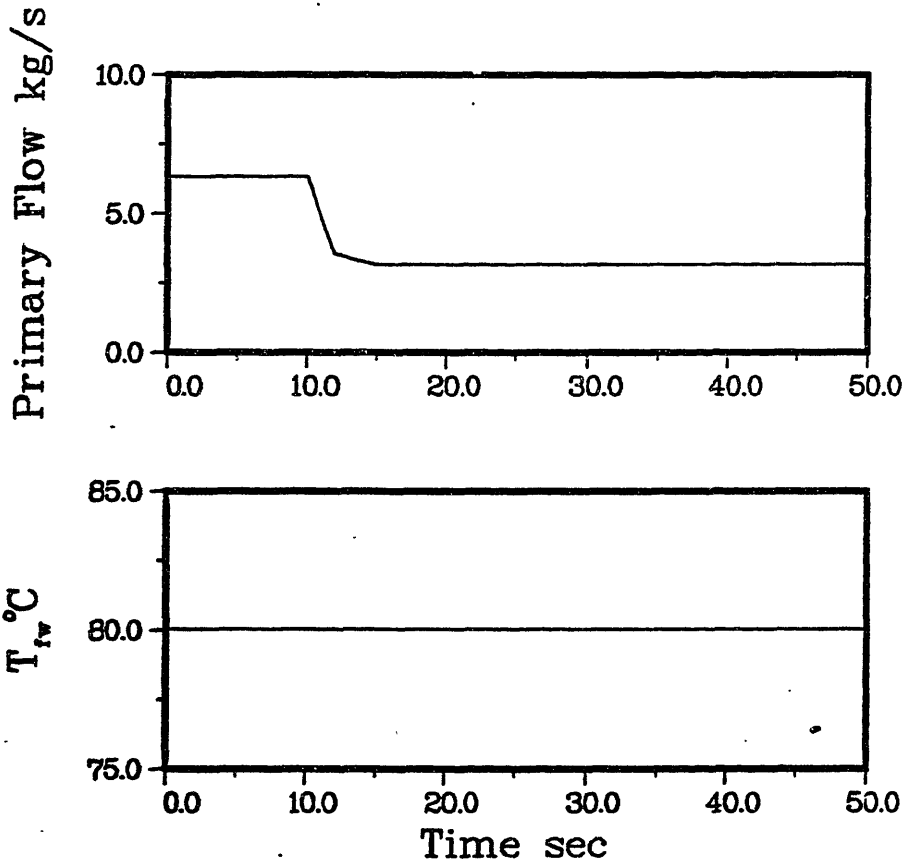


Figure 6.3-13. Input for primary flowrate decrease test.  
(Continued)

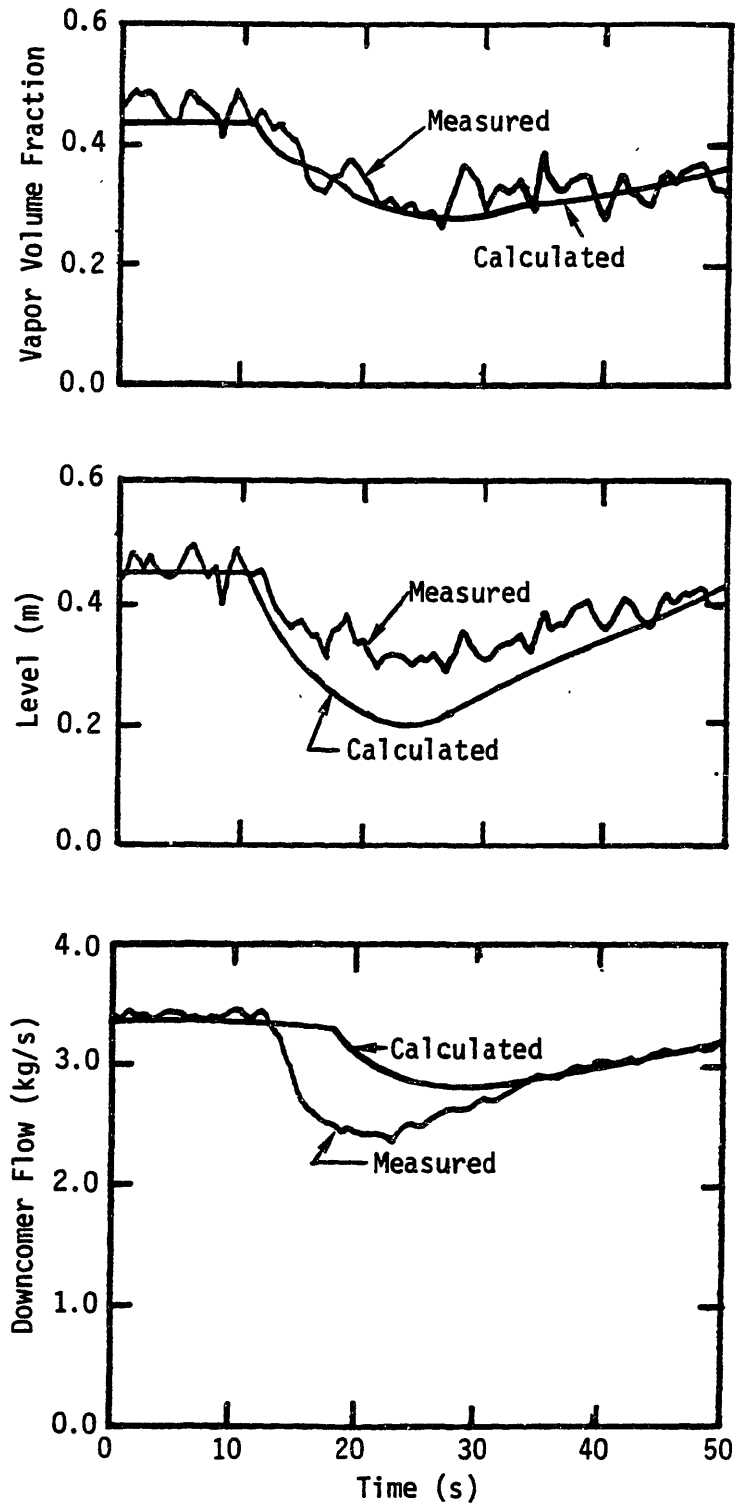


Figure 6.3-14. Steam generator response for primary flowrate decrease test.

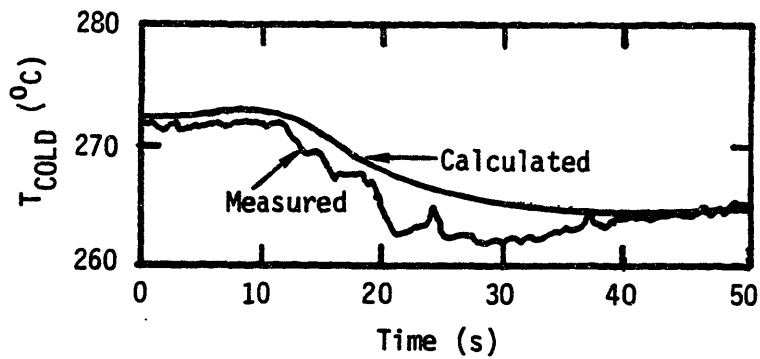
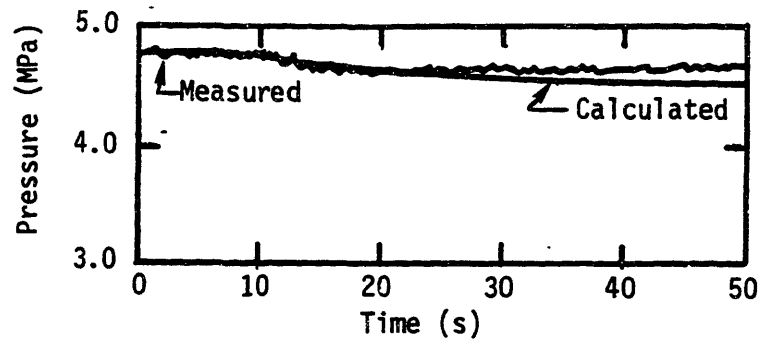


Figure 6.3-14. Steam generator response for primary flowrate decrease test. (Continued)

Table 6.3-4  
Initial Conditions for Primary Flowrate Decrease Test.

Quantity	Value
Power	1.178 MWt
Water Level*	0.4501 m
Downcomer Flowrate	3.383 kg/s
Steam Pressure	4.75 MPa
Steam Flowrate	0.4799 kg/s
Feedwater Temperature	80.05°C
Riser Inlet Vapor Volume Fraction	0.4391
Primary Inlet Temperature	307.5°C
Primary Outlet Temperature	272.7°C
Primary Flowrate	6.317 kg/s

\* Referenced to top of riser.

but with a marked difference in magnitude. The calculated downcomer flowrate is greater than the measured downcomer flowrate, which is consistent with the results obtained for the level. It turns out that there is boiling in the downcomer during this test, as demonstrated by Fig. 6.3-15, which is a plot of the measured downcomer vapor volume fraction versus time. In our model we do not allow boiling in the downcomer. This is a major reason why the calculated

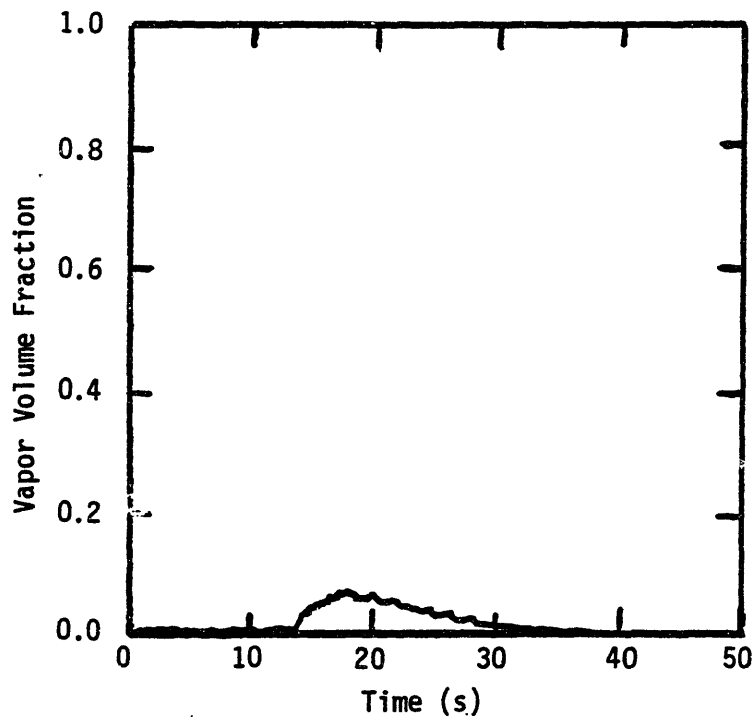


Figure 6.3-15. Downcomer vapor volume fraction during primary flowrate decrease test.

and measured levels and downcomer flowrates do not agree. The presence of vapor in the downcomer decreases the driving head for the recirculation flow and results in a sharp decrease in the measured downcomer flow. In our model we cannot account for this effect, which is why the calculated downcomer flowrate is too high. The boiling in the downcomer also tends to cause a "swell" in the level, so that the measured level does not decrease as much as the calculated level. The fact that the calculated downcomer flowrate is too high also contributes to low calculated value for the level.

The calculated pressure is in good agreement with the measured pressure for the first half of the transient. During the final 25 seconds of the transient the calculated pressure is a little below the measured pressure, which may be the result of error in the input steam flowrate. The calculated cold leg temperature follows the same trend as the measured cold leg temperature, except that it does not respond as sharply as the measured data. Some of this error is due to the approximation made in modeling the preheater.

#### 6.3.7 Primary Flowrate Increase Test

The initial conditions for the primary flowrate increase test are given in Table 6.3-5. The input used to drive the simulation is shown in Fig. 6.3-16. Figure 6.3-17 shows the calculated and measured results for the test.



Table 6.3-5  
Initial Conditions for Primary Flowrate Increase Test.

Quantity	Value
Power	0.7025 MWt
Water Level*	0.1010 m
Downcomer Flowrate	3.147 kg/s
Steam Pressure	4.6 MPa
Steam Flowrate	0.2861 kg/s
Feedwater Temperature	80.05°C
Riser Inlet Vapor Volume Fraction	0.3361
Primary Inlet Temperature	306.6°C
Primary Outlet Temperature	264.8°C
Primary Flowrate	3.159 kg/s

\* Referenced to top of riser.

the calculated result is high. The calculated level is in excellent agreement with the measured level. The calculated level is a little high towards the end of the simulation, which is due, in part, to the integrated effect of input feedwater flowrate errors. The calculated downcomer flowrate follows the same trend as the measured downcomer flow, and reaches a final value somewhat smaller (by about 0.1 kg/s) than the measured value. The response of the

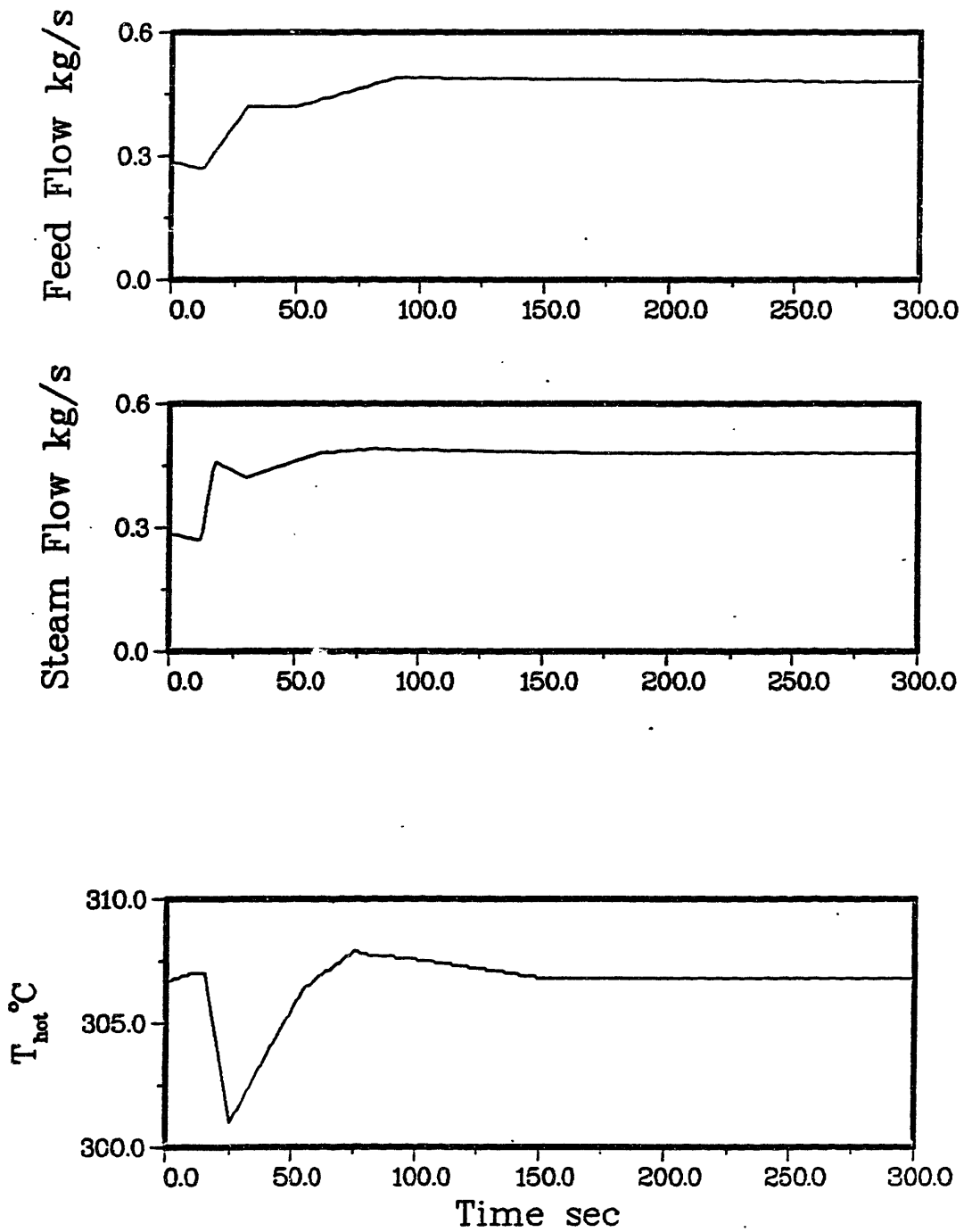


Figure 6.3-16. Input for primary flowrate increase test.

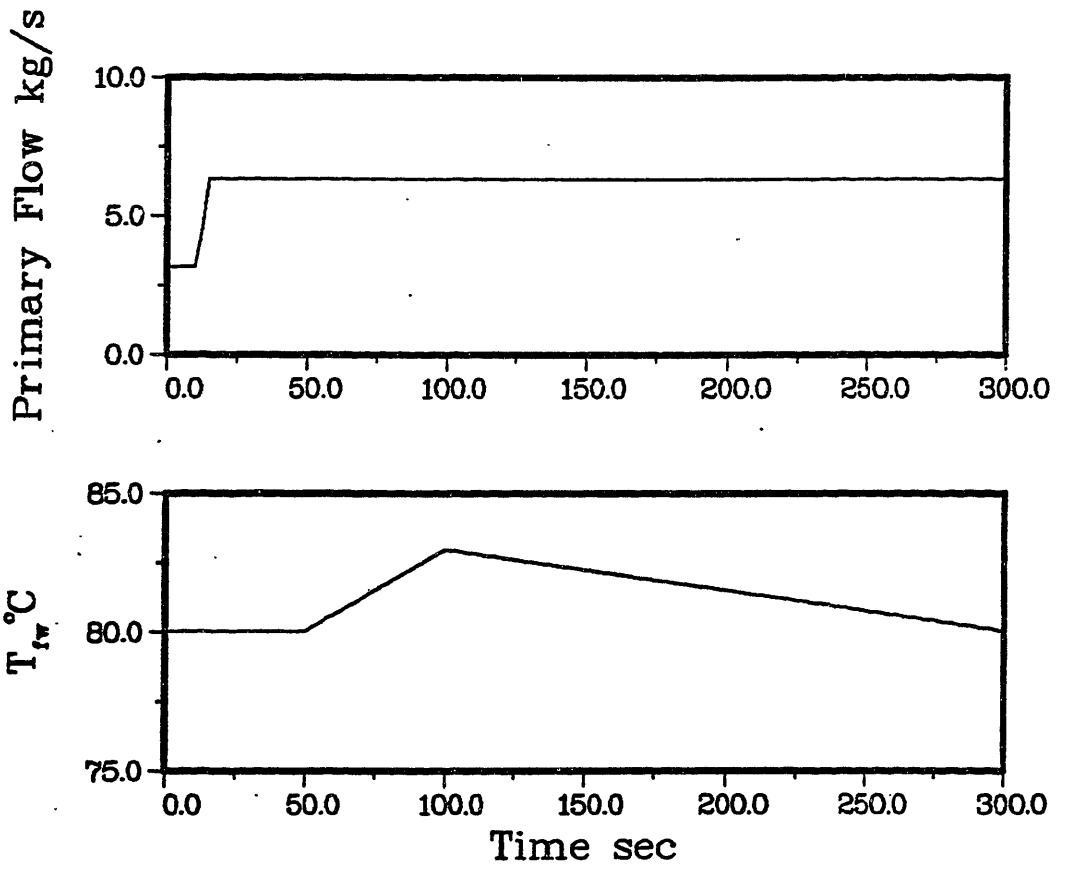


Figure 6.3-16. Input for primary flowrate increase test.  
(Continued)

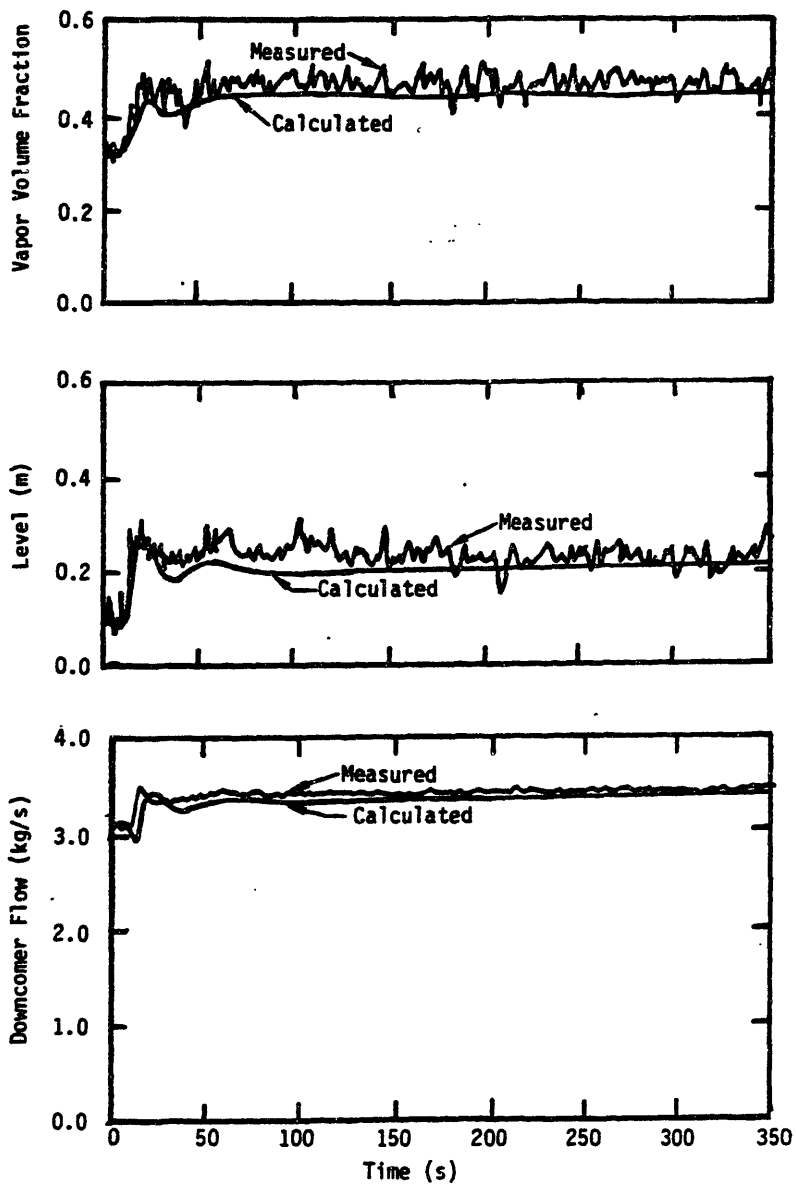


Figure 6.3-17. Steam generator response for primary flowrate increase test.

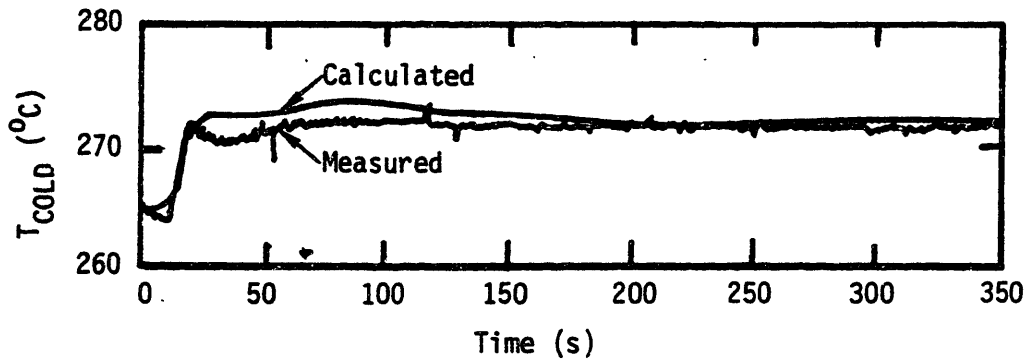
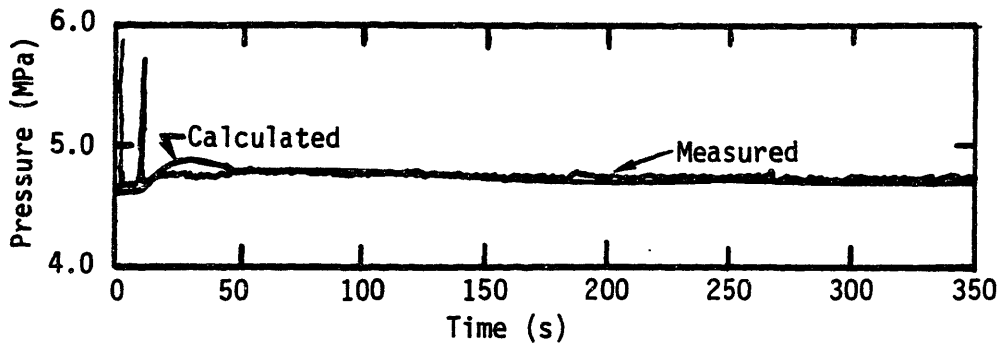


Figure 6.3-17. Steam generator response for primary flowrate increase test. (Continued)

The measured and calculated riser inlet vapor volume fractions are in good agreement, although the calculated vapor volume fraction is a little low. The calculated level shows the same trends as the measured level, correctly exhibiting level swell and shrink. For some portions of the transient the calculated level is less than the measured level, which, to some extent, can be attributed to integration of errors in the input feedwater and steam flowrates. The calculated downcomer flowrate responds in the same manner as the measured flowrate, although it appears to lag behind the measured results.

The calculated pressure is in excellent agreement with the measured pressure, except for a short period at 25 seconds where the calculated pressure is a little high. The calculated cold leg temperature is in good agreement with the measured temperature. Errors in the calculated temperature can be partially accounted for by the approximation made regarding the integral preheater.

#### 6.3.8 Secondary Pressure Increase Test

The initial conditions for the secondary pressure increase test are given in Table 6.3-6. The transient input boundary conditions are shown in Fig. 6.3-18. Figure 6.3-19 shows the measured and calculated results for the test.

The calculated riser inlet vapor volume fraction is in good agreement with the measured vapor volume fraction except for a time span extending from 12 to 20 seconds, where

Table 6.3-6  
Initial Conditions for Secondary Pressure Increase Test.

Quantity	Value
Power	0.8363 MWt
Water Level*	0.4101 m
Downcomer Flowrate	3.235 kg/s
Steam Pressure	4.65 MPa
Steam Flowrate	0.335 kg/s
Feedwater Temperature	70.35°C
Riser Inlet Vapor Volume Fraction	0.3664
Primary Inlet Temperature	293.1°C
Primary Outlet Temperature	268.5°C
Primary Flowrate	6.557 kg/s

\* Referenced to top of riser.

calculated downcomer flowrate at 10 and 18 seconds is more pronounced than the response of the measured flowrate, but this is probably due to using a one-dimensional model as discussed in 6.3.4 and 6.3.5.

The calculated pressure is in good agreement with the measured pressure, although the calculated pressure increases less rapidly than the measured pressure and attains a higher final value than the measured pressure. Some of

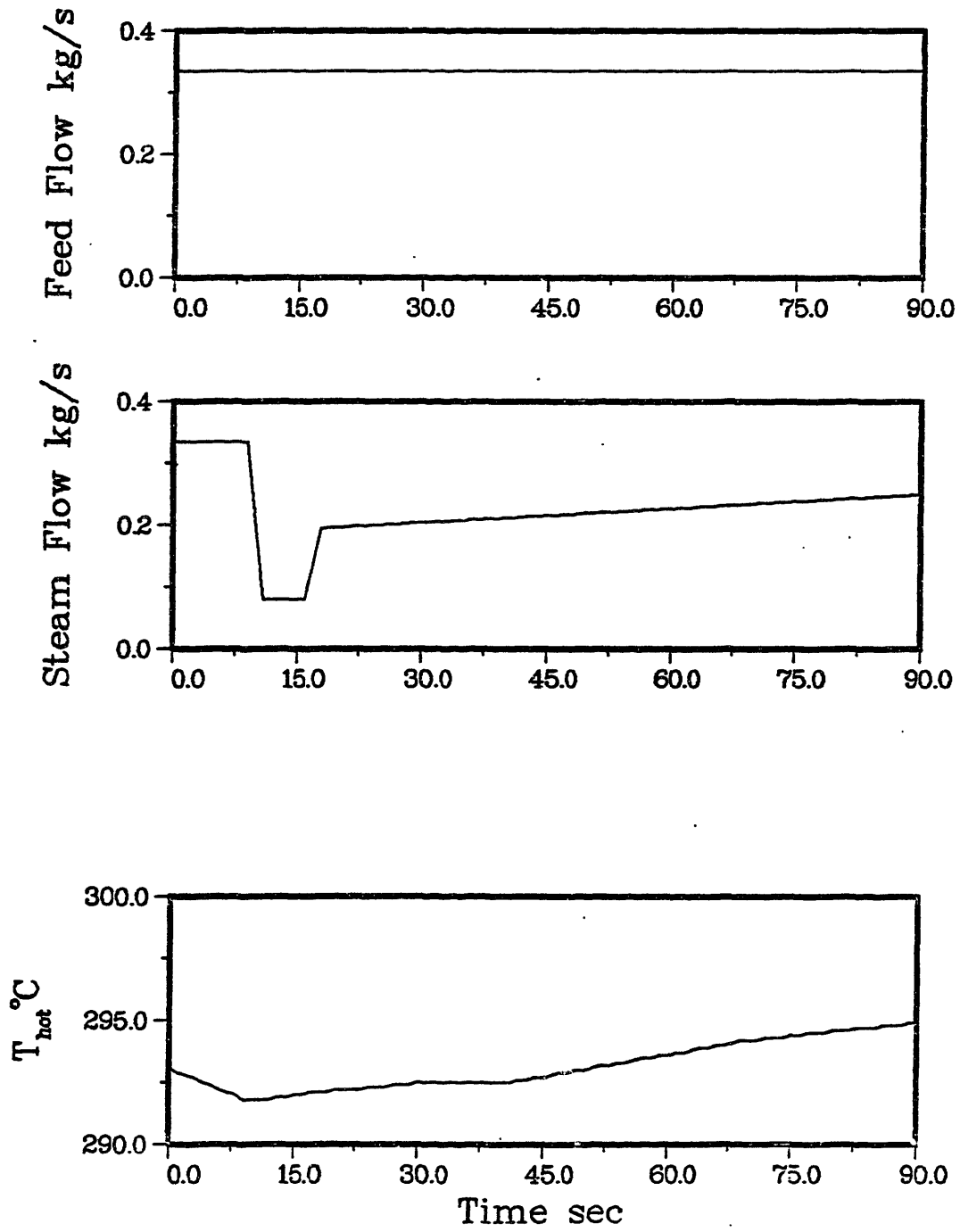


Figure 6.3-18. Input for secondary pressure increase test.



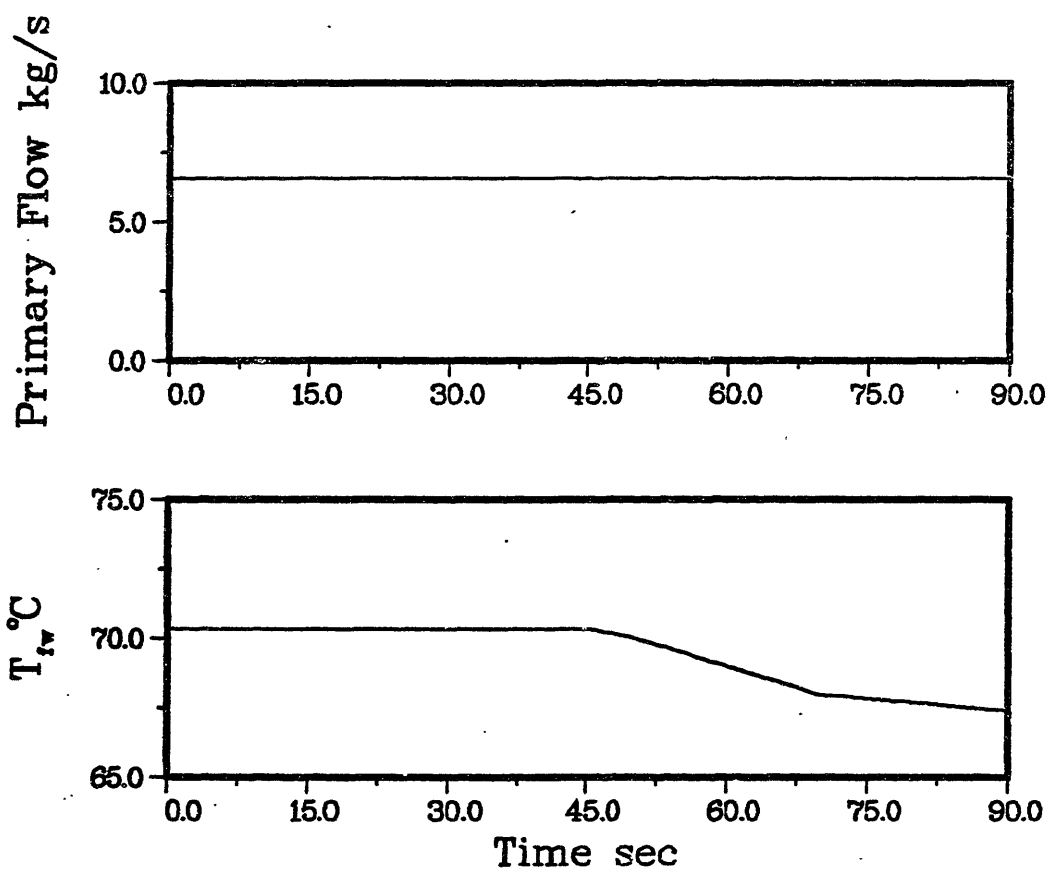


Figure 6.3-18. Input for secondary pressure increase test. (Continued)

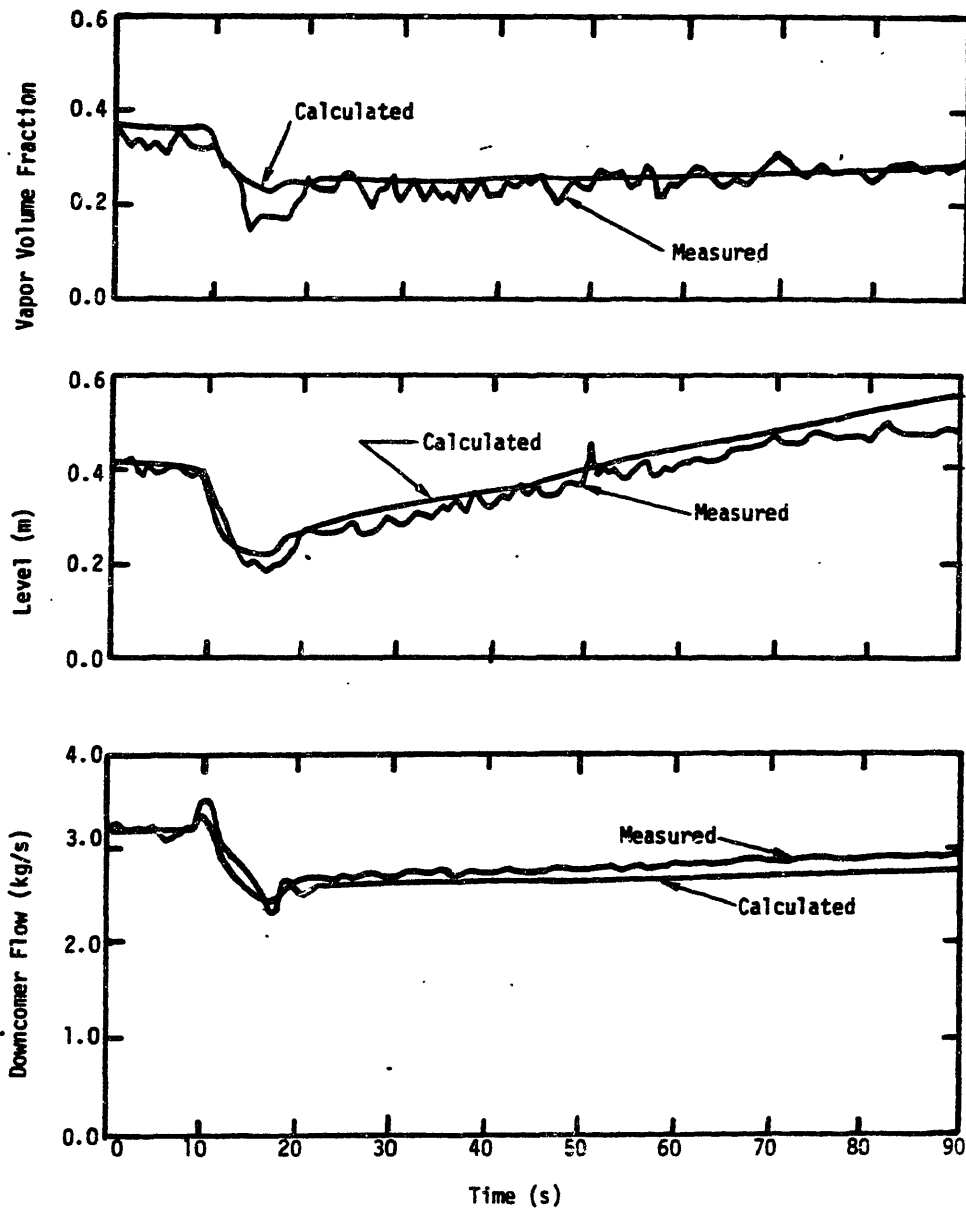


Figure 6.3-19. Steam generator response for secondary pressure increase test.

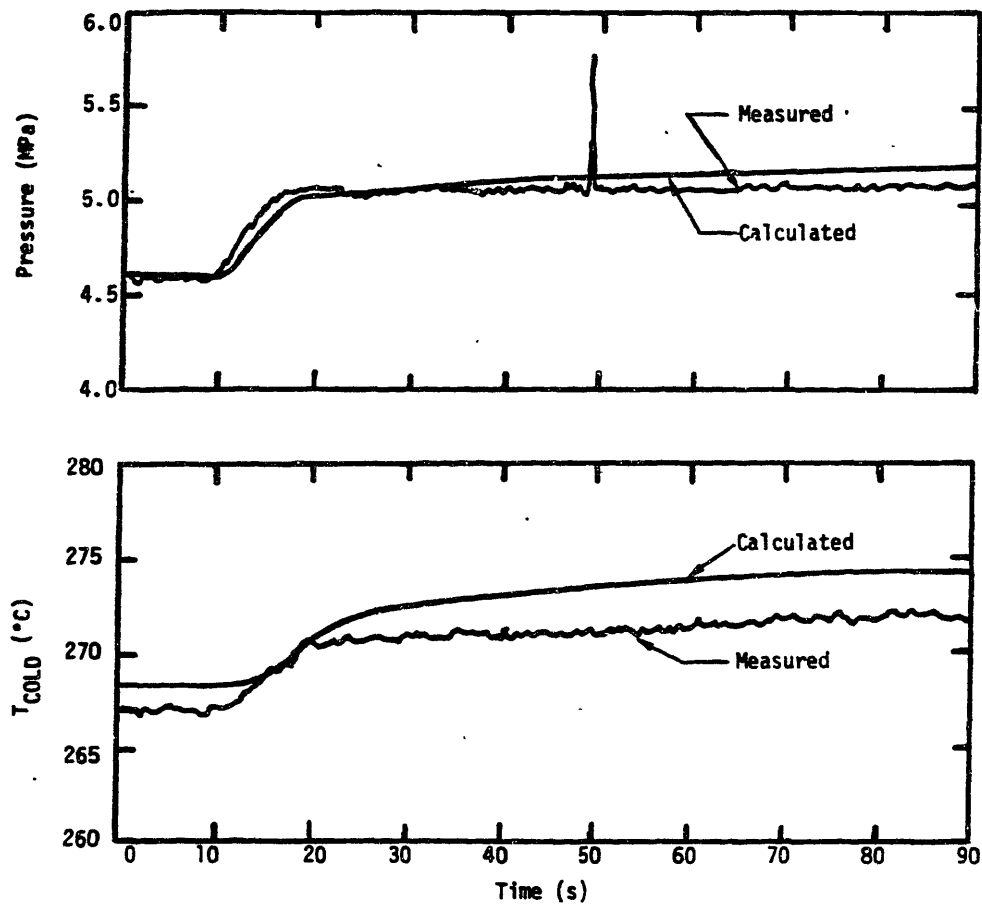


Figure 6.3-19. Steam generator response for secondary pressure increase test. (Continued)

the error observed here is probably due to error in the input steam flowrate. The calculated cold leg temperature is not in good agreement with the measured cold leg temperature, although the calculated temperature follows the correct trend with what appears to be an offset introduced by the different values for the calculated and measured steady state temperature.

#### 6.3.9 Feedwater Transient Test

The initial conditions for the feedwater transient test are given in Table 6.3-7. The inputs used to drive the simulation are shown in Fig. 6.3-20. Calculated and measured results for the test are shown in Figure 6.3-21.

As can be seen in Fig. 6.3-21 the model is able to track the measured water level response for about 230 seconds. After 230 seconds the calculated level decreases faster than the measured level and the calculation terminates at 300 seconds when a breakdown in natural circulation occurs (the model indicates that a breakdown in natural circulation occurs - it is not known whether or not this happens in the experiment.) The downcomer flowrate calculated during the simulation is in good agreement with the measured downcomer flowrate for the first 60 seconds of the test. From about 60 to 200 seconds the calculated flowrate is less than the measured flowrate, although it exhibits the same trend as the measured flowrate. After 220 seconds, the calculated flowrate decreases more rapidly than the measured

Table 6.3-7  
Initial Conditions for Feedwater Transient.

Quantity	Value
Power	1.224 MWt
Water Level*	0.9510 m
Downcomer Flowrate	3.628 kg/s
Steam Pressure	3.85 MPa
Steam Flowrate	0.4902 kg/s
Feedwater Temperature	71.05°C
Riser Inlet Vapor Volume Fraction	0.4854
Primary Inlet Temperature	299.3°C
Primary Outlet Temperature	260.6°C
Primary Flowrate	6.060 kg/s

\* Referenced to top of riser.

flowrate. The reason the downcomer flowrate is nearly constant from 60 to 220 seconds is that for this time span the water level is above the riser exit (zero reference level) where equal static heads for the upflowing fluid and the downflowing fluid cancel so that the flowrate is independent of water level. Once the level falls below the riser exit (below 0.0 m reference level) the decreasing static head causes the downcomer flowrate to decrease.

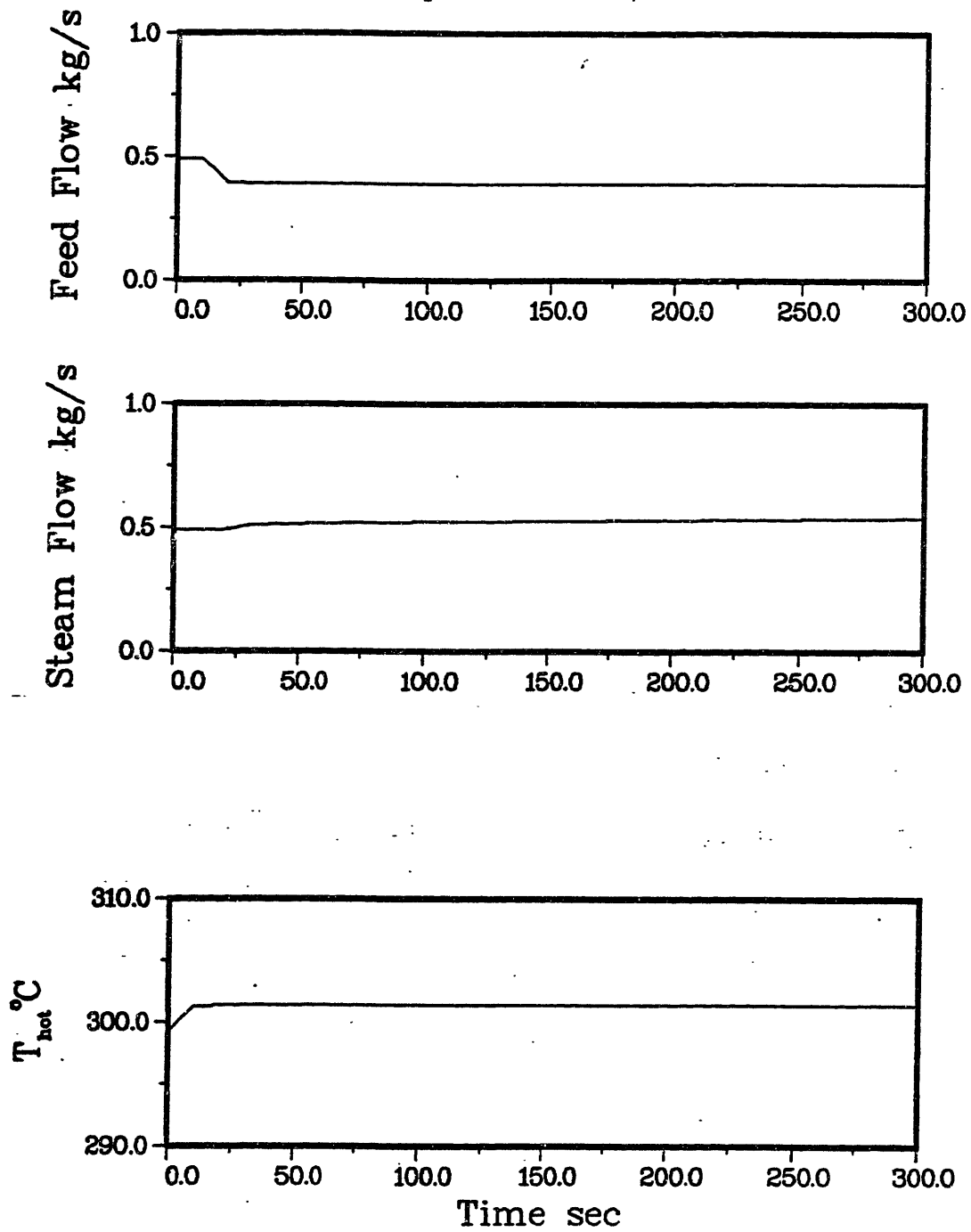


Figure 6.3-20. Input for feedwater transient test.

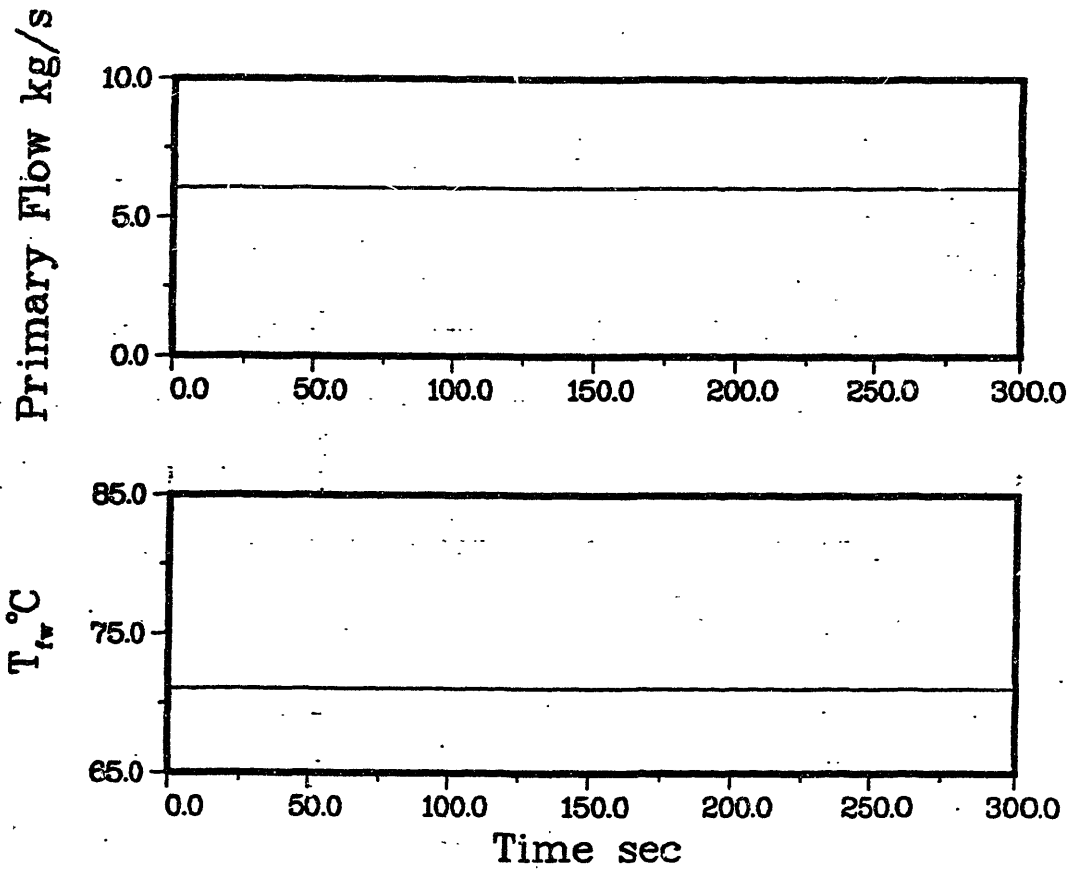


Figure 6.3-20. Input for feedwater transient test.  
(Continued)

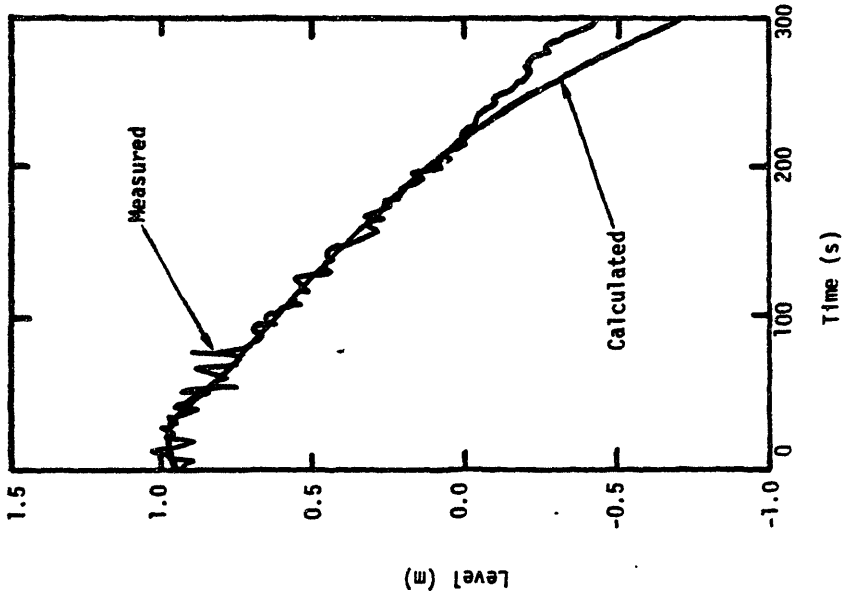
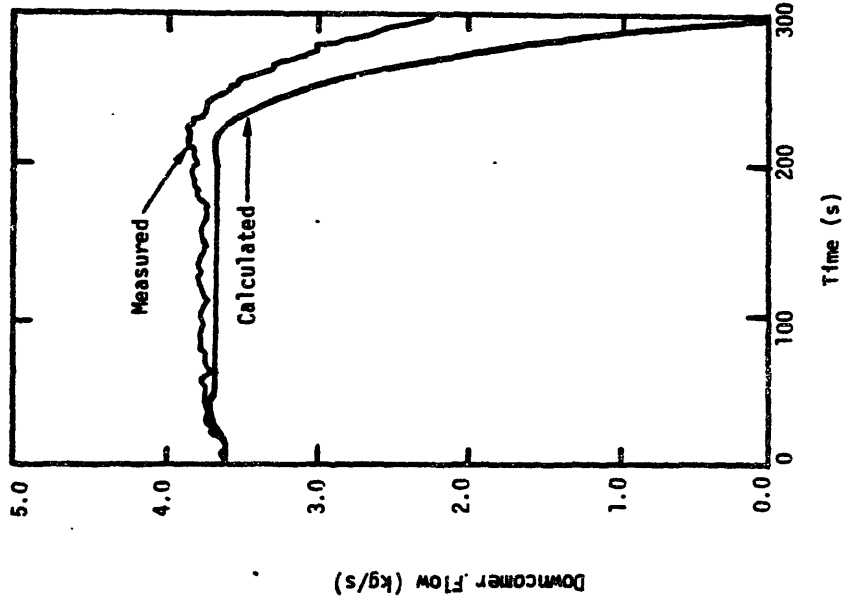


Figure 6.3-21. Steam generator response for feedwater transient test.



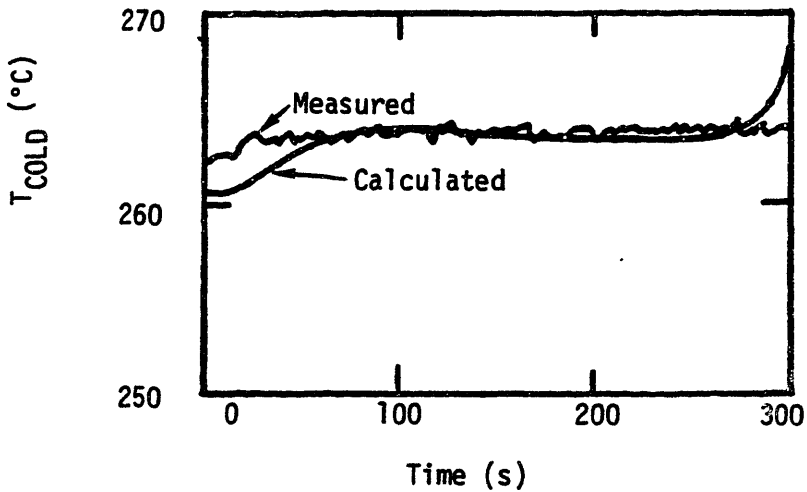
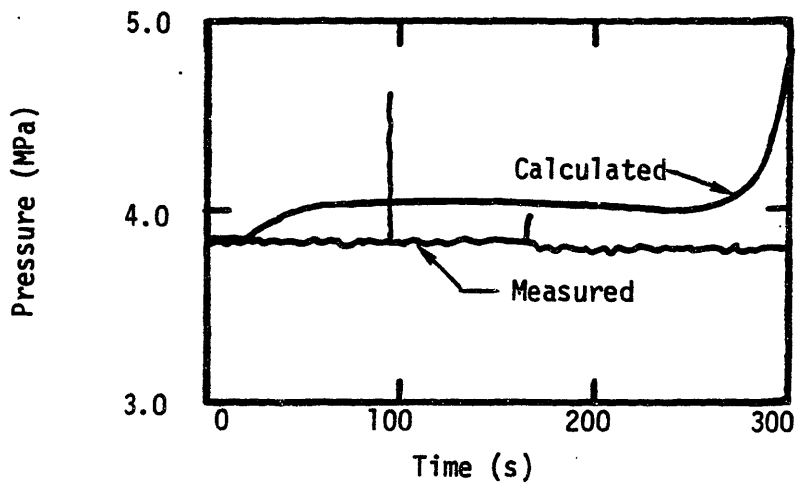


Figure 6.3-21. Steam generator response for feedwater transient test. (Continued)

The calculated pressure is in excellent agreement with the measured pressure for the first 20 seconds of the transient. After this the calculated pressure rises to a constant value about 0.2 MPa above the measured pressure. Towards the end of the simulation the calculated pressure increases rapidly. This happens because the model calculations indicate an approach to a breakdown in natural circulation, where the model rapidly becomes invalid. Thus, model calculations beyond 270 seconds are suspect, since after this time we are attempting to model a situation outside the range of model validity. The calculated cold leg temperature basically follows the trend set by the calculated pressure, so that comments made regarding the validity of the calculated pressure beyond 270 seconds apply equally for the calculated cold leg temperature. Note that the calculated cold leg temperature starts from a lower initial temperature than the measured temperature, which introduces some error in the calculated transient response of the cold leg temperature.

#### 6.3.10 Oscillating Secondary Pressure Test

In this test the condenser pressure was forced to oscillate in a sinusoidal fashion with a 0.2 Hertz frequency and a 0.25 MPa magnitude. This resulted in a sustained oscillation of the secondary pressure and steam flowrate. The measured steam flowrate oscillation is described by the following equation:

$$W_s = 0.38 + 0.21 \sin (1.266 t) \text{kg/s}$$

As mentioned in 6.3.1, attempts to simulate this test were unsuccessful. The major problem encountered is that the calculated downcomer flowrate responds very sharply with larger swings in magnitude than are observed for the measured downcomer flowrate. In fact, the calculated downcomer flowrate becomes negative, indicating reverse flow from the tube bundle to the downcomer; this condition is not observed experimentally. Once the calculated downcomer flowrate becomes negative, the simulation stops since the model developed here cannot handle reverse flow.

It is not clear why the calculated downcomer flowrate oscillation is of larger magnitude than the observed downcomer flowrate oscillation. However, we do know that three-dimensional effects are not accounted for in our one-dimensional, large control volume model, and that these three-dimensional effects tend to damp the downcomer response to transient perturbations (see 6.3.4). Thus, a reasonable explanation of the problem encountered in trying to simulate this test is that three dimensional effects, particularly flow redistribution in the tube bundle, are important, requiring a more detailed spatial model of the steam generator.

## 6.4 ARKANSAS NUCLEAR ONE - UNIT 2

### 6.4.1 Background Information

Arkansas Nuclear One - Unit 2 (ANO-2) is a Combustion Engineering nuclear steam supply system (NSSS) with a rated thermal power of 2815 MWt. The primary loop consists of the reactor, pressurizer, two steam generators and four reactor coolant pumps (see Fig. 6.4-1), with one hot leg and two cold legs per steam generator. Normal operating parameters for the steam generator are listed in Table 6.4-1 and geometric input can be found in Appendix H. Further details concerning plant systems and operation can be found in Refs. (G1) and (F2).

During the initial power ascension test program for ANO-2, four plant transient tests were conducted with the specific objective of adding to the data base used in NSSS design and safety analysis. The tests were:

- 1.) a complete loss of forced primary coolant flow (LOF);
- 2.) a full length control element assembly (CEA) drop (FLCEAD);
- 3.) a part length CEA drop (PLCEAD); and,
- 4.) a turbine trip (TT).

Some of the data generated during these tests were processed (i.e. filtered) to remove noise components (see Ref. (S4) for details on filtering process). According to Ref. (S4) this filtering introduced a time delay between the filtered and unfiltered data which was no greater than

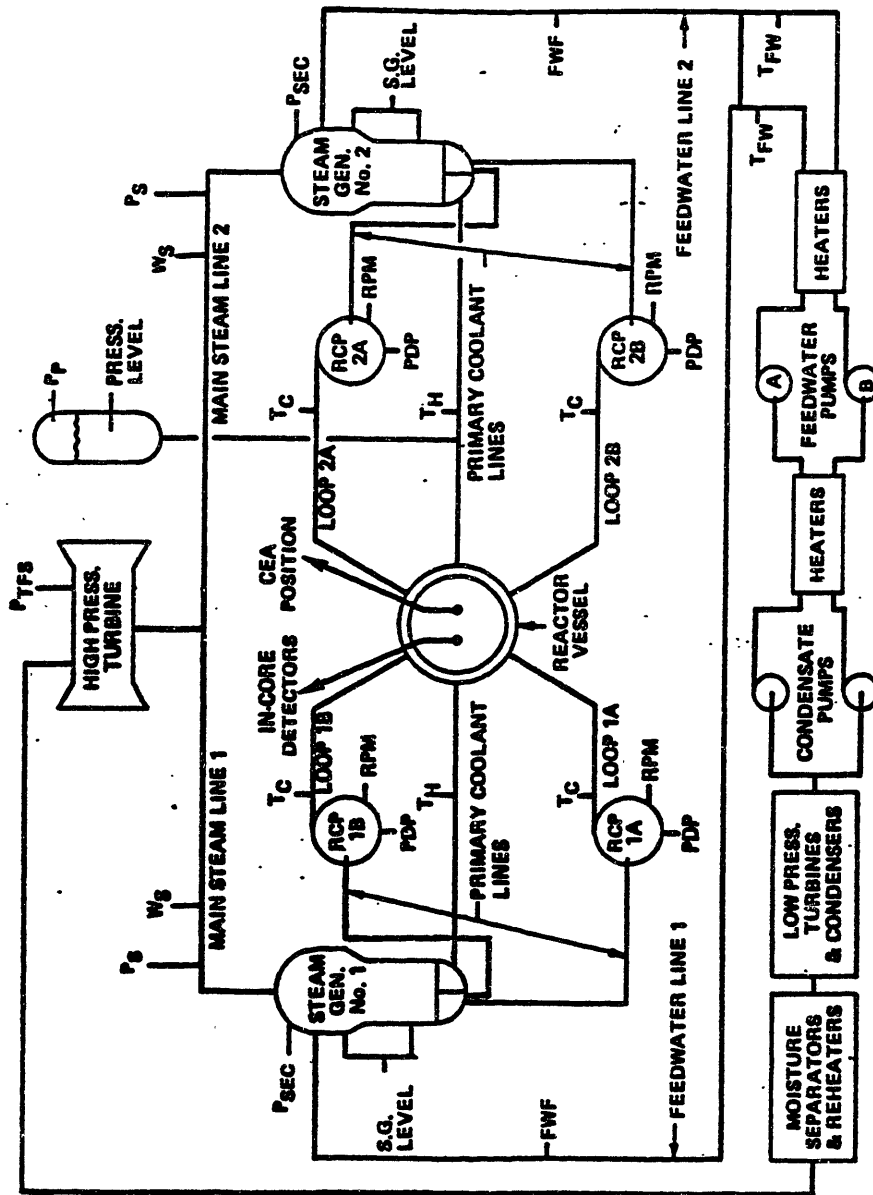


Figure 6.4-1. Arkansas nuclear one - unit 2 schematic (Ref. (E2)).

Table 6.4-1  
Arkansas Nuclear One - Unit 2 Steam Generator  
Design Operating Parameters.

Quantity	Nominal Value
Primary Flowrate/Steam Generator	7592 kg/s
Primary Pressure	15.46 MPa
Primary Inlet Temperature	323°C
Primary Outlet Temperature	290°C
Steam Flowrate/Steam Generator	797 kg/s
Steam Pressure	6.18 MPa
Feedwater Temperature Full Power	233°C
Steam Generator Water Level*	10.43 m

\* Referenced to tube sheet.

1-2 seconds, but generally less than one second. Data acquired during the turbine trip test was not filtered.

An important consideration when comparing computer calculations to measured data is instrument response time. For most of the instruments used in the tests this is on the order of 5 to 180 milliseconds. However, for the temperature sensors, which in this case are resistance temperature detectors (RTDs), the response time, or time constant, is on the order of 5 seconds. This is not a negligible quantity when looking at data acquired over a sixty second interval.

Thus, it is apparent that comparisons of temperature predictions by the computer code to measured temperatures must somehow account for RTD performance. This is done by modeling the sensor response.

The sensor model used in this work is the sensor model presented in Reference (S4) and is given by the following differential equation:

$$\frac{d\phi(t)}{dt} = \frac{I(t) - \phi(t)}{\tau} \quad (6.4-1)$$

where,  $\phi(t) \equiv$  sensor output;

$I(t) \equiv$  sensor input; and,

$\tau \equiv$  time constant of the sensor in seconds.

Equation (6.4-1) is a simple first order lag equation.

Discretizing Eq. (6.4-1) in a fully implicit manner yields

$$\phi^n = \frac{I^n \Delta t + \phi^{n-1} \tau}{\tau + \Delta t} \quad (6.4-2)$$

where  $\phi^n$  is the sensor output for a given input,  $I^n$ , at time level  $n$ . Experimentally derived time constants are listed in Table 6.4-2. Equation (6.4-2) is used to transform calculated cold leg temperatures so that they can be properly compared to measured cold leg temperatures.

Since the hot leg temperature is input to the calculation, we must invert Eq. (6.4-2) to obtain the sensor input

Table 6.4-2  
RTD Response Times

Instrument	Measured Response Time (msec)	Response Time Used in Calculations (msec)
Hot Leg RTD	4753 ± 520	4753
Cold Leg RTD	4898 ± 520	4898

temperature in order to obtain the corrected hot leg temperatures from the measured hot leg temperature. This yields:

$$I^n = \phi^n + \frac{\tau}{\Delta t} (\phi^n - \phi^{n-1}) \quad (6.4-3)$$

Thus, at time level  $n$  we use Eq. (6.4-3) to obtain the true hot leg temperature from the measured hot leg temperature,  $\phi^n$ . For the ANO-2 calculations  $\Delta t$  is 0.25 seconds.

The data for each test is presented in Ref. (S4) in the form of plots of the significant parameters versus time for each of the steam generators. These plots indicate that the two steam generators respond differently during any given transient; therefore, we simulate both steam generators separately for each test, thereby effectively doubling the number of test transients and broadening our data base.



Difficulty in obtaining a steady state heat balance was encountered when performing initialization calculations using steady state data presented in Ref. (S4). There were two sources of trouble. First, the power calculated using the given primary enthalpy drop and flowrate was not equal to the stated power. Second, given the primary temperature difference and the secondary pressure, using the nominal fouling factor (the fouling factor obtained using nominal steam generator parameters) to calculate the heat transfer rate via the log-mean temperature difference yielded a heat transfer different from the stated heat transfer rate. In addition, the power calculated using the primary enthalpy drop, and the power calculated using the log-mean temperature difference were not consistent. To resolve these problems we make two adjustments for steady state calculations. The first adjustment is that we use a value of the primary flowrate that gives us a heat transfer rate that is consistent with the stated power when used in conjunction with the primary enthalpy drop derived from measurements. The second adjustment is that we use a tube fouling factor which gives us the measured power when we use the measured primary and secondary temperatures in the log-mean temperature difference. Both the adjusted primary flowrate and tube fouling factor may be different from measured or nominal values. The adjustments for each test study performed are shown in Table 6.4-3. The reader will observe that only three test transients are shown in Table 6.4-3, while four test

Table 6.4-3  
 Primary Flowrates and Tube Fouling Factors Used in  
 Initialization Calculations for each Transient.

Test Transient	Primary Flowrate	Fouling Factor
Nominal	7592 kg/s	$2.775 \cdot 10^{-5} \text{m}^2$ - °K/W
Turbine Trip Steam Generator 1 Steam Generator 2	104% Nominal 100.4% Nominal	79.7% Nominal 71.3% Nominal
Loss of Primary Flow Steam Generator 1 Steam Generator 2	109.8% Nominal 113.9% Nominal	45.9% Nominal 68.4% Nominal
Full Length CEA Drop Steam Generator 1 Steam Generator 2	100.8% Nominal 98.9% Nominal	56.9% Nominal 66.6% Nominal

transients were actually performed at ANO-2. Simulations of the part length control element assembly drop were not performed, since this is a relatively mild transient in so far as the behavior of the steam generator is concerned, and we felt that simulation of the transient would not yield any significant information.

The feedwater temperature was not given in the test data appearing in Ref. (S4). The steady state feedwater

temperature was inferred from a heat balance on the secondary side of the steam generator. That is,

$$H_{fw} = H_{vs} - \frac{Q_B}{W_s}$$

All the quantities on the right hand side of the above equation are known, so  $H_{fw}$  can be calculated. It is then a simple matter of using steam tables to obtain  $T_{fw}$ . The input time dependent behavior of the feedwater temperature is discussed for each transient separately when the transient itself is presented.

A final note regarding empirical or assignable parameters in the steam generator model. For the drift flux parameters,  $C_0$  and  $u_{vj}$ , we use the expressions given in Appendix C. The loss coefficient at the bottom of the downcomer,  $K_D$ , and the separator loss coefficient,  $K_{SEP}$ , are assigned values that yield a calculated steady state full power recirculation ratio ( $W_0/W_s$ ) in the range of 4 to 5. We use  $K_D$  equal to 0.51 and  $K_{SEP}$  equal to 100, which gives us a calculated full power recirculation ratio of 4.6 with a corresponding downcomer flowrate of 3601 kg/s.

Finally, in plots of cold leg temperature versus time we have two curves corresponding to measured results and one curve for calculated results. This is because the steam generators of ANO-2 have two cold legs and each leg has a separate temperature sensor. For the simulation results, on

the other hand, we calculate only one plenum outlet temperature, which we call the cold leg temperature. If the fluid in the outlet plenum is well mixed then the two measured cold leg temperatures should be the same. Differences in the measured temperatures for the two cold legs could be caused by a bias in the calibration of the RTDs or different RTD response times (e.g., due to displacement of one of the RTDs in its thermowell).

#### 6.4.2 Full Length CEA Drop Test

The full length CEA drop test is a transient in which a reactor trip did not occur. The test is initiated by dropping the full length CEA nearest to the steam generator 2 hot leg and the transient is allowed to proceed until the plant reaches a new equilibrium operating state. Because the dropped full length CEA is near the steam generator 2 hot leg, the system response is asymmetric. That is, steam generator 2 parameters respond faster and exhibit larger swings in value than do parameters associated with steam generator 1.

There is some problem in interpreting the steam and feedwater flowrate data given in Ref. (S4). The measured steady state feedwater flowrate is greater than the measured steady state steam flowrate (by amounts up to 7.2 per cent of full power steam flowrate). It is probable that this difference in measured steady state flowrates can be accounted for by fluid extracted through the steam generator

blowdown line. The model developed in this work does not account for steam generator blowdown flowrates, so we must find a way to reconcile the difference in steam and feedwater flows. One simple way to do this is to bias the feedwater flow so that it is equal to steam flow in the steady state and then apply this bias to the transient feedwater flowrate. This is the method we have chosen to use. We simply equate the steady state feedwater flowrate to the steady state steam flowrate and during transient analyses we subtract the steady state blowdown flowrate (which is simply the difference between the measured feed and steam flows in the steady state) from the measured feedwater flowrate.

#### Steam Generator 1

The initial conditions for steam generator 1 in the full length CEA drop test are given in Table 6.4-4. The input used for the short term (60 second) and long term (600 second) calculations are shown in Figs. 6.4-2 and 6.4-3. The feedwater flowrate is biased by  $-13.5 \text{ kg/s}$  ( $-7.2$  per cent full power steam flowrate) for the entire transient.

The short term response of steam generator 1 is shown in Fig. 6.4-4. The calculated cold leg temperature response is in excellent agreement with the measured data. The calculated pressure is initially in good agreement with the measured pressure, but after about 15 seconds the calculated pressure remains slightly below the measured pressure. The

Table 6.4-4  
Full Length CEA Drop Initial Conditions, Steam Generator 1.

Quantity	Value
Power/Steam Generator	695.5 MWt
Water Level*	10.43 m (70%)†
Downcomer Flowrate	3432 kg/s
Steam Pressure	6.42 MPa
Steam Flowrate	365.2 kg/s
Feedwater Temperature	205.0°C
Primary Inlet Temperature	302.9°C
Primary Outlet Temperature	285.7°C
Primary Flowrate	7651 kg/s
Fouling Factor	$1.580 \cdot 10^{-5} \text{ m}^2 - \text{K/W}$

\* Referenced to tubesheet.

† Percent of instrument span (4.24 m), where lower instrument tap is 7.47 m above tube sheet.

calculated level is also in good agreement with the measured data.

The long term response of steam generator 1 is shown in Fig. 6.4-5. The calculated cold leg temperature is in excellent agreement with the measured data, as is the calculated pressure. The calculated level compares favorably with the measured data at the start of the transient, but after about 60 seconds the calculated level exceeds the

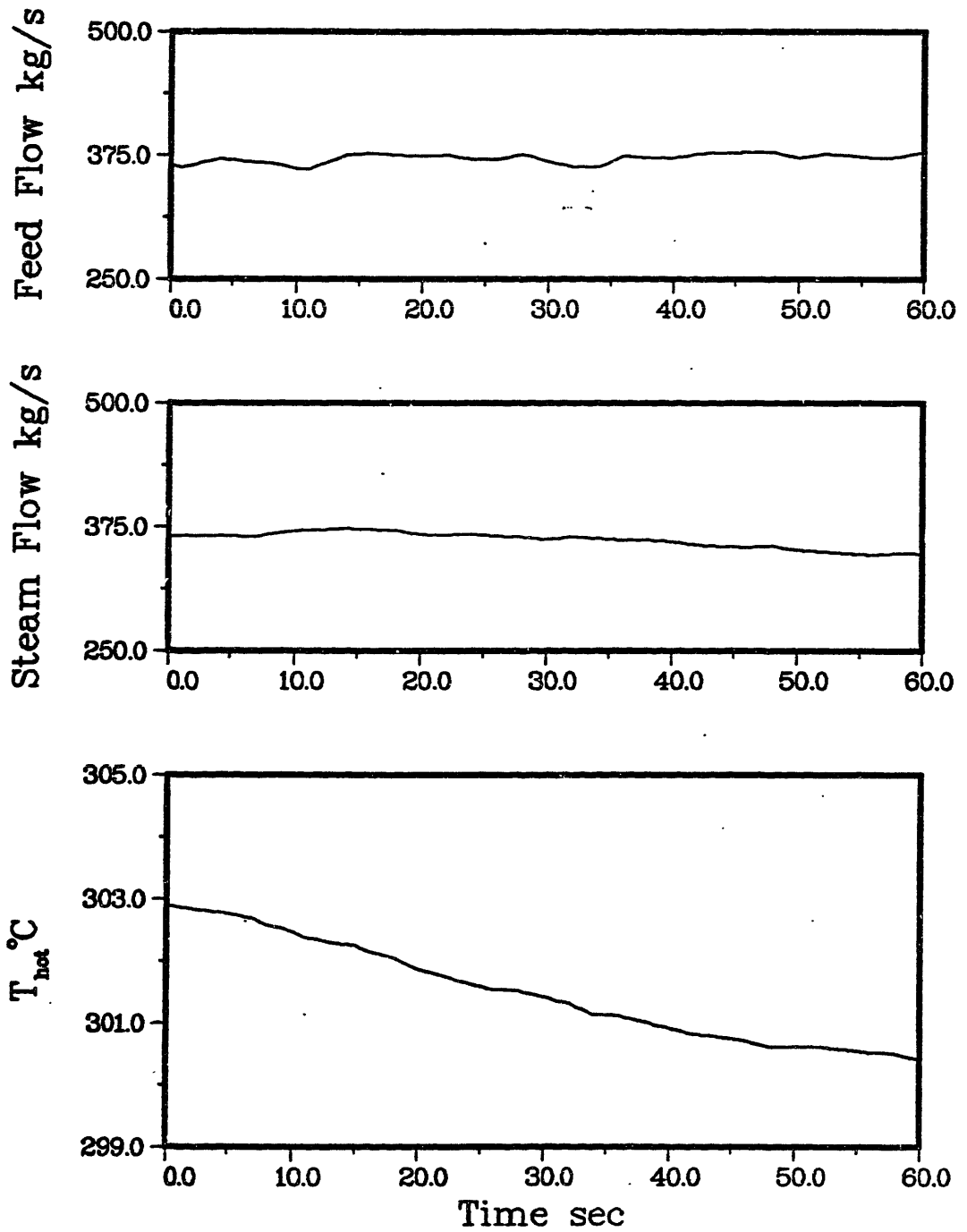


Figure 6.4-2. Short term input for full length CEA drop steam generator 1.

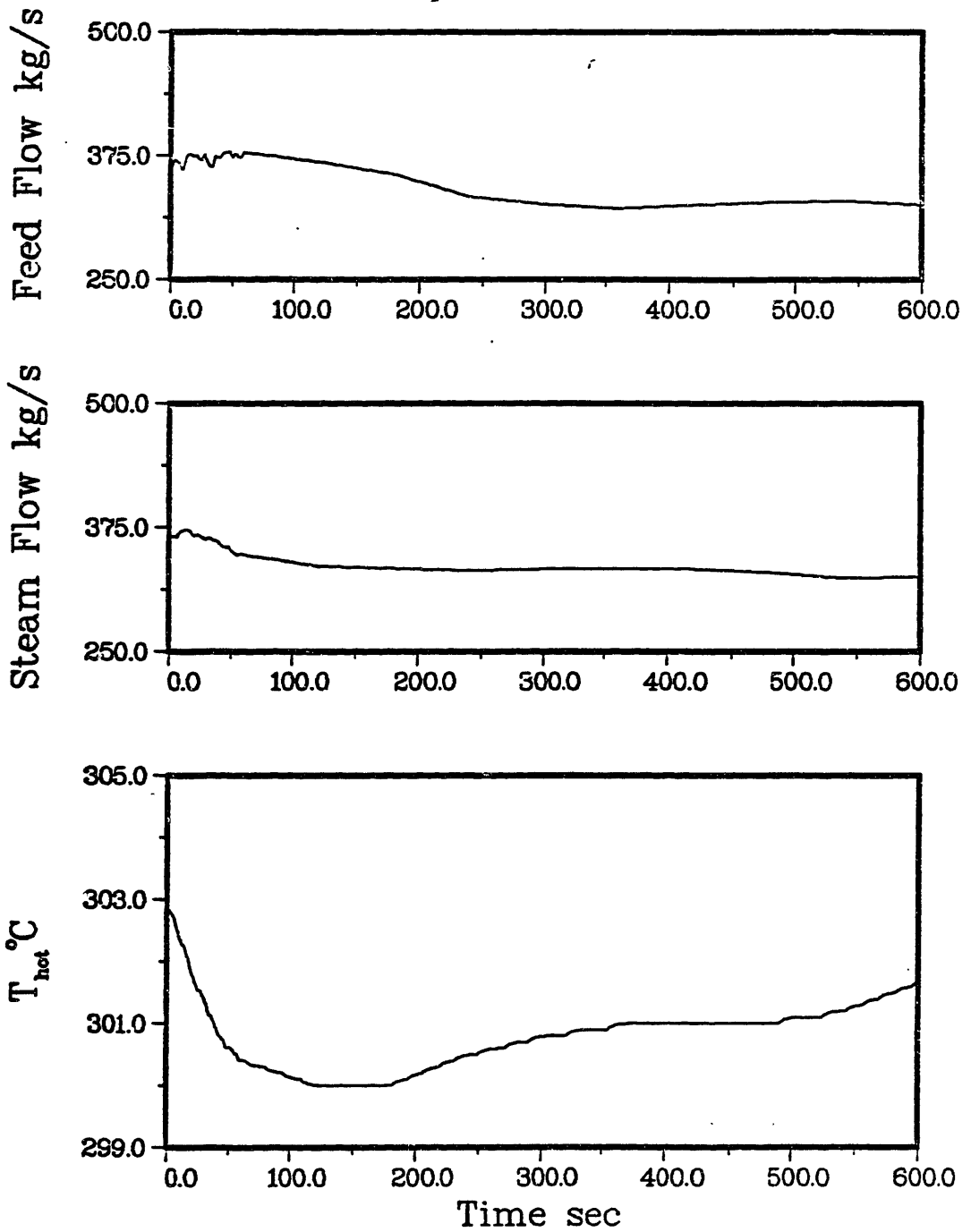


Figure 6.4-3. Long term input for full length CEA drop, steam generator 1.



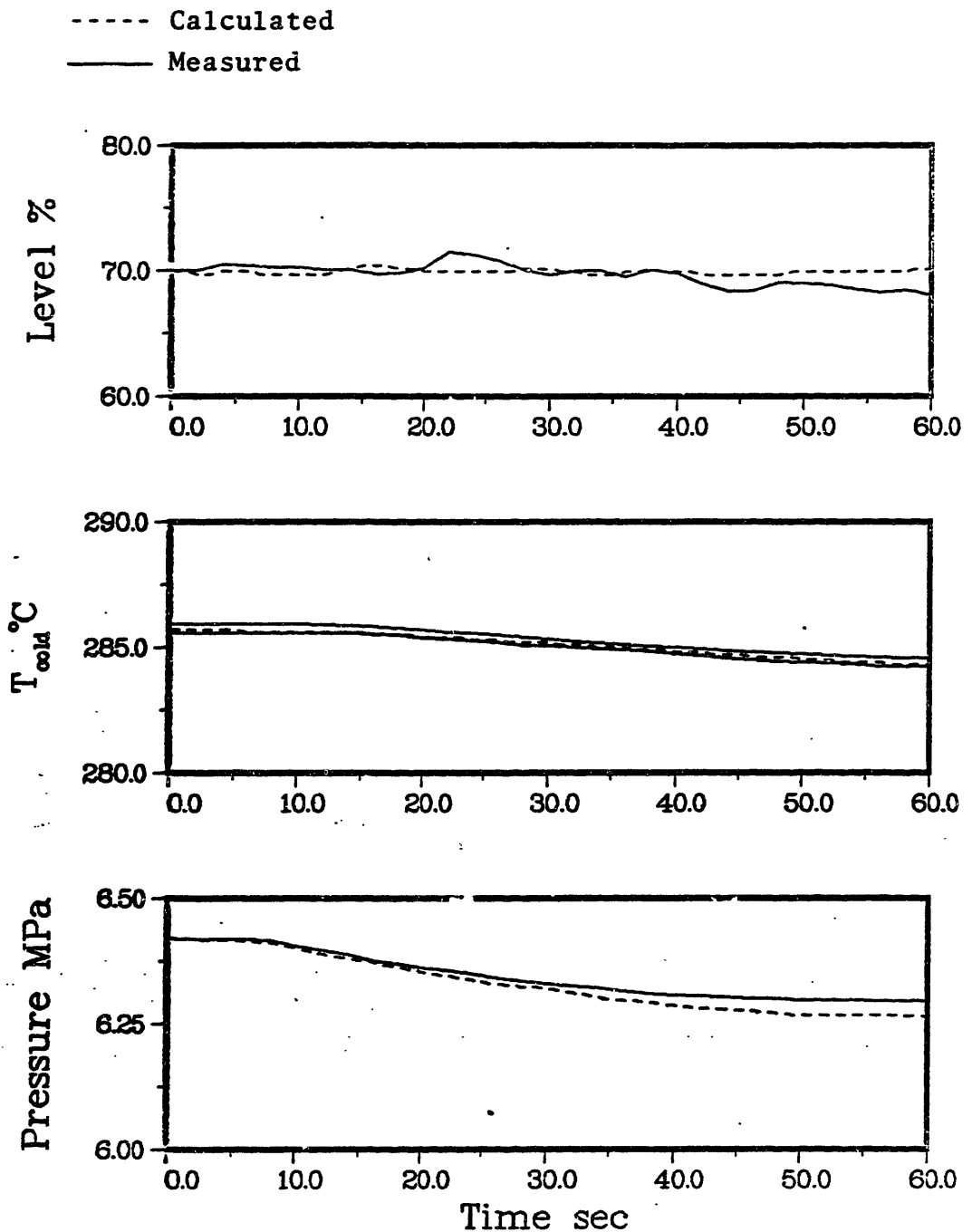


Figure 6.4-4. Short term full length CEA drop response, steam generator 1.

----- Calculated  
 ——— Measured before 60 s  
 ..... Measured after 60 s

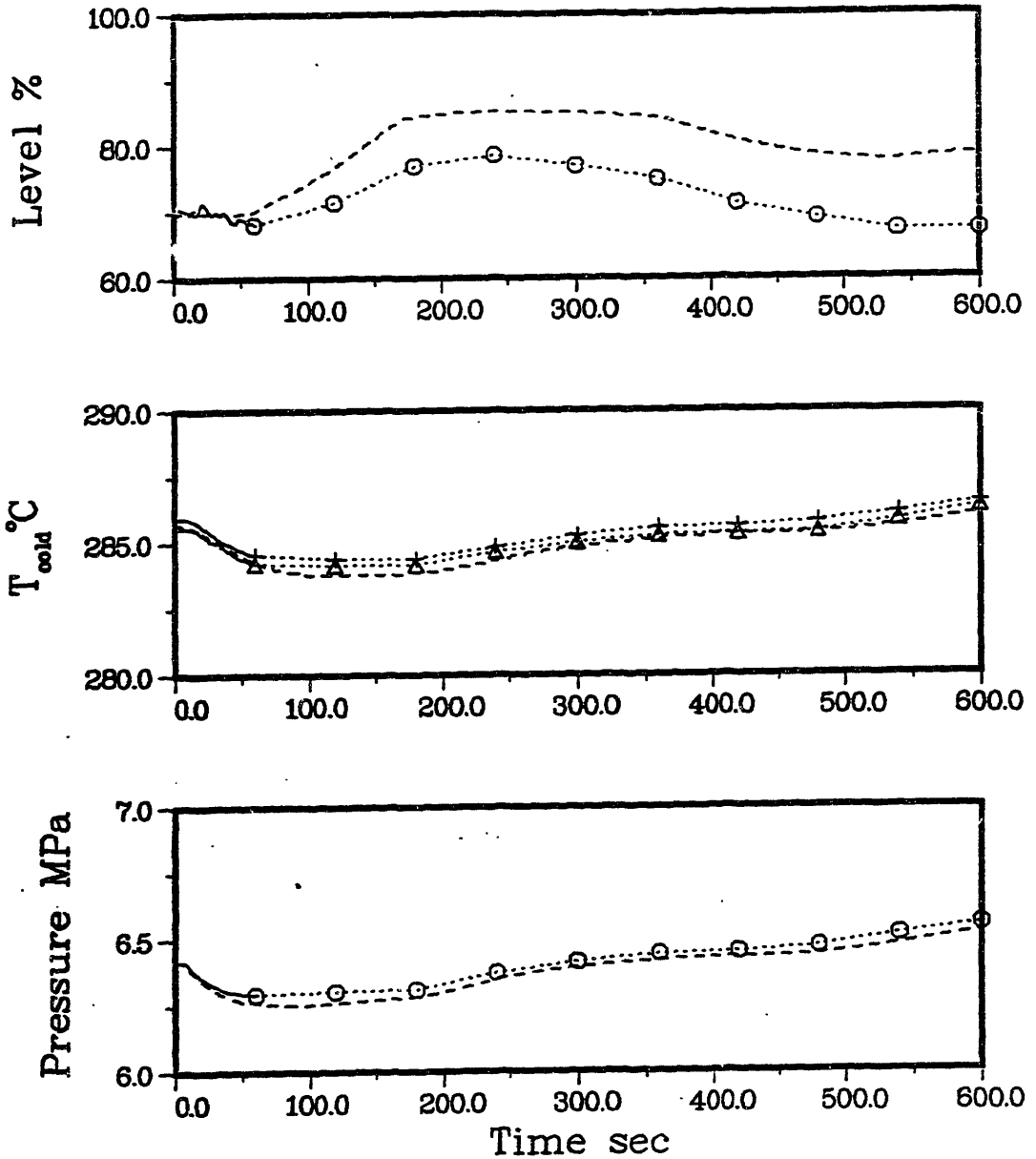


Figure 6.4-5. Long term full length CEA drop response, steam generator 1.

measured level, although it does follow the same general trend as the experimental data. Some of the error in the calculated level can be attributed to idealization of the downcomer geometry in the model (Appendix K) and to the integration of errors in the input feedwater flowrate (see 6.4.3 for discussion of this effect).

### Steam Generator 2

The initial conditions for steam generator 2 are given in Table 6.4-5. The inputs used for the long and short term calculations are shown in Figs. 6.4-6 and 6.4-7. The feedwater flowrate for steam generator 2 is biased by -9 kg/s (-1.1 per cent full power steam flowrate) for the duration of the transient.

The short term response of steam generator 2 is shown in Fig. 6.4-8. The calculated cold leg temperature is in excellent agreement with the measured data. The calculated pressure is also in good agreement with the data, although it is a little high during the last 40 seconds shown. The agreement between the calculated level and the measured level is not good.

The long term response of steam generator 2 is shown in Fig. 6.4-9. As can be seen both the calculated cold leg temperature and the calculated pressure are in good agreement with the plant data. The agreement between the calculated level and the measured level is poor. Some of the error in the level calculation is due to the integrated

Table 6.4-5  
Full Length CEA Drop Initial Conditions, Steam Generator 2.

Quantity	Value
Power/Steam Generator	695.5 MWt
Water Level*	10.39 m (69%)†
Downcomer Flowrate	3415 kg/s
Steam Pressure	6.42 MPa
Steam Flowrate	371.4 kg/s
Feedwater Temperature	212.1°C
Primary Inlet Temperature	303.3°C
Primary Outlet Temperature	285.8°C
Primary Flowrate	7508 kg/s
Fouling Factor	$1.848 \cdot 10^{-5} \text{ m}^2 - \text{K/W}$

\* Referenced to tubesheet.

† Percent of instrument span (4.24 m), where lower instrument tap is 7.47 m above tube sheet.

effect of errors in the input feedwater flowrate, which will now be demonstrated.

### 6.4.3 Sensitivity of Level to Feedwater Flowrate

In Chapter 5 we show that the steam generator model behaves as a free integrator, since one of the eigenvalues of the linearized model equations is zero. We also show that the addition of a feedwater controller model eliminates

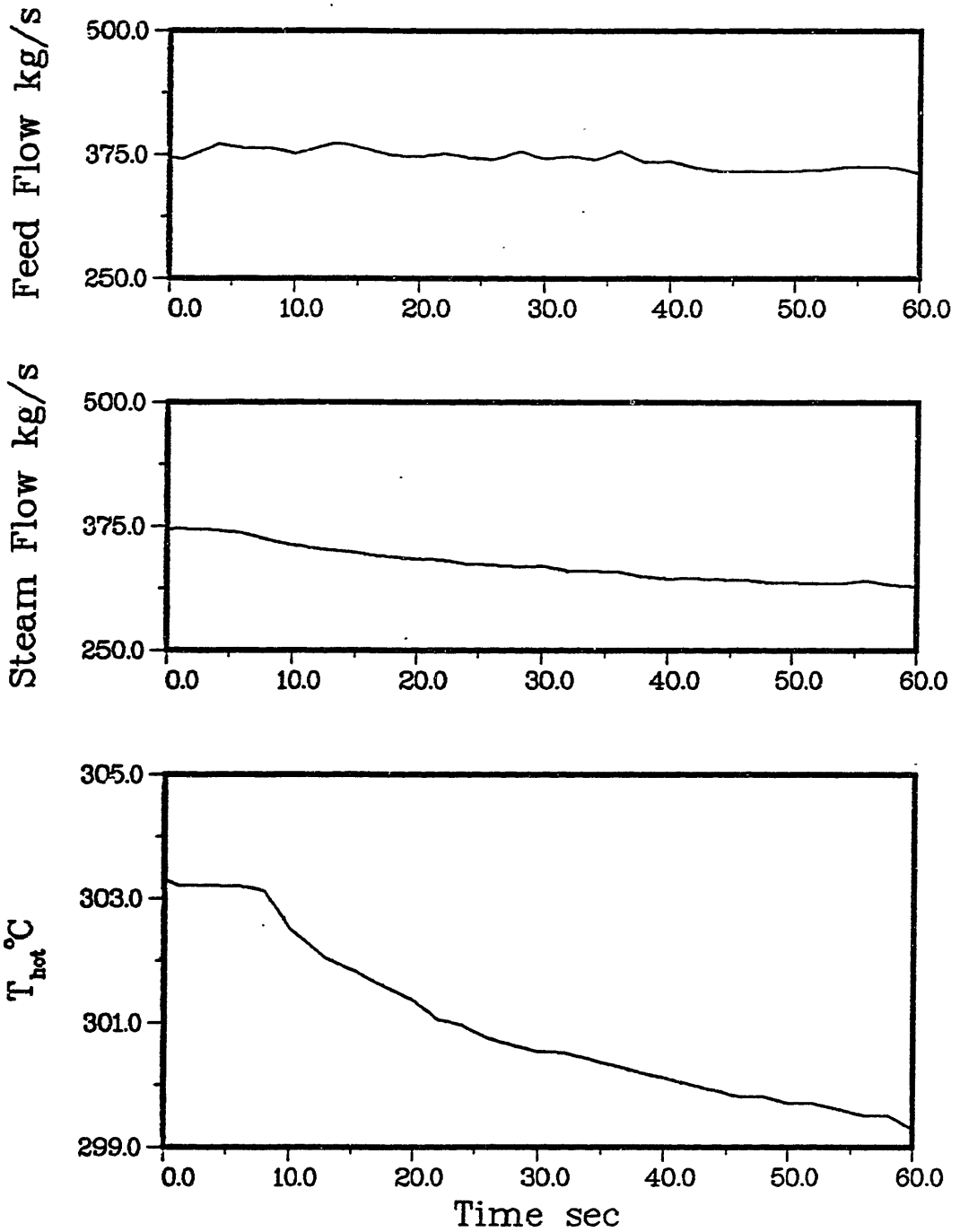


Figure 6.4-6. Short term input for full length CEA drop, steam generator 2.

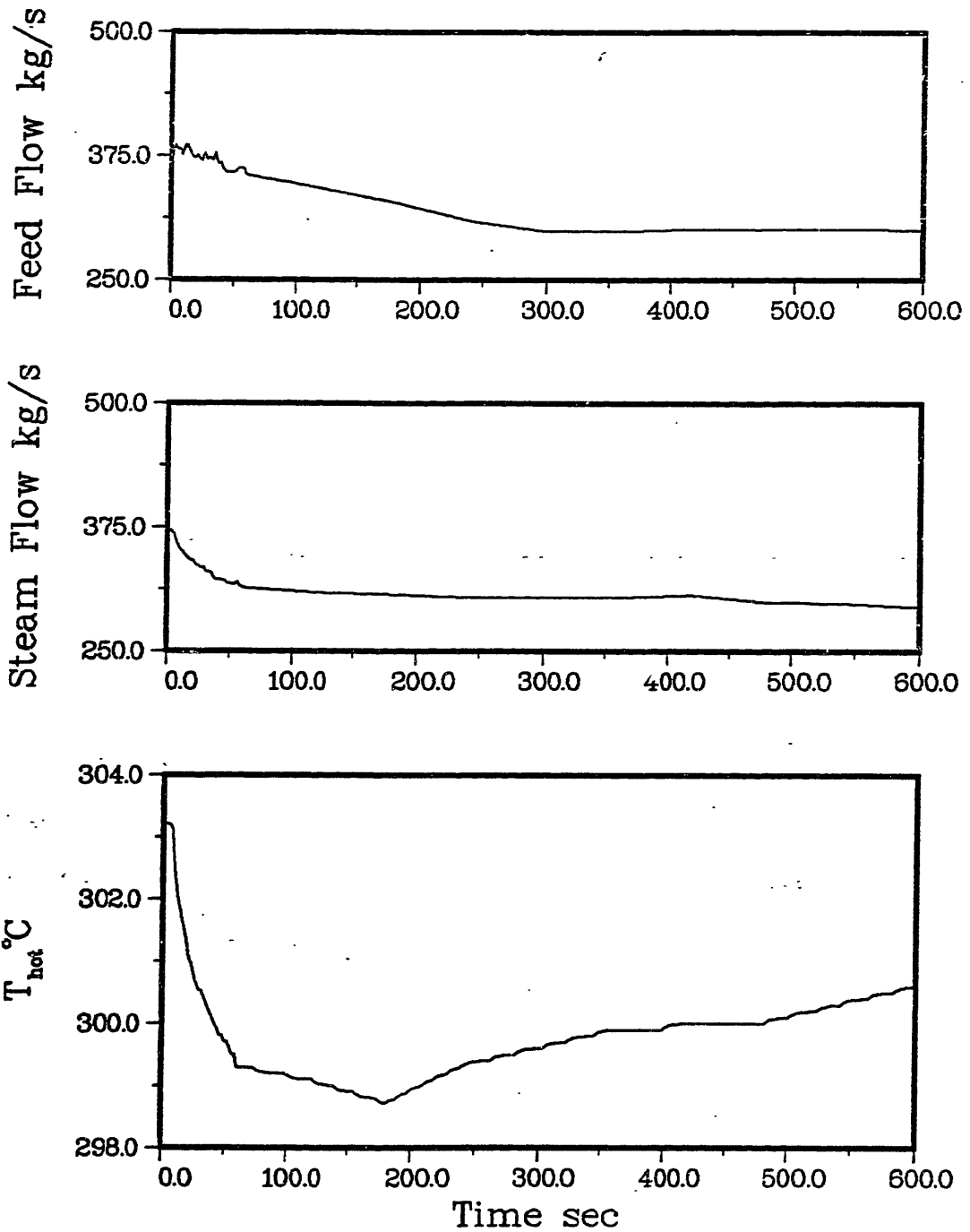


Figure 6.4-7. Long term input for full length CEA drop, steam generator 2.

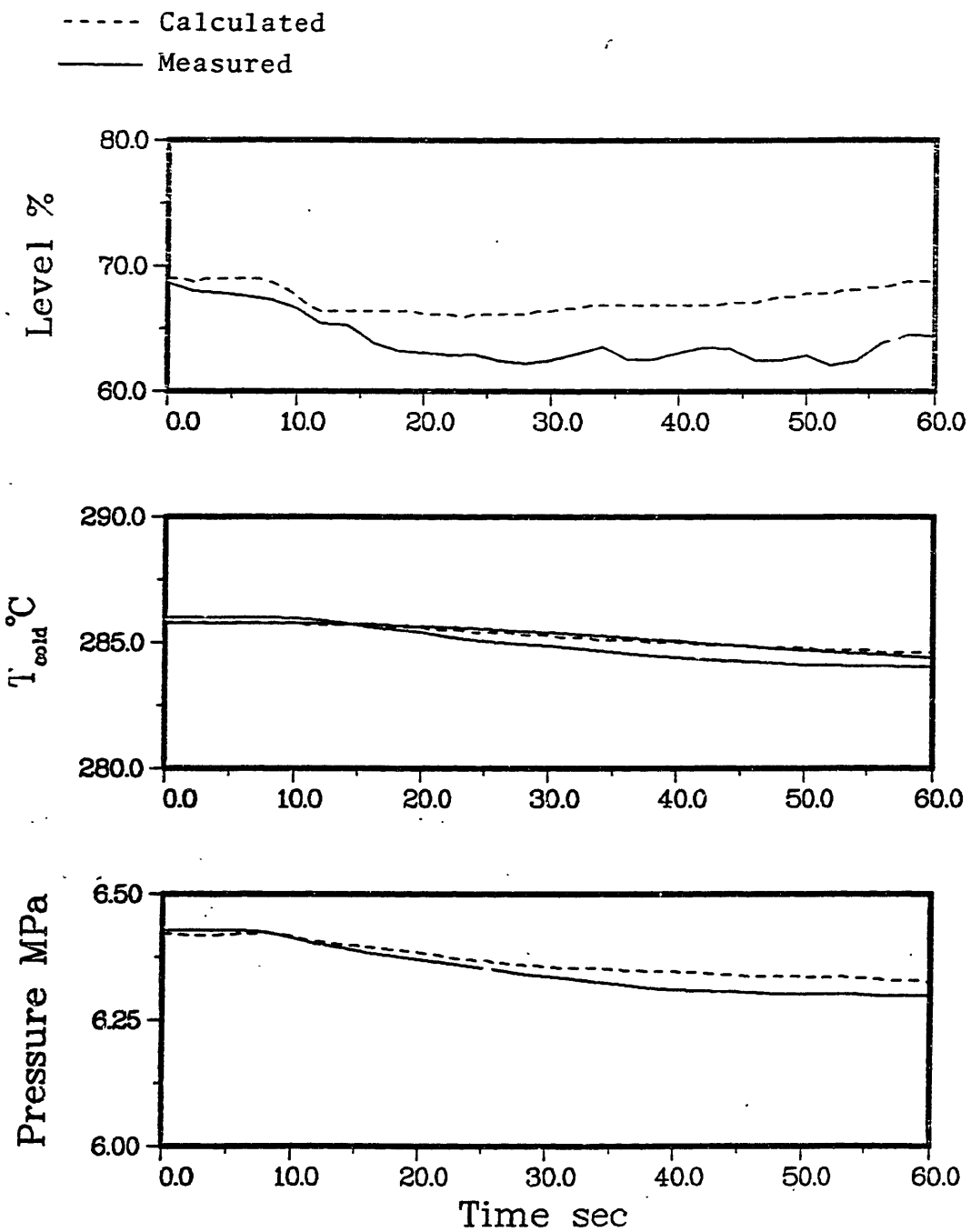


Figure 6.4-8. Short term full length CEA drop response, steam generator 2.

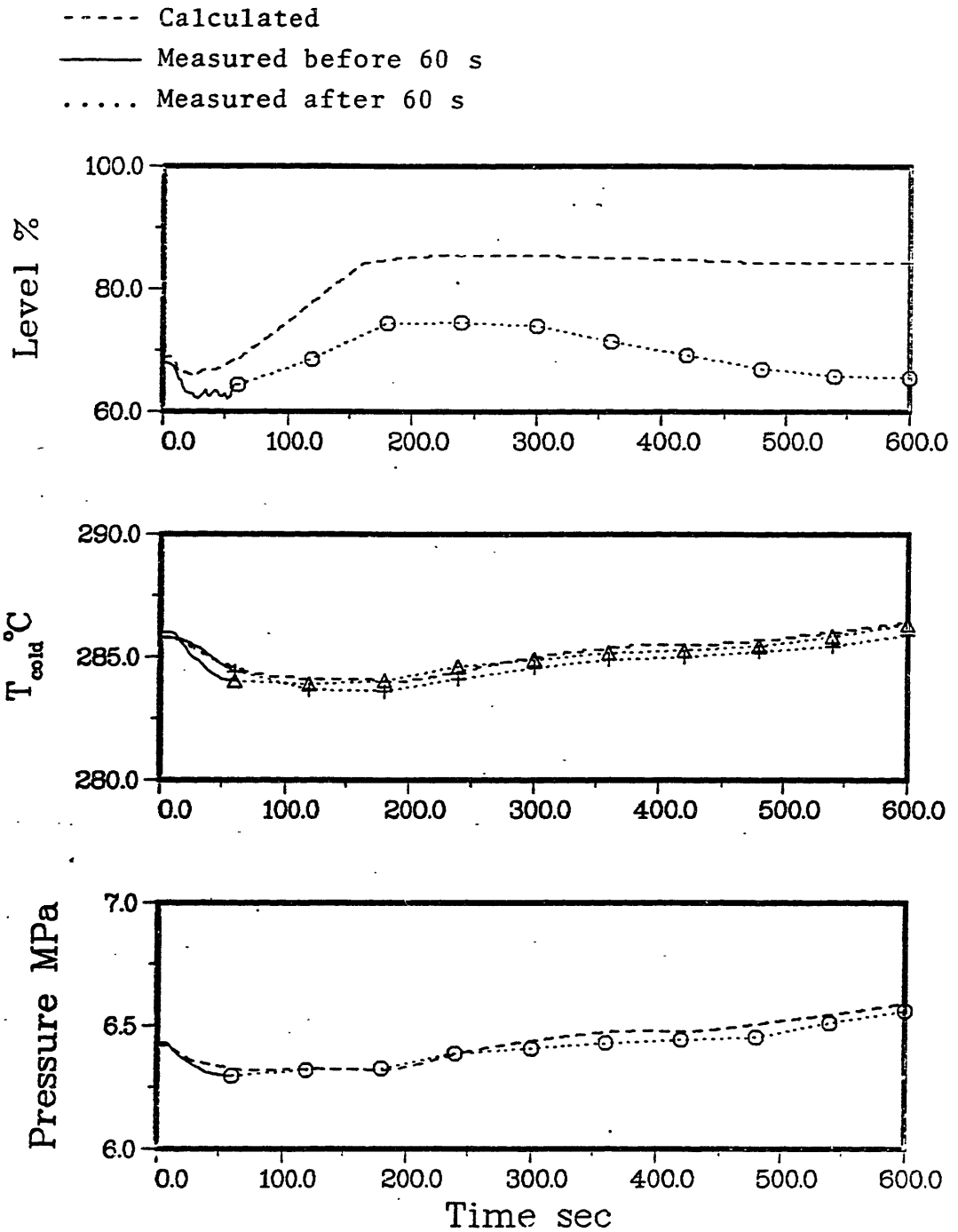


Figure 6.4-9. Long term full length CEA drop response, steam generator 2.



the zero eigenvalue. Therefore, it seems reasonable to conjecture that using a controller model to calculate the feedwater flowrate rather than inputting the measured feedwater flowrate (which may be in error) could help us draw conclusions regarding the sensitivity of level to feedwater flowrate. We use the simple control equation given in Chapter 3, i.e.

$$\frac{dW_{fw}}{dt} = C_w (W_s - W_{fw}) + C_l (l^* - l_w) \quad (6.4-4)$$

Using trial and error to match the calculated level with the measured level shown in Fig. 6.4-9 gives us the following control parameters for Eq. (6.4-4):

$$\begin{aligned} l^* &= 10.43 \text{ m} = \text{Nominal Level} \\ C_w &= 0.02 \\ C_l &= 1.0 \end{aligned}$$

The results obtained for the full length CEA drop (steam generator 2) using the feedwater controller model and keeping all other inputs the same are shown in Fig. 6.4-10. As can be seen by comparing Figs. 6.4-9 and 6.4-10, the calculated cold leg temperature and calculated pressure have not been affected significantly by using the controller model.

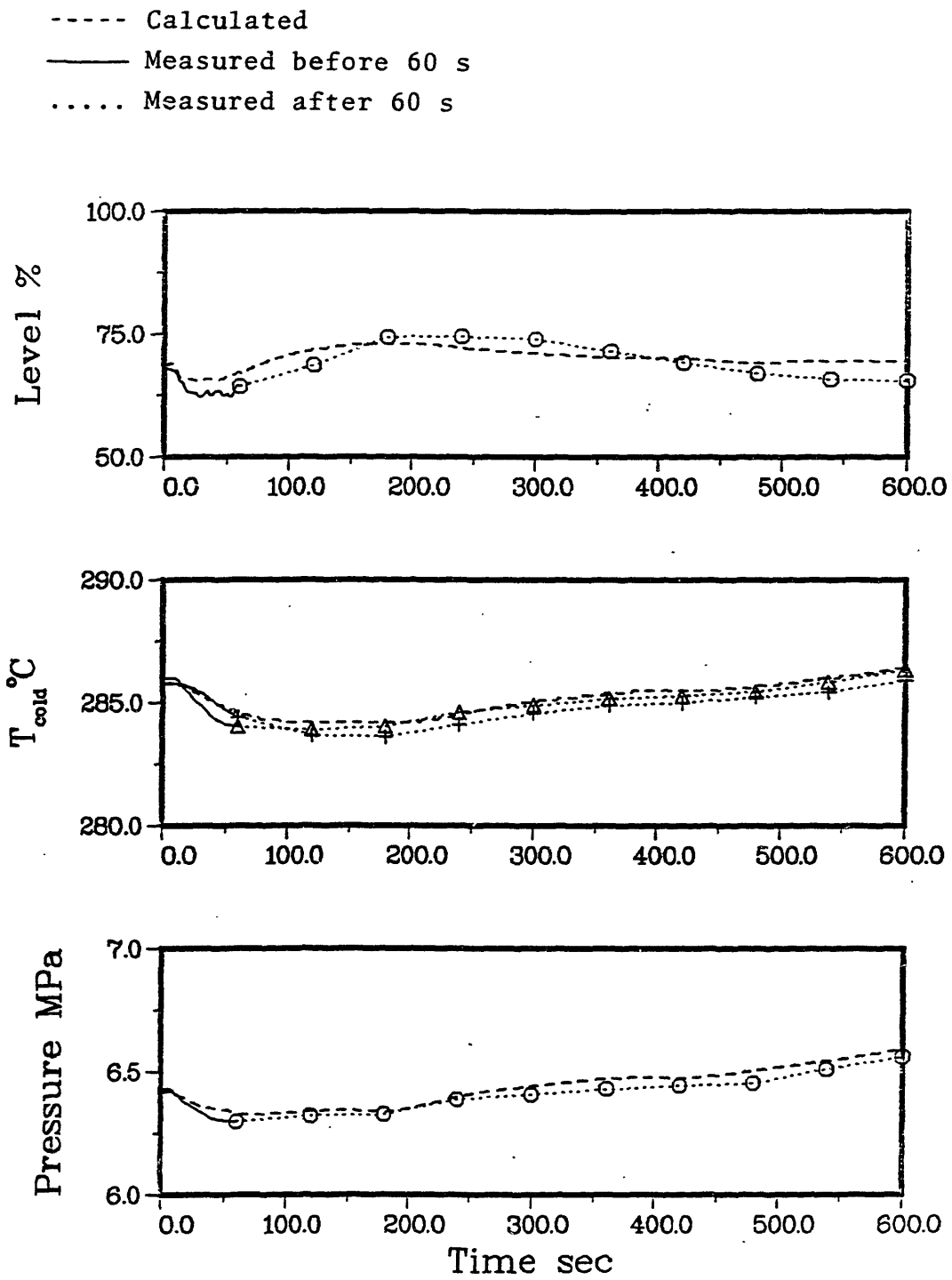


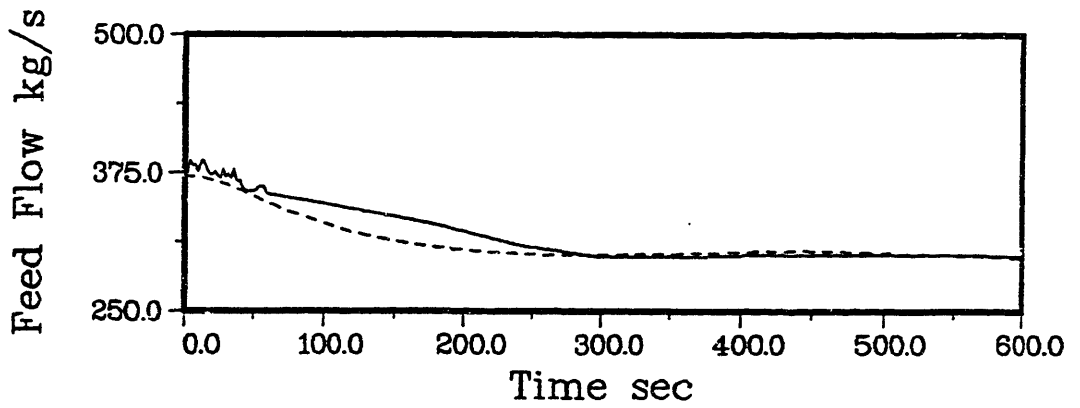
Figure 6.4-10. Long term full length CEA drop response using feedwater controller, steam generator 2.

However, there has been a marked improvement in the agreement between the calculated and measured levels.

The question we must now ask is: How different is the calculated feedwater flowrate from the measured flowrate? This question is answered by looking at Fig. 6.4-11, which is a plot of both the measured and calculated feed flows. Here we see that the difference between the measured and calculated flowrates is not as large as might be expected, demonstrating that the level is sensitive to the feedwater flowrate. In fact, this analysis shows that errors in calculated level are strongly influenced by the integrated error in the feedwater flowrate input to the calculation, a fact that should be kept in mind when making comparisons between measured and calculated levels.

#### 6.4.4 Turbine Trip Test

All the information used to perform the simulations of the turbine trip test are taken from Ref. (S4). For each steam generator there are two sets of calculations. The first set of calculations simulates the first sixty seconds of the transient, since expanded scale plots for this time period are available in Ref. (S4). The second set of calculations simulate the transient for a 200 second interval. For this time period the plots provided in Ref. (S4) are on a compressed scale, making it difficult to accurately pick off the transient boundary conditions for input to the simulation. The long term plots in Ref. (S4) extend for five



----- Feedwater flow from controller model  
—— Feedwater flow from Reference(S4)

Figure 6.4-11. Comparison of feedwater flowrates.

minutes; however, at 200 seconds the reactor coolant pumps are tripped initiating a flow coastdown. Since we already have a flow coast test (see 6.4.5) performed under carefully controlled conditions, we feel that it is unnecessary to simulate the turbine trip beyond 200 seconds.

During the turbine trip test an emergency feedwater actuation signal was generated. This occurred 6.1 seconds after the trip of the main turbine and resulted in the introduction of cold feedwater into the steam generators. The emergency feedwater is drawn from the condensate storage tank, which is maintained at a temperature of 24°C (Ref. (F2)). Unfortunately, data is not available indicating how the feedwater temperature varies with time. We assume that the feedwater temperature ramps down from its initial value to 24°C in three seconds, and that this ramp starts at seven seconds.

#### Steam Generator 1

The initial conditions prevailing for steam generator 1 in the turbine trip test are given in Table 6.4-6. The sequence of events during the test are as follows: At time zero the main turbine is manually tripped. Two seconds into the test the bypass and atmosphere dump valves start to open, and are fully open one second later. At 21 seconds the bypass valves begin to close, while an atmospheric dump valve remains open. The bypass valves are fully closed at 29 seconds. Meanwhile, at 6.1 seconds, the reactor trips

Table 6.4-6  
Turbine Trip Initial Conditions, Steam Generator 1.

Quantity	Value
Power/Steam Generator	1382 MWt
Water Level*	10.52 m (72%)†
Downcomer Flowrate	3572 kg/s
Steam Pressure	6.24 MPa
Steam Flowrate	805.5 kg/s
Feedwater Temperature	246.2°C
Primary Inlet Temperature	320.5°C
Primary Outlet Temperature	289.4°C
Primary Flowrate	7908 kg/s
Fouling Factor	$2.213 \cdot 10^{-5} \text{ m}^2 - \text{K/W}$

\* Referenced to tubesheet.

† Percent of instrument span (4.24 m), where lower instrument tap is 7.47 m above tube sheet.

and an emergency feedwater actuation signal is generated. At 200 seconds the reactor coolant pumps are tripped, initiating a flow coastdown. At this point we stop the turbine trip simulation. Note that from 7 to 10 seconds we ramp down the feedwater temperature from 246.2°C to 23.85°C. The short term and long term inputs for the turbine trip test are shown in Figs. 6.4-12 and 6.4-13.

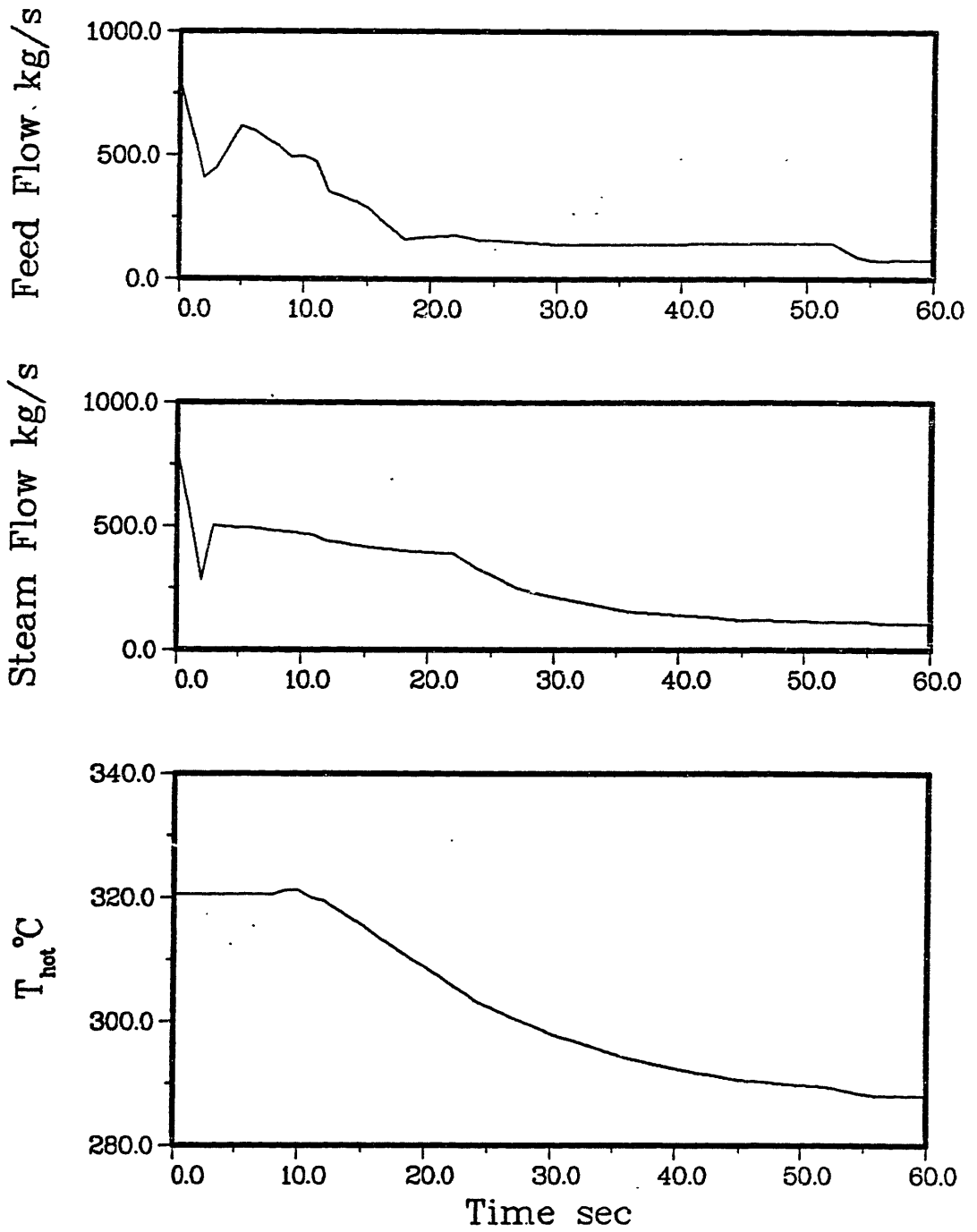


Figure 6.4-12. Short term input for turbine trip, steam generator 1.

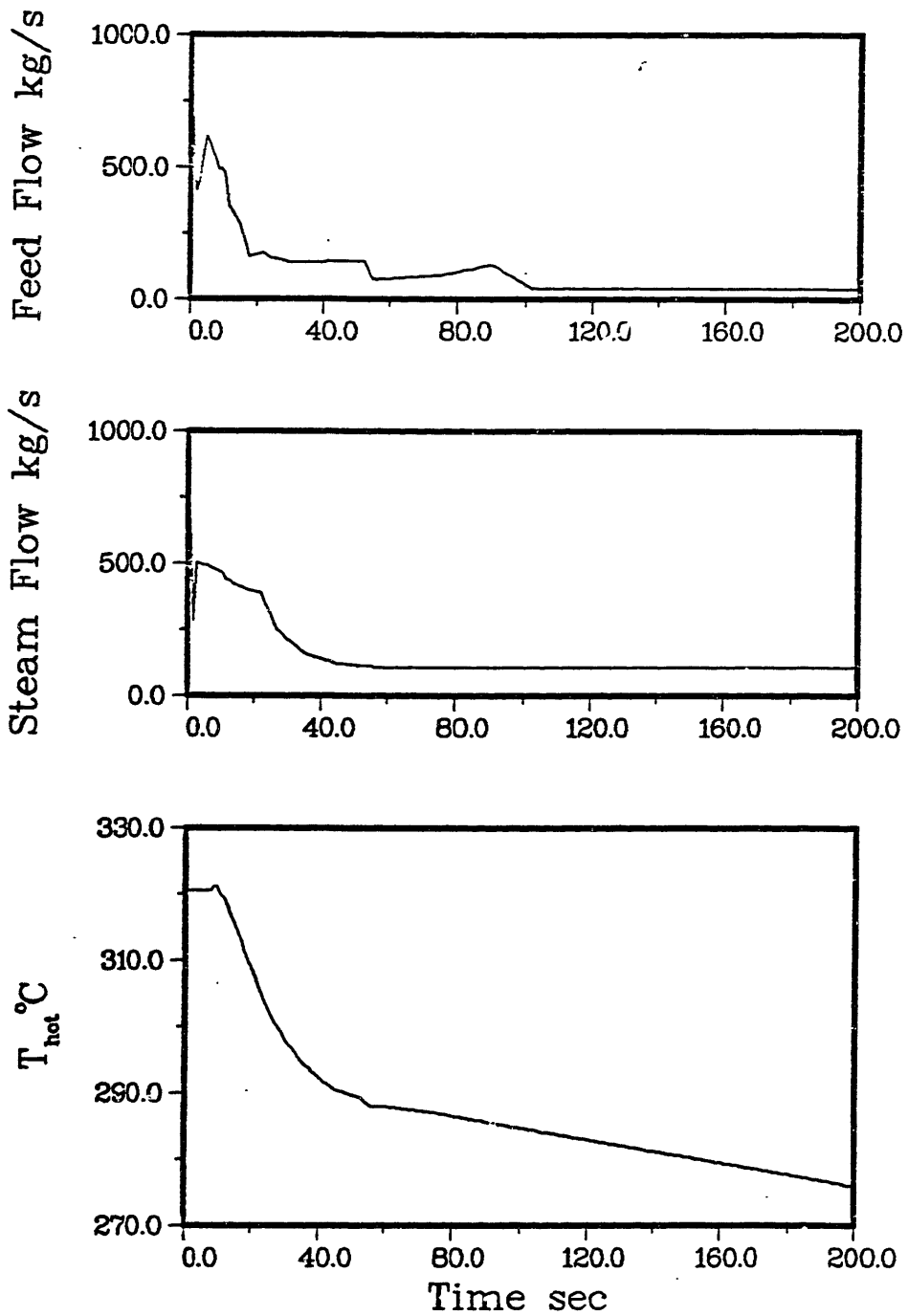


Figure 6.4-13. Long term input for turbine trip, steam generator 1.



The measured and calculated responses of steam generator 1 are shown in Figs. 6.4-14 and 6.4-15.

Looking at Fig. 6.4-14 we see that the short term calculated response of both the steam generator level and cold leg temperature are in excellent agreement with the measured data. The calculated secondary pressure is different in magnitude from the measured pressure, but exhibits essentially the same trend. The differences in the calculated and measured pressure could be due to the following:

- 1.) Inaccuracies in the input steam flowrate history;
- 2.) The use of a thermodynamic equilibrium model; and,
- 3.) Error in the input feedwater temperature.

It should be stressed that the turbine trip transient is, in its initial moments, a rather fast transient and as such is a severe test of our computer model, which was designed to simulate slow transients, such as the later stages of the turbine trip test. Nonetheless, the results for the first sixty seconds are encouraging and demonstrate that the model can be used to simulate this type of transient.

The results of the long term simulation are shown in Fig. 6.4-15. The calculated cold leg temperature response is in excellent agreement with the measured data. The calculated pressure is in excellent agreement with the measured pressure at times greater than 80 seconds. The calculated water level deviates from the measured water level for times

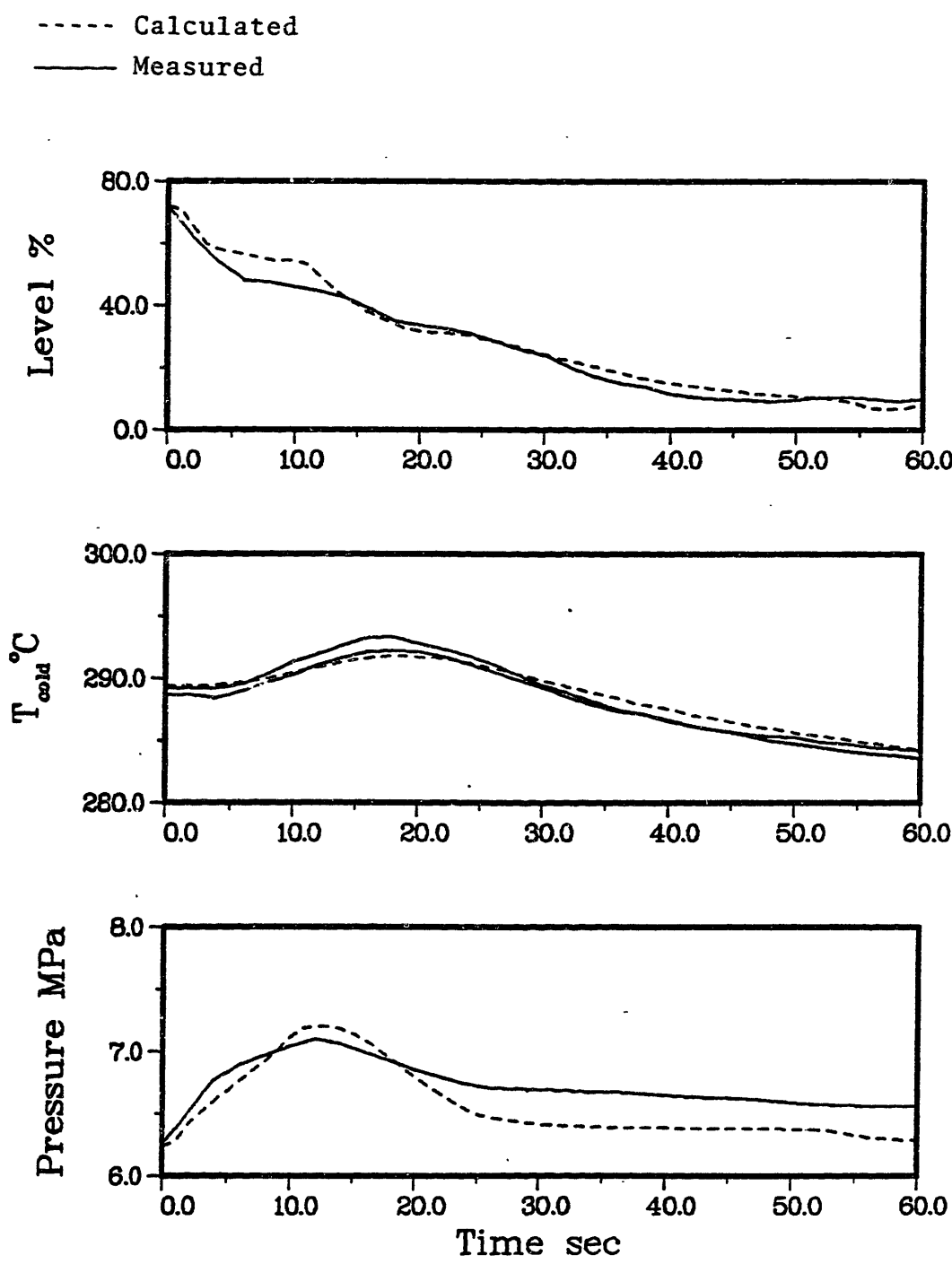


Figure 6.4-14. Short term turbine trip response, steam generator 1.

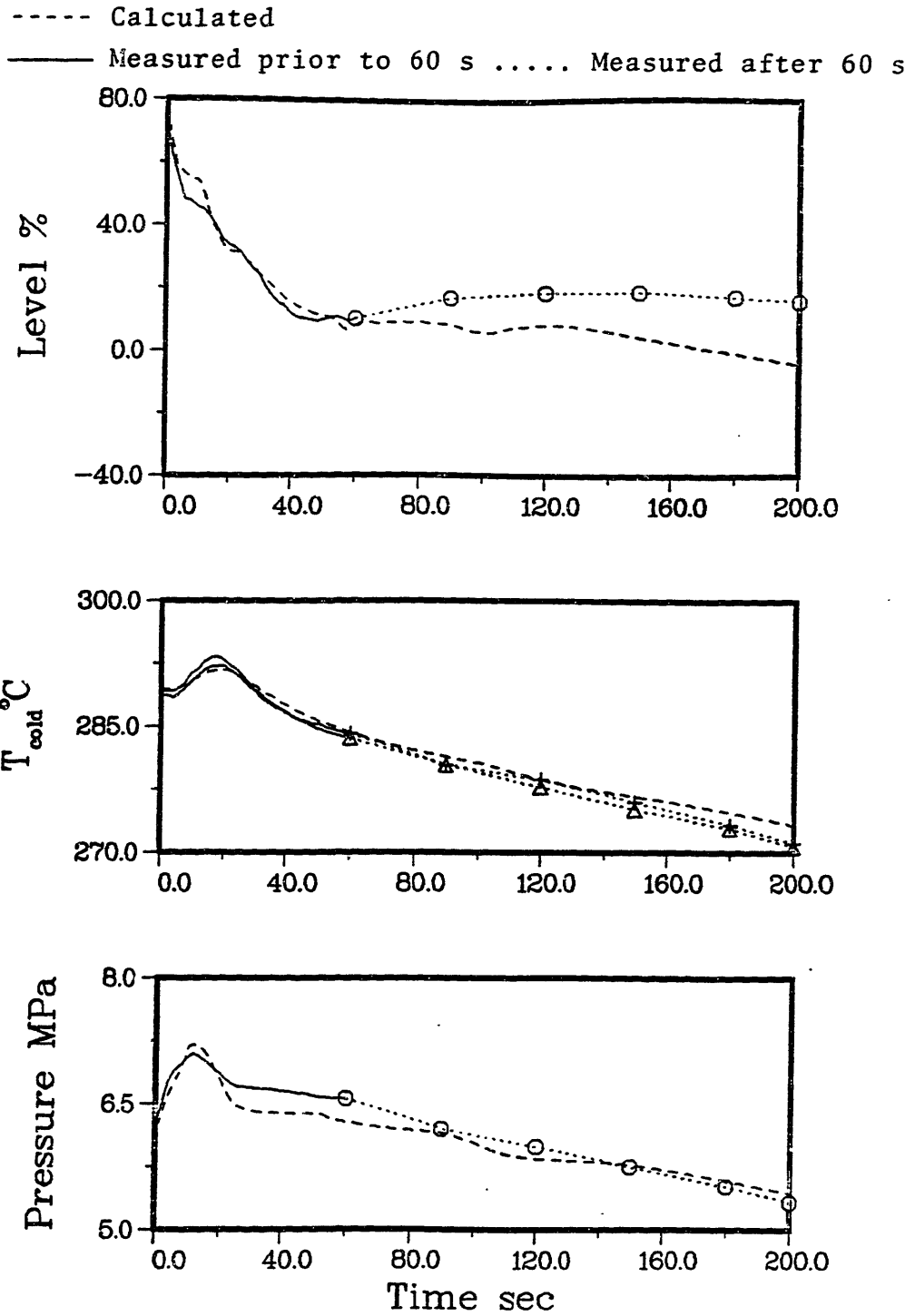


Figure 6.4-15. Long term turbine trip response, steam generator 1.

greater than 60 seconds. Some of the error in the calculated water level can be attributed to the geometric representation of the downcomer in the model. Also, there is the fact that the steam generator model has a free integrator (see Ch. 5.8 and Ch. 6.4.3) and therefore tends to integrate any errors in the input steam and feedwater flowrates resulting in inaccuracies in the calculated level.

### Steam Generator 2

The initial conditions pertaining to steam generator 2 for the turbine trip test are given in Table 6.4-7. The sequence of events for the transient are the same as those given for steam generator 1. The short and long term inputs are shown in Figs. 6.4-16 and 6.4-17.

The calculated short term response for steam generator 2 is shown in Fig. 6.4-18. As can be seen, the calculated pressure exhibits the same trend as the measured pressure with some difference in magnitude. The short term behavior of the cold leg temperature reveals an interesting effect. That is, the measured temperature for one cold leg responds in a very different manner than the measured temperature for the other cold leg, with the calculated cold leg temperature response falling somewhere between. The difference in measured responses is probably due to differences in seating of the RTDs within their thermowells. The transient response of the calculated level compares favorably with the measured level. Part of the error in the calculated error can be

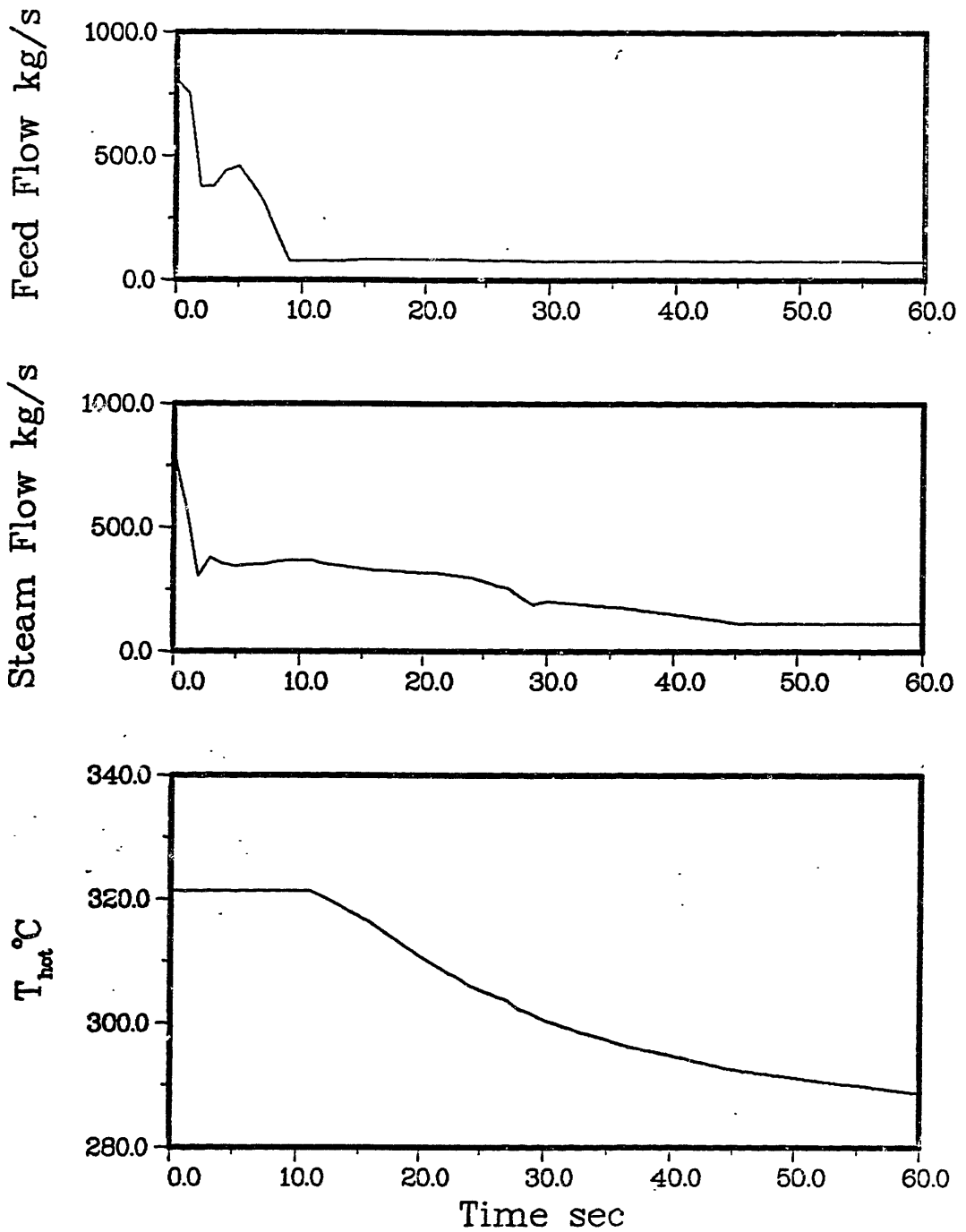


Figure 6.4-16. Short term input for turbine trip, steam generator 2.

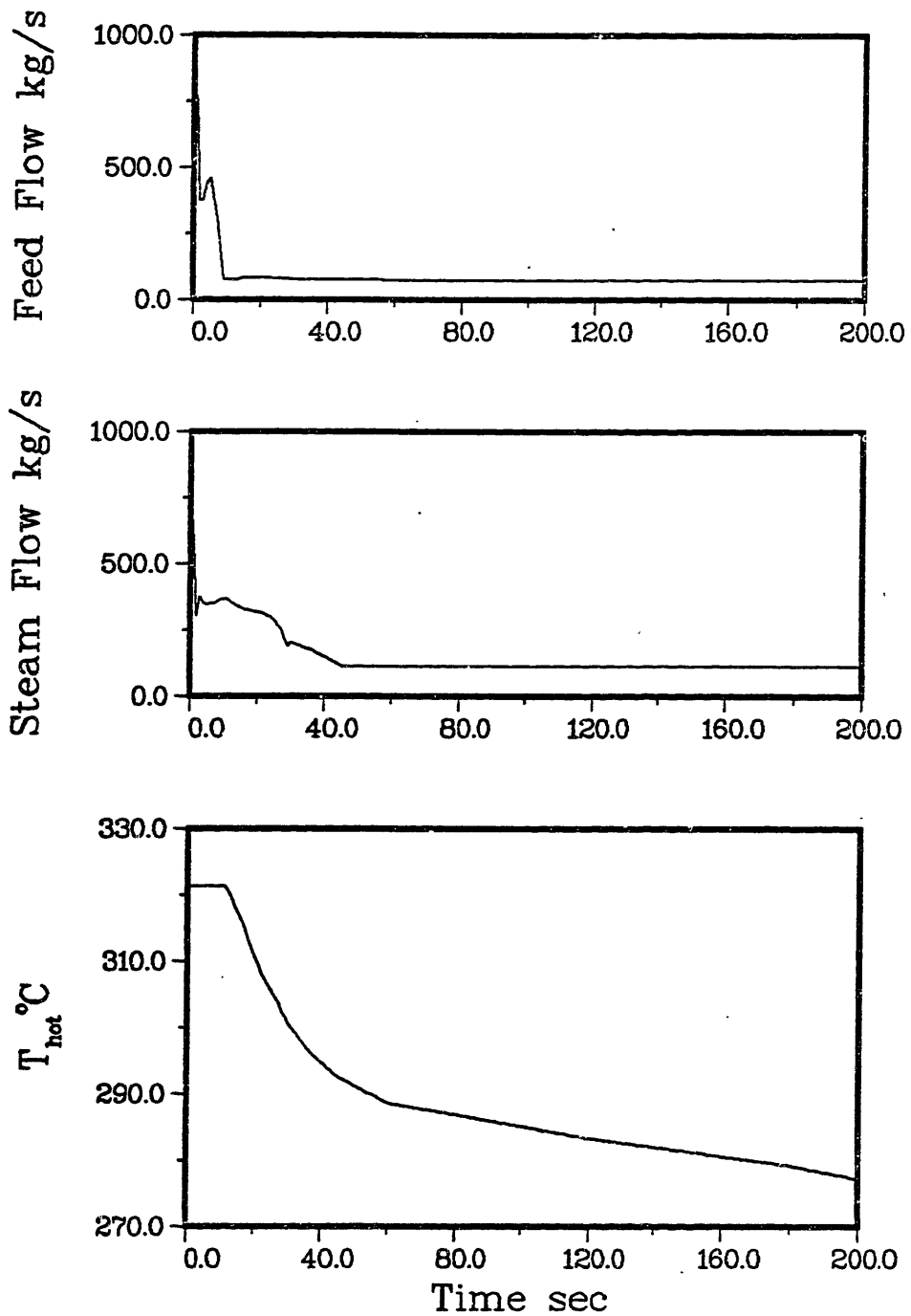


Figure 6.4-17. Long term input for turbine trip, steam generator 2.

----- Calculated  
—— Measured

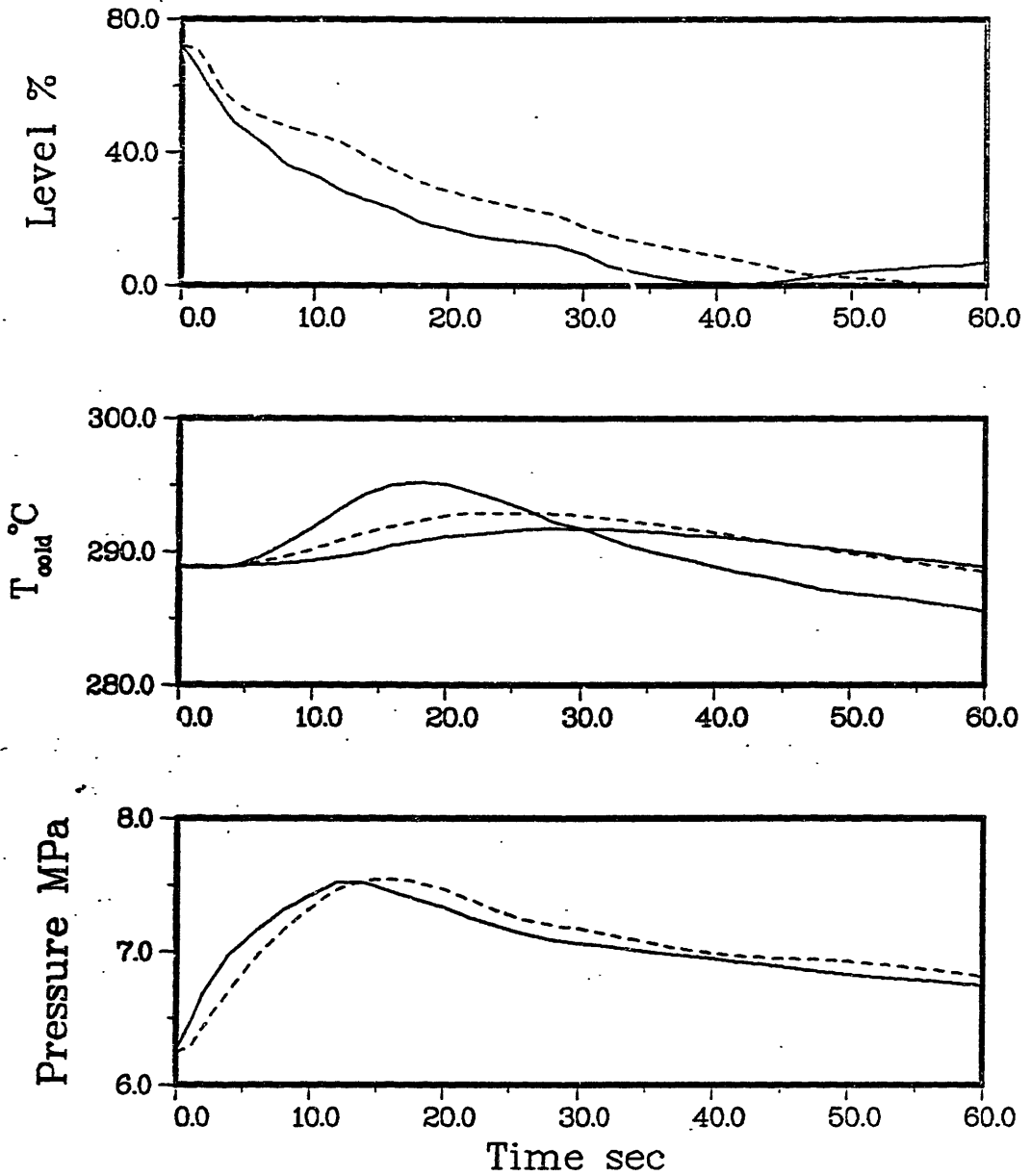


Figure 6.4-18. Short term turbine trip response, steam generator 2.

Table 6.4-7  
Turbine Trip Initial Conditions, Steam Generator 2.

Quantity	Value
Power/Steam Generator	1382 MWt
Water Level*	10.52 (72%)†
Downcomer Flowrate	3572 kg/s
Steam Pressure	6.24 MPa
Steam Flowrate	805.5 kg/s
Feedwater Temperature	246.2°C
Primary Inlet Temperature	321.3°C
Primary Outlet Temperature	288.8°C
Primary Flowrate	7619 kg/s
Fouling Factor	$1.953 \cdot 10^{-5} \text{ m}^2 \text{ K/W}$

\* Referenced to tubesheet.

† Percent of instrument span (4.24 m), where lower instrument tap is 7.47 m above tube sheet.

attributed to the idealized geometry used in the model and to the integration of errors in the input steam and feed-water flowrates.

The long term response of steam generator 2 is shown in Fig. 6.4-19. The calculated pressure is in good agreement with measured data. The calculated cold leg temperature is also in good agreement with the data. Finally the calculated long term level response exhibits dynamics that are





similar to the measured level dynamics with some differences in magnitude.

#### 6.4.5 Loss of Primary Flow

The sequence of events for the test are as follows: All four reactor coolant pumps are manually tripped at 0.0 seconds. At 0.2 seconds a reactor trip occurs, followed by a turbine trip at 0.4 seconds. At one second the turbine bypass valves start to open, and are fully open one second later, at which time the atmospheric dump valve opens. At six seconds the atmospheric dump valve closes. The turbine bypass valves start to close at 12 seconds, and are fully closed at 18 seconds. The simulation continues until 360 seconds after the pumps trip.

The data presented in Ref. (S4) for the time dependent primary flowrate are not adequate for simulation purposes. Therefore, we use our own model for the primary flow coast-down. For this situation we must consider two time periods:

- 1.) The initial part of the transient during which the primary flowrate decreases rapidly; and,
- 2.) The time after which natural circulation in the primary system is established.

For the first time span we use a model developed in Ref. (T1). This model is represented by the following differential equation:

$$\frac{dW}{dt} + aW^2 = 0$$

Integrating this equation subject to the initial condition that  $W = W_i$  at  $t = 0$  yields:

$$\frac{W}{W_i} = \frac{1}{1 + bt} \quad (6.4-5)$$

where  $b = aW_i$ . The constant  $b$  is determined by fitting Eq. (6.4-5) to the initial 30 seconds of the primary flow data presented in Ref. (E1). This fitting gives:

$$\frac{W}{W_i} = \frac{1}{1 + 0.115t} \quad (6.4-6)$$

Once natural circulation is established we must use a different scheme from the one given above to calculate the primary flowrate. Natural circulation conditions are commonly characterized by the flow-to-power ratio, which is defined to be the ratio of the primary flowrate, expressed in percent of the full power flowrate, to the reactor power, expressed in percent of full power. We do not know what this ratio is for ANO-2. However, in Ref. (N1) the flow-to-power ratio for the Calvert Cliffs plant, which is also a Combustion Engineering designed NSSS similar to ANO-2, is given as being in the range of 4.2 to 4.8. Therefore, we choose to use a flow-to-power ratio of 4.5 for ANO-2. In

order to make use of the flow-to-power ratio for calculating the primary flowrate we need to know the reactor decay power. In Ref. (N2) the decay power is modeled as the sum of four decaying exponentials. That is,

$$Q_D(t) = \sum_{i=1}^4 Q_{Di}^0 e^{-\lambda_i t} \quad (6.4-7)$$

where  $Q_D(t) \equiv$  decay power expressed as a fraction of full power;

$Q_{Di}^0 \equiv$  contribution of decay group  $i$  expressed as a fraction of full power; and,

$\lambda_i \equiv$  decay constant of group  $i$ ,  $\text{sec}^{-1}$ .

To obtain the primary flowrate at any time once natural circulation has been established we simply multiply Eq. (6.4-7) by the flow-to-power ratio and the full power primary flowrate. The transition from Eq. (6.4-6) to Eq. (6.4-7) occurs when the primary flowrate calculated using Eq. (6.4-6) becomes less than that obtained using Eq. (6.4-7). The time dependent primary flowrate calculated using the scheme given above and then used in the loss of flow tests is shown in Fig. 6.4-20.

### Steam Generator 1

The initial conditions pertaining to steam generator 1 in the loss of primary flow test are given in Table 6.4-7. The transient calculations consist of both short term

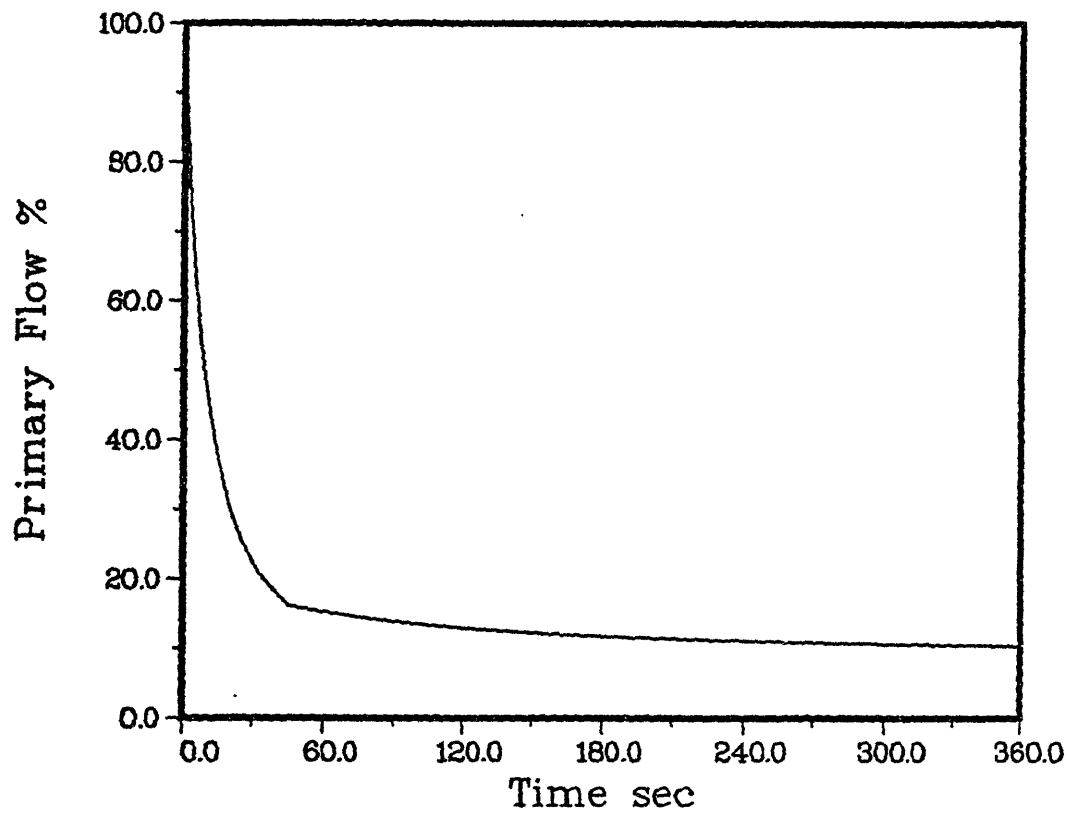


Figure 6.4-20. Primary flowrate used for loss of flow calculations.

Table 6.4-8  
Decay Power Parameters (Ref. (N2)).

Group	$Q_{ni}^0$	$\lambda_i (\text{sec}^{-1})$
1	0.0054	0.7600
2	0.0150	0.1309
3	0.0185	0.01299
4	0.0260	$3.4679 \cdot 10^{-4}$

(60 sec) and long term (360 sec) simulations, and the input for these calculations are shown in Figs. 6.4-21 and 6.4-22.

When the steam and feedwater flowrates presented in Ref. (S4) are used as input to the calculations, the simulation results differ significantly from the measured data. The agreement between model calculations and measured plant data can be improved by adjusting the steam and feedwater flows. In fact, simulations described in Ref. (M5) use steam and feedwater flows adjusted within instrumentation uncertainties to improve agreement between model calculations and plant data. We modify the steam and feedwater flowrates for steam generator 1 by subtracting 17.4 kg/s from the flowrates read off the plots provided in Ref. (S4), effectively biasing the feed and steam flows by -17.4 kg/s, or -2.2 per cent of the full power steam flowrate. This

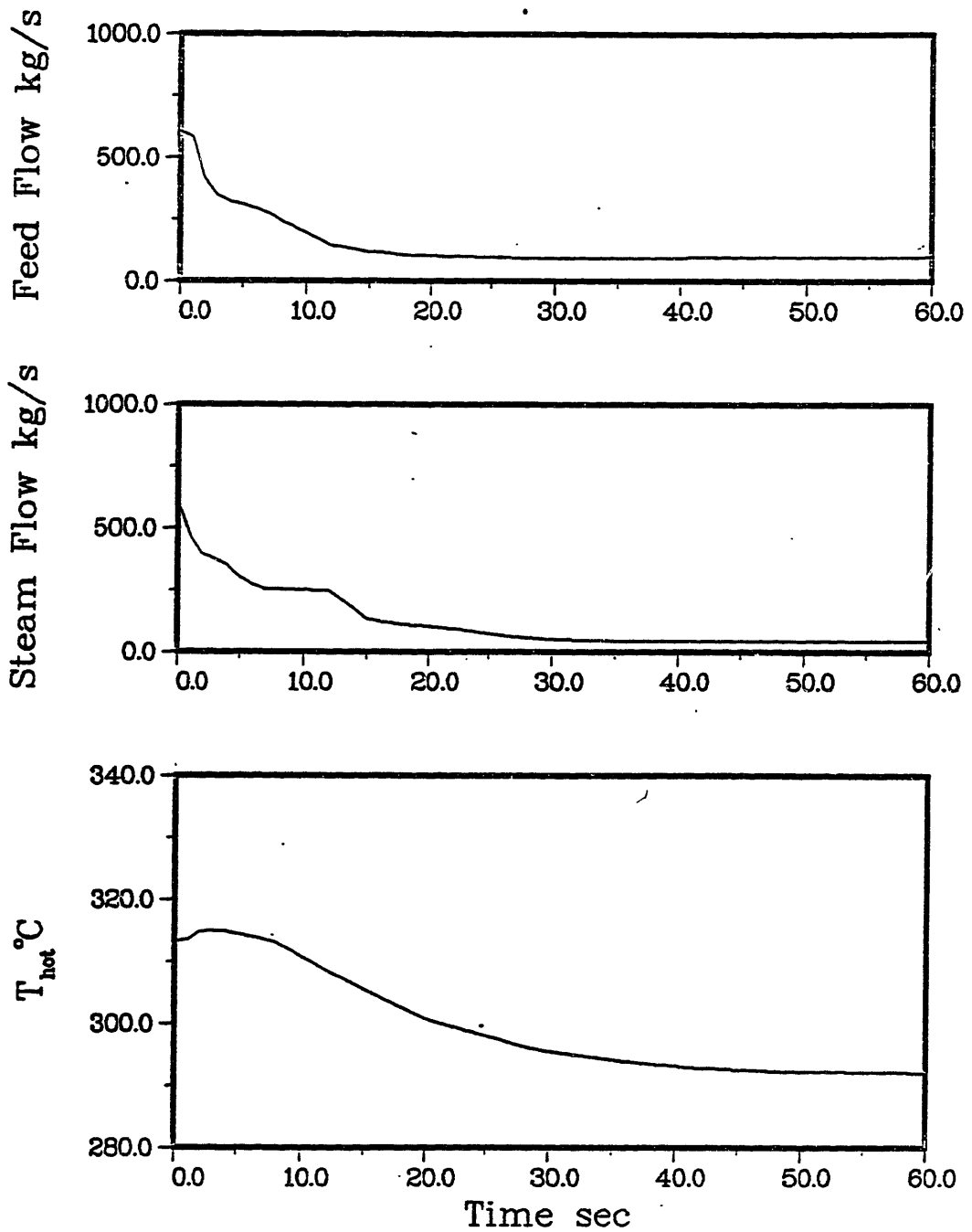


Figure 6.4-21. Short term input for loss of primary flow test, steam generator 1.

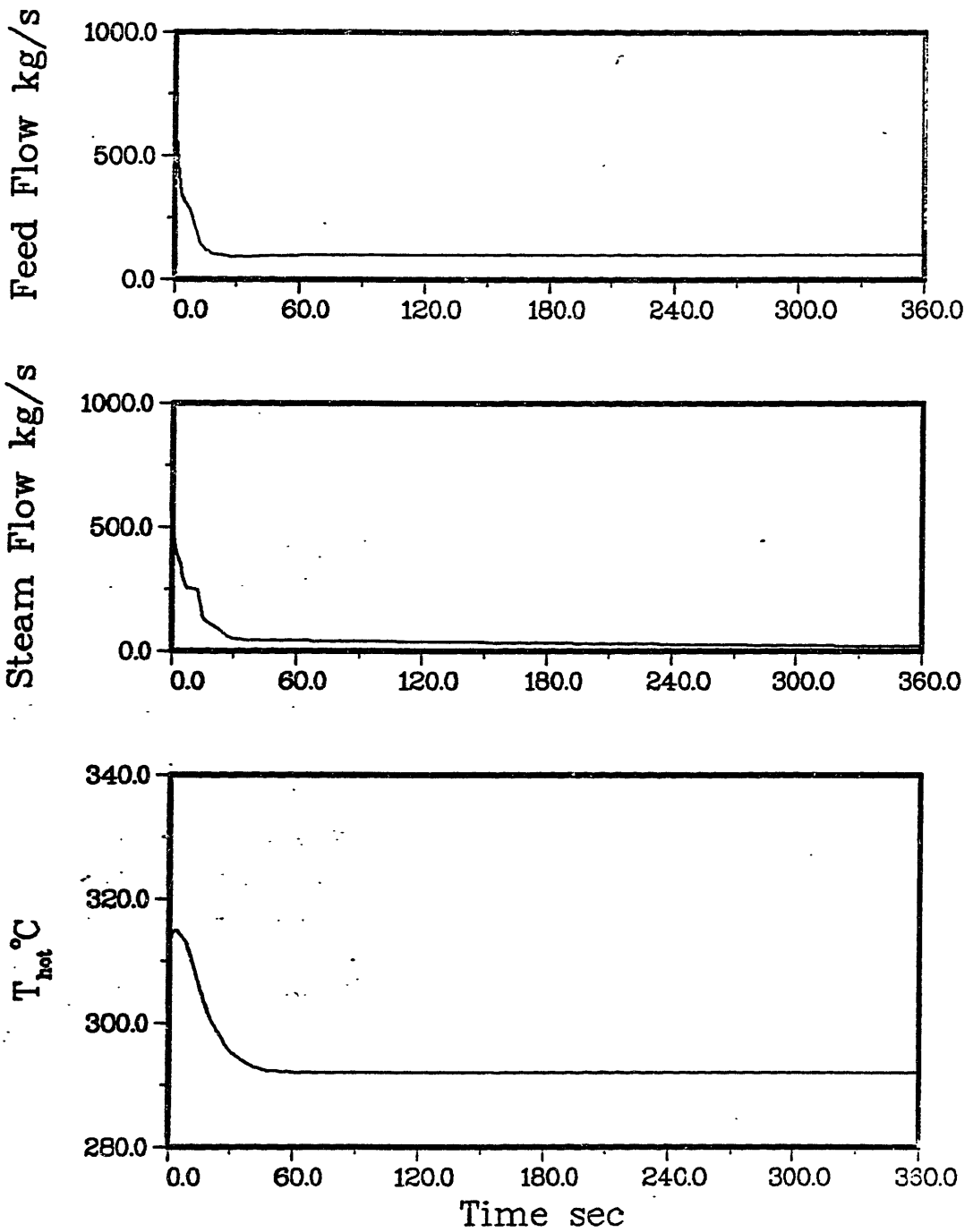


Figure 6.4-22. Long term input for loss of primary flow test, steam generator 1.



Table 6.4-9  
Loss of Primary Flow Initial Conditions, Steam Generator 1.

Quantity	Value
Power/Steam Generator	1148 MWt
Water Level*	10.43 m (70%)†
Downcomer Flowrate	3592 kg/s
Steam Pressure	6.38 MPa
Steam Flowrate	607.9 kg/s
Feedwater Temperature	208.9°C
Primary Inlet Temperature	313.4°C
Primary Outlet Temperature	288.2°C
Primary Flowrate	8336 kg/s
Fouling Factor	$1.273 \cdot 10^{-5} \text{ m}^2 \cdot \text{K/W}$

\* Referenced to tubesheet.

† Percent of instrument span (4.24 m), where lower instrument tap is 7.47 m above tube sheet.

difference can be attributed to instrument calibration error and a possible offset in the plots of the measured steam and feed flows.

The response of steam generator 1 during the first 60 seconds is shown in Fig. 6.4-23. The calculated pressure closely follows the measured pressure, with a slight offset from the measured pressure for times greater than 15 seconds. The calculated cold leg temperature is in good

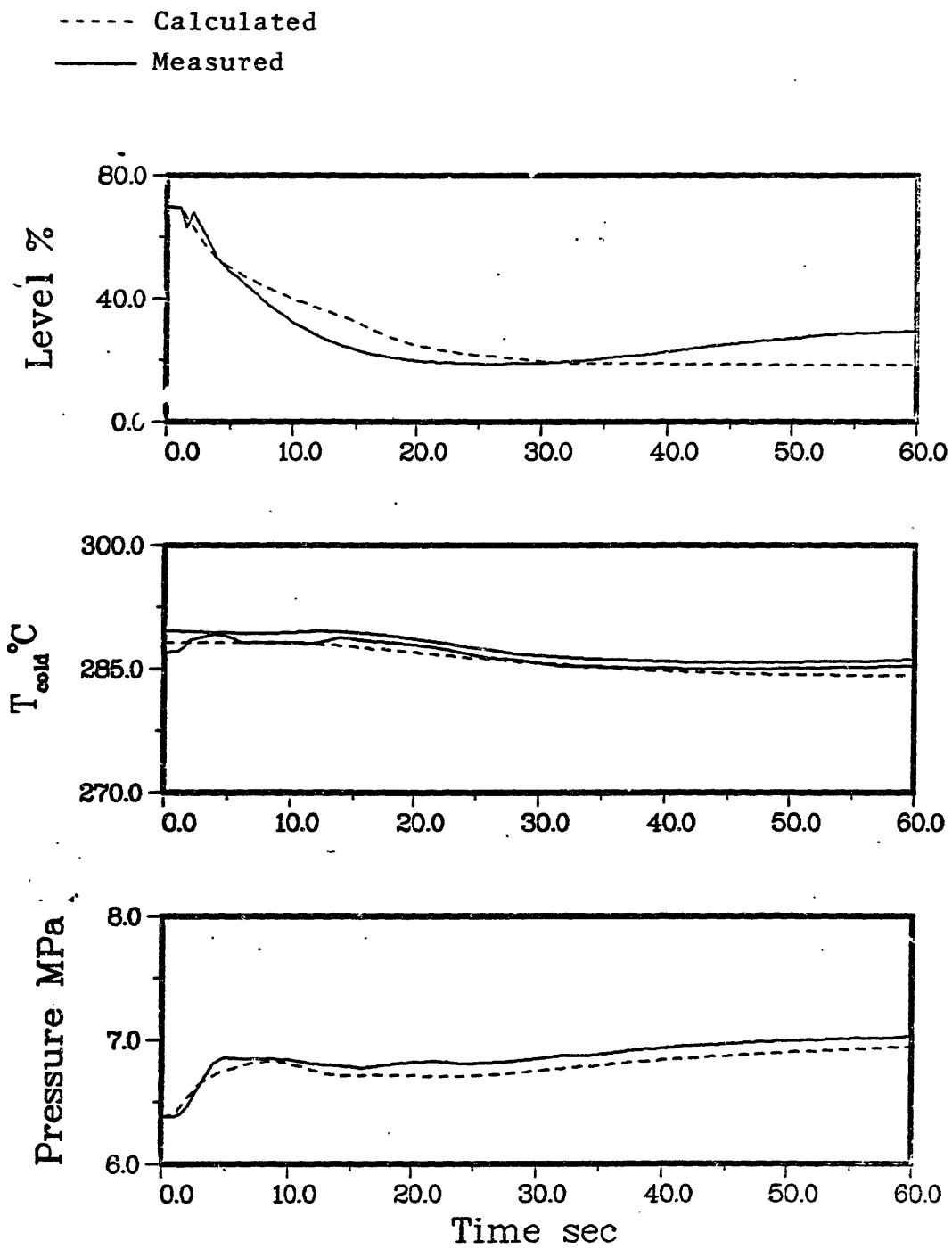


Figure 6.4-25. Short term loss of primary flow response, steam generator 1.

agreement with the measured cold leg temperatures. The calculated level follows the same trend exhibited by the measured level, although it is somewhat greater than the measured level from 4 to 30 seconds and then less than the measured level after 30 seconds. Some of the error in the the calculated level can be attributed to the use of an idealized geometric representation (see Appendix K) of the downcomer geometry and the integration of errors in the input steam and feed flows.

Figure 6.4-24 shows the long term response of steam generator 1 during the loss of primary flow transient. Both the calculated pressure and cold leg temperature are in excellent agreement with the corresponding measured quantities. The calculated water level response is somewhat different from the measured water level response. Some of the error in the calculated water level response is due to idealization of the downcomer geometry and integration of errors in the input steam and feed flows.

#### Steam Generator 2

The initial conditions for steam generator 2 in the primary loss of flow test are shown in Table 6.4-10. As discussed for steam generator 1, the steam and feedwater flowrates are modified to improve agreement between model calculations and plant data. For steam generator 2, the steam and feed flows are modified by subtracting 12.7 kg/s from the measured flowrates throughout the transient. This is equivalent to

----- Calculated  
 ——— Measured before 60 s  
 ..... Measured after 60 s

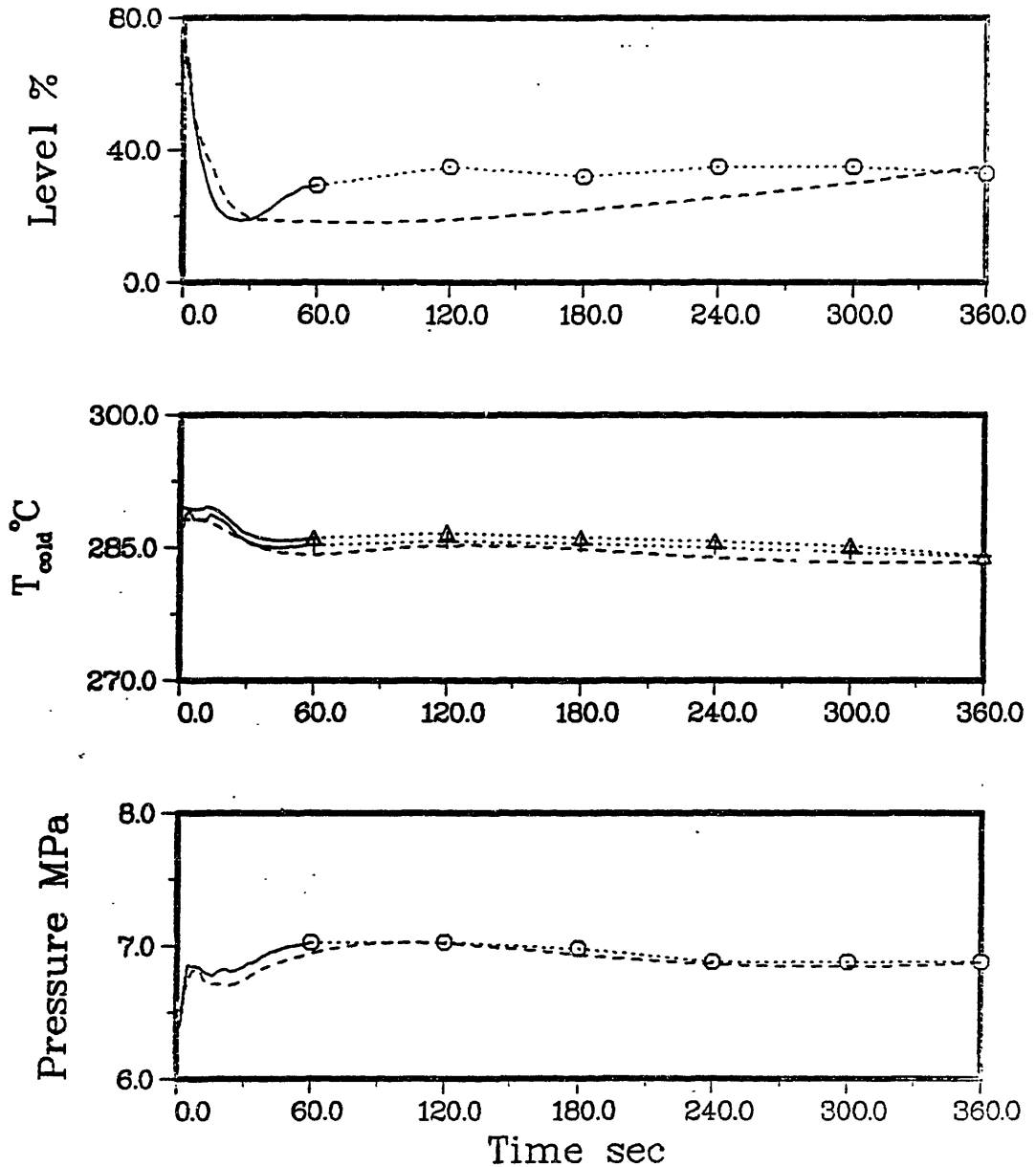


Figure 6.4-24. Long term loss of primary flow response, steam generator 1.

Table 6.4-10  
Loss of Primary Flow Initial Conditions, Steam Generator 2.

Quantity	Value
Power/Steam Generator	1148 MWt
Water Level*	10.43 m (70%)†
Downcomer Flowrate	3585 kg/s
Steam Pressure	6.38 MPa
Steam Flowrate	617.8 kg/s
Feedwater Temperature	215.6°C
Primary Inlet Temperature	313.3°C
Primary Outlet Temperature	289.1°C
Primary Flowrate	8605 kg/s
Fouling Factor	$1.898 \cdot 10^{-5} \text{ m}^2 \text{ - K/W}$

\* Referenced to tubesheet.

† Percent of instrument span (4.24 m), where lower instrument tap is 7.47 m above tube sheet.

using a constant bias in the flowrates of -1.6 per cent of the steam flow at full power. The input used for both the short term and long term calculations are shown in Figs. 6.4-25 and 6.4-26.

The measured pressure for steam generator 2 during the loss of primary flow test is not presented in Ref. (S4). Therefore the measured pressure is not shown in Fig. 6.4-27, which shows the short term response of steam generator 2.

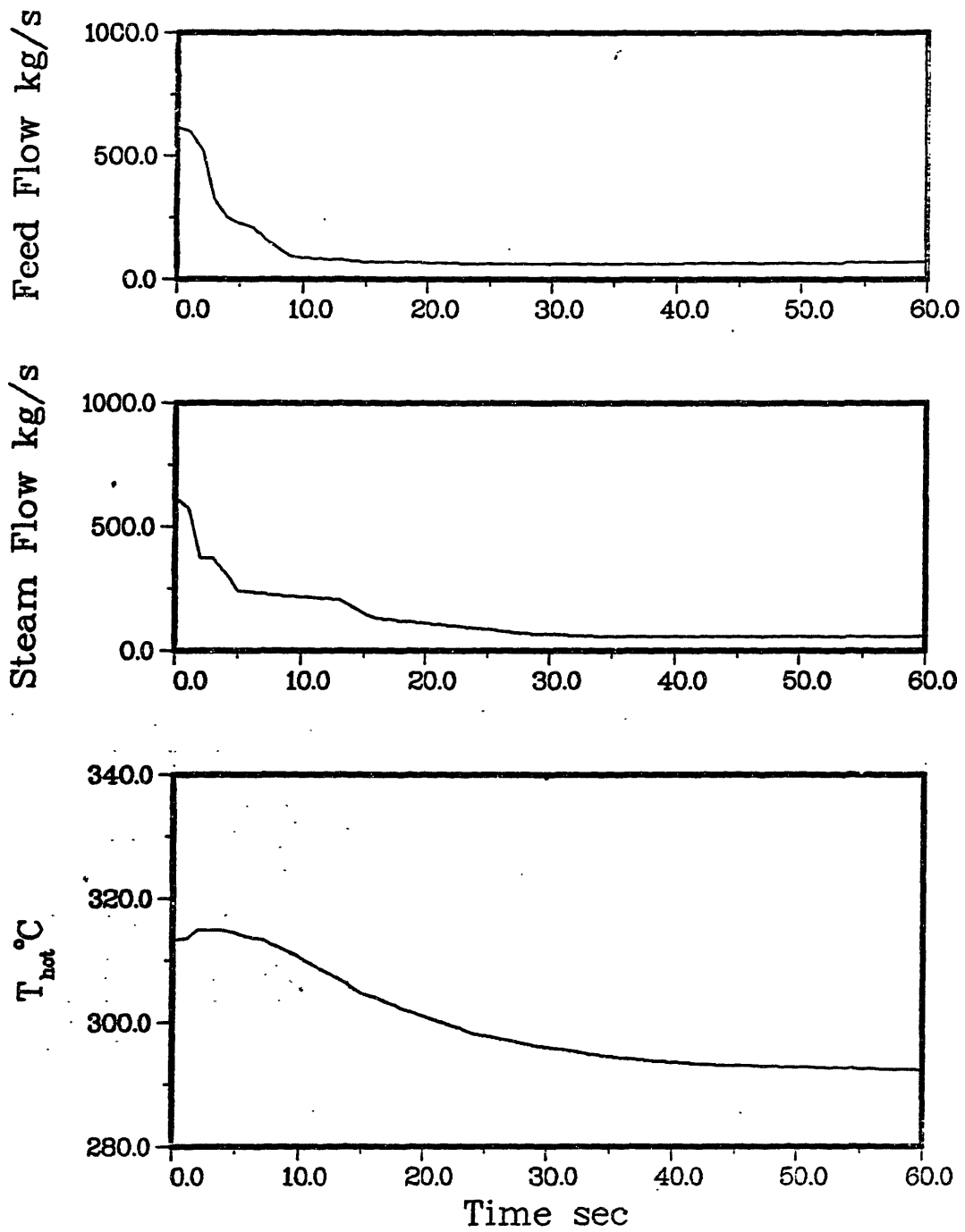


Figure 6.4-25. Short term input for loss of primary flow test, steam generator 2.

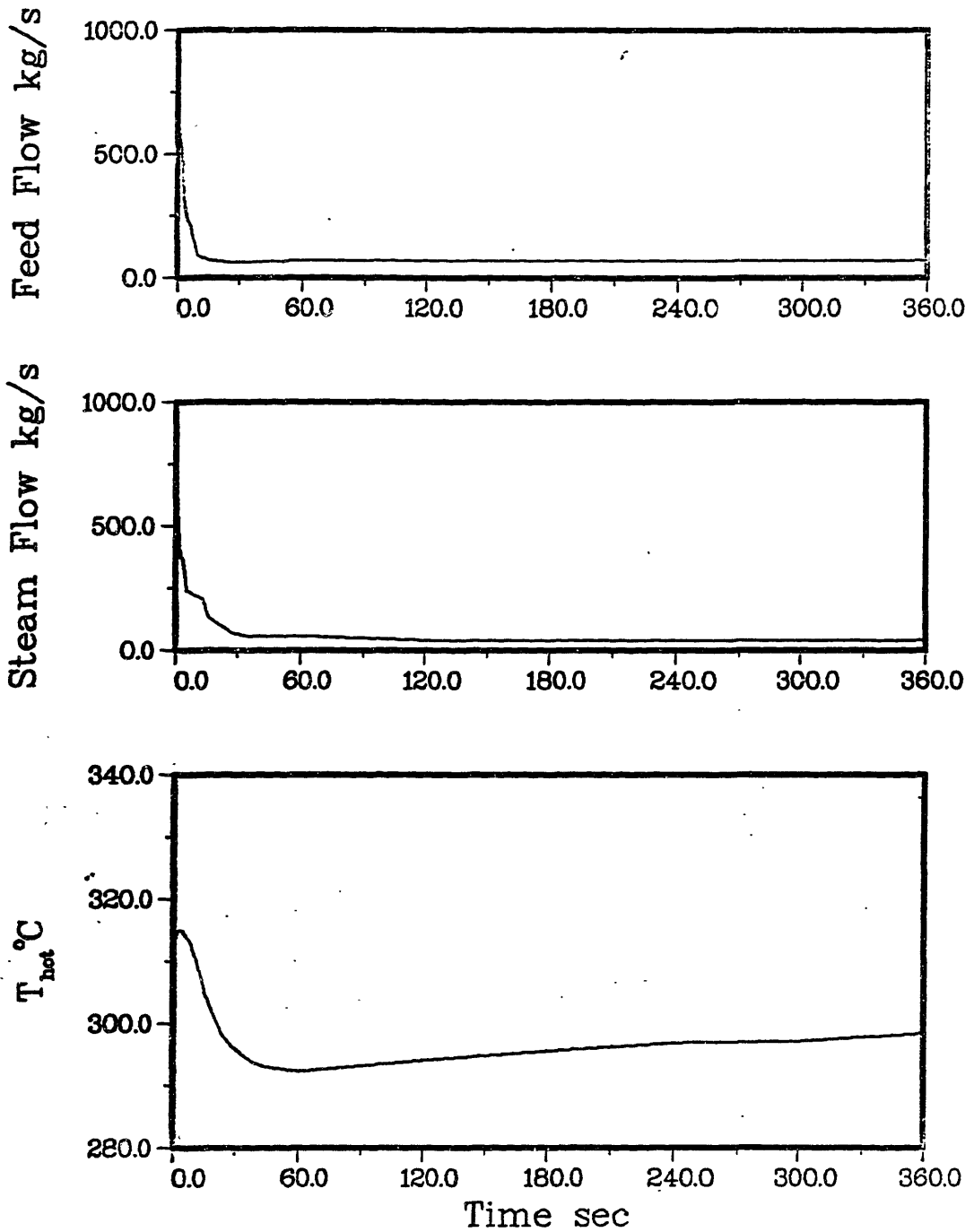


Figure 6.4-26. Long term input for loss of primary flow test, steam generator 2.

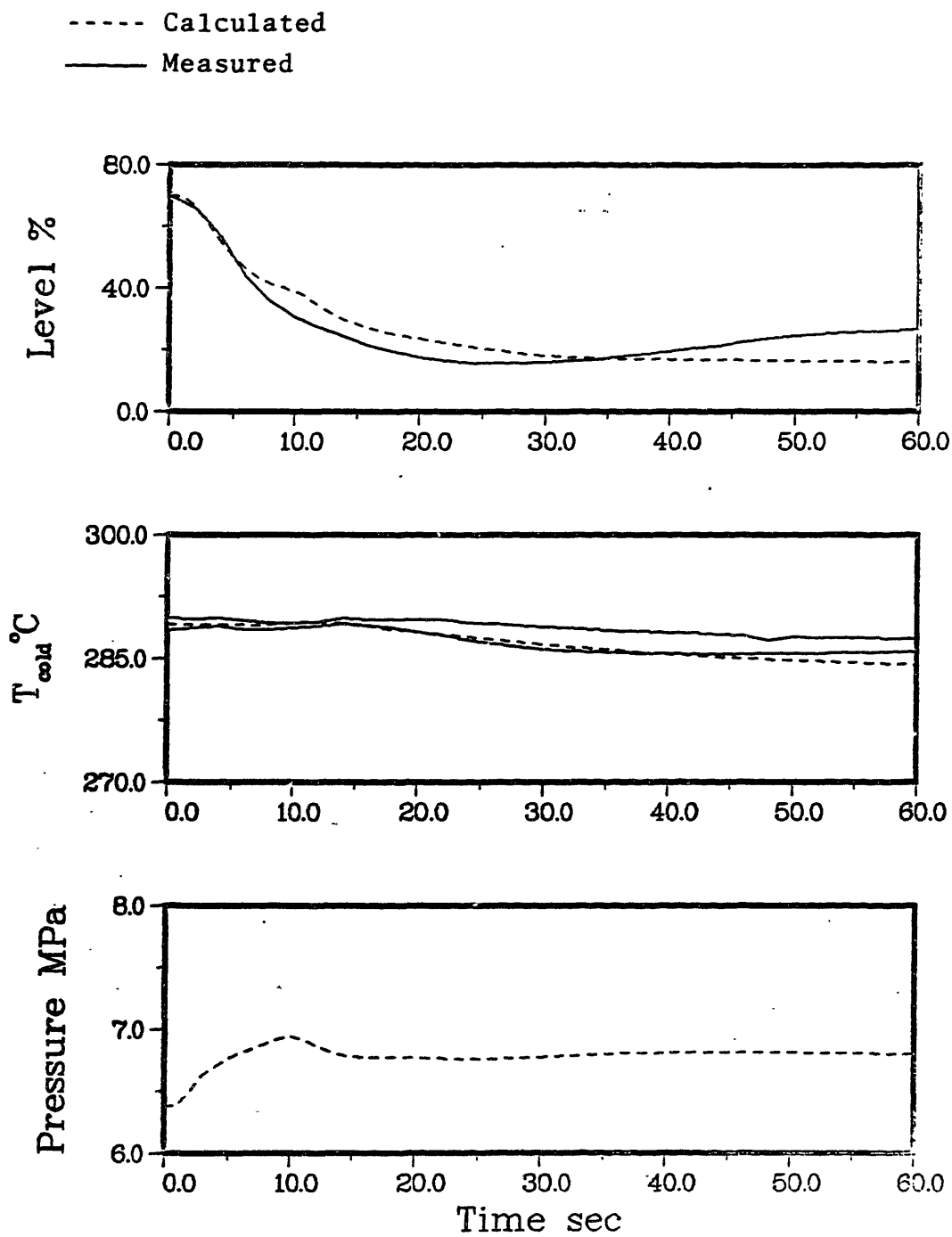


Figure 6.4-27. Short term loss of primary flow response, steam generator 2.



The calculated cold leg temperature is in good agreement with the measured data for the sixty second interval. The calculated short term response of the level is similar to the measured level response. Some of error in the calculated level response can be accounted for by reasons given previously.

The long term response for steam generator 2 is shown in Fig. 6.4-28. The calculated cold leg temperature is in excellent agreement with the measured data except for a slight dip and recovery in the calculated values between 60 and 240 seconds. This calculated cold leg temperature behavior matches the secondary pressure behavior, as it should since the heat transfer link between the primary and secondary systems provides a direct path for the secondary pressure to influence the cold leg temperature. The calculated level exhibits the same trend as the measured level during the early stages of the test. However the calculated level does not follow the measured level from about 45 seconds onward. Instead, the calculated level stays below the measured level and shows signs of recovering as the transient calculation progresses. The error here is due, in part, to the integration of uncertain input steam and feedwater flow-rates, as well as idealizations made in order to model the downcomer geometry.

----- Calculated  
 ——— Measured before 60 s  
 ..... Measured after 60 s

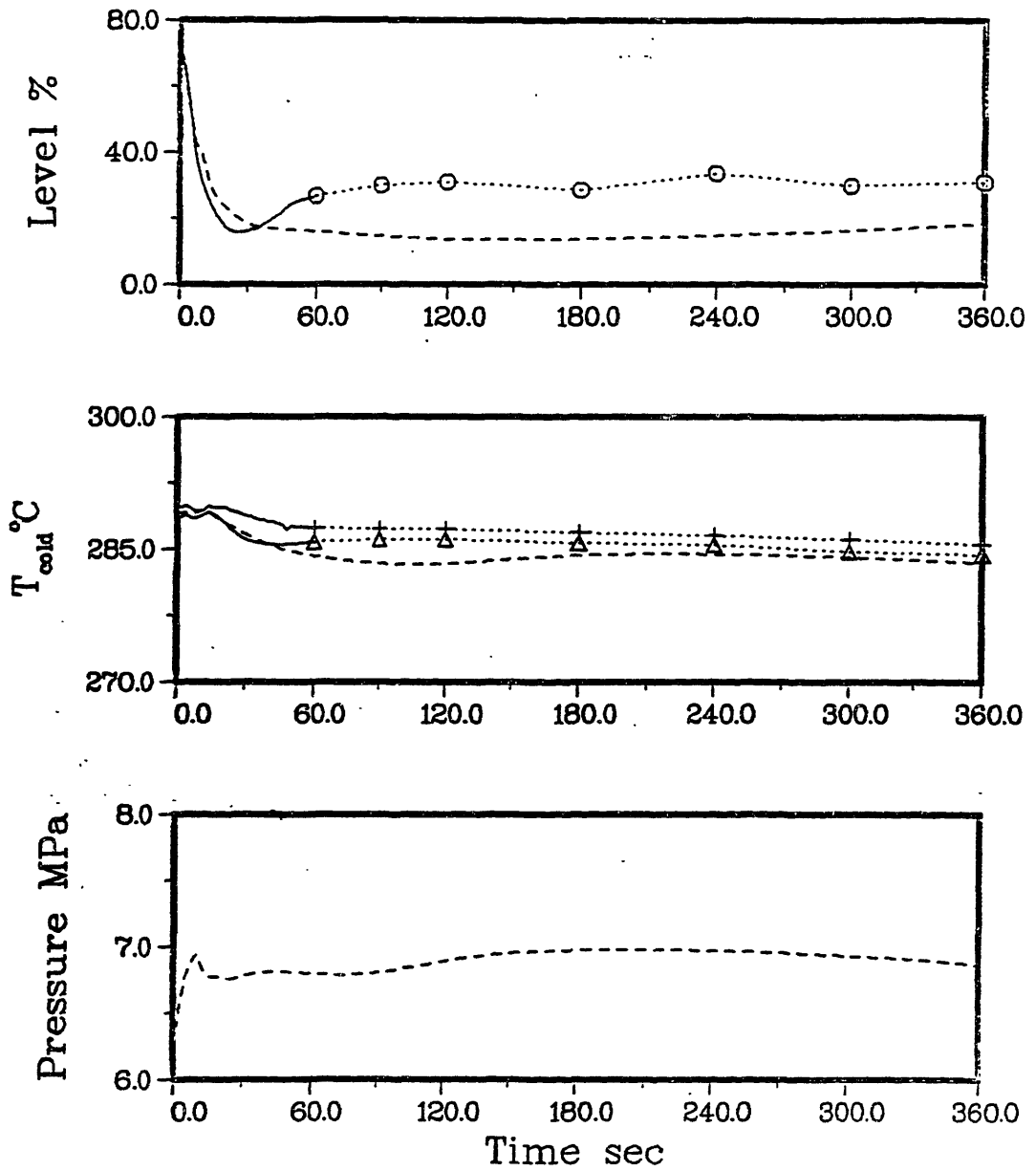


Figure 6.4-28. Long term loss of primary flow response, steam generator 2.

## 6.5 PROGRAM EXECUTION TIME

An important goal of this work is to develop a steam generator model for use in a real time manner during power plant operation. Therefore, we are interested in the program execution time. The parameter of significance here is the Real Time-to-CPU Time ratio. When this ratio is greater than one the program execution is faster than real time.

The computer model was developed using an Amdahl 470 V/8 mainframe computer. This computer is much faster than the on-line computers in power plants, so the Real Time-to-CPU Time ratio for the program run on this machine must be much greater than one if we wish to achieve real time computation on plant process computers. These process computers must also perform other calculations in parallel with the model calculations, reinforcing the need for very fast

Table 6.5-1  
Real Time-to-CPU Time Ratio for Execution  
on Amdahl 470 V/8 System.

Time Step Size(s)	Print Frequency	Real Time-to-CPU With Print
0.10	Every 10 steps	47
0.25	Every 4 steps	107
0.40	Every 5 steps	200

program execution. Table 6.5-1 shows the Real Time-to-CPU Time ratios for a variety of time step sizes with intermediate printing of computation results (no printing of intermediate results yields speeds that are up to 14 per cent faster). The numbers given in Table 6.5-1 indicate that the execution speed of the computer model appears to be sufficiently fast to ensure real time modeling even on a smaller computer system.

In an attempt to gain insight relevant to the execution speed of the program on a plant computer, the model was run on a Digital Equipment Corp. VAX 11/780 computer. This computer is similar in size and speed to the types of computers being used in current generation power plants. The Real Time-to-CPU Time ratio for running the program on the VAX machine using a 0.25 second time step with print outs at every second of simulation time is 11. This result supports our conclusion that the model is probably fast enough for use in a real time manner.

There are two additional comments concerning the program developed in this work:

- 1.) There are no simplifications made with respect to:
  - a.) Reynolds number dependence of friction factors;
  - b.) Used full exponentials rather than approximations;

- c.) No streamlining of property computations by neglecting to update properties with weak dependence on state variables; and,
- d.) No pre-computation and storage of groups of geometric parameters.

This could aid in obtaining even faster computational speeds; and,

- 2.) The amount of computer memory used when performing calculations is not evaluated relative to the amount of storage space available in plant process computers. This may require reducing the storage requirements of the computer model and the difficulty of doing this is not addressed here.

## Chapter 7

### SUMMARY, CONCLUSIONS, AND RECOMMENDATIONS

#### 7.1 SUMMARY

The objective of this work is to develop and validate a fast running computer model of a vertical U-tube steam generator. This model has a variety of applications in power plant technology. The model can be used as part of a Safety Parameter Display System (SPDS). The SPDS is to be used to aid in the rapid and accurate diagnosis of plant faults, as well as routine monitoring of significant plant parameters. These functions require fast running models of important power plant components. The model can also be used to provide information in signal validation efforts and in fault detection and identification (FDI) systems. In addition, this model coupled with other plant component models can be used by operators to make projections of the consequences of contemplated control actions. Finally, this model bridges the gap between simple pot-boiler type models and the more complex, CPU-time-consuming computer codes used for detailed design and safety studies.

The model is developed using a first principles application of the one-dimensional conservation equations of mass, momentum, and energy. The secondary side of the steam generator is divided into four large control volumes. Two of these volumes are the tube bundle region and the unheated

(two-phase) riser region. Two other volumes are obtained by dividing the steam dome - downcomer into a saturated region and a subcooled region. The mass and energy conservation equations are integrated over these large control volumes to eliminate the space derivative, resulting in a set of coupled, nonlinear ordinary differential equations in time. The momentum equation is integrated around the recirculation loop, which results in a single nonlinear ordinary differential equation in time.

The primary side is divided into three volumes: the inlet plenum, the outlet plenum, and the volume within the tubes of the tube bundle. The mass and energy conservation equations are integrated over each primary volume and combined to obtain three coupled, nonlinear ordinary differential equations in time.

The model equations are forward time differenced and solved using the numerical scheme presented in Chapter 5. The stability characteristics of the numerical scheme are investigated by linearizing the equation system.

Two salient features of the model are the incorporation of the loop momentum equation and the retention of all nonlinear effects. The inclusion of the integrated momentum equation allows us to track the water level during transients without having to resort to artifices such as empirical fits of level as a function of inventory or vapor volume. The fact that the model is nonlinear permits us to

model transients with large changes from nominal operating conditions, which would not be the case for a linear model.

The final step in the model development is validation. This step is important because it serves as a check on model fidelity and it allows us to determine the limits of model applicability. The model calculations are compared to experimental results or to results obtained using other computer models. This model is validated over a wide range of steady state operating conditions and a spectrum of transient tests ranging from turbine trip events to a milder full length control element assembly drop test. The results of the validation effort are encouraging, indicating that the model is suitable for application to a broad range of operational transients. Equally important is the execution speed of the computer model. Real Time-to-CPU-Time ratios for running the computer program on an Amdahl 470 V/8 computer range from 47 to 200, with integration time step sizes of 0.1 to 0.4 seconds respectively.

## 7.2 CONCLUSIONS

Based on model development, particularly model validation, we can draw the following conclusions:

- 1.) Execution Time—Real time execution of the model appears to be achievable. Real Time-to-CPU-Time ratios on a large mainframe computer (Amdahl 470 V/8) range from 47 to 200 using integration time step sizes of 0.1



to 0.4 seconds respectively. The Real Time-to-CPU Time ratio for execution on a Digital Equipment Corp. VAX 11/780 computer is 11 with an integration time step size of 0.25 seconds. It should be noted that extrapolating the execution time results obtained here to plant process computers is at best uncertain and can even be misleading. Plant process computers, which are generally mini-computers, come in a variety of sizes and types that are application oriented, making it difficult to draw any definitive conclusions regarding execution time of our computer model on a plant process computer without actually running the model on one of these machines. However, given the Real Time-to-CPU Time ratios achieved on the mainframe computer, it appears that real time use of this model on plant process computers is feasible.

- 2.) Validation—Model calculations agree well with measured data. One requirement for the model is that it be reasonably accurate, but pinpoint accuracy is not necessary. The model developed here fulfills this requirement for transients within its range of applicability. The development goal of real

time execution of the computer model dictates that the model be simple. This implies that some plant events, specifically severe accident scenarios, cannot be followed. However, the model is shown to be applicable to a broad range of operational transients occurring on rather long time scales. It is not intended for use in modeling severe accidents or situations where there is a significant departure from normal operation, such as steam generator dry-out.

- 3.) Sensitivity to Input—The model calculations for secondary pressure and steam generator level are sensitive to the input feedwater and steam flowrates. This sensitivity is due to the fact that the model integrates any persisting error in the input steam and feedwater flowrates thereby affecting the mass and energy storage rates for the entire steam generator. These integrated effects show up as errors in gross steam generator parameters such as secondary pressure and steam generator water level. Using the model on-line would require good "information reliability"; that is, validated steam and feedwater flowrates obtained from sensor

processing software that generates best estimate values of measured quantities.

4.) Sensor Dynamics—When using this model, either on-line or to perform simulations for comparison to real plant data, sensor dynamics must be taken into consideration. The worst known offender, from a response time viewpoint, is the Resistance Temperature Detector (RTD), which can have a time constant on the order of tens of seconds. Sensor outputs used as input to the calculations must be corrected to account for sensor dynamics. Similarly, model calculations should be processed through sensor models in order to obtain quantities that can be compared to measured data.

5.) Adaptation of Model Parameters—The shape and magnitude of downcomer flowrate versus power curves can be modified or adjusted to reproduce measurements by adjusting coefficients used in the calculation of tube bundle inlet and outlet pressure losses. This observation has significant implications with respect to parameter adaptation, which is the process of adjusting model constants, or parameters, in order to improve model agreement with observed plant performance.

- 6.) Drift Flux Parameters—The parameters  $C_0$  and  $u_{vj}$  appearing in the drift flux model should be determined, if possible, for a given application of the model. These constants affect the calculation of the vapor volume fraction in the two-phase regions of the steam generator and therefore have a direct impact on the calculation of downcomer flowrate and steam generator water level, as well as the secondary pressure.
- 7.) Excessive Downcomer Flow Response—The calculated downcomer flowrate responds more strongly to transient perturbations than does the actual downcomer flowrate. This is probably due to multidimensional effects that tend to soften, or damp, the actual downcomer flowrate response. These multidimensional effects are not accounted for in our one-dimensional, large control volume representation, and these effects are most important in the tube bundle region where three-dimensional flow redistribution softens the response of the downcomer flowrate.
- 8.) Alternate Model Inputs—The use of water level and pressure as model inputs (to replace feedwater flow and steam flow) is not practical. The reader is referred to

Appendix G for a complete discussion of this modified steam generator model.

### 7.3 RECOMMENDATIONS FOR FUTURE WORK

We can make several recommendations regarding areas requiring further investigative effort:

1.) Model Realignment—During power plant operation it is expected that the model will drift from actual plant performance. Methods must be developed that will allow realignment of the model with the power plant (e.g. adjust model water level to agree with the measured value). These methods are constrained by:

- the methodology must execute in real time or faster; and,
- the methodology must be able to use existing sensor information to infer the values of model state variables that are not measured.

2.) Parameter Adaptation—Methods for on-line parameter adaption remain to be developed. The adaptation process must correctly identify model deviation from plant performance and having done this select and adapt appropriate model constants (e.g. parameter expressing fouling of heat transfer surface). The

adaptation process should be developed within the following guidelines:

- operation must be real time or faster;
- methods are needed to distinguish between disagreements caused by sensor inconsistencies or by a need to up-date (adapt) model constants; and,
- the model constant adaptation must not negate the validation of the model.

3.) Extended Range of Operation—At sufficiently low powers the steam generator is in a pot-boiler mode of operation, with separate liquid levels in both the upflow and downflow portions of the secondary side. The model developed here is not capable of simulating this situation. The model should be extended to account for this mode of operation and the transition from a natural circulation mode to a pot-boiler mode, as well as the transition from pot boiling to natural circulation.

4.) Tube Bundle Uncovery—This is a further extension of the pot boiler mode of operation to the case where steam generator inventory is low enough to cause uncovering of the tubes in the tube bundle, effectively reducing the heat transfer rate.

- 5.) Downcomer Reverse Flow—The model developed here implicitly assumes flow in one direction only. Although situations where there is net flow from the tube bundle into the downcomer are rare, it may be advisable to be able to simulate these conditions in view of the fact that program execution now terminates when reverse flow conditions are calculated to occur.
- 6.) Alternate Model Inputs—The last recommendation given here applies to work discussed in Appendix G. Here we simply state that methods for using transient water level and pressure to calculate transient steam and feedwater flowrates require further investigation. Since steam pressure and water level are measured by multiply redundant sensors, there are significant fault detection incentives for using this approach. Implementation of this approach is not straightforward; the problems that arise and possible solutions are discussed in Appendix G.

## Appendix A

### TWO PHASE FLOW

The purpose of this appendix is to present basic definitions and principles of two-phase flow. The emphasis here is on aspects of two-phase flow which are of immediate and practical interest for the steam generator model developed in this work. More detailed and sophisticated treatments of the subject may be found in References (C1) and (L1).

In two-phase flow it is important to distinguish between local and average quantities. This is due to the discontinuous nature of a flow field consisting of two distinct phases. We will deal primarily with cross-section averaged quantities. The cross-sectional average of an arbitrary variable,  $F$ , can be written as (Ref. (L1)):

$$\langle F \rangle = \frac{\iint F \, dA}{A} \quad (A-1)$$

where  $A$  is the total flow cross-sectional area.

The local vapor volume fraction, or local void fraction, is defined to be the time-averaged local volumetric fraction of vapor in a two-phase mixture. That is



$$\alpha = \frac{\iiint_V dV_v}{\iiint_V dV} = \frac{V_v}{(V_v + V_l)} \quad (\text{A-2})$$

where the subscript  $l$  indicates the liquid phase and  $v$  denotes the vapor phase.

The cross-sectional averaged vapor volume fraction,  $\langle \alpha \rangle$ , is given by:

$$\langle \alpha \rangle = \frac{\iint \alpha \, dA}{A} \quad (\text{A-3})$$

We will refer to  $\langle \alpha \rangle$  as the vapor volume fraction with the understanding that we mean the cross-sectional vapor volume fraction. Equation (A-3) is often written as:

$$\langle \alpha \rangle = \frac{A_v}{(A_v + A_l)} \quad (\text{A-4})$$

We can also define two other cross-sectional average quantities (Ref. (L1)):

$$\begin{aligned} \langle F_l \rangle_l &= \frac{[\iint F_l (1 - \alpha) \, dA]}{[A(1 - \langle \alpha \rangle)]} \\ &= \frac{\langle (1 - \alpha) F_l \rangle}{(1 - \langle \alpha \rangle)} \end{aligned} \quad (\text{A-5})$$

$$\langle F_v \rangle_v = \frac{[\iint F_v \alpha \, dA]}{(A \langle \alpha \rangle)} = \frac{\langle \alpha F_v \rangle}{\langle \alpha \rangle}$$

These two definitions are essentially averages of phasic parameters over the area of the phase in question.

In general, the velocities of the two phases in a mixture are not equal. For example, in a heated channel with boiling the vapor velocity exceeds that of the liquid. We define the slip ratio,  $S$ , to be the ratio of the average vapor velocity to the average liquid velocity, or:

$$S = \frac{\langle u_v \rangle_v}{\langle u_l \rangle_l} \quad (\text{A-6})$$

The volumetric flux of each phase is defined to be the volumetric flowrate of the phase in question divided by the total cross-sectional flow area, or

$$\langle j_i \rangle = \frac{\langle Q_i \rangle}{A} \quad i = l, v \quad (\text{A-7})$$

where

$$\langle Q_i \rangle = A_i \langle u_i \rangle_i \quad i = l, v \quad (\text{A-8})$$

Using Eqs. (A-2), (A-4) and (A-5) yields

$$\begin{aligned} \langle j_{\ell} \rangle &= (1 - \langle \alpha \rangle) \langle u_{\ell} \rangle_{\ell} = \langle (1 - \alpha) u_{\ell} \rangle \\ \langle j_{\nu} \rangle &= \langle \alpha \rangle \langle u_{\nu} \rangle_{\nu} = \langle \alpha u_{\nu} \rangle \end{aligned} \tag{A-9}$$

The total volumetric flux of the mixture,  $\langle j \rangle$ , is defined to be the sum of the individual volumetric fluxes; it is also the velocity of the center of volume of the mixture.

In the analysis of two-phase flows there are three quantities of interest. The first is the thermodynamic equilibrium quality,  $x_e$ , which is obtained from the energy equation and is written as,

$$x_e = \frac{(H' - H_{\ell S})}{(H_{\nu S} - H_{\ell S})} \tag{A-10}$$

This is the quality one would measure if the flowing mixture was adiabatically isolated and allowed to reach equilibrium. Note that  $x_e$  may be either positive or negative, and can exceed unity.

The second quality of interest is the flow quality, which is defined to be the true flow fraction of vapor, regardless of whether or not a state of thermodynamic equilibrium exists. It can be written as:

$$\begin{aligned}
x &= \frac{W_v}{(W_v + W_l)} \\
&= \frac{\langle \rho_v u_v \rangle_v \langle \alpha \rangle}{\rho_v \langle u_v \rangle_v \langle \alpha \rangle + \rho_l \langle u_l \rangle_l (1 - \langle \alpha \rangle)} \\
&= \frac{\langle \rho_v u_v \rangle_v \langle \alpha \rangle}{\langle \rho u \rangle}
\end{aligned}
\tag{A-11}$$

This can also be written as:

$$x = \frac{(H' - H_l)}{(H_v - H_l)}
\tag{A-12}$$

In Eq. (A-12) we have omitted the subscript *s* since we are not assuming thermodynamic equilibrium. The flow quality is always in the range of 0.0 to 1.0. Comparing Eqs. (A-10) and (A-12) shows that in equilibrium bulk boiling *x* and *x<sub>e</sub>* are equivalent. Note also that by combining Eqs. (A-11) and (A-12), and manipulating the result we obtain:

$$H' = \frac{\langle \rho uH \rangle}{\langle \rho u \rangle}
\tag{A-13}$$

The static quality, *x<sub>s</sub>*, is the last quality of interest. It is simply the mass fraction of vapor, or

$$x_s = \frac{\rho_v A_v}{(\rho_v A_v + \rho_l A_l)} \quad (\text{A-14})$$

The static quality and the flow quality are related by

$$\frac{x}{(1-x)} = \frac{Sx_s}{(1-x_s)} \quad (\text{A-15})$$

Density is defined to be the average mass per unit volume. In keeping with this definition, the density of a two-phase mixture is the volume weighted density, given by

$$\begin{aligned} \bar{\rho} &= [ \iiint \rho_l dV + \iiint \rho_v dV ] \quad (\text{A-16}) \\ &= (1 - \langle \alpha \rangle) \rho_l + \langle \alpha \rangle \rho_v \end{aligned}$$

Other phase weighted quantities may be defined in a similar fashion, e.g.

$$\bar{U} = \frac{[(1 - \langle \alpha \rangle) \rho_l U_l + \langle \alpha \rangle \rho_v U_v]}{\bar{\rho}} \quad (\text{A-17})$$

The mass flux is defined to be the total mass flowrate divided by the cross-sectional area, or

$$\begin{aligned}
 G &= \frac{W}{A} = \frac{\rho_l \langle u_l \rangle_l (1 - \langle \alpha \rangle)}{(1 - x)} \\
 &= \frac{\rho_v \langle u_v \rangle_v \langle \alpha \rangle}{x}
 \end{aligned}$$

(A-18)

This last equation implies

$$\frac{\langle x \rangle}{(1 - \langle x \rangle)} = \left( \frac{\rho_v}{\rho_l} \right) S \left[ \frac{\langle \alpha \rangle}{(1 - \langle \alpha \rangle)} \right] \quad (A-19)$$

Equation (A-15) can be solved for  $\langle \alpha \rangle$  to give the vapor volume fraction-quality relation,

$$\langle \alpha \rangle = \frac{x}{\left[ x + S \left( \frac{\rho_v}{\rho_l} \right) (1 - x) \right]} \quad (A-20)$$

This equation can be used to calculate  $\langle \alpha \rangle$  once  $x$  and  $S$  are known. In reality, however, it is difficult, if not impossible, to determine the slip ratio. To circumvent this problem, the assumption commonly is made that both phases have the same velocity ( $S=1$ ). This is referred to as the homogeneous flow assumption. A more general vapor volume fraction-quality model, known as the drift flux model, was developed by Zuber and Findlay (Ref. Z1) and will be presented here. One can write,

$$u_v = j + (u_v - j)$$

which is simply an identity. Using a local form of Eq. (A-9) yields,

$$j_v = \alpha j + \alpha(u_v - j)$$

Averaging over the cross-sectional area,

$$\langle j_v \rangle = \langle \alpha j \rangle + \langle \alpha(u_v - j) \rangle \quad (\text{A-21})$$

The drift velocity,  $u_{vj}$ , is defined to be the vapor volume weighted average velocity of the vapor phase with respect to the center of volume of the mixture. That is,

$$u_{vj} = \frac{\langle \alpha(u_v - j) \rangle}{\langle \alpha \rangle} \quad (\text{A-22})$$

Zuber and Findlay also defined a distribution parameter,  $C_0$ , such that

$$C_0 = \frac{\langle \alpha j \rangle}{\langle \alpha \rangle \langle j \rangle} \quad (\text{A-23})$$

Thus,  $C_0$  is equal to the ratio of the average of the product of  $j$  and  $\alpha$ , to the product of the averages of each

quantity. Substituting Eqs. (A-22) and (A-23) into Eq. (A-21) yields,

$$\langle j_v \rangle = C_o \langle j \rangle \langle \alpha \rangle + u_{vj} \langle \alpha \rangle \quad (\text{A-24})$$

which can be solved for vapor volume fraction,

$$\langle \alpha \rangle = \frac{\langle j_v \rangle}{(C_o \langle j \rangle + u_{vj})} \quad (\text{A-25})$$

But,  $\langle j_v \rangle = G \frac{x}{\rho_v}$  and  $\langle j_l \rangle = G \frac{(1-x)}{\rho_l}$  so Eq. (A-21) becomes,

$$\langle \alpha \rangle = \frac{x}{\left\{ C_o \left[ x + \left( \frac{\rho_v}{\rho_l} \right) (1-x) \right] + \frac{\rho_v u_{vj}}{G} \right\}} \quad (\text{A-26})$$

The distribution parameter,  $C_o$ , accounts for the effect of a nonuniform vapor volume fraction and volumetric flux distribution and gives a measure of the global slip arising from the averaging of a nonuniform vapor volume fraction profile. The drift velocity,  $u_{vj}$ , accounts for the effect of the local relative velocity of the two phases.

Comparing Eqs. (A-20) and (A-26) we find that the slip ratio in the drift flux model is given by,



$$S = C_o + \frac{[x(C_o - 1)\rho_l]}{[\rho_v(1 - x)]} + \frac{(\rho_l u_{vj})}{[G(1 - x)]}$$

If  $C_o$  is set equal to unity and  $u_{vj}$  is equated to zero, we find that the drift flux model reduces to the homogeneous flow model. See Appendix B for more discussion on the distribution parameter and the drift velocity.

The final topic of interest in this discussion of two-phase flow is the pressure gradient due to frictional losses. In single-phase flow the frictional pressure gradient is commonly expressed in terms of the dynamic head. That is,

$$-\left(\frac{dp}{dz}\right)_l = \frac{K \cdot G^2}{2\rho_l} \quad (A-27)$$

where  $K$  is an empirical, irreversible loss coefficient. In pipe flow, wall friction can be used to find a similar quantity:

$$K = \frac{f}{D_h} \quad (A-28)$$

In Eq. (A-28),  $f$  is the Darcy-Weisbach friction factor and  $D_h$  is the equivalent hydraulic diameter of the flow channel. See Appendix C for further information regarding the Darcy-Weisbach friction factor and the hydraulic diameter.

It has been experimentally observed that the frictional losses in a two-phase flow are, in general, substantially greater than the losses for a single-phase liquid flow having the same mass flux. The standard approach that has been used to correlate two-phase friction losses is to define a two-phase multiplier,  $\phi_{\ell 0}^2$ , which is equal to the ratio of the two-phase frictional pressure gradient to the equivalent saturated single-phase (liquid only) frictional pressure gradient. That is,

$$\phi_{\ell 0}^2 = \frac{-\left(\frac{dp}{dz}\right)_{2\phi}}{-\left(\frac{dp}{dz}\right)_{\ell s}} \quad (\text{A-29})$$

Thus,

$$-\left(\frac{dp}{dz}\right)_{2\phi} = \left(\frac{K_{\ell s} \cdot G^2}{2\rho_{\ell s}}\right) \cdot \phi_{\ell 0}^2 \quad (\text{A-30})$$

The two-phase multiplier is a function of, at least, flow quality, system pressure and the mass flux. See Appendix C for a discussion of the correlations used for the two-phase multiplier.

## Appendix B

### GENERAL CONSERVATION EQUATIONS

In this appendix we will derive a general set of one-dimensional conservation equations for a fixed control volume.\* In the presentation we will use a single reference pressure to evaluate all system fluid properties at any given instant of time. The reference pressure is allowed to vary with time. This assumption allows us to eliminate sonic effects from our model, which is desirable from a numerical standpoint since inclusion of these effects has a negative effect on integration time step size (Refs. (H1), (M2) and (P1)). The single reference pressure assumption also permits us to make fewer entries to fluid property routines during calculations.

The use of a single reference pressure to evaluate all system fluid properties is justifiable on the basis that pressure drops in the system are small compared to the reference pressure and that occurrences on a sonic time scale are not to be followed. The single pressure assumption does not permit compression when the local pressure increases, so pressure and velocity perturbations propagate at an infinite velocity. In this sense, the single pressure assumption is

---

\* Extension to some situations in which the control volume is not fixed is straightforward. See Section 3.3.

analogous to the use of a rigid body in solid mechanics. In reality, local fluid accelerations can be caused by local pressure changes without the immediate acceleration of fluid at locations far removed from the disturbance. In our single pressure model, however, a change in the applied pressure drop will immediately accelerate fluid particles at all locations in the control volume. Therefore, the momentum conservation equation must be integrated over the control volume. The implications of this single pressure assumption with respect to the solution of the conservation equations are discussed in section B.5.

### B.1 MASS CONSERVATION EQUATION

The conservation of mass principle states:

$$\left[ \begin{array}{c} \text{Mass} \\ \text{Storage} \\ \text{Rate} \end{array} \right] - \left[ \begin{array}{c} \text{Mass} \\ \text{Inflow} \\ \text{Rate} \end{array} \right] + \left[ \begin{array}{c} \text{Mass} \\ \text{Outflow} \\ \text{Rate} \end{array} \right] = 0$$

For a fixed control volume,  $V$ , with a surface,  $S$ , this becomes (Ref. (M1)),

$$\frac{\partial}{\partial t} \iiint_V \rho \, dV + \iint_S \rho \vec{u} \cdot d\vec{S} = 0 \quad (\text{B-1})$$

For our purposes we can make the following simplifying assumptions:

- 1) One-dimensional flow, as shown in Figure B-1.
- 2) Flow is predominantly normal to the channel area.

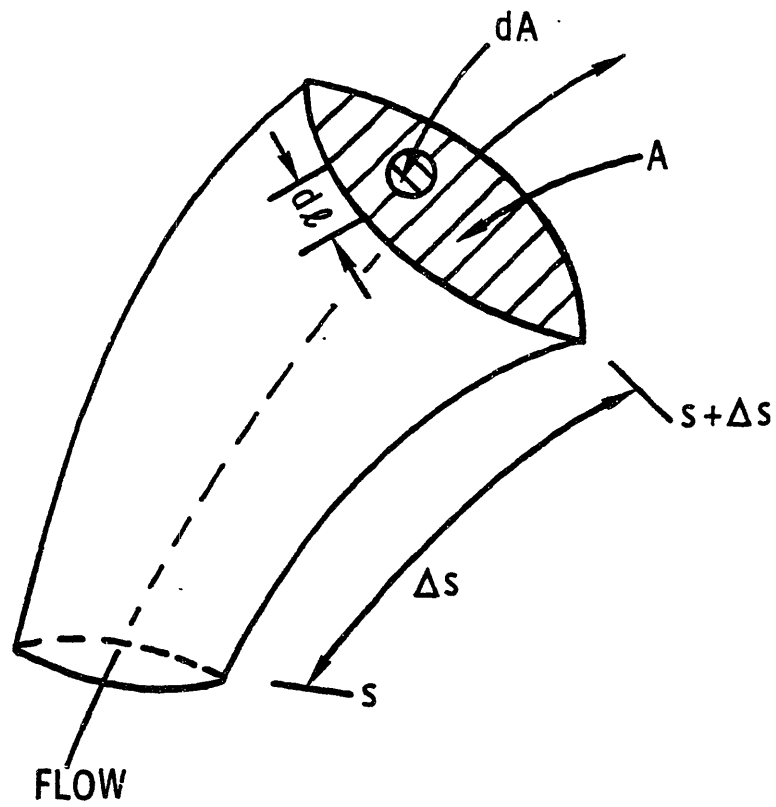


Figure B-1. Channel Geometry

- 3) The thermodynamic state and fluid velocity are uniform (bulk average values) over a given flow area at any instant of time.

As a result of these assumptions, Eq. (B-1) becomes:

$$\frac{dM}{dt} = W_{IN} - W_{OUT} \quad (B-2)$$

where

$$M = \iiint_V \rho dV; \quad \text{and}$$

$$W = \iint_A \rho u_s dA = \rho A u_s$$

## B.2 ENERGY CONSERVATION EQUATION

The conservation of energy principle states:

$$\left[ \begin{array}{c} \text{Energy} \\ \text{Storage} \\ \text{Rate} \end{array} \right] - \left[ \begin{array}{c} \text{Energy} \\ \text{Inflow} \\ \text{Rate} \end{array} \right] + \left[ \begin{array}{c} \text{Energy} \\ \text{Outflow} \\ \text{Rate} \end{array} \right] = 0$$

Mathematically,

$$\frac{\partial}{\partial t} \iiint_V \rho e dV + \iint_S \rho \left( e + \frac{P}{\rho} \right) \vec{u} \cdot d\vec{S} = q - P \quad (B-3)$$

where

$$e = U + \frac{u^2}{2} + gh$$

q = Heat transfer rate to the control volume; and

P = Power extracted from the control volume.

For situations of interest to us, the kinetic and potential energy terms ( $u^2/2$  and  $gh$ ) are negligible when compared to the fluid internal energy term ( $U$ ). So Eq. (B-3) becomes:

$$\frac{\partial}{\partial t} \iiint_V \rho U dV + \iint_S \rho H \vec{u} \cdot d\vec{S} = q - P \quad (B-4)$$

where the definition of enthalpy ( $H = U + p/\rho$ ) has been used in the surface integral. Applying the same assumptions that were used to obtain Eq. (B-2) yields:

$$\frac{dE}{dt} = (WH)_{IN} - (WH)_{OUT} + q - P \quad (B-5)$$

where

$$E = \iiint_V \rho U dV$$

### B.3 MOMENTUM CONSERVATION EQUATION

The conservation of momentum principle is:

$$\left[ \begin{array}{c} \text{Momentum} \\ \text{Storage} \\ \text{Rate} \end{array} \right] - \left[ \begin{array}{c} \text{Momentum} \\ \text{Inflow} \\ \text{Rate} \end{array} \right] + \left[ \begin{array}{c} \text{Momentum} \\ \text{Outflow} \\ \text{Rate} \end{array} \right] = \left[ \begin{array}{c} \text{Sum of} \\ \text{Forces Acting} \\ \text{on the} \\ \text{Control Volume} \end{array} \right]$$

Mathematically this can be written as:

$$\begin{aligned} \frac{\partial}{\partial t} \iiint_V \rho \vec{u} dV + \iint_S (\rho \vec{u}) \vec{u} \cdot d\vec{S} &= - \iint_S p d\vec{S} + \iiint_V \rho \vec{g} dV \\ &+ \iint_S \vec{\tau}_w dS \end{aligned} \quad (B-6)$$

where  $-\iint_S p d\vec{S}$  is due to the normal pressure forces; and  $\iint_S \vec{\tau}_w dS$  is due to the tangential friction forces.

In applying Eq. (B-6) to curved flow paths, we will not deal explicitly with forces generated by centripetal acceleration. We will represent these effects only in cases where turning losses are important, and then by use of appropriate loss coefficients. For our channel model (Fig. B.1) the pressure force term becomes:

$$\begin{aligned} -\iint_S p dS &= -(pA)_{s+\Delta s} + (pA)_s + \int_s^{s+\Delta s} \left( p \frac{dA}{ds} \right) ds \\ &= - \int_s^{s+\Delta s} \left( A \frac{dp}{ds} \right) ds \end{aligned}$$

The frictional force term becomes,

$$\begin{aligned} \iint_S \vec{\tau}_w dS &= - \int_s^{s+\Delta s} \left[ \int_{\text{Wetted Perimeter}} \tau_w d\ell \right] ds \\ &= - \int_s^{s+\Delta s} \left[ \int_{WP} \tau_w d\ell \right] ds \end{aligned}$$

If the magnitude of the gravitational acceleration,  $g$ , is taken to be constant, the body force term can be written as:

$$\iiint_V \rho g dV = - \int_s^{s+\Delta s} (\rho g \sin \theta dA)$$



where  $\theta$  is the angle of the flow direction measured from the horizontal. In addition, the first term of Eq. (B-6) can be replaced by:

$$\iiint_V \rho \vec{u} dV = \int_s^{s+\Delta s} \left( \iint_A \rho u_s dA \right) ds$$

and the second term becomes:

$$\iint_S (\rho \vec{u}) \vec{u} \cdot d\vec{S} = \left( \iint_A \rho u_s^2 dA \right)_{s+\Delta s} - \left( \iint_A \rho u_s^2 dA \right)_s$$

Substituting these results into Eq. (B-6), dividing by  $\Delta s$ , and taking the limit as  $\Delta s$  approaches zero gives:

$$\begin{aligned} \frac{\partial}{\partial t} \left( \iint_A \rho u_s dA \right) + \frac{\partial}{\partial s} \left( \iint_A \rho u_s^2 dA \right) \\ = -A \frac{\partial p}{\partial s} - \int_{WP} \tau_w d\ell - \iint_A \rho g \sin \theta dA \end{aligned}$$

Using assumptions 2 and 3 of Section B.1 yields

$$\frac{\partial W}{\partial t} + \frac{\partial}{\partial s} \left( \frac{v' W^2}{A} \right) = -A \frac{\partial p}{\partial s} - \rho g A \sin \theta - \int_{WP} \tau_w d\ell \quad (B-7)$$

where

$$v' = \frac{A}{W^2} \iint_A \rho u_s^2 dA \quad (B-7a)$$

In order to evaluate the frictional term in Eq. (B-7), an empirical correlation based on the fluid dynamic head is

commonly used. This correlation takes the following form:

$$\int_{WP} \tau_w dl = \frac{fW/W/}{2\rho D_h A}$$

where  $f$  is an empirical friction factor (see Appendix C). Substituting this expression into Eq. (B-7) and dividing by  $A$ , which is constant in time, gives:

$$\frac{\partial}{\partial t} \frac{W}{A} + \frac{1}{A} \frac{\partial}{\partial s} \left( \frac{v'W^2}{A} \right) = - \frac{\partial p}{\partial s} - \frac{fW/W/}{2\rho D_h A^2} - \rho g \sin \theta$$

Because of the single pressure assumption mentioned at the beginning of this appendix we must integrate this expression along the flow path, which results in:

$$\begin{aligned} \int_s^{s+\Delta s} \frac{\partial}{\partial t} \frac{W}{A} ds + \int_s^{s+\Delta s} \frac{1}{A} d \left( \frac{v'W^2}{A} \right) &= (p_{in} - p_{out}) \\ - \int_s^{s+\Delta s} \frac{fW/W/}{2\rho D_h A^2} ds - \int_s^{s+\Delta s} \rho g \sin \theta ds - \int_1 \frac{K_1 W_1^2}{2\rho_1 A_1^2} & \end{aligned} \quad (B-8)$$

The last term in the above equation accounts for shock and turning losses (recoverable and unrecoverable pressure losses). Since the volume is fixed, the first term in this equation becomes:

$$\int_s^{s+\Delta s} \frac{\partial}{\partial t} \left( \frac{W}{A} \right) ds = \frac{d}{dt} \int_s^{s+\Delta s} \left( \frac{W}{A} \right) ds$$

If, in addition, we make the following definitions:

$$I = \int_s^{s+\Delta s} \frac{ds}{A} ;$$

$$\bar{W} = \left[ \int_s^{s+\Delta s} \left( \frac{W}{A} \right) ds \right] / I ;$$

$$\Delta p = p_{in} - p_{out} ; \text{ and,}$$

$$F = \int_s^{s+\Delta s} \frac{1}{A} d \left( \frac{v' W^2}{A} \right) + \int_s^{s+\Delta s} \frac{fW/W/}{2\rho D_h A^2} ds + \int_z^{z+\Delta z} \rho g \sin \theta ds$$

$$+ \sum_i \frac{K_i W_i^2}{2\rho_i A_i^2}$$

then Eq. (B-8) becomes:

$$I \frac{d\bar{W}}{dt} = \Delta p - F \quad (B-9)$$

which is our final form of the control volume momentum equation. Note that  $\bar{W}$  is essentially the average channel flowrate, so that Eq. (B-9) is in fact used to represent the behavior of the average flowrate.

A final note as regards the quantity  $v'$ . The  $v'$  for single-phase flow is simply equal to  $1/\rho$ , if the velocity distribution is considered to be approximately uniform at all cross-sections. In two-phase flows  $v'$  can be determined

by expanding Eq. (B-7a) into components for each phase, as follows:

$$v' = \frac{A}{W^2} \iint_A \rho u_s^2 dA = \frac{A}{W^2} \left[ \iint_{A_v} \rho_v \langle u_{vs} \rangle_v^2 dA + \iint_{A_l} \rho_l \langle u_{ls} \rangle_l^2 dA \right]$$

From Eq. (A-14) we can write:

$$\langle u_{vs} \rangle_v = \frac{xW}{\langle \alpha \rangle \rho_v A}; \quad \text{and}$$

$$\langle u_{ls} \rangle_l = \frac{(1-x)W}{(1-\langle \alpha \rangle) \rho_l A}$$

Thus,

$$\begin{aligned} v' &= \frac{A}{W^2} \left\{ \iint_{A_v} \rho_v \left[ \frac{xW}{\langle \alpha \rangle \rho_v A} \right]^2 dA + \iint_{A_l} \rho_l \left[ \frac{(1-x)W}{(1-\langle \alpha \rangle) \rho_l A} \right]^2 dA \right\} \\ &= \frac{x^2 A_v}{\langle \alpha \rangle^2 A \rho_v} + \frac{(1-x)^2 A_l}{(1-\langle \alpha \rangle)^2 A \rho_l} \end{aligned}$$

But,  $\langle \alpha \rangle = A_v/A$  and  $(1-\langle \alpha \rangle) = A_l/A$  so, in two-phase flow:

$$v' = \frac{x^2}{\langle \alpha \rangle \rho_v} + \frac{(1-x)^2}{(1-\langle \alpha \rangle) \rho_l} \quad (\text{B-10})$$

#### B.4 ENTHALPY REFERENCE POINT AND THE ENERGY EQUATION

The mass and energy conservation equations as derived in Sections B.1 and B.2 are

$$\frac{dM}{dt} = W_{IN} - W_{OUT} \quad (B-2)$$

and

$$\frac{dE}{dt} = (WH)_{IN} - (WH)_{OUT} + q - P \quad (B-5)$$

If we multiply Eq. (B-2) by  $H^*$  and subtract the result from Eq. (B-5), we obtain:

$$\frac{dE}{dt} - H^* \frac{dM}{dt} = [W(H - H^*)]_{IN} - [W(H - H^*)]_{OUT} + q - P \quad (B-11)$$

Equations (B-2) and (B-5) are theoretically correct, and when they are solved simultaneously and precisely, no problem arises. If they are solved approximately or out of step, then Eq. (B-11) is preferred. This can be demonstrated by noting that Eq. (B-5) as it stands is not independent of enthalpy reference point, while Eq. (B-11) is. A change in enthalpy reference point results in a numerical change in Eq. (B-5) if Eq. (B-2) is not satisfied precisely. Equation (B-11), however, does not exhibit this characteristic because only differences in enthalpy appear. To demonstrate that this is the case we will take a closer look at Eq. (B-11). The right hand side of this equation clearly involves only differences in enthalpy. This is not clear for the left hand side of the equation. We will show, however, that the left hand side of Eq. (B-11) is not influenced by enthalpy reference point. Starting with the expression,

$$\frac{dE}{dt} - H^* \frac{dM}{dt}$$

and substituting,

$$E = \int_0^{V_1} (\rho U) dV \quad M = \int_0^{V_1} \rho dV$$

where  $V_1$  is the region volume, yields,

$$\frac{d}{dt} \left[ \int (\rho U) dV \right] - H^* \frac{d}{dt} \left[ \int \rho dV \right]$$

Using the Leibnitz rule for this expression (for generality  $V_1$  is allowed to vary),

$$\int (\partial \rho U / \partial t) dV + (\rho U)_{V_1} (dV_1 / dt) - H^* \left[ \int (\partial \rho / \partial t) dV + \rho_{V_1} (dV_1 / dt) \right]$$

Expanding the derivatives,

$$\begin{aligned} & \int \rho (\partial U / \partial t) dV + \int U (\partial \rho / \partial t) dV - H^* \int (\partial \rho / \partial t) dV \\ & + [(\rho U)_{V_1} - H^* \rho_{V_1}] dV_1 / dt \end{aligned}$$

Substituting  $U = H - p/\rho$ ,

$$\begin{aligned} & \int \rho [\partial H / \partial t - \partial (p/\rho) / \partial t] dV + \int H^* (\partial \rho / \partial t) dV - \int (p/\rho) (\partial \rho / \partial t) dV \\ & - H^* \int (\partial \rho / \partial t) dV + [\rho_{V_1} H_{V_1} - p_{V_1} - H^* \rho_{V_1}] dV_1 / dt \end{aligned}$$

or,

$$\begin{aligned} & \int \rho [\partial H / \partial t - \partial (p/\rho) / \partial t] dV - \int (p/\rho) (\partial \rho / \partial t) dV \quad (B-12) \\ & + [\rho_{V_1} (H_{V_1} - H^*) - p_{V_1}] dV_1 / dt + \int H^* (\partial \rho / \partial t) dV - H^* \int (\partial \rho / \partial t) dV \end{aligned}$$

The first term in this expression involves the derivative of enthalpy, which is independent of reference point. The second term does not involve enthalpy at all and the third term has a difference in enthalpy. To show that the last two terms taken together are independent of enthalpy reference point, we shall assume that the enthalpy reference point is perturbed by a constant amount,  $\delta H_{ref}$ . This yields,

$$\int (H^* + \delta H_{ref})(\partial \rho / \partial t) dV - (H^* + \delta H_{ref}) \int (\partial \rho / \partial t) dV$$

and, since  $\delta H_{ref}$  is a constant, we obtain,

$$\int H^*(\partial \rho / \partial t) dV - H^* \int (\partial \rho / \partial t) dV$$

which is the same expression we started with, demonstrating that the last two terms of Eq. (B-12) are independent of enthalpy reference point. Thus Eq. (B-11) is independent of enthalpy reference point.

## B.5 APPLICATION OF CONSERVATION EQUATIONS

The set of conservation equations we derived in the preceding sections of this appendix constitute the channel integral model (Ref. (M2)), which is a single control volume version of the methods used in the body of this thesis.

These equations are:

Mass

$$\frac{dM}{dt} = W_{IN} - W_{OUT} \quad (B-2)$$

Energy

$$\frac{dE}{dt} - H^* \frac{dM}{dt} = [W(H - H^*)]_{IN} - [W(H - H^*)]_{OUT} + q - P \quad (B-11)$$

Momentum

$$I \frac{d\bar{W}}{dt} = \Delta p - F \quad (B-9)$$

where

$$M = \int_V \rho dV ;$$

$$E = \int_V \rho U dV ;$$

$$I = \int_0^L \frac{ds}{A} ; \quad \text{and}$$

$$\bar{W} = \int_0^L W \frac{ds}{A} / I \quad (B-13)$$

The method used to solve these equations merits further discussion. Consider a vertical, heated channel in which



fluid is flowing upward. The initial conditions for this system are assumed to be known, as is the steady state fluid enthalpy distribution. The pressure drop,  $\Delta p$ , across the channel is fixed and is small relative to the system pressure, which is constant. We also assume that we know the equation of state relating  $H$  and  $\rho$ . The channel inlet enthalpy,  $H_{IN}$ , and the channel heat input are known functions of time. The conservation equations (Eqs. (B-2), (B-11), and (B-9)) together with the definition of  $\bar{W}$  (Eq. (B-13)) allow us to predict the time-dependent behavior of  $W_{IN}$ ,  $W_{OUT}$ ,  $H_{OUT}$ , and  $\bar{W}$ .

In order to evaluate Eq. (B-13) for  $\bar{W}$ , we need to know the transient axial profile of the flowrate. For simplicity we will assume that the profile has been established so that:

$$\bar{W} = \gamma_1 W_{IN} + \gamma_2 W_{OUT} \quad (B-14)$$

where

$$\gamma_1 + \gamma_2 = 1$$

since in steady state  $W_{IN}$  is equal to  $W_{OUT}$ , which is equal to  $\bar{W}$ .

Solving Eq. (B-2) for  $W_{OUT}$  and substituting the result into Eq. (B-14) yields

$$W_{IN} = \bar{W} + \gamma_2 \frac{dM}{dt} \quad (B-15)$$

Substituting Eqs. (B-14) and (B-15) into the energy equation (Eq. (B-11)) gives,

$$\frac{dE}{dt} - \frac{dM}{dt} (H_{IN} + \gamma_1 H_{OUT}) = q - \bar{W}(H_{OUT} - H_{IN}) \quad (B-16)$$

Both E and M can be written as functions of the average channel enthalpy,  $\hat{H}$ . If we assume that the transient enthalpy profile is similar to the steady profile, then

$$\hat{H} = \frac{\int_0^V \rho H dV}{\int_0^V \rho dV} = \gamma_3 H_{IN} + \gamma_4 H_{OUT} \quad (B-17)$$

where  $\gamma_3$  and  $\gamma_4$  can be determined a priori. Thus, Eq. (B-16) becomes

$$\frac{d\hat{H}}{dt} = \frac{1}{c_1} \left[ q - \bar{W}(H_{OUT} - H_{IN}) \right] \quad (B-18)$$

where

$$c_1 = \frac{dE}{d\hat{H}} - \frac{dM}{d\hat{H}} (H_{IN} + \gamma_1 H_{OUT})$$

Equations (B-18) and (B-9) are used to determine  $\hat{H}$ ,  $d\hat{H}/dt$ , and  $\bar{W}$ . Equation (B-17) can then be used to determine  $H_{OUT}$ . We can write Eq. (B-15) as

$$W_{IN} = \bar{W} + \frac{c_2}{c_1} [q - \bar{W}(H_{OUT} - H_{IN})] \quad (B-19)$$

where

$$c_2 = \gamma_2 \frac{dM}{dH}$$

Equation (B-19) gives us  $W_{IN}$  once we know  $d\hat{H}/dt$ . Thus,  $W_{IN}$  is not determined from a differential equation, but from an algebraic relation between our two state variables  $\bar{W}$  and  $\hat{H}$ . Finally, we can rearrange Eq. (B-14) to give us  $W_{OUT}$ :

$$W_{OUT} = \frac{1}{\gamma_2} (\bar{W} - \gamma_1 W_{IN}) \quad (B-20)$$

This example is meant to show how the conservation equations are used to obtain the solution for a simple problem. The method can be easily extended for use in more complex problems.

## Appendix C

### EMPIRICAL CORRELATIONS

The purpose of this appendix is to present the correlations used in this thesis.

#### C.1 VAPOR VOLUME FRACTION

In Appendix A we developed the drift flux model for the calculation of the vapor volume fraction. In this representation we need correlations for the distribution parameter,  $C_o$ , and the drift velocity,  $u_{vj}$ . In order to gain greater insight into the meaning of these parameters, it is useful to rewrite Eq. (A-24) as:

$$\frac{\langle j_v \rangle}{\langle \alpha \rangle} = C_o \langle j \rangle + u_{vj} \quad (C-1)$$

But,

$$\langle u_v \rangle_v = \langle \alpha u_v \rangle / \langle \alpha \rangle$$

so Eq. (C-1) becomes,

$$\langle u_v \rangle_v = C_o \langle j \rangle + u_{vj} \quad (C-2)$$

Equation (C-2) indicates that a plot of the vapor mean velocity,  $\langle u_v \rangle_v$ , versus the average volumetric flux is a

straight line with a slope of  $C_0$  and an intercept equal to  $u_{vj}$ . Such a plot is shown in Fig. (C-1). If both the vapor volume fraction and the volumetric flux profiles are uniform, then the distribution parameter, by definition, is equal to unity. If, in addition, the drift velocity is zero, then the flow is homogeneous, as shown in Fig. (C-1). For a fully developed, saturated two-phase upflow in a round duct, the vapor volume fraction and volumetric flux distributions are not uniform; the profiles tend to be axisymmetric with their maximum values at the center of symmetry. In this case  $C_0$  is greater than one. (See Fig. C-2.) There is also local slip between the phases so that  $u_{vj}$  is greater than zero. This situation is demonstrated by the upper line in Fig. (C-1). For the case of subcooled boiling where the vapor volume fraction is highest near the wall of the duct,  $C_0$  is less than one (Ref. (Z1) and (I1)).

It is apparent from the upper curve in Fig. (C-1) that the mean vapor velocity is equal to the drift velocity where the average volumetric flux,  $\langle j \rangle$ , is zero. This suggests that the drift velocity is closely related to the terminal rise velocity of a vapor bubble. In Reference (L1) the general form of the bubble rise velocity is derived by accounting for the forces acting on a vapor bubble and then performing fractional analysis. The result is:

# Drift Flux Model

## Weighted Mean Vapor Velocity vs Volumetric Flux

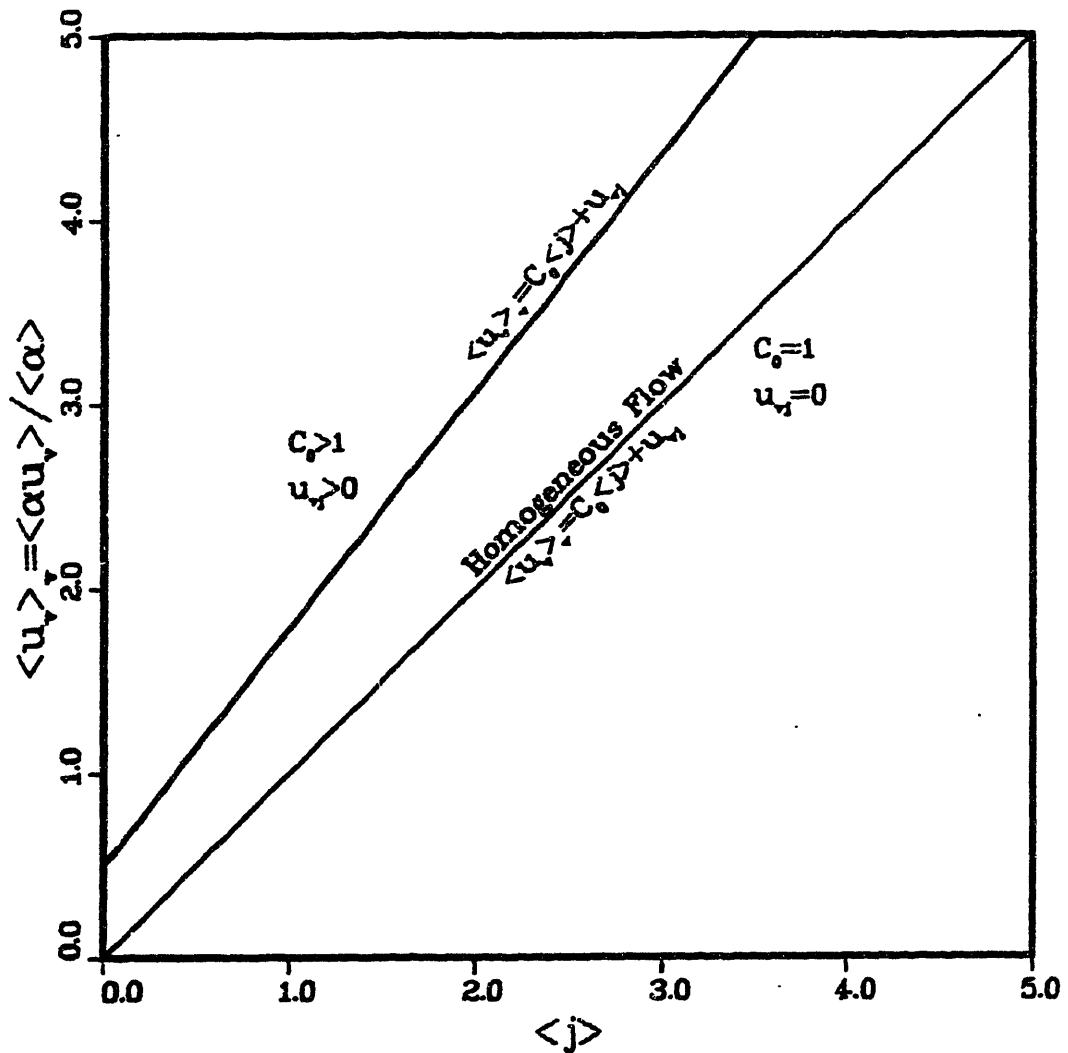


Figure C-1 (Ref. (Z1))

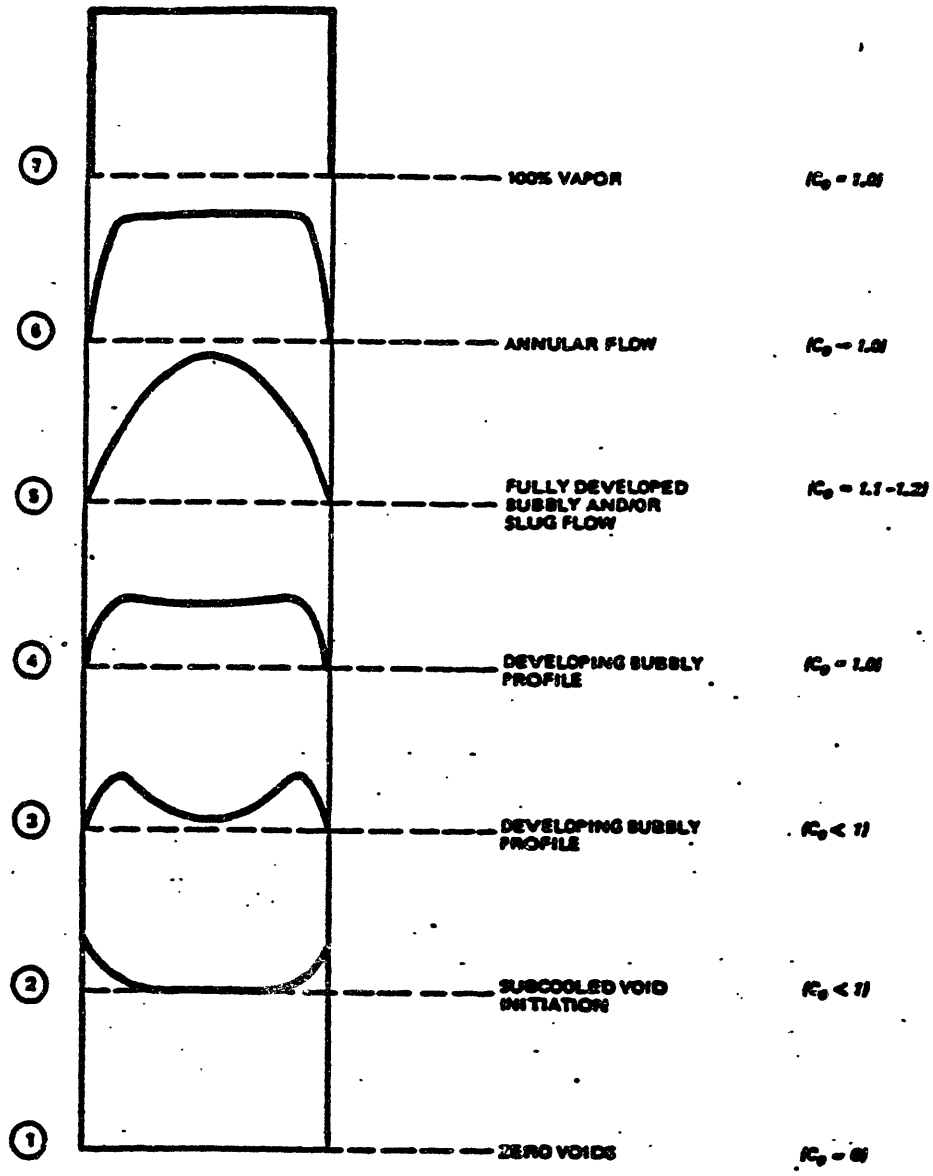


Figure C-2 Void Distribution Profiles in a Round Tube (Ref. (L1))

$$u_{vj} = u_t = K_0 \left[ \frac{\sigma g (\rho_{ls} - \rho_{vs})}{\rho_{ls}^2} \right]^{1/4} \quad (C-3)$$

This equation corresponds to experimental results in the churn-turbulent bubbly flow regime, with the constant,  $K_0$ , given variously as 1.41 or 1.53. It has been found that in vapor-dispersed-flow regimes the effect of vapor volume fraction and volumetric flux profiles dominates the relative motion between the phases (Ref. (11)). Thus, vapor-dispersed-flow regimes are well represented by Eq. (C-3), the churn-turbulent bubbly flow correlation.

As stated previously, the distribution parameter,  $C_0$ , is given by the slope of a plot of the mean vapor velocity versus the average volumetric flux. Experimental results for fully developed bubbly flows plotted in this manner indicate that the value of  $C_0$  lies in the range of 1.1 to 1.2 (Ref. (11)). For the churn-turbulent bubbly flow regime, the data is well represented when  $C_0$  is equal to 1.13.

In this work we are primarily interested in the vapor-dispersed-flow regimes. Consequently we shall adopt Eq. (C-3) with  $K_0$  equal to 1.41 as the correlation for the drift velocity, and we shall use a distribution parameter,  $C_0$ , of 1.13. A good fit to the above equation for  $u_{vj}$  when  $K_0$  is taken to be 1.41 is:

$$u_{vj} = (6.4100 \cdot 10^{-17}) p - (5.7794 \cdot 10^{-9}) p + 2.0957 \cdot 10^{-1}$$



## C.2 FRICTIONAL PRESSURE DROP

In Appendices A and B, we stated that the frictional component of the single-phase pressure gradient is commonly expressed in terms of the dynamic head by:

$$-\left(\frac{dp}{dz}\right)_{1\phi} = f \cdot G^2 / 2\rho L D_h \quad (C-4)$$

where  $f$  is the Darcy-Weisbach friction factor and  $D_h$  is the equivalent hydraulic diameter of the flow channel. The equivalent hydraulic diameter is defined to be equal to four times the flow area divided by the wetted perimeter. The friction factor for turbulent flow is generally written as a function of the Reynolds number ( $Re = GD_h/\mu$ ). Specifically,

$$f = CRe^n$$

where  $C$  is usually given as 0.316 or 0.184 and corresponding values of  $n$  are -0.25 or -0.2 (Ref (R1)). We shall use the second set of numbers,  $C = 0.184$  and  $n = -0.2$ , since these values give a better fit over a wide range of Reynolds numbers.

The two-phase frictional pressure gradient is usually expressed as a multiple of the equivalent saturated liquid frictional pressure gradient. That is,

$$\left(\frac{dp}{dz}\right)_{2\phi} = \phi_{\ell O}^2 \cdot \left(\frac{dp}{dz}\right)_{\ell S}$$

where  $\phi_{\ell O}^2$ , the two-phase multiplier, is a function of at least flow quality, pressure, and mass flux (Refs. (L1) and (E1)). A well-known two-phase multiplier correlation is that developed by Martinelli and Nelson (Ref. (M10)), with a flow effect correction factor developed by Jones (Ref. (J1)). In this correlation  $\phi_{\ell O}^2$  is written as,

$$\phi_{\ell O}^2 = \phi^2(x, \rho_{\ell S}/\rho_{vS}) \cdot \Omega(\langle G \rangle, p) \quad (C-6)$$

where  $\phi^2(x, \rho_{\ell S}/\rho_{vS})$  is the original Martinelli-Nelson correlation, and where  $\Omega(\langle G \rangle, p)$  is the mass flux correction factor developed by Jones. A good fit to the Martinelli correlation is given by (Ref (L1)):

$$\phi^2 = \left\{ 1.2 \left[ \frac{\rho_{\ell S}}{\rho_{vS}} - 1 \right] x^{0.824} \right\} + 1 \quad (C-7)$$

The Jones correction is:

$$\Omega \left\{ \begin{array}{l} 1.43 + \frac{\langle G \rangle - G_0}{G_0} \quad (0.07 - 7.35 \cdot 10^{-8} p) \\ \qquad \qquad \qquad \qquad \qquad \qquad \qquad \qquad \qquad \text{for } \langle G \rangle \leq G_0 \\ \\ 1.43 + \left( \frac{G_0}{\langle G \rangle} - 1 \right) \quad (0.17 - 6 \cdot 10^{-8} p) \\ \qquad \qquad \qquad \qquad \qquad \qquad \qquad \qquad \qquad \text{for } \langle G \rangle > G_0 \end{array} \right. \quad (C-8)$$

where  $p$  is in pascal;  $\langle G \rangle$  is in  $\text{kg/m}^2\text{-s}$ ; and  $G_0 = 950$   $\text{kg/m}^2\text{-s}$ . This two-phase multiplier correlation is the one used in this work.

### C.3 HEAT TRANSFER

In this work we use a log-mean temperature difference approach to calculate the primary to secondary heat transfer rate. The heat transfer equation is simply

$$q_B = U_O A_O \Delta T_{LM} \quad (\text{C-9})$$

where

$U_O \equiv$  overall heat transfer coefficient based on the outer area of the tubes;

$A_O \equiv$  total tube outer area; and

$\Delta T_{LM} \equiv$  log-mean temperature difference.

The overall heat transfer coefficient is:

$$\frac{1}{U_O} = \frac{A_O}{h_p A_i} + \frac{r_o \ln(r_o/r_i)}{K_t} + \frac{1}{h_s} + r_f \quad (\text{C-10})$$

where

$A_i \equiv$  total tube inner area;

$r_o, r_i \equiv$  tube outer and inner radii, respectively;

$K_t \equiv$  tube material thermal conductivity;

$r_f \equiv$  fouling factor to account for degraded heat transfer due to the buildup of corrosion products on tube surfaces;

$h_p$   $\equiv$  primary side convective heat transfer coefficient; and

$h_s$   $\equiv$  secondary side convective heat transfer coefficient.

In order to calculate  $U_o$  from Eq. (C-10) we require correlations for the primary side and secondary side heat transfer coefficients. The primary fluid is a subcooled single-phase fluid, and single-phase convective heat transfer coefficients are correlated by the following equation:

$$Nu = C_1 Re^n Pr^m \quad (C-11)$$

where

$$Nu = \text{Nusselt number} \equiv \frac{hD_h}{K} ;$$

$$Re = \text{Reynolds number} \equiv \frac{GD_h}{\mu} ; \text{ and}$$

$$Pr = \text{Prandtl number} \equiv \frac{C_p \mu}{K} .$$

In the Dittus-Boelter equation for cooling a liquid, the constants appearing in Eq. (C-11) are:

$$C_1 = 0.023$$

$$n = 0.8$$

$$m = 0.3$$

In addition, all fluid properties are evaluated at the fluid bulk temperature. Thus,

$$h_p = \frac{K_{bulk}}{D_h} \left[ 0.023 \left( \frac{GD_h}{\mu_{bulk}} \right)^{0.8} \left( \frac{C_p \mu}{K_{bulk}} \right)^{0.3} \right] \quad (C-12)$$

For the secondary side the situation is somewhat different. If the secondary side is at the saturation temperature, then the heat transfer occurs via nucleate boiling, assuming, of course, that the boiling crisis is not reached or exceeded anywhere within the secondary heat transfer region. In this case, the heat flux is commonly given by an expression of the following form:

$$q'' = \kappa (T_w - T_{sat})^m \quad (C-13)$$

where  $T_w$  is the tube wall temperature. We will use the Thom correlation where,

$$\kappa = \frac{\exp(2p/87 \times 10^5)}{(22.65)^2} ;$$

$$m = 2; \text{ and,}$$

$$p \equiv \text{Pa, } T \equiv \text{°K, } q'' \equiv \text{MW/m}^2$$

Thus,

$$h_s = \frac{q''}{(T_w - T_{SUB})} = \frac{\sqrt{q''}}{22.65} \exp\left(\frac{p}{87 \cdot 10^5}\right) \quad (C-14)$$

Finally, we have made some simple straight line fits for the thermal properties of Inconel 600, which is the alloy currently used as the tube material. These fits are made to data taken from Reference (L-3). The fits are:

$$K_t = 0.016T_t + 9.632 \quad 473^\circ\text{K} \leq T_t \leq 673^\circ\text{K}$$

and

$$(\rho \text{Cp})_t = 1.3677 \cdot 10^3 T_t + 3.3663 \cdot 10^6$$

$$422^\circ\text{K} \leq T_t \leq 755^\circ\text{K}$$

where:

$$K_t \equiv \frac{W}{m - ^\circ\text{K}} ;$$

$$(\rho \text{Cp})_t \equiv \frac{J}{m^3 - ^\circ\text{K}} ; \text{ and,}$$

$$T_t = \frac{\Delta T_{LM}}{2} + T_{SAT} \equiv ^\circ\text{K}$$

## Appendix D

### CROSS FLOW LOSS COEFFICIENT

The purpose of this appendix is to present the methodology used here to calculate the pressure drop experienced by the fluid flowing through the U-bend region of the tube bundle. This calculation is complicated by the following:

- 1.) geometry; and,
- 2.) two phase flow.

The geometry in this region is complex, with the flow being either parallel to the tubes, perpendicular to the tubes, or at some oblique angle to the tubes. In addition, there are open regions where the flow is not obstructed by the presence of tubes. This makes the flow distribution in the U-bend region a truly three-dimensional distribution, which is difficult to represent using a one-dimensional model. Add to this the fact that the flow consists of two phases and one is faced with an intractable modeling challenge.

The approach taken here makes no attempt at dealing with these difficulties in a detailed manner. Rather, the goal is to develop a representation that allows us to account for the physical location of the U-bend pressure drop in the recirculation loop momentum equation in a manner that is physically plausible. To do this we define a U-bend loss coefficient for saturated liquid-only flow,  $K_C$ , by:

$$\Delta P_{UB,\ell 0} = K_c \frac{W W}{2 \rho \ell s} \quad (D-1)$$

Note that this equation is not written in terms of a kinetic head,  $(\frac{W^2}{\rho A})$ , since we cannot associate a single flow area, A, with the U-bend region. Solving for  $K_c$  yields:

$$K_c = \frac{\Delta P_{UB,\ell 0}}{(\frac{W W}{2 \rho \ell s})} \quad (D-2)$$

To obtain  $K_c$  using Eq. (D-2) we need to determine  $\Delta P_{UB,\ell 0}$ .

It should be emphasized here that although Eq. (D-1) is used to calculate the U-bend pressure drop in the computer model, the loss coefficient,  $K_c$ , is specified by the user. Thus, the method given here for determining  $K_c$  is offered as a suggested method and is not part of the computer model. The user, therefore, may or may not opt to use this method, and can select another way to obtain  $K_c$ .

We assume here that the U-bend region may be approximated as consisting of square U-bends so that only parallel and cross flow conditions exist. We then divide the U-bend region into a series of axial segments. For each axial segment we determine the total flow area; that is, the sum of the areas for parallel flow, cross-flow, and flow in the open region. We assume that this total flow area is constant for each axial segment. We then divide the flowrate



by the total flow area in each segment to obtain the average mass velocity in each axial segment,  $G_{avg,i}$ , where the subscript  $i$  is associated with a particular axial segment. We then use this average mass velocity in a cross-flow pressure drop correlation to determine the pressure drop for each axial segment,  $\Delta p_i$ . Summing these pressure drops gives us the total U-bend region pressure drop,  $\Delta p_{UB,\ell 0}$ . That is,

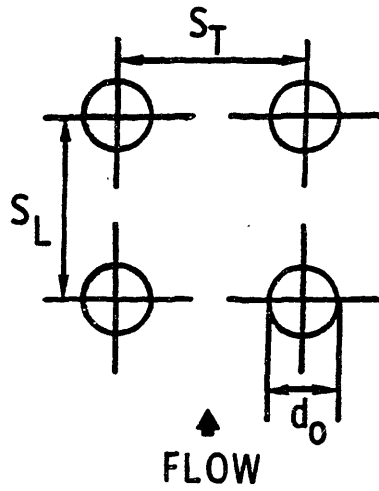
$$\Delta p_{UB,\ell 0} = \sum_i \Delta p_i \quad (D-3)$$

The cross flow pressure drop is calculated using a correlation taken from Ref. (K1). For our system this correlation becomes (see Fig. D-1 for nomenclature):

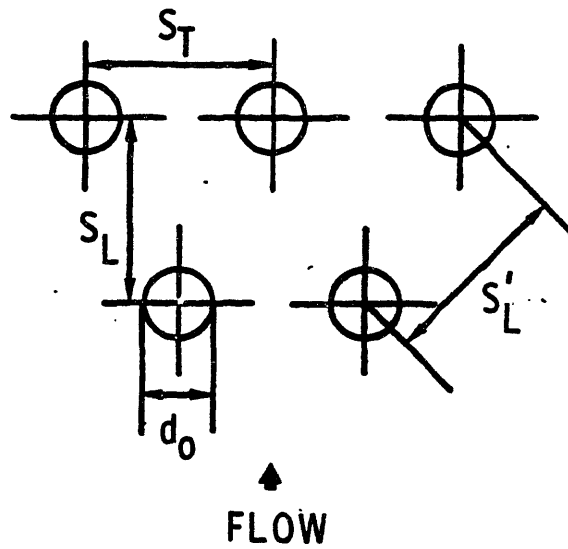
$$Re_{c,i} = \frac{(S_r - d_0)G_{avg,i}}{\mu_{ls}}$$

$$x = \left( \frac{S_T}{d_0} - 1 \right)$$

$N_T$   $\equiv$  Number of rows of tubes transverse to flow.



a) Rectangular array



b) Triangular array

Figure D-1. Arrangement of tubes in tube bundle for cross flow (Ref (K1)).

a.) Rectangular array of tubes:

$$f_{TB,i} = Re_{c,i}^{-0.15} x^{0.15} \left[ 0.044 + \frac{0.08 \left(\frac{S_L}{d_0}\right)}{x^{0.43+1.13 \left(\frac{d_0}{S_L}\right)}} \right]$$

$$N_{T,i} = N_T$$

b.) Triangular array of tubes:

$$f_{TB,i} = Re_{c,i}^{-0.16} x^{0.16} \left[ 0.25 + \frac{0.1175}{x^{1.08}} \right]$$

$$\begin{aligned} N_{T,i} &= N_T \quad \text{for } S_T \leq S'_L \\ &= N_T - 1 \quad \text{for } S_T > S'_L \end{aligned}$$

and,

$$\Delta p_i = 2N_{T,i} f_{TB,i} \frac{G_{avg,i} |G_{avg,i}|}{\rho_l s}$$

The two-phase flow U-bend pressure drop is calculated by multiplying the saturated liquid only pressure drop,  $\Delta P_{UB, \ell 0}$ , by the average two phase multiplier:

$$\Delta P_{UB} = \Delta P_{UB, \ell 0} \frac{(\phi_{\ell 0, p}^2 + \phi_{\ell 0, r}^2)}{2} \quad (D-4)$$

Equation (D-4) is for the steady state pressure drop. In transient situations we use the following equation:

$$\Delta P_{UB} = \frac{K_c}{4\rho_{\ell s}} [W_p/W_p|\phi_{\ell 0, p}^2 + W_r/W_r|\phi_{\ell 0, r}^2]$$

## Appendix E

### LINEAR PROFILE ERRORS

In Chapter 3.1.5 we indicate that the errors introduced by using linear profiles for  $\bar{v}$  and  $\bar{U}$  to calculate the mass and energy content are less than six percent for the mass and in the range of 13 to 22 percent for the energy. The linear profile approximation appears to be a better assumption for the mass content than for the energy content. The energy content error is due primarily to two effects:

- 1) The fluid at the tube bundle inlet becomes less subcooled as power decreases, and
- 2) The axial enthalpy gradient of the tube bundle fluid becomes less pronounced as power decreases.

The first effect is due to the fact that as the power decreases less feedwater is introduced into the steam generator. Performing a steady state energy balance for the downcomer yields:

$$W_0 H_0 = (W_0 - W_s) H_{ls} + W_{fw} H_{fw}$$

In steady state operation the feedwater flowrate is equal to the steam flowrate, so

$$H_0 = \left(1 - \frac{W_s}{W_0}\right) H_{l_s} + \left(\frac{W_s}{W_0}\right) H_{fw}$$

The quantity  $(W_s/W_0)$  is the steady state tube bundle exit quality, which decreases as power decreases. Therefore, according to the last equation, the tube bundle inlet enthalpy,  $H_0$ , approaches  $H_{l_s}$ . This shows that the tube bundle inlet subcooling decreases with decreasing power.

The second effect is demonstrated by the following argument. Since the axial heat flux is assumed to be uniform we have:

$$\frac{dH}{dZ} = \frac{(H_{l_s} - H_0)}{L_{sat}}$$

We have already shown that  $(H_{l_s} - H_0)$  decreases with decreasing power. Table 3.1-3 shows that as power decreases,  $L_{sat}$  increases. The net effect is that  $dH/dZ$  decreases as power decreases.

Figure E-1 shows two plots of  $\bar{U}$  versus fractional tube bundle length: one for high power and one for low power. The solid lines represent the actual profiles, while the dashed lines indicate the hypothesized linear profiles. For the high power case the actual profile of  $\bar{U}$  is kinked, with the amount of deviation from a linear profile determined by both the magnitude of the subcooling and the enthalpy gradi-

ent. For the lower power case we see that the deviation from a linear profile is less pronounced, since both the magnitude of the subcooling and the enthalpy gradient are smaller than for the high power case. Thus, one would expect the error introduced by using a linear profile for  $\bar{U}$  to decrease with decreasing power, which is the result shown in Table 3.1-4.

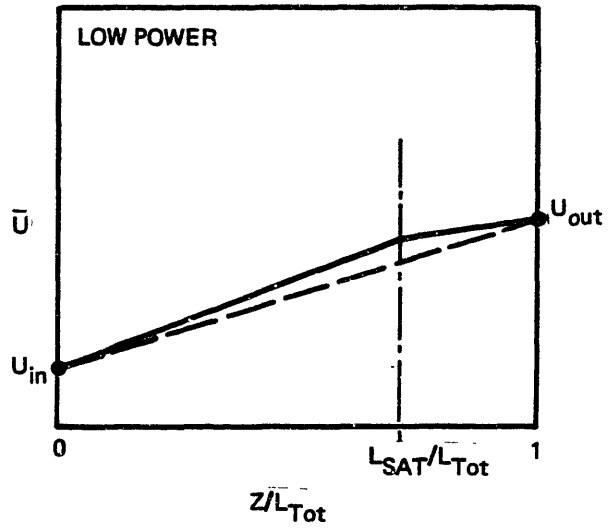
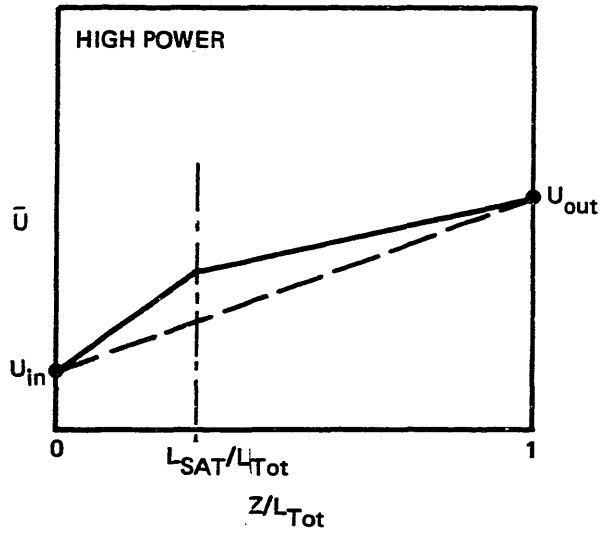


Figure E-1. Internal energy profiles.



## Appendix F

### CONVECTIVE DIFFERENCING SCHEMES

The purpose of this appendix is to present, without proof, some properties of two time differencing schemes for a typical convection equation. A full discussion of the topic can be found in Refs. (B5) and (R2).

The equation we are interested in is the simple one-dimensional convection equation given by:

$$\frac{dH}{dt} = \frac{1}{\tau} (H_{IN} - H_{OUT}) \quad (F-1)$$

where  $\tau$  is the fluid transport time through the control volume ( $\tau = \frac{\Delta z}{u}$ , where  $\Delta z$  is length of control volume and  $u$  is the fluid velocity). If we assume instantaneous, perfect mixing in the control volume, then Eq. (F-1) becomes:

$$\frac{dH_{OUT}}{dt} = \frac{1}{\tau} (H_{IN} - H_{OUT})$$

Using an explicit time difference yields:

$$H_{OUT}^{n+1} = (1 - r)H_{OUT}^n + rH_{IN}^n \quad (F-2)$$

where  $r = \frac{\Delta t}{\tau}$ . Equation (F-2) is an explicit "donor-cell" difference approximation to Eq. (F-1). This scheme has the following properties:

- 1.) When  $r = 1$  Eq. (F-2) gives the exact solution for any change in the inlet enthalpy of the control volume (or volumes if several volumes are connected end-to-end);
- 2.) For a single control volume Eq. (F-2) is stable for  $0 \leq r \leq 2$ ; and,
- 3.) For an infinite line of control volumes Eq. (F-2) is stable for  $0 \leq r \leq 1$ . In practical applications, this is also true for several control volumes connected end-to-end.

In Ref. (B5) the explicit donor cell difference method is referred to as the characteristic method. We point out here that this method is used in the subcooled region of the steam - dome downcomer, and in all the primary side control volumes.

Another method for dealing with Eq. (F-1) is to express the derivative  $\frac{dH}{dt}$  as the derivative of a weighted sum of the inlet and outlet values of H. That is:

$$\gamma \frac{dH_{OUT}}{dt} + (1 - \gamma) \frac{dH_{IN}}{dt} = \frac{1}{\tau} (H_{IN} - H_{OUT})$$

where  $\gamma$  is a weighting factor ( $0 \leq \gamma \leq 1$ ). Explicit time differencing of this equation yields:

$$H_{OUT}^{n+1} = \left(1 - \frac{r}{\gamma}\right)H_{OUT}^n + \left(\frac{1+r}{\gamma} - 1\right)H_{IN}^n + \left(1 - \frac{1}{\gamma}\right)H_{IN}^{n+1} \quad (F-3)$$

If  $\gamma = \frac{1}{2}$  (arithmetic average) Eq. (F-3) becomes:

$$H_{OUT}^{n+1} = (1 - 2r)H_{OUT}^n + (1 + 2r)H_{IN}^n - H_{IN}^{n+1} \quad (F-4)$$

This scheme has the following properties:

- 1.) For a single control volume Eq. (F-4) is stable for  $0 \leq r \leq 1$ ; and,
- 2.) For an infinite line of control volumes Eq. (F-4) is unconditionally unstable.

A scheme similar to Equation (F-3) is used in the tube bundle and riser regions (but  $\gamma \neq \frac{1}{2}$ ).

## Appendix G

### CALCULATING STEAM AND FEEDWATER FLOWRATES USING WATER LEVEL AND PRESSURE AS INPUTS

#### G.1 INTRODUCTION

As mentioned in Chapter 1, one of the applications of the steam generator model developed here is in information reliability. In particular, analytic measurements derived from plant component models can be compared to direct sensor measurements in an attempt to synthesize reliable estimates of measured quantities. The model described in the main text uses input steam and feedwater flows, among other inputs, to calculate steam pressure and water level. In theory, these calculated outputs, along with measured values of steam pressure and water level, could be used as input to decision/estimators (see Chapter 1). However, one may not want to do this in practice, since there are a number of direct sensor measurements of pressure and water level but few direct measurements of steam and feedwater flows. This suggests that analytic measurements of steam and feedwater flows are more useful than analytic measurements of pressure and water level in signal validation efforts. What follows is a description of an attempt to use water level and pressure as input to a modified version of the model that calculates the steam and feedwater flowrates.

## G.2 MODEL MODIFICATION

The secondary side solution (Chapters 3 and 5) requires modification in order to achieve our goal of inputting the level and pressure to calculate the feedwater and steam flowrates. Since we are providing the level and pressure as input we do not need to solve the sixth order differential equation system for the secondary side derived in the main text of this report. The time derivative of the pressure,  $\dot{p}$ , is obtained by taking the difference between successive input values of the pressure and dividing the result by the time interval separating these input values of pressure. Similarly, the time derivative of the volume of saturated vapor in the steam dome - downcomer,  $\dot{V}_v$ , is obtained by first converting successive values of the level into corresponding saturated vapor volumes using the known steam generator geometry, taking the difference of the resulting volumes, and dividing by the time interval. That is:

$$\dot{p}^n = \frac{p^{n+1} - p^n}{t^{n+1} - t^n} \quad (G-1)$$

and,

$$\dot{V}_v^n = \frac{V_v^{n+1}(\ell_w^{n+1}) - V_v^n(\ell_w^n)}{t^{n+1} - t^n} \quad (G-2)$$

We still need to determine  $\dot{U}_0$ ,  $\langle \dot{\alpha}_r \rangle$ ,  $\langle \dot{\alpha}_n \rangle$ , and  $\dot{\bar{W}}$ . In Chapter 5 we indicate that the momentum equation is solved independently of the other differential equations and we retain this feature here. Thus, we need to perform a simultaneous solution for  $\dot{U}_0$ ,  $\langle \dot{\alpha}_r \rangle$ , and  $\langle \dot{\alpha}_n \rangle$ , given  $\dot{p}$  and  $\dot{V}_v$ . This requires three equations. Two of these equations are the tube bundle energy equation and the riser energy equation, which are the first two equations given in the matrix expression of Eq. (5.1-4). Rearranging these equations yields:

$$A_{11}\dot{U}_0 + A_{13}\langle \dot{\alpha}_r \rangle = \bar{W}(H_0 - H_r) + q_B - A_{15}\dot{p} \quad (G-3)$$

and,

$$A_{21}\dot{U}_0 + A_{23}\langle \dot{\alpha}_r \rangle + A_{24}\langle \dot{\alpha}_n \rangle = \bar{W}(H_r - H_n) - A_{25}\dot{p} \quad (G-4)$$

The subcooled and saturated region energy equations are solved for  $W_{fw}$  and  $W_s$  respectively, and the resulting expressions are substituted into the overall steam generator mass balance. This yields:

$$\begin{aligned}
& \left( A_{51} - \frac{A_{31}}{H_{vs} - H_k} - \frac{A_{41}}{H_{fw} - H_k} \right) \dot{U}_0 \\
& + \left( A_{53} - \frac{A_{33}}{H_{vs} - H_k} - \frac{A_{43}}{H_{fw} - H_k} \right) \langle \dot{\alpha}_r \rangle \\
& + \left( A_{54} - \frac{A_{34}}{H_{vs} - H_k} - \frac{A_{44}}{H_{fw} - H_k} \right) \langle \dot{\alpha}_n \rangle \\
= & \bar{W} \left( \frac{H_0 - H_k}{H_{fw} - H_k} - \frac{H_n - H_k}{H_{vs} - H_k} \right) \\
& - \left( A_{52} - \frac{A_{32}}{H_{vs} - H_k} - \frac{A_{42}}{H_{fw} - H_k} \right) \dot{V}_v \\
& - \left( A_{55} - \frac{A_{35}}{H_{vs} - H_k} - \frac{A_{45}}{H_{fw} - H_k} \right) \dot{p}
\end{aligned} \tag{G-5}$$

Equations (G-3) through (G-5) can be written compactly as:

$$\underline{\underline{G}} \dot{\underline{r}} = \underline{z} \tag{G-6}$$

The equations are time differenced as follows:

$$\dot{\underline{r}}^n = [\underline{\underline{G}}^n]^{-1} \underline{z}^n \tag{G-7}$$

where,

$$\dot{\underline{r}}^n = \frac{\underline{r}^{n+1} - \underline{r}^n}{\Delta t}, \quad \Delta t = t^{n+1} - t^n, \text{ and}$$

$$\underline{r}^{n+1} = \underline{r}^n + \Delta t \dot{\underline{r}}^n$$

The values of  $\underline{r}^n$ , along with  $\dot{p}^n$  and  $\dot{V}_v^n$ , are used in Eqs. (5.1-3) and (5.1-2a,b,c) to determine the flowrates  $W_0$ ,  $W_p$ ,  $W_r$ , and  $W_n$ . The flowrate  $W_f$  is found using Eq. (5.1-6). Finally,  $W_{fw}$  and  $W_s$  are obtained from:

$$W_{fw}^n = \frac{\bar{W}^n (H_0 - H_k)^n + \sum_{i=1}^5 A_{4i}^n x_i^n}{(H_{fw} - H_k)^n} \quad (G-8)$$

$$W_s^n = \frac{\bar{W}^n (H_n - H_k)^n - \sum_{i=1}^5 A_{3i}^n x_i^n}{(H_{fw} - H_k)^n} \quad (G-9)$$

where

$$\underline{x}^n = \text{Col}[U_0^n, V_v^n, \langle \alpha_r \rangle^n, \langle \alpha_n \rangle^n, p^n]$$

The solution after this point is the same as that described in Chapter 5 except that the water level is not calculated since it is already known.

### G.3 RESULTS

The base case used to test this modified version of the model is the full-length control-element assembly drop for



steam generator 2 of the Arkansas Nuclear One - Unit 2 power plant (see 6.4.2). In fact, we deal only with the first 60 seconds of this transient and we use the calculated results discussed in 6.4.2 as the numerical standard for our steam and feedwater flowrate calculations.

The transient input hot leg temperature is shown in Fig. 6.4-6 and the transient input level and pressure used here are the calculated values shown in Fig. 6.4-8. The calculated steam and feedwater flowrates obtained when using four digit accuracy in the input level and pressure are shown in Fig. G-1. The level and pressure are input every time step, which is 0.25 seconds. Also shown in this figure are the actual steam and feedwater flows. As can be seen, the calculated steam flowrate is in relatively good agreement with the actual steam flowrate, although there are some jagged, low magnitude fluctuations in the calculated steam flowrate. The calculated feedwater flowrate, on the other hand, shows very marked fluctuations around the actual feedwater flowrate. At first glance it appears that the calculated feedwater flowrate is suspect. As a check on consistency the calculated steam and feedwater flowrates are input to the original steam generator model, and the pressure and level calculated in this manner are compared to the pressure and level originally input to the modified steam generator model. This comparison shows almost exact agreement between the calculated level and pressure, and the input level and pressure.

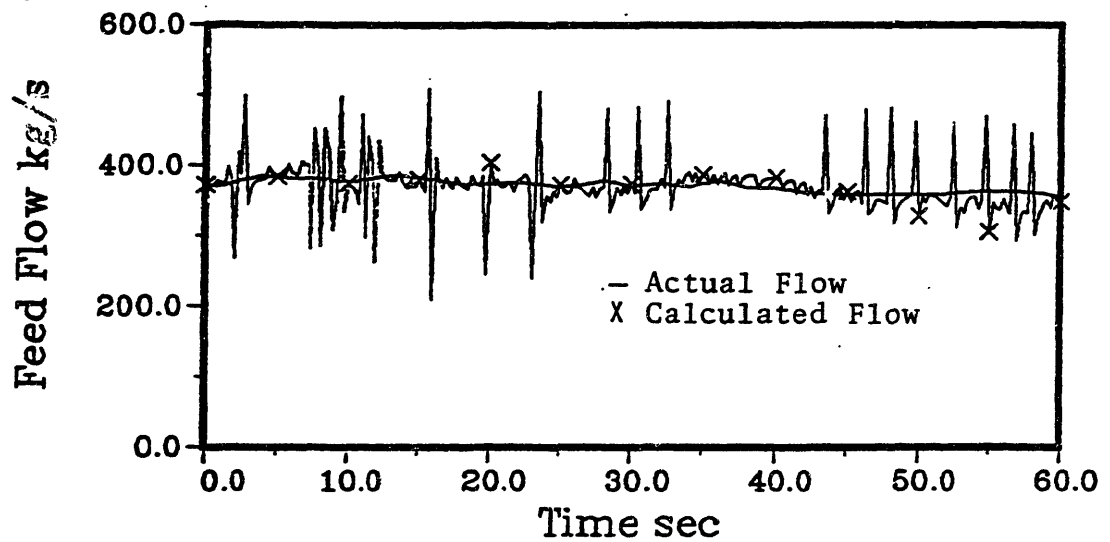
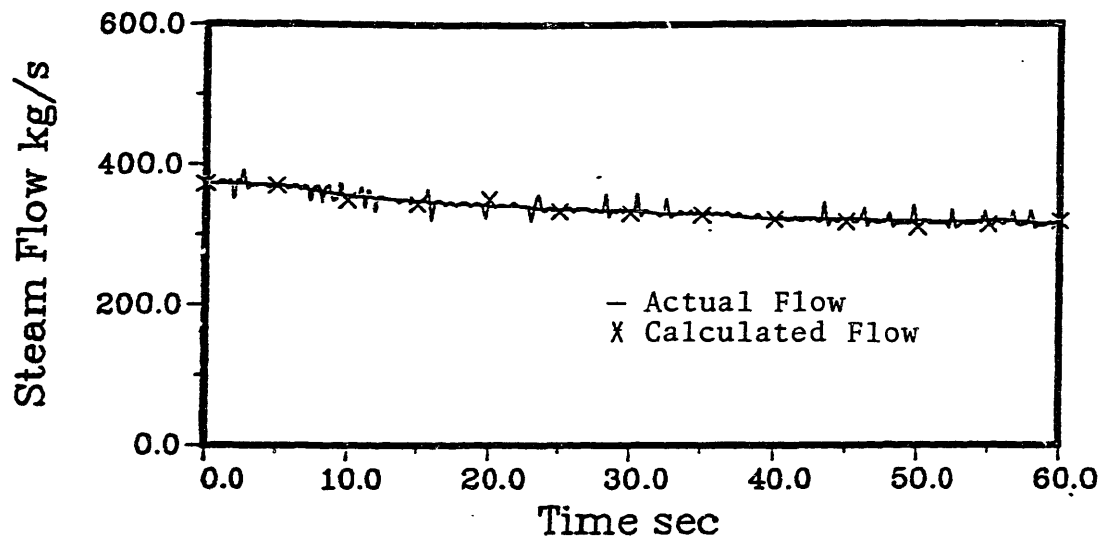


Figure G-1. Steam and feedwater flows obtained using 4-digit accuracy for input level and pressure.

Figure G-2 shows the results obtained using input pressure and level with seven significant digits rather than four. The calculated steam flow is in excellent agreement with the actual steam flow. The calculated feed flow, although slightly different from the actual feedwater flowrate, shows much better agreement and less erratic behavior than the calculated feed flow obtained using four digit level and pressure input. This result is interesting and indicates that the calculated feedwater flowrate is very sensitive to input errors in the pressure and level (in this case the error is caused by using truncated values of the input). This suggests that the derivatives of  $p$  and  $V_V$  must be precisely specified and that simple numerical differentiation using successive values (in time) of  $p$  and  $V_V$  is not adequate.

An attempt was made to improve the calculation of the feedwater flowrate by smoothing the four digit input level and pressure. Let  $\eta_a$  represent the raw input, either  $l_w$  or  $p$ , and let  $\eta_b$  represent the corresponding smoothed value of  $\eta_a$ . The smoothing algorithm used here is then given by:

$$\left( \frac{\eta_b^{n+1} - \eta_b^n}{\Delta t} \right) = \frac{\eta_a^{n+1} - \eta_b^{n+1}}{\tau}$$

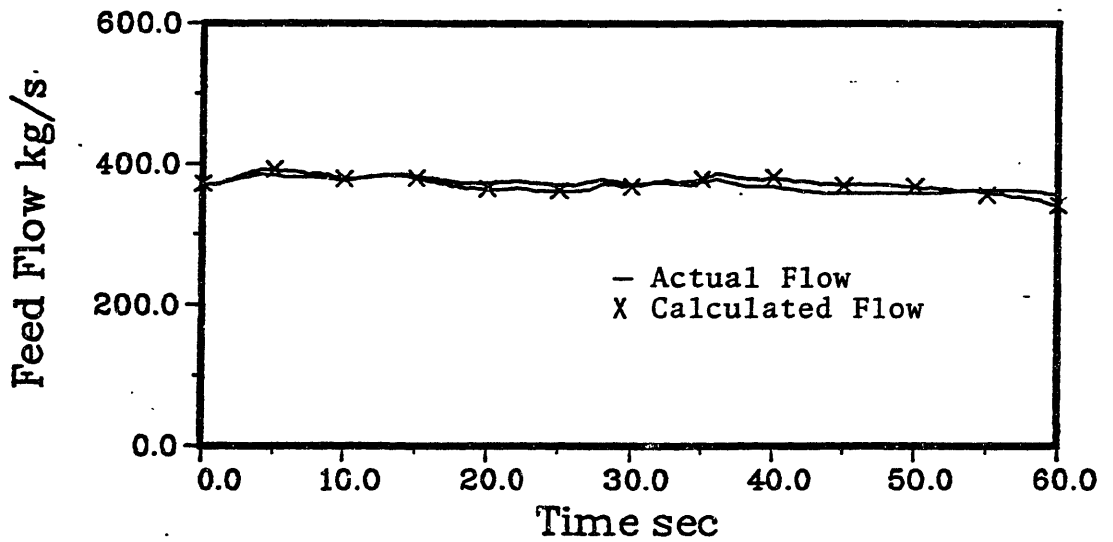
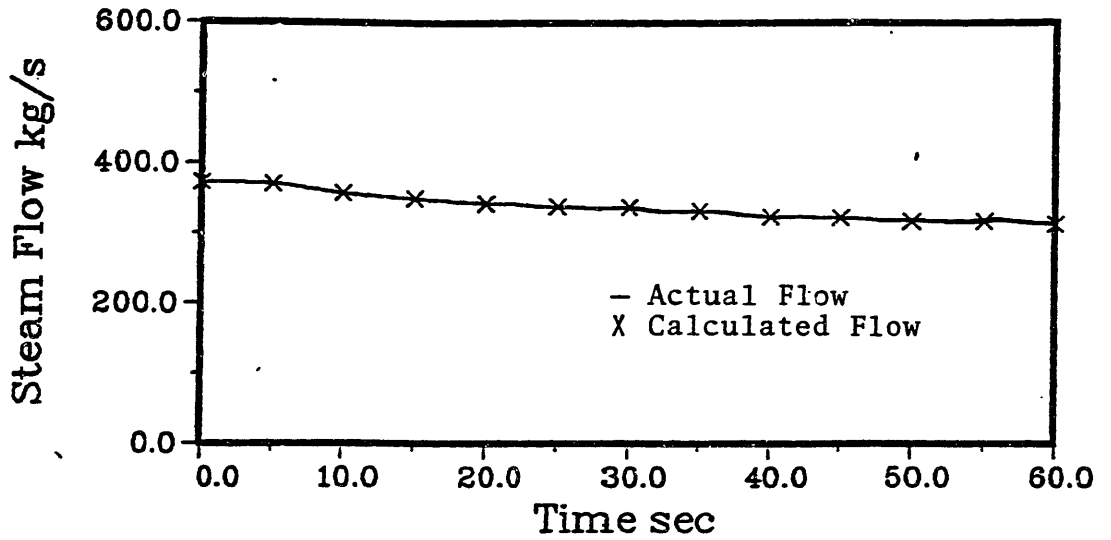


Figure G-2. Steam and feedwater flows obtained using 7-digit accuracy for input level and pressure.

$$\eta_b^{n+1} = \frac{\left(\frac{\tau}{\Delta t}\right)\eta_b^n + \eta_a^{n+1}}{1 + \frac{\tau}{\Delta t}} \quad (G-10)$$

where,

$\Delta t \equiv$  integration time step size

$\tau \equiv$  smoothing "time constant"

Figure G-3 shows results obtained using values for  $\tau$  of 1 and 5 seconds, along with four digit input pressure and level. The plots show that smoothing the input does not significantly improve agreement between calculated and actual feed and steam flowrates, with agreement deteriorating when the larger value of  $\tau$  is used.

#### G.4 CONCLUSIONS AND RECOMMENDATIONS

Calculations show that the method derived in this appendix can be used to calculate the steam and feedwater flowrates using input level and pressure only if the inputs are specified to a high degree of accuracy. However, the stipulation of high accuracy is too stringent for practical application of the model in on-line safety systems since this accuracy is not available from sensors used to measure the level and pressure. In addition, sensor signals will certainly contain noise components, which, even after filtering, will cause greater error in the input pressure and level signals. Finally, high accuracy calculated values of

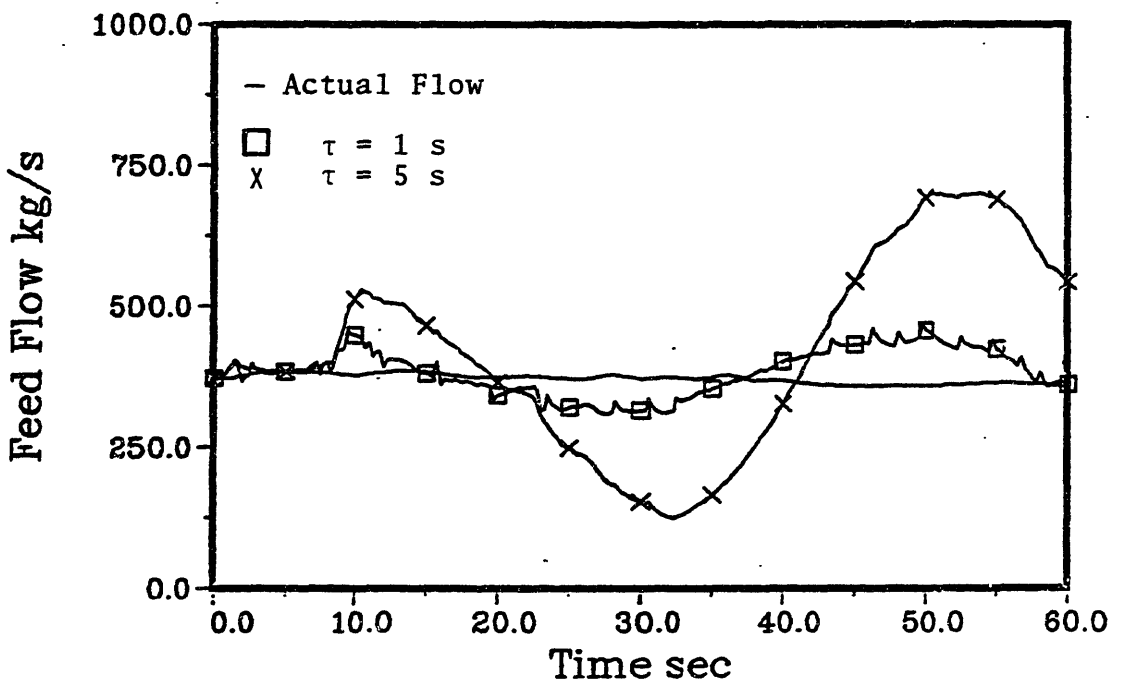
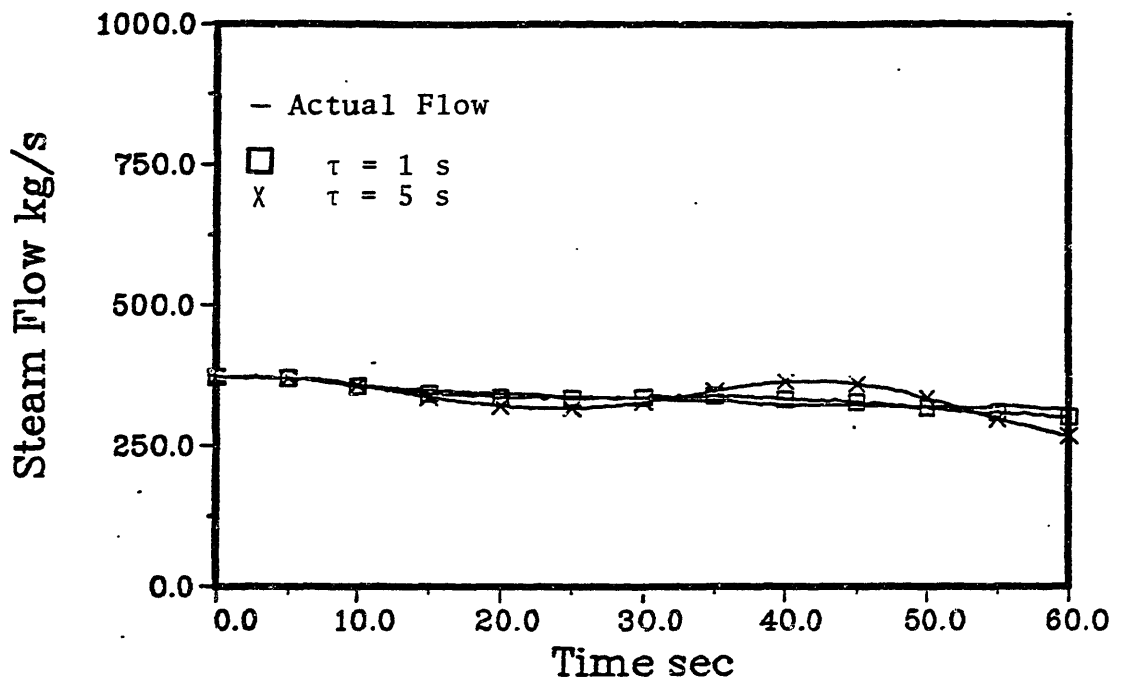


Figure G-3. Steam and feedwater flows obtained using smoothed level and pressure inputs.

pressure and level will not be available from other sources to use as input to this model. Thus, the method described in this appendix for calculating the steam and feedwater flowrates given the pressure and level (among other inputs) is not appropriate for use in operational safety systems as a means of signal validation.

One recommendation that we can make is to use a computing algorithm for the feedwater flowrate that is similar to a three element controller algorithm. In this computing scheme the model can be modified to calculate the steam flowrate and the feed flowrate given the transient pressure. The state vector for this case would be:

$$\text{Col}[ U_0, V_v, \langle \alpha_r \rangle, \langle \alpha_n \rangle, \bar{W} ]$$

Thus,  $\dot{p}^n$  is obtained from the input pressure, while  $\dot{V}_v^n$ , and therefore  $\dot{\ell}_w^{n+1}$ , is obtained from a calculation. The measured water level,  $\ell_m$ , is also input to the model, but it is used in an algorithm that compares it to the calculated level,  $\ell_w$ . This algorithm also compares the steam and feedwater flowrates in order to guarantee equality of the steam and feed flows in steady state operation. The algorithm could be:

$$\frac{dW_{fw}}{dt} = C_w (W_s - W_{fw}) + C_\ell (\ell_m - \ell_w)$$

where  $C_w$  and  $C_\ell$  are algorithm coefficients that must be determined in future research efforts. Using implicit time differencing yields:

$$W_{fw}^{n+1} = \frac{W_{fw}^n + \Delta t C_w W_S^{n+1} + \Delta t C_\ell (\ell_m^{n+1} - \ell_w^{n+1})}{1 + \Delta t C_w}$$

During the initial portions of fast transients the calculated feedwater flowrate will probably be in error, but it will eventually converge on the correct flowrate as the transient proceeds towards a new steady state. Further investigation is required in order to determine the feasibility, accuracy, and limitations of the computational scheme just described.



## APPENDIX H

### ADDITIONAL VALIDATION AND GEOMETRIC INPUT

The purpose of the appendix is to present results obtained for the Maine Yankee and Calvert Cliffs simulations. In addition, the geometric input used for all test cases is presented.

Transient test cases are presented in this appendix for completeness and to demonstrate that the program can be used for licensing type calculations. However, due to a lack of accurate knowledge of the transient steam and feed flows, it is difficult to draw any firm conclusions regarding model fidelity, so results are presented with a minimum of discussion. We also do not know how the cold leg temperature is calculated in the licensing codes to which we compare our results. That is, we do not know if sensor models or first order lags are used to process the calculated cold leg temperature. Unless specifically stated in the text, all cold leg temperatures calculated using our model are not processed through sensor models.

#### H.1 MAINE YANKEE

The Maine Yankee power plant has a Combustion Engineering designed nuclear steam supply system (NSSS). The plant was originally licensed to operate at an NSSS output of 2450 MWt. The NSSS has three steam generators and in all steady

state or transient simulations we assume that the plant is operated symmetrically. Maine Yankee design and operating conditions can be found in Refs. (F1) and (M9).

#### H.1.1 Steady State Results

We have performed a complete set of steady-state calculations for the Maine Yankee plant. In order to perform these calculations we need to provide the feedwater temperature and the primary average temperature as functions of power level. These quantities are shown in Figs. H.1-1 and H.1-2. The primary pressure, primary flowrate, and steam generator level are not functions of power for this plant. Table H.1-1 shows the important operating parameters for this plant; note that both the separator loss coefficient and the fouling factor (used in all calculations) are also listed. The results for the steady-state calculations are shown in Fig. H.1-3.

#### H.1.2 Transient Tests at 106 per cent Power

The transient simulation results shown here are compared to licensing calculations performed for the Maine Yankee plant (Ref. (F1)). All of the transients have the same initial conditions, which are given in Table H.1-2.

There is some difficulty in interpreting the test results given here, primarily because we do not know if the feedwater and steam flowrates used in our calculations match those used in the calculations given in Ref. (F1). In our

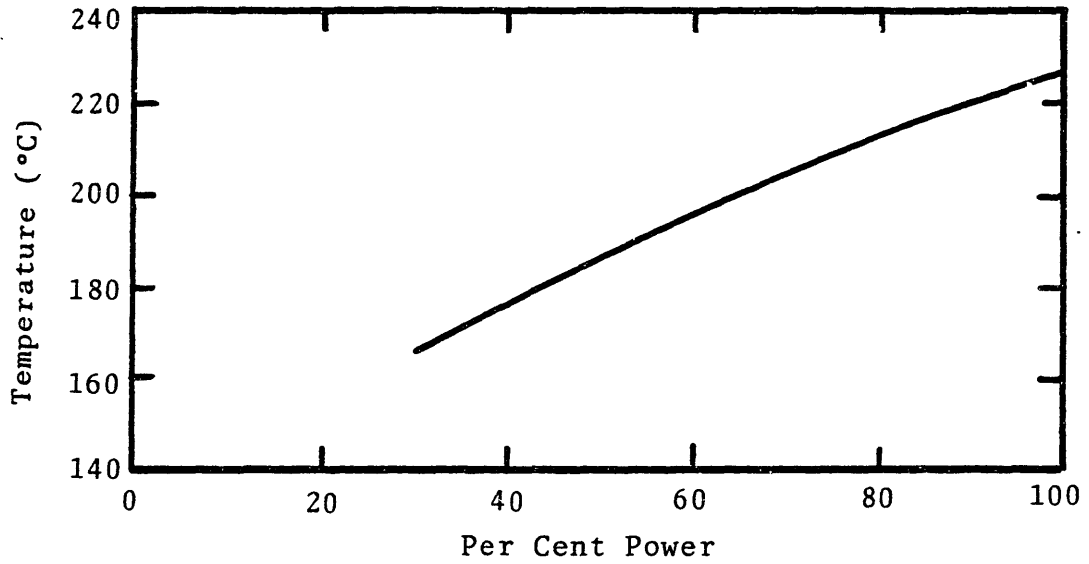


Figure H.1-1. Feedwater temperature vs. power (Ref (M9)).

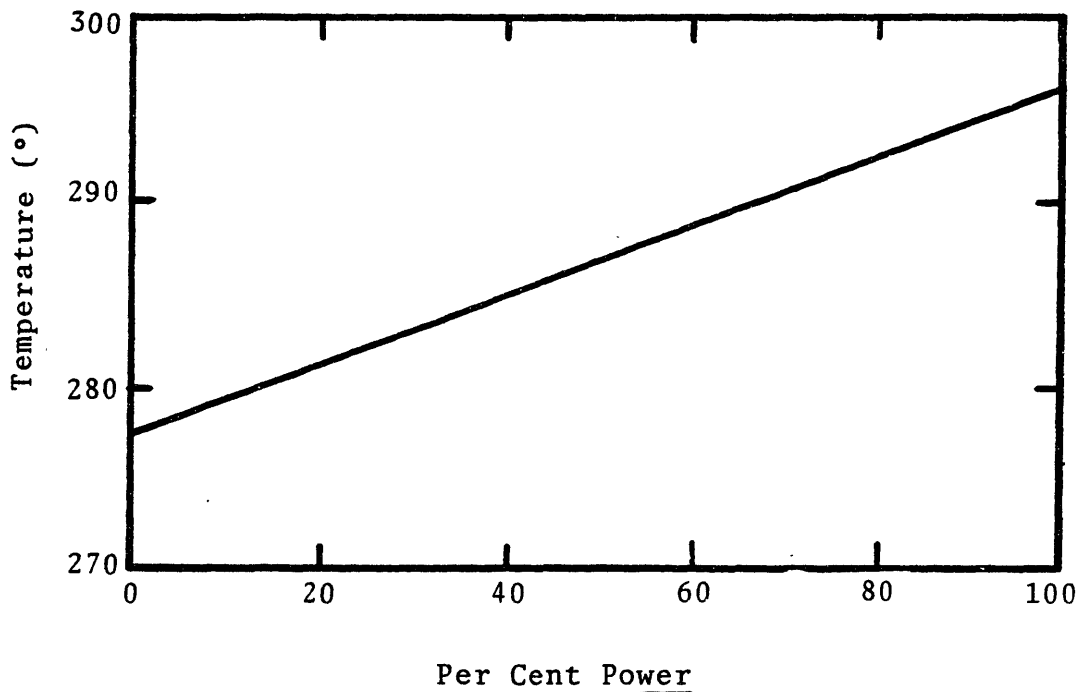


Figure H.1-2. Primary average temperature vs. power (Ref (M9)).

## Steady State Results

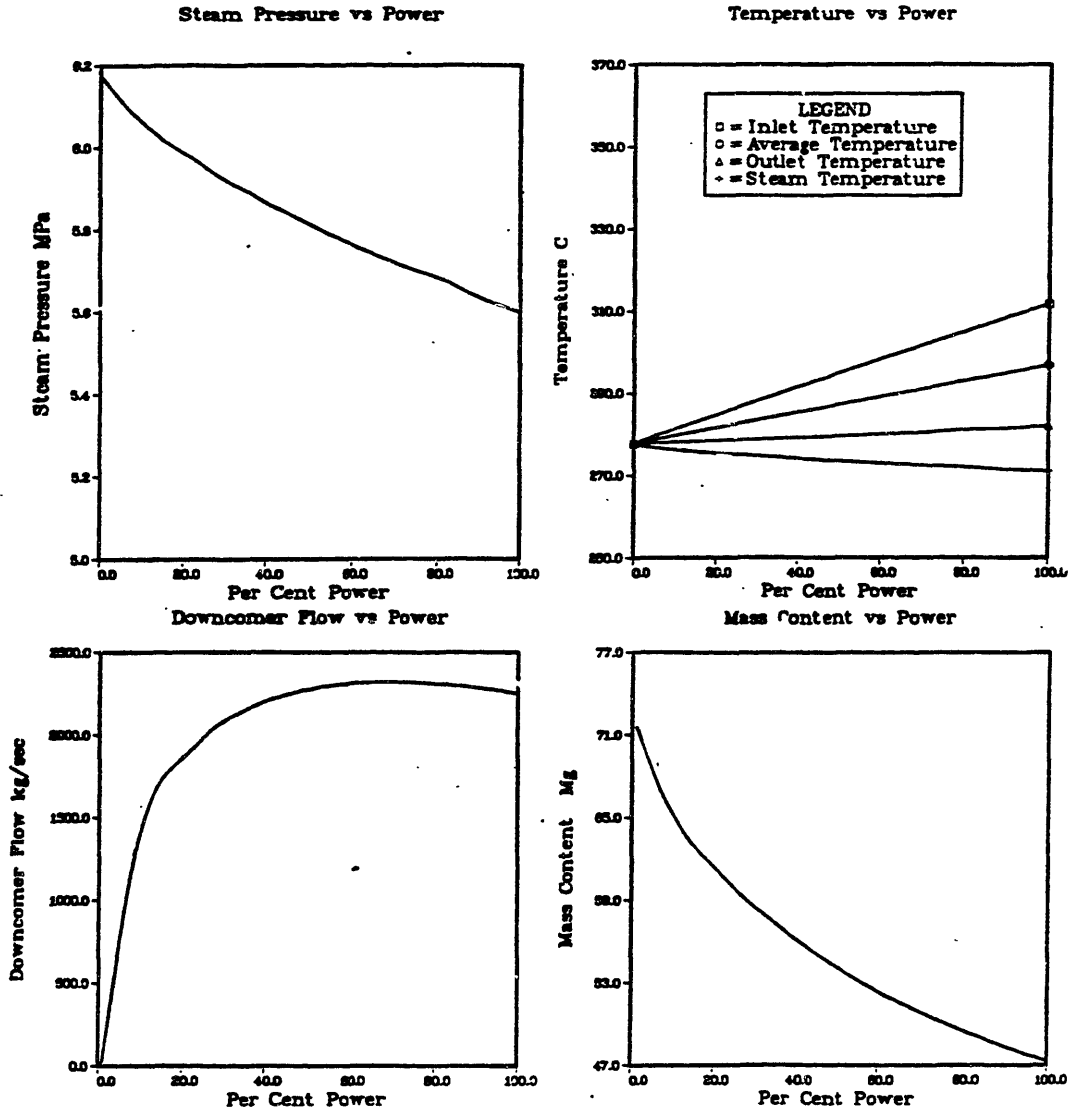


Figure H.1-3.

Table H.1-1  
Steady State Operating Parameters for Maine Yankee.

Quantity	Value
Primary Flowrate/Steam Generator Primary Pressure	5124 kg/s 15.46 MPa
Full Power Primary Average Temperature	297 °C
Full Power Secondary Pressure Reactor Power (100%) Separator Loss Coefficient	5.6 MPa 2450 MWt 282.5
Fouling Factor	$1.93 * 10^{-5} \frac{m^2 - °K}{W}$
Steam Generator Water Level*	10.12 m

\* Measured from tubesheet.

calculations the steam flowrate is obtained from a model of the main steam system (see Chapter 3 and Ref. (M9)). The transient feedwater flowrate behavior is discussed separately for each transient. Discussion of transient results is limited to a brief description of the sequence of events, and comments are made regarding the gross behavior of calculated steam generator parameters.

#### Control Element Withdrawal Incident

The transient inputs used to simulate an uncontrolled withdrawal of a Control Element Assembly (CEA) are shown in Fig. H.1-4. The calculated response of the steam generator

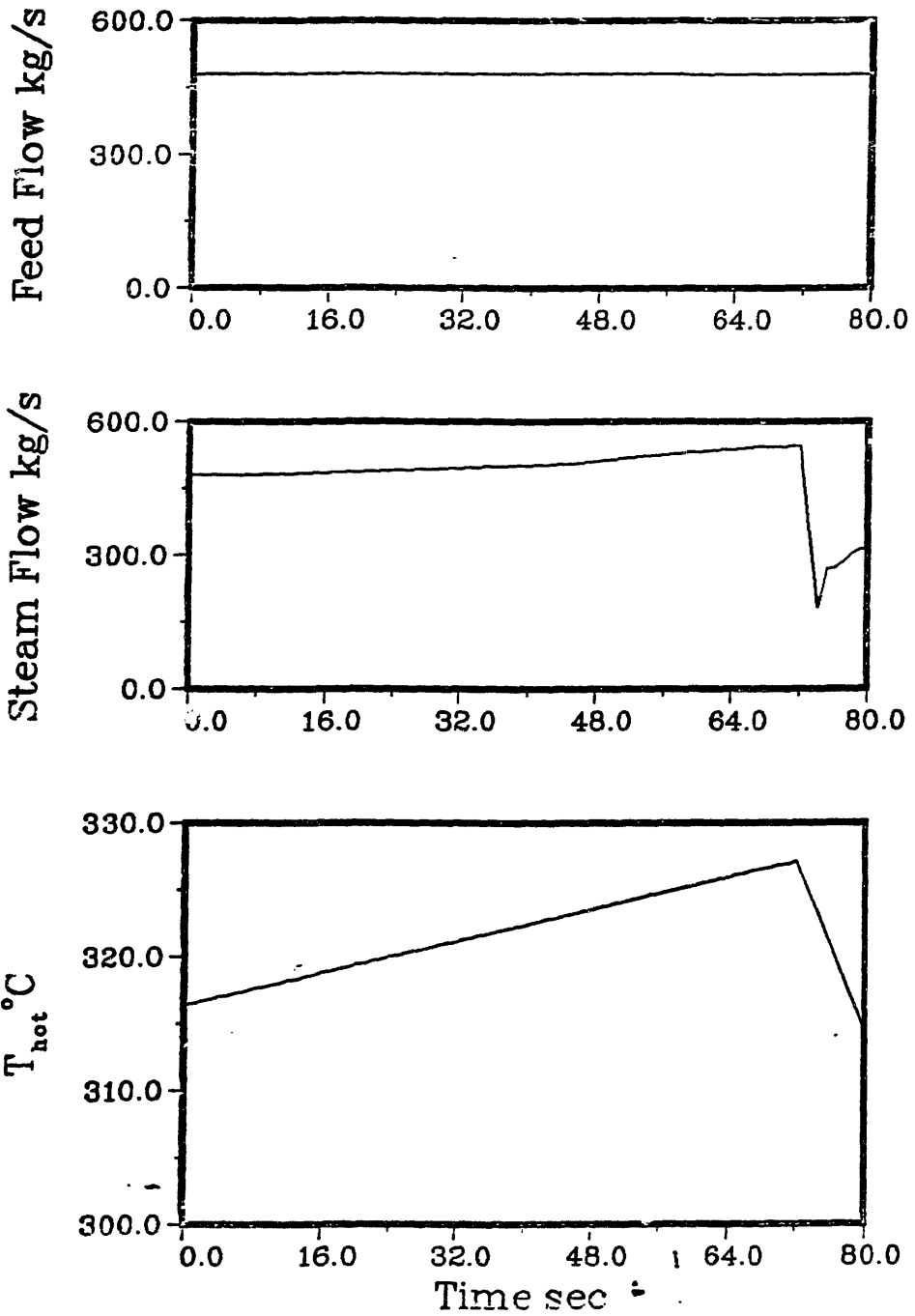


Figure H.1-4. Input for CEA withdrawal incident.

Table H.1-2  
Initial Conditions for Maine Yankee Transient Tests  
at 106 per cent Power.

Quantity	Value
Reactor Power	2611 MWt
Water Level*	10.12 m
Downcomer Flowrate	2231 kg/s
Steam Pressure	5.847 MPa
Steam Flowrate	480.5 kg/s
Feedwater Temperature	225.9°C
Primary Inlet Temperature	316.4°C
Primary Outlet Temperature	285.5°C

\* Measured from tubesheet.

is shown in Fig. H.1-5. The sequence of events is as follows:

- 1.) Transient is initiated by the withdrawal of CEAs;
- 2.) At approximately 43 seconds the turbine bypass valves open; and,
- 3.) At 72 seconds a reactor trip occurs, followed immediately by a turbine trip.

As can be seen in Fig. H.1-5, the results calculated here are in excellent agreement with those presented in Ref. (F1).

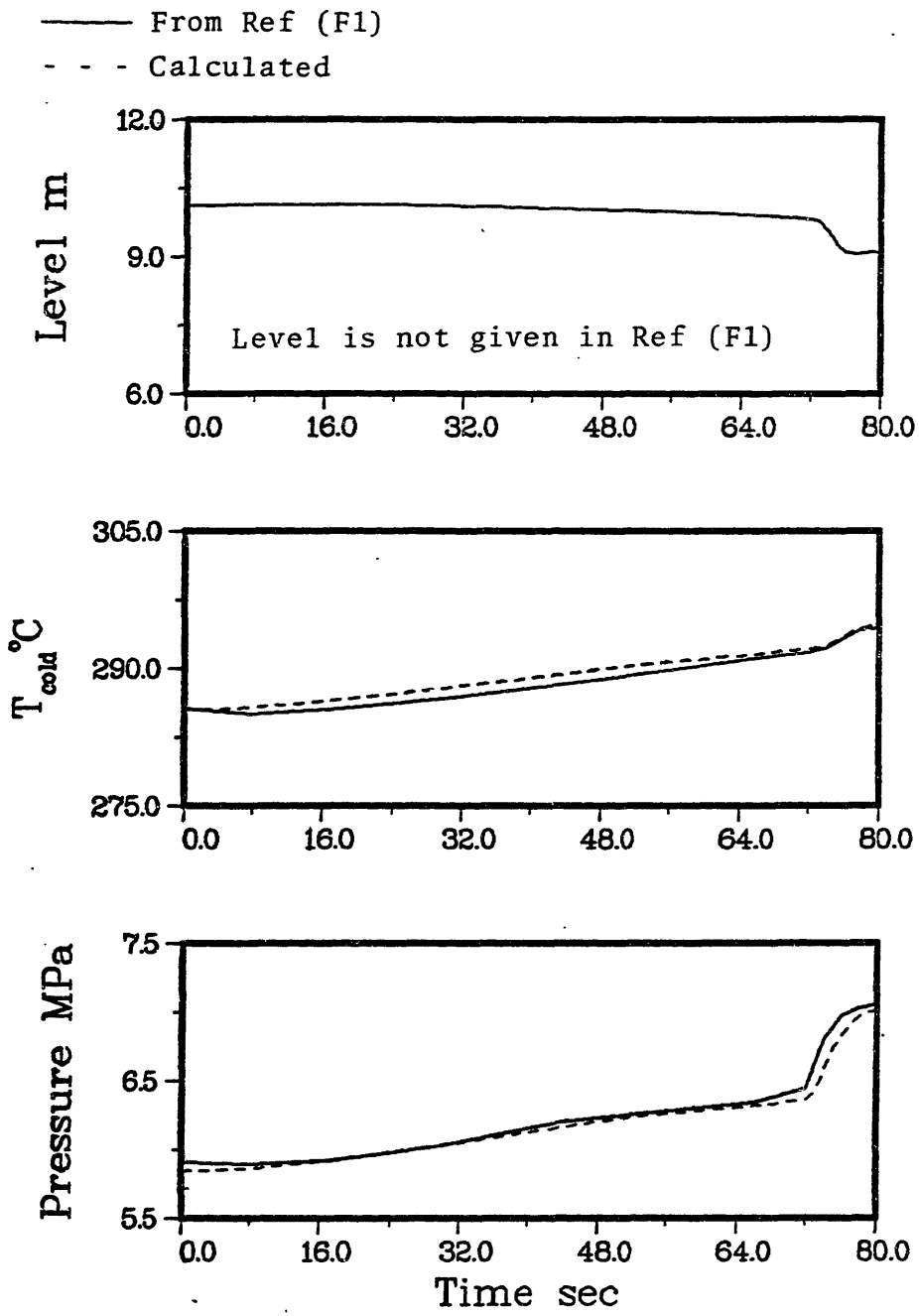


Figure H.1-5. Steam generator response for CEA withdrawal incident.



### Loss of Load Incident

The transient inputs used to simulate the loss of load incident are shown in Fig. H.1-6. The calculated results are shown in Fig. H.1-7. The simulation is run without the benefit of the steam dump or turbine bypass systems. Therefore, secondary pressure relief is accomplished solely by means of the secondary safety valves. The sequence of events is as follows:

- 1.) Main turbine trip initiates transient; turbine stop valves close within 1/2 second; and,
- 2.) Feedwater flowrate is ramped down to 5 per cent of its full power valve in sixty seconds.

As can be seen in Fig. H.1-7, the calculated pressure is in good agreement with the pressure given in Ref. (F1). Differences in our calculated pressure from the calculated pressure given in Ref. (F1) are probably due to differences in the steam flowrate used during the calculations. The calculated cold leg temperatures are in good agreement after 42 seconds; prior to that our calculated cold leg temperature responds faster and reaches a higher peak value than does the cold leg temperature taken from Ref. (F1). The reason for this difference is not known, but it is reasonable to assume that the cold leg temperature from Ref. (F1) is processed through a sensor model or through a first order lag function, while the cold leg temperature we obtain is

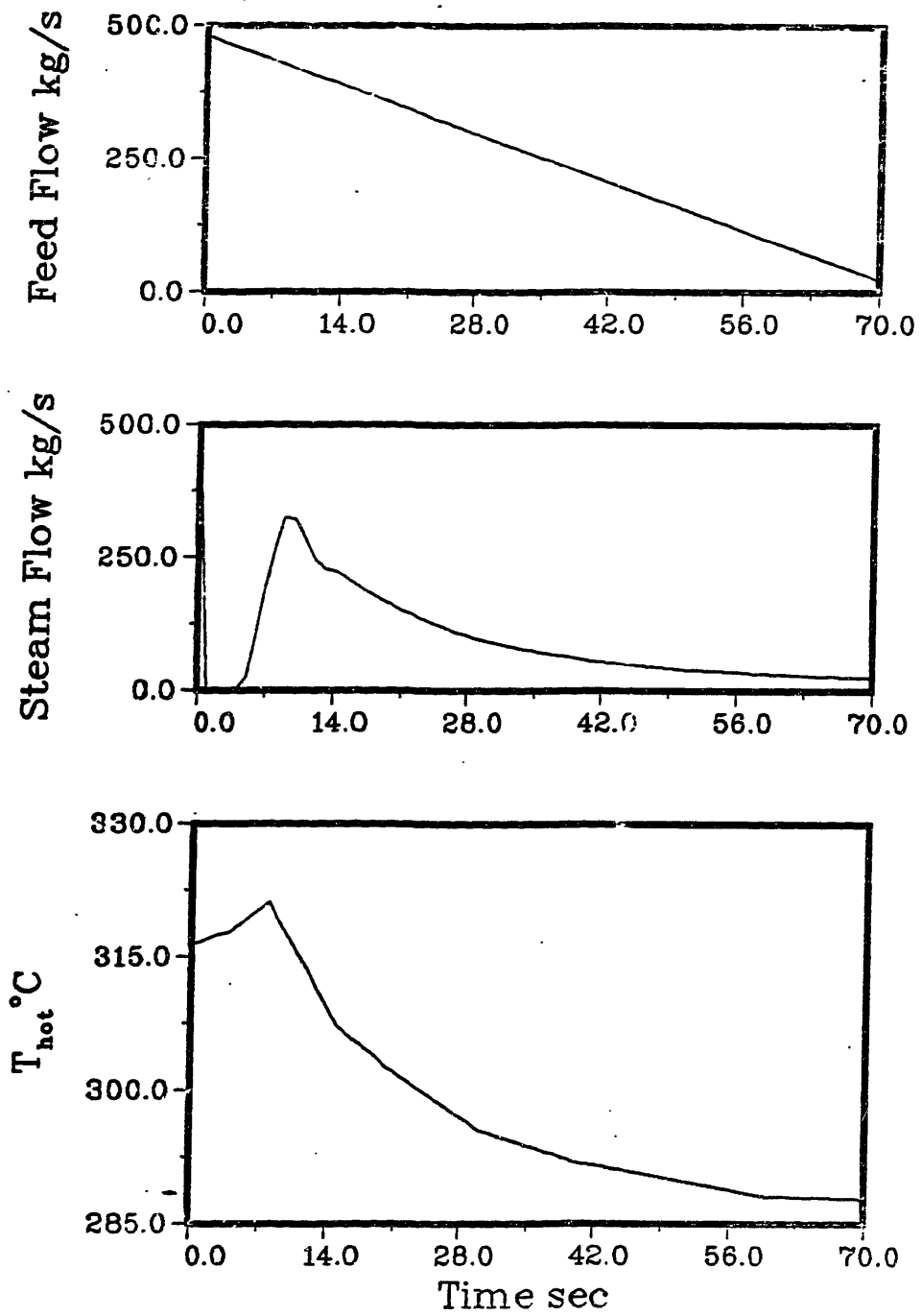


Figure H.1-6. Input for loss of load incident.

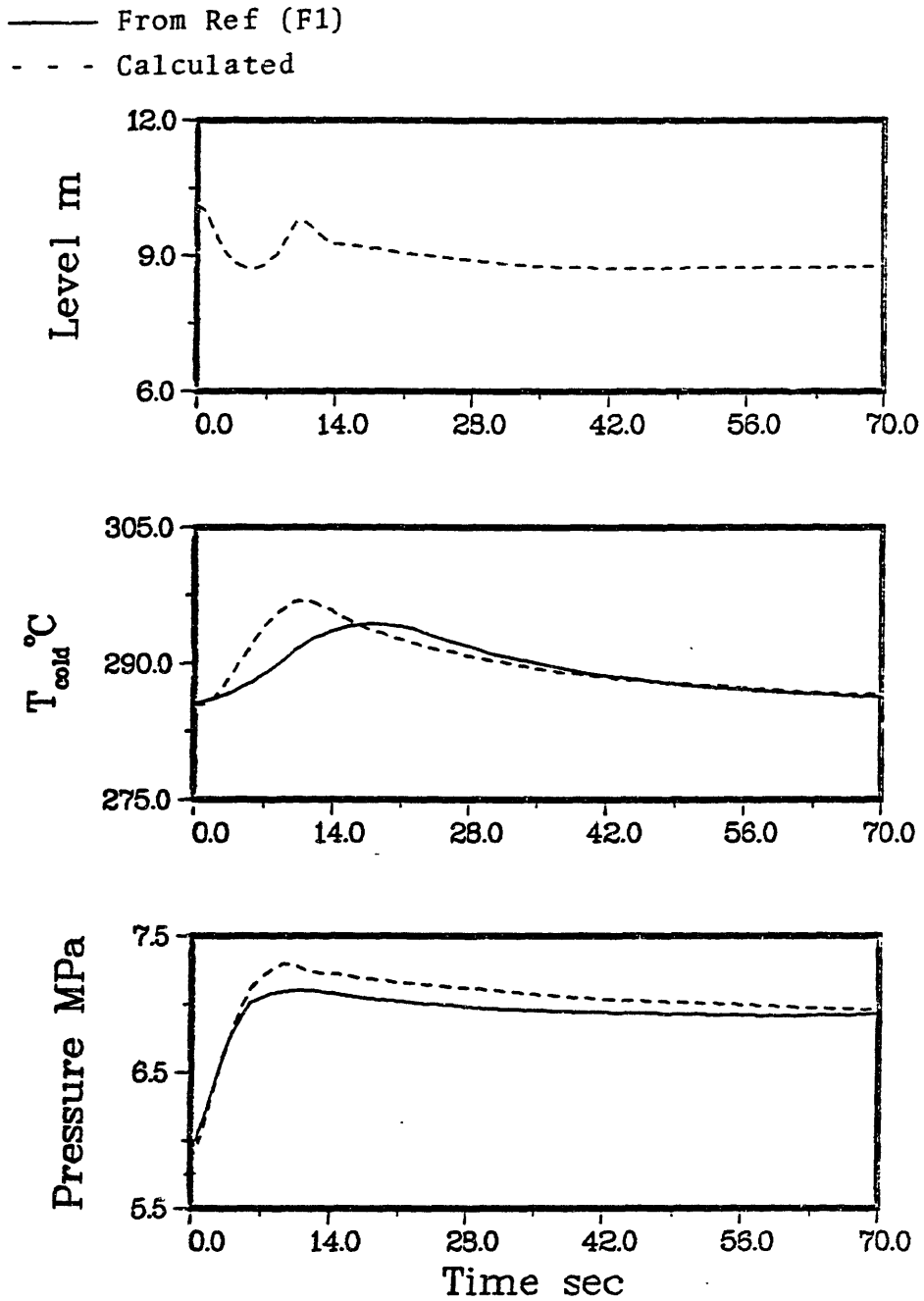


Figure H.1-7. Steam generator response for loss of load incident.

not. This would account for the differences seen in the early part of the transient and would not significantly affect results toward the end of the simulation since the rate of change of the cold leg temperature is slow.

#### Loss of Feedwater Flow Incident

The transient inputs used to simulate the Loss of Feedwater Incident are shown in Fig. H.1-8. The calculated results are shown in Fig. H.1-9. The full main steam system model is used to calculate the transient steam flowrate.

The sequence of events is as follows:

- 1.) The transient is initiated by the instantaneous loss of all feedwater flow; and
- 2.) Reactor and turbine trips occur at 17 seconds.

The results shown in Fig. H.1-9 are not in good agreement, and the reason why is not clear. It appears, however, that the major cause for the difference between the two calculations is that our model predicts an initial decrease in steam generator pressure that is not predicted by the licensing calculation. The pressure calculated by the model never recovers from the initial dip and remains at a nearly constant offset from the pressure calculated using the licensing code. A similar behavior is shown by the calculated cold leg temperature since it is directly influenced by the calculated secondary pressure through the heat transfer rate.

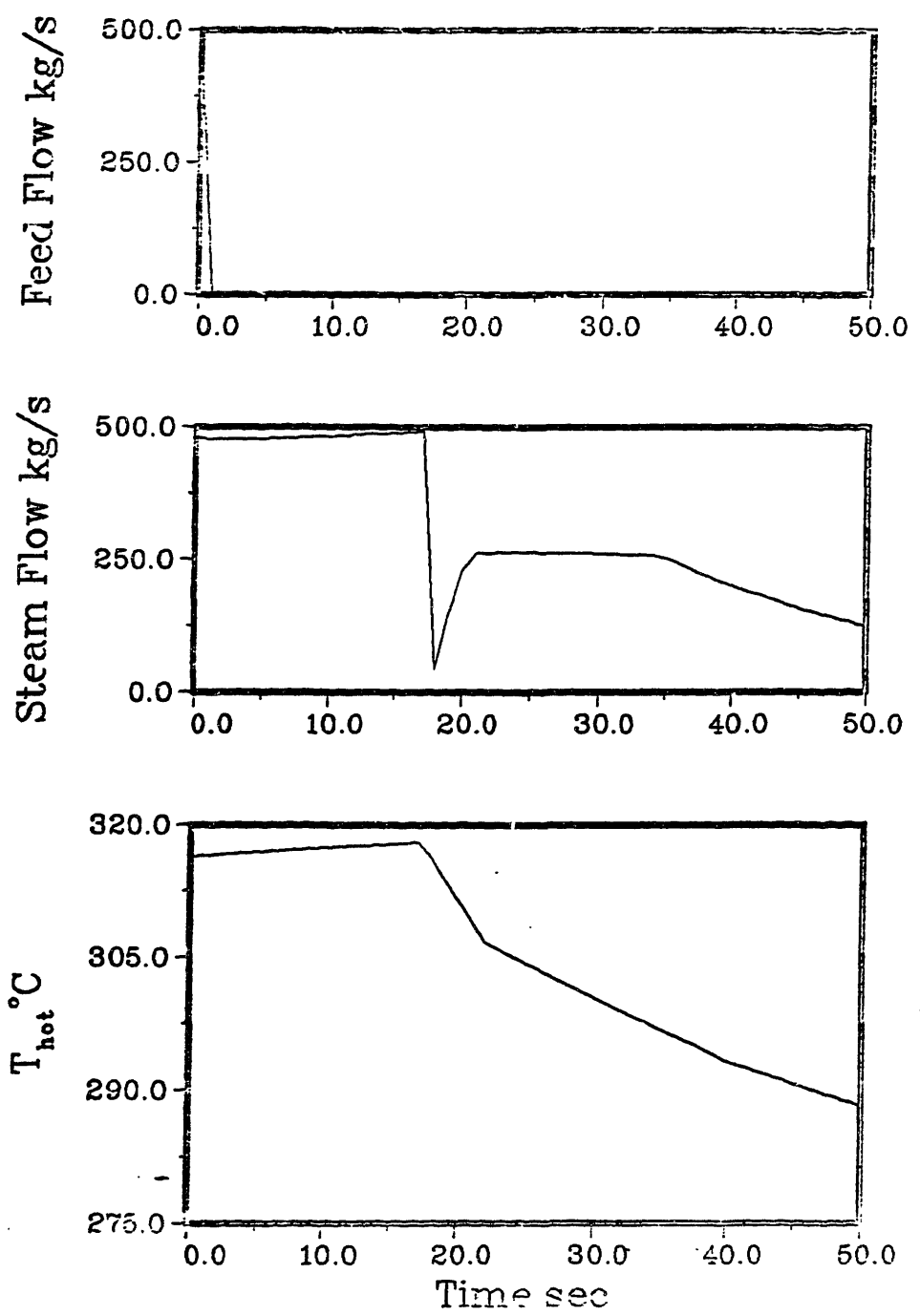


Figure H.1-8. Input for loss of feed incident.

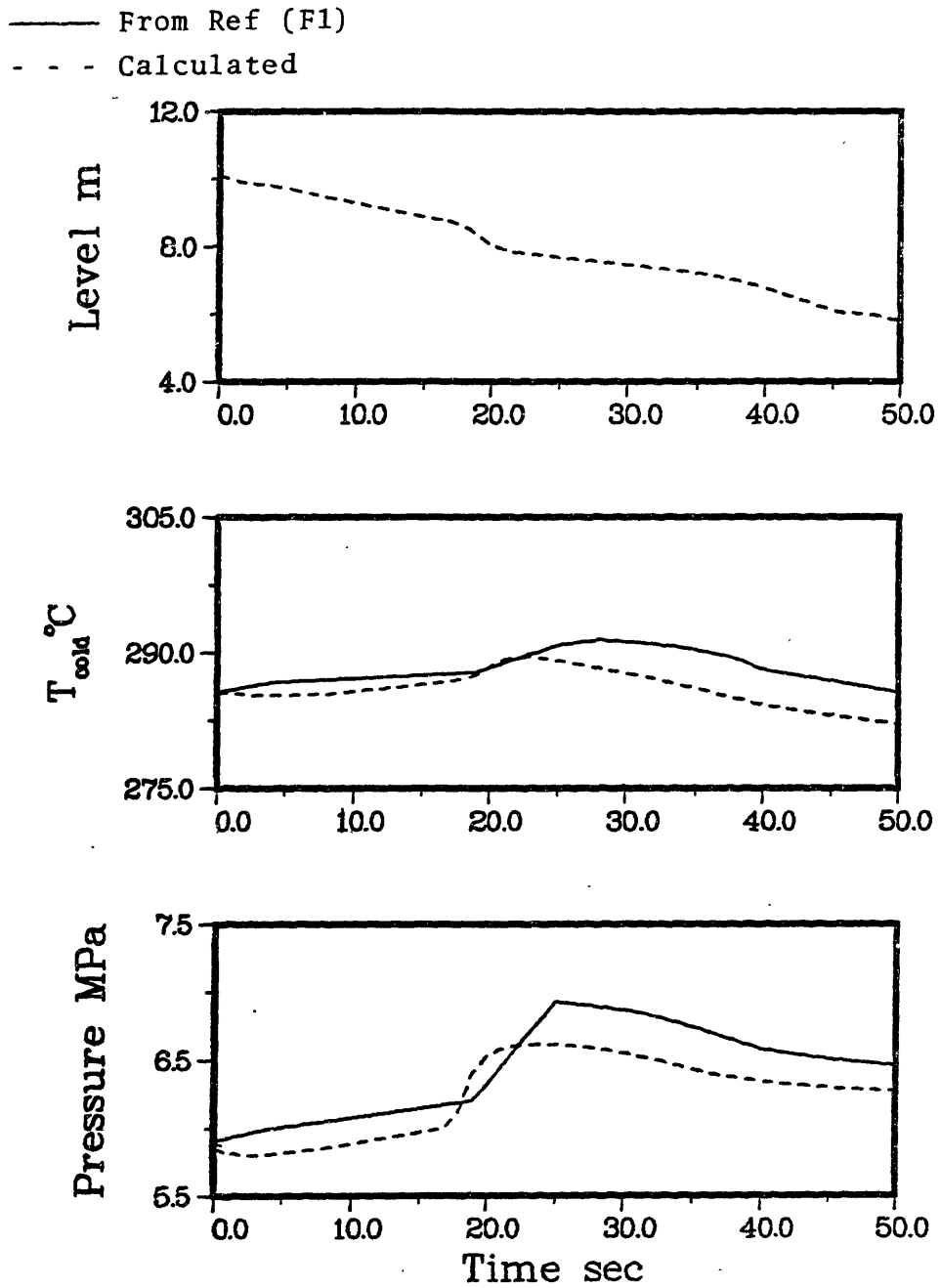


Figure H.1-9. Steam generator response for loss of feed incident.

### H.1.2 Transient Tests at Full Power

The transient simulation results presented in this section are compared to results given in Ref. (M9). The initial conditions for all these transients are the same and are given in Table H.1-3.

Table H.1-3  
Initial Conditions for Maine Yankee Transient  
Tests at Full Power.

Quantity	Value
Reactor Power	2450 MWt
Water Level*	10.12 m
Downcomer Flowrate	2250 kg/s
Steam Pressure	5.6 MPa
Steam Flowrate	450.3 kg/s
Feedwater Temperature	225.9°C
Primary Inlet Temperature	311.7°C
Primary Outlet Temperature	282.1°C

\* Measured from tube sheet.

### Reactor Trip

The transient input for the simulation of the reactor trip are shown in Fig. H.1-10. The calculated steam generator response is shown in Fig. H.1-11. The steam flowrate is obtained using a model of the Maine Yankee main steam

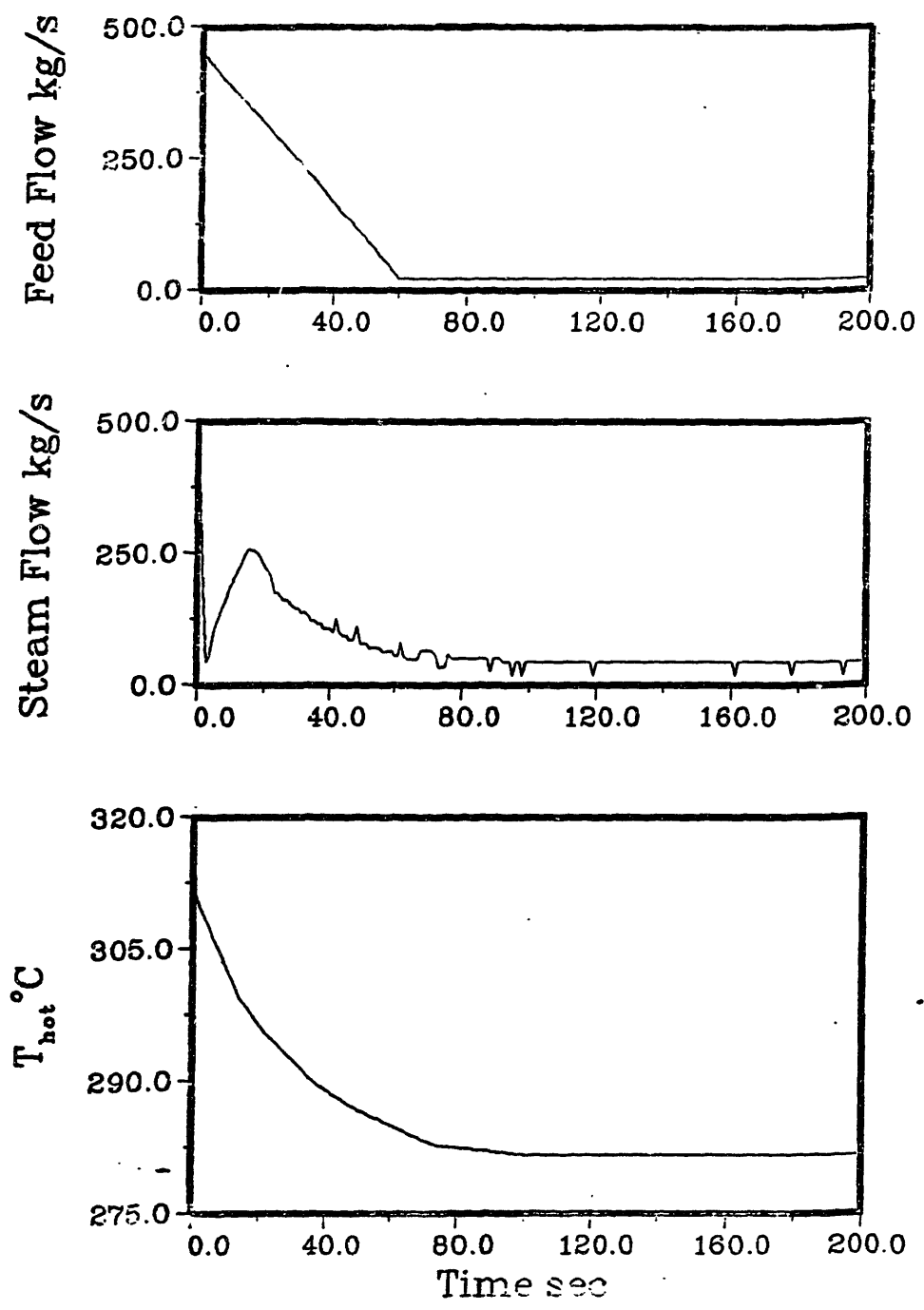


Figure H.1-10. Input for reactor trip.



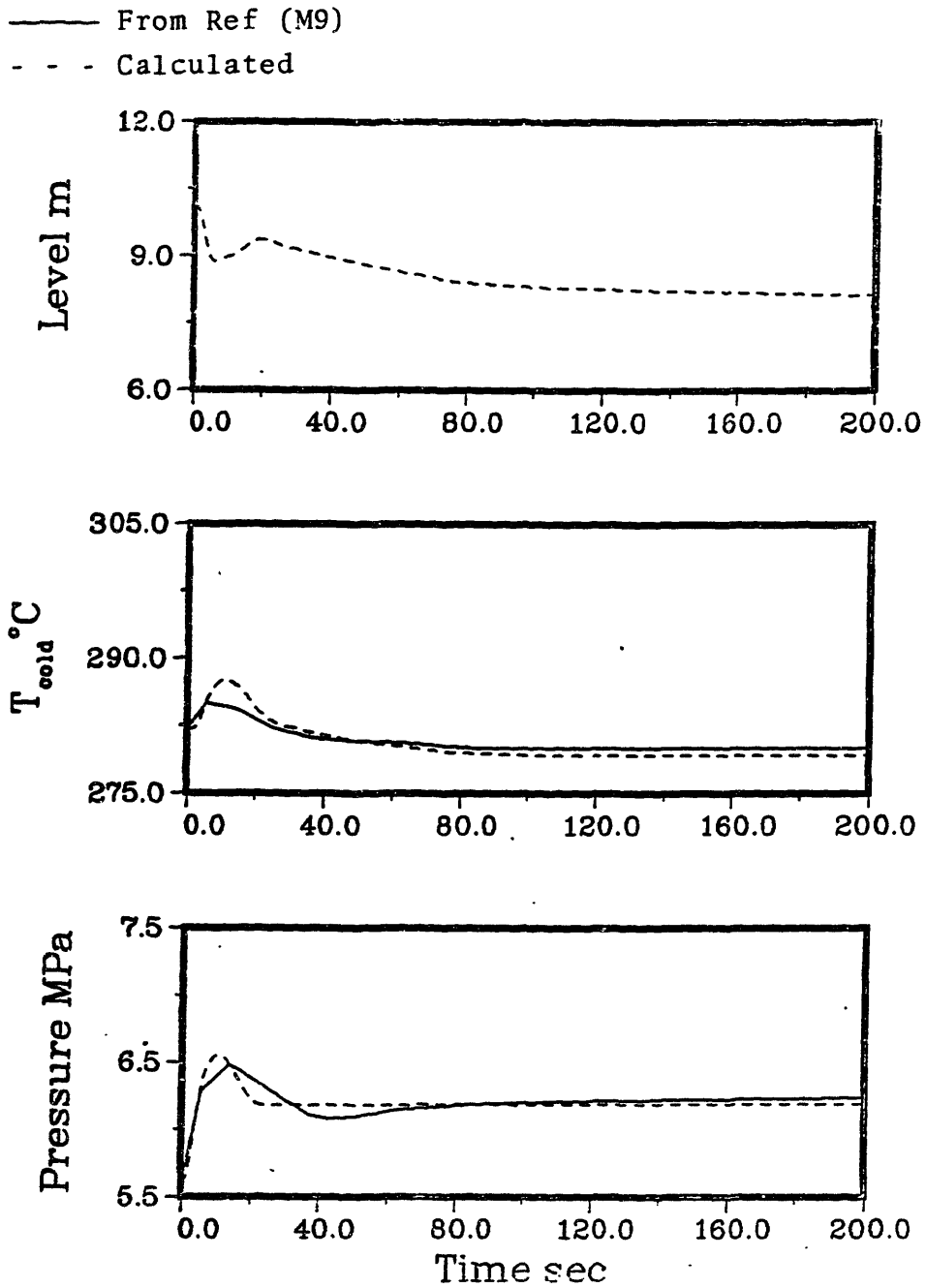


Figure H.1-11. Steam generator response for reactor trip.

system. The transient is initiated by the simultaneous trip of both the reactor and the main turbine. The results obtained using our model compare favorably with the results from Ref. (M9). Some of the differences can be accounted for by inaccuracies and differences in the steam flowrates used to generate each set of results. Unfortunately, the steam flowrate used to generate the results given in Ref. (M9) are not known so no firm conclusion can be drawn.

#### Turbine Trip with Steam Dump

The transient inputs used to simulate the turbine trip with steam dump are shown in Fig. H.1-12. Transient test results are shown in Fig. H.1-13. As can be seen, the calculated pressures are in good agreement and most of the differences seen are probably due to differences in the input steam flows, which cannot be assessed here. Our calculated cold leg temperature responds faster and reaches a higher peak value than the cold leg temperature given in Ref. (M9).

#### Turbine Trip without Steam Dump

The transient inputs used to simulate the turbine trip without steam dump are shown in Fig. H.1-14. The calculated response is shown in Fig. H.1-15. As can be seen the general trends of both the calculated cold leg temperature and the calculated pressure agree with the corresponding trends of the results given in Ref. (M9). Again, the only comment

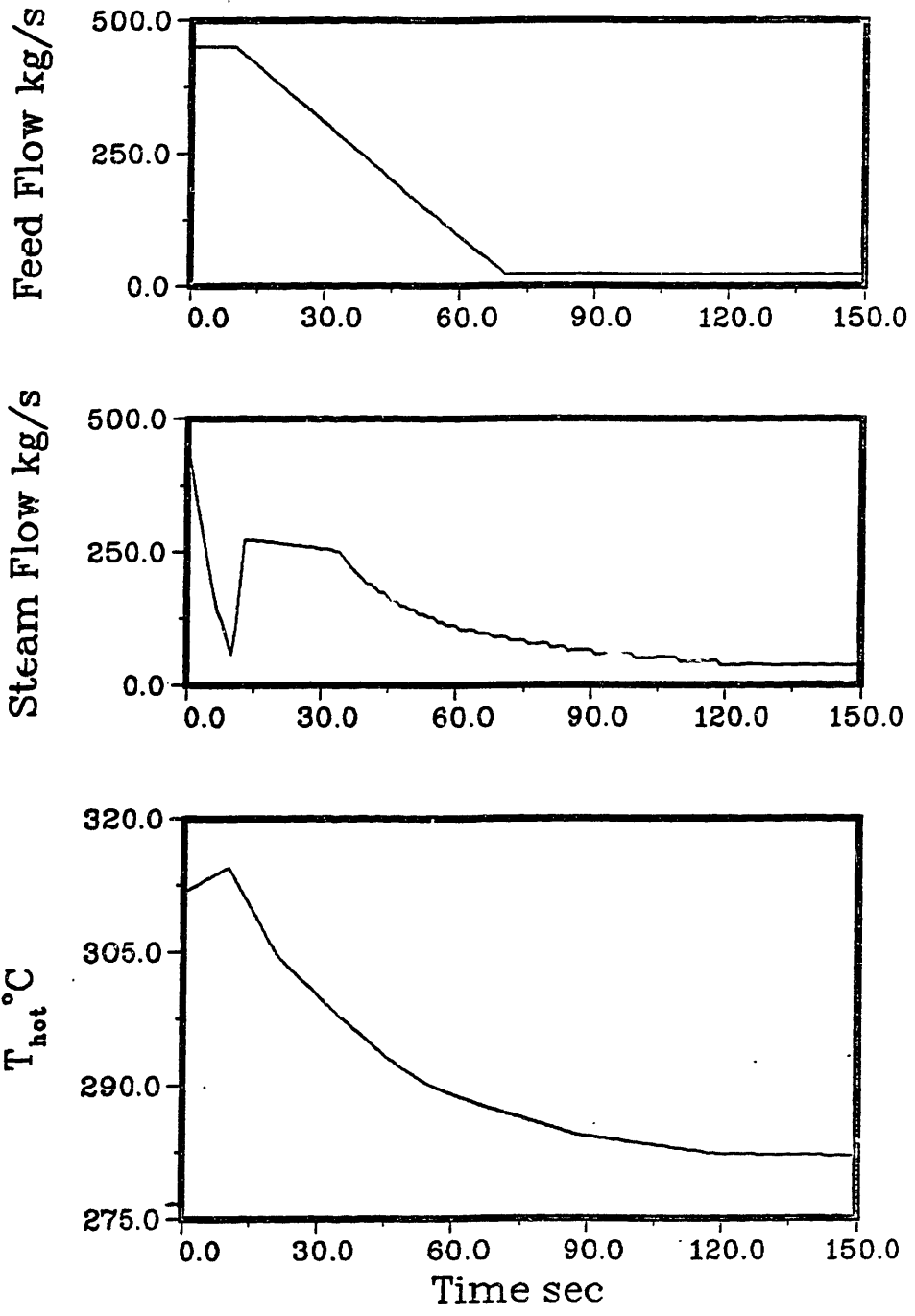


Figure H.1-12. Inputs for turbine trip with steam dump.

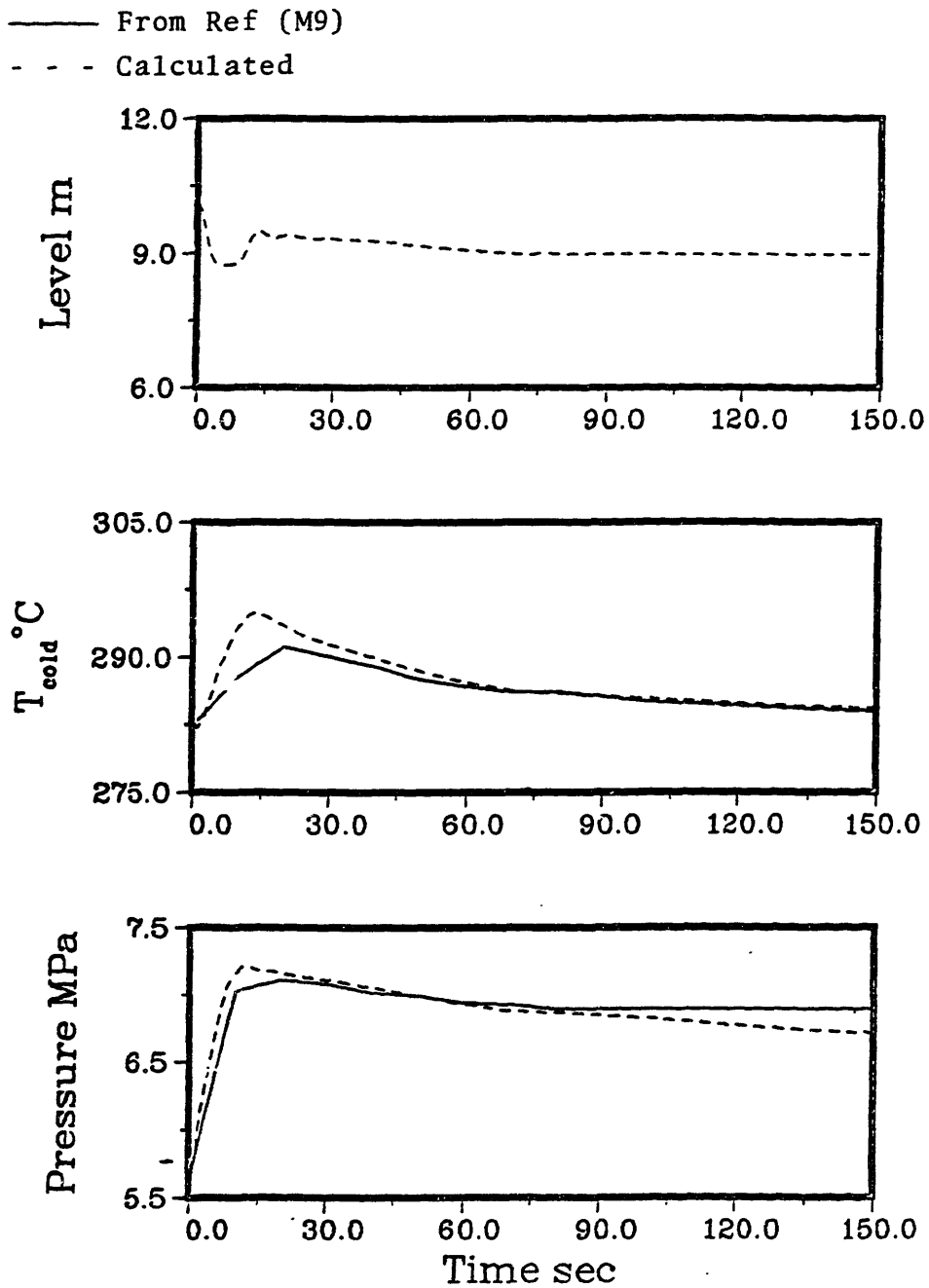


Figure H.1-13. Steam generator response for turbine trip with steam dump.

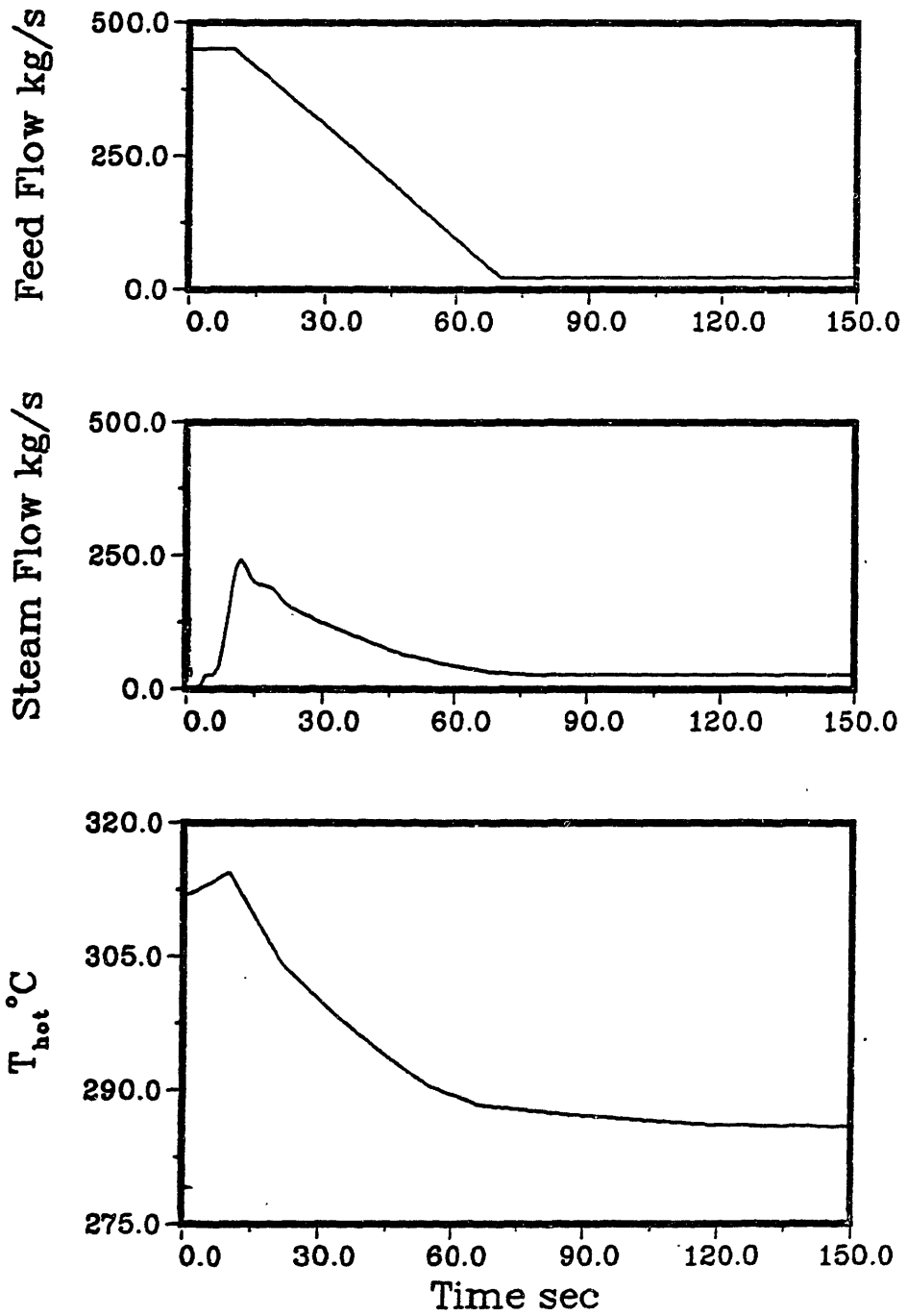


Figure H.1-14. Input for turbine trip without steam dump.

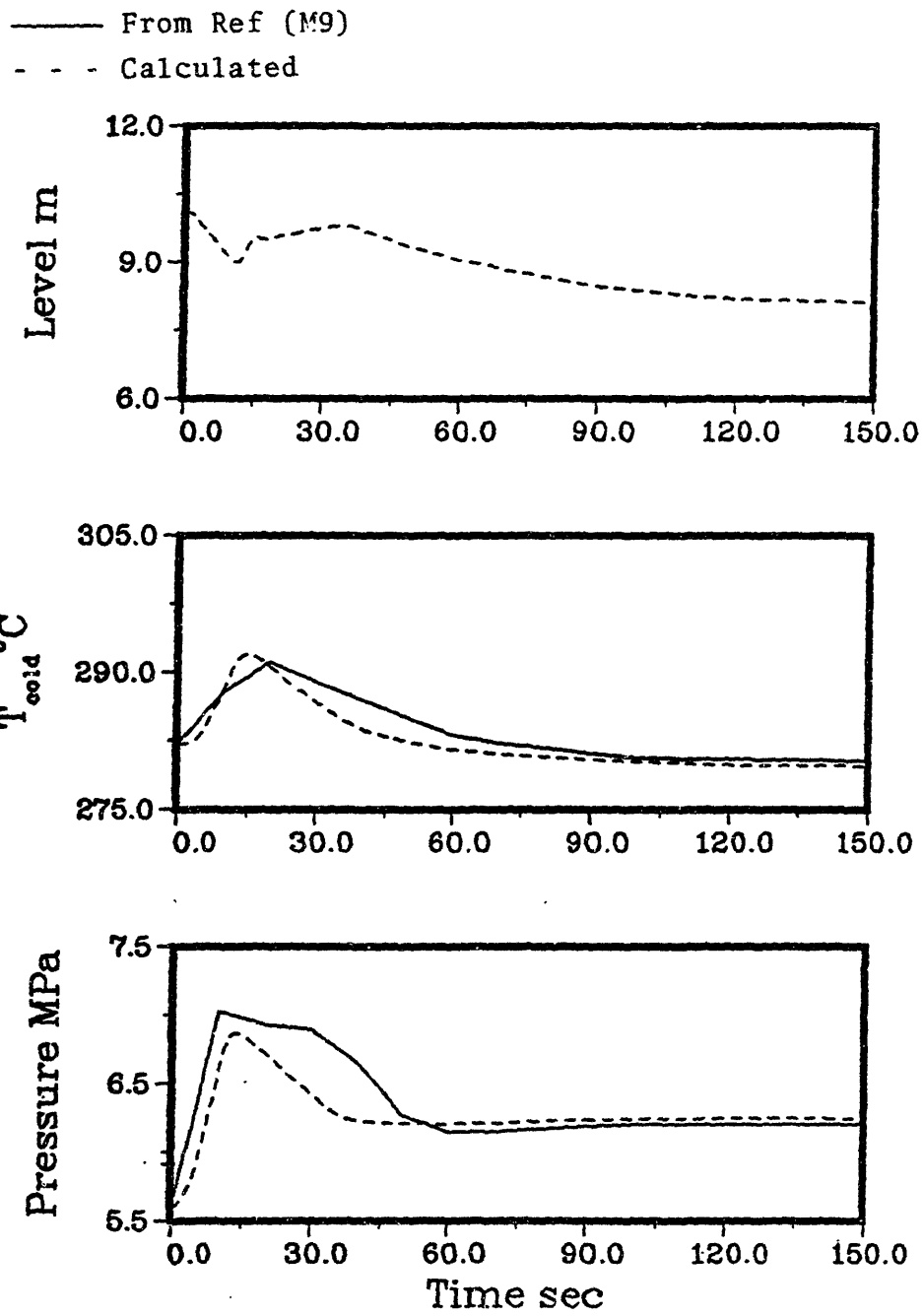


Figure H.1-15. Steam generator response for turbine trip without steam dump.

we can make is that an incomplete knowledge of the transient steam flowrate makes it difficult to draw any specific conclusions regarding model fidelity.

## H.2 CALVERT CLIFFS

The Calvert Cliffs nuclear power plant has a Combustion Engineering designed NSSS. The plant is licensed to operate at an NSSS output of 2560 MWt. The NSSS has two steam generators. Included in the results given here are four transient tests:

- 1.) Control Element Assembly withdrawal at 102% power (Ref. (F3));
- 2.) Loss of Load Incident at 102% power (Ref. - (F3));
- 3.) Loss of Primary Flow at 40% power (Refs. (B4) and (W1); and,
- 4.) Turbine Trip at 100% power (Refs. (B4) and (W1)).

The first two transient tests are taken from licensing calculations (Ref. (F3)), while the last two are reported results from startup tests (Refs. (B4) and (W1)). As is the case for the Maine Yankee plant, we do not know the transient feed and steam flows used to obtain the results to which we compare our calculated results. Thus, it is difficult to draw any firm conclusions from these tests, other than comments regarding general trends of gross steam generator parameters.

### H.2.1 Licensing Calculations

The initial conditions for the licensing type calculations are given in Table H.2-1, which also lists the separator loss coefficient and fouling factor used in the analyses. For all transient tests a model of the main steam system is used to generate the transient steam flowrate.

Table H.2-1  
Initial Conditions for Calvert Cliffs  
Licensing Calculations.

Quantity	Value
Reactor Power	2611 MWt
Water Level*	10.67 m
Downcomer Flowrate	3569 kg/s
Steam Pressure	6.036 MPa
Steam Flowrate	714.8 kg/s
Feedwater Temperature	223.1°C
Primary Inlet Temperature	317.9°C
Primary Outlet Temperature	287.1°C
Primary Flowrate/Steam Generator	7693 kg/s
Fouling Factor	$1.97 \cdot 10^{-5} \frac{\text{m}^2 \cdot \text{K}}{\text{W}}$
Separator Loss Coefficient	100.00

\* Measured from tube sheet.



### Control Element Assembly Withdrawal Incident

The transient inputs for the CEA withdrawal incident are shown in Fig. H.2-1. The steam generator response is shown in Fig. H.2-2. As can be seen the general trends of the cold leg temperature and steam pressure calculated using the model are in good agreement with the results taken from Ref. (F3). Differences in magnitude are probably due to uncertainty in the input steam flowrate, which has a significant effect on the steam pressure and also on the cold leg temperature through the heat transfer rate.

### Loss of Load Incident

The transient inputs for the loss of load incident are shown in Fig. H.2-3. The steam dump and bypass systems are not used in this simulation, so that secondary pressure relief is accomplished solely by the safety valves. The jagged nature of the transient steam flowrate curve is due to the opening and closing of the secondary safety valves.

The steam generator response is shown in Fig. H.2-4. The transient is initiated by closing the turbine stop valves within 1/2 second. Following the reactor trip, which occurs at 7 seconds, the feedwater flowrate is ramped down to 5 per cent of its full load valve in 60 seconds. The calculated pressure using our model is in excellent agreement with the results taken from Ref. (F3). Our calculated cold leg temperature responds faster than the cold leg temperature taken from Ref. (F3).

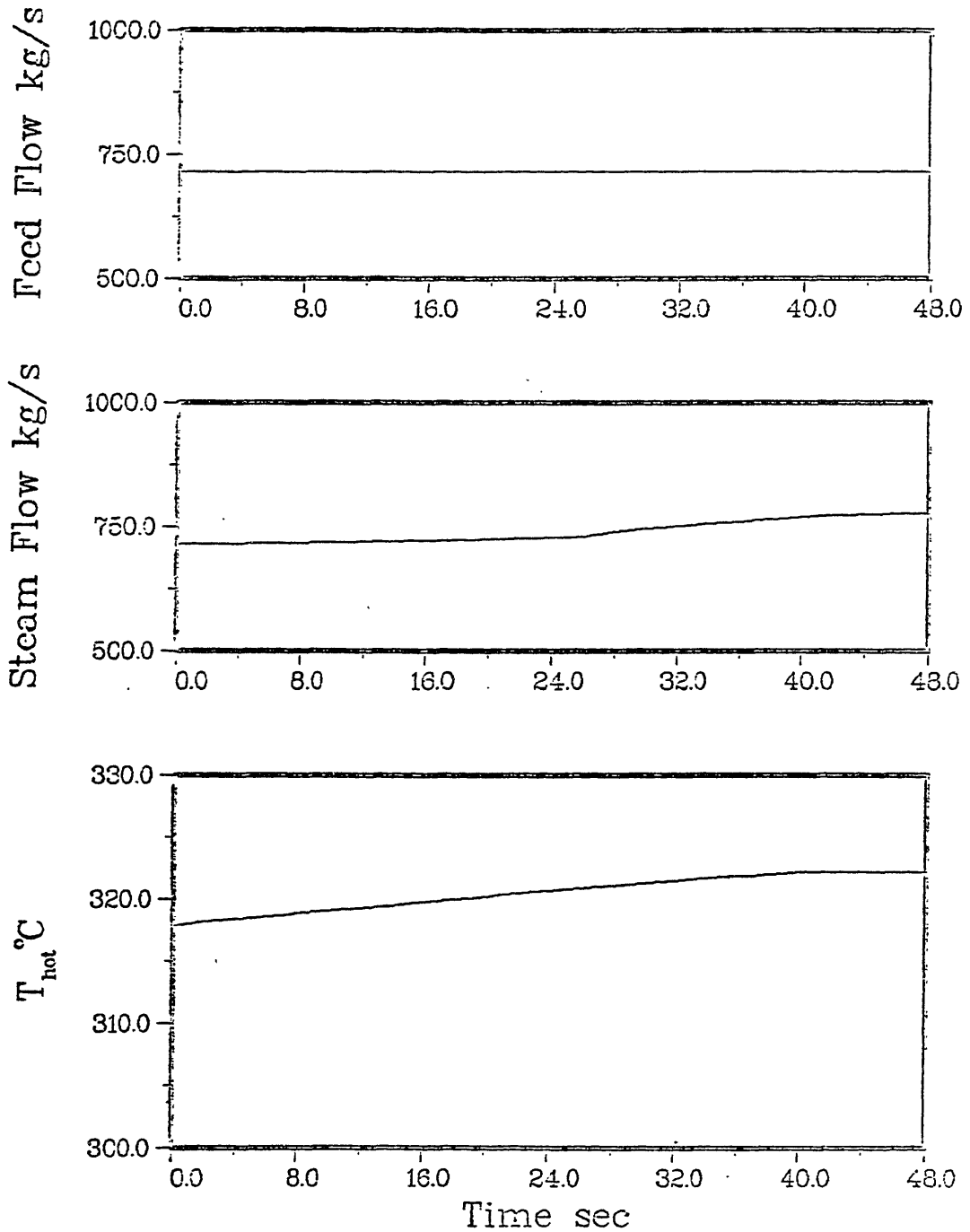


Figure H.2-1. Input for CEA withdrawal incident.

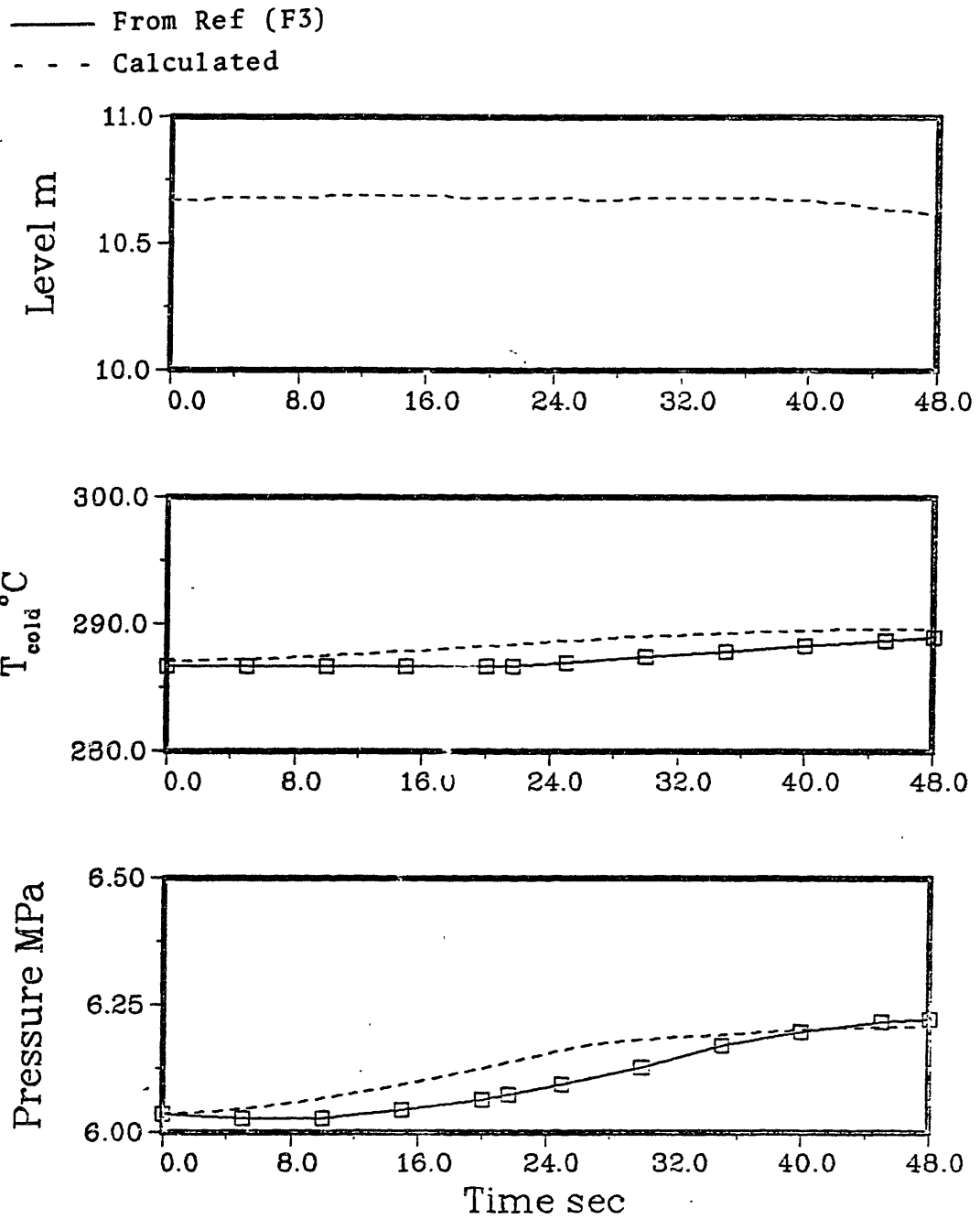


Figure H.2-2. Steam generator response for CEA withdrawal incident.

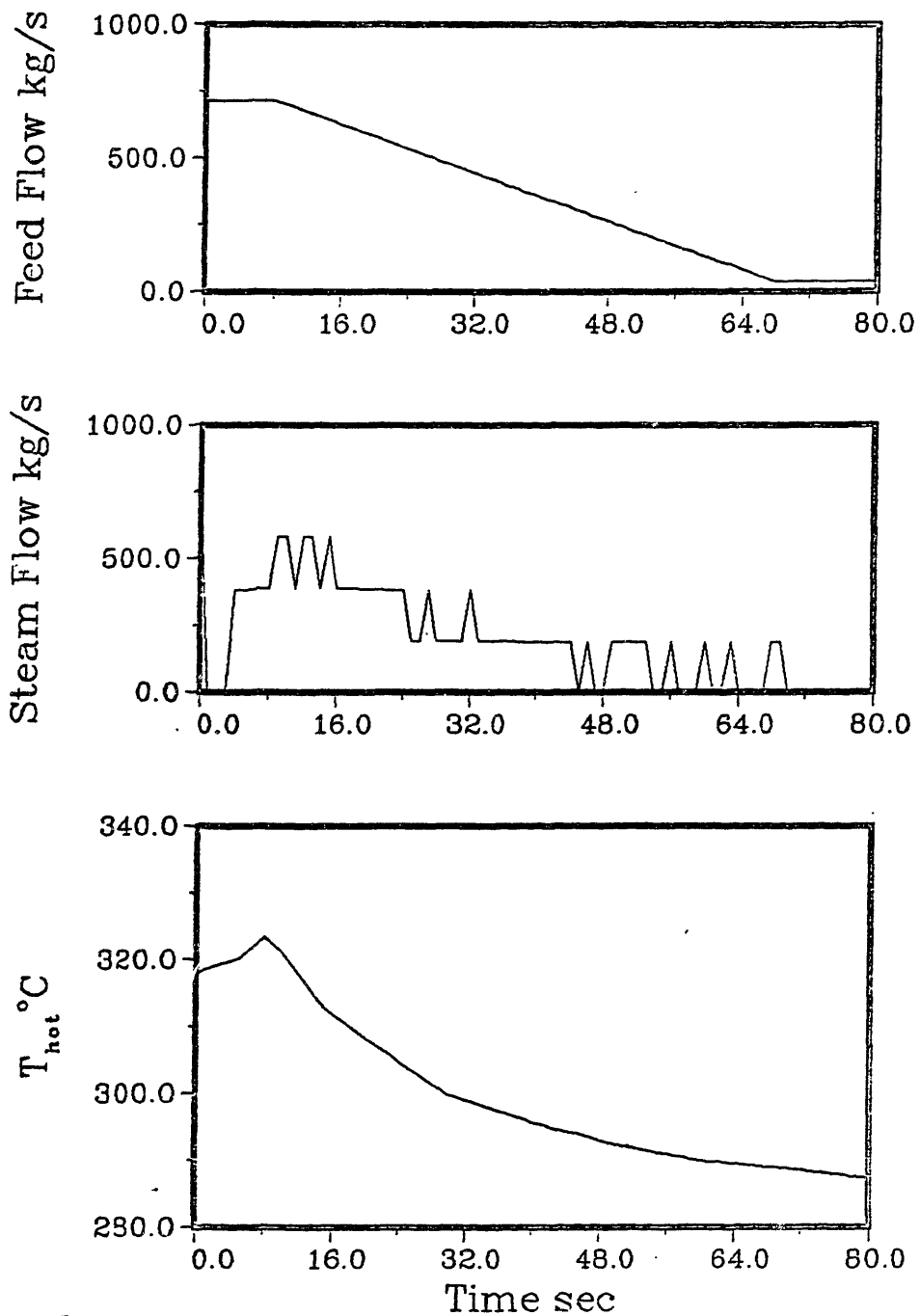


Figure H.2-3. Input for the loss of load incident.

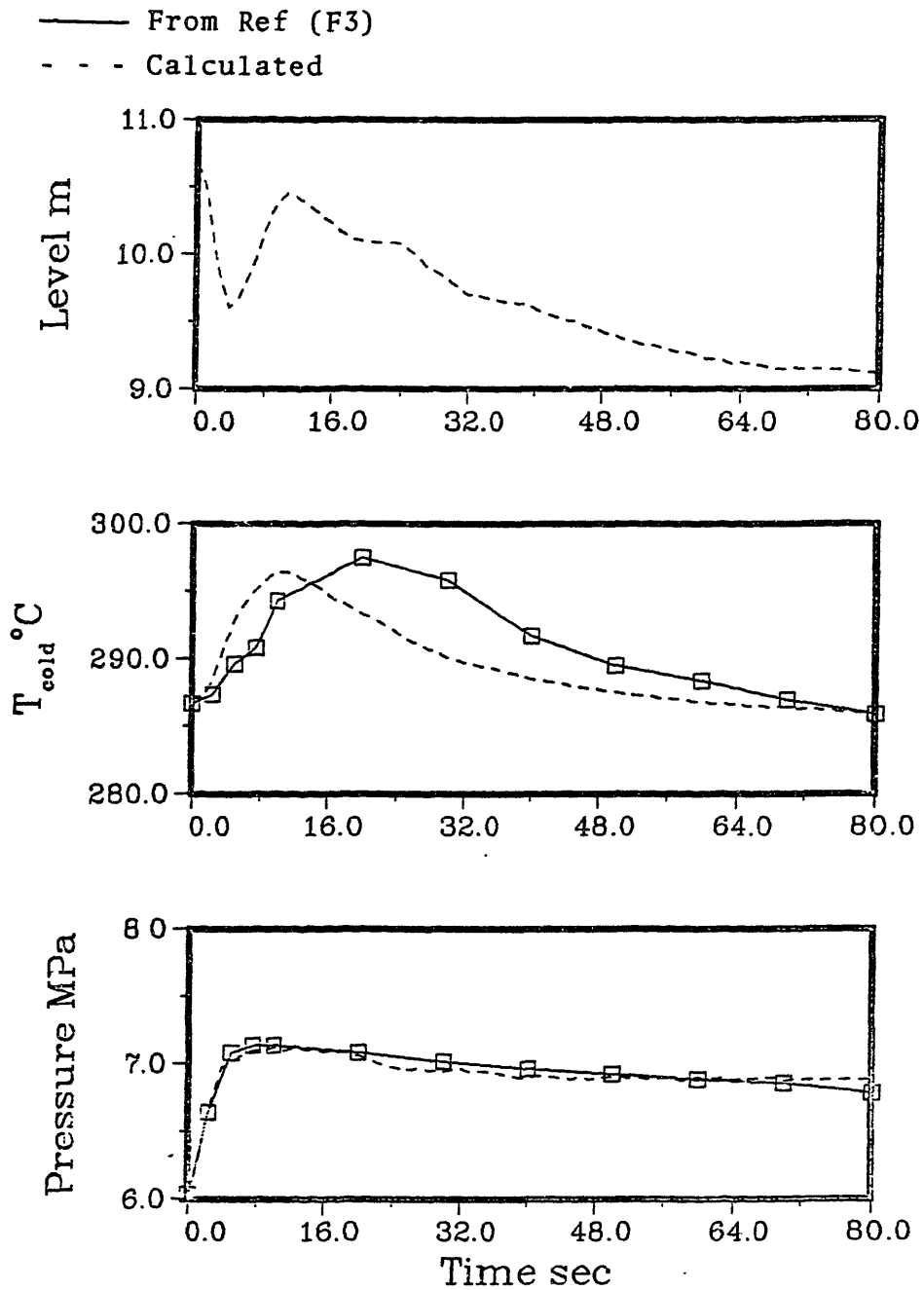


Figure H.2-4. Steam generator response for the loss of load incident.

## H.2.2 Startup Test Results

The results presented in this reaction are taken from Refs. (B4) and (W1). Sensors are modeled using a first order leg (see Chapter 6) with time constants of 2.374 and 2.447 seconds for the hot and cold leg sensors, respectively.

Table H.2-2  
Initial Conditions for Turbine Trip Test.

Quantity	Value
Power/Steam Generator	1280 MWt
Water Level*	11.23 m
Downcomer Flowrate	3800 kg/s
Steam Pressure	5.995 MPa
Steam Flowrate	700.7 kg/s
Feedwater Temperature	223.1°C
Primary Inlet Temperature	311.4°C
Primary Outlet Temperature	285.3°C
Primary Flowrate/Steam Generator	9036 kg/s
Fouling Factor	$5.199 \cdot 10^{-6} \frac{\text{m}^2}{\text{W}} - \text{°K}$
Separator Loss Coefficient	100.00

\* Measured from tube sheet.

### Turbine Trip Test

The initial conditions for the turbine trip test are given in Table H.2-2. The transient inputs used to simulate the turbine trip test are shown in Fig. H.2-5. Neither the steam nor feed flowrate are given in Refs. (B4) and (W1). The steam flowrate is determined using a main steam system model. The feedwater flowrate is ramped down to 5 per cent of its full power value in 10 seconds.

The calculated results are shown in Fig. H.2-6. As can be seen, the calculated pressure and cold leg temperature are in good agreement with the measured data. The calculated level follows the same trend as the measured level but with a larger magnitude. This is most likely due to error in the input feedwater flowrate.

### Loss of Primary Flow at 40 Per Cent Power Test

This test was initiated by tripping the main primary coolant pumps 2 seconds into the test. The resulting primary flow coastdown was modeled using the equations presented in 6.4.5, with the parameter  $b$  appearing in Eq. 6.4-5 equal to 0.1154. The primary flowrate obtained in this manner is shown in Fig. H.2-7.

The initial conditions for this test are given in Table H.2-3, while the transient input is shown in Fig. H.2-8. The steam generator response is shown in Fig. H.2-9. As can be seen, the calculated level follows the same trend as the measured level, with some slight differences in magnitude.

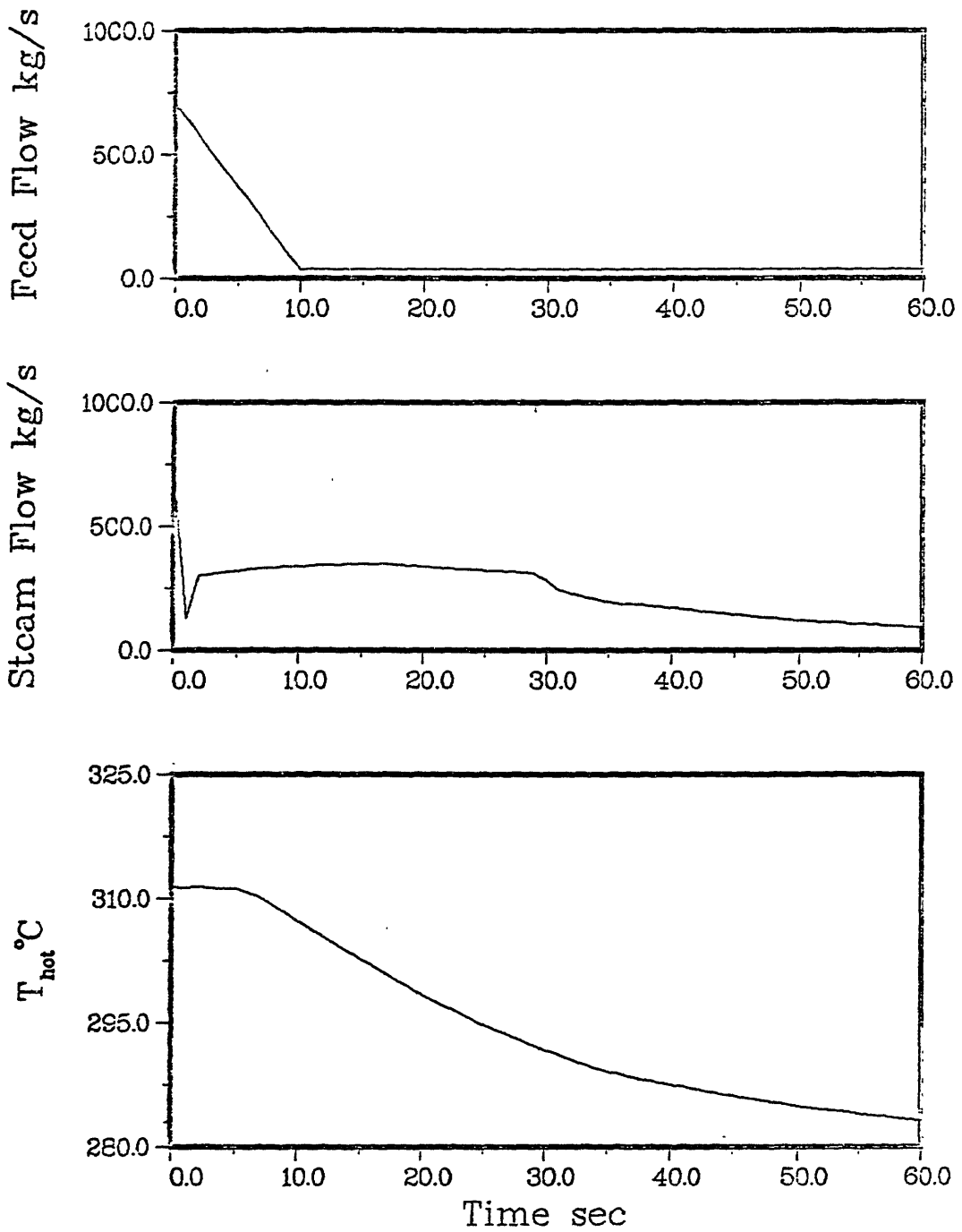


Figure H.2-5. Input for the turbine trip test.



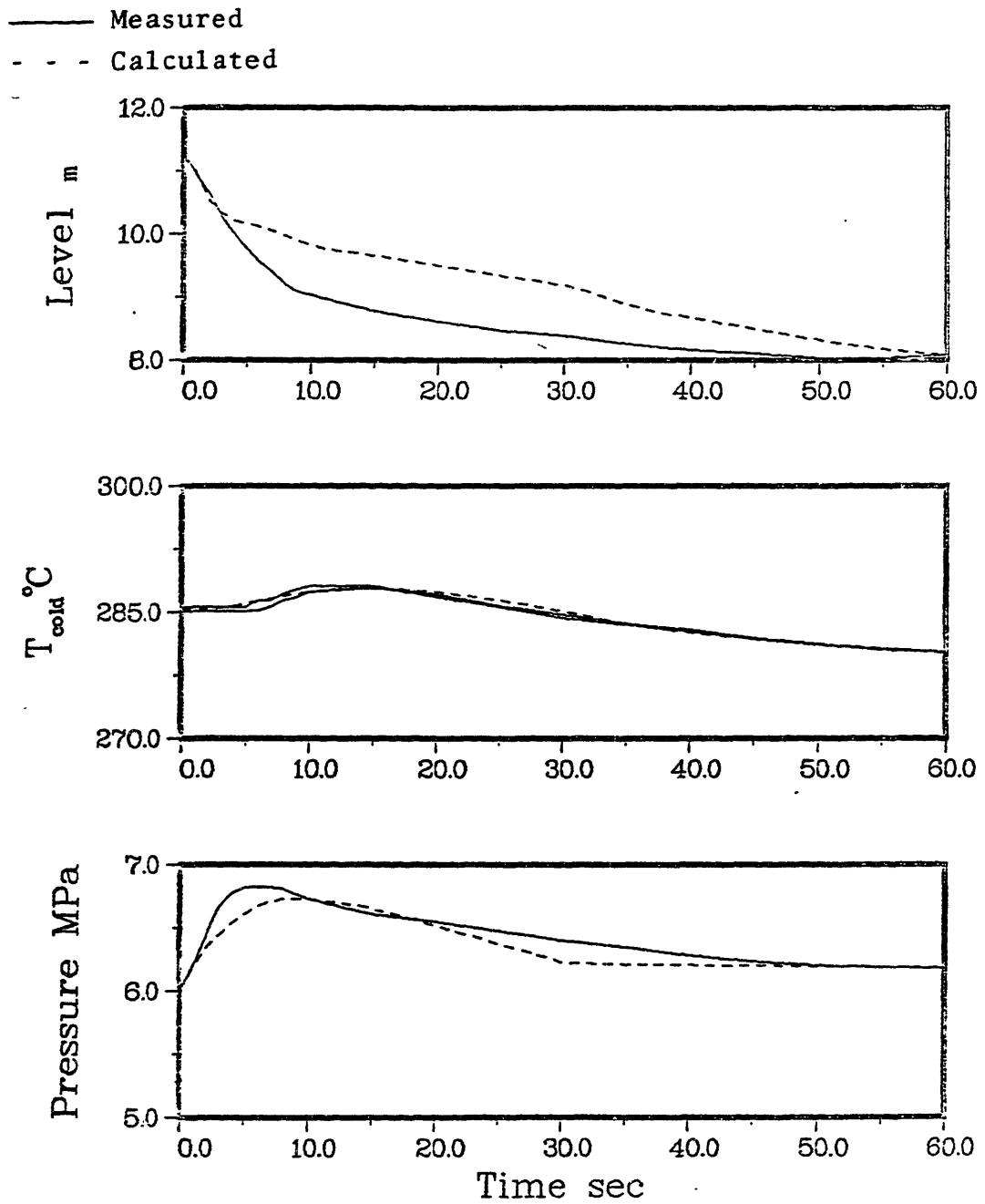


Figure H.2-6. Steam generator response for turbine trip test.

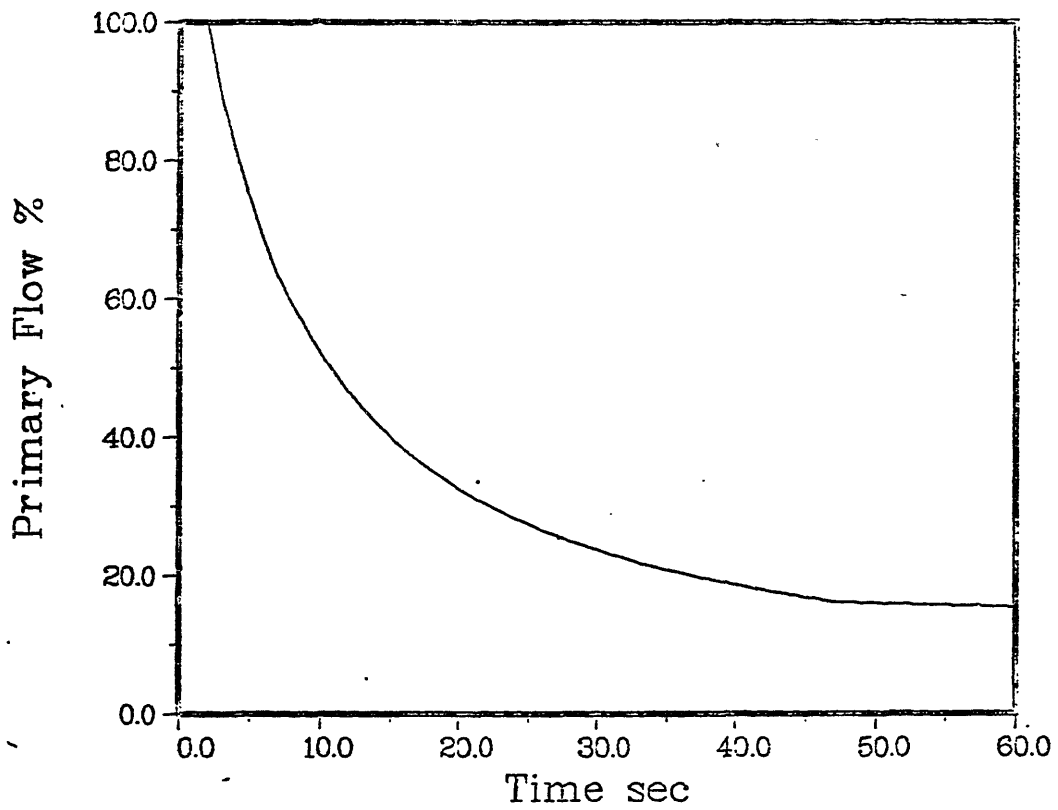


Figure H.2-7. Primary flowrate during loss of primary flow test.

Table H.2-3  
Initial Conditions for Loss of Primary Flow  
at 40 per cent Power.

Quantity	Value
Power/Steam Generator	512 MWt
Water Level*	10.67 m
Downcomer Flowrate	3294 kg/s
Steam Pressure	5.872 MPa
Steam Flowrate	280.1 kg/s
Feedwater Temperature	223.1°C
Primary Inlet Temperature	290.5°C
Primary Outlet Temperature	279.4°C
Primary Flowrate	8922 kg/s
Fouling Factor	$1.518 \cdot 10^{-5} \frac{\text{m}^2 \cdot \text{K}}{\text{W}}$

\* Measured from tube sheet.

The level error is probably due to the fact that we do not know the actual feedwater flowrate for the test and we are using best estimates for the transient feedwater flowrate. The trend of the calculated steam pressure is in fairly good agreement with the trend of the measured steam pressure, although there are differences in magnitude. This is probably due to error in the transient steam flowrate used, since we do not know the actual steam flowrate, but use instead, a

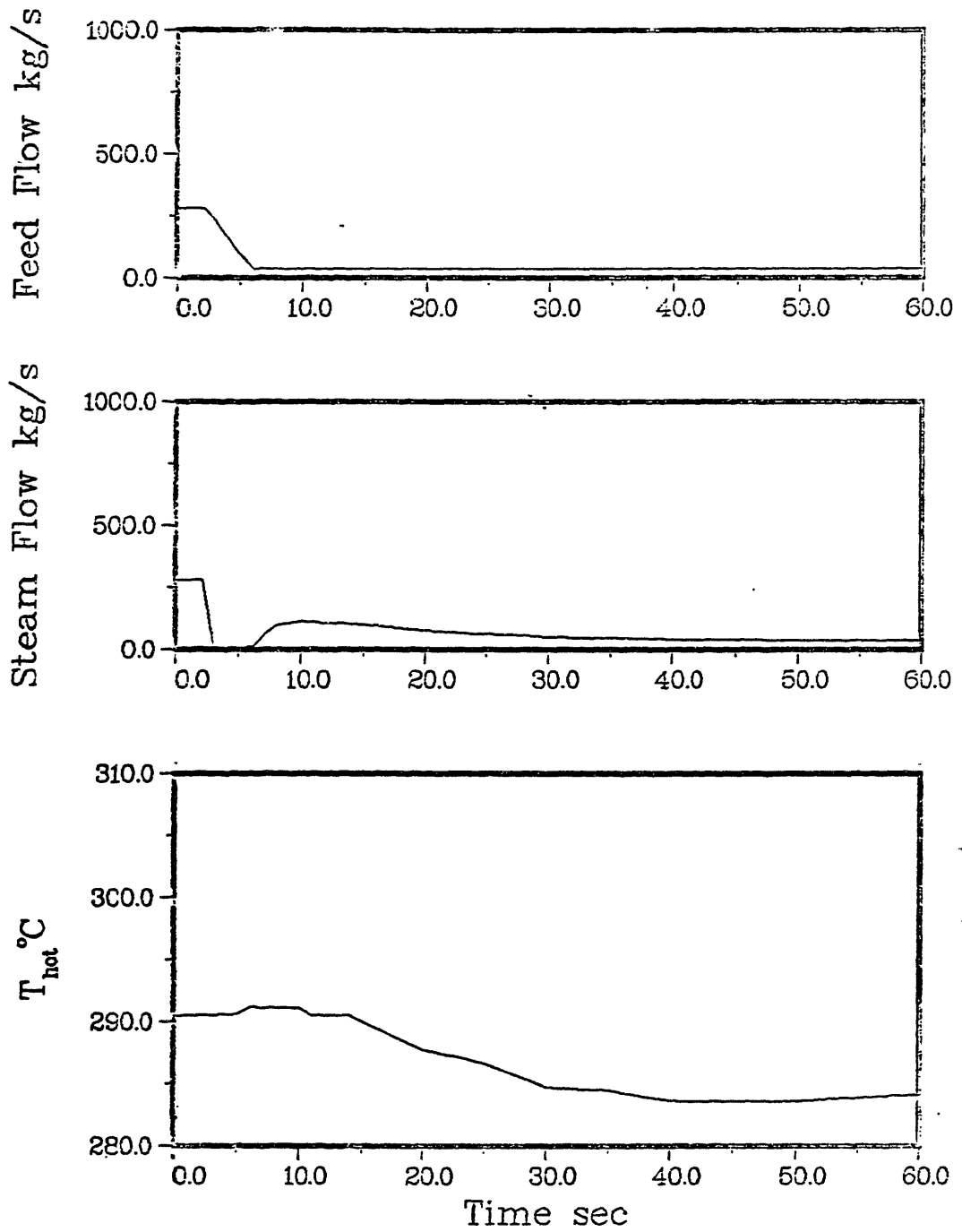


Figure H.2-8. Input for loss of primary flow at 40% power.

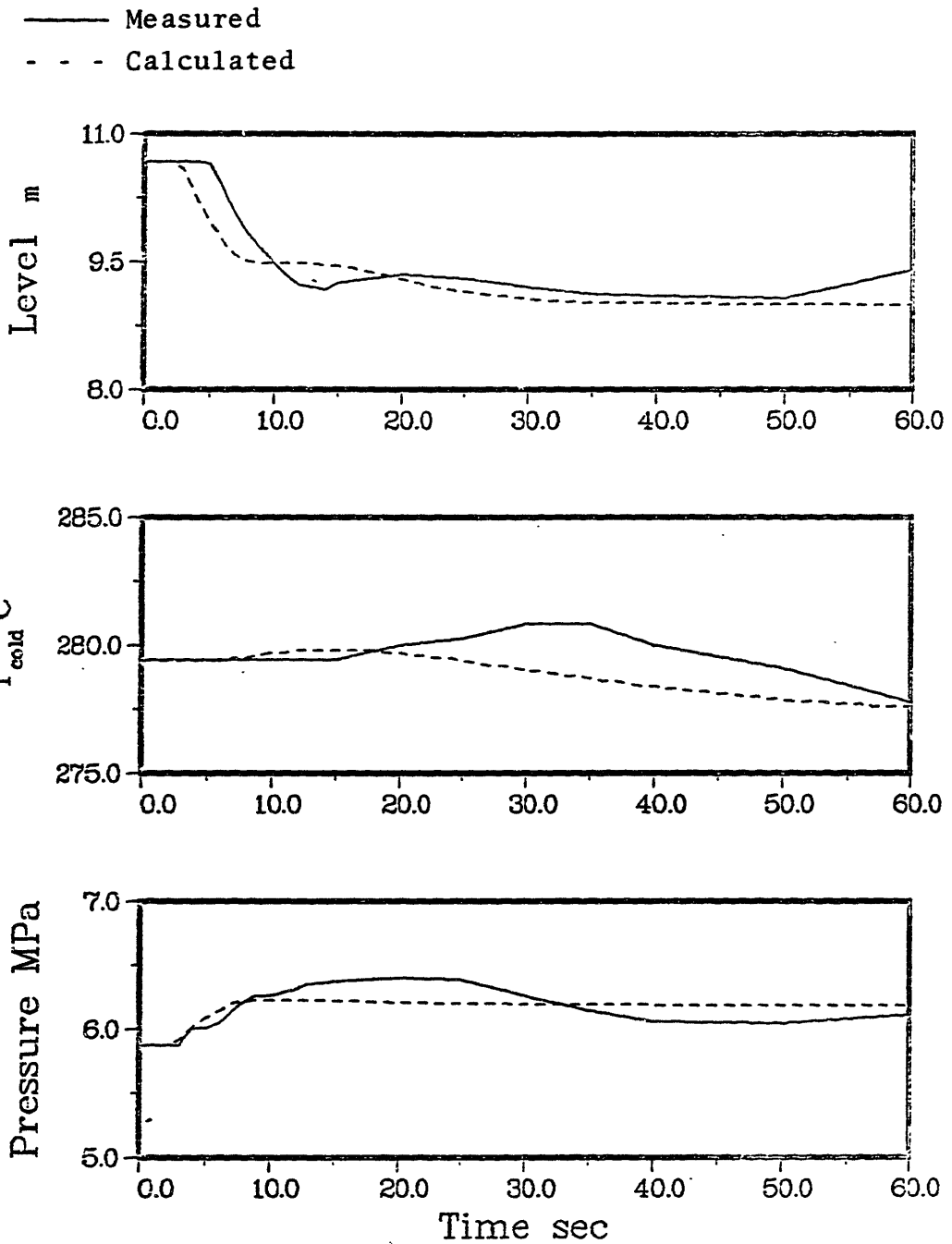


Figure H.2-9. Steam generator response for loss of primary flow at 40% power.

main steam system model. The agreement between the measured cold leg temperature and the calculated cold leg temperature is not good.

### H.3 GEOMETRICAL INPUT FOR ALL TEST CASES AND COMMENTS

#### REGARDING SPECIAL FEATURES IN SOME TEST CASES

The geometric input appearing in the BLOCK DATA routine of the computer program (Appendix J) for each test case is given in Table H.3-1. The variables are identified by their FORTRAN variable names, as used in the program, and each FORTRAN name is clearly defined in the main routine of the program (see Appendix J for variable nomenclature).

The blank spaces appearing under the Argonne National Laboratory (ANL) column of Table H.3-1 are geometric input parameters that do not apply to the ANL test loop. In particular, the primary side model and the heat transfer model were not used since there was not a primary side associated with the ANL test loop. The transient heat transfer rate, which is used only to initiate the stability test (see Chapter 6), is directly input to the code. The water level is determined by dividing the volume of water in the steam dome by the steam dome area. Some comments regarding the special geometry of the RD12 steam generator are made in 6.3.

Table H.3-1  
Input Geometry for Test Cases.

Quantity	Maine Yankee	Calvert Cliffs	ANO-2	RD-12	Argonne National Laboratory
ARO	14.3013	23.86	24.0808	3.36 · 10 <sup>-2</sup>	4.451 · 10 <sup>-4</sup>
ARI	8.2051	13.354	11.4393	5.54 · 10 <sup>-2</sup>	4.451 · 10 <sup>-4</sup>
LR	2.13	2.1082	2.5146	0.4699	1.0573
DHTB	0.0256	0.0252	0.0266	0.0325	0.0238
ATB	4.4084	6.431	6.6698	0.0278	4.45 · 10 <sup>-4</sup>
LTB	8.600	9.1742	8.5296	2.29	0.9144
LP	6.19	6.1976	6.7262	2.032	0.9144
VR	23.6750	36.34	43.6846	0.0213	4.706 · 10 <sup>-4</sup>
VTB	37.9126	63.432	56.8907	0.0637	4.07 · 10 <sup>-4</sup>
KC	0.1217	0.0676	0.0648	326.2	—
Beta(2)	0.9544	0.7133	0.6394	41.1871	1.027 · 10 <sup>-3</sup>
Beta(3)	0.2654	0.1904	0.1887	6.5695	1.188 · 10 <sup>-3</sup>
Beta(4)	0.0745	0.0442	0.0522	6.9926	0.6
KD	0.51	0.51	0.51	39.0	—
AHT	5429.2	8423.9	8841.2	8.1702	—
VOP	4.79	6.6261	6.6261	2.35 · 10 <sup>-2</sup>	—
VTBP	19.633	30.5058	31.998	1.8116 · 10 <sup>-2</sup>	—
RO	9.525 · 10 <sup>-5</sup>	9.525 · 10 <sup>-3</sup>	9.525 · 10 <sup>-3</sup>	6.447 · 10 <sup>-3</sup>	—

Table H.3-1 (Cont.)  
Input Geometry for Test Cases.

Quantity	Maine Yankee	Calvert Cliffs	ANO-2	RD-12	Argonne National Laboratory
RI	$8.3058 \cdot 10^{-3}$	$8.3058 \cdot 10^{-3}$	$8.3058 \cdot 10^3$	$5.3594 \cdot 10^{-3}$	—
APT	1.236	1.8463	1.8229	$3.79 \cdot 10^{-3}$	—
VTM	6.0849	9.6131	10.0851	$3.337 \cdot 10^{-2}$	—
VSTM	57.0	57.0	57.0	0.0	0.0
LD	6.2	6.9834	6.7262	2.4352	1.4732
ZL1	1.37	1.0682	0.997	1.3564	—
ZLF	0.96	0.6953	0.7049	0.100	—
ZL2	3.09	2.6129	2.5083	0.3207	—
ZL3	1.44	1.8002	1.8034	1.8002	—
R1	2.3	2.9226	2.9385	0.1461	—
R2	2.135	2.7682	2.7686	0.1058	—
R3	1.615	1.9082	1.9082	0.135	—
R4	1.695	1.9844	1.986	—	—



## APPENDIX I

### PROGRAM INPUT - OUTPUT

The purpose of this appendix is to describe the input required to run the program and the output generated by the program.

#### I.1 INPUT

The following is a description of the input needed to run the program. The input is described card by card; for each card we give the FORTRAN variable name along with the input format.

- Card 1     TITLE (20A4)  
           Short title (80 characters) identifying the run.
- Card 2     NSTG (I1)  
           Number of steam generators
- Card 3     POWER, TFW, KSEP, WPIN, PPRIM (5E12.3)  
           POWER: Full reactor power (Watts)  
           TFW: Full power feed temperature in (°K)  
           KSEP: Separator loss coefficient (-)  
           WPIN: Full Power Primary Flowrate (kg/s)  
           PPRIM: Full power primary pressure (Pa)
- Card 4     T1, T2 (2E12.3)  
           Parameters giving the primary average temperature  
           as a function of per cent power (°K) i.e.

TAVG = T1 + T2 \* (% Power)

Card 5 PSAT (E12.3)  
Full Power steam pressure (Pa)

Card 6 NTRAN (I1)  
Flag for transient calculation  
NTRAN = 0 Only steady state calculation  
NTRAN = 1 Transient calculation as well as  
steady state calculation.

Card 7 LW (E12.3)  
Steady state water level as measured from  
tubesheet (m)

Card 8 PERP, TFW (2E12.3)  
PERP: Per cent power at initial conditions  
TFW: Feedwater temperature corresponding to PERP  
per cent power (°K)

Card 9 PPRIM, WPIN (2E12.3)  
PPRIM: Pressure corresponding to PERP per cent  
power (Pa)  
WPIN: Primary flowrate corresponding to PERP per  
cent power (Pa)

Card 10 POWER, TAVG (2E12.3)  
This card is only included if PERP is greater than  
1.0  
POWER: Reactor power if PERP greater than 1.0  
(Watts)

TAVG: Primary average temperature corresponding to POWER ( $^{\circ}$ K).

The following cards are only included if NTRAN = 1.

Card 11 NPT, TDT (I2, E12.3)

NPT: Number of time zones.

TDT: Integration time step size (s)

Card 12 NPRIN, MSM, MB, MSV (4I2)

NPRIN: Print every NPRIN time step

MSM: Steam dump flag

MSM = 0 No steam dump

MSM = 1 Steam dump

MB: Turbine bypass flag

MB = 0 No bypass

MB = 1 Bypass

MSV: Secondary safety valve flag

MSV = 0 No secondary safety valves

MSV = 1 Secondary safety valves

Card 13 TMST, TSV, TISO (3E12.3)

TMST: Closing time of turbine stop valve (s)

TSV: Closing (or opening time) of safety valves - not used, but provided if modification is made to code (s)

TISO: Closing time of main steam isolation valve - not used, but provided if modification is made to code (s)

Card 14 TTRIP (E12.3)

Time at which turbine trip occur (s)

Card 15 ISV(4) (4I2)

Flag for secondary safety valves.

ISV(I) = 0 I'th bank of safety valves do not  
operate

ISV(I) = 1 I'th bank of safety valve operate

Up to four banks of valves can be specified.

Card 16 TAUH, TAUC (2E12.3)

TAUH: Hot leg temperature sensor time constant  
(s)

TAUC: Cold leg temperature sensor time constant  
(s)

Card 18 TIM, TPI, TTFW, TWS, TWFW, PVAL (6E12.3)

Card 19 WPI, PPRI, IFW, ISTM (2E12.3, 2I2)

Cards 18 and 19 must be provided for each time zone (NPT times). These cards provide the transient boundary conditions in tabular form. Boundary conditions between successive values of TIM are determined by linear interpolation.

TIM: Time at end of time zone (s)

TPI: Primary inlet temperature at end of time zone (°K)

TTFW: Feedwater temperature at end of time zone (°K)

TWS: Steam flow at end of time zone (kg/s)

TWFW: Feed flow at end of time zone (kg/s)

PVAL: Main steam control valve position, expressed in equivalent position at PVAL per cent power, at end of time zone.

WPI: Primary flowrate at end of time zone (kg/s)

PPRIM: Primary pressure at end of time zone (Pa)

IFW: Flag for feedwater controller model

IFW = 0 No controller model

IFW = 1 Controller model

ISTM: Flag for main steam system model

ISTM = 0 No main steam model

ISTM = 1 Main steam model

- Notes:
- If IFW = 1, then the user must supply a controller model in subroutine CONTRO, and the code ignores the input for TFW
  - If ISTM = 1, then the user must supply a main steam system model in subroutine CHOKE, and the code ignores the input for TWS
  - If ISTM = 0, then the inputs MSM, MB, MSV on Card 12 are ignored, as are the inputs on Cards 13, 14, and 15. The transient steam flow must be specified (TWS). Also PVAL is ignored on Card 18.
  - If IFW = 0, then the transient feed flow must be specified (TFW).

**SAMPLE INPUT FILE WITHOUT FEEDWATER CONTROLLER  
AND MAIN STEAM SYSTEM MODEL**

TURBINE TRIP AND SGI 3 SEC TFW RAMP START AT 7 SEC,SENSOR MODEL

1

1.382E 09 5.194E 02 1.000E 02 7.908E 03 1.546E 07  
 5.579E 02 2.022E 01  
 6.239E 06

1

1.052E 01  
 1.000E 00 5.194E 02  
 1.546E 07 7.908E 03

27 2.500E-01

4 1 1 1

3.000E 00 1.000E 00 1.000E 00  
 0.000E 00

1 1 1 1

4.753E 00 4.898E 00  
 1.000E 00 5.937E 02 5.194E 02 5.801E 02 6.179E 02 1.000E 00  
 7.908E 03 1.557E 07 0 0  
 1.500E 00 5.937E 02 5.194E 02 4.389E 02 3.279E 02 1.000E 00  
 7.908E 03 1.562E 07 0 0  
 2.000E 00 5.937E 02 5.194E 02 2.838E 02 4.099E 02 1.000E 00  
 7.908E 03 1.568E 07 0 0  
 2.500E 00 5.937E 02 5.194E 02 6.243E 02 4.288E 02 1.000E 00  
 7.908E 03 1.573E 07 0 0  
 3.000E 00 5.937E 02 5.194E 02 5.044E 02 4.477E 02 1.000E 00  
 7.908E 03 1.578E 07 0 0  
 5.000E 00 5.937E 02 5.194E 02 4.918E 02 6.179E 02 1.000E 00  
 7.908E 03 1.600E 07 0 0  
 6.000E 00 5.937E 02 5.194E 02 4.918E 02 5.990E 02 1.000E 00  
 7.908E 03 1.611E 07 0 0  
 7.000E 00 5.937E 02 5.194E 02 4.855E 02 5.675E 02 1.000E 00  
 7.908E 03 1.622E 07 0 0  
 8.000E 00 5.937E 02 4.453E 02 4.792E 02 5.360E 02 1.000E 00  
 7.908E 03 1.632E 07 0 0  
 9.000E 00 5.943E 02 3.712E 02 4.767E 02 4.918E 02 1.000E 00  
 7.908E 03 1.602E 07 0 0  
 1.000E 01 5.943E 02 2.970E 02 4.691E 02 4.981E 02 1.000E 00  
 7.908E 03 1.572E 07 0 0  
 1.100E 01 5.932E 02 2.970E 02 4.641E 02 4.754E 02 1.000E 00  
 7.908E 03 1.542E 07 0 0  
 1.200E 01 5.926E 02 2.970E 02 4.414E 02 3.540E 02 1.000E 00  
 7.908E 03 1.512E 07 0 0  
 1.500E 01 5.887E 02 2.970E 02 4.162E 02 2.909E 02 1.000E 00  
 7.908E 03 1.495E 07 0 0  
 1.800E 01 5.845E 02 2.970E 02 3.998E 02 1.611E 02 1.000E 00  
 7.908E 03 1.477E 07 0 0  
 2.200E 01 5.793E 02 2.970E 02 3.884E 02 1.778E 02 1.000E 00  
 7.908E 03 1.439E 07 0 0  
 2.400E 01 5.765E 02 2.970E 02 3.279E 02 1.576E 02 1.000E 00  
 7.908E 03 1.400E 07 0 0  
 2.700E 01 5.737E 02 2.970E 02 2.510E 02 1.513E 02 1.000E 00  
 7.908E 03 1.375E 07 0 0  
 3.000E 01 5.712E 02 2.970E 02 2.119E 02 1.387E 02 1.000E 00  
 7.908E 03 1.349E 07 0 0  
 3.600E 01 5.673E 02 2.970E 02 1.539E 02 1.387E 02 1.000E 00

7.908E 03	1.326E 07 0 0					
3.900E 01	5.659E 02	2.970E 02	1.438E 02	1.400E 02	1.000E 00	
7.908E 03	1.315E 07 0 0					
4.500E 01	5.637E 02	2.970E 02	1.211E 02	1.450E 02	1.000E 00	
7.908E 03	1.292E 07 0 0					
5.200E 01	5.626E 02	2.970E 02	1.135E 02	1.450E 02	1.000E 00	
7.908E 03	1.282E 07 0 0					
5.400E 01	5.618E 02	2.970E 02	1.135E 02	8.954E 01	1.000E 00	
7.908E 03	1.279E 07 0 0					
5.500E 01	5.615E 02	2.970E 02	1.122E 02	7.819E 01	1.000E 00	
7.908E 03	1.278E 07 0 0					
5.600E 01	5.612E 02	2.970E 02	1.072E 02	7.441E 01	1.000E 00	
7.908E 03	1.277E 07 0 0					
6.000E 01	5.612E 02	2.970E 02	1.072E 02	7.819E 01	1.000E 00	
7.908E 03	1.271E 07 0 0					



I.2 SAMPLE OUTPUT

TURBINE TRIP AND 981 3 SEC TPN RAMP START AT 7 SEC.SENSOR MODEL 88000100

TOTAL REACTOR POWER IS 0.1342E+04 MW  
NUMBER OF STEAM GENERATORS 1  
STEADY STATE WATER LEVEL IS 0.1052E+02 METERS  
STEADY STATE POWER LEVEL IS 0.1342E+04 MW PER  
STEAM GENERATOR OR 0.1000E+03 PER CENT RATED FULL POWER

STEADY STATE CONDITIONS

DOMICOMER FLOWRATE IS 0.3522E+04 KG/SEC  
STEAM TEMPERATURE IS 0.2702E+03 C  
STEAM PRESSURE IS 0.6239E+01 MPa  
STEAM FLOW IS 0.0052E+03 KG/SEC  
RISER QUALITY IS 0.2252E+00  
STEAM GENERATOR MASS CONTENT IS 0.7941E+03 KG  
FEEDWATER TEMPERATURE IS 0.2542E+03 C  
PRIMARY INLET TEMPERATURE IS 0.3202E+03 C  
PRIMARY OUTLET TEMPERATURE IS 0.2894E+03 C  
PRIMARY FLOWRATE IS 0.7902E+04 KG/SEC  
FOULING FACTOR IS 0.2212E+04 MW2-K/MHT  
STEADY STATE CPU TIME CENTISECONDS 0





0.5409E+02 0.7040E+01 0.6348E+07 0.2318E+09 0.1138E+03 0.8053E+02 0.7908E+04 0.2108E+02 0.3308E+02 0.1182E+04 0.4708E+03 0.1182E+04  
 0.5290E+02 0.7067E+01 0.6322E+07 0.2247E+09 0.1122E+03 0.2651E+03 0.7908E+04 0.7908E+04 0.2793E+03 0.2793E+03 0.1182E+04 0.4708E+03 0.1182E+04  
 0.5409E+02 0.7764E+01 0.6318E+07 0.2318E+09 0.1078E+03 0.2648E+03 0.7908E+04 0.7908E+04 0.2793E+03 0.2793E+03 0.1182E+04 0.4708E+03 0.1182E+04  
 0.5790E+02 0.7742E+01 0.6308E+07 0.2308E+09 0.1078E+03 0.2648E+03 0.7908E+04 0.7908E+04 0.2793E+03 0.2793E+03 0.1182E+04 0.4708E+03 0.1182E+04  
 0.5808E+02 0.7749E+01 0.6298E+07 0.2298E+09 0.1078E+03 0.2648E+03 0.7908E+04 0.7908E+04 0.2793E+03 0.2793E+03 0.1182E+04 0.4708E+03 0.1182E+04  
 0.5900E+02 0.7772E+01 0.6290E+07 0.2290E+09 0.1078E+03 0.2648E+03 0.7908E+04 0.7908E+04 0.2793E+03 0.2793E+03 0.1182E+04 0.4708E+03 0.1182E+04  
 0.6000E+02 0.7808E+01 0.6280E+07 0.2280E+09 0.1078E+03 0.2648E+03 0.7908E+04 0.7908E+04 0.2793E+03 0.2793E+03 0.1182E+04 0.4708E+03 0.1182E+04  
 0.6000E+03 0.8000E+03 0.6000E+03 0.6000E+03 0.6000E+03 0.6000E+03 0.6000E+03 0.6000E+03 0.6000E+03 0.6000E+03 0.6000E+03 0.6000E+03 0.6000E+03

TRANSPARENT CPU TIME CENTIRECORDS 54  
 END OF PROBLEM

**Appendix J**

**CODE LISTING**

```

CCCCCCCCCCCCCCCCCCCCCCCCCCCCCCCCCCCCCCCCCCCCCCCCCCCCCCCCCCCCCCCC
C   THIS IS THE DRIVING ROUTINE                                     C
C                                                                 C
C   THESIS REFERENCE IS 'DYNAMIC MODELING OF VERTICAL U-TUBE STEAM C
C   GENERATORS FOR OPERATIONAL SAFETY SYSTEMS' BY WALTER          C
C   STROHMAYER, PHD THESIS MIT 1982.                               C
C                                                                 C
C   WE WILL DEFINE VARIABLES BY COMMON BLOCK. ALL UNITS ARE SI.   C
C   TEMPERATURES ARE IN DEGREES KELVIN                            C
C   PRESSURES ARE IN PASCALS                                       C
C   LENGTHS ARE IN METERS                                          C
C   TIME IS IN SECONDS                                             C
C   ENERGY IS IN JOULES                                           C
C   POWER IS IN WATTS                                              C
C   MASS IS IN KILOGRAMS                                           C
C   ALL OTHER UNITS ARE CONSISTENT WITH THE ABOVE                 C
C                                                                 C
C   /GEOM/                                                         C
C                                                                 C
C   KSEP   SEPARATOR LOSS COEFFICIENT                              C
C   LR     RISER LENGTH                                             C
C   LTB    TUBE BUNDLE LENGTH                                       C
C   LP     LENGTH OF PARALLEL FLOW REGION IN TUBE BUNDLE          C
C   KC     CROSS FLOW LOSS COEFFICIENT                              C
C   ARI    FLOW AREA AT RISER INLET                               C
C   ARO    FLOW AREA AT RISER OUTLET                                C
C   ATB    FLOW AREA IN PARALLE FLOW PORTION OF TUBE BUNDLE       C
C   G      ACCELERATION OF GRAVITY                                  C
C   VR     VOLUME OF RISER                                           C
C   VTB    VOLUME OF TUBE BUNDLE                                     C
C   DHTB   HYDRAULIC DIAMETER IN PARALLEL FLOW PORTION OF        C
C           TUBE BUNDLE                                             C
C   BETA(4) GEOMETRIC PARAMETERS APPEARING IN MOMENTUM            C
C           EQUATION. SEE CHAPTER THREE OF THESIS.                 C
C   NSTG   NUMBER OF STEAM GENERATORS ASSOCIATED WITH POWER      C
C           PLANT BEING MODELED                                     C
C   CO     DRIFT FLUX PARAMETER                                       C
C   AHT    HEAT TRANSFER AREA IN THE TUBE BUNDLE                   C
C   RO     OUTER RADIUS OF TUBE                                       C
C   RI     INNER RADIUS OF TUBE                                       C
C   VOP    VOLUME OF PRIMARY PLENA(ASSUMED TO BE SAME FOR         C
C           BOTH INLET AND OUTLET PLENA)                            C
C   VTBP   VOLUME CONTAINED BY TUBES ON PRIMARY SIDE              C
C   APT    TOTAL FLOW AREA OF TUBES ON PRIMARY SIDE               C
C   VTM    TOTAL VOLUME OF TUBE METAL                                C
C                                                                 C
C   /DOME/                                                         C
C                                                                 C
C   VSUB   SUBCOOLED LIQUID VOLUME IN STEAM DOME-DOWNCOMER(SDD)  C
C   VTOT   TOTAL VOLUME OF SDD                                       C
C   VG     VAPOR VOLUME IN SDD                                       C
C   VFO    FIXED VOLUME OF SATURATED LIQUID USED IN MOVING        C
C           INTERFACE CASE FOR THE SDD                               C
C   LSAT   VERTICAL HEIGHT OF SATURATED REGION IN SDD              C

```

C	LSUB	VERTICAL HEIGHT OF SUBCOOLED REGION IN SDD	C
C	VREF	VAPOR VOLUME AT WHICH WE SWITCH FROM A FIXED	C
C		VOLUME SDD TO A MOVING INTERFACE SDD, IF VG	C
C		GREATER THAN VREF.	C
C	LW	WATER LEVEL	C
C	LD	LENGTH OF LOWEST REGION OF SDD. THIS IS EQUAL TO	C
C		L4 IN APPENDIX K OF THESIS; SEE ALSO CHAPTER THREE.	C
C	AD	FLOW AREA OF LOWER DOWNCOMER	C
C	VD	VOLUME OF LOWER DOWNCOMER	C
C	VSD	VOLUME OF STEAM DOME-THAT IS, VOLUME ABOVE FEED RING	C
C	DHD	HYDRAULIC DIAMETER OF LOWER DOWNCOMER	C
C	VT	VOLUME FROM BOTTOM OF SDD TO FEED RING	C
C	LT	VERTICAL HEIGHT CORRESPONDING TO VT	C
C	VSTM	VOLUME OF MAIN STEAM LINE	C
C	DVG	TIME DERIVATIVE OF VAPOR VOLUME IN SDD OBTAINED	C
C		FROM FINITE DIFFERENCING VOLUME CALCULATED USING	C
C		TOTAL STEAM GENERATOR MASS BALANCE	C
C	ASW	FLOW AREA AT VAPOR-LIQUID INTERFACE IN SDD	C
C		FOR FOLLOWING GEOMETRIC PARAMETERS SEE APPENDIX K OF THESIS	C
C	R1	SPHERICAL RADIUS OF STEAM DOME OR INNER RADIUS OF	C
C		STEAM GENERATOR UPPER SHELL	C
C	R2	OUTER RADIUS AT TOP OF RISER SHROUD	C
C	R3	OUTER RADIUS OF TUBE BUNDLE SHROUD	C
C	R4	INNER RADIUS OF STEAM GENERATOR LOWER SHELL	C
C	ZL1	VERTICAL LENGTH FROM SEPARATOR DECK TO BOTTOM OF	C
C		STEAM DOME HEMISPHERE	C
C	ZL2	VERTICAL LENGTH FROM TUBE BUNDLE SHROUD TO TOP OF	C
C		RISER SHROUD	C
C	ZL3	VERTICAL LENGTH OF TRANSITION FROM LOWER SHELL	C
C		RADIUS TO UPPER SHELL RADIUS	C
C	ZLF	VERTICAL LENGTH OF FEED RING ABOVE TUBE BUNDLE SHROUD	C
C			C
C	/STEAM/		C
C			C
C	PSAT	SECONDARY PRESSURE	C
C	TFW(1/2)	FEEDWATER TEMPERATURE(OLD/NEW TIME)	C
C	TSAT	SATURATION TEMPERATURE ON SECONDARY SIDE	C
C	DTSAT	DERIVATIVE OF TSAT WRT PSAT	C
C	HL(1)	ENTHALPY OF SUBCOOLED FLUID IN SDD	C
C	HL(2)	ENTHALPY OF SATURATED LIQUID	C
C	HFW(1/2)	ENTHALPY OF FEEDWATER(OLD/NEW TIME)	C
C	VGJ	DRIFT FLUX PARAMETER-DRIFT VELOCITY	C
C	MU(1/2)	VISCOSITY(SUBCOOLED/SATURATED FLUID)	C
C	HG	SATURATED VAPOR ENTHALPY	C
C	UL	INTERNAL ENERGY OF SUBCOOLED FLUID IN SDD	C
C	RL	SUBCOOLED LIQUID DENSITY	C
C	DRLU	DERIVATIVE OF RL WRT UL	C
C	DRLP	DERIVATIVE OF RL WRT PSAT	C
C	RHOG	SATURATED VAPOR DENSITY	C
C	DRHOG	DERIVATIVE OF RHOG WRT PSAT	C
C	RHOF	SATURATED LIQUID DENSITY	C
C	DRHOF	DERIVATIVE OF RHOF WRT PSAT	C
C	UG	SATURATED VAPOR INTERNAL ENERGY	C
C	DUG	DERIVATIVE OF UG WRT PSAT	C



C	UF	SATURATED LIQUID INTERNAL ENERGY	C
C	DUF	DERIVATIVE OF UF WRT PSAT	C
C	QB	POWER OR HEAT TRANSFER RATE	C
C	POWER	FULL POWER HEAT TRANSFER RATE	C
C	PERP	PER CENT FULL POWER	C
C	HFG	HEAT OF VAPORIZATION	C
C	RFW(1/2)	FEEDWATER DENSITY(OLD/NEW TIME)	C
C			C
C	/FLOWS/		C
C			C
C	WO	DOWNCOMER FLOWRATE	C
C	WS(1/2)	STEAM FLOWRATE(OLD/NEW TIME)	C
C	WFW(1/2)	FEEDWATER FLOWRATE(OLD/NEW TIME)	C
C	WF	FLOWRATE OF SATURATED LIQUID FROM SATURATED REGION	C
C		OF SDD TO SUBCOOLED REGION OF SDD	C
C	WF	FLOWRATE AT PARALLEL TO CROSS FLOW TRANSITION IN	C
C		TUBE BUNDLE REGION	C
C	WR	FLOWRATE AT RISER INLET	C
C	WN	FLOWRATE AT RISER OUTLET	C
C	DINERT	INERTANCE OF RECIRCULATION LOOP	C
C			C
C	/TRANS/		C
C			C
C	VOID(1/2/3)	VAPOR VOLUME FRACTION AT:	C
C		1 TUBE BUNDLE OUTLET	C
C		2 RISER OUTLET	C
C		3 PARALLEL TO CROSS FLOW TRANSITION IN TUBE BUNDLE	C
C	XQ(1/2/3)	FLOW QUALITY AT:	C
C		1 TUBE BUNDLE OUTLET	C
C		2 RISER OUTLET	C
C		3 PARALLEL TO CROSS FLOW TRANSITION IN TUBE BUNDLE	C
C	RB(1/2)	VOLUME WEIGHTED DENSITY(INLET/OUTLET OF RISER)	C
C	DRP(1/2)	DERIVATIVE OF(RB(1)WRT PSAT/RB(2)WRT PSAT)	C
C	DRA	DERIVATIVE OF RB(1/2) WRT VOID(1/2)	C
C	UB(1/2)	WEIGHTED INTERNAL ENERGY(INLET/OUTLET OF RISER)	C
C	DUP(1/2)	DERIVATIVE OF(UB(1)WRT PSAT/UB(2)WRT PSAT)	C
C	DUA(1/2)	DERIVATIVE OF(UB(1)WRT VOID(1)/UB(2)WRT VOID(2))	C
C	MFD(1/2)	NOT USED	C
C	MR(1/2)	MASS OF RISER REGION(OLD/NEW TIME)	C
C	MTB(1/2)	MASS OF TUBE BUNDLE REGION(OLD/NEW TIME)	C
C	MTBC(1/2)	MASS OF CROSS FLOW REGION(OLD/NEW TIME)	C
C	MSD	MASS OF STEAM DOME WIHT VOLUME VSD GIVEN ABOVE	C
C	MTOT(1/2)	TOTAL MASS OF STEAM GENERATOR(OLD/NEW TIME)	C
C	HR	ENTHALPY AT RISER INLET	C
C	HN	ENTHALPY AT RISER OUTLET	C
C	S(5)	RIGHT HAND SIDES OF STATE EQUATIONS	C
C	M(5)	MOMENTUM EQUATION PARAMETERS, SEE CHAPTER 3 OF THESIS	C
C	VP(1/2/3)	MOMENTUM DENSITY AT:	C
C		1 TUBE BUNDLE OUTLET	C
C		2 RISER OUTLET	C
C		3 PARALLEL TO CROSS FLOW TRANSITION IN TUBE BUNDLE	C
C	R(9,5)	DERIVATIVES RELATED TO MASS AND ENERGY EQUATIONS	C
C			C
C	/TIME/		C

C			C
C	T	SIMULATION TIME	C
C	DT	INTEGRATION TIME STEP SIZE	C
C	ITRAN	FLAG FOR STEADY STATE CALCULATION(=0) OR TRANSIENT	C
C		CALCULATION(=1)	C
C	WFWF	FULL POWER FEED FLOW	C
C	WSF	FULL POWER STEAM FLOW	C
C	ITC	FLAG USED IN HEAT TRANSFER CALCULATION	C
C	ICLK	FLAG FOR INITIAL FULL POWER CALCULATION	C
C		=0 DO FULL POWER CALCULATION AND GET FOULING FACTOR	C
C		=1 FULL POWER CALCULATION ALREADY DONE	C
C			C
C	/RESP/		C
C			C
C	VALK	TURBINE STOP AND CONTROL VALVE FLOW COEFFICIENT	C
C		FOR CHOKED FLOW CALCULATION	C
C	VALK0	VALK AT FULL POWER	C
C	IFW	FLAG FOR FEED CONTROLLER	C
C		=0 NO CONTROLLER-FEED FLOW INPUT	C
C		=1 CONTROLLER-NO FEED FLOW INPUT	C
C	ISTM	FLAG FOR MAIN STEAM SYSTEM MODEL	C
C		=0 NO MODEL-STEAM FLOW INPUT	C
C		=1 MODEL- NO STEAM FLOW INPUT	C
C	PVALV	TURBINE STOP AND CONTROL VALVE OPENING IN TERMS OF	C
C		OPENING AT PVALV PER CENT POWER	C
C	TTRIP	TIME WHEN TURBINE TRIP OCCURS	C
C	AK	FLOW COEFFICIENT FOR STEAM DUMP CHOKED FLOW	C
C	AKB	FLOW COEFFICIENT FOR BYPASS CHOKED FLOW	C
C	MB	FLAG FOR BYPASS SYSTEM OPERATION.	C
C		=0 NO BYPASS SYSTEM	C
C		=1 BYPASS SYSTEM	C
C	MSM	FLAG FOR STEAM DUMP SYSTEM	C
C		=0 NO STEAM DUMP	C
C		=1 STEAM DUMP	C
C	MSV	FLAG FOR SAFETY VALVES	C
C		=0 NO SAFETY VALVES	C
C		=1 SAFETY VALVES	C
C	TMST	CLOSING TIME OF TURBINE STOP AND CONTROL VALVE	C
C	TSV	TSV CLOSING TIME FOR SAFETY VALVES-NOT USED PROVIDED	C
C		FOR CONVENIENCE IF MODIFICATION IS MADE	C
C	TISO	CLOSING TIME OF ISOLATION VALVE-NOT USED PROVIDED	C
C		FOR CONVENIENCE IF ISOLATION VALVE IS TO BE MODELED	C
C	ISV(1/2/3/4)	FLAGS FOR INDIVIDUAL SAFETY VALVE BANKS. UP TO	C
C		FOUR BANKS CAN BE MODELED.	C
C		=0 THIS BANK INOPERATIVE	C
C		=1 THIS BANK OPERATIVE	C
C			C
C	/VALVES/		C
C			C
C	F	FRACTIONAL OPENING OF DUMP VALVES	C
C	FMST	FRACTIONAL OPENING OF TURBINE STOP AND CONTROL VALVE	C
C	FB	FRACTIONAL OPENING OF BYPASS VALVES	C
C	FS1	FRACTIONAL OPENING OF SAFETY VALVE BANK 1	C
C	FS2	FRACTIONAL OPENING OF SAFETY VALVE BANK 2	C

C	FS3	FRACTIONAL OPENING OF SAFETY VALVE BANK 3	C
C	FS4	FRACTIONAL OPENING OF SAFETY VALVE BANK 4	C
C			C
C	/PRIME/		C
C			C
C	PPRIM	PRIMARY PRESSURE	C
C	TLMTD	LOG-MEAN TEMPERATURE DIFFERENCE	C
C	UO	OVERALL HEAT TRANSFER COEFFICIENT	C
C	TP(1/2/3)	PRIMARY TEMPERATURES(INLET PLENUM OUTLET/ TUBES OUTLET/OUTLET PLENUM OUTLET)	C
C	HP(1/2/3)	PRIMARY FLUID ENTHALPY CORRESPONDING TO TP(1/2/3)	C
C	RP(1/2/3)	PRIMARY FLUID DENSITIES(INLET PLENUM/TUBES/ OUTLET PLENUM)	C
C	DRPT(1/2/3)	DERIVATIVE OF RP(I) WRT TP(I)	C
C	UP(1/2/3)	PRIMARY FLUID INTERNAL ENERGY(INLET PLENUM/ TUBES/OUTLET PLENUM)	C
C	DUPT(1/2/3)	DERIVATIVE OF UP(I) WRT TP(I)	C
C	TPIN(1/2)	PRIMARY INLET TEMPERATURE(OLD/NEW TIME)	C
C	HPIN(1/2)	PRIMARY INLET ENTHALPY(OLD/NEW TIME)	C
C	WPIN(1/2)	PRIMARY INLET FLOWRATE(OLD/NEW TIME)	C
C	MUP	VISCOSITY OF PRIMARY FLUID IN TUBES	C
C	TKL	THERMAL CONDUCTIVITY OF FLUID IN TUBES	C
C	CPL	HEAT CAPACITY OF FLUID IN TUBES	C
C	CPT	VOLUMETRIC HEAT CAPACITY OF TUBE METAL	C
C			C
C	/HTS/		C
C			C
C	HPR	PRIMARY HEAT TRANSFER COEFFICIENT	C
C	HS	SECONDARY HET TRANSFER COEFFICIENT	C
C	RTUBE	TUBE METAL HEAT TRANSFER RESISTANCE	C
C	RFOUL	FOULING FACTOR OR RESISTANCE	C
C			C
C	/DOWCO/		C
C			C
C	KD	PRESSURE DROP COEFFICIENT FOR SHOCK AND TURNING LOSSES AT BASE OF DOWNCOMER	C
C			C
C	/AVE/		C
C			C
C	WBAR	GEOMETRICALLY WEIGHTED AVERAGE RECIRCULATION FLOW	C
C			C
C	/FILTER/		C
C			C
C	TFOLD	OLD TIME VALUE OF PRIMARY OUTLET PLENUM EXIT TEMPERATURE (IN DEGREES C) FOR SENSOR DYNAMICS MODEL	C
C			C
C	TAUC	COLD LEG TEMPERATURE SENSOR RESPONSE TIME	C
C	CC		
	REAL LW,KSEP,LR,LD,LTB,LP,MU,KC,LF,M,MFD,MR,MTB,		
	INTBC,MSD,MTOT,LT,MUP,LSAT,LSUB,KD		
	DIMENSION TITLE(20)		
	COMMON /GEOM/ KSEP,LR,LTB,LP,KC,ARI,ATB,ARO,G,		
	1VR,VTB,DHTB,BETA(4),NSTG,CO,		
	2AHT,RO,RI,VOP,VTBP,APT,VTM		

```

COMMON /DOME/ VSUB,VTOT,VG,VFO,LSAT,LSUB,VREF,LW,
1LD,AD,VD,VSD,DHD,VT,LT,VSTM,DVG,ASN,R1,R2,R3,R4,
2ZL1,ZL2,ZL3,ZLF
COMMON /STEAM/ PSAT,TFW(2),TSAT,UL,HL(2),HFW(2),VGJ,MU(2),
1HG,RL,RHOG,RHOF,DUG,UG,DRHOG,DUF,UF,DRHOF,DRLP,DRLU,
2QB,POWER,PERP,HFG,RFW(2),DTSAT
COMMON /FLOWS/ WO,WS(2),WFW(2),WF,WP,WR,WN,DINERT
COMMON /TRANS/ VOID(3),XQ(3),RB(2),UB(2),DUP(2),DUA(2),DRP(2),
1DRA,MFD(2),MR(2),MTB(2),MTBC(2),HR,HN,MSD,
2MTOT(2),S(5),M(5),VP(3),R(9,5)
COMMON /TIME/ T,DT,ITRAN,WFWF,WSF, ITC,ICLK
COMMON /RESP/ VALK,IFW(31),PVALV,TTRIP,AK,AKB,VALKO,MB,MSH,
1MSV,THST,TSV,TISO,ISTM(31),ISV(4)
COMMON /VALVES/ F,FMST,FB,FS1,FS2,FS3,FS4
COMMON /PRIME/ PPRIM,TLMTD,UO,TP(3),HP(3),RP(3),UP(3),DRPT(3),
1DUPT(3),TPIN(2),HPIN(2),WPIN(2),MUP,CPL,TKL,CPT
COMMON /HTS/ HPR,HS,RTUBE,RFOUL
COMMON /DOWCO/ KD
COMMON /AVE/ WBAR
COMMON /FILTER/ TFOLD,TAUC

```

```

C
CCCCCCCCCCCCCCCCCCCCCCCCCCCCCCCCCCCCCCCCCCCCCCCCCCCCCCCCCCCC
C   INITIALIZE FLAGS FOR STEADY STATE CALCULATIONS C
CCCCCCCCCCCCCCCCCCCCCCCCCCCCCCCCCCCCCCCCCCCCCCCCCCCCCCCCCCCC
C

```

```

      ITRAN=0
      ICHK=0

```

```

C
CCCCCCCCCCCCCCCCCCCCCCCCCCCCCCCCCCCCCCCCCCCCCCCCCCCCCCCCCCCC
C   READ IN PROBLEM TITLE,NUMBER OF STEAM GENERATORS, FULL POWER   C
C   HEAT TRANSFER RATE,FULL POWER FEEDWATER TEMPERATURE,         C
C   SEPARATOR LOSS COEFFICIENT, PRIMARY FLOWRATE, PRIMARY PRESSURE C
CCCCCCCCCCCCCCCCCCCCCCCCCCCCCCCCCCCCCCCCCCCCCCCCCCCCCCCCCCCC
C

```

```

      READ(5,600) TITLE
      WRITE(6,601) TITLE
600  FORMAT(20A4)
601  FORMAT('1',20A4)
      READ(5,100) NSTG
      READ(5,115) POWER,TFW(2),KSEP,WPIN(1),PPRIM
      PERP=1.0
      QB=POWER*PERP/NSTG
      TFW(1)=TFW(2)
      WPIN(2)=WPIN(1)
      CALL ITER
      ICHK=1

```

```

C
CCCCCCCCCCCCCCCCCCCCCCCCCCCCCCCCCCCCCCCCCCCCCCCCCCCCCCCCCCCC
C   INITIALIZE FULL POWER STEAM AND FEED FLOWS, AS WELL AS C
C   CHOKED FLOW COEFFICIENT FOR TURBINE STOP VALVE                C
CCCCCCCCCCCCCCCCCCCCCCCCCCCCCCCCCCCCCCCCCCCCCCCCCCCCCCCCCCCC
C

```

```

      WFWF=WS(1)
      WSF=WS(1)

```

```

      VALK0=NSF*SQRT(TSAT)/PSAT
C
CCCCCCCCCCCCCCCCCCCCCCCCCCCCCCCCCCCCCCCCCCCCCCCCCCCCCCCCCCCCCCCC
C   READ IN FLAG FOR TRANSIENT CALCULATION(NTRAN=0 STEADY STATE C
C   CALCULATION ONLY, NTRAN=1 TRANSIENT CALCULATION AS WELL      C
CCCCCCCCCCCCCCCCCCCCCCCCCCCCCCCCCCCCCCCCCCCCCCCCCCCCCCCCCCCCCCCC
C
      READ(5,100) NTRAN
      IO=ITIME(IDUMMY)
C
CCCCCCCCCCCCCCCCCCCCCCCCCCCCCCCCCCCCCCCCCCCCCCCCCCCCCCCCCCCCCCCC
C   DO STEADY STATE CALCULATION C
CCCCCCCCCCCCCCCCCCCCCCCCCCCCCCCCCCCCCCCCCCCCCCCCCCCCCCCCCCCCCCCC
C
      CALL STEADY
      IO1=ITIME(IDUMMY)
      IZ=IO1-IO
      WRITE(6,150) IZ
150  FORMAT(' ', 'STEADY STATE CPU TIME CENTISECONDS',I4)
C
CCCCCCCCCCCCCCCCCCCCCCCCCCCCCCCCCCCCCCCCCCCCCCCCCCCCCCCCCCCCCCCC
C   IF NTRAN=1 DO TRANSIENT CALCULATION C
CCCCCCCCCCCCCCCCCCCCCCCCCCCCCCCCCCCCCCCCCCCCCCCCCCCCCCCCCCCCCCCC
C
      IF(NTRAN.NE.1) GO TO 5
      IO2=ITIME(IDUMMY)
      CALL TRANST
      IO3=ITIME(IDUMMY)
      IZ1=IO3-IO2
      WRITE(6,160) IZ1
160  FORMAT(' ', 'TRANSIENT CPU TIME CENTISECONDS',I4)
5    WRITE(6,200)
100  FORMAT(I1)
115  FORMAT(5E12.3)
200  FORMAT('-', 'END OF PROBLEM')
      STOP
      END

```

SUBROUTINE ALPHA

```

C
CCCCCCCCCCCCCCCCCCCCCCCCCCCCCCCCCCCCCCCCCCCCCCCCCCCCCCCCCCCCCCCC
C   THE PURPOSE OF THIS ROUTINE IS TO CALCULATE STEADY STATE   C
C   VAPOR VOLUME FRACTIONS AND BOTH STEADY STATE AND         C
C   TRANSIENT MOMENTUM SPECIFIC VOLUMES FOR SPATIAL ACCELERATION C
CCCCCCCCCCCCCCCCCCCCCCCCCCCCCCCCCCCCCCCCCCCCCCCCCCCCCCCCCCCCCCCC
C
  REAL LM,KSEP,LR,LD,LTB,LP,MU,KC,LF,M,MFD,MR,MTB,
  IMTBC,MSD,MTOT,LT,MUP,LSAT,LSUB
  COMMON /GEOM/ KSEP,LR,LTB,LP,KC,ARI,ATB,ARO,G,
  IVR,VTB,DHTB,BETA(4),NSTG,CO,
  ZAHT,RO,RI,VOP,VTBP,APT,VTM
  COMMON /DOME/ VSUB,VTOT,VG,VFO,LSAT,LSUB,VREF,LW,
  1LD,AD,VD,VSD,DHD,VT,LT,VSTM,DVG,ASH,R1,R2,R3,R4,
  2ZL1,ZL2,ZL3,ZLF
  COMMON /STEAM/ PSAT,TFW(2),TSAT,UL,HL(2),HFW(2),VGJ,MU(2),
  IHG,RL,RHOG,RHOF,DUG,UG,DRHOG,DUF,UF,DRHOF,DRLP,DRLU,
  2QB,POWER,PERP,HFG,RFW(2),DTSAT
  COMMON /FLOWS/ WO,WS(2),WFW(2),WF,WP,WR,MN,DINERT
  COMMON /TRANS/ VOID(3),XQ(3),RB(2),UB(2),DUP(2),DUA(2),DRP(2),
  1DRA,MFD(2),MR(2),MTB(2),MTBC(2),HR,HN,MSD,
  2MTOT(2),S(5),M(5),VP(3),R(9,5)
  COMMON /TIME/ T,DT,ITRAN,WFWF,WSF, ITC,ICLK
  IF(ITRAN.EQ.1) GO TO 5
C
CCCCCCCCCCCCCCCCCCCCCCCCCCCCCCCCCCCCCCCCCCCCCCCCCCCCCCCCCCCCCCCC
C   CALCULATE STEADY STATE VAPOR VOLUME FRACTIONS   C
CCCCCCCCCCCCCCCCCCCCCCCCCCCCCCCCCCCCCCCCCCCCCCCCCCCCCCCCCCCCCCCC
C
  XQ(2)=XQ(1)
  RX=RHOG/RHOF
  X1=CO*(XQ(1)+(1.0-XQ(1))*RAT)
  X2=VGJ*RHOG/WO
  VOID(1)=XQ(1)/(X1+X2*ARI)
  VOID(2)=XQ(2)/(X1+X2*ARO)
  DO 2 I=1,2
  2  RB(I)=VOID(I)*RHOG+(1.0-VOID(I))*RHOF
  RBP=1.0/(1.0/RL+(1.0/RB(1)-1.0/RL)*LP/LTB)
  VOID(3)=(RHOF-RBP)/(RHOF-RHOG)
  X3=CO*RAT+RHOG*ATB*VGJ/WO
  X4=CO*(1.0-RAT)
  XQ(3)=(VOID(3)*X3)/(1.0-VOID(3)*X4)
C
CCCCCCCCCCCCCCCCCCCCCCCCCCCCCCCCCCCCCCCCCCCCCCCCCCCCCCCCCCCCCCCC
C   CALCULATE SPECIFIC VOLUME FOR SPATIAL ACCELERATION C
CCCCCCCCCCCCCCCCCCCCCCCCCCCCCCCCCCCCCCCCCCCCCCCCCCCCCCCCCCCCCCCC
C
  5  DO 10 J=1,3
  DY=XQ(J)**2/VOID(J)
  DX=((1.0-XQ(J))**2)/(1.0-VOID(J))
  10  VP(J)=DY/RHOG+DX/RHOF
  RETURN
  END

```

BLOCK DATA

C

CC

C THIS ROUTINE CONTAINS GEOMETRIC DATA FOR THE STEAM C  
C GENERATOR BEING MODELED. THE NUMBERS SHOWN HERE ARE C  
C THOSE USED IN THE ARKANSAS NUCLEAR ONE-UNIT 2 STUDY C  
CC

C

REAL LW,KSEP,LR,LD,LTB,LP,MJ,KC,LF,M,MFD,MR,MTB,  
INTBC,MSD,MTOT,LT,MUP,LSAT,LSUB,KD  
COMMON /GEOM/ KSEP,LR,LTB,LP,KC,ARI,ATB,ARO,G,  
IVR,VTB,DHTB,BETA(4),NSTG,CO,  
2AHT,RO,RI,VOP,VTBP,APT,VTM  
COMMON /DOME/ VSUB,VTOT,VG,VFO,LSAT,LSUB,VREF,LN,  
ILD,AD,VD,VSD,DHD,VT,LT,VSTM,DVG,ASH,R1,R2,R3,R4,  
2ZL1,ZL2,ZL3,ZLF  
COMMON /DOWCO/ KD  
DATA G/9.8/,ARO/24.0808/,ARI/11.4393/,LR/2.5146/,DHTB/0.0266/  
DATA ATB/6.6698/,LTB/8.5296/,LP/6.7262/,VR/43.6846/,VTB/56.8907/  
DATA CO/1.13/,KC/0.06479/,BETA(2)/0.6394/,BETA(3)/0.1887/  
DATA BETA(4)/0.0522/,KD/0.51/,AHT/8841.2219/,VOP/6.6261/  
DATA VTBP/31.998/,RO/9.525E-03/,RI/8.3058E-03/,APT/1.8229/  
DATA VTM/10.0851/,VSTM/57.0/  
DATA LD/6.7262/,ZL1/0.9970/,ZLF/0.7049/,ZL2/2.5083/,ZL3/1.8034/  
DATA R1/2.9385/,R2/2.7686/,R3/1.9082/,R4/1.986/  
END

SUBROUTINE CHOKE

```
C
CCCCCCCCCCCCCCCCCCCCCCCCCCCCCCCCCCCCCCCCCCCCCCCCCCCCCCCCCCCCCCCC
C   THIS ROUTINE SIMULATES CONTROL ACTION IMPACT ON THE STEAM C
C   FLOW. THAT IS IT SIMULATES THE MAIN STEAM LINE VALVES. C
C   THE VERSION SHOWN HERE IS THE ONE USED FOR MAINE YANKEE. C
C   THE USER MAY CHANGE THIS ROUTINE TO SIMULATE OTHER PLANTS C
CCCCCCCCCCCCCCCCCCCCCCCCCCCCCCCCCCCCCCCCCCCCCCCCCCCCCCCCCCCCCCCC
C
COMMON /STEAM/ PSAT,TFW(2),TSAT,UL,HL(2),HFW(2),VGJ,MU(2),
1HG,RL,RHOG,RHOF,DUG,UG,DRHOG,DUF,UF,DRHOF,DRLP,DRLU,
2QB,POWER,PERP,HFG,RFW(2),DTSAT
COMMON /FLOWS/ WD,WS(2),WFW(2),WF,WP,WR,WN,DINERT
COMMON /TIME/ T,DT,ITRAN,WFWF,WSF, ITC,ICLK
COMMON /PRIME/ PPRIM,TLMTD,UO,TP(3),HP(3),RP(3),UP(3),DRPT(3),
1DUPT(3),TPIN(2),HPIN(2),WPIN(2),MUP,CPL,TKL,CPT
COMMON /RESP/ VALK,IFW(31),PVALV,TTRIP,AK,AKB,VALK0,MB,MSM,
1MSV,TMST,TSV,TISO,ISTM(31),ISV(4)
COMMON /VALVES/ F,FMST,FB,FS1,FS2,FS3,FS4
DATA C1/117.8/,C2/0.223/,C3/255.2/,A14/1.0E-05/,C12/2.5896E06/
DATA C13/6.35E-03/,C14/-1.0582E-09/,C15/1.0764/,C16/3.625E-10/
DATA C17/-9.063E-17/,SL0/-1.465568E06/,SL1/6.926955E03/
DATA SL2/-7.742307/,SL3/7.280301E-03/,C47/1000.0/,C45/1.0E-06/
DATA C48/-0.15E03/,C49/-20.0/,C51/0.657E-06/
DATA C9/1.066555/,PSET1/6.1840E 06/,PSET2/6.3215E 06/
DATA C10/1.02E-08/,C11/-2.548E-15/,C8/3.403E05/,C7/-4.995E10/
DATA C6/2619410.618/,SH0/-8.9/,SH1/2.363444E04/,SH2/-77.434017/
DATA SH3/7.021557E-02/,AKSV/3.2198E-04/
DATA PSV1/6.8712E06/,PSV2/7.0086E06/,PSV3/7.1117E06/
DATA PSV4/7.2147E06/,ACCUM/0.00/,BDOWN/0.00/
C
CCCCCCCCCCCCCCCCCCCCCCCCCCCCCCCCCCCCCCCCCCCCCCCCCCCCCCCCCCCCCCCC
C   ACCUM AND BDOWN ARE THE SAFETY VALVE ACCUMULATION AND C
C   BLOWDOWN, RESPECTIVELY. THESE EFFECTS ARE MODELED ONLY C
C   APPROXIMATELY IN THIS PARTICULAR SUBROUTINE, BUT THE C
C   MODEL COULD BE IMPROVED TO HANDLE THIS BETTER. C
CCCCCCCCCCCCCCCCCCCCCCCCCCCCCCCCCCCCCCCCCCCCCCCCCCCCCCCCCCCCCCCC
C
WS(2)=0.0
PTSAT=PSAT/SQRT(TSAT)
IF(PSAT.LE.3.2844E06) GO TO 50
IF(T.ST.DT) GO TO 1
C
CCCCCCCCCCCCCCCCCCCCCCCCCCCCCCCCCCCCCCCCCCCCCCCCCCCCCCCCCCCCCCCC
C   INITIALIZE PARAMETERS C
CCCCCCCCCCCCCCCCCCCCCCCCCCCCCCCCCCCCCCCCCCCCCCCCCCCCCCCCCCCCCCCC
C
F=0.0
FMST=1.0
FB=0.0
FS1=0.0
FS2=0.0
FS3=0.0
FS4=0.0
```



```

1   IF(T.GE.TTRIP) GO TO 20
C
CCCCCCCCCCCCCCCCCCCCCCCCCCCCCCCCCCCCCCCCCCCCCCCCCCCCCCCCCCCCCCCC
C   DO CALCULATIONS FOR MANIPULATION OF STOP AND CONTROL VALVE C
CCCCCCCCCCCCCCCCCCCCCCCCCCCCCCCCCCCCCCCCCCCCCCCCCCCCCCCCCCCCCCCC
C
   IF(PERP.GT.1.0) GO TO 17
   PS=(5.95-(0.35*PVALV))*(1.0E06)
   TF=(-45.83)*(PVALV**2)+150.83*PVALV+394.0
   TS=C1*((A14*PS)**C2)+C3
   IF(PS.GE.2.0E06) GO TO 2
   US=C6+C7*(1.0/(C8+PS))
   GS=C9+(C11*PS+C10)*PS
   GO TO 3
2   CONTINUE
   US=C12+(C14*PS+C13)*PS
   GS=C15+(C17*PS+C16)*PS
   DGS=C16+2.0*C17*PSAT
   DUG=C13+2.0*C14*PSAT
3   RG=PS/((GS-1.0)*US)
   HGS=US*GS
   IF(TF.GE.573.15) GO TO 6
   UFS=SL0+SL1*TF+SL2*(TF**2.0)+SL3*(TF**3.0)
   GO TO 7
6   UFS=SH0+SH1*TF+SH2*(TF**2.0)+SH3*(TF**3.0)
7   RFS=C47+(C45*UFS)*(C48*C45*UFS+C49)+C51*PS
   HFS=UFS+PS/RFS
   NST=QB*PVALV/(HGS-HFS)
   VALK=NST*(TS**0.5)/PS
17  WS(2)=VALK*PTSAT
C
CCCCCCCCCCCCCCCCCCCCCCCCCCCCCCCCCCCCCCCCCCCCCCCCCCCCCCCCCCCCCCCC
C   IF TURBINE TRIP HAS OCCURED RAMP DOWN STEAM FLOW C
CCCCCCCCCCCCCCCCCCCCCCCCCCCCCCCCCCCCCCCCCCCCCCCCCCCCCCCCCCCCCCCC
C
20  IF (T.LT.TTRIP) GO TO 30
   DVALK=(VALK0-VALK)/VALK0
   IF(FMST.EQ.0.0) GO TO 21
   FMST=1.0-((T-TTRIP)/TMST)-DVALK
   IF(FMST.LE.0.0) FMST=0.0
21  WS(2)=FMST*VALK0*PTSAT
   IF(MSM) 30,30,22
C
CCCCCCCCCCCCCCCCCCCCCCCCCCCCCCCCCCCCCCCCCCCCCCCCCCCCCCCCCCCCCCCC
C   IF DUMP SYSTEM IS OPERATIONAL SIMULATE IT C
CCCCCCCCCCCCCCCCCCCCCCCCCCCCCCCCCCCCCCCCCCCCCCCCCCCCCCCCCCCCCCCC
C
22  TAVE=(TPIN(2)+TP(3))/2.0
   DTAVE=TAVE-550.93
   TCH=T-TTRIP
   IF(TCH.GE.DT) GO TO 25
   F=0.0
   ITR=0
   IF(DTAVE.GE.13.89) GO TO 23

```

```

      2F(DTAVE.SE.4.44) GO TO 24
      FO=0.0
      GO TO 25
23    FO=1.0
      GO TO 25
24    FO=0.0818*DTAVE-0.1362
25    IF(ITR.EQ.1) GO TO 28
      IF(F.LT.FO) GO TO 26
      ITR=1
      GO TO 28
26    IF(FO.LT.1.0) GO TO 27
      F=(T-TTRIP)/3.0
      IF(F.GE.1.0) F=1.0
      GO TO 36
27    F=(T-TTRIP)/15.0
      IF(F.GE.FO) F=FO
      GO TO 36
28    IF(DTAVE.LT.13.89) GO TO 29
      IF(F.EQ.1.0) GO TO 36
      F=F+DT/15.0
      IF(F.GE.1.0) F=1.0
      GO TO 36
29    IF(F.EQ.0.0) GO TO 35
      F1=DTAVE*0.0818-0.1362
      IF(F-F1) 31,32,33
31    SIGN=1.0
      GO TO 34
32    SIGN=0.0
      GO TO 34
33    SIGN=-1.0
34    F=F+SIGN*DT/15.0
      IF(F.GE.1.0) F=1.0
      IF(F.LE.0.0) F=0.0
      GO TO 36
35    IF(DTAVE.LT.4.44) GO TO 36
      F2=DTAVE*0.818-0.1362
      F=F+DT/15.0
      IF(F.GE.F2) F=F2
      GO TO 36
37    F=1.0
36    NS(2)=NS(2)+F*AK*PTSAT
30    IF(MB) 50,50,39
C
CCCCCCCCCCCCCCCCCCCCCCCCCCCCCCCCCCCCCCCCCCCCCCCCCCCCCCCCCCCC
C   IF BYPASS SYSTEM IS OPERATIONAL SIMULATE IT C
CCCCCCCCCCCCCCCCCCCCCCCCCCCCCCCCCCCCCCCCCCCCCCCCCCCCCCCCCCCC
C
39    IF(PSAT.LE.PSET1) GO TO 40
      IF(PSAT.GE.PSET2) GO TO 41
      FB=(PSAT-PSET1)/(PSET2-PSET1)
      GO TO 42
40    FB=0.0
      GO TO 42
41    FB=1.0

```

```

42  WS(2)=WS(2)+FB*AKB*PTSAT
C
CCCCCCCCCCCCCCCCCCCCCCCCCCCCCCCCCCCCCCCCCCCCCCCCCCCCCCCCCCCC
C   IF SAFETY VALVES ARE WORKING SIMULATE THEM C
CCCCCCCCCCCCCCCCCCCCCCCCCCCCCCCCCCCCCCCCCCCCCCCCCCCCCCCCCCCC
C
50  IF(MSV.NE.1) RETURN
     IF(ISV(1).NE.1) GO TO 53
     PSA1=(1.0+ACCUM)*PSV1
     PSB1=(1.0-BDOWN)*PSV1
     IF(PSAT.GE.PSA1) GO TO 51
     IF(PSAT.LE.PSB1) GO TO 52
     FS1=(PSAT-PSB1)/(PSA1-PSB1)
     GO TO 53
51  FS1=1.0
     GO TO 53
52  FS1=0.0
53  WS(2)=WS(2)+FS1*AKSV*PTSAT
     IF(ISV(2).NE.1) GO TO 56
     PSA2=(1.0+ACCUM)*PSV2
     PSB2=(1.0-BDOWN)*PSV2
     IF(PSAT.GE.PSA2) GO TO 54
     IF(PSAT.LE.PSB2) GO TO 55
     FS2=(PSAT-PSB2)/(PSA2-PSB2)
     GO TO 56
54  FS2=1.0
     GO TO 56
55  FS2=0.0
56  WS(2)=WS(2)+FS2*AKSV*PTSAT
     IF(ISV(3).NE.1) GO TO 59
     PSA3=(1.0+ACCUM)*PSV3
     PSB3=(1.0-BDOWN)*PSV3
     IF(PSAT.GE.PSA3) GO TO 57
     IF(PSAT.LE.PSB3) GO TO 58
     FS3=(PSAT-PSB3)/(PSA3-PSB3)
     GO TO 59
57  FS3=1.0
     GO TO 59
58  FS3=0.0
59  WS(2)=WS(2)+2.0*FS3*AKSV*PTSAT
     IF(ISV(4).NE.1) GO TO 62
     PSA4=(1.0+ACCUM)*PSV4
     PSB4=(1.0-BDOWN)*PSV4
     IF(PSAT.GE.PSA4) GO TO 60
     IF(PSAT.LE.PSB4) GO TO 61
     FS4=(PSAT-PSB4)/(PSA4-PSB4)
     GO TO 62
60  FS4=1.0
     GO TO 62
61  FS4=0.0
62  WS(2)=WS(2)+2.0*FS4*AKSV*PTSAT
     RETURN
     END

```

SUBROUTINE CONTRO

```
C
CCCCCCCCCCCCCCCCCCCCCCCCCCCCCCCCCCCCCCCCCCCCCCCCCCCCCCCCCCCC
C   THIS SUBROUTINE SIMULATES THE ACTION OF A THREE ELEMENT C
C   FEEDWATER CONTROLLER. THE ROUTINE MAY BE REPLACED BY C
C   ONE OF THE USERS CHOICE. THIS CONTROLLER MODEL'S C
C   PARAMETERS ARE THOSE USED FOR PART OF THE ARKANSAS C
C   NUCLEAR ONE-UNIT 2 STUDY C
CCCCCCCCCCCCCCCCCCCCCCCCCCCCCCCCCCCCCCCCCCCCCCCCCCCCCCCCCCCC
C
REAL LW,KSEP,LR,LD,LTB,LP,MU,KC,LF,M,MFD,MR,MTB,
INTBC,MSD,MTOT,LT,MUP,LSAT,LSUB
COMMON /GEOM/ KSEP,LR,LTB,LP,KC,ARI,ATB,ARO,G,
IVR,VTB,DHTB,BETA(4),NSTG,CO,
2AHT,RO,RI,VOP,VTBP,APT,VTH
COMMON /DOME/ VSUB,VTOT,VG,VFO,LSAT,LSUB,VREF,LW,
1LD,AD,VD,VSD,DHD,VT,LT,VSTM,DVG,ASW,R1,R2,R3,R4,
2ZL1,ZL2,ZL3,ZLF
COMMON /FLOWS/ WO,WS(2),WFW(2),WF,WP,WR,WN,DINERT
COMMON /TIME/ T,DT,ITRAN,WFWF,WSF, ITC,ICLK
CL=1.0000E+00
CW=0.02
WDOT=CW*(WS(1)-WFW(1))+CL*(10.43-LW)
WFW(2)=WFW(1)+WDOT*DT
RETURN
END
```

SUBROUTINE DODEN

```
C
CCCCCCCCCCCCCCCCCCCCCCCCCCCCCCCCCCCCCCCCCCCCCCCCCCCCCCCCCCCCCCCC
C   THIS ROUTINE PERFORM A STEADY STATE MIXING CALCULATION FOR   C
C   THE DOWNCOMER(SUBCOOLED REGION)                               C
CCCCCCCCCCCCCCCCCCCCCCCCCCCCCCCCCCCCCCCCCCCCCCCCCCCCCCCCCCCCCCCC
C
  REAL LW,KSEP,LR,LD,LTB,LP,MU,KC,LF,M,MFD,MR,MTB,
  1MTBC,MSD,MTOT,LT,MUP,LSAT,LSUB
  COMMON /STEAM/ PSAT,TFW(2),TSAT,UL,HL(2),HFW(2),VGJ,MU(2),
  IHG,RL,RHOG,RHOF,DUG,UG,DRHOG,DUF,UF,DRHOF,DRLP,DRLU,
  2QB,POWER,PERP,HFG,RFW(2),DTSAT
  COMMON /TRANS/ VOID(3),XQ(3),RB(2),UB(2),DUP(2),DUA(2),DRP(2),
  1DRA,MFD(2),MR(2),MTB(2),MTBC(2),HR,HN,MSD,
  2MTOT(2),S(5),M(5),VP(3),R(9,5)
  COMMON /TIME/ T,DT,ITRAN,WFWF,MSF, ITC,ICHK
  DATA A/-1.2083E-10/,B/-4.1089E-05/,C/986.3/
  DATA C45/1.0E-06/,C47/1000.0/,C48/-0.15E03/
  DATA C49/-20.0/,C51/0.657E-06/
C
CCCCCCCCCCCCCCCCCCCCCCCCCCCCCCCCCCCCCCCCCCCCCCCCCCCCCCCCCCCCCCCC
C   CALCULATE SUBCOOLED REGION ENTHALPY   C
CCCCCCCCCCCCCCCCCCCCCCCCCCCCCCCCCCCCCCCCCCCCCCCCCCCCCCCCCCCCCCCC
C
  HL(1)=XQ(1)*HFW(1)+(1.0-XQ(1))*HL(2)
C
CCCCCCCCCCCCCCCCCCCCCCCCCCCCCCCCCCCCCCCCCCCCCCCCCCCCCCCCCCCCCCCC
C   USE NEWTON'S METHOD TO FIND DOWNCOMER DENSITY   C
C   FROM PROPERTY FITS                               C
CCCCCCCCCCCCCCCCCCCCCCCCCCCCCCCCCCCCCCCCCCCCCCCCCCCCCCCCCCCCCCCC
C
  RL=A*HL(1)**2+B*HL(1)+C
  C1=(C45**2)*C48
  C2=C49*C45
  C3=C47+C51*PSAT
  P=(-1.0)*(C1*HL(1)**2+C2*HL(1)+C3)
  Q=2.0*PSAT*HL(1)*C1+C2*PSAT
  RD=-1.0*C1*(PSAT**2)
  RN=RL
  GO TO 5
10  RN=RHO
  5  F=RN**3+P*RN**2+Q*RN+RD
  FP=3.0*RN**2+2.0*P*RN+Q
  RHO=RN-F/FP
  DEL=RHO-RN
  ADEL=ABS(DEL)
  IF (ADEL.LT.1.0E-02) GO TO 20
  GO TO 10
20  RL=RHO
C
CCCCCCCCCCCCCCCCCCCCCCCCCCCCCCCCCCCCCCCCCCCCCCCCCCCCCCCCCCCCCCCC
C   CALCULATE DOWNCOMER INTERNAL ENERGY   C
CCCCCCCCCCCCCCCCCCCCCCCCCCCCCCCCCCCCCCCCCCCCCCCCCCCCCCCCCCCCCCCC
C
```

```
      UL=HL(1)-PSAT/RL
C
CCCCCCCCCCCCCCCCCCCCCCCCCCCCCCCCCCCCCCCC
C   EVALUATE OTHER PROPERTIES   C
CCCCCCCCCCCCCCCCCCCCCCCCCCCCCCCCCCCCCCCC
C
      CALL THERM1
      RETURN
      END
```

SUBROUTINE HEAT

```
C
CCCCCCCCCCCCCCCCCCCCCCCCCCCCCCCCCCCCCCCCCCCCCCCCCCCCCCCCCCCCCCCC
C   THE PURPOSE OF THIS ROUTINE IS TO CALCULATE THE STEADY C
C   STATE STEAM AND FEED FLOWS, AS WELL AS THE TURBINE STOP C
C   AND CONTROL VALVE CHOKED FLOW COEFFICIENT C
CCCCCCCCCCCCCCCCCCCCCCCCCCCCCCCCCCCCCCCCCCCCCCCCCCCCCCCCCCCCCCCC
C
COMMON /GEOM/ KSEP,LR,LTB,LP,KC,ARI,ATB,ARO,G,
1VR,VTB,DHTB,BETA(4),NSTG,CO,
2AHT,RO,RI,VOP,VTBP,APT,VTM
COMMON /STEAM/ PSAT,TFW(2),TSAT,UL,HL(2),HFW(2),VGJ,MU(2),
1HG,RL,RHOG,RHOF,DUG,UG,DRHOG,DUF,UF,DRHOF,DRLP,DRLU,
2QB,POWER,PERP,HFG,RFW(2),DTSAT
COMMON /FLOWS/ NO,WS(2),WFW(2),WF,WP,WR,WN,DINERT
COMMON /RESP/ VALK,IFW(31),PVALV,TTRIP,AK,AKB,VALK0,MB,MSM,
1MSV,THST,TSV,TISO,ISTH(31),ISV(4)
C
CCCCCCCCCCCCCCCCCCCCCCCCCCCCCCCCCCCCCCCCCCCCCCCCCCCCCCCCCCCCCCCC
C   USE STEADY STATE HEAT BALANCE TO CALCULATE STEAM FLOW C
CCCCCCCCCCCCCCCCCCCCCCCCCCCCCCCCCCCCCCCCCCCCCCCCCCCCCCCCCCCCCCCC
C
WS(1)=QB/(HG-HFW(1))
WFW(1)=WS(1)
C
CCCCCCCCCCCCCCCCCCCCCCCCCCCCCCCCCCCCCCCCCCCCCCCCCCCCCCCCCCCCCCCC
C   CALCULATE TURBINE STOP AND CONTROL VALVE FLOW COEFFICIENT C
CCCCCCCCCCCCCCCCCCCCCCCCCCCCCCCCCCCCCCCCCCCCCCCCCCCCCCCCCCCCCCCC
C
VALK=WS(1)*(TSAT**0.5)/PSAT
IF(PERP.GE.1.0) VALK0=VALK
RETURN
END
```

```

SUBROUTINE ITER
C
CCCCCCCCCCCCCCCCCCCCCCCCCCCCCCCCCCCCCCCCCCCCCCCCCCCCCCCCCCCCCCCC
C   THIS ROUTINE CALCULATES THE STEADY STATE PRIMARY TEMPERATURE C
C   DISTRIBUTION AND FOULING FACTOR. IT ALSO CALCULATES THE      C
C   SECONDARY PRESSURE IF THE REACTOR IS NOT AT FULL POWER.      C
C   THE SECONDARY STEADY STATE FLOW PATTERN IS ALSO CALCULATED.  C
CCCCCCCCCCCCCCCCCCCCCCCCCCCCCCCCCCCCCCCCCCCCCCCCCCCCCCCCCCCCCCCC
C
REAL LW,KSEP,LR,LD,LTB,LP,MU,KC,LF,MFD,MR,MTB,
INTBC,MSD,HTOT,LT,MUP,LSAT,LSUB,KD
COMMON /GEOM/ KSEP,LR,LTB,LP,KC,ARI,ATB,ARO,G,
1VR,VTB,DHTB,BETA(4),NSTG,CO,
2AHT,RO,RI,VOP,VTBP,APT,VTM
COMMON /RESP/ VALK,IFW(31),PVALV,TTRIP,AK,AKB,VALKO,MB,MSM,
1MSV,TMST,TSV,ISO,ISTM(31),ISV(4)
COMMON /DOME/ VSUB,VTOT,VG,VFO,LSAT,LSUB,VREF,LW,
1LD,AD,VD,VSD,DHD,VT,LT,VSTM,DVG,ASW,R1,R2,R3,R4,
2ZL1,ZL2,ZL3,ZLF
COMMON /STEAM/ PSAT,TFW(2),TSAT,UL,HL(2),HFW(2),VGJ,MU(2),
1HG,RL,RHOG,RHOF,DUG,UG,DRHOG,DUF,UF,DRHOF,DRLP,DRLU,
2QB,POWER,PERP,HFG,RFW(2),DTSAT
COMMON /FLOWS/ NO,WS(2),WFW(2),WF,WP,WR,WN,DINERT
COMMON /TRANS/ VOID(3),XQ(3),RB(2),UB(2),DUP(2),DUA(2),DRP(2),
1DRA,MFD(2),MR(2),MTB(2),MTBC(2),HR,HN,MSD,
2HTOT(2),S(5),H(5),VP(3),R(9,5)
COMMON /TIME/ T,DT,ITRAN,WFWF,WSF,ITC,ICHK
COMMON /PRIME/ PPRIM,TLMTD,UO,TP(3),HP(3),RP(3),UP(3),DRFT(3),
1DUPT(3),TPIN(2),HPIN(2),WPIN(2),MUP,CPL,TKL,CPT
COMMON /HTS/ HPR,HS,RTUBE,RFOUL
COMMON /DOWCO/ KD
COMMON /AVE/ WBAR
DATA A1,A2,A4,A5 /255.2,117.8,0.223,87.0E05/
C
CCCCCCCCCCCCCCCCCCCCCCCCCCCCCCCCCCCCCCCCCCCCCCCCCCCCCCCCCCCCCCCC
C   CHECK IF THIS IS THE INITIAL FULL POWER CALCULATION C
C   FOR THE FOULING FACTOR C
CCCCCCCCCCCCCCCCCCCCCCCCCCCCCCCCCCCCCCCCCCCCCCCCCCCCCCCCCCCCCCCC
C
IF(ICHK.EQ.1) GO TO 80
C
CCCCCCCCCCCCCCCCCCCCCCCCCCCCCCCCCCCCCCCCCCCCCCCCCCCCCCCCCCCCCCCC
C   READ IN THE PARAMETERS T1 AND T2 FOR LINEAR FUNCTION C
C   OF TAVE WITH POWER: TAVE=T1+T2*PERP C
CCCCCCCCCCCCCCCCCCCCCCCCCCCCCCCCCCCCCCCCCCCCCCCCCCCCCCCCCCCCCCCC
C
READ(5,201) T1,T2
201  FORIAT(2E12.3)
80   IF(PERP.LE.1.0) GO TO 90
C
CCCCCCCCCCCCCCCCCCCCCCCCCCCCCCCCCCCCCCCCCCCCCCCCCCCCCCCCCCCCCCCC
C   IF THE REACTOR IS OPERATING ABOVE FULL POWER READ IN TAVE C
CCCCCCCCCCCCCCCCCCCCCCCCCCCCCCCCCCCCCCCCCCCCCCCCCCCCCCCCCCCCCCCC
C

```



```

      READ(5,200) TAVE
200  FORMAT(E12.3)
      GO TO 91
90   TAVE=T1+T2*PERP
C
CCCCCCCCCCCCCCCCCCCCCCCCCCCCCCCCCCCCCCCCCCCCCCCCCCCCCCCCCCCC
C    CALCULATE PRIMARY TEMPERATURES USING BISECTION C
CCCCCCCCCCCCCCCCCCCCCCCCCCCCCCCCCCCCCCCCCCCCCCCCCCCCCCCCCCCC
C
91   ICT=0
      DHSTAR=QB/WPIN(1)
      CRIT=5.0E-03*DHSTAR
      TP(1)=TAVE+100.0
      TP0=TP(1)
100  TP(2)=2.0*TAVE-TP(1)
      ITC=1
      CALL PRMPRO
      DH=HP(1)-HP(2)
      EDH=DH-DHSTAR
      AEDH=ABS(EDH)
      IF(AEDH.LE.CRIT) GO TO 103
      IF(EDH.LE.0.0) GO TO 102
      IF(ICT.EQ.1) GO TO 101
      TP0=TP(1)
      TP(1)=(TP0+TAVE)/2.0
      GO TO 100
101  TP0=TP(1)
      TP(1)=(TP0+TN)/2.0
      GO TO 100
102  TN=TP(1)
      TP(1)=(TP0+TN)/2.0
      ICT=1
      GO TO 100
103  TPIN(1)=TP(1)
      TPIN(2)=TPIN(1)
      TP(3)=TP(2)
C
CCCCCCCCCCCCCCCCCCCCCCCCCCCCCCCCCCCCCCCCCCCCCCCCCCCCCCCCCCCC
C    IF THE REACTOR IS AT LESS THAN FULL POWER C
C    CALCULATE SECONDARY PRESSURE USING THE C
C    FOULING FACTOR OBTAINED FROM A FULL POWER C
C    CALCULATION C
CCCCCCCCCCCCCCCCCCCCCCCCCCCCCCCCCCCCCCCCCCCCCCCCCCCCCCCCCCCC
C
      IF (PERP.NE.1.0) GO TO 107
C
CCCCCCCCCCCCCCCCCCCCCCCCCCCCCCCCCCCCCCCCCCCCCCCCCCCCCCCCCCCC
C    IF THIS IS THE INITIAL FULL POWER CALCULATION C
C    READ IN THE SECONDARY PRESSURE AND DETERMINE C
C    THE FOULING FACTOR C
CCCCCCCCCCCCCCCCCCCCCCCCCCCCCCCCCCCCCCCCCCCCCCCCCCCCCCCCCCCC
C
      IF(ICHK.EQ.0) READ(5,203) PSAT
203  FORMAT(E12.3)

```

```

ITC=0
CALL PRMPRO
CALL THERM
CALL HEAT
Z1=TP(1)-TSAT
Z2=TP(2)-TSAT
TLMTD=(TP(1)-TP(2))/ALOG(Z1/Z2)
CALL NEWPR1
UO=QB/(AHT*TLMTD)
RFOUL=1.0/UO-RTUBE-(RO/RI)/HPR-1.0/HS
IF (ICLK.NE.1) RETURN
GO TO 106

```

```

C
CCCCCCCCCCCCCCCCCCCCCCCCCCCCCCCCCCCCCCCCCCCCCCCCCCCCCCCCCCCCCCCC
C THIS SECTION CALCULATES THE SECONDARY PRESSURE AT C
C POWERS OTHER THAN FULL POWER, GIVEN THE FOULING FACTOR C
CCCCCCCCCCCCCCCCCCCCCCCCCCCCCCCCCCCCCCCCCCCCCCCCCCCCCCCCCCCCCCCC
C

```

```

107 ITC=0
CALL PRMPRO
A3=1.0/A4
QP=QB/AHT
QP1=QP/1.0E06
RE=2.0*RI*WPIN(2)/(APT*MUP)
PR=MUP*CPL/TKL
HPR=(0.023)*(RE**0.8)*(PR**0.4)*TKL/(2.0*RI)
RPF=(RO/RI)/HPR+RFOUL
TS2=TAVE-30.0
104 TS1=TS2
AS=(TS1-A1)/A2
PS1=(AS**A3)*1.0E05
Z1=TP(1)-TS1
Z2=TP(2)-TS1
TL=(TP(1)-TP(2))/ALOG(Z1/Z2)
TT=0.016*(TL/2.0+TS1)+9.632
F1=QP*(RPF+RO*ALOG(RO/RI)/TT)
F2=22.65*SQRT(QP1)*EXP(-PS1/AS)
F=F1+F2-TL
DTL=(-1.0)*(TL**2.0)/(Z1*Z2)
DPS=A3*(AS**A3)*1.0E05/A2
FP1=(-1.0*QP)*(RO*ALOG(RO/RI)/TT**2.0)*(0.016)*(DTL/2.0+1.0)
FP=FP1+(F2/AS)*DPS-DTL
TS2=TS1-F/FP
DTS=TS2-TS1
ADTS=ABS(DTS)
IF (ADTS.LE.0.1) GO TO 105
GO TO 104
105 TSAT=TS2
PS=(TSAT-A1)/A2
PSAT=(PS**A3)*1.0E05
CALL THERM
CALL HEAT
Z1=TP(1)-TSAT
Z2=TP(2)-TSAT

```

```

      TLMTD=(TP(1)-TP(2))/ALOG(Z1/Z2)
106  CONTINUE
C
CCCCCCCCCCCCCCCCCCCCCCCCCCCCCCCCCCCCCCCCCCCCCCCCCCCCCCCCCCCC
C   CALCULATE THE STEADY STATE DOWNCOMER FLOWRATE   C
C   AND SECONDARY FLOW PATTERN USING BISECTION     C
CCCCCCCCCCCCCCCCCCCCCCCCCCCCCCCCCCCCCCCCCCCCCCCCCCCCCCCCCCCC
C
      XQ(1)=0.01
      WO=WS(1)/XQ(1)
      IPT=0
10   CONTINUE
      XQ(1)=WS(1)/WO
      CALL DODEN
      WP=WO
      WF=WO-WS(1)
      WR=WO
      WN=WO
      CALL MOMEN
      DP=(M(1)+M(2)+M(3)+M(4))*WO+M(5)
      ADP=ABS(DP)
      IF (ADP.LT.1.0E-01) GO TO 40
      IF(DP.LT.0.0) GO TO 30
      IF(IPT.NE.0) GO TO 20
      XQ(1)=XQ(1)+0.05
      WOP=WO
      WO=WS(1)/XQ(1)
      IF(XQ(1).GT.1.0) RETURN
      GO TO 10
20   CONTINUE
      WOP=WO
      WO=(WOP+WON)/2.0
      IPT=1
      GO TO 10
30   CONTINUE
      WON=WO
      WO=(WOP+WON)/2.0
      IPT=1
      GO TO 10
40   CONTINUE
C
CCCCCCCCCCCCCCCCCCCCCCCCCCCCCCCCCCCCCCCCCCCCCCCCCCCCCCCCCCCC
C   CALCULATE THE STEADY STATE MASSES AND OTHER PARAMETERS   C
C   AND WRITE OUT THE RESULTS OF THE STEADY STATE CALCULATION C
CCCCCCCCCCCCCCCCCCCCCCCCCCCCCCCCCCCCCCCCCCCCCCCCCCCCCCCCCCCC
C
      CALL NEWPR
      CALL OUT
      RETURN
      END

```

SUBROUTINE LEVEL

```

C
CCCCCCCCCCCCCCCCCCCCCCCCCCCCCCCCCCCCCCCCCCCCCCCCCCCCCCCCCCCCCCCC
C   THE PURPOSE OF THIS ROUTINE IS TO CALCULATE THE DOWNCOMER C
C   LEVEL GIVEN THE STEAM VOLUME IN THE STEAM DOME-DOWNCOMER. C
C   THE DOWNCOMER GEOMETRY IS REPRESENTED ANALYTICALLY; THE C
C   LEVEL IS OBTAINED BY DIRECT INVERSION OF A CUBIC EQUATION.C
C   THE ROUTINE ALSO CALCULATES THE HEIGHT OF SUBCOOLED LIQ- C
C   UID, AS WELL AS THE LENGTH OF SATURATED LIQUID IN THE C
C   DOWNCOMER. C
CCCCCCCCCCCCCCCCCCCCCCCCCCCCCCCCCCCCCCCCCCCCCCCCCCCCCCCCCCCCCCCC
C
    REAL LW,KSEP,LR,LD,LTB,LP,MJ,KC,LF,M,MFD,MR,MTB,
    1MTBC,MSD,MTOT,LT,MUP,LSAT,LSUB
    COMMON /GEOM/ KSEP,LR,LTB,LP,KC,ARI,ATB,ARO,G,
    1VR,VTB,DHTB,BETA(4),NSTG,CO,
    2AHT,RO,RI,VOP,VTBP,APT,VTH
    COMMON /DOME/ VSUB,VTOT,VS,VFO,LSAT,LSUB,VREF,LW,
    1LD,AD,VD,VSD,DHD,VT,LT,VSTM,DVS,ASH,R1,R2,R3,R4,
    2ZI : ZL2,ZL3,ZLF
    COMMON /TRANS/ VOID(3),XQ(3),RB(2),UB(2),DUP(2),DUA(2),DRP(2),
    1DRA,MFD(2),MR(2),MTB(2),MTBC(2),HR,HN,MSD,
    2MTOT(2),S(5),M(5),VP(3),R(9,5)
    COMMON /TIME/ T,DT,ITRAN,MFWF,MSF,ITC,ICLK
    IF(ITRAN.EQ.1) GO TO 10
C
CCCCCCCCCCCCCCCCCCCCCCCCCCCCCCCCCCCCCCCCCCCCCCCCCCCCCCCCCCCCCCCC
C   INITIALIZATION OF STEAM DOME-DOWNCOMER GEOMETRY: CALCULATE C
C   REGION VOLUMES. C
CCCCCCCCCCCCCCCCCCCCCCCCCCCCCCCCCCCCCCCCCCCCCCCCCCCCCCCCCCCCCCCC
C
    PI=3.141593
    V1=(2.0/3.0)*PI*(R1**3)
    V2=PI*(R1**2)*ZL1
    V12=V1+V2
    C1=(R2-R3)/ZL2
    V3=PI*(R1**2*ZL2-(R2**3-R3**3)/(3.0*C1))
    V123=V12+V3
    VLF=PI*((R1**2)*ZLF-((C1*ZLF+R3)**3-R3**3)/(3.0*C1))
    ZL2M=LW-ZL3-LD
    V2M=PI*((R1**2)*ZL2M-((C1*ZL2M+R3)**3-R3**3)/(3.0*C1))
    VFO=(V2M-VLF)/4.0
    ZL1234=ZL1+ZL2+ZL3+LD
    LT=ZLF+ZL3+LD
    ZL234=ZL1234-ZL1
    C2=(R1-R4)/ZL3
    V4=PI*((R1**3-R4**3)/(3.0*C2)-ZL3*R3**2)
    V1234=V123+V4
    AD=PI*(R4**2-R3**2)
    VD=LD*AD
    VTOT=V1234+VD
    VT=VD+V4+VLF
    VSD=VTOT-VT
    VREF=VSD-VFO

```

```

    ASW=PI*(R1**2-(C1*ZL2W+R3)**2)
    VR1=V1234-VFO
    VR2=VTOT-VFO
    LSUB=LT
    LSAT=LW-LSUB
    DHD=(2.0*AD)/((R4+R3)*PI)
    VG=VTOT-V2W-V4-VD
    RETURN
10  IF(VG.GT.V1) GO TO 15
    TEST=1.0
    ANG=ARCOS(ANS)/3.0+4.0*PI/3.0
    SL=2.0*R1*COS(ANG)
    LW=SL+ZL1234
    LSUB=LT
    LSAT=LW-LT
    ASW=PI*(R1**2.0-R2**2.0)
    RETURN
15  IF(V6.GE.V12) GO TO 20
    SL=(V12-V6)/(PI*R1**2.0)
    LW=SL+ZL234
    LSUB=LT
    LSAT=LW-LSUB
    ASW=PI*(R1**2.0-R2**2.0)
    RETURN
20  IF(V6.GT.VREF) GO TO 25
    B=3.0*C1*(V123-V6)/PI+(3.0*(R1**2)-(R3**2))*R3
    ARG=B/(-2.0*(R1**3.0))
    ANG=ARCOS(ARG)/3.0+4.0*PI/3.0
    SL1=COS(ANG)*2.0*R1
    SL=(SL1-R3)/C1
    ASW=PI*((R1**2)-((C1*SL+R3)**2.0))
    LW=SL+LD+ZL3
    LSUB=LT
    LSAT=LW-LSUB
    RETURN
25  IF(V6.GT.V123) GO TO 30
    IF(V4.LE.VFO) GO TO 100
    B=3.0*C1*(V123-V6)/PI+(3.0*R1**2-R3**2)*R3
    ARG=B/(-2.0*R1**3.0)
    ANG=ARCOS(ARG)/3.0+4.0*PI/3.0
    SL1=COS(ANG)*2.0*R1
    SL=(SL1-R3)/C1
    ASW=PI*(R1**2-(C1*SL+R3)**2.0)
    LW=SL+LD+ZL3
    VI=VG+VFO
    B=(3.0*R3**2.0-R4**2.0)*R4-3.0*C2*(V1234-VI)/PI
    ARG=B/(-2.0*R3**3)
    ANG=ARCOS(ARG)/3.0
    SL2=2.0*R3*COS(ANG)
    SL=(SL2-R4)/C2
    LSUB=SL+LD
    LSAT=LW-LSUB
    RETURN
30  IF(V6.GT.VR1) GO TO 35

```

```

IF(V4.LE.VFO) GO TO 100
B=(3.0*R3**2.0-R4**2.0)*R4-3.0*C2*(V1234-VG)/PI
ARG=B/(-2.0*R3**3)
ANG=ARCOS(ARG)/3.0
SL2=2.0*R3*COS(ANG)
SL=(SL2-R4)/C2
LW=SL+LD
VI=VG+VFO
ASW=PI*((C2*SL+R4)**2.0-R3**2.0)
B=(3.0*R3**2.0-R4**2.0)*R4-3.0*C2*(V1234-VI)/PI
ARG=B/(-2.0*R3**3)
ANG=ARCOS(ARG)/3.0
SL2=2.0*R3*COS(ANG)
SL=(SL2-R4)/C2
LSUI=SL+LD
LSAT=LW-LSUB
RETURN
35 IF(VG.GE.V1234) GO TO 40
B=(3.0*R3**2.0-R4**2.0)*R4-3.0*C2*(V1234-VG)/PI
ARG=B/(-2.0*R3**3)
ANG=ARCOS(ARG)/3.0
SL2=2.0*R3*COS(ANG)
SL=(SL2-R4)/C2
LW=SL+LD
VI=VG+VFO
ASW=PI*((C2*SL+R4)**2.0-R3**2.0)
LSUB=(VTOT-VI)/AD
LSAT=LW-LSUB
RETURN
40 IF(VG.GE.VR2) GO TO 45
LW=(VTOT-VG)/AD
VI=VG+VFO
LSUB=(VTOT-VI)/AD
ASW=AD
LSAT=LW-LSUB
RETURN
45 LW=(VTOT-VG)/AD
LSAT=LW
LSUB=0.0
RETURN
100 IF(VG.GE.V1234) GO TO 40
B=(3.0*R3**2.0-R4**2.0)*R4-3.0*C2*(V1234-VG)/PI
ARG=B/(-2.0*R3**3)
ANG=ARCOS(ARG)/3.0
SL2=2.0*R3*COS(ANG)
SL=(SL2-R4)/C2
LW=SL+LD
VI=VG+VFO
ASW=PI*((C2*SL+R4)**2.0-R3**2.0)
LSUB=(VTOT-VI)/AD
LSAT=LW-LSUB
RETURN
END

```

```

SUBROUTINE MINV(R,A,N,D,L,M)
C
CCCCCCCCCCCCCCCCCCCCCCCCCCCCCCCCCCCCCCCCCCCCCCCCCCCCCCCCCCCC
C   DOCUMENTATION : PAGE 118, IBM SCIENTIFIC SOFTWARE DOCUMENT   C
C
C   PURPOSE: INVERT A MATRIX                                     C
C
C   USAGE: CALL MINV(R,A,N,D,L,M)                               C
C
C   DESCRIPTION OF PARAMETERS:                                   C
C     R   -INPUT MATRIX.                                         C
C     A   -INVERSE.                                             C
C     N   -ORDER OF MATRIX A.                                    C
C     D   -RESULTANT DETERMINANT.                               C
C     L   -WORK VECTOR OF LENGTH N.                             C
C     M   -WORK VECTOR OF LENGTH N.                             C
C
C   REMARKS: MATRIX A MUST BE A GENERAL MATRIX.               C
C
C   SUBROUTINES AND FUNCTION SUBPROGRAMS REQUIRED: NONE.        C
C
C   METHOD:                                                       C
C     THE STANDARD GAUSS-JORDAN METHOD IS USED. THE DETERMINANT C
C     IS ALSO CALCULATED. A DETERMINANT OF ZERO INDICATES THAT C
C     THE MATRIX IS SINGULAR                                     C
CCCCCCCCCCCCCCCCCCCCCCCCCCCCCCCCCCCCCCCCCCCCCCCCCCCCCCCCCCCC
C
DIMENSION A(1),L(N),M(N),R(1)
N2=N*N
DO 5 I=1,N2
5  A(I)=R(I)
C
CCCCCCCCCCCCCCCCCCCCCCCCCCCCCCCCCCCCCCCCCCCCCCCCCCCCCCCCCCCC
C   SEARCH FOR LARGEST ELEMENT C
CCCCCCCCCCCCCCCCCCCCCCCCCCCCCCCCCCCCCCCCCCCCCCCCCCCCCCCCCCCC
C
D=1.0
NK=-N
DO 80 K=1,N
NK=NK+N
L(K)=K
M(K)=K
KK=NK+K
BIGA=A(KK)
DO 20 J=K,N
IZ=N*(J-1)
DO 20 I=K,N
IJ=IZ+I
IF(ABS(BIGA)-ABS(A(IJ))) 15,20,20
15  BIGA=A(IJ)
L(K)=I
M(K)=J
20  CONTINUE
C

```

```

CCCCCCCCCCCCCCCCCCCCCCCCCCCC
C   INTERCHANGE ROWS C
CCCCCCCCCCCCCCCCCCCCCCCCCCCC
C
      J=L(K)
      IF(J-K) 35,35,25
25   KI=K-N
      DO 30 I=1,N
      KI=KI+N
      HOLD=-A(KI)
      JI=KI-K+J
      A(KI)=A(JI)
30   A(JI)=HOLD
C
CCCCCCCCCCCCCCCCCCCCCCCCCCCC
C   INTERCHANGE COLUMNS C
CCCCCCCCCCCCCCCCCCCCCCCCCCCC
C
35   I=M(K)
      IF(I-K) 45,45,38
38   JP=N*(I-1)
      DO 40 J=1,N
      JK=NK+J
      JI=JP+J
      HOLD=-A(JK)
      A(JK)=A(JI)
40   A(JI)=HOLD
C
CCCCCCCCCCCCCCCCCCCCCCCCCCCCCCCCCCCCCCCCCCCCCCCCCCCCCCCCCCCC
C   DIVIDE COLUMN BY MINUS PIVOT (VALUE OF PIVOT ELEMENT IS C
C   CONTAINED IN BIGA) C
CCCCCCCCCCCCCCCCCCCCCCCCCCCCCCCCCCCCCCCCCCCCCCCCCCCCCCCCCCCC
C
45   IF(BIGA) 48,46,48
46   D=0.0
      RETURN
48   DO 55 I=1,N
      IF(I-K) 50,55,50
50   IK=NK+I
      A(IK)=A(IK)/(-BIGA)
55   CONTINUE
C
CCCCCCCCCCCCCCCCCCCCCCCCCCCC
C   REDUCE MATRIX C
CCCCCCCCCCCCCCCCCCCCCCCCCCCC
C
      DO 65 I=1,N
      IK=NK+I
      HOLD=A(IK)
      IJ=I-N
      DO 65 J=1,N
      IJ=IJ+N
      IF(I-K) 60,65,60
60   IF(J-K) 62,65,62

```



```

62   KJ=IJ-I+K
      A(IJ)=HOLD*A(KJ)+A(IJ)
65   CONTINUE
C
CCCCCCCCCCCCCCCCCCCCCCCCCCCCCCCC
C   DIVIDE ROW BY PIVOT C
CCCCCCCCCCCCCCCCCCCCCCCCCCCCCCCC
C
      KJ=K-N
      DO 75 J=1,N
      KJ=KJ+N
      IF(J-K) 70,75,70
70   A(KJ)=A(KJ)/BIGA
75   CONTINUE
C
CCCCCCCCCCCCCCCCCCCCCCCCCCCCCCCC
C   PRODUCT OF PIVOTS C
CCCCCCCCCCCCCCCCCCCCCCCCCCCCCCCC
C
      D=D*BIGA
C
CCCCCCCCCCCCCCCCCCCCCCCCCCCCCCCC
C   REPLACE PIVOT BY RECIPROCAL C
CCCCCCCCCCCCCCCCCCCCCCCCCCCCCCCC
C
      A(KK)=1.0/BIGA
80   CONTINUE
C
CCCCCCCCCCCCCCCCCCCCCCCCCCCCCCCC
C   FINAL ROW AND COLUMN INTERCHANGE C
CCCCCCCCCCCCCCCCCCCCCCCCCCCCCCCC
C
      K=N
100  K=K-1
      IF(K) 150,150,105
105  I=L(K)
      IF(I-K) 120,120,108
108  JQ=N*(K-1)
      JR=N*(I-1)
      DO 110 J=1,N
      JK=JQ+J
      HOLD=A(JK)
      JI=JR+J
      A(JK)=-A(JI)
110  A(JI)=HOLD
120  J=M(K)
      IF(J-K) 100,100,125
125  KI=K-N
      DO 130 I=1,N
      KI=KI+N
      HOLD=A(KI)
      JI=KI-K+J
      A(KI)=-A(JI)
130  A(JI)=HOLD

```

```
GO TO 100  
150 RETURN  
END
```

```

SUBROUTINE MOMEN
C
CCCCCCCCCCCCCCCCCCCCCCCCCCCCCCCCCCCCCCCCCCCCCCCCCCCCCCCCCCCC
C   THE PURPOSE OF THIS ROUTINE IS TO CALCULATE THE      C
C   PARAMETERS M(I) APPEARING IN THE MOMENTUM EQUATION  C
CCCCCCCCCCCCCCCCCCCCCCCCCCCCCCCCCCCCCCCCCCCCCCCCCCCCCCCCCCCC
C
  REAL LW,KSEP,LR,LD,LTB,LP,MU,KC,LF,M,MFD,MR,MTB,
  IMTBC,MSD,MTOT,LT,MUP,LSAT,LSUB,KD
  DIMENSION RE(3),F(3)
  COMMON /GEOM/ KSEP,LR,LTB,LP,KC,ARI,ATB,ARO,G,
  IVR,VTB,DHTB,BETA(4),NSTG,CO,
  2AHT,RO,RI,VOP,VTBP,APT,VTM
  COMMON /DOME/ VSUB,VTOT,VG,VFO,LSAT,LSUB,VREF,LW,
  1LD,AD,VD,VSD,DHD,VT,LT,VSTM,DVG,ASH,R1,R2,R3,R4,
  2ZL1,ZL2,ZL3,ZLF
  COMMON /STEAM/ PSAT,TFW(2),TSAT,UL,HL(2),HFW(2),VGJ,MU(2),
  1HG,RL,RHOG,RHOF,DUG,UG,DRHOG,DUF,UF,DRHOF,DRLP,DRLU,
  2QB,POWER,PERP,HFG,RFW(2),DTSAT
  COMMON /FLOWS/ WO,WS(2),WFW(2),WF,WP,WR,WN,DINERT
  COMMON /TRANS/ VOID(3),XQ(3),RB(2),UB(2),DUP(2),DUA(2),DRP(2),
  1DRA,MFD(2),MR(2),MTB(2),MTBC(2),HR,HN,MSD,
  2MTOT(2),S(5),M(5),VP(3),R(9,5)
  COMMON /TIME/ T,DT,ITRAN,WFW,WSF, ITC,ICLK
  COMMON /DOWCO/ KD
C
CCCCCCCCCCCCCCCCCCCCCCCCCCCCCCCCCCCCCCCCCCCCCCCCCCCCCCCCCCCC
C   SUBSCRIPTS ON RE AND F MEAN      C
C   1 DOWNCOMER OUTLET                C
C   2 TUBE BUNDLE INLET                C
C   3 TUBE BUNDLE CROSSFLOW TRANSITION C
CCCCCCCCCCCCCCCCCCCCCCCCCCCCCCCCCCCCCCCCCCCCCCCCCCCCCCCCCCCC
C
  RE(1)=(WO*DHD)/(MU(1)*AD)
  RE(2)=(WO*DHTB)/(MU(1)*ATB)
  RE(3)=(WP*DHTB)/(MU(2)*ATB)
  DO 5 I=1,3
5   F(I)=0.184/(ABS(RE(I))*0.2)
C
CCCCCCCCCCCCCCCCCCCCCCCCCCCCCCCCCCCCCCCCCCCCCCCCCCCCCCCCCCCC
C   OBTAIN VPRIME IN TRANSIENT CALCULATION C
C   AND VAPOR VOLUME FRACTIONS IN STEADY  C
C   STATE CALCULATIONS                    C
CCCCCCCCCCCCCCCCCCCCCCCCCCCCCCCCCCCCCCCCCCCCCCCCCCCCCCCCCCCC
C
  CALL ALPHA
  AM11=(LP*F(2)*ABS(WO))/(4.0*DHTB*ATB**2)
  AM12=WO/ATB**2
  FRIC=LD
  IF(LW.LE.LD) FRIC=LW
  AM13=(F(1)*FRIC*ABS(WO))/(2.0*DHD*AD**2)
  AM14=((1.0/AD**2-1.0/ASH**2)/2.0)*WO
  AM15=(KD*WO)/(2.0*AD**2.0)
  M(1)=(AM11-AM12+AM13+AM14+AM15)/RL

```

```

AM21=(LP*F(3))/(4.0*DHTB*(ATB**2))+KC/2.0
AM22=VP(3)/(2.0*ATB)*WP*(1.0/ATB-1.0/ARI)
B=ABS(WP)/ATB
M(2)=AM21*PHILO(XQ(3),B)*ABS(WP)/RHOF+AM22
AM31=(VP(1)/(2.0*ARI))*(1.0/ATB-1.0/ARO)*WR
B=ABS(WR)/ARI
M(3)=KC*PHILO(XQ(1),B)*ABS(WR)/(2.0*RHOF)+AM31
M(4)=(VP(2)/(2.0*ARO))*(1.0/ARI+(KSEP+1.0)/ARO)*WN
AM51=LTB*RL*RB(1)*ALOG(RL/RB(1))/(RL-RB(1))+((LR/2.0)*(RB(1)+RB(2)))
AM52=LSAT*RHOF+RL*LSUB
M(5)=G*(AM51-AM52)
RETURN
END

```

SUBROUTINE NEWPR

```

C
CCCCCCCCCCCCCCCCCCCCCCCCCCCCCCCCCCCCCCCCCCCCCCCCCCCCCCCCCCCC
C   THE PURPOSE OF THIS ROUTINE IS TO CALCULATE:           C
C       1) TWO-PHASE PROPERTIES;                            C
C       2) QUALITIES GIVEN THE VAPOR VOLUME FRACTIONS      C
C           USING THE DRIFT FLUX MODEL;                     C
C       3) REGION MASSES;                                   C
C       4) VAPOR VOLUME IN THE STEAM DOME-DOWNCOMER        C
C           FOR LEVEL CALCULATION; AND,                     C
C       5) HEAT TRANSFER RATE.                              C
CCCCCCCCCCCCCCCCCCCCCCCCCCCCCCCCCCCCCCCCCCCCCCCCCCCCCCCCCCCC
C
   REAL LW,KSEP,LR,LD,LTB,LP,MU,KC,LF,M,MFD,MR,MTB,
   IMTBC,MSD,MTOT,LT,MUP,LSAT,LSUB,MCUT
   COMMON /GEOM/ KSEP,LR,LTB,LP,KC,ARI,ATB,ARO,G,
   IVR,VTB,DHTB,BETA(4),NSTG,CO,
   2AHT,RO,RI,VOP,VTBP,APT,VTM
   COMMON /DOME/ VSUB,VTOT,VG,VFO,LSAT,LSUB,VREF,LW,
   1LD,AD,VD,VSD,DHD,VT,LT,VSTM,DVG,ASW,R1,R2,R3,R4,
   2ZL1,ZL2,ZL3,ZLF
   COMMON /STEAM/ PSAT,TFW(2),TSAT,UL,HL(2),HFW(2),VGJ,MU(2),
   1HG,RL,RHOG,RHOF,DUG,UG,DRHOG,DUF,UF,DRHOF,DRLP,DRLU,
   2QB,POWER,PERP,HFG,RFW(2),DTSAT
   COMMON /FLOWS/ WO,WS(2),MFW(2),WF,WP,WR,WN,DINERT
   COMMON /TRANS/ VOID(3),XQ(3),RB(2),UB(2),DUP(2),DUA(2),DRP(2),
   1DRA,MFD(2),MR(2),MTB(2),MTBC(2),HR,HN,MSD,
   2MTOT(2),S(5),M(5),VP(3),R(9,5)
   COMMON /TIME/ T,DT,I TRAN,WFW,WSF, ITC,ICLK
   COMMON /PRIME/ PPRIM,TLMTD,UO,TP(3),HP(3),RP(3),UP(3),DRPT(3),
   1DUPT(3),TPIN(2),HPIN(2),WPIN(2),MUP,CPL,TKL,CPT
   COMMON /HTS/ HPR,HS,RTUBE,RFOUL
   COMMON /AVE/ WBAR
   DRA=RHOG-RHOF
C
CCCCCCCCCCCCCCCCCCCCCCCCCCCCCCCCCCCCCCCCCCCCCCCCCCCCCCCCCCCC
C   CALCULATE RHOBAR AND UBAR, AND THEIR DERIVATIVES      C
CCCCCCCCCCCCCCCCCCCCCCCCCCCCCCCCCCCCCCCCCCCCCCCCCCCCCCCCCCCC
C
   DO 5 I=1,2
   RB(I)=VOID(I)*RHOG+(1.0-VOID(I))*RHOF
   UB(I)=(VOID(I)*UG*RHOG+(1.0-VOID(I))*UF*RHOF)/RB(I)
   DUA(I)=(RHOG*UG-RHOF*UF-DRA*UB(I))/RB(I)
   DRP(I)=VOID(I)*DRHOG+(1.0-VOID(I))*DRHOF
   A=VOID(I)*(UG*DRHOG+RHOG*DUG)
   B=(1.0-VOID(I))*(RHOF*DUF+UF*DRHOF)
5   DUP(I)=(A+B-UB(I)*DRP(I))/RB(I)
C
CCCCCCCCCCCCCCCCCCCCCCCCCCCCCCCCCCCCCCCCCCCCCCCCCCCCCCCCCCCC
C   CALCULATE QUALITIES C
CCCCCCCCCCCCCCCCCCCCCCCCCCCCCCCCCCCCCCCCCCCCCCCCCCCCCCCCCCCC
C
   RAT=RHOG/RHOF
   X1=CO*RAT+RHOG*ARI*VGJ/WR

```

```

X2=CO*(1.0-RAT)
XQ(1)=(VOID(1)*X1)/(1.0-VOID(1)*X2)
X3=CO*RAT+RHOG*ARO*VGJ/WN
XQ(2)=(VOID(2)*X3)/(1.0-VOID(2)*X2)
HR=HL(2)+XQ(1)*HFG
HN=HL(2)+XQ(2)*HFG
RBP=1.0/(1.0/RL +(1.0/RB(1)-1.0/RL )*LP/LTB)
VOID(3)=(RHOF-RBP)/(RHOF-RHOG)
X4=CO*RAT+RHOG*ATB*VGJ/WP
XQ(3)=(VOID(3)*X4)/(1.0-VOID(3)*X2)
C
CCCCCCCCCCCCCCCCCCCCCCCCCCCC
C   CALCULATE MASSES   C
CCCCCCCCCCCCCCCCCCCCCCCCCCCC
C
IF(ITRAN.NE.1) GO TO 10
MR(1)=MR(2)
MTB(1)=MTB(2)
MTBC(1)=MTBC(2)
10 CONTINUE
MR(2)=(VR/2.0)*(RB(1)+RB(2))
C=RL/RB(1)
D=RBP/RB(1)
MTB(2)=VTB*RB(1)*RL*ALOG(C)/(RL-RB(1))
MTBC(2)=MTB(2)*ALOG(D)/ALOG(C)
IF(ITRAN.EQ.1) GO TO 15
C
CCCCCCCCCCCCCCCCCCCCCCCCCCCCCCCCCCCCCCCCCCCCCCCCCCCCCCCCCCCC
C   INITIALIZE INERTANCE, WBAR, STEAM DOME-   C
C   DOWNCOMER MASS, AND TOTAL MASS.           C
CCCCCCCCCCCCCCCCCCCCCCCCCCCCCCCCCCCCCCCCCCCCCCCCCCCCCCCCCCCC
C
B1=(LW-LD)*(1.0/ASH-1.0/AD)/2.0
B2=LD/AD+LP/(2.0*ATB)
BETA(1)=B1+B2
DINERT=BETA(1)+BETA(2)+BETA(3)+BETA(4)
WBAR=(BETA(1)*WO+BETA(2)*WP+BETA(3)*WR+BETA(4)*WN)/DINERT
DVG=0.0
VSUB=VT
MSD=(VG+VSTM)*RHOG+(VSD-VG)*RHOF+VT*RL
MTOT(2)=MR(2)+MTB(2)+MSD
GO TO 60
15 CONTINUE
MTOT(1)=MTOT(2)
MTOT(2)=MTOT(1)+(MFW(2)-WS(2))*DT
C
CCCCCCCCCCCCCCCCCCCCCCCCCCCCCCCCCCCCCCCCCCCCCCCCCCCCCCCCCCCC
C   CALCULATE STEAM DOME-DOWNCOMER MASS   C
CCCCCCCCCCCCCCCCCCCCCCCCCCCCCCCCCCCCCCCCCCCCCCCCCCCCCCCCCCCC
C
MSD=MTOT(2)-MTB(2)-MR(2)
C
CCCCCCCCCCCCCCCCCCCCCCCCCCCCCCCCCCCCCCCCCCCCCCCCCCCCCCCCCCCC
C   CALCULATE VAPOR VOLUME IN STEAM DOME-DOWNCOMER   C

```

```

CCCCCCCCCCCCCCCCCCCCCCCCCCCCCCCCCCCCCCCCCCCCCCCCCCCCCCCCCCCC
C
      MCUT=(VREF+VSTM)*RHOG+VFO*RHOF+VT*RL
      VG1=VG
      IF(MSD.GE.MCUT) GO TO 16
      VG=(VSTM*RHOG+VFO*RHOF+(VTOT-VFO)*RL-MSD)/(RL-RHOG)
      DVG=(VG-VG1)/DT
      VSUB=VTOT-VG-VFO
      GO TO 17
16     VG=(VSD*RHOF+VT*RL+VSTM*RHOG-MSD)/(RHOF-RHOG)
      VSUB=VT
      DVG=(VG-VG1)/DT
C
CCCCCCCCCCCCCCCCCCCCCCCCCCCCCCCCCCCCCCCCCCCCCCCCCCCCCCCCCCCC
C   CALCULATE LEVEL FROM VAPOR VOLUME   C
CCCCCCCCCCCCCCCCCCCCCCCCCCCCCCCCCCCCCCCCCCCCCCCCCCCCCCCCCCCC
C
17     CALL LEVEL
      ENTRY NEWPR1
C
CCCCCCCCCCCCCCCCCCCCCCCCCCCCCCCCCCCCCCCCCCCCCCCCCCCCCCCCCCCC
C   CALCULATE TUBE METAL PROPERTIES   C
CCCCCCCCCCCCCCCCCCCCCCCCCCCCCCCCCCCCCCCCCCCCCCCCCCCCCCCCCCCC
C
60     TTUBE=TLMTD/2.0+TSAT
      TK=0.016*TTUBE+9.632
      CPT=(1.3677E03)*TTUBE+3.3663E06
C
CCCCCCCCCCCCCCCCCCCCCCCCCCCCCCCCCCCCCCCCCCCCCCCCCCCCCCCCCCCC
C   CALCULATE REYNOLDS AND PRANDTL NUMBERS FOR   C
C   PRIMARY FLOW                               C
CCCCCCCCCCCCCCCCCCCCCCCCCCCCCCCCCCCCCCCCCCCCCCCCCCCCCCCCCCCC
C
      RE=(WPI*(2)*2.0*RI)/(MUP*APT)
      PR=MUP*CPL/TKL
      P=PSAT/1.0E05
      D=AHT*TLMTD
C
CCCCCCCCCCCCCCCCCCCCCCCCCCCCCCCCCCCCCCCCCCCCCCCCCCCCCCCCCCCC
C   CALCULATE PRIMARY HEAT TRANSFER COEFFICIENT   C
CCCCCCCCCCCCCCCCCCCCCCCCCCCCCCCCCCCCCCCCCCCCCCCCCCCCCCCCCCCC
C
      HPR=(0.023)*(RE**0.8)*(PR**0.4)*TKL/(2.0*RI)
      IF(ITRAN.EQ.1)GO TO 40
C
CCCCCCCCCCCCCCCCCCCCCCCCCCCCCCCCCCCCCCCCCCCCCCCCCCCCCCCCCCCC
C   STEADY STATE HEAT TRANSFER PARAMETERS   C
CCCCCCCCCCCCCCCCCCCCCCCCCCCCCCCCCCCCCCCCCCCCCCCCCCCCCCCCCCCC
C
      RTUBE=RO*ALOG(RO/RI)/TK
      QF=(QB/AHT)/1.0E06
      DTS=22.65*SQRT(QF)*EXP(-P/87.0)
      HS=(QF/DTS)*1.0E06
      GO TO 50

```

```

C
CCCCCCCCCCCCCCCCCCCCCCCCCCCCCCCCCCCCCCCCCCCCCCCCCCCCCCCC
C   CALCULATE TRANSIENT HEAT TRANSFER RATE C
CCCCCCCCCCCCCCCCCCCCCCCCCCCCCCCCCCCCCCCCCCCCCCCCCCCCCCCC
C
40  B=RO/(RI*HPR)+(RO*ALOG(RO/RI)/TK)+RFOUL
    C=22.65*((AHT/1.0E06)**0.5)*EXP(-P/87.0)
    F=C**2.0+4.0*B*D
    SQB=(SQRT(F)-C)/(2.0*B)
    QB=SQB**2.0
50  CONTINUE
    RETURN
    END

```



```

SUBROUTINE OUT
C
CCCCCCCCCCCCCCCCCCCCCCCCCCCCCCCCCCCCCCCCCCCCCCCCCCCCCCCCCCCC
C   THIS SUBROUTINE WRITES OUT THE STEADY STATE CONDITIONS   C
C   CALCULATED BY THE CODE                                     C
CCCCCCCCCCCCCCCCCCCCCCCCCCCCCCCCCCCCCCCCCCCCCCCCCCCCCCCCCCCC
C
  REAL LW,KSEP,LR,LD,LTB,LP,MU,KC,LF,M,MFD,MR,MTB,
  1MTBC,MSD,MTOT,LT,MUP,LSAT,LSUB
  COMMON /STEAM/ PSAT,TFW(2),TSAT,UL,HL(2),HFW(2),VGJ,MU(2),
  1HG,RL,RHOG,RHOF,DUG,UG,DRHOG,DUF,UF,DRHOF,DRLP,DRLU,
  2QB,POWER,PERP,HFG,RFW(2),DTSAT
  COMMON /FLCWS/ WO,WS(2),WFW(2),WF,WP,WR,WN,DINERT
  COMMON /TRANS/ VOID(3),XQ(3),RB(2),UB(2),DUP(2),DUA(2),DRP(2),
  1DRA,MFD(2),MR(2),MTB(2),MTBC(2),HR,HN,MSD,
  2MTOT(2),S(5),M(5),VP(3),R(9,5)
  COMMON /TIME/ T,DT,ITRAN,WFWF,WSF, ITC,ICLK
  COMMON /PRIME/ PPRIM,TLMTD,UO,TP(3),HP(3),RP(3),UP(3),DRPT(3),
  1DUPT(3),TPIN(2),HPIN(2),WPIN(2),MUP,CPL,TKL,CPT
  COMMON /HTS/ HPR,HS,RTUBE,RFOUL
  WRITE(6,100) WO
C
CCCCCCCCCCCCCCCCCCCCCCCCCCCCCCCCCCCCCCCCCCCCCCCCCCCCCCCCCCCC
C   ALL TEMPERATURES ARE CONVERTED TO DEGREES CELSIUS AND   C
C   THE SECONDARY PRESSURE IS CONVERTED TO MEGAPASCAL       C
CCCCCCCCCCCCCCCCCCCCCCCCCCCCCCCCCCCCCCCCCCCCCCCCCCCCCCCCCCCC
C
  TSATC=TSAT-273.15
  WRITE(6,110) TSATC
  PSATM=PSAT/(1.0E06)
  WRITE(6,120) PSATM
  WRITE(6,130) WS(1)
  WRITE(6,140) XQ(1)
  WRITE(6,150) MTOT(2)
  TFWC=TFW(1)-273.15
  WRITE(6,160) TFWC
  TC1=TPIN(1)-273.15
  TC2=TP(3)-273.15
  WRITE(6,170) TC1
  WRITE(6,180) TC2
  WRITE(6,190) MPIN(2)
  WRITE(6,200) RFOUL
100  FORMAT('-', 'DOWNCOMER FLOWRATE IS',E12.4,1X,'KG/SEC')
110  FORMAT(' ', 'STEAM TEMPERATURE IS',E12.4,1X,'C')
120  FORMAT(' ', 'STEAM PRESSURE IS',E12.4,1X,'MPA')
130  FORMAT(' ', 'STEAM FLOW IS',E12.4,1X,'KG/SEC')
140  FORMAT(' ', 'RISER QUALITY IS',E12.4)
150  FORMAT(' ', 'STEAM GENERATOR MASS CONTENT IS',E12.4,1X,'KG')
160  FORMAT(' ', 'FEEDWATER TEMPERATURE IS',E12.4,1X,'C')
170  FORMAT(' ', 'PRIMARY INLET TEMPERATURE IS',E12.4,1X,'C')
180  FORMAT(' ', 'PRIMARY OUTLET TEMPERATURE IS',E12.4,1X,'C')
190  FORMAT(' ', 'PRIMARY FLOWRATE IS',E12.4,1X,'KG/SEC')
200  FORMAT(' ', 'FOULING FACTOR IS',E12.4,1X,'M**2-K/WATT')
RETURN

```

**END**

SUBROUTINE OUT1

```

C
CCCCCCCCCCCCCCCCCCCCCCCCCCCCCCCCCCCCCCCCCCCCCCCCCCCCCCCCCCCC
C   THIS ROUTINE WRITES OUT STEADY STATE HEADING C
CCCCCCCCCCCCCCCCCCCCCCCCCCCCCCCCCCCCCCCCCCCCCCCCCCCCCCCCCCCC
C
      REAL LW,KSEP,LR,LD,LTB,LP,MU,KC,LF,M,MFD,MR,MTB,
      1MTBC,MSD,MTOT,LT,MUP,LSAT,LSUB
      COMMON /GEOM/ KSEP,LR,LTB,LP,KC,ARI,ATB,ARO,G,
      1VR,VTB,DHTB,BETA(4),NSTG,C0,
      2AHT,RO,RI,VOP,VTBP,APT,VTH
      COMMON /DOME/ VSUB,VTOT,VG,VFO,LSAT,LSUB,VREF,LW,
      1LD,AD,VD,VSD,DHD,VT,LT,VSTM,DVG,ASW,R1,R2,R3,R4,
      2ZL1,ZL2,ZL3,ZLF
      COMMON /STEAM/ PSAT,TFW(2),TSAT,UL,HL(2),HFW(2),VGJ,MU(2),
      1HG,RL,RHOG,RHOF,DUG,UG,DRHOG,DUF,UF,DRHOF,DRLP,DRLU,
      2QB,POWER,PERP,HFG,RFW(2),DTSAT
      COMMON /FLOWS/ WO,WS(2),WFW(2),WF,WP,WR,WN,DINERT
      COMMON /TRANS/ VOID(3),XQ(3),RB(2),UB(2),DUP(2),DUA(2),DRP(2),
      1DRA,MFD(2),MR(2),MTB(2),MTBC(2),HR,HN,MSD,
      2MTOT(2),S(5),M(5),VP(3),R(9,5)
      QPOWER=POWER/(1.0E 06)
      WRITE(6,100) QPOWER
100  FORMAT('-', 'TOTAL REACTOR POWER IS',E12.4,1X,'MWT')
      WRITE(6,120) NSTG
120  FORMAT(' ', 'NUMBER OF STEAM GENERATORS',3X,I1)
      WRITE(6,130) LW
130  FORMAT(' ', 'STEADY STATE WATER LEVEL IS',E12.4,1X,'METERS')
      SPOWER=QPOWER*PERP/NSTG
      IF(PERP.GT.1.0) SPOWER=QPOWER/NSTG
      WRITE(6,140) SPOWER
140  FORMAT(' ', 'STEADY STATE POWER LEVEL IS',E12.4,1X,'MWT PER')
      P=PERP*100.0
      WRITE(6,150) P
150  FORMAT(' ', 'STEAM GENERATOR OR',E12.4,1X,'PER CENT RATED ',
      1'FULL POWER')
      WRITE(6,160)
160  FORMAT('-', '25X, 'STEADY STATE CONDITIONS')
      RETURN
      END

```

SUBROUTINE PDERIV

```

C
CCCCCCCCCCCCCCCCCCCCCCCCCCCCCCCCCCCCCCCCCCCCCCCCCCCCCCCCCCCC
C   THE PURPOSE OF THIS SUBROUTINE IS TO CALCULATE C
C   PRIMARY SIDE TIME DERIVATIVES AND THEN TO UPDATE C
C   PRIMARY SIDE PROPERTIES BY CALLING PRMPRO C
CCCCCCCCCCCCCCCCCCCCCCCCCCCCCCCCCCCCCCCCCCCCCCCCCCCCCCCCCCCC
C
      DIMENSION RA(3),CA(3),DTP(3)
      REAL LW,KSEP,LR,LD,LTB,LP,MU,KC,LF,M,MFD,MR,MTB,
      INTBC,MSD,MTOT,LT,MUP,LSAT,LSUB
      COMMON /GEOM/ KSEP,LR,LTB,LP,KC,ARI,ATB,ARO,G,
      IVR,VTB,DHTB,BETA(4),NSTG,CO,
      2AHT,RO,RI,VOP,VTBP,APT,VTM
      COMMON /DOME/ VSUB,VTOT,VG,VFO,LSAT,LSUB,VREF,LW,
      1LD,AD,VD,VSD,DHD,VT,LT,VSTM,DVG,ASH,R1,R2,R3,R4,
      2ZL1,ZL2,ZL3,ZLF
      COMMON /STEAM/ PSAT,TFW(2),TSAT,UL,HL(2),HFW(2),VGJ,MU(2),
      IHG,RL,RHOG,RHOF,DUG,UG,DRHOG,DUF,UF,DRHOF,DRLP,DRLU,
      2QB,POWER,PERP,HFG,RFW(2),DTSAT
      COMMON /TIME/ T,DT,ITRAN,WFWF,WSF, ITC,ICLK
      COMMON /PRIME/ PPRIM,TLMTD,UO,TP(3),HP(3),RP(3),UP(3),DRPT(3),
      IDUPT(3),TPIN(2),HPIN(2),WPIN(2),MUP,CPL,TKL,CPT
      DATA EPS/1.0/
      RA(1)=VOP*(RP(1)*DUPT(1)+(UP(1)-(HPIN(1)+HP(1))/2.0)*DRPT(1))
      RA(2)=VTBP*(RP(2)*DUPT(2)+(UP(2)-(HP(2)+HP(1))/2.0)*DRPT(2))+
      IVTM*CPT/2.0
      RA(3)=VOP*(RP(3)*DUPT(3)+(UP(3)-(HP(3)+HP(2))/2.0)*DRPT(3))
C
CCCCCCCCCCCCCCCCCCCCCCCCCCCCCCCCCCCCCCCCCCCCCCCCCCCCCCCCCCCC
C   USE HPIN(2) IN FOLLOWING EQUATION BECAUSE WE HAVE C
C   NOT YET UPDATED HPIN(I) TO CORRESPOND TO C
C   CURRENT VALUES OF TPIN(I) C
CCCCCCCCCCCCCCCCCCCCCCCCCCCCCCCCCCCCCCCCCCCCCCCCCCCCCCCCCCCC
C
      CA(1)=WPIN(1)*(HPIN(2)-HP(1))
      CA(2)=WPIN(1)*(HP(1)-HP(2))-QB
      CA(3)=WPIN(1)*(HP(2)-HP(3))
      DO 5 I=1,3
      DTP(I)=CA(I)/RA(I)
      5 TP(I)=TP(I)+DTP(I)*DT
C
CCCCCCCCCCCCCCCCCCCCCCCCCCCCCCCCCCCCCCCCCCCCCCCCCCCCCCCCCCCC
C   UPDATE PRIMARY PROPERTIES C
CCCCCCCCCCCCCCCCCCCCCCCCCCCCCCCCCCCCCCCCCCCCCCCCCCCCCCCCCCCC
C
      CALL PRMPRO
C
CCCCCCCCCCCCCCCCCCCCCCCCCCCCCCCCCCCCCCCCCCCCCCCCCCCCCCCCCCCC
C   CALCULATE LOG-MEAN TEMPERATURE DIFFERENCE AND C
C   CHECK THAT TCOLD MINUS TSAT IS POSITIVE. IF NOT C
C   APPROXIMATE MEAN TEMPERATURE DIFFERENCE C
CCCCCCCCCCCCCCCCCCCCCCCCCCCCCCCCCCCCCCCCCCCCCCCCCCCCCCCCCCCC
C

```

```
DELT=TP(2)-TSAT
IF(DELT.LE.EPS) GO TO 10
TD=(TP(1)-TSAT)/DELT
TLMTD=(TP(1)-TP(2))/ALOG(TD)
RETURN
10 TH=TP(1)-TSAT
TLN=(TP(1)-TSAT-EPS)/ALOG(TH/EPS)
FAC=(TLN-EPS)/(TP(1)-TSAT-EPS)
TLMTD=FAC*TH+(1.0-FAC)*DELT
RETURN
END
```



SUBROUTINE PRMPRO

C  
 CCC  
 C THE PURPOSE OF THIS ROUTINE IS TO EVALUATE THE PROPERTIES C  
 C OF THE SUBCOOLED PRIMARY FLUID. THE INPUTS ARE THE PRIMARY C  
 C PRESSURE, PPRIM, AND TEMPERATURES, TP(I). THIS ROUTINE IS C  
 C ALSO USED TO DETERMINE PROPERTIES OF THE SUBCOOLED FEED- C  
 C WATER. FITS ARE TAKEN FROM THERMIT. C  
 CCC

C  
 REAL LM,KSEP,LR,LD,LTB,LP,MU,KC,LF,M,MFD,MR,MTB,  
 IMTBC,MSD,MTOT,LT,MJP,LSAT,LSUB  
 DIMENSION UFW(2),RPIN(2),UPIN(2)  
 COMMON /STEAM/ PSAT,TFW(2),TSAT,UL,HL(2),HFW(2),VGJ,MU(2),  
 IHG,RL,RHOG,RHOF,DUG,UG,DRHOG,DUF,UF,DRHOF,DRLP,DRLU,  
 2QB,POWER,PERP,HFG,RFW(2),DTSAT  
 COMMON /TIME/ T,DT,ITRAN,WFWF,WSF, ITC,ICLK  
 COMMON /PRIME/ PPRIM,TLMTD,UO,TP(3),HP(3),RP(3),UP(3),DRPT(3),  
 IDUPT(3),TPIN(2),HPIN(2),WPIN(2),MJP,CPL,TKL,CPT  
 DATA SL0,SL1,SL2,SL3,SL4 /-460.26818E03,-2.864305E03,27.450693,  
 1 -4.810832E-02,3.205932E-05/  
 DATA SH0,SH1,SH2,SH3,SH4 /1.242646E09,-8.608225E06,2.236456E04,  
 1 -2.581596E01,1.117877E-02/  
 DATA D1/-1.836607E-04/,D2/7.567076E-05/,D3/-1.647879E-05/  
 DATA D4/1.416458E-06/,H00/3.892077E-06/,D0/3.026032E-04/  
 DATA PR/6.894575E05/  
 DATA E0/1.452605E-03/,E1/-6.988009E-09/,E2/1.521023E-14/  
 DATA E3/-1.23032E-20/,F0/-3.806351E-11/,F1/3.928521E-16/  
 DATA F2/-1.25858E-21/,F3/1.286018E-27/,B0L/2.394907E-04/  
 DATA B1L/-5.19625E-13/,C0L/1.193203E-11/,C1L/2.412704E-18/  
 DATA D0L/-3.944067E-17/,D1L/-1.680771E-24/,TK1/0.686/  
 DATA TK2/-5.87E-06/,TREF/415.0/,TK3/7.3E-10/  
 DATA RL0,RL1,RL2,RL3 /1735.332,-4.640684,  
 1 1.043109E-02,-9.436709E-06/  
 DATA RHO,RH1,RH2,RH3,RH4 /-1.175598E06,8.143736E03,  
 1 -2.113656E01,2.43816E-02,-1.054975E-05/  
 DATA RP0,RP1,RP2 /-14.64389,1.128336E-03,1.267037E-02/  
 DATA SP0,SP1,SP2,SP3 /-42.0218,0.2116,-4.4587E-04,3.251E-07/  
 IF(ITRAN.EQ.1) GO TO 10

C  
 CCC  
 C STEADY STATE CALCULATIONS. C  
 C NOTATION: UP-INTERNAL ENERGY C  
 C RP-DENSITY C  
 C HP-ENTHALPY C  
 CCC

C  
 IF(ITC.NE.1) GO TO 10  
 DO 6 I=1,2  
 DP=PPRIM-15.0E06  
 DELDP=-EXP(SP0+TP(I))\*(SP1+TP(I))\*(SP2+TP(I)\*SP3))  
 DRLDP=EXP(RP0+RP1\*EXP(RP2\*TP(I)))  
 DEL=DELDP\*DP  
 DRL=DRLDP\*DP

```

IF(TP(I).GT.576.5) GO TO 5
UP(I)=SL0+TP(I)*(SL1+TP(I)*(SL2+TP(I)*(SL3+TP(I)*SL4)))+DEL
RP(I)=RL0+TP(I)*(RL1+TP(I)*(RL2+TP(I)*RL3))+DRL
GO TO 6
5 UP(I)=SH0+TP(I)*(SH1+TP(I)*(SH2+TP(I)*(SH3+TP(I)*SH4)))+DEL
RP(I)=RH0+TP(I)*(RH1+TP(I)*(RH2+TP(I)*(RH3+TP(I)*RH4)))+DRL
6 HP(I)=UP(I)+PPRIM/RP(I)
RETURN
10 CONTINUE
C
CCCCCCCCCCCCCCCCCCCCCCCCCCCCCCCCCCCC
C TRANSIENT CALCULATION. C
CCCCCCCCCCCCCCCCCCCCCCCCCCCCCCCCCCCC
C
DP=PPRIM-15.0E06
DO 11 I=1,2
DELDP=-EXP(SP0+TPIN(I))*(SP1+TPIN(I))*(SP2+TPIN(I)*SP3))
DRLDP=EXP(RP0+RP1*EXP(RP2*TPIN(I)))
DEL=DELDP*DP
DRL=DRLDP*DP
IF(TPIN(I).GT.576.5) GO TO 14
UPIN(I)=SL0+TPIN(I)*(SL1+TPIN(I)*(SL2+TPIN(I)*(SL3+TPIN(I)*SL4))
)+DEL
RPIN(I)=RL0+TPIN(I)*(RL1+TPIN(I)*(RL2+TPIN(I)*RL3))+DRL
GO TO 11
14 UPIN(I)=SH0+TPIN(I)*(SH1+TPIN(I)*(SH2+TPIN(I)*(SH3+TPIN(I)*SH4))
)+DEL
RPIN(I)=RH0+TPIN(I)*(RH1+TPIN(I)*(RH2+TPIN(I)*(RH3+TPIN(I)*RH4))
)+DRL
11 HPIN(I)=UPIN(I)+PPRIM/RPIN(I)
DO 20 I=1,3
DELDP=-EXP(SP0+TP(I))*(SP1+TP(I)*(SP2+TP(I)*SP3))
DRLDP=EXP(RP0+RP1*EXP(RP2*TP(I)))
DEL=DELDP*DP
DRL=DRLDP*DP
IF(TP(I).GT.576.5) GO TO 15
UP(I)=SL0+TP(I)*(SL1+TP(I)*(SL2+TP(I)*(SL3+TP(I)*SL4)))+DEL
DUPT(I)=SL1+TP(I)*(2.0*SL2+TP(I)*(3.0*SL3+4.0*TP(I)*SL4))
+DEL*(SP1+TP(I)*(2.0*SP2+3.0*SP3*TP(I)))
RP(I)=RL0+TP(I)*(RL1+TP(I)*(RL2+TP(I)*RL3))+DRL
DRPT(I)=RL1+TP(I)*(2.0*RL2+TP(I)*3.0*RL3)+DRL*RP1*RP2
+DEL*EXP(RP2*TP(I))
GO TO 20
15 UP(I)=SH0+TP(I)*(SH1+TP(I)*(SH2+TP(I)*(SH3+TP(I)*SH4)))+DEL
DUPT(I)=SH1+TP(I)*(2.0*SH2+TP(I)*(3.0*SH3+4.0*TP(I)*SH4))
+DEL*(SP1+TP(I)*(2.0*SP2+3.0*SP3*TP(I)))
RP(I)=RH0+TP(I)*(RH1+TP(I)*(RH2+TP(I)*(RH3+TP(I)*RH4)))+DRL
DRPT(I)=RH1+TP(I)*(2.0*RH2+TP(I)*(3.0*RH3+TP(I)*4.0*RH4))
+DRL*RP1*RP2*EXP(RP2*TP(I))
20 HP(I)=UP(I)+PPRIM/RP(I)
Y=HP(2)*(D0L+D1L*PPRIM)+C0L+C1L*PPRIM
C
CCCCCCCCCCCCCCCCCCCCCCCCCCCCCCCCCCCC
C CALCULATE SUBCOOLED LIQUID HEAT CAPACITY, CPL. C

```



```

CCCCCCCCCCCCCCCCCCCCCCCCCCCCCCCCCCCCCCCCCCCCCCCCCCCCCCCCCCCC
C
      CPL=1.0/(HP(2)*Y+B0L+B1L*PPRIM)
C
CCCCCCCCCCCCCCCCCCCCCCCCCCCCCCCCCCCCCCCCCCCCCCCCCCCCCCCCCCCC
C   CALCULATE SUBCOOLED LIQUID THERMAL CONDUCTIVITY, TKL. C
CCCCCCCCCCCCCCCCCCCCCCCCCCCCCCCCCCCCCCCCCCCCCCCCCCCCCCCCCCCC
C
      TKL=TK1+TK2*(TP(2)-TREF)**2.0+TK3*PPRIM
C
CCCCCCCCCCCCCCCCCCCCCCCCCCCCCCCCCCCCCCCCCCCCCCCCCCCCCCCCCCCC
C   CALCULATE SUBCOOLED LIQUID VISCOSITY, MUP. C
CCCCCCCCCCCCCCCCCCCCCCCCCCCCCCCCCCCCCCCCCCCCCCCCCCCCCCCCCCCC
C
      IF(HP(2).GE.3.94E05) GO TO 30
      E=E0+E1*HP(2)+E2*(HP(2)**2.0)+E3*(HP(2)**3.0)
      F=F0+F1*HP(2)+F2*(HP(2)**2.0)+F3*(HP(2)**3.0)
      MUP=E-F*(PPRIM-PR)
      GO TO 40
30   Z=(HP(2)-401467.1)*H00
      MUP=D0+D1*Z+D2*(Z**2)+D3*(Z**3)+D4*(Z**4)
40   CONTINUE
      RETURN
      ENTRY PRMPRI
C
CCCCCCCCCCCCCCCCCCCCCCCCCCCCCCCCCCCCCCCCCCCCCCCCCCCCCCCCCCCC
C   SUBCOOLED FEEDWATER CALCULATION. C
CCCCCCCCCCCCCCCCCCCCCCCCCCCCCCCCCCCCCCCCCCCCCCCCCCCCCCCCCCCC
C
      DO 46 I=1,2
      DP=PSAT-15.0E06
      DELDP=-EXP(SP0+TFW(I))*(SP1+TFW(I))*(SP2+TFW(I)*SP3)))
      DRLDP=EXP(RP0+RP1*EXP(RP2*TFW(I)))
      DEL=DELDP*DP
      DRL=DRLDP*DP
      IF(TFW(I).GT.576.5) GO TO 45
      UFW(I)=SL0+TFW(I)*(SL1+TFW(I)*(SL2+TFW(I)*(SL3+TFW(I)*SL4)))+DEL
      RFW(I)=RL0+TFW(I)*(RL1+TFW(I)*(RL2+TFW(I)*RL3))+DRL
      GO TO 46
45   UFW(I)=SH0+TFW(I)*(SH1+TFW(I)*(SH2+TFW(I)*(SH3+TFW(I)*SH4)))+DEL
      RFW(I)=RH0+TFW(I)*(RH1+TFW(I)*(RH2+TFW(I)*(RH3+TFW(I)*RH4)))+DRL
46   HFW(I)=UFW(I)+PSAT/RFW(I)
      RETURN
      END

```

SUBROUTINE STEADY

```
C
CCCCCCCCCCCCCCCCCCCCCCCCCCCCCCCCCCCCCCCCCCCCCCCCCCCCCCCCCCCC
C   THIS ROUTINE DRIVES THE STEADY-STATE CALCULATION C
CCCCCCCCCCCCCCCCCCCCCCCCCCCCCCCCCCCCCCCCCCCCCCCCCCCCCCCCCCCC
C
    REAL LW,KSEP,LR,LD,LTB,LP,MU,KC,LF,M,MFD,MR,MTB,
    1MTBC,MSD,MTOT,LT,MUP,LSAT,LSUB,KD
    COMMON /GEOM/ KSEP,LR,LTB,LP,KC,ARI,ATB,ARO,G,
    1VR,VTB,DHTB,BETA(4),NSTG,CO,
    2AHT,RO,RI,VOP,VTBP,APT,VTM
    COMMON /DOME/ VSUB,VTOT,VG,VFO,LSAT,LSUB,VREF,LW,
    1LD,AD,VD,VSD,DHD,VT,LT,VSTM,DVG,ASW,R1,R2,R3,R4,
    2ZL1,ZL2,ZL3,ZLF
    COMMON /STEAM/ PSAT,TFW(2),TSAT,UL,HL(2),HFW(2),VGJ,MU(2),
    1HG,RL,RHOG,RHOF,DUG,UG,DRHOG,DUF,UF,DRHOF,DRLP,DRLU,
    2QB,POWER,PERP,HFG,RFW(2),DTSAT
    COMMON /FLOWS/ WQ,WS(2),WFW(2),WF,WP,WR,WN,DINERT
    COMMON /TRANS/ VOID(3),XQ(3),RB(2),UB(2),DUP(2),DUA(2),DRP(2),
    1DRA,MFD(2),MR(2),MTB(2),MTBC(2),HR,HN,MSD,
    2MTOT(2),S(5),M(5),VP(3),R(9,5)
    COMMON /TIME/ T,DT,ITRAN,WFWF,WSF, ITC,ICLK
    COMMON /PRIME/ PPRIM,TLMTD,UO,TP(3),HP(3),RP(3),UP(3),DRPT(3),
    1DUPT(3),TPIN(2),HPIN(2),WPIN(2),MUP,CPL,TKL,CPT
    COMMON /HTS/ HPR,HS,RTUBE,RFOUL
    COMMON /DOWCO/ KD
    COMMON /AVE/ WBAR
C
CCCCCCCCCCCCCCCCCCCCCCCCCCCCCCCCCCCCCCCCCCCCCCCCCCCCCCCCCCCC
C   READ IN STEADY-STATE OPERATING LEVEL C
CCCCCCCCCCCCCCCCCCCCCCCCCCCCCCCCCCCCCCCCCCCCCCCCCCCCCCCCCCCC
C
    READ(5,120) LW
C
CCCCCCCCCCCCCCCCCCCCCCCCCCCCCCCCCCCCCCCCCCCCCCCCCCCCCCCCCCCC
C   INITIALIZE STEAM DOME-DOWNCOMER GEOMETRY C
CCCCCCCCCCCCCCCCCCCCCCCCCCCCCCCCCCCCCCCCCCCCCCCCCCCCCCCCCCCC
C
    CALL LEVEL
C
CCCCCCCCCCCCCCCCCCCCCCCCCCCCCCCCCCCCCCCCCCCCCCCCCCCCCCCCCCCC
C   READ IN PER CENT FULL POWER AND FEEDWATER TEMPERATURE C
C   READ IN PRIMARY PRESSURE AND FLOWRATE C
CCCCCCCCCCCCCCCCCCCCCCCCCCCCCCCCCCCCCCCCCCCCCCCCCCCCCCCCCCCC
C
    READ(5,110) PERP,TFW(2)
    TFW(1)=TFW(2)
    READ(5,110) PPRIM,WPIN(1)
    WPIN(2)=WPIN(1)
    IF(PERP.GT.1.0) GO TO 10
C
CCCCCCCCCCCCCCCCCCCCCCCCCCCCCCCCCCCCCCCCCCCCCCCCCCCCCCCCCCCC
C   CALCULATE HEAT TRANSFER RATE PER STEAM GENERATOR C
CCCCCCCCCCCCCCCCCCCCCCCCCCCCCCCCCCCCCCCCCCCCCCCCCCCCCCCCCCCC
```

```

C
      QB=POWER*PERP/NSTG
      GO TO 15
C
CCCCCCCCCCCCCCCCCCCCCCCCCCCCCCCCCCCCCCCCCCCCCCCCCCCCCCCCCCCC
C      IF REACTOR IS OPERATING AT GREATER THAN FULL POWER C
C      READ IN POWER VALUE AND CALCULATE HEAT TRANSFER C
C      RATE PER STEAM GENERATOR C
CCCCCCCCCCCCCCCCCCCCCCCCCCCCCCCCCCCCCCCCCCCCCCCCCCCCCCCCCCCC
C
10     READ(5,120) POWER
      QB=POWER/NSTG
C
CCCCCCCCCCCCCCCCCCCCCCCCCCCCCCCCCCCCCCCCCCCCCCCCCCCCCCCCCCCC
C      CALL STEADY STATE HEADING OUTPUT ROUTINE C
CCCCCCCCCCCCCCCCCCCCCCCCCCCCCCCCCCCCCCCCCCCCCCCCCCCCCCCCCCCC
C
15     CALL OUT1
C
CCCCCCCCCCCCCCCCCCCCCCCCCCCCCCCCCCCCCCCCCCCCCCCCCCCCCCCCCCCC
C      CALCULATE STEADY STATE CONDITIONS C
CCCCCCCCCCCCCCCCCCCCCCCCCCCCCCCCCCCCCCCCCCCCCCCCCCCCCCCCCCCC
C
      CALL ITER
110    FORMAT(2E12.3)
120    FORMAT(E12.3)
      RETURN
      END

```

SUBROUTINE THERM

```

C
CCCCCCCCCCCCCCCCCCCCCCCCCCCCCCCCCCCCCCCCCCCCCCCCCCCCCCCCCCCC
C   THE PURPOSE OF THIS ROUTINE IS TO EVALUTE SATURATED C
C   FLUID PROPERTIES USING ALGEBRAIC FITS TAKEN FROM C
C   THE TRAC CODE. THE INPUT FOR THIS CALCULATION IS THE C
C   SECONDARY PRESSURE, PSAT. C
CCCCCCCCCCCCCCCCCCCCCCCCCCCCCCCCCCCCCCCCCCCCCCCCCCCCCCCCCCCC
C
    REAL LM,KSEP,LR,LD,LTB,LP,MU,KC,LF,M,MFD,MR,MTB,
    1MTBC,MSD,MTOT,LT,MUP,LSAT,LSUB
    DIMENSION UFW(2)
    COMMON /STEAM/ PSAT,TFW(2),TSAT,UL,HL(2),HFW(2),VGJ,MU(2),
    1HG,RL,RHOG,RHOF,DUG,UG,DRHOG,DUF,UF,DRHOF,DRLP,DRLU,
    2QB,POWER,PERP,HFS,RFW(2),DTSAT
    COMMON /TIME/ T,DT,ITRAN,WFWF,WSF, ITC,ICLK
    DATA C1/!17.8/,C2/0.223/,C3/255.2/,A14/1.0E-05/,C12/2.5896E06/
    DATA C13/6.35E-03/,C14/-1.0582E-09/,C15/1.0764/,C16/3.625E-10/
    DATA C17/-9.063E-17/,SL0/-1.465568E06/,SL1/6.926955E03/
    DATA SL2/-7.742307/,SL3/7.280301E-03/,C47/1000.0/,C45/1.0E-06/
    DATA C48/-0.15E03/,C49/-20.0/,C51/0.657E-06/,D0/3.026032E-04/
    DATA D1/-1.836607E-04/,D2/7.567076E-05/,D3/-1.647879E-05/
    DATA D4/1.416458E-06/,H00/3.892077E-06/,C9/1.066555/
    DATA C10/1.02E-08/,C11/-2.548E-15/,C8/3.403E05/,C7/-4.995E10/
    DATA C6/2619410.618/,SH0/-8.9/,SH1/2.363444E04/,SH2/-77.434017/
    DATA SH3/7.021557E-02/,H0/8.58129E-06/,EH0/6.484504E-06/
    DATA PR/6.894575E05/,A0/1.29947E-03/,A1/-0.264032E-04/
    DATA A2/3.910471E-04/,A3/-8.219445E-05/,A4/7.022438E-06/
    DATA B0/0.0/,B1/0.0/,B2/0.0/,B3/0.0/,B4/0.0/
    DATA E0/1.452605E-03/,E1/-6.988009E-09/,E2/1.521023E-14/
    DATA E3/-1.23032E-20/,F0/-3.806351E-11/,F1/3.928521E-16/
    DATA F2/-1.25858E-21/,F3/1.286018E-27/

C
CCCCCCCCCCCCCCCCCCCCCCCCCCCCCCCCCCCCCCCCCCCCCCCCCCCCCCCCCCCC
C   CALCULATE THE SATURATION TEMPERATURE, TSAT. C
CCCCCCCCCCCCCCCCCCCCCCCCCCCCCCCCCCCCCCCCCCCCCCCCCCCCCCCCCCCC
C
    TSAT=C1*((A14*PSAT)**C2)+C3
    DTSAT=C1*C2*A14*((A14*PSAT)**(C2-1.0))

C
CCCCCCCCCCCCCCCCCCCCCCCCCCCCCCCCCCCCCCCCCCCCCCCCCCCCCCCCCCCC
C   CALCULATE PROPERTIES FOR SATURATED STEAM. C
CCCCCCCCCCCCCCCCCCCCCCCCCCCCCCCCCCCCCCCCCCCCCCCCCCCCCCCCCCCC
C
    IF(PSAT.GE.2.0E06) GO TO 2
    UG=C6+C7*(1.0/(C8+PSAT))
    GS=C9+(C11*PSAT+C10)*PSAT
    DGS=C10+2.0*C11*PSAT
    DUG=-C7/((C8+PSAT)**2.0)
    GO TO 3
2. CONTINUE
    UG=C12+(C14*PSAT+C13)*PSAT
    GS=C15+(C17*PSAT+C16)*PSAT
    DGS=C16+2.0*C17*PSAT

```

```

DUG=C13+2.0*C14*PSAT
3  RHOG=PSAT/((GS-1.0)*UG)
   DRHOG=RHOG*(1.0/PSAT-DGS/(GS-1.0))-DUG/UG
   HG=UG*GS
C
CCCCCCCCCCCCCCCCCCCCCCCCCCCCCCCCCCCCCCCCCCCCCCCCCCCCCCCCCCCC
C  EVALUATE THE DRIFT VELOCITY FOR DRIFT FLUX MODEL.  C
CCCCCCCCCCCCCCCCCCCCCCCCCCCCCCCCCCCCCCCCCCCCCCCCCCCCCCCCCCCC
C
   VGJ=(6.41E-17)*(PSAT**2.0)-(5.7794E-09)*PSAT+2.0957E-01
C
CCCCCCCCCCCCCCCCCCCCCCCCCCCCCCCCCCCCCCCCCCCCCCCCCCCCCCCCCCCC
C  EVALUATE LIQUID PROPERTIES.  C
CCCCCCCCCCCCCCCCCCCCCCCCCCCCCCCCCCCCCCCCCCCCCCCCCCCCCCCCCCCC
C
   IF(TSAT.GE.573.15) GO TO 4
   UF=SL0+SL1*TSAT+SL2*(TSAT**2.0)+SL3*(TSAT**3.0)
   DUF=(SL1+2.0*SL2*TSAT+3.0*SL3*(TSAT**2.0))*DTSAT
   GO TO 5
4  UF=SH0+SH1*TSAT+SH2*(TSAT**2.0)+SH3*(TSAT**3.0)
   DUF=(SH1+2.0*SH2*TSAT+3.0*SH3*(TSAT**2.0))*DTSAT
5  RHOF=C47+(C45*UF)*(C48*C45*UF+C49)+C51*PSAT
   DRHOF=(2.0*(C45**2.0)*C48*UF+C45*C49)*DUF+C51
   HL(2)=UF+PSAT/RHOF
   HFG=HG-HL(2)
C
CCCCCCCCCCCCCCCCCCCCCCCCCCCCCCCCCCCCCCCCCCCCCCCCCCCCCCCCCCCC
C  EVALUATE FEEDWATER PROPERTIES USING SUBCOOLED TABLE.  C
CCCCCCCCCCCCCCCCCCCCCCCCCCCCCCCCCCCCCCCCCCCCCCCCCCCCCCCCCCCC
C
   CALL PRMPR1
   IF(ITRAN.EQ.1) GO TO 8
   N=2
   GO TO 10
   ENTRY THERM1
8  N=1
   RL=C47+(C45*UL)*(C48*C45*UL+C49)+C51*PSAT
   DRLP=C51
   DRLU=2.0*C48*(C45**2.0)*UL+C45*C49
   HL(1)=UL+PSAT/RL
C
CCCCCCCCCCCCCCCCCCCCCCCCCCCCCCCCCCCCCCCCCCCCCCCCCCCCCCCCCCCC
C  EVALUTE FLUID VISCOSITY.  C
CCCCCCCCCCCCCCCCCCCCCCCCCCCCCCCCCCCCCCCCCCCCCCCCCCCCCCCCCCCC
C
10 DO 13 J=N,2
   IF(HL(J).GE.2.76E05) GO TO 11
   X=(HL(J)-42658.4)*H0
   Y=(HL(J)-55358.8)*EHO
   A=A0+A1*X+A2*(X**2)+A3*(X**3)+A4*(X**4)
   B=B0+B1*Y+B2*(Y**2)+B3*(Y**3)+B4*(Y**4)
   MU(J)=A-B*(PSAT-PR)
   GO TO 13
11 IF(HL(J).GE.3.94E05) GO TO 12

```

```
E=E0+E1*HL(J)+E2*(HL(J)**2.0)+E3*(HL(J)**3.0)
F=F0+F1*HL(J)+F2*(HL(J)**2.0)+F3*(HL(J)**3.0)
MU(J)=E-F*(PSAT-PR)
GO TO 13
12 Z=(HL(J)-401467.1)*H00
    MU(J)=D0+D1*Z+D2*(Z**2)+D3*(Z**3)+D4*(Z**4)
13 CONTINUE
    RETURN
    END
```

SUBROUTINE TOUT

```

C
CCCCCCCCCCCCCCCCCCCCCCCCCCCCCCCCCCCCCCCCCCCCCCCCCCCCCCCCCCCC
C   THIS ROUTINE WRITES OUT TRANSIENT INFORMATION. C
C   ALL TEMPERATURES ARE CONVERTED TO DEGREES C
C   CELSIUS AND PRESSURES TO MEGAPASCALS. C
C   OUTLET PLENUM EXIT TEMPERATURE IS PROCESSED C
C   THROUGH A SENSOR MODEL. C
CCCCCCCCCCCCCCCCCCCCCCCCCCCCCCCCCCCCCCCCCCCCCCCCCCCCCCCCCCCC
C
      REAL LW,KSEP,LR,LD,LTB,LP,MU,KC,LF,M,MFD,MR,MTB,
      INTBC,MSD,MTOT,LT,MUP,LSAT,LSUB
      COMMON /GEOM/ KSEP,LR,LTB,LP,KC,ARI,ATB,ARO,G,
      1VR,VTB,DHTB,BETA(4),NSTG,CO,
      2AHT,RO,RI,VOP,VTBP,APT,VTM
      COMMON /DOME/ VSUB,VTOT,VG,VFO,LSAT,LSUB,VREF,LW,
      1LD,AD,VD,VSD,DHD,VT,LT,VSTM,DVG,ASW,R1,R2,R3,R4,
      2ZL1,ZL2,ZL3,ZLF
      COMMON /STEAM/ PSAT,TFW(2),TSAT,UL,HL(2),HFW(2),VGJ,MU(2),
      1HG,RL,RHOG,RHOF,DUG,UG,DRHOG,DUF,UF,DRHOF,DRLP,DRLU,
      2QB,POWER,PERP,HFG,RFW(2),DTSAT
      COMMON /FLOWS/ NO,WS(2),WFW(2),WF,WP,WR,WN,DINERT
      COMMON /TRANS/ VOID(3),XQ(3),RB(2),UB(2),DUP(2),DUA(2),DRP(2),
      1DRA,MFD(2),MR(2),MTB(2),MTBC(2),HR,HN,MSD,
      2HTOT(2),S(5),M(5),VP(3),R(9,5)
      COMMON /TIME/ T,DT,ITRAN,WFWF,WSF, ITC,ICLK
      COMMON /PRIME/ PPRIM,TLMTD,UO,TP(3),HP(3),RP(3),UP(3),DRPT(3),
      1DUPT(3),TPIN(2),HPIN(2),WPIN(2),MUP,CPL,TKL,CPT
      COMMON /FILTER/ TFOLD,TAUC
      CTFW=TFW(2)-273.15
      TCIN=TPIN(2)-273.15
      TC1=TP(1)-273.15
      TC2=TP(2)-273.15
      TF=(TP(3)*DT+TFOLD*TAUC)/(DT+TAUC)
      TFOLD=TF
      TC3=TF-273.15
      CTSAT=TSAT-273.15
      TAVE=(TCIN+TC3)/2.0
      WRITE(6,100) T,LW,PSAT,QB,WS(2),WFW(2),CTFW,NO,MTOT(2),XQ(1)
      WRITE(6,110) TCIN,TC1,TC2,TC3,WPIN(2),CTSAT,PPRIM,TAVE
100  FORMAT(' ',9(E12.4,3X),E12.4)
110  FORMAT(' ',15X,7(E12.4,3X),E12.4)
      RETURN
      END

```

```

SUBROUTINE TOUT1(TDT,NPRIN)
C
CCCCCCCCCCCCCCCCCCCCCCCCCCCCCCCCCCCCCCCCCCCCCCCCCCCCCCCCCCCC
C   THIS ROUTINE WRITES OUT TRANSIENT OUTPUT HEADINGS C
CCCCCCCCCCCCCCCCCCCCCCCCCCCCCCCCCCCCCCCCCCCCCCCCCCCCCCCCCCCC
C
WRITE(6,100)
WRITE(6,110) TDT
WRITE(6,115) NPRIN
WRITE(6,120)
WRITE(6,130)
WRITE(6,140)
WRITE(6,150)
WRITE(6,160)
100  FORMAT('1',15X,'TRANSIENT EDIT')
110  FORMAT('-', 'TIME STEP SIZE IS',E12.4,1X,'SEC')
115  FORMAT(' ', 'EDIT EVERY',1X,I2,1X,'TIME STEPS')
120  FORMAT('-',4X,'TIME',10X,'WATER',9X,'PRESSURE',8X,'POWER',
110X,'STEAM',10X,'FEED',11X,'FEED',10X,'DOWNCOMER',7X,'MASS',
210X,'TUBE EXIT')
130  FORMAT(' ',4X,'(S)',10X,'LEVEL (M)',9X,'(PA)',9X,'(WATTS)',7X,
1'FLOW (KG/S)',4X,'FLOW (KG/S)',4X,'TEMP (C)',7X,'FLOW (KG/S)',
23X,'CONTENT (KG)',5X,'QUALITY')
140  FORMAT(' ',18X,'PRIMARY',8X,'TUBE',12X,'TUBE',10X,'PRIMARY'
1,8X,'PRIMARY',8X,'SATURATION',6X,'PRIMARY',8X,'PRIMARY')
150  FORMAT(' ',18X,'INLET',10X,'INLET',10X,'OUTLET',9X,'OUTLET'
1,9X,'FLOW',11X,'TEMPERATURE',5X,'PRESSURE',7X,'TAVE')
160  FORMAT(' ',17X,'TEMPERATURE',4X,'TEMPERATURE',4X,'TEMPERATURE'
1,4X,'TEMPERATURE')
RETURN
END

```



SUBROUTINE TRANST

```

C
CCCCCCCCCCCCCCCCCCCCCCCCCCCCCCCCCCCCCCCCCCCCCCCCCCCCCCCCCCCC
C   THIS IS THE MAIN TRANSIENT CALCULATION DRIVING ROUTINE C
CCCCCCCCCCCCCCCCCCCCCCCCCCCCCCCCCCCCCCCCCCCCCCCCCCCCCCCCCCCC
C
    REAL LN,KSEP,LR,LD,LTB,LP,MU,KC,LF,M,MFD,MR,MTB,
    1MTBC,MSD,MTOT,LT,MUP,LSAT,LSUB,KD
    DIMENSION TIM(41),TPI(41),TWS(41),TWF(41),TTFW(41),PVAL(41)
    1,WPI(41),PPRI(41),IPRINT(5),TPINF(2)
    COMMON /RESP/ VALK,IFW(41),PVALV,TTRIP,AK,AKB,VALK0,MB,MSM,
    1MSV,TMST,TSV,TISO,ISTM(41),ISV(4)
    COMMON /VALVES/ F,FMST,FB,FS1,FS2,FS3,FS4
    COMMON /GEOM/ KSEP,LR,LTB,LP,KC,ARI,ATB,ARO,G,
    1VR,VTB,DHTB,BETA(4),NSTG,CO,
    2AHT,RO,RI,VOP,VTBP,APT,VTM
    COMMON /DOME/ VSUB,VTOT,VG,VFO,LSAT,LSUB,VREF,LW,
    1LD,AD,VD,VSD,DHD,VT,LT,VSTM,DVG,ASW,R1,R2,R3,R4,
    2ZL1,ZL2,ZL3,ZLF
    COMMON /STEAM/ PSAT,TFW(2),TSAT,UL,HL(2),HFW(2),VGJ,MU(2),
    1HG,RL,RHOG,RHOF,DUG,UG,DRHOG,DUF,UF,DRHOF,DRLP,DRLU,
    2QB,POWER,PERP,HFG,RFW(2),DTSAT
    COMMON /FLOWS/ WO,WS(2),WFW(2),WF,WP,WR,WN,DINERT
    COMMON /TRANS/ VOID(3),XQ(3),RB(2),UB(2),DUP(2),DUA(2),DRP(2),
    1DRA,MFD(2),MR(2),MTB(2),MTBC(2),HR,HN,MSD,
    2MTOT(2),S(5),M(5),VP(3),R(9,5)
    COMMON /TIME/ T,DT,ITRAN,WFW,WSF, ITC,ICLK
    COMMON /PRIME/ PPRIM,TLMTD,UO,TP(3),HP(3),RP(3),UP(3),DRPT(3),
    1DUPT(3),TPIN(2),HPIN(2),WPIN(2),MUP,CPL,TKL,CPT
    COMMON /HTS/ HPR,HS,RTUBE,RFOUL
    COMMON /DOWCO/ KO
    COMMON /AVE/ WBAR
    COMMON /FILTER/ TFOLD,TAUC
C
CCCCCCCCCCCCCCCCCCCCCCCCCCCCCCCCCCCCCCCCCCCCCCCCCCCCCCCCCCCC
C   INITIALIZE PARAMETERS C
CCCCCCCCCCCCCCCCCCCCCCCCCCCCCCCCCCCCCCCCCCCCCCCCCCCCCCCCCCCC
C
    IF(ITRAN.EQ.1) GO TO 40
    TFOLD=TP(3)
    DO 70 L=1,5
    S(L)=0.0
    DO 70 N=1,9
70  R(N,L)=0.0
    ITRAN=1
    NSTEP=0
    K=0
    J=2
    T=0.0
    TIM(1)=0.0
    TTFW(1)=TFW(1)
    PVAL(1)=PERP
    TWS(1)=WS(1)
    TWF(1)=WS(1)

```

```

WFW(1)=WS(1)
WFW(2)=WFW(1)
WS(2)=WS(1)
TPI(1)=TPIN(2)
TPIN(1)=TPIN(2)
TPINF(1)=TPIN(2)
TPINF(2)=TPIN(2)
WPI(1)=WPIN(1)
PPRI(1)=PPRIM
C
CCCCCCCCCCCCCCCCCCCCCCCCCCCCCCCCCCCCCCCCCCCCCCCCCCCCCCCCCCCC
C   READ IN NUMBER OF TIME ZONES AND TIME STEP SIZE   C
CCCCCCCCCCCCCCCCCCCCCCCCCCCCCCCCCCCCCCCCCCCCCCCCCCCCCCCCCCCC
C
      READ(5,100) NPT,TDI
      NPT=NPT+1
100  FORMAT(I2,E12.3)
C
CCCCCCCCCCCCCCCCCCCCCCCCCCCCCCCCCCCCCCCCCCCCCCCCCCCCCCCCCCCC
C   READ IN PRINT FREQUENCY AND FLAGS FOR DUMP,BYPASS AND SAFETY   C
C   SYSTEMS OPERATION                                           C
CCCCCCCCCCCCCCCCCCCCCCCCCCCCCCCCCCCCCCCCCCCCCCCCCCCCCCCCCCCC
C
      READ(5,110) NPRIN,MSM,MB,MSV
110  FORMAT(4I2)
C
CCCCCCCCCCCCCCCCCCCCCCCCCCCCCCCCCCCCCCCCCCCCCCCCCCCCCCCCCCCC
C   READ IN TURBINE STOP AND CONTROL VALVE CLOSING SPEED, SAFETY   C
C   VALVE CLOSING SPEED(NOT USED HERE BUT PROVIDED IF MODIFICATION C
C   IS DESIRED), ISOLATION VALVE CLOSING SPEED(NOT USED HERE BUT   C
C   PROVIDED FOR CONVENIENCE IF MODIFICATION IS DESIRED)       C
CCCCCCCCCCCCCCCCCCCCCCCCCCCCCCCCCCCCCCCCCCCCCCCCCCCCCCCCCCCC
C
      READ(5,112) TMST,TSV,TISO
112  FORMAT(3E12.3)
C
CCCCCCCCCCCCCCCCCCCCCCCCCCCCCCCCCCCCCCCCCCCCCCCCCCCCCCCCCCCC
C   READ IN TURBINE TRIP TIME(NOT USED IF STEAM FLOWS ARE PROVIDED)C
CCCCCCCCCCCCCCCCCCCCCCCCCCCCCCCCCCCCCCCCCCCCCCCCCCCCCCCCCCCC
C
      READ(5,111) TTRIP
111  FORMAT(E12.3)
      KPRIN=NPRIN
C
CCCCCCCCCCCCCCCCCCCCCCCCCCCCCCCCCCCCCCCCCCCCCCCCCCCCCCCCCCCC
C   READ IN FLAGS FOR EACH SAFETY VALVE BANK   C
CCCCCCCCCCCCCCCCCCCCCCCCCCCCCCCCCCCCCCCCCCCCCCCCCCCCCCCCCCCC
C
      READ(5,203) (ISV(I),I=1,4)
203  FORMAT(4I2)
C
CCCCCCCCCCCCCCCCCCCCCCCCCCCCCCCCCCCCCCCCCCCCCCCCCCCCCCCCCCCC
C   READ IN TIME CONSTANTS FOR TEMPERATURE SENSORS   C
CCCCCCCCCCCCCCCCCCCCCCCCCCCCCCCCCCCCCCCCCCCCCCCCCCCCCCCCCCCC

```

```

C
  READ(5,900) TAUH,TAUC
900  FORMAT(2E12.3)
C
CCCCCCCCCCCCCCCCCCCCCCCCCCCCCCCCCCCCCCCCCCCC
C  READ IN TRANSIENT INPUT TABLE  C
CCCCCCCCCCCCCCCCCCCCCCCCCCCCCCCCCCCCCCCCCCCC
C
  DO 5 I=2,NPT
  READ(5,120) TIM(I),TPI(I),TTFW(I),TWS(I),TWFW(I),PVAL(I)
  5  READ(5,121) WPI(I),PPRI(I),IFW(I),ISTH(I)
120  FORMAT(6E12.3)
121  FORMAT(2E12.3,2I2)
C
CCCCCCCCCCCCCCCCCCCCCCCCCCCCCCCCCCCCCCCCCCCC
C  WRITE OUT TRANSIENT OUTPUT HEADINGS AND INITIAL CONDITIONS  C
CCCCCCCCCCCCCCCCCCCCCCCCCCCCCCCCCCCCCCCCCCCC
C
  CALL TOUT1(TDT,NPRIN)
  DT=TDT
  CALL TOUT
  40 CONTINUE
C
CCCCCCCCCCCCCCCCCCCCCCCCCCCCCCCCCCCCCCCCCCCC
C  DETERMINE NUMBER OF TIME STEPS IN THIS TIME ZONE  C
C  NOTE THAT TIME STEP SIZE IS FIXED  C
CCCCCCCCCCCCCCCCCCCCCCCCCCCCCCCCCCCCCCCCCCCC
C
  DT=TDT
  DEL=TIM(J)-TIM(J-1)
  X=DEL/DT
  Y=X+0.50
  IZ=IFIX(X)
  IZ1=IFIX(Y)
  IF (IZ.EQ.IZ1) GO TO 10
  N=IZ1
  GO TO 11
10  N=IZ
11  CONTINUE
  DO 12 I=1,N
  NSTEP=NSTEP+1
  T=NSTEP*DT
C
CCCCCCCCCCCCCCCCCCCCCCCCCCCCCCCCCCCCCCCCCCCC
C  UPDATE FORCING FUNCTIONS USING LINEAR INTERPOLATION  C
C  ON INPUT TABLE FOR THE APPROPRIATE TIME ZONE  C
CCCCCCCCCCCCCCCCCCCCCCCCCCCCCCCCCCCCCCCCCCCC
C
  WS(1)=WS(2)
  WFW(1)=WFW(2)
  IF(ISTH(J).EQ.1) GO TO 20
  WS(2)=WS(1)+DT*(TWS(J)-TWS(J-1))/DEL
  20  IF(IFW(J).EQ.1) GO TO 21
  WFW(2)=WFW(1)+DT*(TWFW(J)-TWFW(J-1))/DEL

```

```

21 TFW(1)=TFW(2)
   TFW(2)=TFW(1)+DT*(TTFW(J)-TTFW(J-1))/DEL
   TPINF(1)=TPINF(2)
   TPINF(2)=TPINF(1)+DT*(TPI(J)-TPI(J-1))/DEL
C
CCCCCCCCCCCCCCCCCCCCCCCCCCCCCCCCCCCCCCCCCCCCCCCCCCCCCCCCCCCC
C   USE SENSOR MODEL TO CALCULATE APPROPRIATE      C
C   PRIMARY INLET TEMPERATURE                      C
CCCCCCCCCCCCCCCCCCCCCCCCCCCCCCCCCCCCCCCCCCCCCCCCCCCCCCCCCCCC
C
   TPIN(1)=TPIN(2)
   TPIN(2)=(TPI(J)-TPI(J-1))/DEL*TAUH+TPINF(2)
   WPIN(1)=WPIN(2)
   WPIN(2)=WPIN(1)+DT*(WPI(J)-WPI(J-1))/DEL
   PPRIM=PPRIM+DT*(PPRI(J)-PPRI(J-1))/DEL
C
CCCCCCCCCCCCCCCCCCCCCCCCCCCCCCCCCCCCCCCCCCCCCCCCCCCCCCCCCCCC
C   CALCULATE ADVANCED TIME STATE VARIABLES FOR SECONDARY SIDE C
CCCCCCCCCCCCCCCCCCCCCCCCCCCCCCCCCCCCCCCCCCCCCCCCCCCCCCCCCCCC
C
   CALL UPDATE
C
CCCCCCCCCCCCCCCCCCCCCCCCCCCCCCCCCCCCCCCCCCCCCCCCCCCCCCCCCCCC
C   DETERMINE NEW SECONDARY PROPERTIES      C
CCCCCCCCCCCCCCCCCCCCCCCCCCCCCCCCCCCCCCCCCCCCCCCCCCCCCCCCCCCC
C
   CALL THERM
C
CCCCCCCCCCCCCCCCCCCCCCCCCCCCCCCCCCCCCCCCCCCCCCCCCCCCCCCCCCCC
C   CALCULATE ADVANCED TIME PRIMARY STATE VARIABLES AND PROPERTIES C
CCCCCCCCCCCCCCCCCCCCCCCCCCCCCCCCCCCCCCCCCCCCCCCCCCCCCCCCCCCC
C
   CALL PGERIV
C
CCCCCCCCCCCCCCCCCCCCCCCCCCCCCCCCCCCCCCCCCCCCCCCCCCCCCCCCCCCC
C   CHECK FLAGS FOR MAIN STEAM AND FEEDWATER SYSTEM MODELS C
CCCCCCCCCCCCCCCCCCCCCCCCCCCCCCCCCCCCCCCCCCCCCCCCCCCCCCCCCCCC
C
   IF(IFW(J).NE.1) GO TO 22
   CALL CONTRO
22  IF(ISTM(J).NE.1) GO TO 23
   PVALV=PVAL(J-1)+(PVAL(J)-PVAL(J-1))/DEL*(T-TIM(J-1))
   CALL CHOKE
C
CCCCCCCCCCCCCCCCCCCCCCCCCCCCCCCCCCCCCCCCCCCCCCCCCCCCCCCCCCCC
C   UPDATE MASSES, TWO-PHASE PROPERTIES, LEVEL,      C
C   AND HEAT TRANSFER RATE. GET MOMENTUM           C
C   EQUATION PARAMETERS, M(I)                     C
CCCCCCCCCCCCCCCCCCCCCCCCCCCCCCCCCCCCCCCCCCCCCCCCCCCCCCCCCCCC
C
23  CALL NEWPR
   CALL MOMEN
C
CCCCCCCCCCCCCCCCCCCCCCCCCCCCCCCCCCCCCCCCCCCCCCCCCCCCCCCCCCCC

```

```

C SOLVE MOMENTUM EQUATION AND UPDATE WBAR C
CCCCCCCCCCCCCCCCCCCCCCCCCCCCCCCCCCCCCCCCCCCCCCCCCCCCCCCC
C
WBDOT=(-1.0)*(M(1)*WO+M(2)*WP+M(3)*WR+M(4)*WN+M(5))/DINERT
WBAR=WBAR+DT*WBDOT
300 K=K+1
C
CCCCCCCCCCCCCCCCCCCCCCCCCCCCCCCCCCCCCCCCCCCCCCCCCCCCCCCC
C CHECK FOR TRANSIENT PRINT C
CCCCCCCCCCCCCCCCCCCCCCCCCCCCCCCCCCCCCCCCCCCCCCCCCCCCCCCC
C
IF(K.NE.KPRIN) GO TO 12
CALL TOUT
KPRIN=KPRIN+NPRIN
12 CONTINUE
C
CCCCCCCCCCCCCCCCCCCCCCCCCCCCCCCCCCCCCCCCCCCCCCCCCCCCCCCC
C CHECK FOR END OF TRANSIENT SIMULATION C
CCCCCCCCCCCCCCCCCCCCCCCCCCCCCCCCCCCCCCCCCCCCCCCCCCCCCCCC
C
IF (J.EQ.NPT) GO TO 14
J=J+1
GO TO 40
14 CONTINUE
RETURN
END

```

SUBROUTINE UPDATE

```

C
CCCCCCCCCCCCCCCCCCCCCCCCCCCCCCCCCCCCCCCCCCCCCCCCCCCCCCCCCCCCCCCCCCCC
C   THE PURPOSE OF THIS SUBROUTINE IS TO EVALUATE THE REDUCED   C
C   STATE EQUATION WITH THE STATE VECTOR (UO,VG,VOID(1),VOID(2), C
C   PSAT) TO OBTAIN THE TIME DERIVATIVE OF THE STATE VECTOR.   C
C   THE FLOWRATES ARE THEN CALCULATED. FINALLY, THE STATE VECTOR C
C   IS UPDATED.                                                 C
CCCCCCCCCCCCCCCCCCCCCCCCCCCCCCCCCCCCCCCCCCCCCCCCCCCCCCCCCCCCCCCCCCCC
C

```

```

REAL LW,KSEP,LR,LD,LTB,LP,MU,KC,LF,M,MFD,MR,MTB,
IMTB,MSD,MTOT,LT,MUP,LSAT,LSUB
DIMENSION RA(5,5),RAINV(5,5),E(4),XG(5)
COMMON /GEOM/ KSEP,LR,LTB,LP,KC,ARI,ATB,ARO,G,
1VR,VTB,DHTB,BETA(4),NSTG,CO,
2AHT,RO,RI,VOP,VTBP,APT,VTM
COMMON /DOME/ VSUB,VTOT,VG,VFO,LSAT,LSUB,VREF,LW,
1LD,AD,VD,VSD,DHD,VT,LT,VSTM,DVG,ASW,R1,R2,R3,R4,
2ZL1,ZL2,ZL3,ZLF
COMMON /STEAM/ PSAT,TFW(2),TSAT,UL,HL(2),HFW(2),VGJ,MU(2),
1HG,RL,RHOG,RHOF,DUG,UG,DRHOG,DUF,UF,DRHOF,DRLP,DRLU,
2QB,POWER,PERP,HFG,RFW(2),DTSAT
COMMON /FLOWS/ WQ,W3(2),WFW(2),WF,WP,WR,WN,DINERT
COMMON /TRANS/ VOID(3),XQ(3),RB(2),LB(2),DUP(2),DUA(2),DRP(2),
1DRA,MFD(2),MR(2),MTB(2),MTBC(2),HR,HN,MSD,
2MTOT(2),S(5),M(5),VP(3),R(9,5)
COMMON /TIME/ T,DT,ITRAN,WFWF,MSF, ITC,ICLK
COMMON /PRIME/ PPRIM,TLMTD,UO,TP(3),HP(3),RP(3),UP(3),DRPT(3),
1DUPT(3),TPIN(2),HPIN(2),WPIN(2),MUP,CPL,TKL,CPT
COMMON /AVE/ MBAR
DATA RA(1,2)/0.0/,RA(2,2)/0.0/

```

```

C
CCCCCCCCCCCCCCCCCCCCCCCCCCCCCCCCCCCCCCCCCCCCCCCCCCCCCCCCCCCCCCCCCCCC
C   EVALUATE THE VARIOUS DERIVATIVES OF THE MASS AND ENERGY CONTENTS C
C   OF THE STEAM GENERATOR SECONDARY REGIONS.                   C
CCCCCCCCCCCCCCCCCCCCCCCCCCCCCCCCCCCCCCCCCCCCCCCCCCCCCCCCCCCCCCCCCCCC
C

```

```

DEL=RL-RB(1)
Q1=RL/RB(1)
RAT=ALOG(Q1)
DEL2=DEL**2
RAT2=RAT**2
DELU=UL-UB(1)
GAM=LP/LTB
R(1,1)=(RB(1)/DEL)*(VTB-MTB(2)/RL)*DRLU
R(1,3)=(RL/DEL)*(MTB(2)/RB(1)-VTB)*DRA
R(1,5)=R(1,1)*DRLP/DRLU+R(1,3)*DRP(1)/DRA
SR1=MTB(2)*DELU*(1.0/(RL*RAT2)-RB(1)/DEL2)
SR2=MTB(2)*DELU*(RL/DEL2-1.0/(RB(1)*RAT2))
SR3=MTB(2)*(1.0/RAT-RB(1)/DEL)
SR4=MTB(2)*(RL/DEL-1.0/RAT)
R5=(-1.0*DELU)/RAT+(RL*UL-RB(1)*UB(1))/DEL
R(2,1)=R(1,1)*R5+SR4+SR1*DRLU
R(2,3)=R(1,3)*R5+SR2*DRA+SR3*DUA(1)

```

```

R(2,5)=R(1,5)*R5+SR1*DRLP+SR2*DRP(1)+SR3*DUP(1)
1+(VTM*CPT/2.0)*DTSAT
R61=(VTB*(1.-GAM)*(RB(1)**2))/(DEL*(GAM*RL+(1.0-GAM)*RB(1)))
R62=MTBC(2)*RB(1)/(RL*DEL)
Ro=R61-R62
R71=(RL/DEL)*(MTBC(2)/RB(1)-VTB)
R72=(VTB*GAM*(RL**2))/(DEL*(GAM*RL+(1.0-GAM)*RB(1)))
R7=R71+R72
R(3,1)=R6*DRLU
R(3,3)=R7*DRA
R(3,5)=R6*DRLP+R7*DRP(1)
R(4,3)=DRA*VR/2.0
R(4,4)=R(4,3)
R(4,5)=(DRP(1)+DRP(2))*VR/2.0
C
CCCCCCCCCCCCCCCCCCCCCCCCCCCCCCCCCCCC
C   CALCULATE THE INERTANCE C
CCCCCCCCCCCCCCCCCCCCCCCCCCCCCCCCCCCC
C
B1=(LM-LD)*(1.0/ASH-1.0/AD)/2.0
B2=LD/AD+LP/(2.0*ATB)
BETA(1)=B1+B2
B3=BETA(2)+BETA(3)+BETA(4)
DINERT=BETA(1)+B3
E(1)=(BETA(2)*R(3,1)-B3*R(1,1))/DINERT
E(2)=(BETA(2)*R(3,3)-B3*R(1,3)-BETA(4)*R(4,3))/DINERT
E(3)=-BETA(4)*R(4,4)/DINERT
E(4)=(BETA(2)*R(3,5)-B3*R(1,5)-BETA(4)*R(4,5))/DINERT
DO 5 I=1,2
5 R(5,I+2)=(UB(I)*DRA+RB(I)*DUA(I))*VR/2.0
R(5,5)=(UB(1)*DRP(1)+RB(1)*DUP(1)+UB(2)*DRP(2)+RB(2)*DUP(2)
1*VR/2.0
R8=HL(1)-HR
C
CCCCCCCCCCCCCCCCCCCCCCCCCCCCCCCCCCCC
C   CALCULATE MATRIX COMPONENTS FOR TUBE BUNDLE AND C
C   RISER ENERGY EQUATIONS C
CCCCCCCCCCCCCCCCCCCCCCCCCCCCCCCCCCCC
C
RA(1,1)=R(2,1)-HR*R(1,1)+E(1)*R8
RA(1,3)=R(2,3)-HR*R(1,3)+E(2)*R8
RA(1,4)=E(3)*R8
RA(1,5)=R(2,5)-HR*R(1,5)+E(4)*R8
R81=HR-HN
RA(2,1)=(R(1,1)+E(1))*R81
RA(2,3)=R(5,3)-HN*R(4,3)+(R(1,3)+E(2))*R81
RA(2,4)=R(5,4)-HN*R(4,4)+E(3)*R81
RA(2,5)=R(5,5)-HN*R(4,5)+(R(1,5)+E(4))*R81
R72=RHOG*UG-RHOF*UF
R751=RHOG*DUG+UG*DRHOG
R752=RHOF*DUF+UF*DRHOF
C
CCCCCCCCCCCCCCCCCCCCCCCCCCCCCCCCCCCC
C   CALCULATE THE SATURATED AND SUBCOOLED MATRIX COMPONENTS FOR C

```





```

R(9,2)=-RL*UL
R(9,5)=VSUB*UL*DRLP
R04=HN-HL(K)
RA(3,1)=(R(1,1)+E(1))*R04
RA(3,2)=R(7,2)-HL(K)*R(6,2)+PSAT
RA(3,3)=(R(1,3)+R(4,3)+E(2))*R04
RA(3,4)=(R(4,4)+E(3))*R04
RA(3,5)=R(7,5)-HL(K)*R(6,5)+(R(1,5)+R(4,5)+E(4))*R04
R05=HL(1)-HL(K)
RA(4,1)=R(9,1)-HL(K)*R(8,1)-E(1)*R05
RA(4,2)=R(9,2)-HL(K)*R(8,2)-PSAT
RA(4,3)=-E(2)*R05
RA(4,4)=-E(3)*R05
RA(4,5)=R(9,5)-HL(K)*R(8,5)-E(4)*R05
C
CCCCCCCCCCCCCCCCCCCCCCCCCCCCCCCCCCCCCCCCCCCCCCCCCCCCCCCCCCCC
C   CALCULATE THE RIGHT HAND SIDES OF THE SATURATED AND C
C   SUBCOOLED ENERGY EQUATIONS FOR THE CASE WHEN THE C
C   VOLUMES ARE NOT FIXED C
CCCCCCCCCCCCCCCCCCCCCCCCCCCCCCCCCCCCCCCCCCCCCCCCCCCCCCCCCCCC
C
S(3)=MBAR*R04-WS(1)*(HG-HL(K))
S(4)=HFW(1)*(HFW(1)-HL(K))-MBAR*R05
11 CONTINUE
C
CCCCCCCCCCCCCCCCCCCCCCCCCCCCCCCCCCCCCCCCCCCCCCCCCCCCCCCCCCCC
C   CALCULATE MATRIX COMPONENTS FOR THE OVERALL MASS BALANCE C
CCCCCCCCCCCCCCCCCCCCCCCCCCCCCCCCCCCCCCCCCCCCCCCCCCCCCCCCCCCC
C
DO 12 I=1,5
12 RA(5,I)=R(1,I)+R(4,I)+R(6,I)+R(8,I)
C
CCCCCCCCCCCCCCCCCCCCCCCCCCCCCCCCCCCCCCCCCCCCCCCCCCCCCCCCCCCC
C   CALCULATE THE RIGHT HAND SIDES OF THE RISER AND TUBE BUNDLE C
C   ENERGY EQUATIONS AND THE OVERALL MASS BALANCE EQUATIONS C
CCCCCCCCCCCCCCCCCCCCCCCCCCCCCCCCCCCCCCCCCCCCCCCCCCCCCCCCCCCC
C
S(1)=MBAR*R0+QB
S(2)=MBAR*R01
S(5)=HFW(1)-WS(1)
C
CCCCCCCCCCCCCCCCCCCCCCCCCCCCCCCCCCCC
C   INVERT THE MATRIX C
CCCCCCCCCCCCCCCCCCCCCCCCCCCCCCCCCCCC
C
CALL MINV(RA,RAINV,5,DD,L,M)
C
CCCCCCCCCCCCCCCCCCCCCCCCCCCCCCCCCCCCCCCCCCCCCCCCCCCCCCCCCCCC
C   OBTAIN THE DERIVATIVE OF THE STATE VECTOR BY MULTIPLYING C
C   THE INVERSE OF RA BY TH VECTOR S C
CCCCCCCCCCCCCCCCCCCCCCCCCCCCCCCCCCCCCCCCCCCCCCCCCCCCCCCCCCCC
C
DO 20 I=1,5
XG(I)=0.0

```

```

DO 20 J=1,5
20  XG(I)=XG(I)+RAINV(I,J)*S(J)
C
CCCCCCCCCCCCCCCCCCCCCCCCCCCCCCCCCCCCCCCCCCCCCCCCCCCCCCCC
C   CALCULATE THE OLD TIME DOWNCOMER FLOWRATE  C
CCCCCCCCCCCCCCCCCCCCCCCCCCCCCCCCCCCCCCCCCCCCCCCCCCCCCCCC
C
      ESUM=XG(1)*E(1)
      DO 21 K=3,5
21   ESUM=ESUM+XG(K)*E(K-1)
      WO=WBAR-ESUM
C
CCCCCCCCCCCCCCCCCCCCCCCCCCCCCCCCCCCCCCCCCCCCCCCCCCCCCCCC
C   CALCULATE MASS STORAGE RATES  C
CCCCCCCCCCCCCCCCCCCCCCCCCCCCCCCCCCCCCCCCCCCCCCCCCCCCCCCC
C
      DMTBC=0.0
      DMTB=0.0
      DMR=0.0
      DO 22 I=1,5
      DMTBC=DMTBC+XG(I)*R(3,I)
      DMTB=DMTB+XG(I)*R(1,I)
22   DMR=DMR+XG(I)*R(4,I)
C
CCCCCCCCCCCCCCCCCCCCCCCCCCCCCCCCCCCCCCCCCCCCCCCCCCCCCCCC
C   CALCULATE OLD TIME RECIRCULATION FLOW PATTERN  C
CCCCCCCCCCCCCCCCCCCCCCCCCCCCCCCCCCCCCCCCCCCCCCCCCCCCCCCC
C
      WN=WO-DMTB-DMR
      WR=WN+DMR
      WP=WR+DMTBC
C
CCCCCCCCCCCCCCCCCCCCCCCCCCCCCCCCCCCCCCCCCCCCCCCCCCCCCCCC
C   CALCULATE OLD TIME SATURATED LIQUID FLOW FROM SATURATED  C
C   REGION TO SUBCOOLED REGION  C
CCCCCCCCCCCCCCCCCCCCCCCCCCCCCCCCCCCCCCCCCCCCCCCCCCCCCCCC
C
      VG=VG+XG(2)*DT
      IF(VG.GT.VREF) GO TO 30
      WF=R(8,1)*XG(1)+R(8,5)*XG(5)-WFW(2)+WO
      GO TO 31
30   WF=R(8,1)*XG(1)+(RHOF+R(8,2))*XG(2)+R(8,5)*XG(5)-WFW(2)+WO
C
CCCCCCCCCCCCCCCCCCCCCCCCCCCCCCCCCCCCCCCCCCCCCCCCCCCCCCCC
C   UPDATE UL,VOID (1 AND 2),AND PSAT  C
CCCCCCCCCCCCCCCCCCCCCCCCCCCCCCCCCCCCCCCCCCCCCCCCCCCCCCCC
C
31   UL=UL+DT*XG(1)
      VOID(1)=VOID(1)+DT*XG(3)
      VOID(2)=VOID(2)+DT*XG(4)
      PSAT=PSAT+DT*XG(5)
      RETURN
      END

```

## Appendix K

### DOWNCOMER GEOMETRIC REPRESENTATION FOR WATER LEVEL CALCULATION

The purpose of this appendix is to discuss the geometric representation of the steam dome - downcomer used to calculate the water level given the volume of saturated steam present in the steam dome - downcomer. Figure K-1 is a schematic of this idealized geometry showing the nomenclature used in this presentation.

Table K-1 gives the volume of the five regions making up our idealized steam dome - downcomer. Also given in this table is the liquid volume within a given region  $i$ ,  $V_{LIQ}^i$ , assuming that the volume is neither empty nor full of water. The region liquid volume is given as a function of the liquid level,  $L$ , measured from the bottom of the region.

The water level is calculated as follows:

- 1.) Using  $V_v$  determine in which region the water level is located. That is, compare  $V_v$  to  $V_1$ ,  $V_1 + V_2$ ,  $V_1 + V_2 + V_3$ , and so forth until  $V_v$  is less than the sum of the region volumes and call the sum  $\sum v$ . The last region volume appearing in the summation used to obtain  $\sum v$  corresponds to the region where the water level is located.

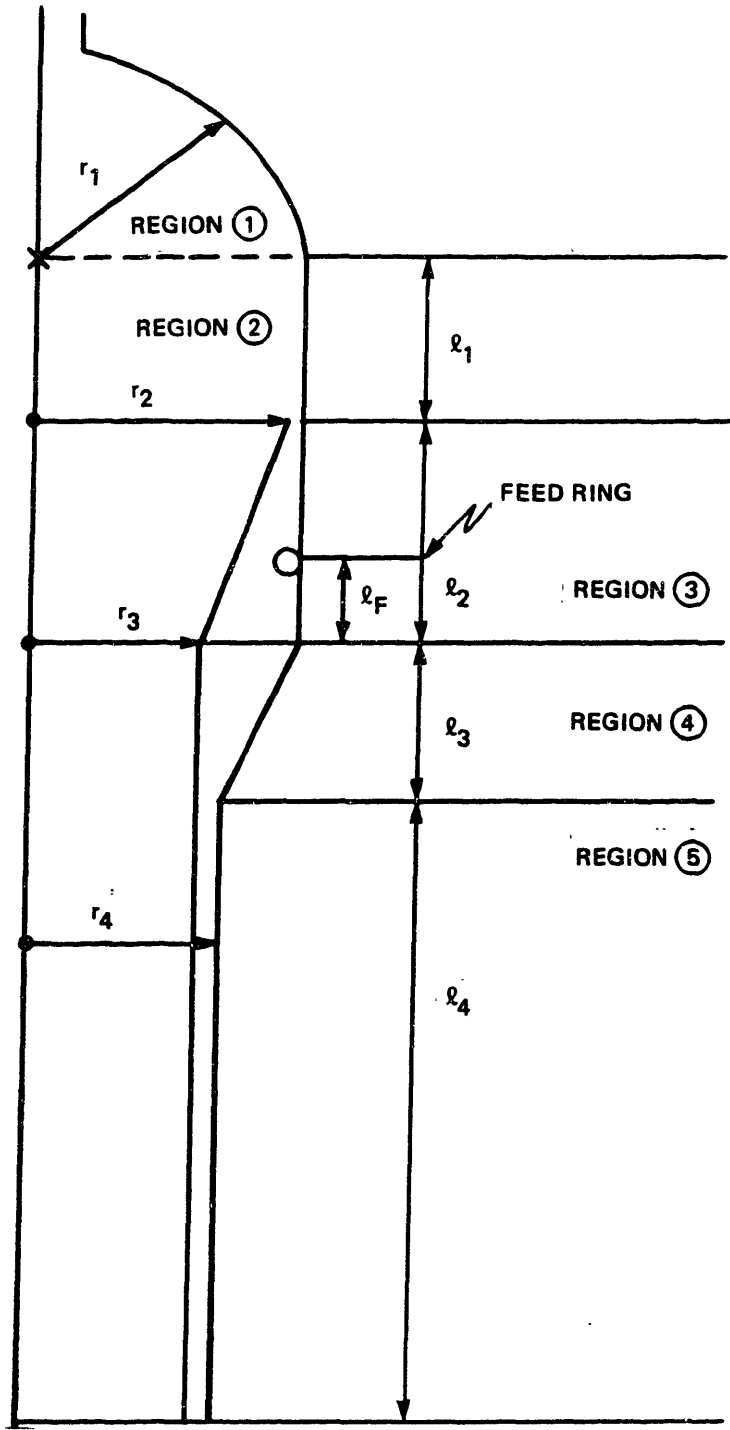


Figure K-1. Idealized steam dome - downcomer representation.

- 2.) Subtract  $V_v$  from  $\sum v$  to obtain the liquid volume contained in the region determined in Step 1. That is,

$$V_{LIQ}^I = \sum v - V_v$$

where the superscript I corresponds to the region where the water level is located. The form of  $V_{LIQ}^I$  as a function of the level, L, as measured from the bottom of the region, for each region, is given in Table K-1.

- 3.) Solve the resulting algebraic equation for L. As can be seen from Table K-1, this equation is either linear in L or cubic in L. The solution of the linear equation is trivial. It turns out that the cubic equation is always of the form:

$$L^3 + aL + b = 0$$

where  $ab \neq 0$ . This equation has an analytic solution, which is obtained using the transformation,  $L = m \cos \theta$ . The solution is:

$$L = m \cos \left( \theta_1 + \frac{2n\pi}{3} \right) \quad n = 0, 2, 4.$$

Table K-1  
Region Volumes.

Region	Volume of Region	Liquid Volume in Region as Function of Liquid Level Measured from Lower Boundary of Region (L).
1	$V_1 = \frac{2}{3} \pi r_1^3$	$V_{LIQ}^1 = \pi r_1^2 L - \frac{\pi}{3} L^3$
2	$V_2 = \pi r_1^2 l_1$	$V_{LIQ}^2 = \pi r_1^2 L$
3	$V_3 = \pi r_1^2 l_2 - \frac{\pi l_2 (r_2^3 - r_3^3)}{r_2 - r_3}$	$V_{LIQ}^3 = \pi r_1^2 L - \frac{\pi}{3b} [(bL + r_3)^3 - r_3^3]$ $b = \frac{(r_2 - r_3)}{l_2}$

Table K-1  
Region Volumes (Cont.)

Region	Volume of Region	Liquid Volume in Region as Function of Liquid Level Measured from Lower Boundary of Region (L).
4	$V_4 = \frac{\pi r_3(r_1^3 - r_4^3)}{r_1 - r_4}$	$V_{LIQ}^4 = \frac{\pi}{3b} [(bL + r_4)^3 - r_4^3] - \pi r_3^2 L$ $b = \frac{(r_1 - r_4)}{r_3}$
5	$V_5 = \pi r_4(r_4^2 - r_3^2)$	$V_{LIQ}^5 = \pi L(r_4^2 - r_3^2)$

where,

$$m = 2\sqrt{\frac{a}{3}}$$

$$\theta_1 = \frac{1}{3} \cos^{-1} \left( \frac{3b}{am} \right)$$

- 4.) The water level,  $l_w$ , is then obtained by adding  $L$  to the vertical height of the bottom of the region in which the water level is located.

The water level equations as functions of  $V_v$  are given in Table K-2.

Another calculation performed using the idealized steam dome - downcomer representation is the determination of the quantities  $l_{SAT}$  and  $l_{SUB}$ , which are used in the momentum equation. We must consider two cases (see Chapter 3 Section 3):

- 1.) fixed interface between saturated and sub-cooled volumes; and,
- 2.) moving interface between saturated and sub-cooled volumes.

The first quantity we must determine is the vapor volume at which the transition from a stationary to a moving interface occurs; we call this vapor volume  $V_{ref}$ . In Chapter 5 we state that the transition occurs when the liquid volume is equal to the volume of the downcomer plus 25 percent of the volume of saturated liquid present in the steam dome at



Table K-2  
Water Level Equations

Vapor Volume	Equation Solved	Water Level
$V_V < V_1$	$V_{LIQ}^1 = V_1 - V_V$	$h_W = L + h_1 + h_2 + h_3 + h_4$ $L = 2r_1 \cos\left(\theta + \frac{4\pi}{3}\right)$ $\theta = \frac{1}{3} \cos^{-1} \frac{-3(V_1 - V_V)}{2\pi r_1^3}$ $A_W = \pi(r_1^2 - r_2^2)$
$V_1 \leq V_V < V_1 + V_2$	$V_{LIQ}^2 = V_1 + V_2 - V_V$	$h_W = L + h_2 + h_3 + h_4$ $L = \frac{(V_1 + V_2 - V_V)}{\pi r_1^2}$ $A_W = \pi(r_1^2 - r_2^2)$

Table K-2  
Water Level Equations (Cont.)

Vapor Volume	Equation Solved	Water Level
$V_1 + V_2 < V_v \leq V_1 + V_2 + V_3$	$V_{LIQ}^3 = V_1 + V_2 + V_3 - V_v$	$\begin{aligned} \ell_w &= L + \ell_3 + \ell_4 \\ L &= \frac{(z - r_3)}{b} \\ b &= \frac{(r_2 - r_3)}{\ell_2} \\ z &= 2r_1 \cos\left(\theta + \frac{4\pi}{3}\right) \\ \theta &= \frac{1}{3} \cos^{-1}\left(\frac{-b}{2r_1}\right) \\ A_w &= \pi[r_1^2 - (bL + r_3)^2] \end{aligned}$

Table K-2  
Water Level Equations (Cont.)

Vapor Volume	Equation Solved	Water Level
$V_1 + V_2 + V_3 < V_V$ $< V_1 + V_2 + V_3 + V_4$	$V_{LIQ}^4 = V_1 + V_2 + V_3 + V_4 - V_V$	$l_w = L + l_4$ $L = \frac{(z - r_4)}{b}$ $b = \frac{(r_1 - r_4)}{l_3}$ $z = 2r_3 \cos \theta$ $\theta = \frac{1}{3} \cos^{-1} \left( -\frac{b}{2r_3} \right)$
		$A_w = \pi [(bL + r_4)^2 - r_3^2]$

Table K-2  
Water Level Equations (Cont.)

Vapor Volume	Equation Solved	Water Level
$V_v > V_1 + V_2 + V_3 + V_4$	$V_{LIQ}^5 = V_1 + V_2 + V_3 + V_4 + V_5 - V_v$	$z_w = \frac{(V_{TOT} - V_v)}{\pi(r_4^2 - r_3^2)}$ $V_{TOT} = V_1 + V_2 + V_3 + V_4 + V_5$ $A_w = A_D = \pi(r_4^2 - r_3^2)$

normal full power operation. Thus,  $V_{ref}$  is simply the total volume of the steam dome - downcomer,  $V_{TOT}$  ( $V_{TOT} = \sum_{i=1}^5 V_i$ ), minus this liquid volume. The volume of the downcomer,  $V_D$ , is simply the volume extending from the bottom of the steam dome - downcomer to the feedwater ring, or:

$$V_D = V_5 + V_4 + V_{LIQ}^3(l_F)$$

where  $V_{LIQ}^3(l_F)$  indicates that the expression for  $V_{LIQ}^3$  given in Table K-1 is to be evaluated at  $L = l_F$ . We assume that the water level at normal full power conditions,  $l_{w0}$ , is located in region 3 and is above the feedwater ring. Letting  $V_{f0}$  denote 25 percent of the volume of saturated liquid present in the steam dome at normal full power, we get:

$$V_{f0} = 0.25 [ V_{LIQ}^3(l_{w0} - l_3 - l_4) - V_{LIQ}^3(l_F) ]$$

Thus,

$$V_{ref} = V_{TOT} - V_{f0} - V_D$$

When  $V_v$  is less than or equal to  $V_{ref}$ , the interface between the saturated and subcooled regions is fixed, so the

height of the subcooled liquid,  $l_{\text{SUB}}$ , is fixed and is given by:

$$l_{\text{SUB}} = l_{\text{F}} + l_3 + l_4 \quad V_{\text{v}} \leq V_{\text{ref}}$$

In Chapter 3 we assume that when  $V_{\text{v}}$  is greater than  $V_{\text{ref}}$ , the volume of saturated liquid is constant and equal to  $V_{\text{f0}}$ . In this situation the interface between the saturated and subcooled regions is moving and  $l_{\text{SUB}}$  is no longer constant. We can determine  $l_{\text{SUB}}$  by using the same scheme used to determine the water level except that we replace  $V_{\text{v}}$  by  $V_{\text{v}} + V_{\text{f0}}$ . Thus, for  $V_{\text{v}}$  greater than  $V_{\text{ref}}$ ,  $l_{\text{SUB}}$  is determined using the water level equations given in Table K-2 with  $V_{\text{v}}$  replaced by  $V_{\text{v}} + V_{\text{f0}}$  and  $l_{\text{w}}$  replaced by  $l_{\text{SUB}}$ .

Finally, once  $l_{\text{SUB}}$  and  $l_{\text{w}}$  are known,  $l_{\text{SAT}}$  is determined from the relationship,

$$l_{\text{SAT}} = l_{\text{w}} - l_{\text{SUB}}$$

which is always true.

The final quantity that we must determine is the area at the liquid-vapor interface in the steam dome - down-comer. These areas are listed in Table K-2. Note that the areas in regions 1 and 2, where we would not expect to find the water level, are given by the minimum flow area located at the top of region 3.

## NOMENCLATURE

Most of the nomenclature is defined locally in the text. This is a brief list of some symbols for convenience.

A	Areas (m <sup>2</sup> )
A <sub>D</sub>	Lower Downcomer Area (m <sup>2</sup> )
A <sub>RI</sub>	Riser Inlet Flow Area (m <sup>2</sup> )
A <sub>RO</sub>	Riser Outlet Flow Area (m <sup>2</sup> )
A <sub>w</sub>	Area at Liquid-Vapor Interface (m <sup>2</sup> )
C <sub>p</sub>	Specific Heat Capacity ( $\frac{J}{kg \cdot ^\circ K}$ )
D <sub>h</sub>	Hydraulic Diameter (m)
E	Energy Content (J)
f	Friction Factor (-)
g	Acceleration of Gravity ( $\frac{m}{s^2}$ )
H	Specific Enthalpy ( $\frac{J}{kg}$ )
H'	Specific Enthalpy of Flowing Mixture ( $H_l + xH_{vs}$ ) ( $\frac{J}{kg}$ )
h	Heat Transfer Coefficient ( $\frac{W}{m^2 \cdot ^\circ K}$ )
	Subscript s for secondary
	Subscript p for primary
I	Inertance (m <sup>-1</sup> ) or $\sqrt{-1}$
K <sub>C</sub>	Crossflow Loss Coefficient (m <sup>-2</sup> )
K <sub>D</sub>	Loss Coefficient at Downcomer Exit (-)
K <sub>SEP</sub>	Separator Loss Coefficient (-)
L	Length (m)
L <sub>D</sub>	Length of Lower Downcomer (m)

$L_p$	Length of Parallel Flow Portion of Tube Bundle (m)
$M$	Mass Content (kg)
$M_i$	Momentum Equation Parameters ( $\frac{\text{Pa} \cdot \text{s}}{\text{kg}}$ )
$p$	Pressure (Pa)
$q_B$	Power or Heat Transfer Rate (W)
$q''$	Heat Flux ( $\frac{\text{W}}{\text{m}^2}$ )
$r_f$	Fouling Factor ( $\frac{\text{m}^2 \cdot \text{K}}{\text{W}}$ )
$r_i$	Tube Inner Radius (m)
$r_o$	Tube Outer Radius (m)
$s$	Coordinate for Integration Around Recirculation Loop (m)
$T$	Temperature ( $^{\circ}\text{K}$ )
$\Delta T_{LM}$	Log-Mean Temperature Difference ( $^{\circ}\text{K}$ )
$t$	Time(s)
$\Delta t$	Time Step Size
$U$	Specific Internal Energy ( $\frac{\text{J}}{\text{kg}}$ )
$u$	Velocity ( $\frac{\text{m}}{\text{s}}$ )
$V$	Volume ( $\text{m}^3$ )
$V_D$	Volume of Lower Downcomer ( $\text{m}^3$ )
$v'$	Momentum Specific Volume ( $\frac{\text{m}^3}{\text{kg}}$ )
$W$	Flowrate ( $\frac{\text{kg}}{\text{s}}$ )
$W_s$	Saturated Steam Flow ( $\frac{\text{kg}}{\text{s}}$ )
$x$	Quality (-)



### Greek

$\alpha_2$	Vapor Volume Fraction (-)
$\phi_{l0}$	Two-Phase Multiplier (-)
$\rho$	Density ( $\frac{\text{kg}}{\text{m}^3}$ )
$\tau$	Transport Time or Time Constant (s)
$\lambda$	Eigenvalue (-)

### Subscripts

fw	Feedwater
l	Liquid
l0	Liquid Only
ls	Saturated Liquid
lvs	Indicates $\xi_{lvs} = \xi_{vs} - \xi_{ls}$
n	Riser Outlet
o	Downcomer Exit
p	Parallel-to-Crossflow Transition
r	Riser Inlet
R	Riser
SAT	Saturated
STM	Main Steam Line
SUB	Subcooled
t	Tube Metal
TB	Tube Bundle
TBC	Tube Bundle Crossflow Region
TBP	Tube Bundle Primary Side
TM	Tube Metal Volume

v Vapor  
vs Saturated Vapor

Other Notation

$\underline{\xi}$  Indicates that  $\xi$  is a Matrix  
 $\underline{\xi}$  Indicates that  $\xi$  is a Vector  
 $\dot{\xi}$  Indicates Time Derivative of  $\xi$   
 $\bar{\xi}$   
 $\langle \xi \rangle$  Defined in Appendix A.  
 $\langle \xi \rangle_v$   
 $\langle \xi \rangle_l$

## REFERENCES

- (A1) R.P. Anderson, et al., "An Analog Simulation of the Transient Behavior of Two-Phase Natural Circulation Systems," Chemical Engineering Progress Symposium Series 59, No. 41, 96-103 (1963).
- (A2) R.P. Anderson, et al., "Transient Analysis of Two-Phase Natural-Circulation Systems," ANL-6653, Argonne National Laboratory (1962).
- (B1) N.W.S. Bruens, "U-Tube Steam Generator Dynamics Modeling and Verification," Proceedings of the Second International Conference on Boiler Dynamics and Control in Nuclear Power Stations, Bournemouth, United Kingdom, October 1979.
- (B2) R.B. Bird, W.E. Stewart, and E.N. Lightfoot, Transport Phenomena, John Wiley and Sons, New York, 1960.
- (B3) F.W. Barclay, et al., "RD-12 Facility Description," WNRE-496, December 1980.
- (B4) "Baltimore Gas and Electric Company, Calvert Cliffs Nuclear Power Plant, Unit 1, Startup Test Report," Docket 50-317-463, 1975.
- (B5) G. Birkhoff and T.F. Kimes, "CHIC Programs for Thermal Transients," WAPD-TM-245, February 1962.
- (B6) W.E. Boyce and R.C. DiPrima, Elementary Differential Equations and Boundary Value Problems, John Wiley and Sons, Inc., New York, 1977.

- (C1) J.G. Collier, Convective Boiling and Condensation, McGraw-Hill Book Company, New York, 1971.
- (C2) W.G. Clarke, "Transient Analysis of Steam Generators in Nuclear Power Plants using Digital Computer Techniques," M.S. Thesis, University of Pittsburgh, 1965.
- (D1) J.C. Deckert, et al., "On-Line Power Plant Signal Validation Technique Utilizing Parity - Space Representation and Analytic Redundancy," EPRI NP-2110, November 1981.
- (E1) M.M. El-Walkil, Nuclear Heat Transport, International Textbook Company, New York, 1971.
- (E2) "Summary and Evaluation of Scoping and Feasibility Studies for Disturbance Analysis and Surveillance Systems (DASS)," EPRI NP-1684, December 1980.
- (F1) "Maine Yankee Atomic Power Station, Final Safety Analysis Report," Docket 30309, Maine Yankee Atomic Power Company, 1971.
- (F2) "Arkansas Nuclear One, Unit 2 License Application, Final Safety Analysis Report," Docket 50368-R1, Arkansas Power and Light Company, 1974.
- (F3) "Calvert Cliffs Nuclear Power Plant, Units 1 and 2, Final Safety Analysis Report," Docket 50317-R1, Baltimore Gas and Electric Company, 1973.
- (G1) P.A. Gagne, "NSSS Design and Cycle 1 Operating History Data for Arkansas Nuclear One, Unit 2," EPRI NP-1707, March 1981.

- (H1) C.A. Hall, et al., "Numerical Methods for Thermally Expandable Two-Phase Flow—Computational Techniques for Steam Generator Modeling," EPRI NP-1416, May 1980.
- (H2) J.P. Holman, Heat Transfer, McGraw-Hill Book Company, New York, 1972.
- (H3) A.C. Hindmarsh, "Linear Multistep Methods for Ordinary Differential Equations: Method Formulations, Stability, and the Methods of Nordsieck and Gear," UCRL-51186 Rev. 1, March 1972.
- (H4) J.H. Hopps, "Safety Parameter Display Systems: A High Information Reliability Design Concept," Preprint. Presented at ASME Second International Computer Engineering Conference, San Diego, August 15-19, 1982.
- (H5) A. Hoeld, "A Theoretical Model for the Calculation of Large Transients in Nuclear Natural - Circulation U-Tube Steam Generators (Digital Code UTSG)," Nuclear Engineering and Design 47, 1-23 (1978)
- (I1) M. Ishii, "One-Dimensional Drift-Flux Model and Constitutive Equations for Relative Motion Between Phases in Various Two-Phase Flow Regimes," ANL-77-47, Argonne National Laboratory, October 1977.
- (I2) W.W.R. Inch and R.H. Shill, "Thermal-Hydraulics of Nuclear Steam Generators: Analysis and Parameter Study," ASME Paper 80-C2/NE-7, 1980.

- (J1) A.B. Jones, "Hydrodynamic Stability of a Boiling Channel," KAPL-2170, October 1961.
- (K1) J.G. Knudsen and D.C. Katz, Fluid Dynamics and Heat Transfer, McGraw-Hill Book Company, New York, 1958.
- (K2) L.W. Keeton, et al., "The URSULA2 Computer Program," EPRI NP-1315 Vols. 1-4, January 1980.
- (K3) J.E. Kelly et al. "User's Guide for THERMIT-2: A Version of THERMIT for both Core-Wide and Subchannel Analysis of Light Water Reactors," MIT Energy Lab. Report No. MIT-EL-81-029, August 1981.
- (L1) R.T. Lahey, Jr., and F.J. Moody, The Thermal-Hydraulics of a Boiling Water Nuclear Reactor, American Nuclear Society, LaGrange Park, Illinois, 1977.
- (L2) J.C. Lee, et al., "Review of Transient Modeling of Steam Generator Units in Nuclear Power Plants," EPRI NP-1576, October 1980.
- (L3) J.C. Lee, et al., "Transient Modeling of Steam Generator Units in Nuclear Power Plants: Computer Code TRANSG-01," EPRI NP-1368, March 1980.
- (L4) "TRAC-P1: An Advanced Best Estimate Computer Program for PWR LOCA Analysis," LA-7279-MS Vol. 1, Los Alamos Scientific Laboratory, June 1978.
- (M1) J.E. Meyer, "Conservation Laws in One-Dimensional Hydrodynamics," WAPD-BT-20, September 1960.
- (M2) J.E. Meyer, "Hydrodynamic Models for the Treatment of Reactor Thermal Transients," Nuclear Science and Engineering 19, 269-277 (1961).

- (M3) C.G. Mewdell, et al., "Development and Verification of a Space Dependent Dynamic Model of a Natural Circulation Steam Generator," Proceedings of the Second International Conference on Boiler Dynamics and Control in Nuclear Power Stations, Bournemouth, United Kingdom, October 1979.
- (M4) C.G. Mewdell, et al., "Verification of the Computer Code Boiler 2 Using the RD12 Boiler Test Results," unpublished data.
- (M5) R.C. Mitchell, et al., "Verification of Best-Estimate Nuclear Power Plant Simulation Models," EPRI WS-81-212, Proceedings of Simulation Methods for Nuclear Power Systems, Tucson, Arizona, May 1981.
- (M6) C.H. Meijer and B.J. Frogner, "On-Line Power Plant Alarm and Disturbance Analysis Systems," EPRI NP-1379, April 1980.
- (M7) E.O. Marchand, et al., "Predictions of Operation Transients for a Steam Generator of a PWR Nuclear Power System," ASME Paper 80-C2/NE-5, 1980.
- (M8) J.H. McFadden, et al., "RETRAN-02—A Program for Transient Thermal-Hydraulic Analysis of Complex Fluid Flow Systems," EPRI NP-1850 Vols. 1-4, May, 1981.
- (M9) R.P. McCarty, "Maine Yankee Plant Reactor Coolant System," System Description No. 4467-010 Rev. 0, Combustion Engineering, Inc., Windsor, CT, April 1971.

- (M10) R.C. Martinelli and D.B. Nelson, "Prediction of Pressure Drop during Forced-Circulation Boiling of Water," Trans. ASME 70, 695 (1948).
- (N1) "Generic Evaluation of Feedwater Transients and Small Break Loss of Coolant Accidents in Combustion Engineering Designed Operating Plants," NUREG-0635, January 1980.
- (N2) G.Y. Nakayama, "Linearized Model Real Time Reactor Simulation," S.B. and S.M. Thesis, Massachusetts Institute of Technology, 1981.
- (P1) T.A. Porsching, "A Finite Difference Method for Thermally Expandable Fluid Transients," Nuclear Science and Engineering 64, 269-277(1977).
- (P2) M.A. Pulick and S.G. Margolis, "CRIB-1—A Steam Generator Stability Analysis Program for the Philco-2000 Computer," WAPD-TM-530, December 1965.
- (R1) W.M. Rohsenow and H.Y. Choi, Heat, Mass, and Momentum Transfer, McGraw-Hill Book Company, New York, 1958.
- (R2) P.J. Roache, Computational Fluid Dynamics, Hermosa Publishers, Albuquerque, NM, 1976.
- (S1) G. Slovik, et al., "Transient Studies on BRENDA - A Breeder Reactor Model," Proceedings of the Fourth Power Plant Dynamics, Control, and Testing Symposium, Gatlinburg, Tennessee, March 1980.



- (S2) C.W. Stewart, et al., "Improvements to the COBRA-TF (EPRI) Computer Code for Steam Generator Analysis," EPRI NP-1509, September 1980.
- (S3) G. Strang, Linear Algebra and its Applications, Academic Press, New York, 1980.
- (S4) D.P. Siska, "NSSS Transient Tests at ANO-2," EPRI NP-1708, May 1981.
- (T1) L.S. Tong and J. Weisman, Thermal Analysis of Pressurized Water Reactors, American Nuclear Society, La Grange Park, Illinois, 1970.
- (V1) G.J. Van Tuyle, "Linearized Transient Analysis of Nuclear Steam Generators," Ph.D. Thesis, University of Michigan, 1978.
- (W1) D.H. Williams, Letter with Calvert Cliffs Startup Test Results, Docket 50-368-557, 1978.
- (Z1) N. Zuber and J.A. Findlay, "Average Volumetric Concentration in Two Phase Flow Systems," J. Heat Transfer 87, 453-468 (1965).

## BIOGRAPHICAL NOTE

Walter H. Strohmayer was born May 10, 1955 in St. Louis, Missouri. He spent the first eight years of his life in the United States. From 1963 to 1973 the author lived in Brussels, Belgium, and graduated from the International School of Brussels.

In September 1973 the author enrolled at Rensselaer Polytechnic Institute. He graduated cum Laude and received the degree of Bachelor of Science in Nuclear Engineering, with a minor in Economics, in December of 1976. During his undergraduate studies, the author spent one summer working as an Engineering Aide at the Babcock and Wilcox Company in Lynchburg, Virginia, and another summer as an Engineering Aide with the Nuclear Energy Liability and Property Insurance Association in Farmington, Connecticut.

The author entered the graduate school at the Massachusetts Institute of Technology in February, 1977. In June of 1978 he was awarded the degree of Master of Science in Nuclear Engineering. In September of 1982 the author received the degree of Doctor of Philosophy in Nuclear Engineering and subsequently began employment with the General Atomic Company in San Diego, California, as a Senior Engineer.

During his graduate career the author was awarded a three year National Science Foundation Fellowship and a Charles Stark Draper Laboratory Fellowship. The author is a

member of Tau Beta Pi and an associate member of Sigma Xi.  
He is also a student member of the American Nuclear Society  
and the American Society of Mechanical Engineers.